Synthesis of Pyrrolo-Coumarins, Indolizidines, C-N Bond Cleavage of Mannich Bases, and Alkylation of Tetrahydroisoquinolines

A THESIS SUBMITTED IN PARTIAL FULFILLMENT for THE DEGREE of

DOCTOR OF PHILOSOPHY

IN THE SCHOOL OF CHEMICAL SCIENCES
GOA UNIVERSITY

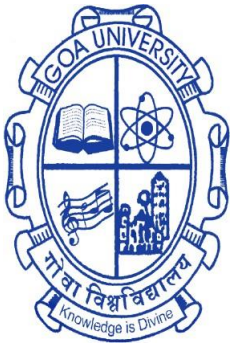

By

KETAN SHARAD MANDREKAR
GOA UNIVERSITY
TALEIGAO
GOA

MARCH 2022

Synthesis of Pyrrolo-Coumarins, Indolizidines, C-N Bond Cleavage of Mannich Bases, and Alkylation of Tetrahydroisoquinolines

A THESIS SUBMITTED IN PARTIAL FULFILLMENT for THE DEGREE of

DOCTOR OF PHILOSOPHY

IN THE SCHOOL OF CHEMICAL SCIENCES
GOA UNIVERSITY

By

KETAN SHARAD MANDREKAR
GOA UNIVERSITY
Taleigao
GOA

MARCH 2022

DECLARATION

I, Ketan Sharad Mandrekar hereby declare that this thesis represents work which has been carried out by me and that it has not been submitted, either in part or full, to any other University or Institution for the award of any research degree.

Place: Taleigao Plateau.
Date: 15-03-2022

Ketan Sharad Mandrekar
Research Scholar
School of Chemical Sciences
Goa University, Goa.

CERTIFICATE

I hereby certify that the above Declaration of the candidate, Ketan Sharad Mandrekar is true and the work was carried out under my supervision.

Prof. Santosh G. Tilve
Research Guide
School of Chemical Sciences
Goa University, Goa.

ACKNOWLEDGEMENT

Life is a journey of moments and experiences we gain in this endless and unbound time of the universe. The Ph.D. work, the thesis, and the moments spent during this time form an important part of my life which would not have been possible without the support, guidance, and unconditional help provided by many people. I owe a big thanks to all of them.

I would like to express my sincere gratitude to my thesis supervisor ***Prof. Santosh G. Tilve****. His patience, enthusiasm, co-operation, and suggestions made me present this research work in the existing form. His brilliant, skillful supervision enriched this study higher than my expectations. I could not remain any more without giving heartfelt thanks to him for his painstaking supervision throughout the study period. This research work would not be possible without his stimulation, inspiration, and cooperation. Special thanks to my subject experts* ***Prof. V. S. Nadkarni*** *and* ***Dr. Sandesh T. Bugde.*** *Your encouraging words and thoughtful, detailed feedback have been very important to me.*

I take this opportunity to thank all my teachers and faculty members of the School of Chemical Sciences ***Prof. V. M. S. V. Verenkar***, ***Prof. R. N. Shirsat***, ***Prof. A. V. Salkar***, *and* ***Prof. S. N. Dhuri*** *for their encouragement and support. I would also like to thank* ***Dr. Rohan Kunkalekar, Dr. Vinod Mandrekar, Dr. Prem Lama, Dr. Mahesh Majik***, ***Dr. G. Santosh***, ***Dr. Hari Kadam***, ***Dr. Rupesh Patre***, ***Dr. Pranay P. Morajkar,*** *and* ***Prof. Sheshnath V. Bhosale*** *for their timely motivation, help and constant support. Special thanks go out to* ***Dr. Sagar Patil*** *and* ***Dr. Prajesh Volvoikar****. Their knowledge and ingenuity are something I will always keep aspiring to.*

I wish to thank ***Syngenta Biosciences*** *for the NMR facility in time of need. Also, my thank goes to* ***Prof. Mainak Banerjee*** *for the valuable suggestions during my SRF interview which helped me carry out my research in an impactful way.*

I owe my gratitude to my group seniors ***Dr. Mayuri Naik, Dr. Durga Kamat, Dr. Pratibha Bakre*** *for their constant help, advice, and training. Also, I am thankful to other seniors from the department* ***Dr. Mira Parmekar, Dr. Satu Gawas, Dr. Daniel***

Coutinho, Dr. Shambhu Parab, ***Dr. Mithil Fal Desai***, ***Dr. Diptesh Naik***, ***Dr. Savita Kundaikar***, *and* ***Dr. Rita Jyai*** *for their help and advice and my lab-mates* ***Dr. Shashank Mhaldar, Ms. Gayatri Kotkar, Ms. Madhuri Gaikwad*** *and* ***Mr. Savio Dias*** *for creating a positive and friendly working environment.*

It is important to strike a balance with life outside the dark depths of the lab. As such, I cannot stress enough about the importance of the support and constant motivation of my friends and colleagues. I would thank ***Dr. Pooja Bhargao, Dr. Sudesh Morajkar, Dr. Abhijit Shetgaonkar, Dr. Neha Parsekar***, ***Dr. Rahul Kerkar***, ***Dr. Prajyoti Gauns Dessai***, ***Dr. Pratik Asogekar***, ***Dr. Vishnu Chari***, ***Dr. Celia Braganza***, ***Dr. Vishal Pawar***, ***Dr. Akshay Salkar, Dr. Amarja Naik, Dr. Saeesh Mangaokar***, ***Dr. Priyanka Kole, Ms. Lalitprabha Salgaonkar*** *and my juniors* ***Mangala***, ***Wilma***, ***Seneca***, ***Sonam***, ***Geeta***, ***Pritesh***, ***Vipul***, ***Sanjali***, ***Ratan***, ***Dinesh***, ***Kerba***, ***Vishal***, ***Vilas*** *and* ***Harshad*** *for their support.*

I sincerely thank the ***non-teaching staff*** *of the School of Chemical Sciences-Goa University, the librarian, and other staff in the library of Goa University for being kind and helpful. Special gratitude goes out to* ***UGC-New Delhi*** *for the UGC-NFOBC fellowship for providing the funding for the work.*

Further, yet importantly, heartfelt and due respect to my mother ***Mrs. Savita S. Mandrekar***, *father* ***Mr. Sharad D. Mandrekar***, *my sisters and brother for their strong moral support and timely encouragement in every step to bring me to this present stage. Similarly, other friends* ***Dr. Tanya Raghava***, ***Dr. Shilpa Raghava***, *and* ***Mr. Agnelo Silveira*** *are also subject to special thanks for their inspiration and cooperation in my study.*

Finally, I thank Lord ***Shree Krishna*** *for all the bounties and blessings he has bestowed upon me and for granting me the strength and patience to complete my research.*

*…….****Ketan Sharad Mandrekar***

Dedicated to my family

And

I want to thank me for believing in me, I want to thank me for trying to do more rights than wrong, I want to thank me for just being me at all times, I want to thank me for never quitting, I want to thank me for always being a giver and trying to give more than I receive.

Table of Contents

Section II: Synthetic studies of isoindolo[1,2-*a*]isoquinoline compounds

Section III: *In Silico* molecular docking study of pyrrolo[2,1-*a*]isoquinoline moieties with sars-cov-2 proteins

3 Oxidative cleavage of the C–N bond of aryl and heteroaryl (dimethylamino)methyl groups into aldehydes

GENERAL REMARKS

- ✓ The compound numbers, figure numbers, scheme numbers, and reference numbers given in each chapter (Section) refer to that particular chapter (Section) only.
- ✓ Commercial reagents were used without any further purification.
- ✓ Organic solvents were distilled before use and stored over specified dehydrated agents whenever necessary.
- ✓ Reactions were monitored by thin-layer chromatography (TLC Silica gel 60 F254 purchased from Merck) and visualization of the spots on TLC plates was achieved by I_2 staining and UV chamber.
- ✓ Chromatographic purification was conducted by column chromatography using silica gel (60-120 mesh size) or by flash chromatography using silica gel (230-400 mesh size) on the Combiflash Companion instrument.
- ✓ All melting points and boiling points were recorded using Thiele's tube and are uncorrected.
- ✓ Infrared spectroscopy was performed on a Shimadzu Prestige-21 FT-IR spectrometer by the KBr sample holder method.
- ✓ ^{1}H NMR and ^{13}C NMR experiments were carried out on a Bruker Avance 400 MHz spectrometer at 25℃ using deuterated solvents such as $CDCl_3$, DMSO-d_6, D_2O, and TMS as an internal standard.
- ✓ Electron spray ionization mass spectra (ESI-MS) were obtained using Shimadzu single quadrupole LC-MS-2020 instrument performed in positive ion mode and HRMS were recorded with Micromass Q-ToF ESI instrument.
- ✓ XRD measurements were performed on a Bruker D8 FOCUS diffractometer using a Cu target radiation source (λ = 0.15418 nm).

List of Abbreviation

General abbreviations

g	-	Gram/s
mg	-	Milligram/s
mmol	-	Millimole
mL	-	Milliliter
m.p.	-	Melting point
b.p.	-	Boiling point
dil.	-	Dilute
lit.	-	Literature
d	-	Day/s
h	-	Hour/s
min	-	Minute/s
sec	-	Second/s
Z	-	Zussamen (together)
E	-	Eentegegen (opposite)
R	-	Rectus
S	-	Sinister
Fig.	-	Figure
conc.	-	Concentrated
glac.	-	Glacial
sat.	-	Saturated
aq.	-	Aqueous
anhyd.	-	Anhydrous
°C	-	Degree Celcius
hυ	-	Irradiation
%	-	Percentage
rt	-	Room temperature
Expt.	-	Experiment
Temp.	-	Temperature
MW	-	Microwave
o	-	Ortho

m	-	Meta
p	-	Para
MS	-	Molecular sieves
cat.	-	Catalytic
atm.	-	Atmospheric
et al.	-	Et alia (and others)
equiv	-	Equivalent
psi	-	Pounds per square inch
TLC	-	Thin layer chromatography

Compound Abbreviations

Ac	-	Acetyl
Ac_2O	-	Acetic anhydride
Ts	-	*p*-Toluene sulfonyl
Ar	-	Aryl
Boc	-	tert-Butyl carbonyl
Bn	-	Benzyl
Bz	-	Benzoyl
t-Bu	-	*tert*-Butyl
TFA	-	Trifluoro acetic acid
TFAA	-	Trifluoro acetic anhydride
AcOH	-	Acetic acid
MeOH	-	Methanol
EtOH	-	Ethanol
m-CPBA	-	*m*-Chloroperbenzoic acid
p-TsOH	-	*p*-Toluene sulfonic acid
DMSO	-	Dimethyl sulfoxide
DMF	-	*N*,*N*-Dimethylformamide
THF	-	Tetrahydrofuran
Et	-	Ethyl
Me	-	Methyl
LDA	-	Lithium diisopropylamide
Py	-	Pyridine
TBHP	-	*tert*-Butyl hydroperoxide

EtOAc	-	Ethyl acetate
*n*BuLi	-	*n*Butyl lithium
t-BuOK	-	Potassium tertiary butoxide
PMB	-	*p*-Methoxybenzyl
Ph	-	Phenyl
MOM	-	Methoxymethyl ether
Ms	-	Methane sulfonyl
TMS	-	Trimethylsilyl
TMSCN	-	Cyanotrimethyl silane
PPA	-	Polyphosphoric acid
CAN	-	Cerric ammonium nitrate
NBS	-	*N*-Bromosuccinimide
DMP	-	Dess-Martin periodinane
Boc_2O	-	*tert*-Butyl dicarbonate
Pet. ether	-	Petroleum ether
TsCl	-	Tosyl chloride
AIBN	-	Azobisisobutyronitrile
DMAP	-	4-Dimethyl amino pyridine
HMPA	-	Hexamethylphosphoramide
DIAD	-	Diisopropyl azodicaboxylate
DCC	-	Dicyclohexyl cabodiimide
TBAF	-	Tetrabutylammonium fluoride
TBAF	-	Tetrabutyl ammonium fluoride
LAH	-	Lithium aluminium hydride
DIBALH	-	Diisobutyl aluminium hydride
DDQ	-	2,3-Dichloro-5,6-dicyanobenzoquinone
Pd/C	-	Palladium on activated charcoal
i-PrOH	-	Iso-propanol

Spectroscopic Abbreviations

IR	-	Infrared
υ_{max}	-	Frequency maximum
cm^{-1}	-	Frequency in wavenumber

UV	-	Ultra violet
MHz	-	Megahertz
Hz	-	Hertz
J	-	Coupling constant
bs	-	Broad singlet
ppm	-	Parts per million
$CDCl_3$	-	Deuterated chloroform
s	-	Singlet
d	-	Doublet
t	-	Triplet
q	-	Quartet
m	-	Multiplet
dd	-	Doublet of doublet
δ	-	Chemical shift in ppm
m/z	-	Mass to charge ratio
M^+	-	Molecular ion
$CDCl_3$	-	Deuterated chloroform
DMSO-d_6	-	Deuterated dimethyl sulfoxide
HRMS	-	High Resolution Mass Spectrum
DEPT	-	Distortionless Enhancement by Polarization Transfer
NMR	-	Nuclear magnetic resonance

List of Schemes

Chapter 1

Chapter 2

Section I

Section II

Chapter 3

Chapter 4

List of Tables

Chapter 4

List of Figures

Chapter 1

Chapter 2

Section I

Section II

Section III

Chapter 3

Chapter 4

ABSTRACT OF THESIS

The thesis entitled "**Synthesis of pyrrolo-coumarins, indolizidines, C-N bond cleavage of mannich bases, and alkylation of tetrahydroisoquinolines**" consists of four chapters with thorough literature studies and analysis.

The ***First*** chapter, "Synthetic studies of pyrrolo-coumarin alkaloids: Lamellarins" presents the syntheses of lamellarin analogs from a highly convergent synthetic route (Scheme 1). A tandem process of, Bischler Napieralski- Michael addition- oxidation sequence was developed for the synthesis of lamellarin skeleton. Simple, commercially available chemicals like phenylethylamine, phenylacetic acid, salicylaldehyde proxies, and ethyl bromoacetate are used to build the pentacyclic molecules. Overall, three lamellarin analogs were prepared successfully.

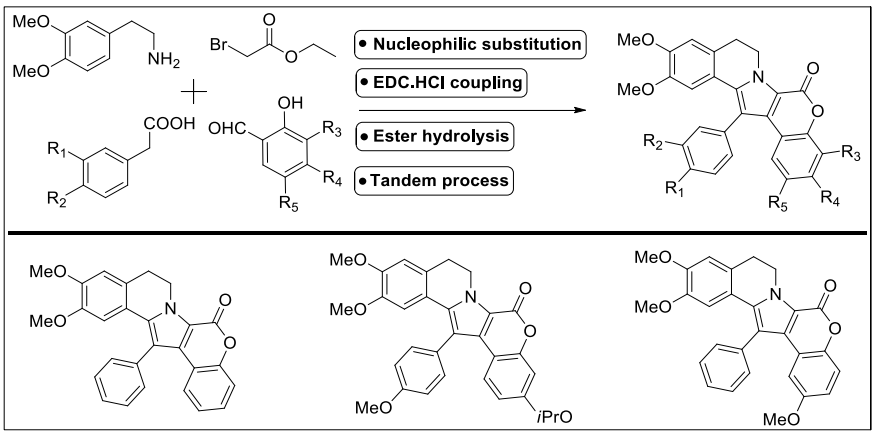

Scheme 1

The ***Second*** chapter, "Synthetic studies of benzoindolizidine derived alkaloids**"** describes the construction of an indolizidine ring core adjacent to the benzene rings using the simple condensation-cyclization methodology. This chapter is further divided into three sections depending upon its type of ring system and application. The first section gives an account of three methods tried for the syntheses of pyrrolo[2,1-*a*]isoquinoline moieties. In the first method, we attempted an intramolecular aza-ene cyclization of the cyclic iminium ion with an attached allyl group (Scheme 2, strategy 1). In the second method, we have attempted the δ-amino aldehyde cyclization strategy to build an indolizidine ring around a dimethoxy substituted benzene ring (Scheme 2, strategy 2). We had anticipated one-pot oxidation of δ-hydroxy amine followed by a cyclization reaction to form a cyclic iminium ion but failed at the oxidation step reaction. Protection of NH with the Boc anhydride group helped in oxidizing the hydroxy group on the other end. Later the deprotection-

cyclization failed to give the expected product. Concisely, we developed a tandem approach to synthesize pyrrolo[2,1-*a*]isoquinoline molecules starting from easily available compounds like phenethylamine and dicarboxylic acids using 8.3 wt% P_4O_{10}/TfOH (Scheme 2, strategy 3). Corresponding naturally occurring compounds such as (±)-crispine A, (±)-trolline/oleracein E, (±)-mescalotam, (±)-harmicine were synthesized along with a trihydroxy analog of mescalotam.

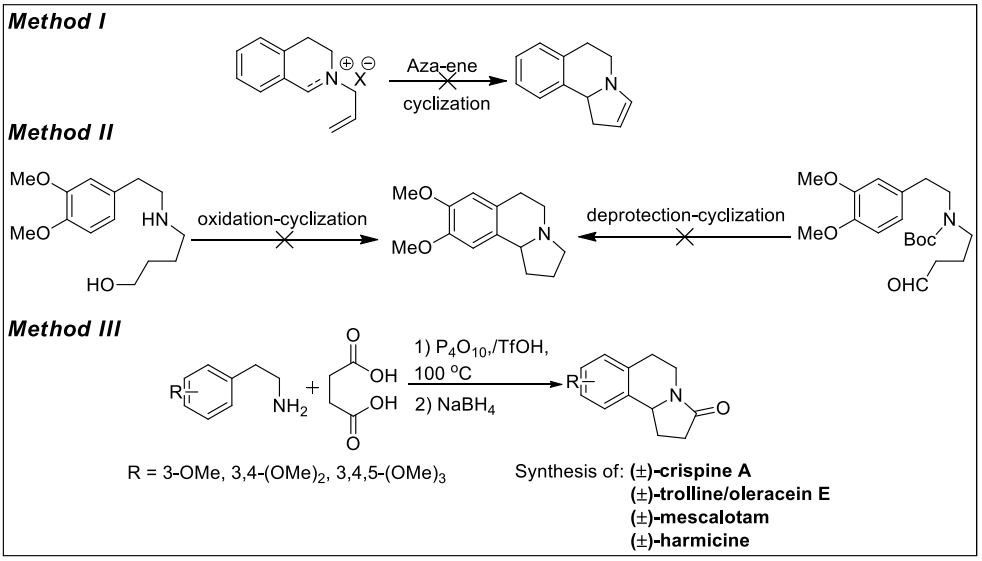

Scheme 2

This second section describes the attempted synthesis of isoindolo[2,1-*a*]isoquinoline compounds *via* intramolecular C-C coupling reaction strategy using iodine and copper catalysts (Scheme 3, method I). Further, the goal of constructing isoindolo[2,1-*a*]isoquinolinone was achieved using the one-pot condensation-cyclization reaction between phenethylamine and phthalic acid derivatives using an 8.3 wt% P_4O_{10}/TfOH reagent system (Scheme 3, method II).

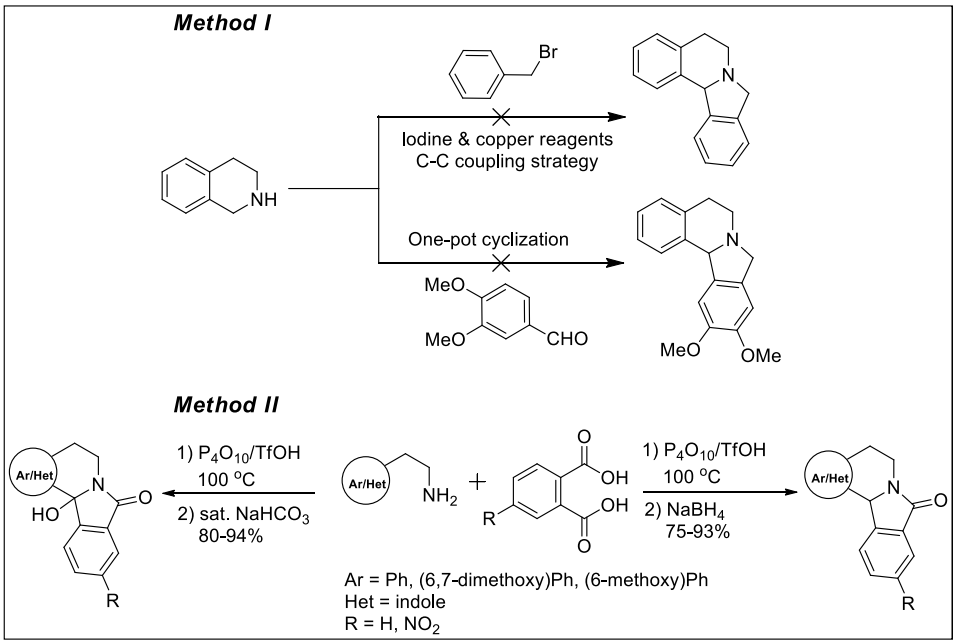

Scheme 3

In the third section, we have performed the molecular docking studies of pyrrolo[2,1-*a*]isoquinoline moieties and favipiravir drug as a standard against $3CL^{PRO}$ proteases (PDB: 6LU7) in Autodock 4.2.6 software followed by studying its interactions in BIOVIA Discovery software. We have seen a better performance of our ligands against 6LU7 than the favipiravir drug.

The ***Third*** chapter, "Oxidative cleavage of the C–N bond of aryl and heteroaryl (dimethylamino)methyl groups into aldehydes" deals with our efforts in developing a methodology using an iodine mediated conversion of aryl and heteroaryl (dimethylamino)methyl groups into aldehydes at ambient temperature. We have synthesized around twenty such aldehydes of substituted indoles, aryl, coumarin, and thiophene. We have also prepared acetophenone and benzophenone from their respective Mannich adducts (Scheme 4). We have studied the reaction mechanism pathway using NMR spectroscopy.

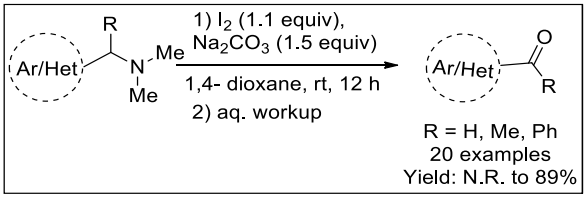

Scheme 4

The ***Fourth*** chapter, "Intermolecular cross dehydrogenative Csp_3-Csp_3 coupling reactions of N-phenyl-THIQ employing ternary oxide nanocomposite of $CuO{\cdot}NiO{\cdot}TiO_2$" describes the methodology using a bimetallic-TiO_2 catalyst, which synergistic catalytic

ability facilitated an intermolecular CDC coupling of *N*-phenyltetrahydroisoquinoline with various nucleophiles under an oxygen atmosphere. Three catalysts were screened to study the synergistic effect of bimetals i.e. 5% Cu·TiO_2, 5% NiO·TiO_2, 5% CuO·NiO·TiO_2, out of which 5% CuO·NiO·TiO_2 showed good performance. The use of solvent mostly resulted in the formation of a side product (its amide compound) in greater yield than the expected product. So, a neat heating reaction condition is developed to synthesize several *N*-phenyltetrahydroisoquinoline derivatives with different nucleophiles in good yields (Scheme 5).

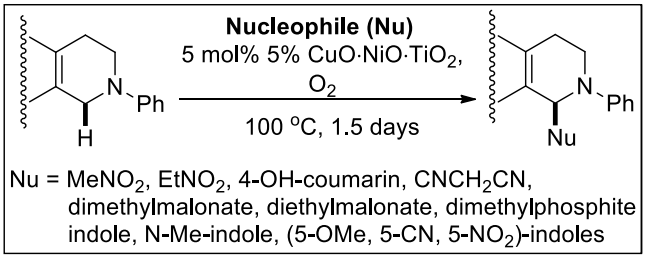

Scheme 5

List of publications

Appended to thesis:

1) Domino Bischler–Napieralski – Michael Reaction and Oxidation – New Route to Coumarin-Pyrrole-Isoquinoline Fused Pentacycles. **Mandrekar, K. S.**; Kadam, H. K.; Tilve, S. G. *Eur. J. Org. Chem.* **2018**, *2018*, 6665.
2) *Cover Feature*: Domino Bischler–Napieralski – Michael Reaction and Oxidation – New Route to Coumarin-Pyrrole-Isoquinoline Fused Pentacycles. **Mandrekar, K. S.**; Kadam, H. K; Tilve, S. G. *Eur. J. Org. Chem.* **2019**, *2019*, 863.
3) Molecular iodine mediated oxidative cleavage of the C–N bond of aryl and heteroaryl (dimethylamino)methyl groups into aldehydes. **Mandrekar K. S.;** Tilve S. G. *New J. Chem.*, **2021**, *45*, 4152.
4) P_4O_{10}/TfOH mediated domino condensation-cyclization of amines with diacids: A route to indolizidine alkaloids under catalyst and solvent-free conditions. **Mandrekar K. S.;** Tilve S. G. *Manuscript communicated for publication.*
5) Aerobic intermolecular cross dehydrogenative coupling reaction using CuO.NiO.TiO_2 trimetallic nanocomposites: A profound version of synergistic catalysis. *Manuscript under preparation.*

Other publications:

1) Facile convergent route to indoloquinolines. Kadam, H. K.; Malik, D. D.; Salgaonkar, L.; **Mandrekar, K. S.;** Tilve, S. G. *Synthetic communications*, **2017**, *47*, 1980.
2) Solventless Mechanosynthesis Of Bis(Indolyl)Methanes. Mhaldar S. N.; **Mandrekar K. S.;** Gawde M. K.; Shet R. V.; Tilve S. G. *Synthetic Communications*, **2019**, *49*, 94.
3) CuO-NiO-TiO_2 bimetallic nanocomposites for catalytic applications. Bakre P. V.; Kamat D. P.; **Mandrekar K. S.**; Tilve S. G.; Ghosh N. N. *Molecular Catalysis*, **2020**, *496*, 111193.
4) Alternate oxidative pathways for synthesis of amides *via* alpha oxygenation of amines. (Review). **Mandrekar, K. S.**; Kadam, H. K.; Tilve, A. S.; Tilve, S. G. *Manuscript communicated for publication.*

Conferences Attended & Poster Presentation:

1) **Mandrekar, K. S.;** Tilve, S. G. "Tandem Bischler–Napieralski – Michael Reaction and Oxidation: Access to the pyrrole ring formation leading to lamellarins scaffolds", 3rd National conference 2019 organized by Department of Chemistry, **BITS Pilani KK Birla Goa campus**.
2) **Mandrekar, K. S.;** Tilve, S. G. "Efficient transition metal-free synthesis of lamellarin core via electrophilic- nucleophilic cascades of Bischler- Napieralski reaction – Michael reaction and oxidation," **24th CRSI National Symposium 2019 organized by CSIR- Central Leather Research Institute (CLRI) and Indian Institute of Technology Madras**.
3) **Mandrekar, K. S.;** Tilve, S. G. Participated in "**Syngenta Agro Science Symposium: Sustainable Chemistry & Technology - 2019**" organized by **Syngenta Biosciences Pvt. Ltd., Goa**.
4) **Mandrekar, K. S.;** Tilve, S. G. "Domino Bischler Napieralski – Michael Reaction and Oxidation: New Synthetic Route To Lamellarin Scaffolds," **National Conference on Recent Developments in Chemical Sciences, RDCS-2018, Department of Chemistry, University of Mumbai, Mumbai** (8-9th March 2018).
5) **Mandrekar, K. S.;** Tilve, S. G. attended **"New Frontiers in Chemistry – From Fundamentals to Applications,"** 2nd National Conference 2017 organized by Department of Chemistry, **BITS Pilani KK Birla Goa campus**.
6) **Mandrekar, K. S.;** Tilve, S. G. "Tandem Bischler-Napieralski - Michael reaction and oxidation: New synthetic route to Lamellarin scaffolds", **"Emerging Trends in Agro science- Chemistry & Technology - 2016"** organized by **Syngenta Biosciences Pvt. Ltd., Goa**.

Chapter 1

Synthetic studies of pyrrolo-coumarin alkaloids: Lamellarins

1.1 Introduction:

In 1985, Faulkner and co-workers[1] isolated lamellarins from prosobranch mollusc *Lamellaria* sp., a group of DOPA-(2-amino-3-(3', 4'-dihydroxyphenyl)propionic acid)-derived pyrrole alkaloids. So far more than 70 different lamellarins (A-Z, α-χ, and A1-A6, including their acetate and sulfate derivatives) have been isolated from various marine organisms such as tunicates and sponges.[2] Initially, lamellarins were first named alphabetically from A to Z, and then subsequent Greek alphabets were used. Three types of classification are done for lamellarin, in which pentacyclic framework of the *6H*-chromeno[4',3':4,5]pyrrolo-[2,1-*a*]isoquinolin-6-one type is characterized as type 1a (partially saturated) and 1b (fully unsaturated) lamellarins, while the less abundant and structurally simpler as type 2 lamellarins which contain an unfused 3,4-diarylpyrrole core (Figure 1).[3]

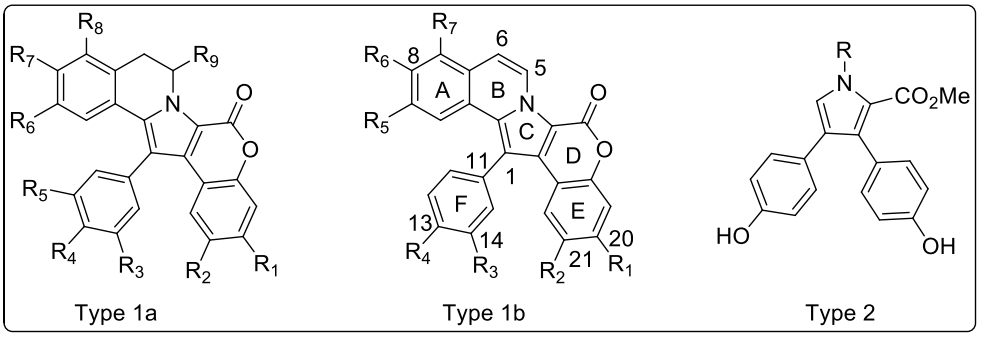

Figure 1. Representation of types of lamellarin compounds

Table 1. Lamellarins (Type 1a)

No.	lamellarin	R_1	R_2	R_3	R_4	R_5	R_6	R_7	R_8	R_9
1	A	OH	OMe	H	OH	OMe	OMe	OMe	OMe	OH
2	A triacetate	OAc	OMe	H	OAc	OMe	OMe	OMe	OMe	OAc
3	C	OH	OMe	H	OH	OMe	OMe	OMe	OMe	H
4	C diacetate	OAc	OMe	H	OAc	OMe	OMe	OMe	OMe	H
5	C 20-sulfate	OSO_3^-	OMe	H	OH	OMe	OMe	OMe	OMe	H
6	E	OH	OMe	H	OMe	OH	OMe	OMe	OH	H
7	F	OH	OMe	H	OMe	OMe	OMe	OMe	OH	H
8	G	OMe	OH	H	OMe	OH	OMe	OH	H	H
9	G 8-sulfate	OMe	OH	H	OMe	OH	OMe	OSO_3^-	H	H
10	I	OH	OMe	H	OMe	OMe	OMe	OMe	OMe	H

11	J	OH	OMe	H	OMe	OMe	OMe	OH	H	H
12	K	OH	OMe	H	OH	OMe	OMe	OMe	OH	H
13	K diacetae	OAc	OMe	H	OAc	OMe	OMe	OMe	OH	H
14	K triacetate	OAc	OMe	H	OAc	OMe	OMe	OMe	OAc	H
15	L	OH	OMe	H	OMe	OH	OMe	OH	H	H
16	L triacetate	OAc	OMe	H	OMe	OAc	OMe	OAc	H	H
17	L 20-sulfate	OSO_3^-	OMe	H	OMe	OH	OMe	OH	H	H
18	S	OH	OH	H	OH	OH	OMe	OH	H	H
19	T	OH	OMe	H	OMe	OH	OMe	OMe	OMe	H
20	T diacetate	OAc	OMe	H	OMe	OAc	OMe	OMe	OMe	H
21	T 20-sulfate	OSO_3Na	OMe	H	OMe	OH	OMe	OMe	OMe	H
22	U	OH	OMe	H	OMe	OH	OMe	OMe	H	H
23	U 20-sulfate	OSO_3Na	OMe	H	OMe	OH	OMe	OMe	H	H
24	V	OH	OMe	H	OMe	OH	OMe	OMe	OMe	OH
25	V 20-sulafte	OSO_3Na	OMe	H	OMe	OH	OMe	OMe	OMe	OH
26	Y	OH	OMe	H	OMe	OH	OH	OMe	H	H
27	Y 20-sulfate	OSO_3Na	OMe	H	OMe	OH	OH	OMe	H	H
28	Z	OMe	OH	H	OH	OH	OMe	OH	H	H
29	β	OH	OH	H	OMe	OH	OH	OH	H	H
30	γ	OH	OMe	OMe	H	OMe	OMe	OMe	OH	H
31	χ	OAc	OMe	H	OAc	OMe	OMe	OAc	H	H

Table 2. Lamellarins (Type 1b)

No.	**lamellarin**	**R^1**	**R^2**	**R^3**	**R^4**	**R^5**	**R^6**	**R^7**
32	B	OH	OMe	OH	OMe	OMe	OMe	OMe
33	B diacetate	OAc	OMe	OAc	OMe	OMe	OMe	OMe
34	B 20-sulfate	OSO_3^-	OMe	OH	OMe	OMe	OMe	OMe
35	D	OH	OMe	OH	OMe	OMe	OH	H
36	D triacetate	OAc	OMe	OAc	OMe	OMe	OAc	H
37	H	OH	OH	OH	OH	OH	OH	H
38	M	OH	OMe	OH	OMe	OMe	OMe	OH
39	M triacetate	OAc	OMe	OAc	OMe	OMe	OMe	OAc
40	N	OH	OMe	OMe	OH	OMe	OH	H
41	N triacetate	OAc	OMe	OMe	OAc	OMe	OAc	H
42	W	OH	OMe	OMe	OH	OMe	OMe	OMe
43	X	OH	OMe	OMe	OH	OMe	OMe	OH

44	X triacetate	OAc	OMe	OMe	OAc	OMe	OMe	OAc
45	α	OH	OMe	OMe	OH	OMe	OMe	H
46	α 20-sulfate	OSO_3Na	OMe	OMe	OH	OMe	OMe	H
47	α 13,20-disulfate	OSO_3Na	OMe	OMe	OSO_3Na	OMe	OMe	H
48	ϵ	OH	OMe	OMe	OMe	OMe	OMe	OH
49	ξ	OH	OMe	OMe	OMe	OMe	OMe	OMe
50	η	OH	OMe	OMe	OMe	OMe	OMe	H
51	ϕ	OAc	OMe	OAc	OMe	OAc	OAc	OMe

1.1.1: Isolation:

Lamellarins have been mainly isolated from various marine organisms such as mollusks, tunicates, and sponges. Faulkner and his colleagues isolated Lamellarins A-D. Fenical's group isolated Lamellarins E-H.[4] Bowden's group reported lamellarins I-M. Lamellarin O-R were isolated from the Australian marine sponge *Dendrilla cactos*.[5,6] Lamellarin S from near Durras, New South Wales, Australia.[7] Lamellarin Z from Great Barrier Reef ascidian.[8] Sulfated derivatives at the C-20 (Fig. 1) were also isolated and characterized, such as lamellarins T, U, V, or Y 20-sulfate, but these are generally not very stable.[9] C-20-sulfated derivatives of lamellarins B, C, and L, and the 8-sulfated derivative of lamellarin G were isolated from *Didemnum chartaceum*, a Great Barrier Reef ascidian.[10] Lamellarin α, lamellarin γ, and lamellarin ε, lamellarins C-diacetate, I, K, K-diacetate, K-triacetate, M, U, X-triacetate were isolated from *Didemnum obscurum*, a small orange lattice ascidian collected in Tiruchandur coast in the Gulf of Mannar, Tamilnadu, India, which are also responsible for chemical defenses in ascidians.[11] Similarly from the same habitat, lamellarins ξ, η, ϕ, χ, lamellarins F, I, J, K, lamellarin K triacetate, lamellarin L triacetate, lamellarin T diacetate from red colonial ascidian *Didemnum obscurum* were isolated.[12] From Australian tunicate *Didemnum sp.* of Durras, New South Wales, was isolated lamellarin S by Urban and Capon in 1996.[13] Lamellarin N, T-X was isolated from unidentified ascidian species, Trivandrum coast of India.[14] Besides, lamellarin U was isolated from Prosobranch mollusc *Coriocella hibyae*, Landaa Giraavaru (Maldives, Baa Atoll).[15] After 2001, Plisson et al. isolated lamellarins A1 to A5, from a *Didemnum* species collected near Wasp Island, New South Wales.[16]

Even though less active than the pentacyclic condensed forms, the trisubstituted pyrrole structures (type 2) are also of great interest. Neolamellarin A (R = $COCH_2$-C_6H_4-*p*-OH,

type 2 Fig. 1) is a metabolite isolated from the sponge *Dendrilla nigra* from the Gulf of Mannar.

1.1.2: Biological activity:

Lamellarins (type 1a, 1b, 2) have shown a wide range of biological activities such as cytotoxicity antitumor activity, multidrug resistance reversal (MDR) activity, inhibition of HIV-1 integrase, MCV topoisomerase, inhibition of ATP-citrate lyase, human aldose reductase (h-ALR2), cell division inhibition, immunomodulatory activity, and antioxidant activity. Table 3 displays various biological activities exhibited by lamellarins.

Table 3. Lamellarin alkaloids displaying different biological activities

Biological Activities	Lamellarin derivatives and their potency
Cytotoxicity and Antitumor Activity	Lamellarin D, K, M (exhibit cytotoxicity in the range of 38-110 nM towards cancer cell lines).[17] Lamellarin C and U (inhibit human tumor cell lines A549, HCT-116, LOX IMVI, MALME-3M, MCF-7, and MOLT-4 with IC50's ranging from 0.4 to 19.4 nM).[18] Lamellarins I, K, and L (shows cytotoxicity against P388 and A549 cultured cancer cell lines with IC50 = 0.5 nM).[19] Lamellarin H, lamellarin α, and lamellarin α 13, 20-disulfate (cytotoxicity against HeLa cell lines with LD50s of 5.7, 5.1, and 29 μM, respectively was measured using MTT as a dye).[20]
Inhibitors of acquired Multidrug Resistance (MDR) cancer cell lines	Lamellarin O and lukianol A (exhibit moderate cytotoxic activity against wild-type and MDR tumor cell lines)[21]
Inhibition of HIV-1 Integrase	Lamellarin α-20 sulfate (inhibit integrase terminal cleavage activity with an IC50 of 16 μM. Also, strand transfer activity growth of the HIV-1 virus in cell culture with an IC50s of 22 μM, 8 μM respectively).[22]
MCV Topoisomerase	Lamellarin H, lamellarin R, and lamellarin R 13,20-disulfate (inhibition of the type 1B topoisomerase of the Molluscum contagiosum virus with IC50 of 0.23 μM, 70 μM, and 170 μM, respectively)[23]
Human Aldose Reductase (h-ALR2)	Lukianol B (Type 2 lamellarin class)[24]
Cell Division Inhibition	Lamellarin D and C (shows inhibition with 78% and 15 % of cell division of sea urchin egg at concentrations of 19 μg/mL respectively).[25]

Immunomodulatory Activity	Lamellarin K and L (exhibit steady immunomodulatory activity at LcV = MLR 147, 98 respectively).[26]
Antioxidant Activity	Lamellarins γ, K, U, I, and C-diacetate (possess antioxidant properties at active millimolar range with IC50 and TEAC order: I > γ > K > C-diacetate > U)[27]

Due to their diverse range of bioactivity and medical treatment importance, they are studied much widely and are important subjects for the research.

1.2 Literature Review:

To the best of our knowledge, since the discovery of lamellarin compounds Heonjoong Kang and William Fenical's report is the only report on biogenesis in 1997.[28] They considered amino acid tyrosine (DOPA) as a biosynthetic precursor for lamellarin compounds among sponges and molluscs. They postulated that ningalins can be derived by condensing two DOPA fragments, which implies, ningalin A becomes a sole precursor for lamellarins and ningalins B, C, D (Scheme 1).

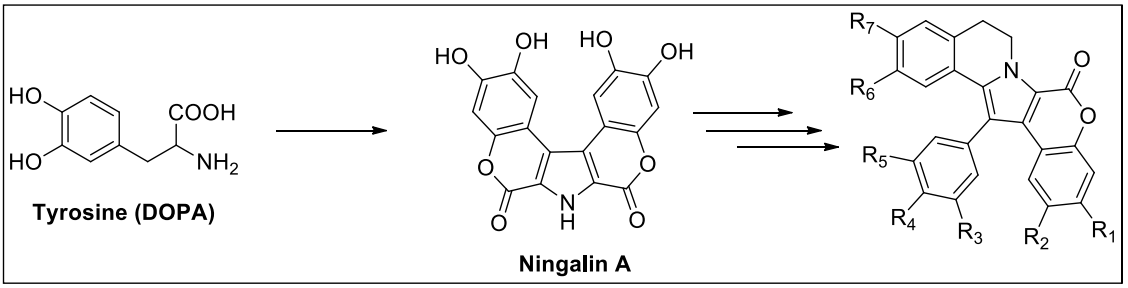

Scheme 1. Biosynthetic pathway of lamellarin scaffolds

In 2006, Peschko et al.[29] reported a biomimetic synthesis of lamellarin alkaloids by forming 3,4-diarylpyrrole-2,5-dicarboxylic acids from arylpyruvic acids and 2-arylethylamines (Scheme 2). Pyrrole-2,5-dicarboxylic acid was synthesized by coupling of 2 moles of 3-(3-isopropoxy-4-methoxyphenyl)pyruvic acid using *n*BuLi and 1 mol of molecular iodine and further condensed with 2-(6-bromo-3-isopropoxy-4-methoxyphenyl)ethylamine. The resultant pyrrole compound upon treatment with lead(IV)acetate in EtOAc furnished monolactone, which was stitched to form lamellarin G using a palladium catalyst and further dealkylation to get lamellarin K.

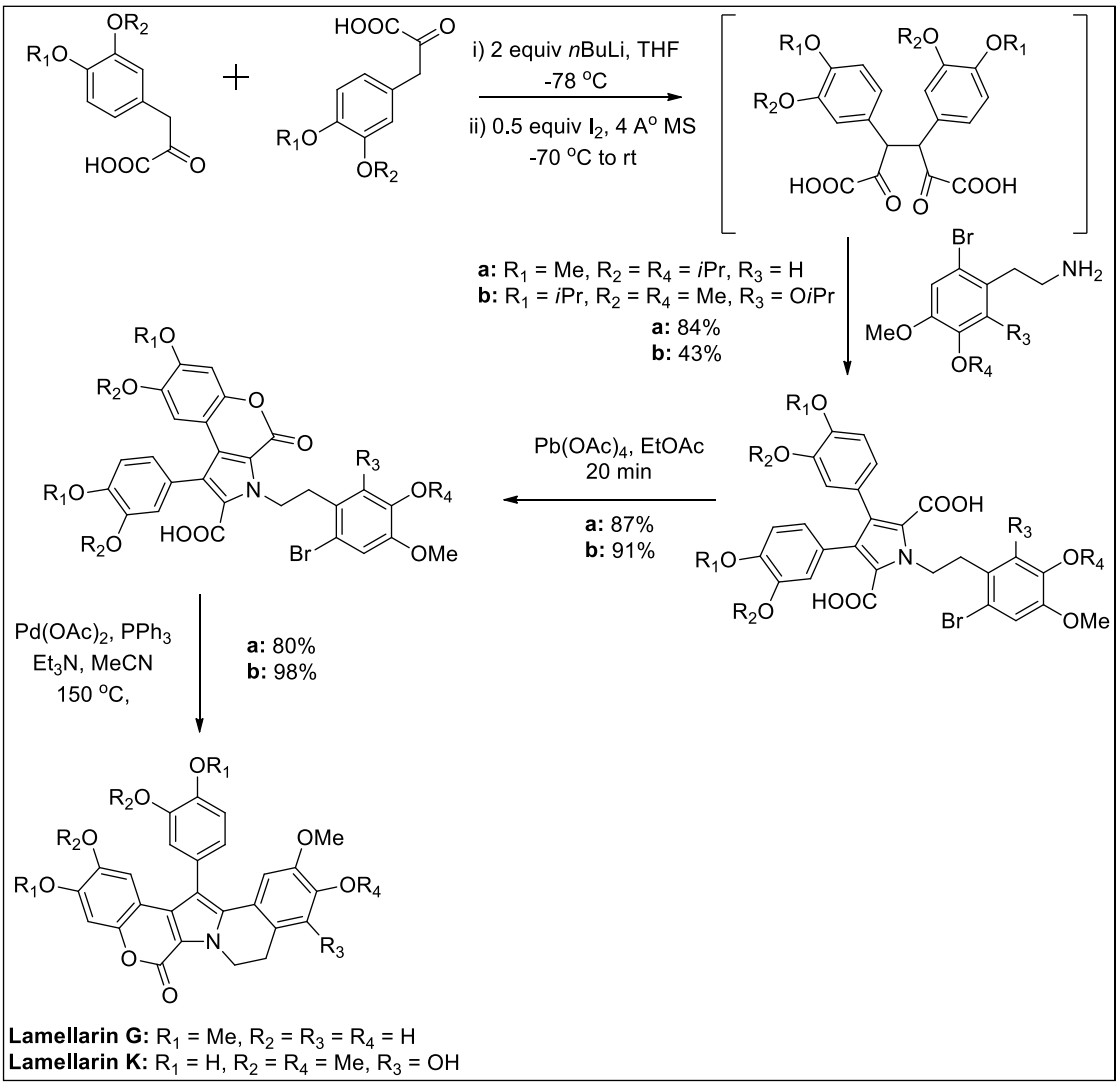

Scheme 2. Total syntheses of lamellarin G and K

Paal-Knorr approach to synthesize lamellarin O and Q has been depicted by Vazquez et al. (Scheme 3).[30] They started with Knoevenagel condensation reaction between substituted benzaldehydes and corresponding phenylacetonitriles to get acrylonitriles. The conjugate addition of cyanide using $NaCN/NH_4Cl$ produced a racemic mixture of succinonitriles. DIBAL-H reduction of the resultant product followed by heating with NaH_2PO_4 resulted in corresponding 3, 4-diaryl-substituted pyrroles. Smooth acylation of 3, 4-diaryl-substituted pyrroles with trichloroacetyl chloride in the presence of DMAP followed by trans-esterification using NaOMe yielded Fürstner intermediate. Further OBn deprotection using hydrogenolysis gave lamellarin Q. Similarly, *N*-alkylation of Fürstner intermediate with 2-bromo-4′-methoxyacetophenone using K_2CO_3 in refluxing acetone, followed by hydrogenolysis gave lamellarin O.

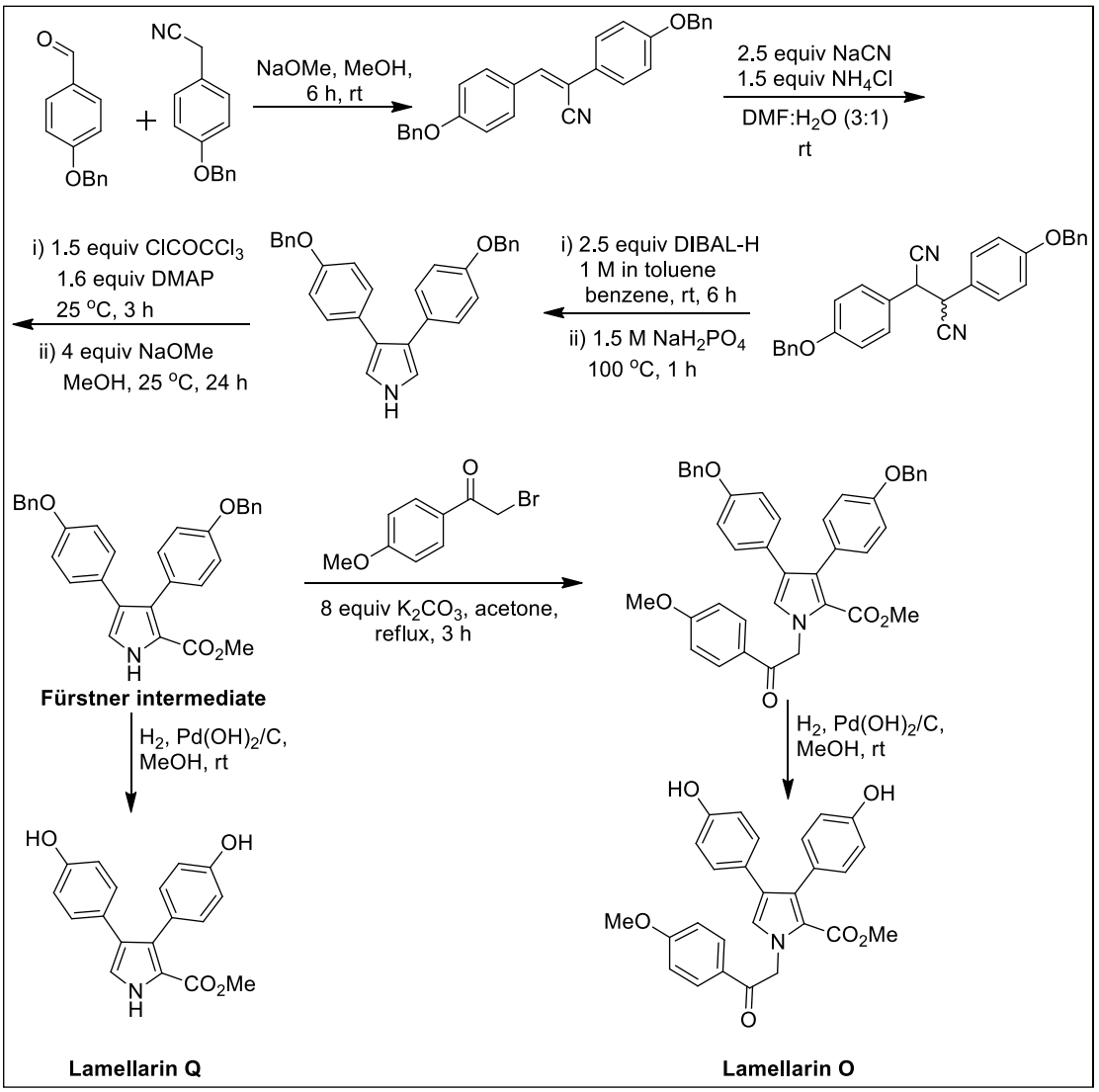

Scheme 3. Total syntheses of lamellarin Q and O

Opatz and co-workers[31] have shown a high-yielding modular synthesis to prepare lamellarin G trimethyl ether, lamellarin η and dihydrolamellarin η (Scheme 4). The reaction of α-aminonitrile (prepared from homoveratryl amine) and α,β-unsaturated aldehydes (prepared using phenylacetonitrile and veratraldehyde) furnished pyrroles upon dehydration/dehydrocyanation in excellent yield. The resultant pyrroles were subjected to Vilsmeier formylation to give the corresponding carbaldehydes, which produced carboxylic acid derivatives further upon Pinnick oxidation. These acids under microwave irradiation using copper(I)-thiophene-2-carboxylate (CuTC) resulted in lamellarin G trimethyl ether and benzyl lamellarin G dimethyl ether. The benzyl lamellarin G dimethyl ether upon debenzylation was converted into dihydolamellarin η. Further, it was subjected to complete aromatization by using DDQ followed by debenzylation with BCl_3 to obtain

lamellarin η.

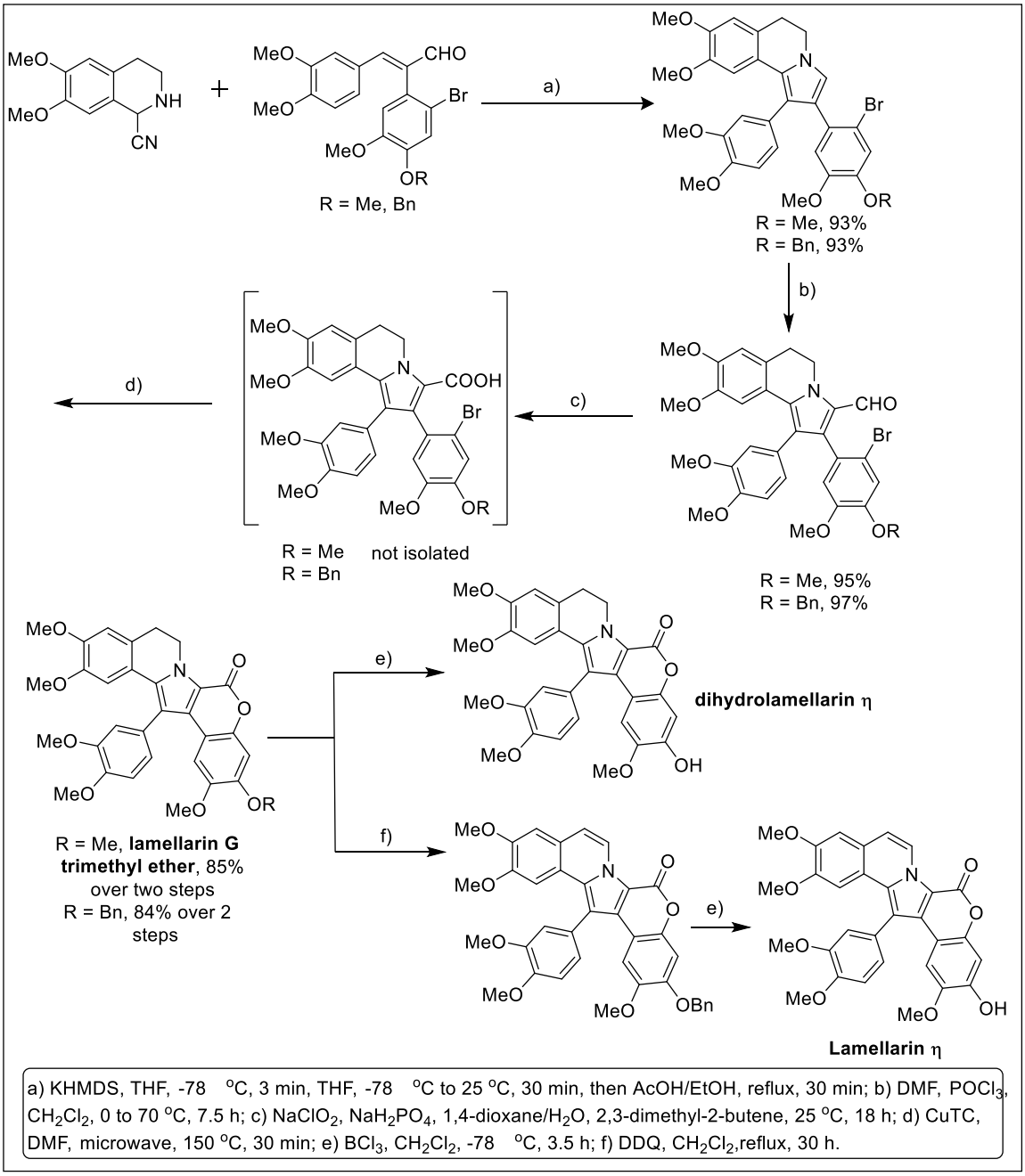

Scheme 4. Total syntheses of lamellarin G trimethyl ether, η and dihydrolamellarin η

Yamaguchi group[32] has synthesized lamellarin C and I by *β*-selective C-H arylation of pyrroles with aryl iodides (Scheme 5). They have constructed pyrrole ring from commercially available 2, 3, 4-trimethoxy benzaldehyde by a three-step sequence of nitroaldol condensation, reduction of the corresponding nitro-styrene, followed by pyrrole ring construction from 2, 5-dimethoxy tetrahydrofuran. Selective C-H arylation at the β

position of pyrrole using rhodium catalyst in excellent result rendered the strategy to avoid reactions like selective bromination and Suzuki Miyaura cross-coupling. The resultant C3 substituted pyrrole was subjected to C5 acylation with trichloroacetyl chloride, pyridine to give carboxylic acid, followed by EDC.HCl, DMAP coupling with substituted phenol to furnish respective esters. Intramolecular double C-H/C-H coupling of esters with stoichiometric $Pd(OAc)_2$, $Cu(OAc)_2$, and K_2CO_3 successfully provided lamellarin C and I after removing the *i*-Pr group selectively by treatment with BCl_3 both in overall 3% yield.

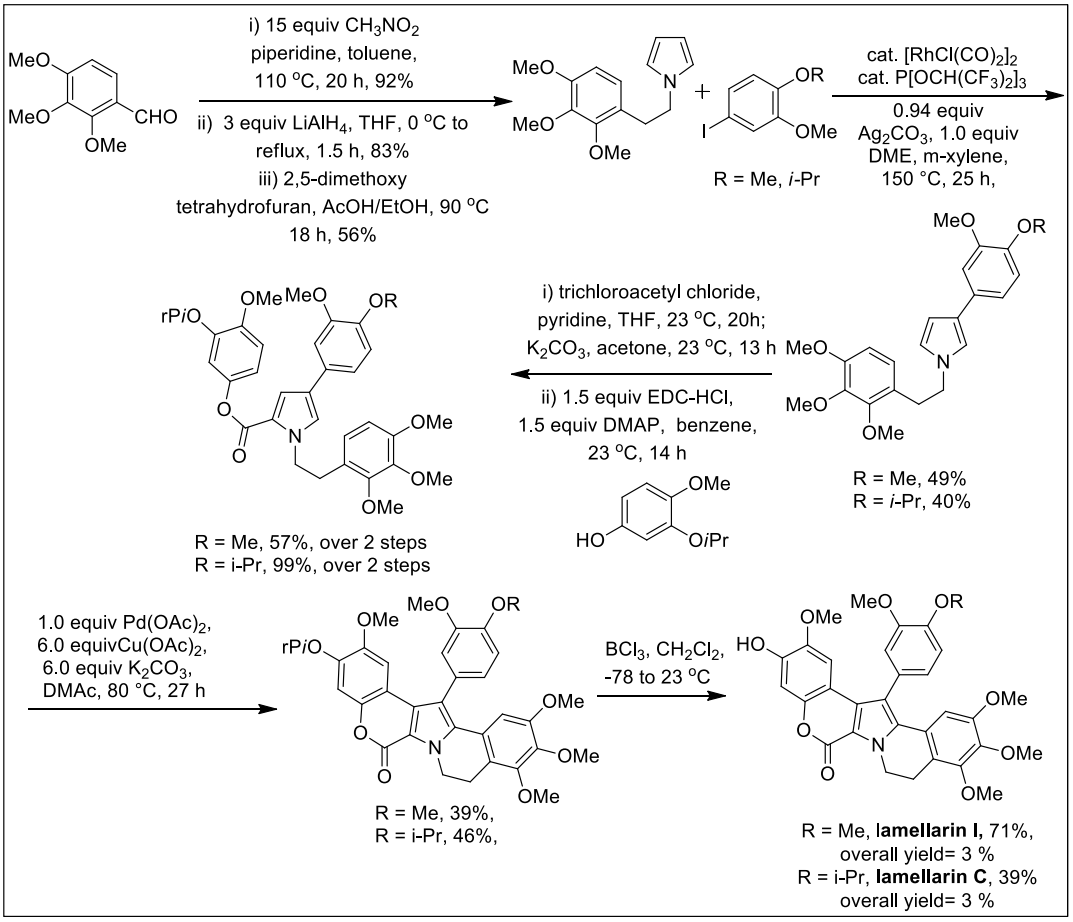

Scheme 5. Total syntheses of lamellarin I and C

Masatomo et al.[33] established regioselective construction of 3, 4, 5-differentially arylated pyrrol-2-carboxylate intermediates to synthesize lamellarin L and N (Scheme 6). The introduction of methoxyester at the C5 position was carried out by a controlled Br-Li exchange reaction of *N*-Boc-2,5-dibrompyrrole. The pyrrole ester was arylated at the C2 position with respective boronic acids using Suzuki Miyaura coupling.

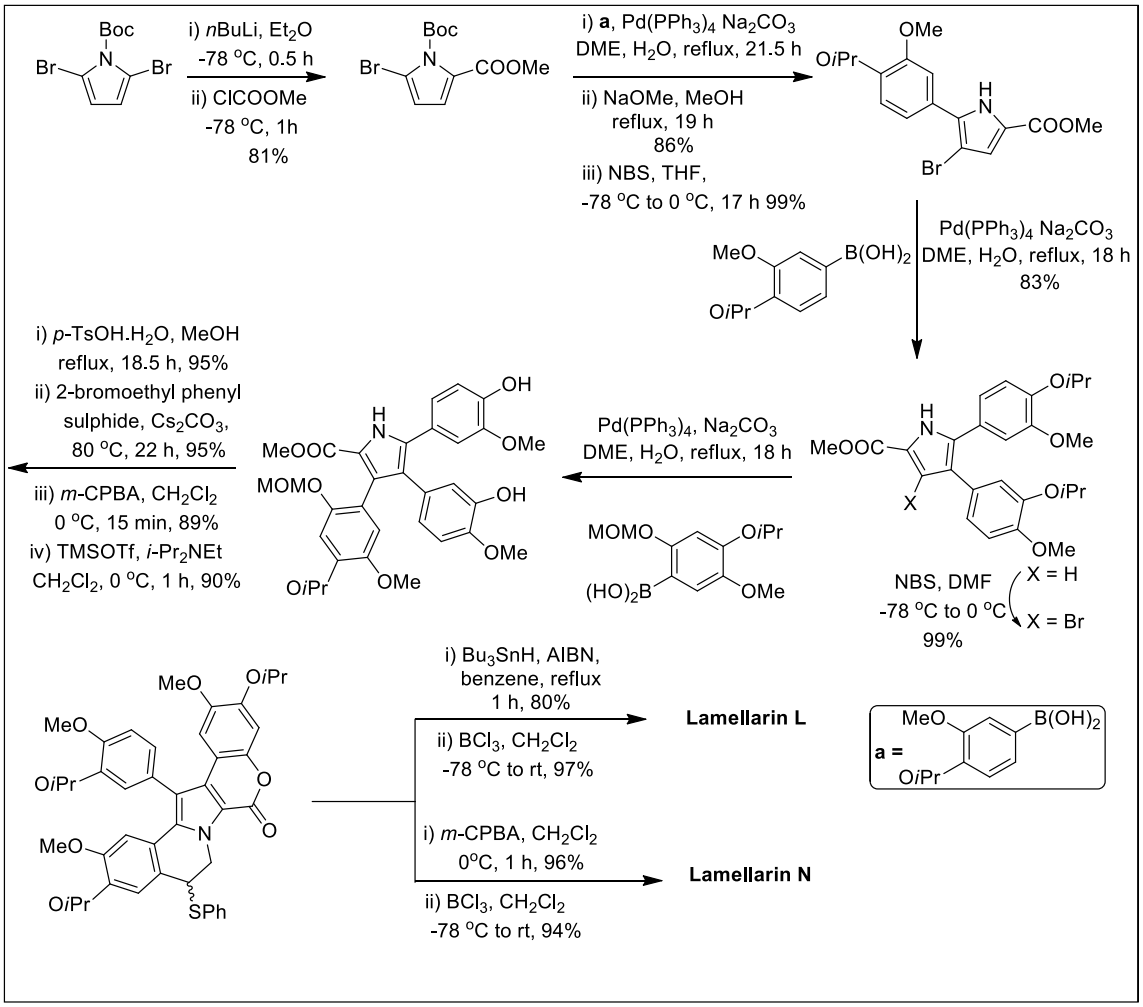

Scheme 6. Total syntheses of lamellarin L and N

Further upon consecutive double bromination - Suzuki Miyaura coupling triarylpyrrole was obtained in substantial yield. Corresponding triarylpyrrole compound was subjected to alkylation and Pummerer cyclization sequence to construct lamellarin-C6-phenylsulfane. The resultant sulfane compound was desulfurized using Bu_3SnH, AIBN in refluxing benzene, upon deisopropylation with BCl_3 furnished lamellarin L (C5-C6 saturated). In another experiment, to bring unsaturation at the C5-C6 bond, *m*-CPBA was used to knock out phenylsulfinyl group. Further, deisopropylation by BCl_3 produced lamellarin N.

From the laboratory of Opatz,[34] one more excellent strategy was developed for the synthesis of lamellarin D trimethyl ether and lamellarin H (Scheme 7). They have shown an efficient construction of trisubstituted pyrrole core of the lamellarin alkaloids by generating in situ 2-azapentadienyl anion from a chalcone and glycine ester *via* an electrocyclic ring closure as a key step. Commercially available veratraldehyde was treated

with elemental bromine in methanol, followed by aldol condensation with commercial acetoveratrone furnished chalcone. Upon reaction of this chalcone with glycine ethyl ester hydrochloride in refluxing pyridine, followed by oxidation with stoichiometric amounts of copper(II) acetate and regioselective iodination of the resulting pyrrole with *N*-iodosuccinimide gave iodopyrrole. Suzuki-Miyaura coupling between iodopyrrole and 3, 4-dimethoxyphenylboronic acid resulted in tetrasubstituted pyrrole ring. Pomeranz-Fritsch isoquinoline synthesis was used to build the pyrrolo[2,1-*a*]isoquinole moiety from the corresponding tetrasubstituted pyrrole. Ester hydrolysis using NaOH and Ullmann using copper(I) thiophene-2-carboxylate (CuTC) under microwave irradiation yielded lamellarin D trimethyl ether in 43% overall yield over 9 linear steps. Further upon complete O-demethylation with BBr_3 gave lamellarin H in 41% overall yield over 10 steps.

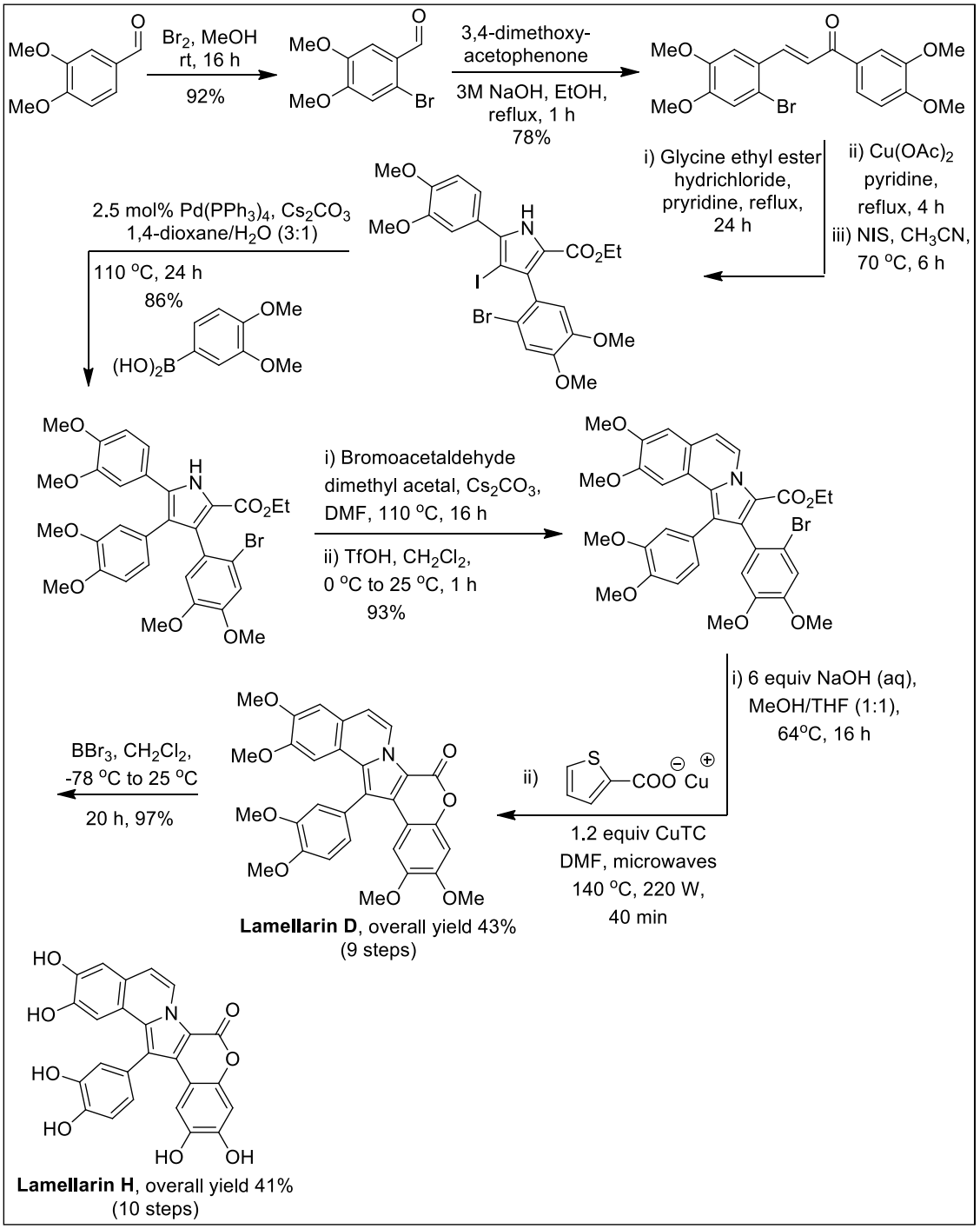

Scheme 7. Total syntheses of lamellarin D and H

Yang et al.[35] have developed a visible light promoted and $Yb(OTf)_3$-catalyzed construction method for lamellarin core, in which synthesis of lamellarin D trimethyl ether and lamellarin H is shown (Scheme 8). Lewis acid-catalyzed coupling of 4-chloro-3-nitrocoumarin and 1-benzyl-isoquinoline derivatives in refluxing xylene was carried out. $Yb(OTf)_3$ was the best Lewis acid with a yield of 17%. One-step synthesis of lamellarin D trimethyl ether was achieved in 14% yield. Lamellarin D trimethyl ether was synthesized

by coupling 4-chloro-6, 7-dimethoxy-3-nitrocoumarin, and papaverine for 2 days. Exhaustive demethylation of lamellarin D trimethyl ether with boron tribromide produced lamellarin H in a 12% overall yield.

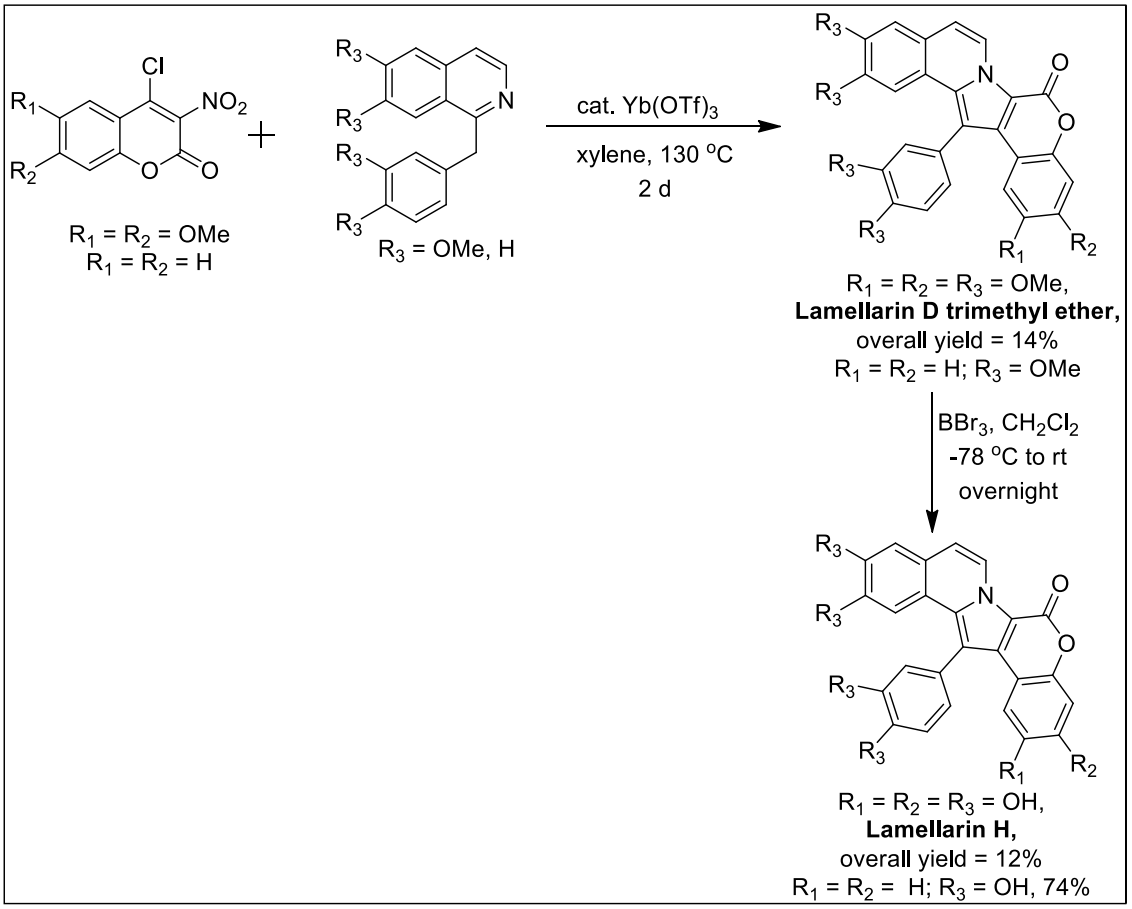

Scheme 8. Total syntheses of lamellarin D trimethyl ether and H

Recently, in 2017 Wu and his team[36] developed a straightforward strategy of electrophilic substitution and palladium-catalyzed Suzuki−Miyaura cross-coupling reactions to synthesize lamellarin core and lamellarin G trimethyl ether (Scheme 9). A one-pot acid-mediated [3+2] cycloaddition reaction between 1,2,3,4-tetrahydroisoquinoline, arylglyoxal, and nitrostyrene proxies in refluxing toluene led to the formation of 1-dearyllamellarin core. This 1-dearyllamellarin moiety was brominated using NBS followed by a Suzuki−Miyaura cross-coupling reaction with phenylboronic acid surrogates to yield lamellarin core and lamellarin G trimethyl ether in overall 24% yield.

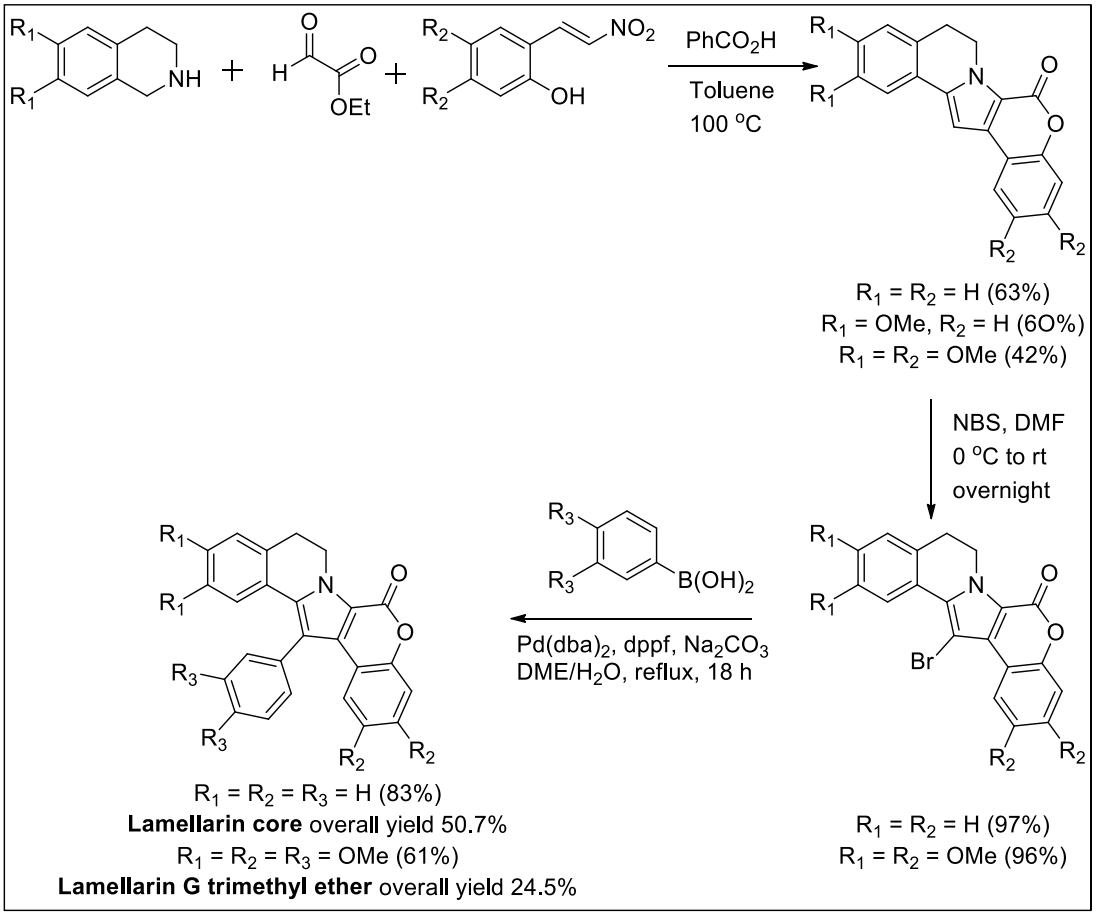

Scheme 9. Total synthesis of lamellarin G trimethyl ether

In the same year, Manjappa and co-workers[37] published similar work to that of Yang et al. regarding starting substrates (Scheme 10). A simple utilization of Grob coupling for the lamellarin D trimethyl ether, lamellarin H, lamellarin 501, and lamellarin D is shown. Lamellarin D trimethyl ether was synthesized by coupling 6,7-dimethoxy-3-nitrocoumarin, and papaverine in a sealed tube. The corresponding nitrocoumarin derivative was prepared by piperidine-catalyzed Knovenagal condensation of commercial 2-hydroxy-3,4-dimethoxybenzaldehyde with ethyl nitroacetate in Dean-Stark trap. Lamellarin D trimethyl ether was converted into lamellarin H, by exhaustive demethylation with an excess boron tribromide. Also, deprotection of benzyl group of corresponding O-Bn protected lamellarin D was carried out with two different time intervals to produce lamellarin D (8 h) and lamellarin 501 (18 h) using $Pd(OH)_2/C$ and Pd/C respectively. Wherein, partial dearomatization of C5-C6 bond was seen in O-Bn protected lamellarin D resulting in lamellarin 501.

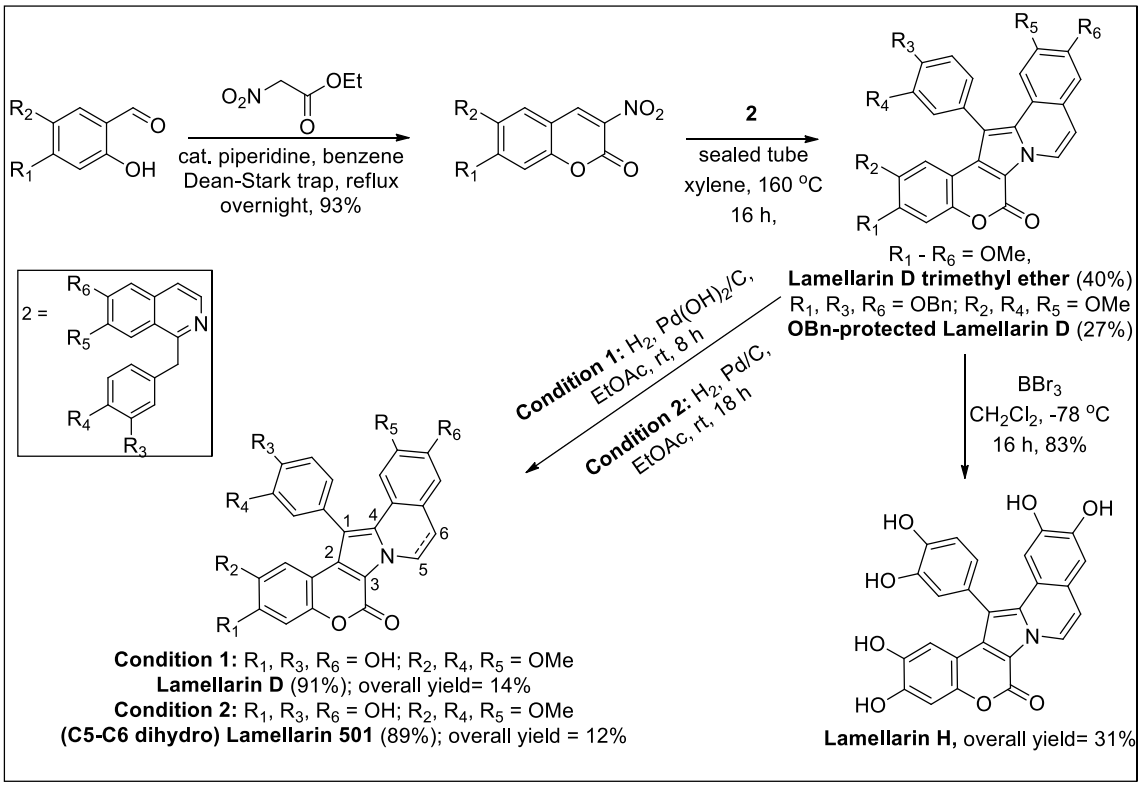

Scheme 10. Total syntheses of lamellarin D, 501, H and D trimethyl ether

From two different labs, similar kinds of synthetic strategies were developed to synthesize lamellarin D and H in the same year (Scheme 11). In the second quarter of 2017, Chandrasekhar et al.[38] showed an excellent pathway to construct a central pyrrole ring from Ru(II)-catalyzed [3+2] annulation of enamides and diarylalkynes as a key step leading to the construction of lamellarin D and H. In the third quarter of the same year, Lutz Ackermann and co-workers[39] synthesized lamellarin D and H by using Ru(II)-catalyzed [3+2] annulation of enamides and alkynes strategy with slight modifications. Both strategies include annulation, lactonization, Pomeranz−Fritsch-type cyclization, and dealkylation steps to construct lamellarin moieties (Scheme 12). In the first step, [3+2] annulation between enamide and diarylalkyne was studied using only one catalyst i.e. $[Ru(p\text{-cymene})Cl_2]_2$ in a green solvent like PEG-400 by Chandrasekhar's group. But, Ackermann's group screened various transition metal catalysts like cobalt, rhodium, palladium, ruthenium, and AgSbF6 in various solvent mixtures to observe which conditions best serve. They found that the use of PEG-400 was less selective as compared to other polar/non-polar solvent mixtures. With the resultant pyrrole in hand, both groups have followed bromination using NBS, followed by Suzuki-Miyaura coupling reaction with phenylboronic acid derivative with $Pd(dba)_2$ in the presence of 1,1′-

bis(diphenylphosphino)ferrocene (dppf). TsOH mediated lactonization was carried out on tetra substituted pyrrole compound, which was converted into the desired lamellarins H and D through a Pomeranz–Fritsch approach.

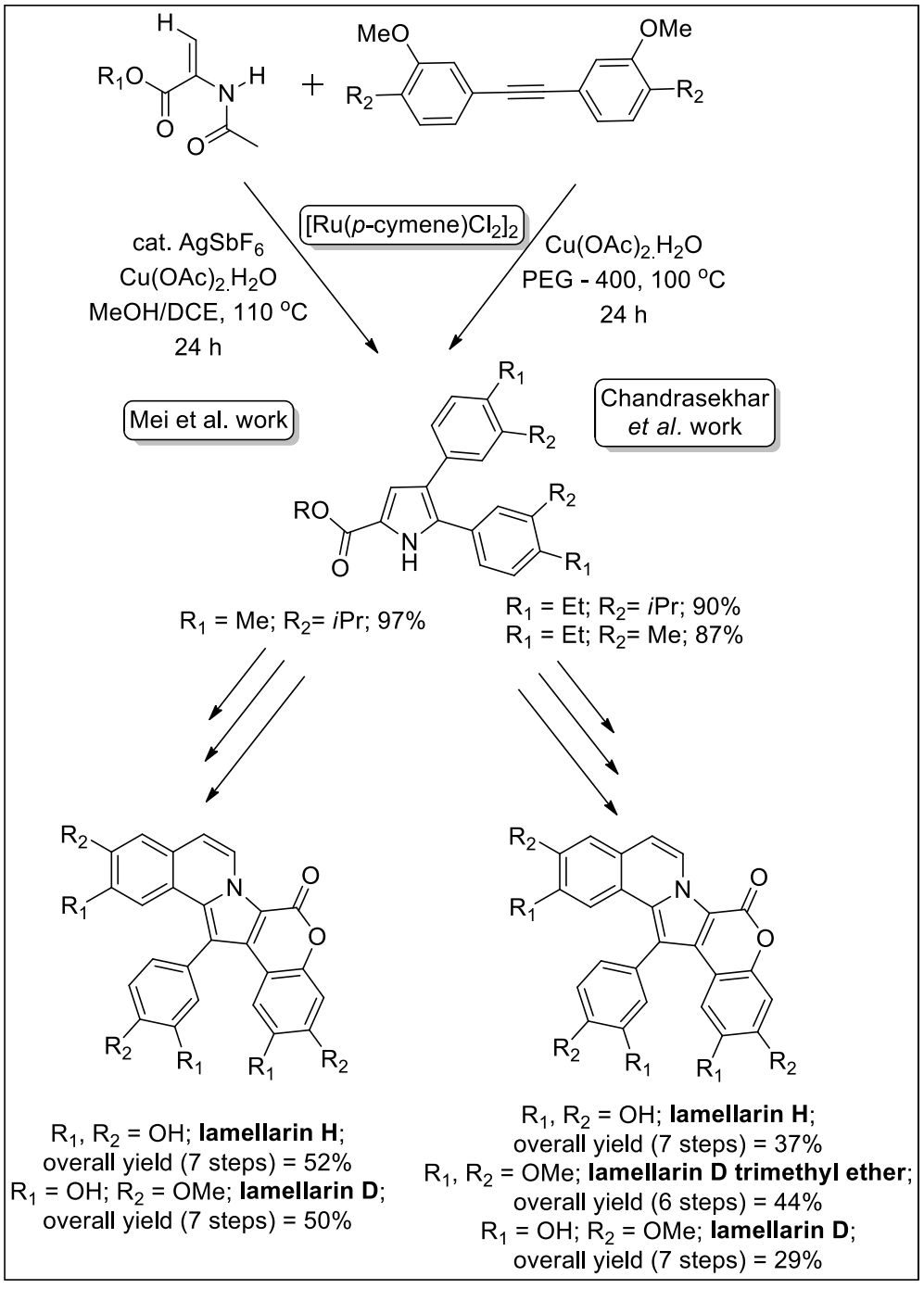

Scheme 11. Schematic representation of Mei et al. and Chandrashekhar et al. works

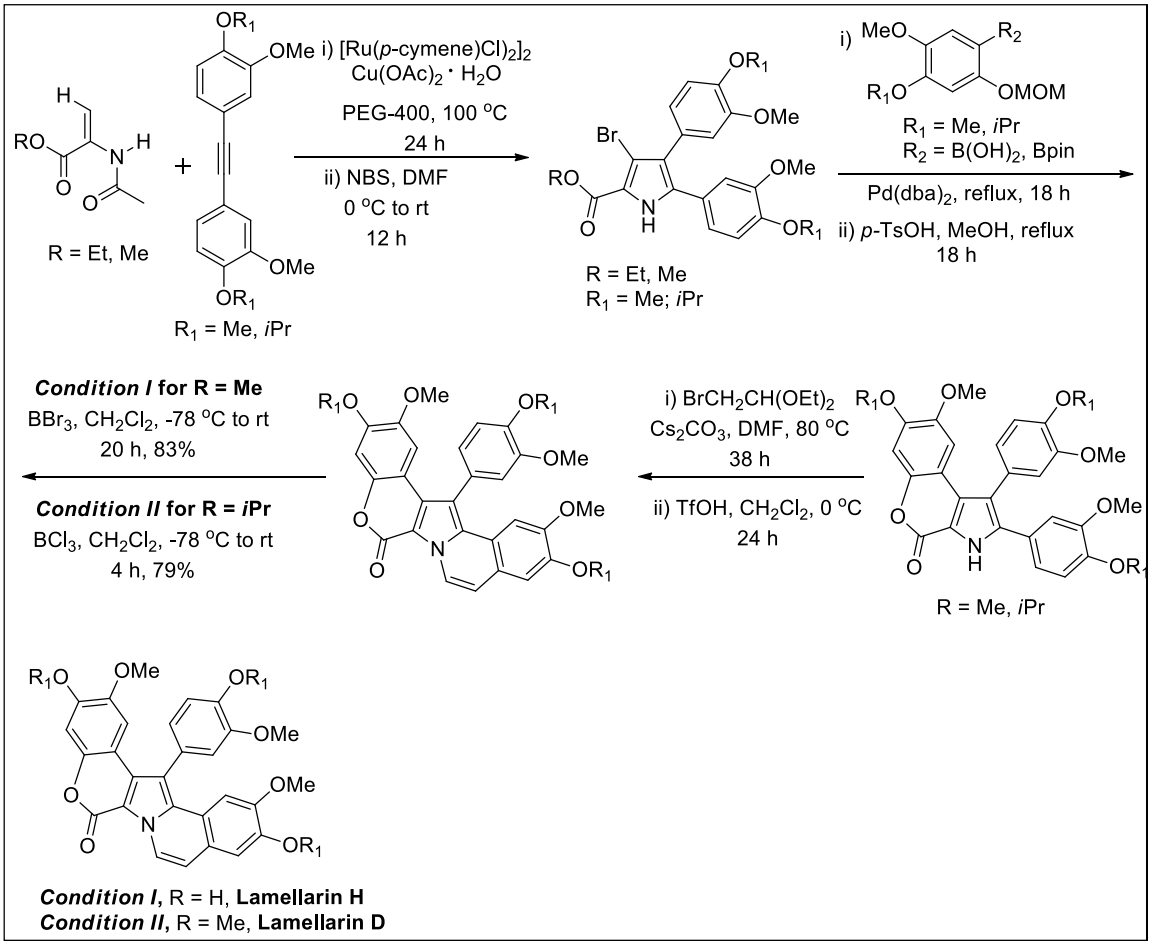

Scheme 12. Total syntheses of lamellarin H and D

A succinct synthesis of lamellarin G trimethyl ether *via* a von Miller–Plöchl-type cyclocondensation as a key step is developed by Opatz et al. (Scheme 13).[40] This method generalizes the construction of pyrrolo[2,1-*a*]isoquinoline structure in one step. The lamellarin G trimethyl ether synthesis is accessed by two routes splitting from 2-bromo-1-phenyl-5,6-dihydropyrrolo[2,1-*a*]isoquinoline-3-carbaldehyde. Homoveratryl amine was converted to the corresponding formamide and later to dihydroisoquinoline using PCl_5 *via* Bischler-Napieralski reaction. α-Amino cyanation was carried out on dihydroisoquinoline to set a primary synthon for the von Miller–Plöchl-type cyclocondensation. On the other hand, secondary synthon dimethoxy-enone was obtained from aldol condensation between veratraldehyde and 1,1-dimethoxypropan-2-one. Modified von Miller–Plöchl-type cyclocondensation was performed on both synthons to achieve pyrrolo[2,1-*a*]isoquinolino carbaldehyde in good yield.

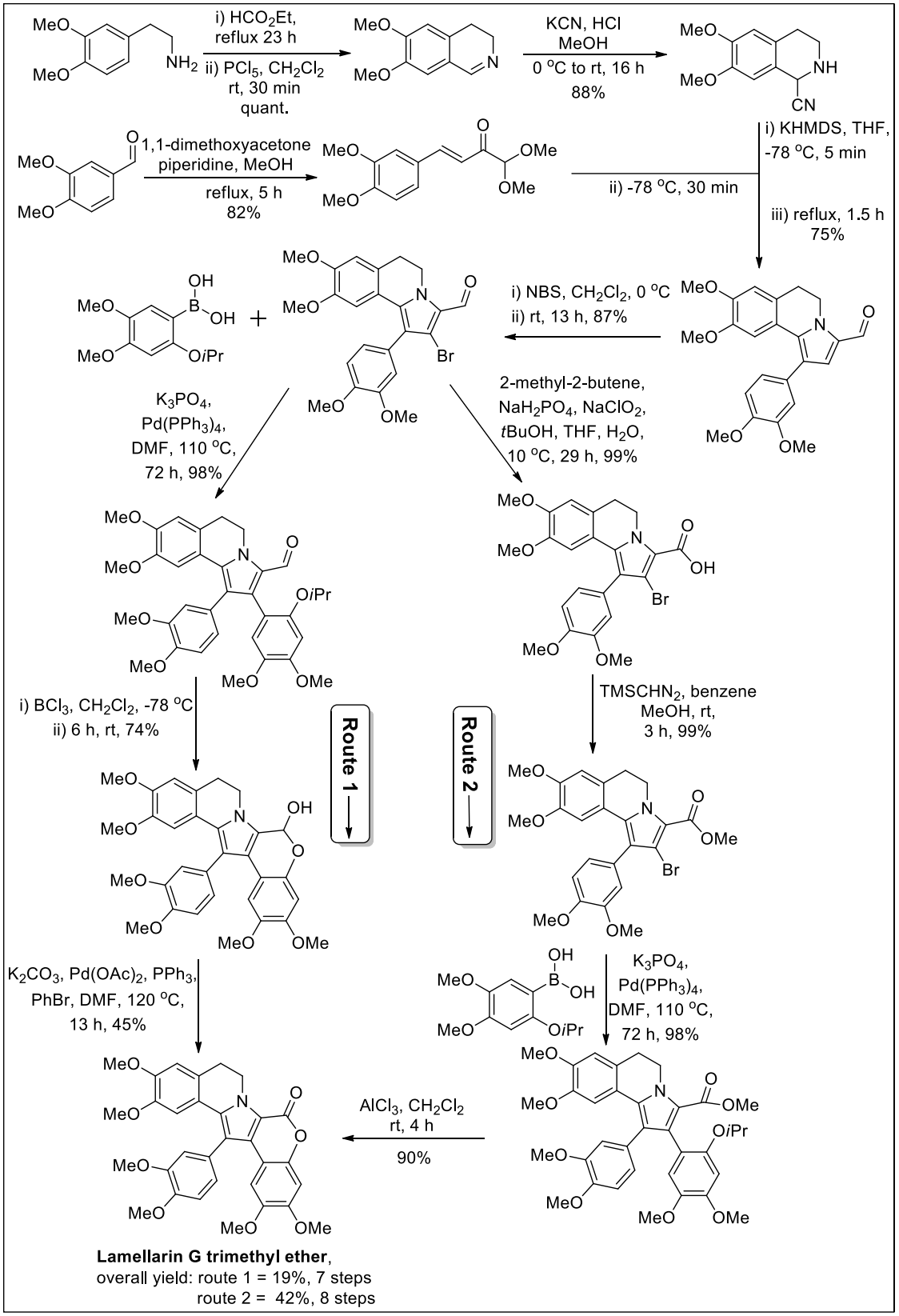

Scheme 13. Total synthesis of lamellarin G trimethyl ether

Further, this carbaldehyde was brominated at C3 of pyrrole using NBS taking this strategy

to its path divergent step. The first route describes the synthesis of lamellarin G trimethyl ether in 3 steps whereas, the second route describes it in 4 steps. In route 1, brominated pyrrolo[2,1-*a*]isoquinolino carbaldehyde was put through cross-coupling with corresponding phenyl boronic acid derivative using $Pd(PPh_3)_4$ in degassed DMF at 110 °C. Selective deprotection of the O-*i*Pr group using BCl_3 at low temperature leads to the formation of hemiacetal product, which gave undesired product upon simple oxidizing agents. But with the combination of $Pd(OAc)_2/PPh_3$ the hemiacetal product was successfully converted to lamellarin G trimethyl ether in 19% yield over 7 steps. Route 2 was simplified to overcome the demerits of route 1 to avoid the formation of quinone wherein at an earlier stage, oxidation of aldehyde was done to respective carboxylic acid using Pinnick oxidation. Methyl ester of carboxylic acid was prepared using $TMSCHN_2$ just in case to avoid any complication before Suzuki-Miyaura coupling with phenylboronic acid derivative. Finally, selective deprotection of the O-*i*Pr group with $AlCl_3$ leads to the target molecule in 42% yield over 8 steps. This strategy complies with independent variation of the substitution pattern.

Michael et al. [41] have developed a green method to synthesize lamellarin G trimethyl ether from environmentally benign precursors and solvents. Efficient development of first, dihydropapaverine followed by enanmionone intermediate formation with a strong base like *n*BuLi, and second, pyrrole formation in low energy microwave synthesizer using *o*-benzylated-4,5-dimethoxy-ethyl salicylate and ethyl bromoacetate. The corresponding substituted pyrrolo-isoquinoline was converted to lamellarin G trimethyl ether *via* benzyl deprotection and lactone formation with catalytic NEt_3 (Scheme 14).

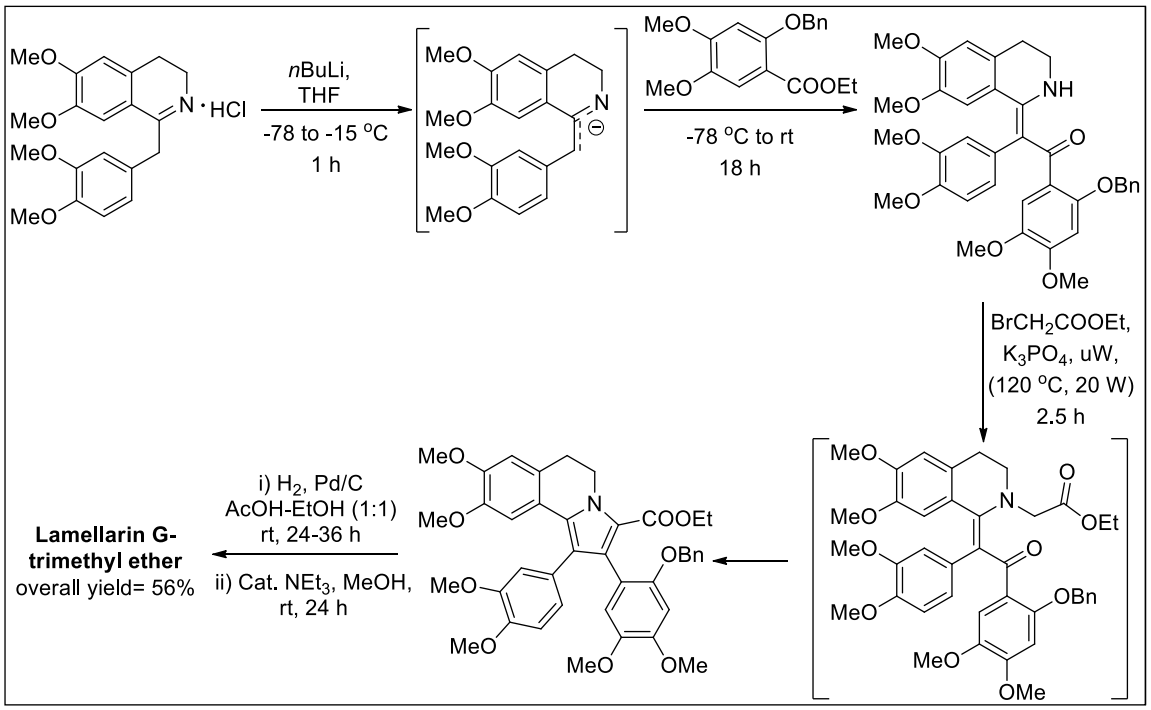

Scheme 14. Total synthesis of lamellarin G trimethyl ether

Intermediates like α-keto acids are found to be important in metabolic pathways. Donohoe and co-workers[42] have designed a synthetic route for the synthesis of lamellarin D using pyruvic acid. Bioinspired conversion of pyruvic acid to OBO (oxabicyclo[2.2.2]octyl) orthoester masked pyruvic acid is shown as a key intermediate. They have synthesized lamellarin D in two approaches as one in 8 steps and another in 6 steps. Eight steps synthesis involves the construction of - 1) pyrrole 2) coumarin 3) isoquinoline in sequence whereas, the 6 steps approach shows - 1) pyrrolo-isoquinoline and then 2) coumarin formation. Both the approaches include C3 C-H arylation of pyrrole using bromo compound and deprotection of isopropyl group in the later stage. Both the 8 steps and 6 steps routes effectively gave the target molecule an excellent overall yield of 40% and 22%, respectively (Scheme 15). Similarly, a 7 steps synthesis of lamellarin Q is achieved in overall 22% yield using methyl-OBO-ketone of pyruvic acid with isopropyl protected aryl bromide and α-bromo benzyl nitrile proxies. HBr mediated pyrrole aromatization, OBO hydrolysis, and transesterification of β-cyano ketone to tetrasubstituted bromo pyrrole compound led to the formation of lamellarin Q.

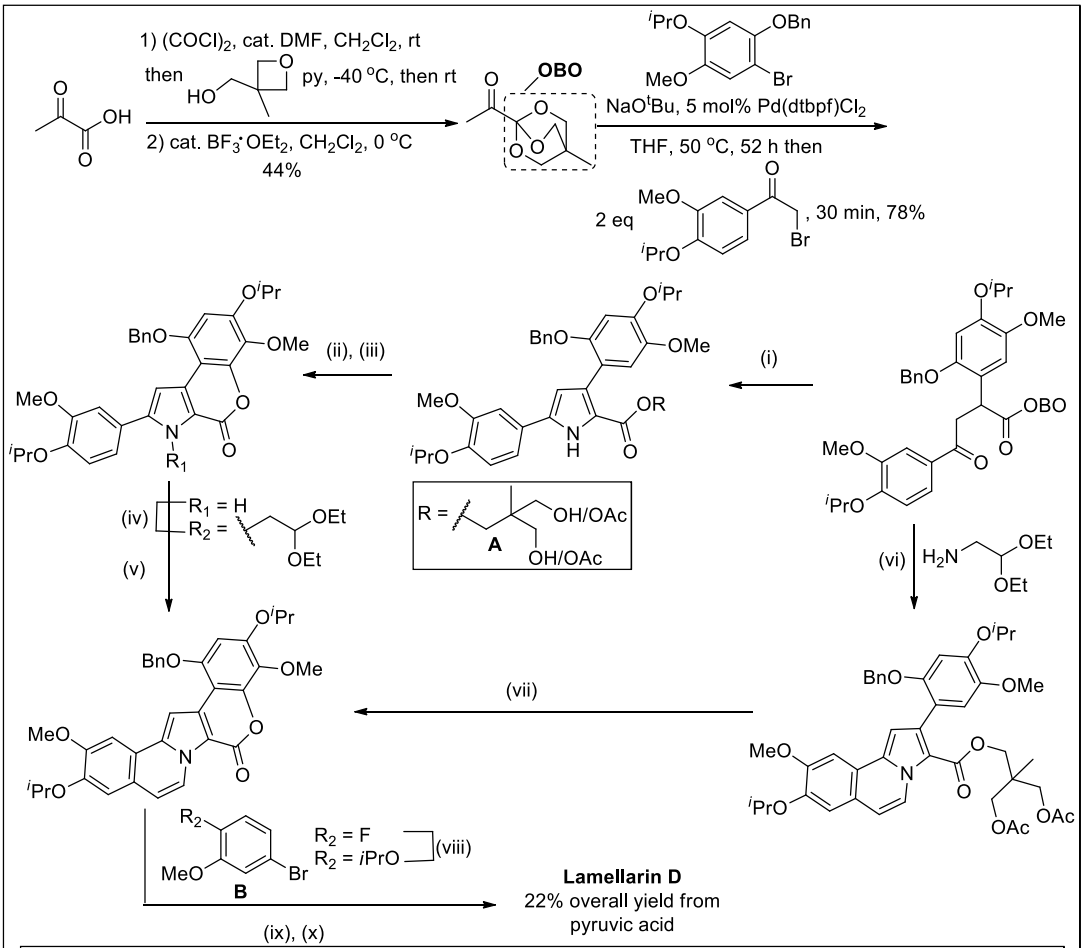

(i) 10 equiv NH_4OAc, AcOH, 110 °C, 30 min; (ii) H_2, Pd/C, EtOH, rt, 6.5 h; (iii) 2 equiv K_2CO_3, EtOH, 90 °C, 2 h, 95% over 3 steps; (iv) 6.6 equiv $BrCH_2CH(OEt)_2$, 6.5 equiv Cs_2CO_3, DMF, 110 °C, 24 h, 86%; (v) TfOH (1 M in CH_2Cl_2), CH_2Cl_2, 10 to 5 °C, 24 h, 88%; (vi) 9 equiv **A**, AcOH, 1 mol% H_2O, 1 mol% HCO_2H, 100 °C, 16 h, 89%; (vii) 20% $Pd(OH)_2$/C, 25 equiv 1,4-cyclohexadiene, MeOH/EtOAc, 60 °C, 6 h then K_2CO_3, 89%. (i) 4.5 equiv *i*PrOH, 4.0 equiv KOtBu, PhMe, DMPU, 80 °C, 30 min, then 1 equiv 15, 3 h, 82%; (ii) 5 mol% $Pd(PPh_3)_2Cl_2$, 2 equiv KOAc, 2.5 **equiv B**, DMA, 150 °C, 22 h, 80%; (iii) 9 equiv BCl_3 (1 M in heptane), CH_2Cl_2, 78 °C to rt, 3.5 h, 99%.

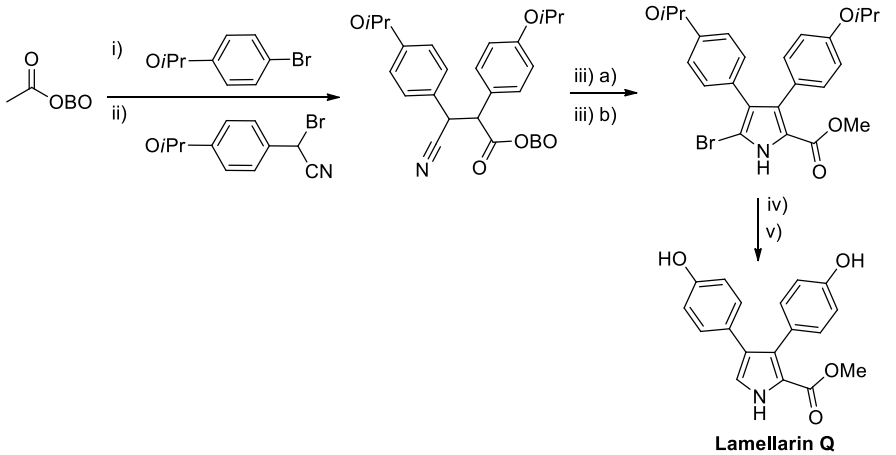

i) $Pd(dtbpf)Cl_2$ (5 mol%), 2.5 equiv NaOtBu, THF, 55 °C, 20 h; ii), 3 h, 75%; iii) a) 33% HBr in AcOH, CH_2Cl_2/Et_2O (1:1), 0 °C to rt, 3.5 h; (b) 2 equiv K_2CO_3, MeOH, 65 °C, 62% over 2 steps; iv) H_2, 10% Pd/C, 2.1 equiv NaOAc, MeOH, rt, 1 h, >99%; (v) 3 equiv BBr_3, CH_2Cl_2, 78 °C to rt, >99%.

Scheme 15. Total syntheses of lamellarin D and Q

Khan et al.[43] have constructed 1,2,4-trisubstituted pyrrole ring synthesis in a highly regioselective manner *via* a one-pot [3+2] cycloaddition/elimination/aromatization sequence-based domino process. Subsequently, a Pd-mediated double CH oxidative coupling reaction sequence was achieved to form a pentacyclic framework in a single step.

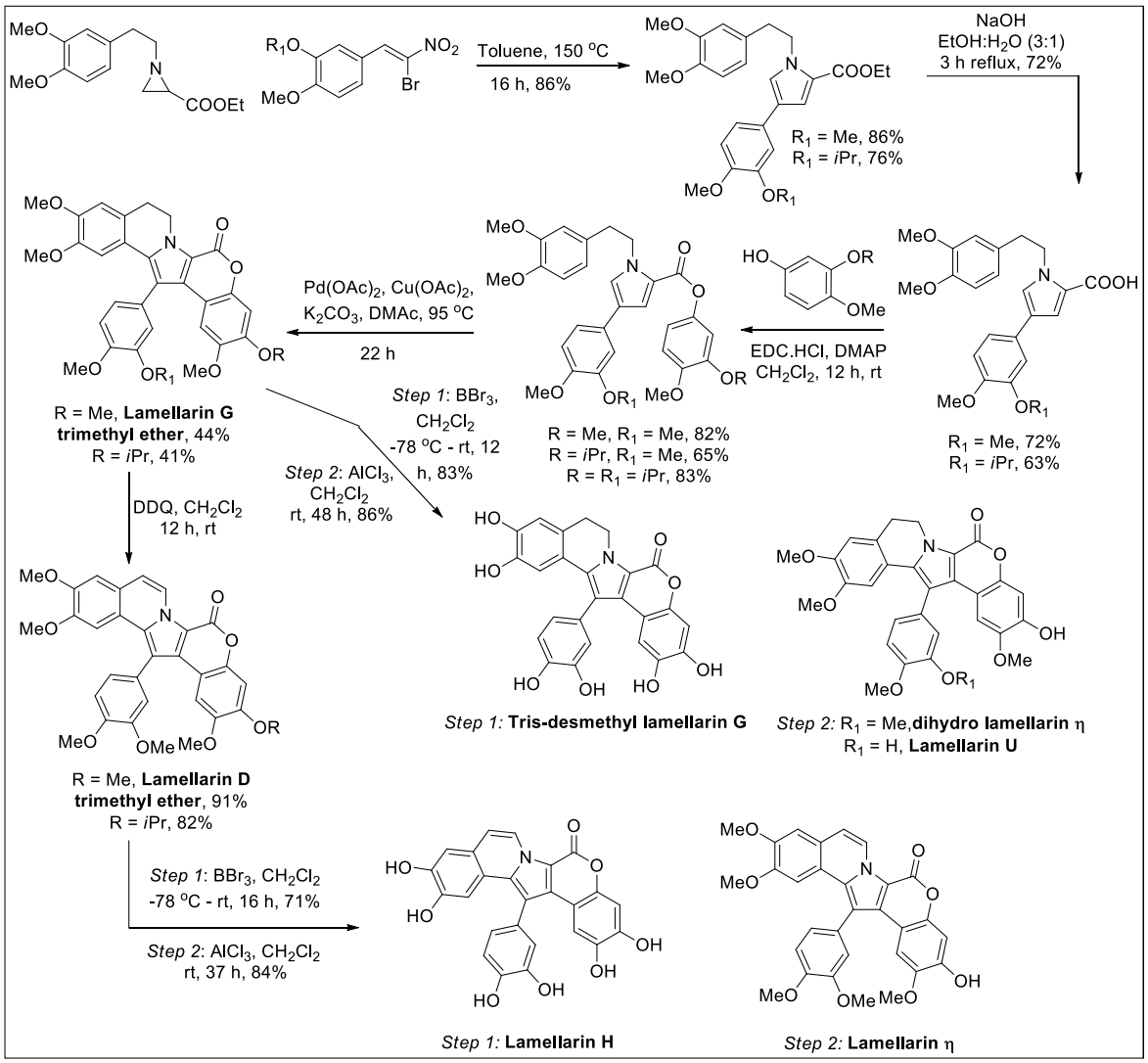

Scheme 16. Total syntheses of lamellarin D trimethyl ether, H, η and dihydro lamellarin η

Aziridine ester and *β*-bromo-*β*-nitrostyrene were subjected to their key step, i.e., [3+2] cycloaddition/elimination/aromatization sequence to provide central 1,2,4-trisubstituted pyrrole ring. Saponification of the ester group was achieved using sodium hydroxide, followed by EDC coupling with substituted phenol gave 2-phenyl ester-1,4-trisubstituted pyrrole. Further, a single step CH oxidative coupling converted 2-phenyl ester-1,4-trisubstituted pyrrole to the pentacyclic framework of lamellarin G trimethyl ether using

Pd/Cu catalysts. Aromatization of pentacyclic compound using DDQ led to lamellarin D trimethyl ether, which was fully demethylated to lamellarin H using BBr_3, and mono depropylation using $AlCl_3$ gave lamellarin η. Similarly, complete and mono dealkylation of lamellarin G trimethyl ether using BBr_3 and $AlCl_3$ gave tris-desmethyllamellarin G and dihydrolamellarin η, lamellarin U respectively.

Hwu et al.[44] synthesized lamellarin R in one pot method involving five sequential steps. (Methoxy)-silylphenyl triflate, Schiff base, and bis(methoxyphenyl)acetylene assembled into lamellarin R through 1,2-elimination, their alkylation by Schiff bases through 1,2-addition, 1,4-intramolecular proton transfer, Huisgen 1,3-dipolar cycloaddition, and dehydrogenative aromatization reaction sequence. They have also utilized this methodology to synthesize various polysubstituted pyrroles in good yields (Scheme 17).

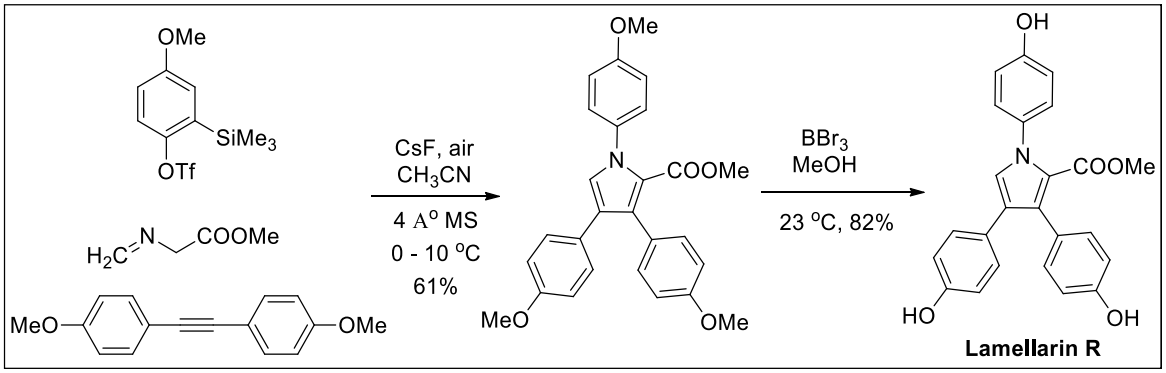

Scheme 17. Total synthesis of lamellarin R

A very distinct methodology has been developed to synthesize multisubstituted 4*H*-pyrrole compounds. Jin[45] and his team have shown an efficient C−C bond carbenoid formal insertion/cyclization/[1,5]-shift cascade reaction *via* AgOTf-catalyzed coupling of enaminones with donor/acceptor or donor/donor carbenes in successfully developing pyrrole ring by [4+1C] insert approach. A corresponding enaminone of isopropyl protected 4-methoxydopamine and ethyl(*3E*)-4-ethoxy-2-oxo-3-butenoate was converted to tetrasubstituted pyrrole, which upon demethylation using BBr_3 gave bromopyrrole. Subsequently, chromeno[3,4-*b*]pyrrol-4(3*H*)-one was obtained by Suzuki coupling of bromopyrrole with corresponding phenylboronic acid and intramolecular transesterification reaction under strong acidic condition. Further, the authors have synthesized lamellarin L by known decarboxylation coupling cyclization and deprotection of pyrrole (scheme 18).

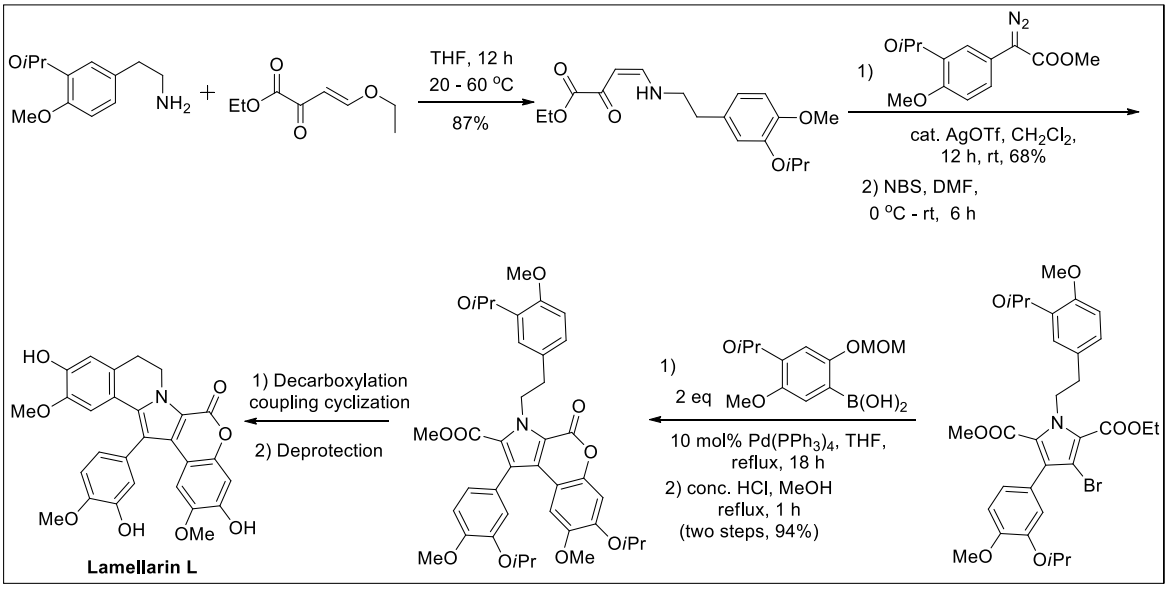

Scheme 18. Total synthesis of lamellarin L

3,4-Diarylpyrrole-2-carboxylate and pyrrolocoumarin cores of lamellarins are synthesized by Semenov[46] and his team, using a metal-free approach and Barton – Zard reaction. Respective nitrostilbene and ethyl isocyanoacetate in the presence of mild base formed 3,4-diarylpyrrole-2-carboxylate. Using this as a key intermediate, they synthesized lamellarin Q and lamellarin Q ethyl ester *via* simple transesterification-demethylation and demethylation steps, respectively.

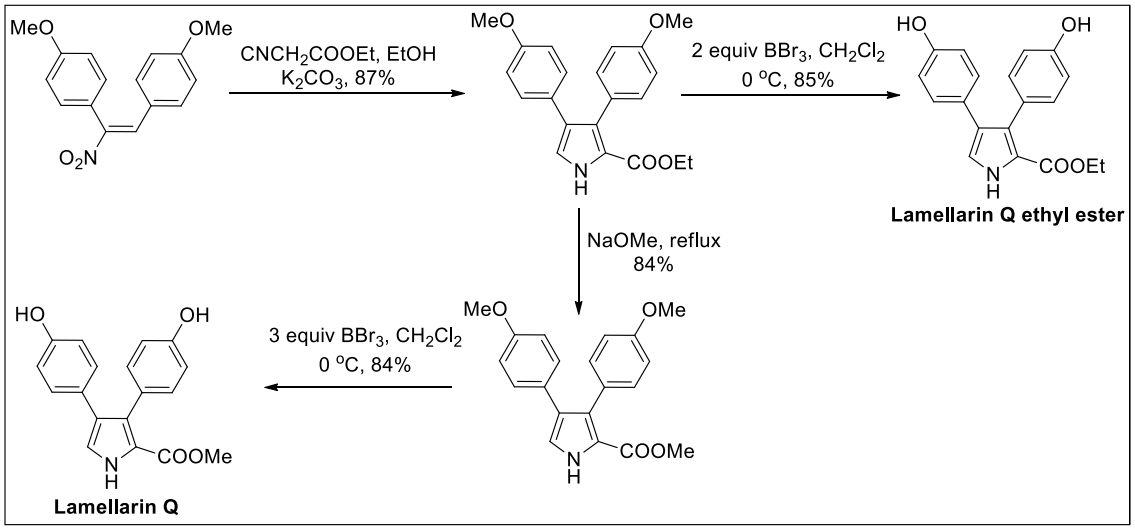

Scheme 19. Total syntheses of lamellarin Q and Q ethyl ester

Michael et al.[47] have described a high-yielding synthesis of lamellarin G trimethyl ether, lamellarin D trimethyl ether, lamellarin H, and lamellarin A4. A novel demethylative

lactonization reaction between aryl methyl ether and a neighboring carboxylic acid to construct courmarin ring is shown. A Friedel-Crafts acylation between homoveratroyl chloride (prepared from homoveratric acid using oxalyl chloride and used as such in situ) and 1,2,4-trimethoxybenzene followed by bromination furnished bromo keto compound.

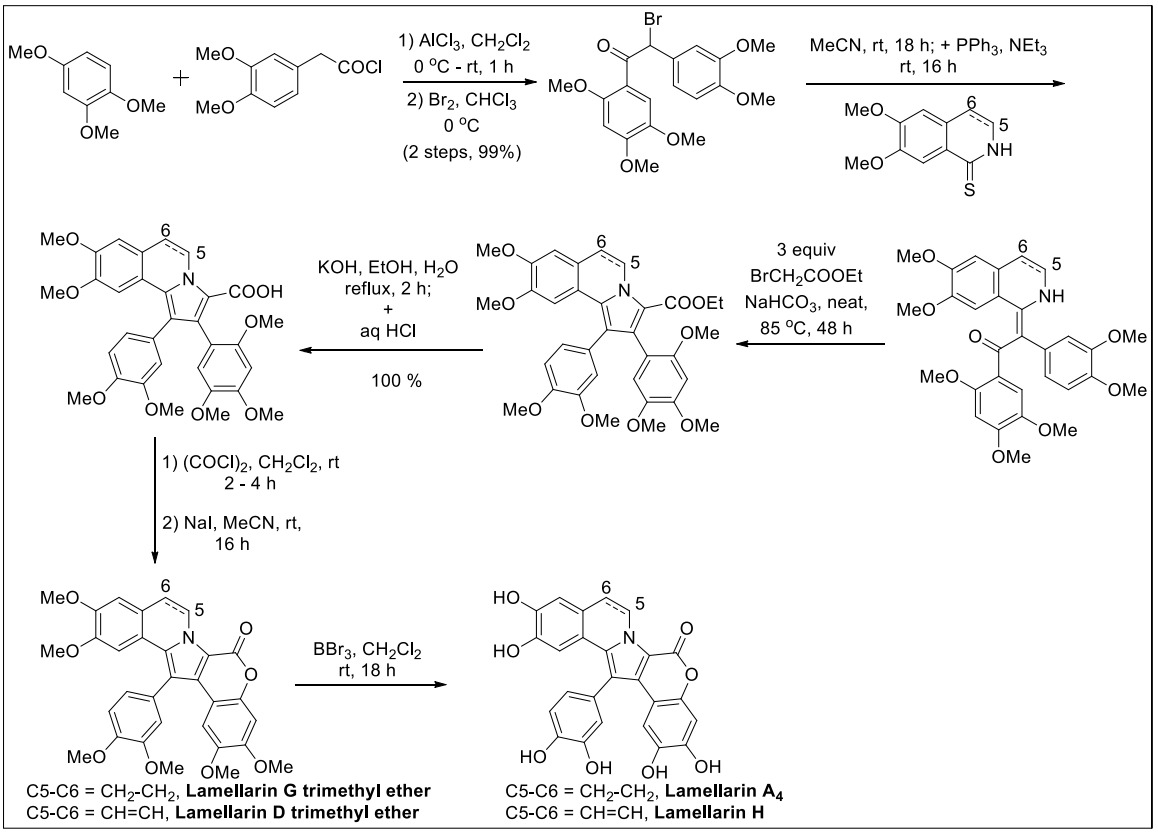

Scheme 20. Total syntheses of lamellarin G trimethyl ether, D trimethyl ether, A_4 and H

Eschnemoser sulfide contraction strategy is used with thiolactum to get heptamethoxylated enaminone. This enaminone was converted to pyrrole ester under neat heating with ethyl bromoacetate in the presence of a mild base. The resultant pyrrole ester compound was saponified using KOH to get a pivotal core to perform the novel demethylative lactonization step. In this step, the acid was first treated with oxalyl chloride then with sodium iodide when a pentacyclic core of lamellarin G trimethyl ether was obtained in high yield. This lamellarin G trimethyl ether was converted to lamellarin A_4 by complete demethylation using boron tribromide. To synthesize lamellarin D, they first aromatized pyrrole ester to get the double bond at C5-C6 bond and then carried out further operations of saponification, demethylative lactonization. Similarly, lamellarin D was fully demethylated to lamellarin H using boron tribromide.

Saito et al.[48] have shown a unique strategy to synthesize lamellarin compounds by first constructing coumarin ring and then pyrrole followed by isoquinoline ring. 4,5-Dimethoxy salicylaldehyde on treatment with methyl aminoacetate followed by bromination using NBS furnished corresponding 3-amino-4-bromo coumarin moiety. Simple Sonogahsira coupling under modified Stoddart's conditions with substituted phenyl acetylene helped construct coumarin-pyrrole fused ring core *via* their key method using ruthenium catalyst. Further, the strategy was applied for the formal synthesis of ningalin B,[49] lamellarin G trimethyl ether,[50] and lamellarin H. [43]

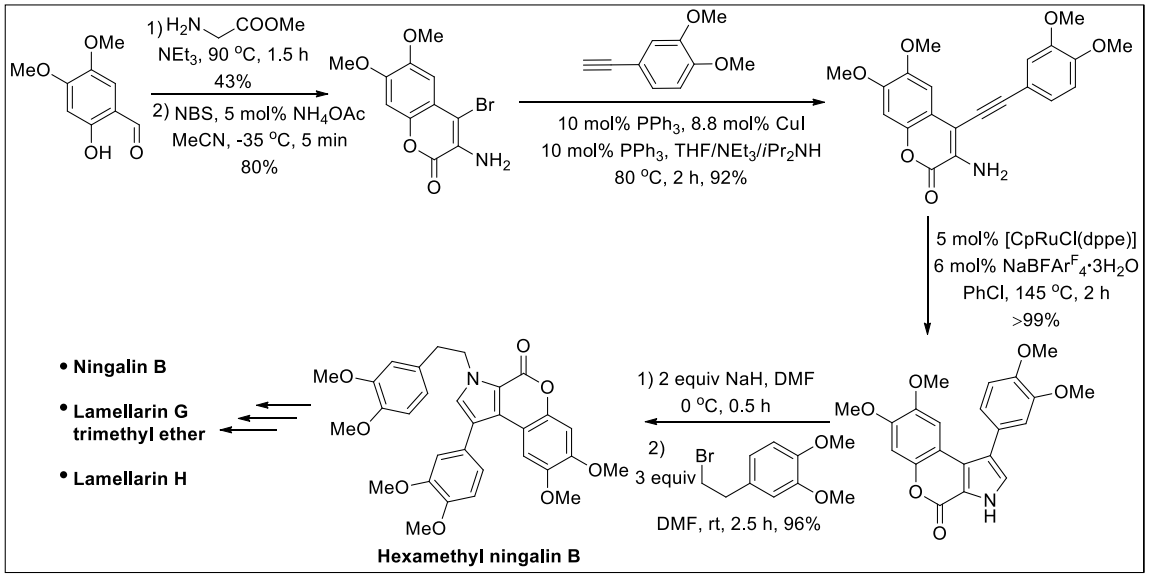

Scheme 21. Total syntheses of lamellarin G trimethyl ether, H and ningalin B

Total synthesis of lamellarin S, Z, ningalin B, lukianol A, B were achieved in 7 – 9 steps by Okano group[51] starting from dibromopyrrole ester. They have shown the construction of lukianol A and B by simple Suzuki coupling, SEM deprotection, and nucleophilic substitution on pyrrole, hydrolysis of the ester by $KOSiMe_3$, and finally cyclization. Lukianol A was synthesized in an overall 16% yield, whereas lukianol B is achieved in 1.6% (Scheme 22). Similarly, dibromopyrrole ester remained the key synthon for synthesizing lamellarin S, Z, and ningalin B. A convergent route was performed on pyrrole ring to form, first, the fused coumarin ring and then isoquinoline ring *via* Suzuki coupling, hydrolysis of ester, lactonization, and then *N*-alkylation using phenylethyl alcohol. Lamellarin S, Z, and ningalin B were prepared in overall 6%, 6%, and 9% respectively (Scheme 23).

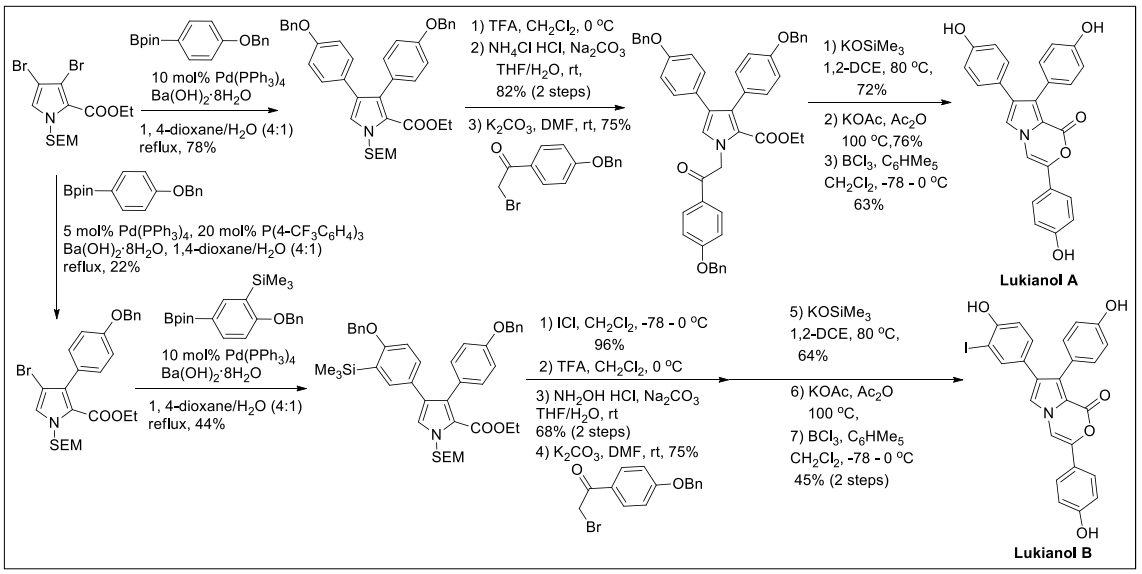

Scheme 22. Total Syntheses of lukianol A and B

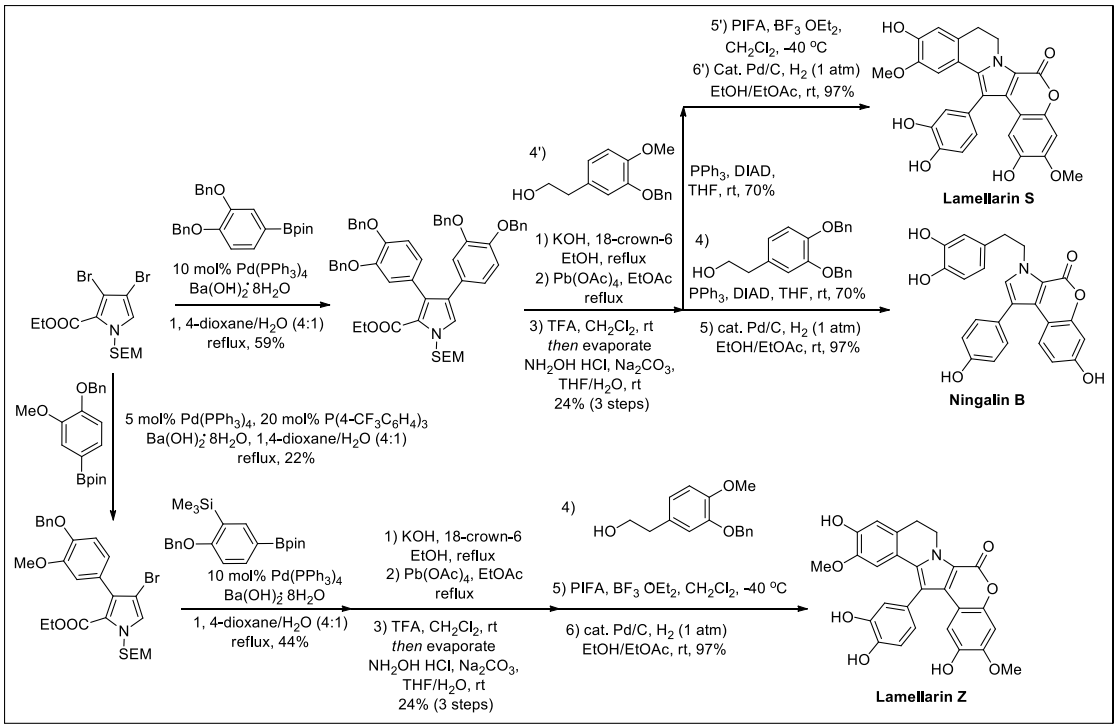

Scheme 23. Total syntheses of ningalin B, lamellarin S, and Z

1.3 Results and Discussion:

From the literature methods presented, we can see that most of the methods stress building pyrrole-isoquinoline ring structure in a single step and then performing Suzuki, Stille coupling reactions to get the lamellarin compounds in hand. To avoid coupling reaction steps, we thought of building lamellarin skeleton to synthesize pyrrolo-isoquinoline-

coumarin ring structure in an efficient metal-free manner. The lamellarin core is depicted below, showing different groups on different rings at different positions (Figure 2).

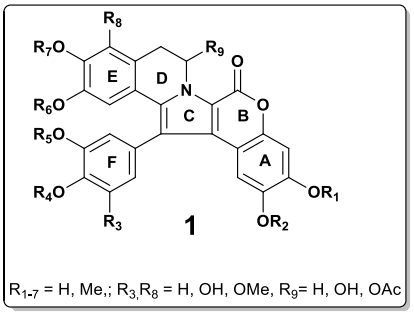

Figure 2. Pictorial depiction of substituents positions on lamellarin core

Our retrosynthesis of lamellarin core is depicted in scheme 24. The coumarin ring could be synthesized first by a classical Perkin reaction followed by a Bischler-Napieralski reaction to form the isoquinoline, which could undergo an intramolecular Michael reaction in the same vessel in the presence of Michael donor enamine and coumarin the Michael acceptor. Further oxidation could give us the required lamellarin core in a metal-free approach. If successful, this could be a unique approach that differs from common metal-mediated routes.

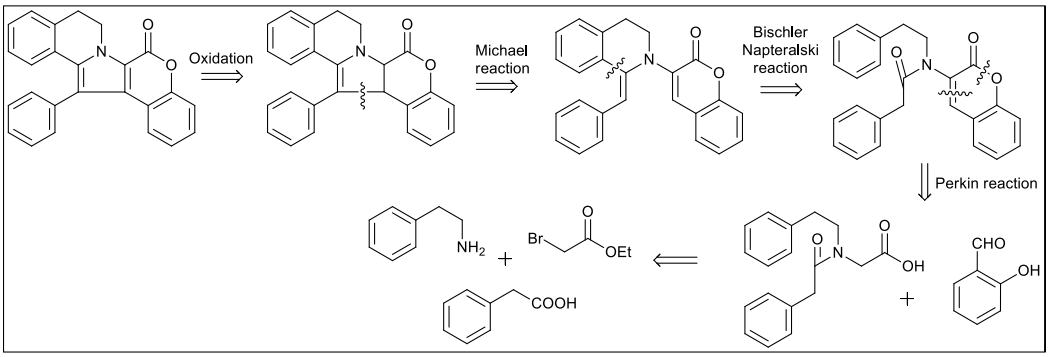

Scheme 24. Retrosynthetic pathway

To begin with, we implemented the reported procedure for nucleophilic substitution reaction between homoveratryl amine **2** and ethyl bromoacetate to obtain the secondary amine-ester in an excellent yield, which could be used for further reactions without column purification (Scheme 25).

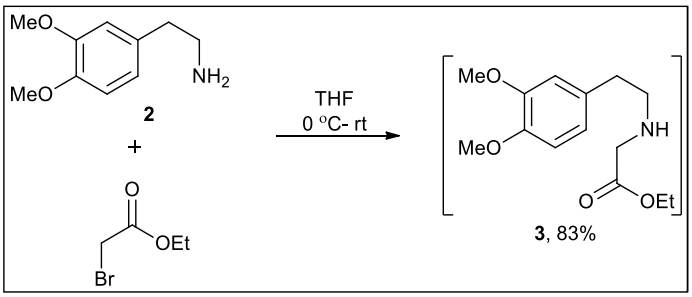

Scheme 25. Synthesis of ethyl 2-((3,4-dimethoxyphenethyl)amino)acetate 3

Once the secondary amine was in hand, it was immediately coupled with phenylacetic acid to avoid self-coupling. The reaction was first carried out with DCC (*N*,*N*′-dicyclohexylcarbodiimide) in dry CH_2Cl_2 to see the productivity of amide-ester from phenylacetic acid with **3**. But the workup of the reaction turned out to be problematic. Hence, it's another alternative, EDC (1-Ethyl-3-(3-dimethylaminopropyl)carbodiimide) coupling agent, was used to facile this reaction, whose workup was found to be much easier. Accordingly, compound **3** was reacted with homoveratric acid **4a** in the presence of EDC.HCl/HOBT to give amide-ester **5a** as pale yellow viscous oil in 79% yield (Scheme 26).

Similarly, parent phenylacetic acid was subjected to EDC coupling and converted to its corresponding amide-ester **5b** in an 82% yield. Mono methoxy derivative of phenylacetic acid gave its amide-ester **5c**. The structures of amides were characterized by spectroscopic techniques and the analytical data of **5a** is mentioned below in the experimental section.

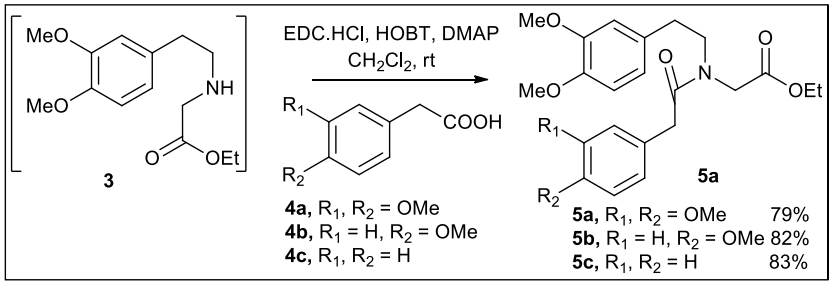

Scheme 26. Syntheses of various amide-ester 5a-c

Amide-ester with salicylaldehyde cannot give coumarin ring under standard Perkin reaction to build ring B. So, it was essential to hydrolyze it to its corresponding acid. First, a mild base like K_2CO_3 was used, which was inefficient to hydrolyze compound **5a**,

whereas LiOH resulted in amide and ester hydrolysis. Fortunately, Cs_2CO_3/EtOH-H_2O mixture hydrolyzed **5a** to amide-acid **6a** in 81% yield (Scheme 27). A white foamy sticky mass was formed, which confirmed the formation of compound **6a**. Similarly, amide-esters **5b** and **5c** were also hydrolyzed to get compounds **6b** and **6c** in 79% and 81%, respectively.

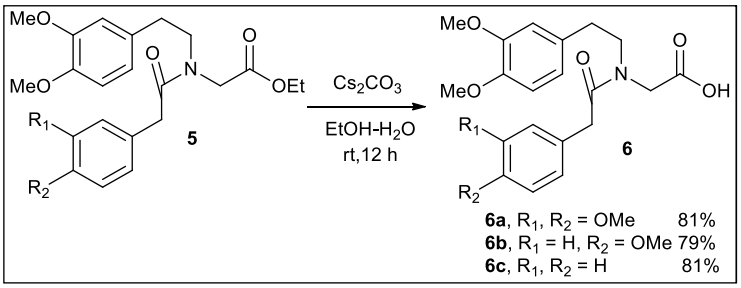

Scheme 27. Syntheses of amide-ester 6a-c

With the amide-acid **6a** in hand, it was planned first to synthesize lamellarin G trimethyl ether, so it was reacted with 4,5-dimethoxysalicylaldehyde under Perkin reaction condition using freshly distilled Ac_2O and catalytic triethylamine (Table 4, entry 1). But it failed to furnish amide-coumarin **7a**. Other bases like piperidine, pyrrolidine, and NaOAc could not show any formation of **7a** (Table 4, entries 2, 3, 4). So, we thought of using hitherto unreported P_4O_{10} as an alternative to acetic anhydride for the coumarin ring synthesis. The rationale to choose P_4O_{10} was because it is a well-known reagent for preparing anhydrides and the Bischler-Napieralski reaction, which was the subsequent reaction in the planned synthesis. After optimizing the reaction conditions, P_4O_{10} at 80 °C gave amide-coumarin **7a** in a 73% yield in just 2 hours (Table 4, entry 5). Prolonging the reaction at a higher temperature (110 °C) to check the possibility of further Bischler-Napieralski response in the same vessel resulted in getting the coumarin in 31% as the only isolable product (Table 4, entry 6). Employment of another phosphorous cyclization agent like PPA failed to give the product (Table 4, entry 7).

Table 4. Reagent selection for Perkin reaction

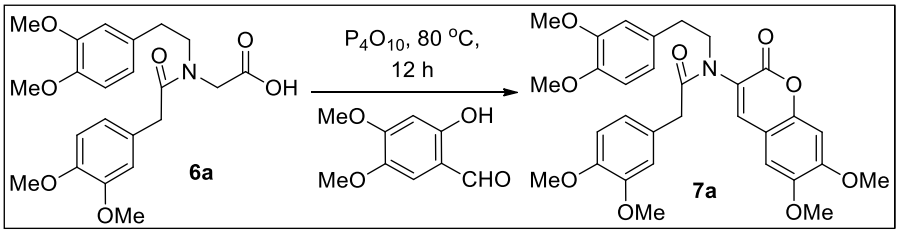

Entry	Reaction condition	Result
1	Acetic anhydride, Et_3N, reflux, 36 h	No reaction
2	Acetic anhydride, piperidine, reflux, 24 h	No reaction
3	Acetic anhydride, pyrrolidine, reflux, 24 h	No reaction
4	Acetic anhydride, NaOAc, rt - reflux, 24 h	No reaction
5	**$P_4O_{10,}$ 80 ^oC, 2 h**	**73 %**
6	$P_4O_{10,}$ 110 ^oC, 12 h	31%
7	PPA, 70 – 100 ^oC, 12 h	No reaction

With the successful synthesis of **7a**, we synthesized five more derivatives of amide-coumarins using different salicylaldehyde compounds (Scheme 28). The reaction of salicylaldehyde went smoothly with **6c** to construct its corresponding amide-coumarin **7b** in 76% yield. To prepare compound **8c**, we first had to prepare its isopropoxy derivative **9** of β-resorcylaldehyde **8**. Its synthesis was done in the heating condition in dry dimethylformamide in the presence of anhydrous K_2CO_3 (Scheme 29). 2-hydroxy-4-isopropoxybenzaldehyde was later fused with compound **6b** to get **7c** in 71% yield. Also, 4-methoxysalicylaldehyde was subjected to our reaction condition with compound **5c** to construct compound **7d** in a 74% yield. A distinct compound was synthesized using 3-ethoxysalicylaldehyde to construct C22 substituted lamellarin compound. So, it was reacted with compound **5b** and successfully converted into compound **7e** in a 33% yield. The low productivity may be due to the ortho-position hindrance caused by the ethoxy group in the cyclization process. Later an amide-coumarin precursor for C13, C14-bisdemethoxylamellarin G trimethyl ether **7f** was synthesized in 54% using 4,5-dimethoxysalicylaldehyde.

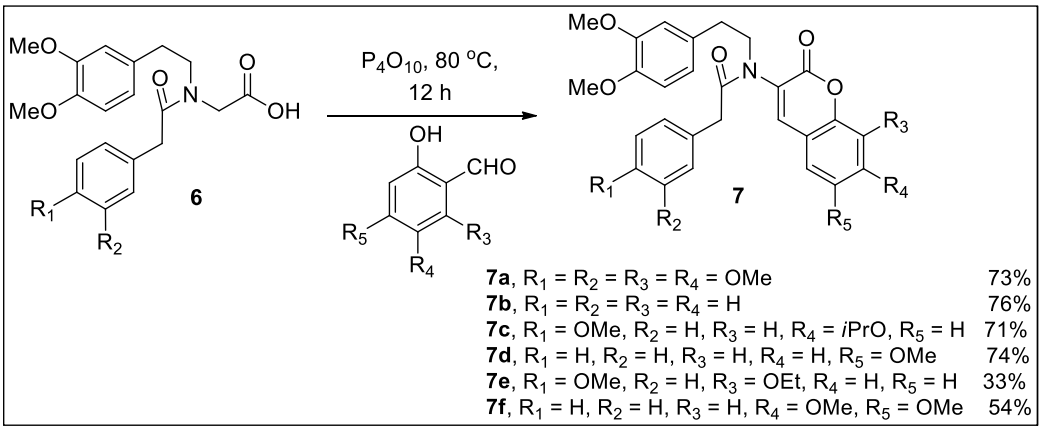

Scheme 28. Syntheses of different amide-coumarin 7a-f

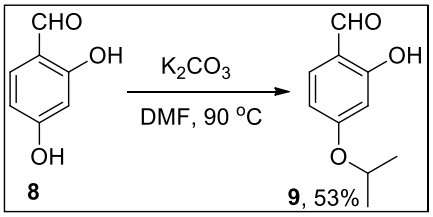

Scheme 29. Synthesis of 2-hydroxy-4-isopropoxybenzaldehyde 9

To synthesize lamellarin G trimethyl ether we treated compound **7a** with standard Bischler-Napieralski condition using reported reaction condition. As mentioned earlier, Perkin condensation reaction to get **7a** using P_4O_{10} was continued heating for another 10 hours, to see the possibility of formation of final lamellarin G trimethyl ether (Table 5, entry 1). However, this gave a complex mixture. Hence, the amide-coumarin **7a** was reacted with freshly distilled $POCl_3$ in refluxing toluene. But unfortunately, it failed to construct the pentacyclic core of lamellarin G trimethylether (Table 5, entry 2). We tried various reported reaction conditions available for the Bischler-Napieralski reaction. Reaction in refluxing xylene failed to deliver the product (Table 5, entry 3). Solvents like 1,2-dichloroethane could not facilitate the Bischler-Napieralski reaction (Table 5, entry 4). Triflic acid and Eaton's reagent failed to facilitate the product (Table 5, entry 5, 6). Under no conditions, we could get any pure product, and in most cases, starting was also not traceable.

Table 5. Bischler–Napieralski reaction of 7a

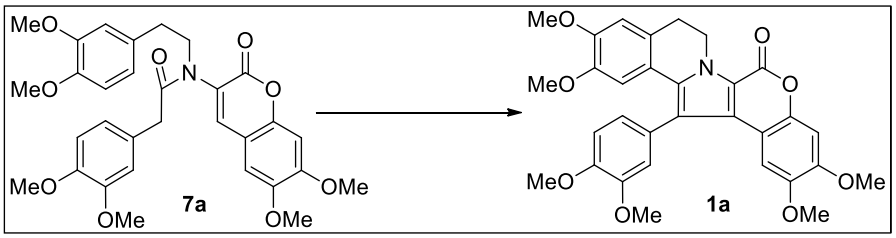

Entry	Reaction conditions	% Yield
1	P_4O_{10}, 110 °C, 12 h	Complex Mixture
2	$POCl_3$, dry toluene, reflux, 12 h	Complex Mixture
3	$POCl_3$, dry xylene, reflux, 12 h	Complex Mixture
4	$POCl_3$, 1,2-DCE, reflux, 11h	Complex Mixture
5	TfOH, CH_2Cl_2, 0 °C – rt, 12 h	Complex Mixture
6	Eatons's reagent	Complex Mixture

Unable to synthesize our target molecule, we tried the same reaction condition on **6b** (Table 2, entry 2) and observed a bright fluorescent spot on TLC, giving us hope about the formation of the final compound **1b**. After basic workup and chromatographic separation, that fluorescent compound was isolated and, with dry methanol washing, facilitated a white solid compound. Interestingly, spectroscopic analysis of the reaction product obtained revealed the structure to be lamellarin scaffold **1b**. The spectral details were consistent with the data available in the literature.[52,53] In this reaction, a domino Bischler-Napieralski reaction - Michael reaction - oxidation sequence took place directly, giving the final product **1b** in 34% yield.

We synthesized three new lamellarin analogs bearing different substituents on A and F rings with the standard condition. Compound **1c** bearing isopropoxy group at C21 position was synthesized in 43% yield. Derivative like **1d** containing methoxy group on **A** ring was formed in 31% yield. Unfortunately, the synthesis of compounds **1e** and **1f** bearing ethoxy group and dimethoxy groups on **A** ring could not be achieved with any of the reaction conditions tried. The presence of the dimethoxy group on ring A seemed crucial for the Bischler Napieralski reaction step (Scheme 30).

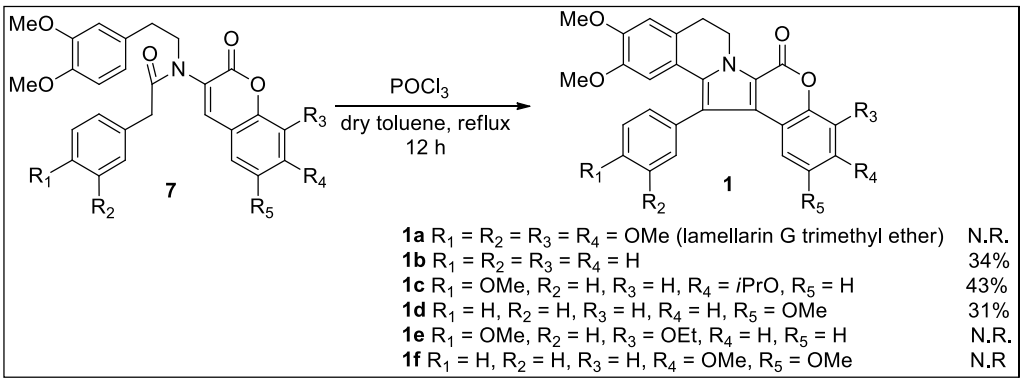

Scheme 30. Syntheses of different lamellarin compounds

A probable mechanism is given below successfully synthesizing six-membered lamellarin core using tandem Bischler-Napieralski - Michael reaction - oxidation sequence (Scheme 31). Carrying out the reaction under atmospheric oxygen was essential for facile oxidation in the final step.

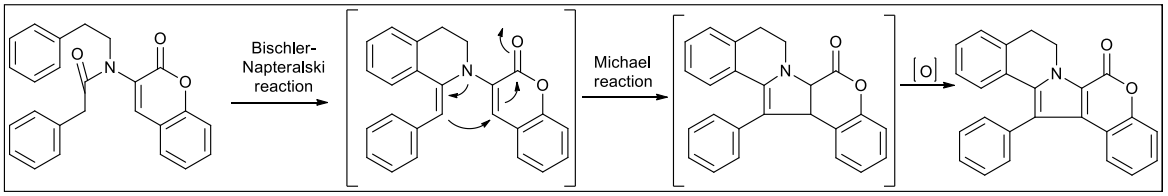

Scheme 31. Probable mechanism of tandem Bischler-Napieralski - Michael reaction - oxidation sequence

Similarly, an attempt was made to synthesize indole-based lamellarin **10** core having a structure shown in figure 3. Referring to indole shows various biological activities, and fusing it in lamellarin core can make it more potent towards the biological activities offered by lamellarin alkaloids.

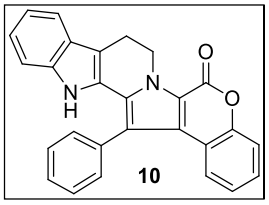

Figure 3. Structure of indole containing lamellarin core

At first, tryptamine was reacted with ethyl bromoacetate to get corresponding secondary amine-ester using reported reaction conditions without protecting NH of indole moiety, and it was used for the further reaction without purification (Scheme 32).

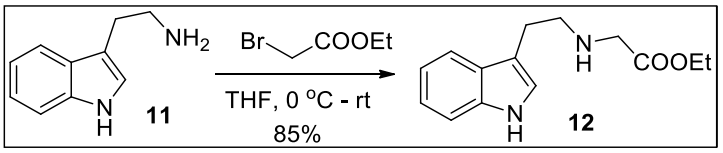

Scheme 32. Synthesis of ethyl 2-((2-(1*H*-indol-3-yl)ethyl)amino)acetate 12

To avoid any complication in the final two steps, a simple phenylacetic acid was coupled with compound **12** using EDC.HCl coupling (Scheme 33).

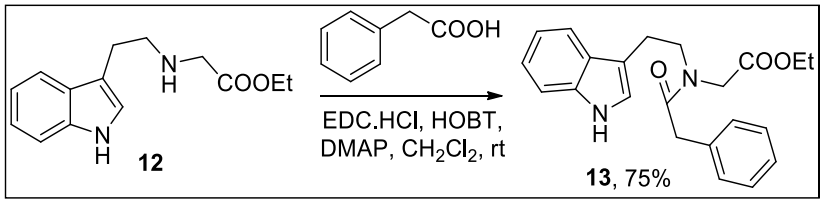

Scheme 33. Synthesis of amide-ester 13

Later, the hydrolysis of amide-ester **13** was done using Cs_2CO_3 to obtain the corresponding amide-acid in 77% yield (Scheme 34). A white foamy compound was obtained whose analytical data were consistent with the above-recorded data of other amide-acids.

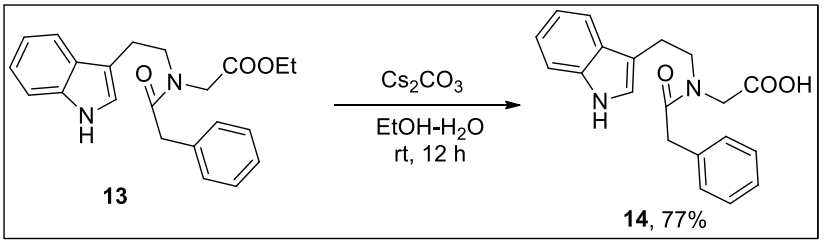

Scheme 34. Synthesis of amide-acid 14

The Perkin reaction of compound **14** didn't go as planned. Its reaction with parent salicylaldehyde under neat heating in P_4O_{10} was carried out, and it was observed no formation of amide-coumarin **15** on TLC. Besides that, we further did workup of that reaction and carried out its purification over flash chromatography but unfortunately, none of the isolated compounds could suggest the formation of amide-coumarin **15** in NMR (Scheme 35).

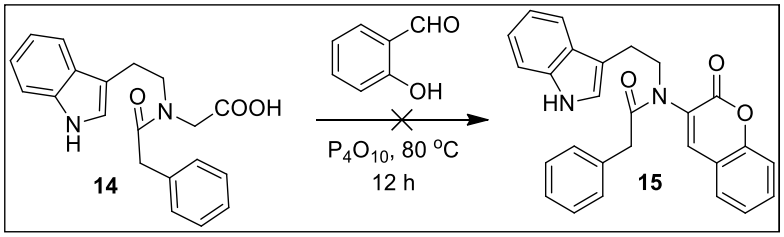

Scheme 35. Attempted synthesis of amide-coumarin 15

As this method fails to construct indole-based lamellarin compound with free NH of indole, one can think of using our strategy to develop *N*-protected indole-based lamellarin compounds. The use of electron-donating groups like methyl, ethyl, propyl, etc. on the nitrogen may give good results.

1.4 Conclusion:

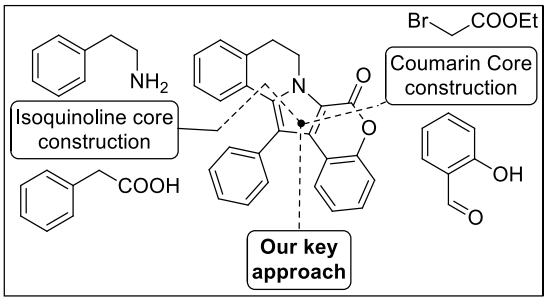

Figure 4. Depiction of various small molecules to construct pentacyclic core

A metal-free convergent route for the pentacyclic framework is developed starting from commercially available starting synthons. Three lamellarin analogs were successfully synthesized by tandem Bischler-Napieralski-Michael reaction-oxidation sequence. Preparation of ethoxy substituted lamellarin core and lamellarin G trimethyl ether failed in the final step. Indole-based lamellarin analog synthesis failed during the Perkin reaction. The highlight of the route was the development of a tandem Bischler-Napieralski-Michael reaction-oxidation sequence for the pentacyclic core. Further modifications in the standard Bischler-Napieralski are awaited to make the synthesis of natural products viable by this route or maybe flow chemistry could benefit the process.

1.5 Experimental:

1.5.1: Ethyl 2-((3,4-dimethoxyphenethyl)amino)acetate (3):

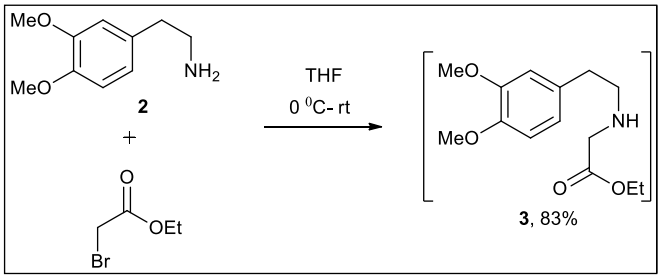

Homoveratryl amine (3.62 g, 20 mmol) **2** was dissolved in dry THF (20 mL), and to it, ethyl bromoacetate (1.67 g, 10 mmol) was added and stirred at room temperature for 12 h. The resulting heterogeneous mixture (secondary amine-ester and HBr salt of homoveratryl amine) was filtered through a Whatman filter paper. The filtrate evaporated to get the secondary amine **3** in 83 % (2.35 g) yield, which was as such used for the next reaction.

1.5.2: Ethyl 2-((2-(1*H*-indol-3-yl)ethyl)amino)acetate (12):

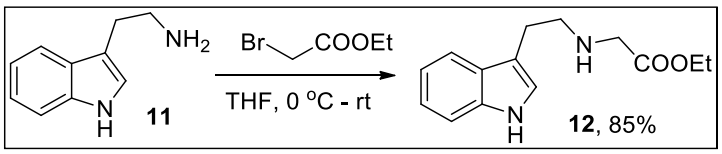

Following the similar procedure mentioned in 1.5.1 with tryptamine **11** gave the product **12** in 85% yield as a dark brown liquid, which was as such used for the next reaction.

1.5.3: Ethyl 2-(*N*-(3,4-dimethoxyphenethyl)-2-(3,4-dimethoxyphenyl)-acetamido)acetate (5a):

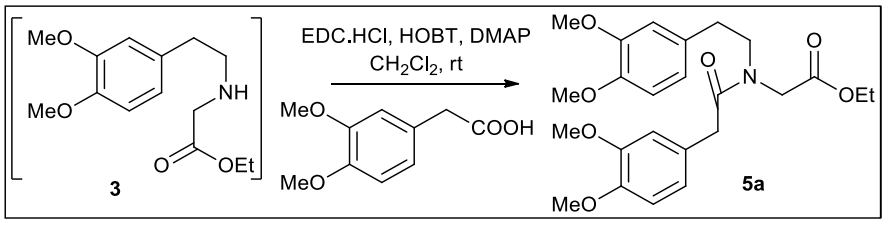

10 mmol of secondary amine prepared above, 12 mmol substituted phenylacetic acid, 13 mmol of HOBT, and catalytic DMAP were dissolved in 20 mL dry CH_2Cl_2 and cooled to 0 °C. 15 mmol EDC was added and stirred at 0 °C - rt for 24 h. The suspension was cooled to 0 °C and filtered. The filtrate was evaporated to dryness. Fresh 20 mL CH_2Cl_2 was added and the solution was cooled to 0 °C and filtered again. The evaporation, addition of CH_2Cl_2, cooling, and filtering was repeated thrice. The organic layer was washed with water, brine, and dried over Na_2SO_4. The solvent was removed under vacuum, and the crude product was purified by flash chromatography (CH_2Cl_2) to give pure product **5a** in 79% yield.

Viscous oil. IR (neat) ν_{max}: 2936, 2835, 1746, 1643, 1589, 1261 cm^{-1}. ^1H NMR (400 MHz, $CDCl_3$): δ = 1.19 (t, *J* = 7.2 Hz, 3H), 2.61 [2.71] (t, *J* = 7.2 Hz, 2H), 3.43 (s, 3H), 3.46 [3.52] (m, 2H), 3.77-3.79 (m, 12H), 3.97 (s, 2H), 4.12 (q, *J* = 7.2 Hz, 2H), 6.53-6.57 (m, 1 H), 6.61-6.63 (m, 1H), 6.65-6.69 (m, 1H), 6.71-6.74 (m, 3H) ppm. ^{13}C NMR (100 MHz, $CDCl_3$): δ = 14.1 (CH_3), 34.55 [33.4] (CH_2), 39.8 [40.6] (CH_2), 47.9 [49.9] (CH_2), 51.2 [50.6] (CH_2), 55.7 (CH_3), 55.8 (CH_3), 55.8 (CH_3), 55.8 (CH_3), 61.1 [61.5] (CH_2), 111.1 (CH), 111.3 (CH), 111.8 (CH), 111.8 (CH), 120.6 (2XCH), 120.7 (CH), 127.2 (Cq), 130.5 (Cq), 147.8 (Cq), 149.0 (2XCq), 169.2 (Cq), 171.7 (Cq) ppm. HRMS (m/z): calculated for $C_{24}H_{31}NO_7Na$ $[M+Na]^+$ 468.1998; found 468.1998.

1.5.4: Ethyl 2-(*N*-(3,4-dimethoxyphenethyl)-2-(4-methoxyphenyl)acetamido)acetate (5b):

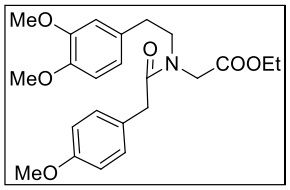

Following the similar procedure mentioned in 1.5.3 with 4-methoxyphenyl acetic acid **4b** gave the product **5b** in 85% yield.

Viscous oil. IR (neat) ν_{max}: 2934, 2829, 1751, 1648, 1593, 1267 cm^{-1}. ^1H NMR (400 MHz, $CDCl_3$): δ = 1.28 (t, *J* =7.2 Hz, 3H), 2.69 [2.79] (t, *J* = 7.2 Hz, 2H), 3.51 (s, 2H), 3.57 [3.60] (m, 1H), 3.78 (s, 3H), 3.86 (s, 6H), 4.04 (s, 1H), 4.16-4.22 (m, 2H), 6.60-6.63 (m, 1H), 6.79 (d, *J* = 8.0 Hz, 1H), 6.84-6.87 (m, 3H), 7.12 (d, *J* = 8.8 Hz, 2H) ppm. ^{13}C NMR (100 MHz, $CDCl_3$): δ = 14.1 (CH_3), 34.6 [33.4] (CH_2), 39.4 [40.1] (CH_2), 48.0 [49.0]

(CH_2), 51.3 [50.6] (CH_2), 55.92 (CH_3), 55.9 (CH_3), 61.1 [61.6] (CH_2), 111.9 (CH), 114.0 (2XCH), 120.7 (CH), 126.7 (Cq), 129.7 (2XCH), 130.5 (Cq), 131.4 (CH), 147.8 (Cq), 149.0 (Cq), 158.4 (Cq), 169.3 (Cq), 171.8 (Cq) ppm. HRMS (m/z): calculated for $C_{23}H_{29}NO_6Na$ $[M+Na]^+$ 438.1893; found 438.1894.

1.5.5: Ethyl 2-(*N*-(3,4-dimethoxyphenethyl)-2-phenylacetamido)acetate (5c):

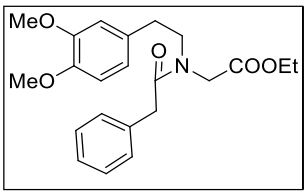

Following the similar procedure mentioned in 1.5.3 with phenylacetic acid **4c** gave the product **5c** in an 85% yield.

Viscous oil. IR (neat) ν_{max}: 2928, 2827, 1749, 1645, 1584, 1261 cm^{-1}. ^1H NMR (400 MHz, $CDCl_3$): δ = 1.25 (t, *J* = 7.6 Hz, 3H), 2.64 (t, *J* = 7.2 Hz, 2H), 3.52-3.61 (m, 2H), 3.63 (s, 2H), 3.79 (s, 1H), 3.43 (s, 6H), 4.04 (s, 1H), 4.13 (m, 2H), 6.58-6.80 (m, 3H), 7.20-7.24 (m, 3H), 7.25-7.32 (m, 2H) ppm. ^{13}C NMR (100 MHz, $CDCl_3$): δ = 14.1 (CH_3), 34.6 [33.44] (CH_2), 40.3 [41.0] (CH_2), 48.0 [49.8] (CH_2), 51.3 [50.6] (CH_2), 51.3 (CH_3), 55.8 (CH_3), 61.6 [61.6] (CH_2), 111.5 (CH), 112.0 (CH), 120.7 (CH), 126.8 (CH), 128.6 (2XCH), 128.8 (2XCH), 130.5 (Cq), 131.5 (Cq), 134.8 (Cq), 147.9 (Cq), 149.1 (Cq), 169.3 (Cq), 171.5 (Cq) ppm. HRMS (m/z): calculated for $C_{22}H_{27}NO_5H$ $[M+H]^+$ 386.1967 ; found 386.1978.

1.5.6: Ethyl 2-(*N*-(2-(1*H*-indol-3-yl)ethyl)-2-phenylacetamido)acetate (13):

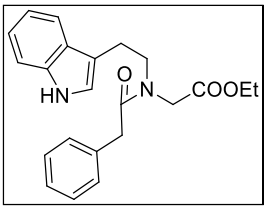

Following the similar procedure mentioned in 1.5.3 with phenylacetic acid **4b** and **12** gave the product **7** in an 85% yield.

Light brown oil. IR (neat) ν_{max}: 3119, 3018, 2942, 1730, 1686, 1616, 1528, 1489, 1278, 1189 cm^{-1}. ^1H NMR (400 MHz, $CDCl_3$): δ = 1.31 (t, *J* = 7.2 Hz, 3H), 2.82 (t, *J* = 6.8 Hz, 2H), 3.36 (s, 2H), 3.53 (t, *J* = 7.2 Hz, 2H), 3.99 (s, 2H), 4.04-4.09 (m, 2H), 6.75-6.79 (m, 1H), 6.97-7.03 (m, 3H), 7.06-7.11 (m, 1H), 7.12-7.15 (m, 3H), 7.17-7.23 (m, 2H), 7.37 (d, *J* = 8 Hz, 1H), 8.61 (s, 1H) ppm. ^{13}C NMR (100 MHz, $CDCl_3$): δ = 13.0 (CH_3), 23.5 (CH_2), 38.9 (CH_2), 47.1 (CH_2), 49.0 (CH_2), 60.1 (CH_2), 110.2 (Cq), 110.6 (CH), 116.9 (Cq), 118.3 (CH), 121.0 (CH), 121.7 (CH), 125.6 (CH), 125.8 (CH), 127.5 (2XCH), 127.7 (2XCH), 133.7 (Cq), 135.3 (Cq), 168.4 (Cq), 170.9 (Cq) ppm. LCMS (m/z): calculated for $C_{22}H_{24}N_2O_3H$ $[M+H]^+$ 365.4; Found: 365.6.

1.5.7: 2-(*N*-(3,4-Dimethoxyphenethyl)-2-(3,4-dimethoxyphenyl)acetamido)acetic acid (6a):

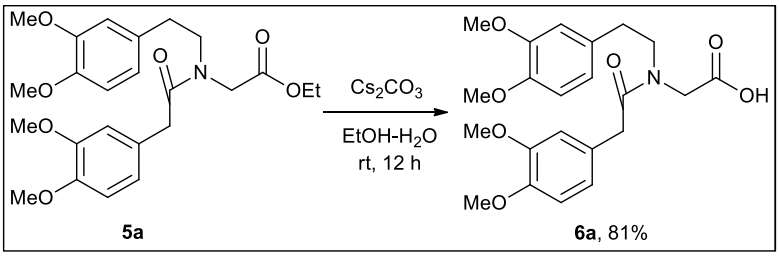

A mixture of 5 mmol amide-ester **5a**, 7 mmol Cs_2CO_3, and 2 mL H_2O in 10 mL EtOH was stirred at room temperature for 12 h. The reaction mixture then dried under vacuum, and to it, 20 mL aqueous saturated Na_2CO_3 was added. The basic aqueous layer was washed with Et_2O (2 X 15 mL) and acidified with 1N HCl. The product was extracted in CH_2Cl_2 (2 X 20 mL), dried over Na_2SO_4, and concentrated under vacuum to give analytically pure product **6a**.

Light brown oil. IR (neat) ν_{max}: 3205, 3017, 2935, 1732, 1662, 1608, 1514, 1458, 1261, 1155 cm^{-1}. ^1H NMR (400MHz, $CDCl_3$): δ = 2.60 [2.70] (t, *J* = 6.8 Hz, 2H), 3.42 (s, 2H), 3.48 (m, 2H), 3.75 – 3.78 (m, 12H), 4.00 (s, 2H), 5.77 (bs, 1H), 6.52 – 6.73 (m, 6H) ppm. ^{13}C NMR (100 MHz, $CDCl_3$): δ = 34.5 [34.4] (CH_2), 39.8 [40.6] (CH_2), 48.4 [50.0] (CH_2), 51.6 [50.3] (CH_2), 55.8 (CH_3), 55.8 (CH_3), 55.9 (CH_3), 55.9 (CH_3), 111.2 (CH), 111.4 (CH), 111.7 (CH), 111.9 (CH), 120.7 (2X CH), 126.8 (Cq), 130.2 (Cq), 147.9 (2X Cq), 149.1 (2X Cq), 172.5 (Cq), 172.8 (Cq) ppm. HRMS (m/z): calculated for $C_{22}H_{27}NO_7Na$ $[M+Na]^+$ 440.1685; found 440.1681.

1.5.8: 2-(*N*-(3,4-Dimethoxyphenethyl)-2-(4-methoxyphenyl)acetamido)acetic acid (6b):

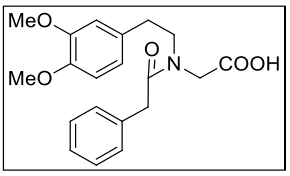

Following the similar procedure mentioned in the 1.5.7 compound, **5b** gave the product **6b** in 79% yield.

Colourless oil. IR (neat) ν_{max}: 3200, 3007, 2935, 1731, 1666, 1606, 1518, 1462, 1263, 1151 cm^{-1}. ^1H NMR (400 MHz, $CDCl_3$): δ = 2.66 (t, *J* = 7.2 Hz, 2H), 3.50 (s, 2H), 3.54-3.59 (m, 2H), 3.74 (s, 3H), 3.82 (s, 3H), 3.84 (s, 3H), 4.07 (s, 2H), 6.59-6.66 (m, 2H), 6.78 (s, 1H), 6.81 (d, *J* = 8.4 Hz, 2H), 7.07 (d, *J* = 8.4 Hz, 2H), 8.48 (bs, 1H) ppm. ^{13}C NMR (100 MHz, $CDCl_3$): δ = 34.4 [33.5] (CH_2), 39.2 [40.0] (CH_2), 48.3 [49.8] (CH_2), 51.5 [50.3] (CH_2), 55.2 (CH_3), 55.9 (CH_3), 55.9 (CH_3), 111.5 (CH), 111.9 (CH), 114.1 (2XCH), 120.7 (CH), 126.3 (Cq), 129.8 (2XCH), 130.3 (Cq), 147.9 (Cq), 149.0 (Cq), 158.5 (Cq), 172.5 (Cq), 173.0 (Cq) ppm. HRMS (m/z): calculated for $C_{21}H_{25}NO_5Na$ $[M+Na]^+$ 394.1360; found 394.1358.

1.5.9: 2-(*N*-(3,4-dimethoxyphenethyl)-2-phenylacetamido)acetic acid (6c):

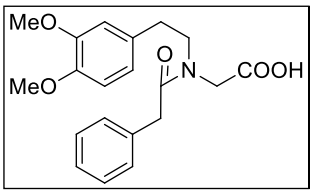

Following the similar procedure mentioned in the 1.5.7 compound **5c** gave the product **6c** in an 81% yield.

Colourless oil. IR (neat) ν_{max}: 3219, 3010, 2939, 1725, 1672, 1611, 1520, 1459, 1269, 1149 cm-1. ^1H NMR (400 MHz, $CDCl_3$): δ = 2.65 (t, *J* = 6.8 Hz , 2H), 3.54 (s, 2H), 3.63 (s, 1H), 3.77 (s, 1H), 3.83 (s, 3H), 3.85 (s, 3H), 4,07 (s, 2H), 6.59-6.66 (m, 2H), 6.79 (d, *J* = 8 Hz, 1H), 7.15-7.32 (m, 5H) ppm. ^{13}C NMR (100 MHz, $CDCl_3$): δ = 34.5 [33.4] (CH_2), 40.2 [41.0] (CH_2), 48.5 [49.8] (CH_2), 51.7 [50.3] (CH_2), 55.9 (CH_3), 55.9 (CH_3), 111.5 (CH), 111.9 (CH), 120. 7 (CH), 126.9 (CH), 128.6 (2XCH), 128.8 (2XCH), 129.3 (Cq), 134.3

(Cq), 147.9 (Cq), 149.1 (Cq), 172.7 (Cq), 173.0 (Cq) ppm. LCMS (m/z): calculated for $C_{20}H_{23}NO_5H$ $[M+H]^+$: 358.1654; found 358.1666. HRMS (m/z): calculated for $C_{20}H_{23}NO_5Na$ $[M+Na]^+$: 380.1474; found 380.1479.

1.5.10: 2-(*N*-(3,4-dimethoxyphenethyl)-2-phenylacetamido)acetic acid (14):

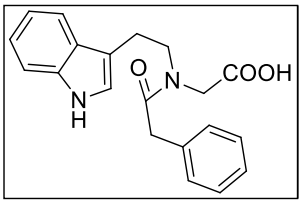

Following the similar procedure mentioned in the 1.5.7 compound **14** gave the product **15** in 77% yield.

Colourless oil. IR (neat) ν_{max}: 3119, 3018, 2942, 1730, 1686, 1616, 1528, 1489, 1278, 1189 cm^{-1}. ^1H NMR (400 MHz, $CDCl_3$): δ = 2.87 (t, *J* = 6.8 Hz, 2H), 3.31 (s, 2H), 3.58 (t, *J* = 6.4 Hz, 2H), 4,00 (s, 2H), 7.04-7.07 (m, 2H), 7.11-7.17 (m, 5H), 7.21 (1H), 7.25-7.28 (m, 1H), 7.40 (d, *J* = 8 Hz, 1H) ppm. ^{13}C NMR (100 MHz, $CDCl_3$): δ = 24.4 (CH_2), 39.7 [40.9] (CH_2), 49.1 (CH_2), 50.3 (CH_2), 111.2 (Cq), 111.6 (CH), 118.0 (CH), 119.7 (CH), 122.3 (CH), 123.1 (CH), 126.8 (Cq), 126.9 (CH), 128.6 (2XCH), 128.8 (2XCH), 128.9 (Cq), 129.3 (Cq), 134.2 (Cq), 136.3 (Cq), 172.4 (Cq), 173.4 (Cq) ppm. LCMS (m/z): calculated for $C_{20}H_{20}N_2O_3H$ $[M+H]^+$: 337.3; found: 337.5. HRMS (m/z): calculated for $C_{20}H_{20}N_2O_3Na$ $[M+Na]^+$: 359.1372; Found 359.1374.

1.5.11: 2-hydroxy-4-isopropoxybenzaldehyde (9):

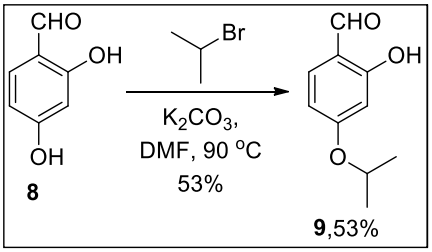

In a two-neck round bottom flask equipped with stirring bar, refluxing condenser, and septum was added 1 mmol of 2,4-dihydroxybenzaldehdye **8** in 10 mL dry dimethylformamide and 1 mmol of anhydrous K_2CO_3. The mixture was stirred for 30 minutes and at room temperature 1 mmol of 2-bromopropane was added slowly. Then the

mixture was heated at 90 °C for 8 hours. After the disappearance of compound **8** on TLC, the reaction was quenched with 20 mL water and extracted using ethyl acetate (3 X 10 mL). The organic layer was dried over anhydrous Na_2SO_4 and concentrated on the rotary evaporator to get the crude compound. Further to get the analytically pure compound, the crude mixture was purified over combiflash on silica gel (Pet. ether and ethyl acetate) to give pale yellow oil.

Pale yellow oil. IR (neat) ν_{max}: 3024, 2930, 1708, 1662, 1600, 1509, 1459, 1255, 1147 cm^{-1}. ^1H NMR (400 MHz, $CDCl_3$): δ = 1.38 (s, 3H), 1.40 (s, 3H), 4.59-4.68 (m, 1H), 6.42 (s, 1H), 6.51 (d, *J* = 8.8 Hz, 1H), 7.42 (d, *J* = 8.4 Hz, 1H), 9.71 (s, 1H), 11.50 (s, 1H) ppm. ^{13}C NMR (100 MHz, $CDCl_3$): δ = 21.8 (CH_3), 70.6 (CH), 101.7 (CH), 109.5 (CH), 114.8 (Cq), 135.3 (CH), 164.5 (Cq), 165.4 (Cq), 194.2 (O=Cq) ppm.

1.5.12: *N*-(6,7-dimethoxy-2-oxo-2*H*-chromen-3-yl)-*N*-(3,4-dimethoxyphenethyl)-2-(3,4-dimethoxyphenyl)acetamide (7a):

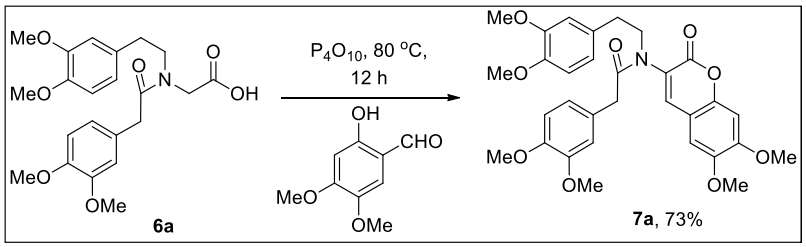

A mixture of 2 mmol of amide-acid **6a**, 4 mmol 4,5-dimethoxy-2-hydroxybenzaldehyde, and 3 equiv P_4O_{10} were heated neat at 80 °C for 2 h. To the reaction flask, 30 mL ice-cold water was added and then extracted with CH_2Cl_2 (4 X 10 mL). The organic layer was dried over Na_2SO_4 and concentrated under vacuum and directly purified by flash column chromatography (Pet. ether and ethyl acetate) to afford the pure product **7a** in 73% yield.

Light brown oil. IR (neat) ν_{max}: 3028, 2926, 1707 1665, 1611, 1509, 1461, 1257, 1149 cm^{-1}. ^1H NMR (400 MHz, $CDCl_3$): δ = 2.74-2.91 (m, 2H), 3.30-3.42 (m, 2H), 3.49-3.53 (m, 1H), 3.65 (s, 3H), 3.71 (s, 3H), 3.76 (s, 3H), 3.77 (s, 3H), 3.84 (s, 3H), 3.90 (s, 3H), 4.16-4.23 (m, 1H), 6.48-6.53 (m, 3H), 6.57-6.61 (m, 2H), 6.63-6.65 (m, 3H), 6.80 (s, 1H) ppm. ^{13}C NMR (100 MHz, $CDCl_3$): δ 33.69 (CH_2), 41.55 (CH_2), 49.52 (CH_2), 55.72 (CH_3), 55.86 (CH_3), 55.88 (CH_3), 55.91 (CH_3), 56.38 (CH_3), 56.55 (CH_3), 99.73 (CH), 107.82 (CH), 110.68 (Cq), 111.14 (CH), 111.20 (CH), 112.13 (CH), 112.22 (CH), 120.98 (CH), 121.03 (CH), 125.66 (Cq), 127.60 (Cq), 131.33 (Cq), 142.17 (CH), 146.82 (CH), 147.59

(Cq), 147.88 (Cq), 148.92 (Cq), 148.98 (Cq), 149.28 (Cq), 153.43 (Cq), 159.30 (Cq), 171.28 (Cq) ppm. HRMS (m/z): calculated for $C_{31}H_{33}NO_9H$ $[M+H]^+$: 563.2155; found 563.2158.

1.5.13: *N*-(3,4-dimethoxyphenethyl)-*N*-(2-oxo-2*H*-chromen-3-yl)-2-phenylacetamide (7b):

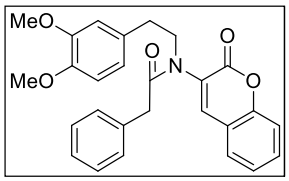

Following the similar procedure mentioned in the 1.5.12 with salicylaldehyde and compound, **6c** gave the product **7b** in 76% yield.

Light brown oil. IR (neat) ν_{max}: 3024, 2930, 1708, 1662, 1600, 1509, 1459, 1255, 1147 cm^{-1}. ^1H NMR (400 MHz, $CDCl_3$): δ = 2.73-2.85 (m, 2H), 3.33-3.36 (m, 2H), 3.51-3.55 (m, 1H), 3.67 (s, 3H), 3.71 (s 3H), 4.21 (m, 1H), 6.55-6.61 (m, 2H), 6.67 (s, 1H), 6.96 (s, 1H), 7.11 (s, 3H), 7.19-7.26 (m, 3H), 7.46-7.50 (m, 1H) ppm. ^{13}C NMR (100 MHz, $CDCl_3$): δ = 33.7 (CH_2), 41.9 (CH_2), 49.4 (CH_2), 55.8 (CH_3), 55.8 (CH_3), 111.2 (CH), 112.1 (CH), 116.6 (Cq), 118.2 (CH), 120.9 (Cq), 125.0 (Cq), 126.9 (2XCH), 128.2 (Cq), 128.5 (Cq), 128.6 (CH), 128.9 (CH), 131.1 (CH), 132.4 (CH), 134.8 (Cq), 141.8 (2XCH), 147.5 (CH), 148.9 (Cq), 153.0 (CH), 158.9 (Cq), 170.97 (Cq) ppm. HRMS (m/z): calculated for $C_{27}H_{25}NO_5H$ $[M+H]^+$: 444.1811; found 444.1819.

1.5.14: *N*-(3,4-dimethoxyphenethyl)-*N*-(7-isopropoxy-2-oxo-2*H*-chromen-3-yl)-2-(4-methoxyphenyl)acetamide (7c):

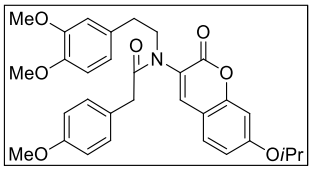

Following the similar procedure mentioned in the 1.5.12 with 4-isopropoxy-2-hydroxybenzaldehyde and compound, **6b** gave the product **7c** in 71% yield.

Light brown oil. IR (neat) ν_{max}: 3028, 2931, 1709, 1659, 1596, 1518, 1455, 1262, 1142 cm^{-1}. ^1H NMR (400 MHz, $CDCl_3$): δ = 1.31 (s, 3H), 1.33 (s, 3H), 2.70-2.90 (m, 2H), 3.32-3.37 (m, 2H), 3.44-3.48 (m, 1H), 3.69 (s, 3H), 3.71 (s, 3H), 3.75 (s, 3H), 4.15-4.53 (m, 1H), 4.54-4.59 (m, 1H), 6.57-6.62 (m, 3H), 6.64-6.70 (m, 3H), 6.74-6.6.79 (m, 2H), 6.91 (d, *J* = 8.4 Hz, 2H), 7.04 (d, *J* = 8.4 Hz, 1H) ppm. ^{13}C NMR (100 MHz, $CDCl_3$): δ = 21.7 (CH_3), 33.6 (CH_2), 40.8 (CH_2), 49.4 (CH_2), 55.2 (CH_3), 55.8 (CH_3), 55.8 (CH_3), 70.9 (CH), 101.9 (CH), 111.1 (CH), 111.3 (Cq), 112.1 (CH) 113.9 (CH), 114.4 (CH), 120.9 (2XCH), 125.0 (Cq), 127.0 (Cq), 129.2 (CH), 129.9 (CH) 131.2 (Cq), 142.0 (2XCH), 147.5 (CH), 148.8 (Cq), 155.1 (CH), 158.4 (Cq), 159.3 (Cq) 161.8 (Cq), 171.4 (Cq) ppm. HRMS (m/z): calculated for $C_{31}H_{33}NO_7Na$ $[M+H]^+$: 532.2335; found 532.2322.

1.5.15: *N*-(3,4-dimethoxyphenethyl)-*N*-(6-methoxy-2-oxo-2*H*-chromen-3-yl)-2-phenylacetamide (7d):

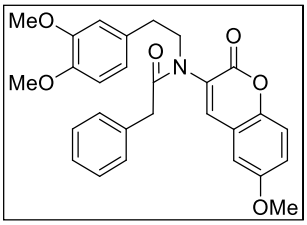

Following the similar procedure mentioned in the 1.5.12 with 5-methoxy-2-hydroxybenzaldehyde and compound, **6c** gave the product **7d** in 74% yield.

Light brown oil. IR (neat) ν_{max}: 3026, 2935, 1706, 1667, 1602, 1503, 1456, 1255, 1143 cm^{-1}. ^1H NMR (400 MHz, $CDCl_3$): δ = 2.83-2.94 (m, 2H), 3.45- 3.49 (m, 2H), 3.61-3.65 (m, 1H), 3.77 (s, 3H), 3.82 (s, 3H), 3.84 (s, 3H), 4.29 (bs, 1H), 6.60 (s, 1H), 6.65-6.71 (m, 4H), 7.07 (s, 2H), 7.12-7.15 (m, 1H), 7.22 (m, 3H), 7.27-7.29 (m, 2H) ppm. ^{13}C NMR (100 MHz, $CDCl_3$): δ = 33.7 (CH_2), 41.9 (CH_2), 49.5 (CH_2), 55.8 ($2XCH_3$), 55.9 (CH_3), 110.0 (CH), 111.2 (CH), 112.2 (CH), 117.7 (2XCH), 118.6 (CH), 120.1 (Cq), 120.9 (CH), 126.8 (CH), 128.5 (2XCH), 128.9 (2XCH), 131.2 (Cq), 134.9 (Cq), 141.6 (Cq), 147.5 (Cq), 147.6 (Cq), 149.0 (Cq), 156.4 (Cq), 158.9 (Cq), 170.9 (Cq) ppm. HRMS (m/z): $C_{28}H_{27}NO_6H$ $[M+H]^+$: 474.1917; found 474.1927.

1.5.16: *N*-(3,4-dimethoxyphenethyl)-*N*-(8-ethoxy-2-oxo-2*H*-chromen-3-yl)-2-(4-methoxyphenyl)acetamide (7e):

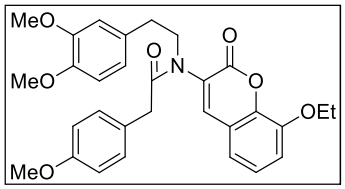

Following the similar procedure mentioned in the 1.5.12 with 3-ethoxy-2-hydroxybenzaldehyde and compound **6b** gave the product **7e** in 33% yield.

Light brown oil. IR (neat) ν_{max}: 3028, 2932, 1705, 1667, 1601, 1507, 1460, 1251, 1148 cm^{-1}. ^1H NMR (400 MHz, $CDCl_3$): δ = 1.46 (t, *J* = 7.2 Hz, 3H), 2.73-2.88 (m, 2H), 3.30-3.44 (m, 2H), 3.46-3.52 (m, 1H), 3.70 (s, 6H), 3.75 (s, 3H), 4.11-4.19 (m, 1H), 6.57-6.64 (m, 3H), 6.69-6.71 (broad doublet, 3H), 6.90-6.93 (m, 2H), 7.02-7.05 (m, 1H), 7.12-7.16 (m, 1H) ppm. ^{13}C NMR (100 MHz, $CDCl_3$): δ = 14.7 (CH_3), 33.7 (CH_2), 40.8 (CH_2), 49.5 (CH_2), 55.2 (CH_3), 55.8 (CH_3), 55.8 (CH_3), 65.0 (CH_2), 111.1 (CH), 112.1 (CH), 113.9 (2XCH), 115.2 (CH), 119.3 (CH), 120.9 (CH), 124.9 (CH), 127.0 (Cq), 128.7 (Cq), 129.9 (2XCH), 131.1 (Cq), 141.9 (Cq), 142.9 (CH), 146.5 (Cq), 147.5 (Cq), 148.9 (Cq), 158.4 (Cq), 171.2 (Cq) ppm. LCMS (m/z): $C_{30}H_{31}NO_7H$ $[M+H]^+$: 518.5; found 518.3.

1.5.17: *N*-(6,7-dimethoxy-2-oxo-2*H*-chromen-3-yl)-*N*-(3,4-dimethoxyphenethyl)-2-phenylacetamide (7f):

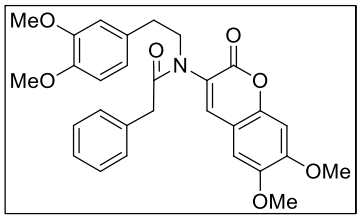

Following the similar procedure mentioned in the 1.5.12 with 2-hydroxy-4,5-dimethoxybenzaldehyde and compound **6c** gave the product **7f** in 54% yield.

Light brown oil. IR (neat) ν_{max}: 3029, 2933, 1710, 1667, 1557, 1502, 1458, 1249, 1140, 1145 cm^{-1}. ^1H NMR (400 MHz, $CDCl_3$): δ = 2.72-2.78 (m, 1H), 2.84-2.92 (m, 1H), 3.20-3.42 (m, 2H), 3.53-3.57 (m, 1H), 3.70 (s, 3H), 3.76 (s, 3H), 3.84 (s, 3H), 3.90 (s, 3H), 4.18-

4.25 (m, 1H), 6.46 (s, 1H), 6.54 (s, 1H), 6.59-6.66 (m, 3H), 6.78 (s, 1H), 6.98-7.00 (m, 2H), 7.15 (s, 3H) ppm. ^{13}C NMR (100 MHz, $CDCl_3$): δ = 33.7 (CH_2), 41.8 (CH_2), 49.5 (CH_2), 55.8 (CH_3), 55.9 (CH_3), 56.3 (CH_3), 56.5 (CH_3), 99.7 (CH), 107.9 (CH), 110.6 (Cq), 11.2 (CH), 112.3 (CH), 120.9 (CH), 125.7 (Cq), 126.7 (CH), 128.5 (2XCH), 128.9 (2XCH), 131.3 (Cq), 135.0 (Cq), 142.1 (CH), 146.8 (Cq), 147.6 (Cq), 149.0 (Cq), 149.3 (Cq), 153.4 (Cq), 159.2 (Cq), 171.1 (Cq). LCMS (m/z): $C_{29}H_{29}NO_7H$ $[M+H]^+$: 504.5; found 504.8.

1.5.18: 11,12-dimethoxy-14-phenyl-8,9-dihydro-6*H*-chromeno[4',3':4,5]pyrrolo[2,1-*a*]isoquinolin-6-one (1b):

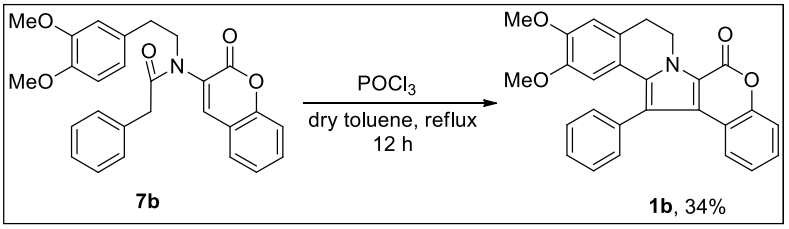

A solution of 1 mmol amide-coumarin **7b**, 3 mL freshly distilled $POCl_3$, and 10 mL toluene were refluxed at 120 °C for 12 h. The reaction mixture was cautiously poured over ice, basified with Na_2CO_3, and extracted in CH_2Cl_2 (3 X 30 mL). The crude product was purified by flash column chromatography (CH_2Cl_2: MeOH) to afford the pure product **1b**. Brown solid, m.p. 239-241 °C. IR (KBr) ν_{max}: 3019, 1701, 1523, 1480, 1321, 1214 cm^{-1}. ^{1}H NMR (400 MHz, $CDCl_3$): δ = 3.041 (t, *J* = 6.8 Hz , 2H), 3.206 (s, 3H), 3.816 (s, 3H), 4.745 (t, *J* = 7.2 Hz, 2H), 6.418 (s, 1H), 6.684 (s, 1H), 6.880 (m, 1H), 7.083 (m, 1H), 7.298 (m, 1H), 7.431 (m, 5H) ppm. ^{13}C NMR (100 MHz, $CDCl_3$): δ = 28.7 (CH_2), 42.5 (CH_2), 55.0 (CH_3), 55.9 (CH_3), 108.7 (CH), 110.9 (CH), 114.6 (Cq), 116.0 (Cq), 117.1 (CH), 118.3 (Cq), 119.9 (CH), 123.3 (2XCH), 123.7 (Cq), 126.6 (CH), 127.2 (Cq), 128.1 (2XCH), 129.4 (2XCH), 131.1 (Cq), 135.72 (Cq), 136.0 (Cq), 147.4 (Cq), 148.9 (Cq), 151.2 (Cq), 155.3 (Cq) ppm. HRMS (m/z): calculated for $C_{27}H_{21}NO_4H$ $[M+H]^+$: 424.1549; found 424.1558.

1.5.19: 3-isopropoxy-11,12-dimethoxy-14-(4-methoxyphenyl)-8,9-dihydro-6*H*-chromeno[4',3':4,5]pyrrolo[2,1-*a*]isoquinolin-6-one (1c):

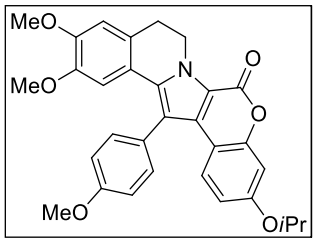

Following the similar procedure mentioned in the 1.5.18, compound **7c** gave the product **1c** in 43% yield.

Yellow solid, m.p. 242-246 °C. IR (KBr) ν_{max}: 3019, 1707, 1531, 1478, 1338, 1244 cm^{-1}. ^1H NMR (400 MHz, $CDCl_3$): δ = 1.25 (s, 3H), 1.27 (s, 3H), 3.04 (t, *J* = 6.8 Hz, 2H), 3.27 (s, 3H), 3.82 (s, 3H), 3.84 (s, 3H), 4.41-4.50 (septet, 1H), 4.72 (d, *J* = 6.8 Hz, 2H), 6.48-6.50 (m, 2H), 6.68 (s, 1H), 6.81 (s, 1H), 7.00 (m, 3H), 7.34 (d, *J* = 8.8 Hz, 2H) ppm. ^{13}C NMR (100 MHz, $CDCl_3$): δ = 21.9 (CH_3), 28.7 (CH_2), 42.3 (CH_2), 55.1 (CH_3), 55.4 (CH_3), 55.9 (CH_3), 70.2 (CH), 103.3 (CH), 108.6 (CH), 110.9 (CH), 111.3 (Cq), 112.8 (CH), 113.3 (Cq), 114.8 (2XCH), 114.9 (Cq), 120.1 (Cq), 123.9 (CH), 126.6 (Cq), 127.6 (Cq), 128.2 (Cq), 132.2 (2XCH), 136.2 (Cq), 147.3 (Cq), 148.3 (Cq), 152.5 (Cq), 155.5 (Cq), 157.4 (Cq), 159.4 (Cq) ppm. HRMS (m/z): calculated for $C_{31}H_{30}NO_6$ $[M+H]^+$: 512.2073; found 512.2077.

1.5.20: 2,11,12-trimethoxy-14-(4-methoxyphenyl)-8,9-dihydro-6*H*-chromeno[4',3':4,5]pyrrolo[2,1-*a*]isoquinolin-6-one (1d):

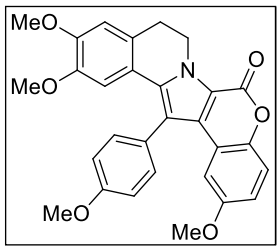

Following the similar procedure mentioned in the 1.5.18, compound **7d** gave the product **1d** in 31% yield.

Brown solid, m.p. 229-232 °C. IR (KBr) υ_{max}: 3015, 1712, 1515, 1469, 1329, 1215 cm^{-1}.

^{1}H NMR (400 MHz, $CDCl_3$): δ = 3.04 (t, *J* = 6.4 Hz, 2H), 3.21 (s, 3H), 3.35 (s, 3H), 3.82 (s, 3H), 4.75 (t, *J* = 7.2 Hz, 2H), 6.49 (s, 1H), 6.54 (d, 1H), 6.69 (s, 1H), 6.75 (m, 1H), 7.20 (s, 1H), 7.42 (s, 1H), 7.45 (m, 3H), 7.49 (m, 1H) ppm. ^{13}C NMR (100 MHz, $CDCl_3$): δ = 28.68 (CH_2), 41.4 (CH_2), 53.9 (CH_3), 54.9 (CH_3), 104.7 (CH), 107.6 (2XCH), 109.9 (Cq), 113.7 (CH), 114.1 (Cq), 114.9 (2XCq), 116.9 (2XCH), 117.5 (CH), 118.9 (CH), 125.5 (Cq), 127.1 (2XCH), 128.3 (2XCq), 130.2 (Cq), 134.7 (Cq), 144.6 (Cq), 146.4 (Cq), 147.9 (Cq), 154.4 (Cq) ppm. HRMS (m/z): calculated for $C_{28}H_{23}NO_5H$ $[M+H]^+$: 454.1654; found 454.1669.

1.6 References:

1) Anderson, R. J.; Faulkner, D. J.; He, C. H.; Van, Duyne, G. D.; Clardy, J. *J. Am. Chem. Soc.* **1985,** *107*, 5492.

2) (a) Lindquist, N.; Fenical, W. *J. Org. Chem*. **1988**, *53*, 4570. (b) Carroll, A. R.; Bowden, B. F.; Coll, J. C. *Aust. J. Chem*. **1993**, *46*, 489. (c) Urban, S.; Butler, M. S.; Capon, R. J. *Aust. J. Chem*. **1994**, *47*, 1919. (d) Urban, S.; Hobbs, L.; Hooper, J. N. A.; Capon, R. J. *Aust. J. Chem*. **1995**, *48*, 1491. (e) Urban, S.; Capon, R. J. *Aust. J. Chem*. **1996**, *49*, 711.

3) (a) Bailly, C. *Anti-Cancer Agents Med. Chem*. **2004**, *4*, 363. (b) Fan, H.; Peng, J.; Hamann, M. T.; Hu, J.-F. *Chem. Rev*. **2008**, *108*, 264. (c) Pla, D.; Albericio, F.; Alvarez, M. *Med. Chem. Comm.* **2011**, *2*, 689. (d) Handy, S. T.; Zhang, Y. *Org. Prep. Proced. Int*. **2005**, *37*, 411. (e) Pla, D.; Albericio, F.; Alvarez, M. *Anti-Cancer Agents Med. Chem*. **2008**, *8*, 746.

4) Lindquist, N.; Fenical, W.; Van Duyne, G. D.; Clardy, J. *J. Org. Chem.* **1998**, *53*, 4570.

5) Bailly, C. *Phytochem Rev* **2014**, *13*, 171.

6) Ballot, C.; Kluza, J.; Martoriati, A.; Nyman, U.; Formstecher, P.; Joseph, B.; Bailly, C.; Marchetti, P. *Mol. Cancer Ther*. **2009**, *8*, 3307.

7) Urban, S.; Capon, R. J. *Aust. J.Chem.* **1996**, *49*, 711.

8) Davis, R. A.; Carroll, A. R.; Pierens, G. K.; Quinn, R. J. *J. Nat. Prod.* **1999**, *62*, 419.

9) Ballot, C.; Kluza, J.; Lancel, S.; Martoriati, A.; Hassoun, S. M.; Mortier, L.; Vienne, J. C.; Briand, G.; Formstecher, P.; Bailly, C.; Neviere, R.; Marchetti, P. *Apoptosis* **2010**, *15*, 769.

10) Baunbaek, D.; Trinkler, N.; Ferandin, Y.; Lozach, O.; Ploypradith, P.; Rucirawat, S.; Ishibashi, F.; Iwao, M.; Meijer, L. *Mar. Drugs* **2008**, *6*, 514.

11) Krishnaiah, P.; Reddy, V. L. N.; Venkataramana, G.; Ravinder, K.; Srinivasulu, M.; Raju, T. V.; Ravikumar, K.; Chandrasekar, D.; Ramakrishna, S.; Venkateswarlu, Y. *J. Nat. Prod.* **2004**, *67*, 1168.

12) Reddy, S. M.; Srinivasulu, M.; Satyanarayana, N.; Kondapi, A. K.; Venkateswarlu, Y. *Tetrahedron* **2005**, *61*, 9242.

13) Urban, S.; Capon, R. J. *Aust. J. Chem.* **1996**, *49*, 711.

14) Reddy, M. V. R.; Faulkner, D. J.; Venkateswarlu, Y.; Rao, M. R. *Tetrahedron* **1997**, *53*, 3457.

15) Cantrell, C. L.; Groweiss, A.; Gustafson, K. R.; Boyd, M. R. *Nat. Prod. Lett.* **1999**, *14*, 39.

16) Plisson, F.; Huang, X.-C.; Zhang, H.; Khalil, Z.; Capon, R. J. *Chem. Asian J.* **2012**, *7*, 1616.

17) Yoshida, W. Y.; Lee, K. K.; Carroll, A. R.; Scheuer, P. J. *HelV. Chim. Acta* **1992**, *75*, 1721.

18) Rudi, A.; Goldberg, I.; Stein, Z.; Frolow, F.; Benayahu, Y.; Schleyer, M.; Kashman, Y. *J. Org. Chem.* **1994**, *59*, 999.

19) Rudi, A.; Evan, T.; Aknin, M.; Kashman, Y. *J. Nat. Prod*. **2000**, *63*, 832.

20) Palermo, J. A.; Brasco, M. F. R.; Seldes, A. M. *Tetrahedron* **1996**, *52*, 2727.

21) Vervoort, H. C.; Richards-Gross, S. E.; Fenical, W.; Lee, A. Y.; Clardy, J. *J. Org. Chem.* **1997**, *62*, 1486.

22) Berlinck, R. G. S.; Britton, R.; Piers, E.; Lim, L.; Roberge, M.; Da Rocha, R. M.; Andersen, R. J. *J. Org. Chem.* **1998**, *63*, 9850.

23) Vervoort, H. C.; Fenical, W.; Keifer, P. A. *J. Nat. Prod.* **1999**, *62*, 389.

24) Kang, H.; Fenical, W. *J. Org. Chem.* **1997**, *62*, 3254.

25) Chan, G. W.; Francis, T.; Thureen, D. R.; Offen, P. H.; Pierce, N. J.; Westley, J. W.; Johnson, R. K.; Faulkner, D. J. *J. Org. Chem.* **1993**, *58*, 2544.

26) Urban, S.; Hickford, S. J. H.; Blunt, J. W.; Munro, M. H. G. *Curr. Org. Chem.* **2000**, *4*, 765.

27) Bowden, B. F. Stud. *Nat. Prod. Chem.* **2000**, *23*, 233.

28) Bailly, C. *Anti-Cancer Agents Med. Chem.* **2004**, *4*, 363.

29) Peschko, C.; Winklhofer, C.; Terpin, A.; Steglich, W. *Synthesis* **2006**, 3048.

30) Ramírez-Rodríguez, A.; Méndez, J. M.; Jiménez, C. C.; León, F.; Vazquez, A. *Synthesis* **2012**, *44*, 3321.

31) Imbri, D.; Tauber, J.; Opatz, T. *Chem. - A Eur. J.* **2013**, *19*, 15080.

32) Ueda, K.; Amaike, K.; Maceiczyk, R. M.; Itami, K.; Yamaguchi, J. *J. Am. Chem. Soc.* **2014**, *136*, 13226.

33) Komatsubara, M.; Umeki, T.; Fukuda, T.; Iwao, M. *J. Org. Chem.* **2014**, *79*, 529.

34) Dialer, C.; Imbri, D.; Hansen, S. P.; Opatz, T. *J. Org. Chem.* **2015**, *80*, 11605.

35) Manjappa, K. B.; Syu, J. R.; Yang, D. Y. *Org.Lett*. **2016**, 332.

36) Zheng, K. L.; You, M. Q.; Shu, W. M.; Wu, Y. D.; Wu, A. X. *Org. Lett.* **2017**, *19*, 2262.

37) Manjappa, K. B.; Lin, J. M.; Yang, D. Y. *J. Org. Chem.* **2017**, *82*, 7648.

38) Lade, D. M.; Pawar, A. B.; Mainkar, P. S.; Chandrasekhar, S. *J. Org. Chem.* **2017**, *82*, 4998.

39) Mei, R.; Zhang, S. K.; Ackermann, L. *Synlett* **2017**, *28*, 1715.

40) Colligs, V. C.; Dialer, C.; Opatz, T. *Eur. J. Org. Chem.* **2018**, *2018*, 4064.

41) Klintworth, R.; De Koning, C. B.; Opatz, T.; Michael, J. P. *J. Org. Chem.* **2019**, *84*, 11025.

42) Shirley, H. J.; Koyioni, M.; Muncan, F.; Donohoe, T. J. *Chem. Sci.* **2019**, *10*, 4334.

43) Kumar, V.; Awasthi, A.; Salam, A.; Khan, T. *J. Org. Chem.* **2019**, *84*, 11596.

44) Hwu, J. R.; Roy, A.; Panja, A.; Huang, W.-C.; Hu, Y.-C.; Tan, K.-T.; Lin, C.-C.; Hwang, K.-C.; Hsu, M.-H.; Tsay, S.-C. *J. Org. Chem.* **2020**, *85*, 9835.

45) Luo, K.; Mao, S.; He, K.; Yu, X.; Pan, J.; Lin, J.; Shao, Z.; Jin, Y. *ACS Catal.* **2020**, *10*, 3733.

46) Silyanova, E. A.; Samet, A. V.; Salamandra, L. K.; Khrustalev, V. N.; Semenov, V. V. *Eur. J. Org. Chem.* **2020**, *2020*, 2093.

47) Klintworth, R.; de Koning, C. B.; Michael, J. P. *Eur. J. Org. Chem.* **2020**, *2020*, 3860.

48) Watanabe, T.; Mutoh, Y.; Saito, S. *Org. Biomol. Chem.* **2019**, *18*, 81.

49) D. L. Boger, D. R. Soenen, C. W. Boyce, M. P. Hendrick, Q. Jin, *J. Org. Chem.* **2000**, *65*, 2479.

50) Iwao, M.; Takeuchi, T.; Fujikawa, N.; Fukuda, T.; Ishibashi, F. *Tetrahedron Lett.* **2003**, *44*, 4443.

51) Morikawa, D.; Morii, K.; Yasuda, Y.; Mori, A.; Okano, K. *J. Org. Chem.* **2020**, *85*, 8603.

52) Ploypradith, P.; Kagan, R. K.; Ruchirawat, S. *J. Org. Chem.* **2005**, *70*, 5119.

53) (a) Nyerges, M.; Toke, L. *Tetrahedron Lett.* **2005**, *46*, 7531. (b) Ploypradith, P.; Jinaglueng, W.; Pavaro, C.; Ruchirawat, S. *Tetrahedron Lett.* **2003**, *44*, 1363. (c) Ruchirawat S.; Mutarapat, T. *Tetrahedron Lett.* **2001**, *42*, 1205.

NMR Spectra

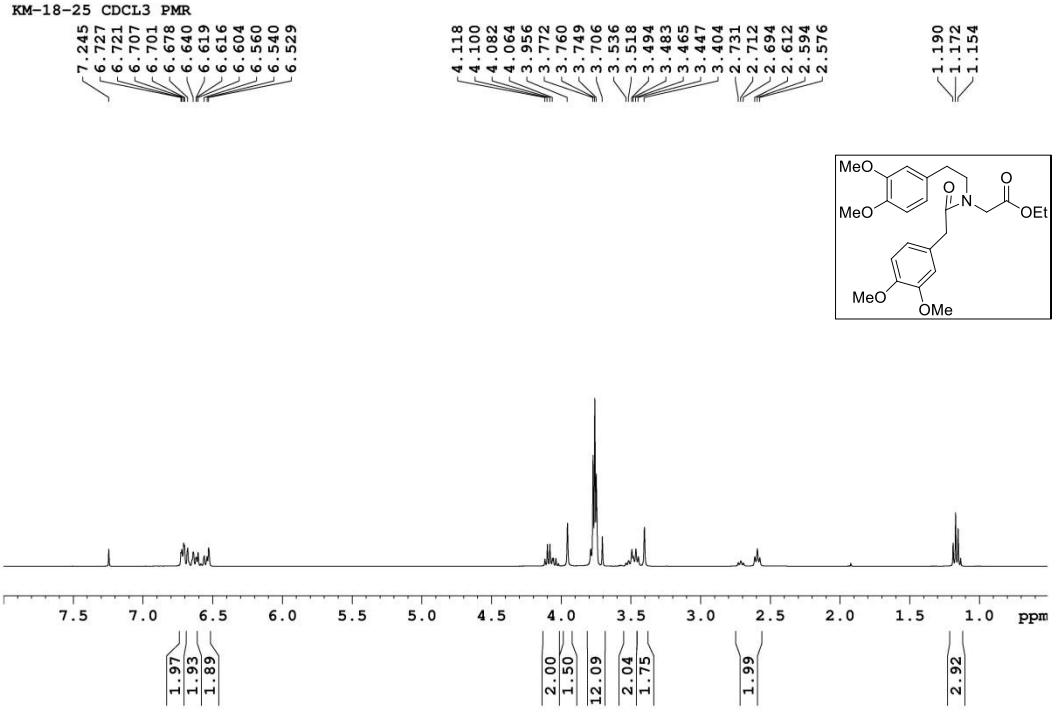
KM-18-25 CDCL3 PMR
7.245
6.727
6.721
6.707
6.701
6.678
6.640
6.619
6.616
6.604
6.560
6.540
6.529
4.118
4.100
4.082
4.064
3.956
3.772
3.760
3.749
3.706
3.536
3.518
3.494
3.483
3.465
3.447
3.404
2.731
2.712
2.694
2.612
2.594
2.576
1.190
1.172
1.154
MeO
MeO
O
N
O
OEt
MeO
OMe
7.5
7.0
6.5
6.0
5.5
5.0
4.5
4.0
3.5
3.0
2.5
2.0
1.5
1.0
ppm
1.97
1.93
1.89
2.00
1.50
12.09
2.04
1.75
1.99
2.92

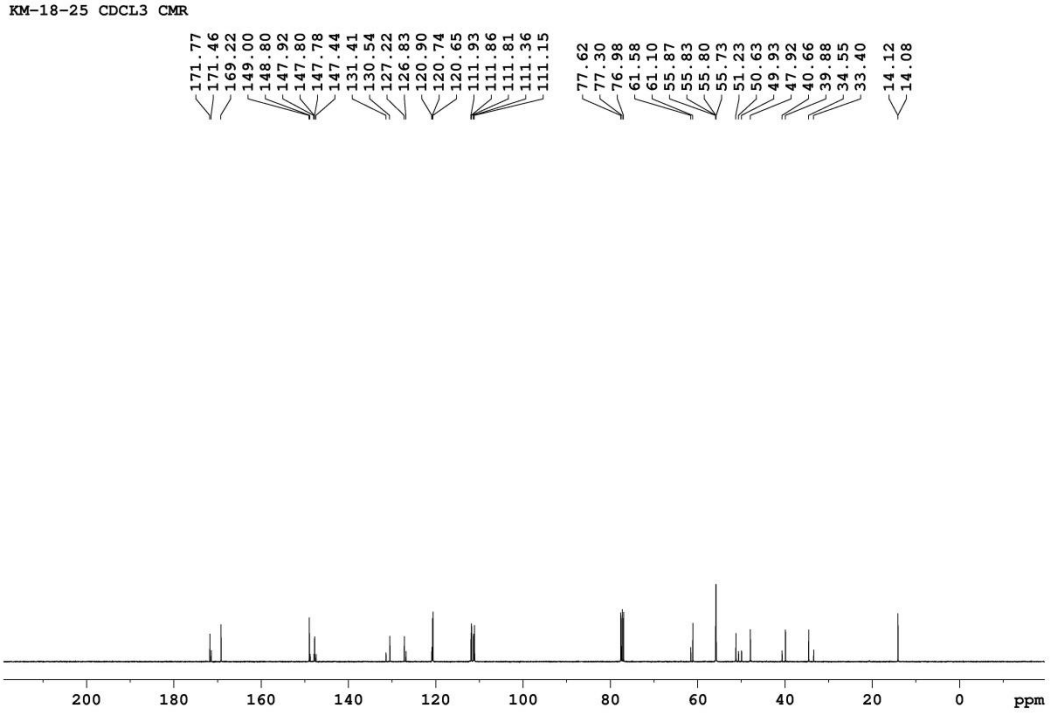
KM-18-25 CDCL3 CMR
171.77
171.46
169.22
149.00
148.80
147.92
147.80
147.78
147.44
131.41
130.54
127.22
126.83
120.90
120.74
120.65
111.93
111.86
111.81
111.36
111.15
77.62
77.30
76.98
61.58
61.10
55.87
55.83
55.80
55.73
51.23
50.63
49.93
47.92
40.66
39.88
34.55
33.40
14.12
14.08
200
180
160
140
120
100
80
60
40
20
0
ppm

KM-18-25 CDCL3 DEPT

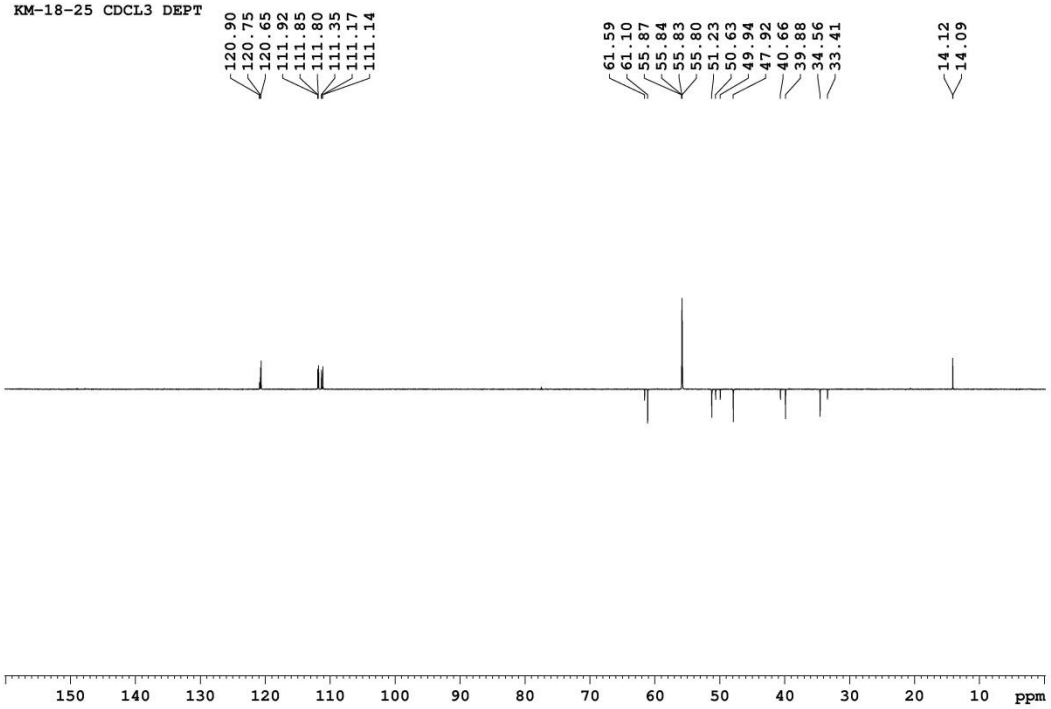

KM-18-27 CDCL3 PMR

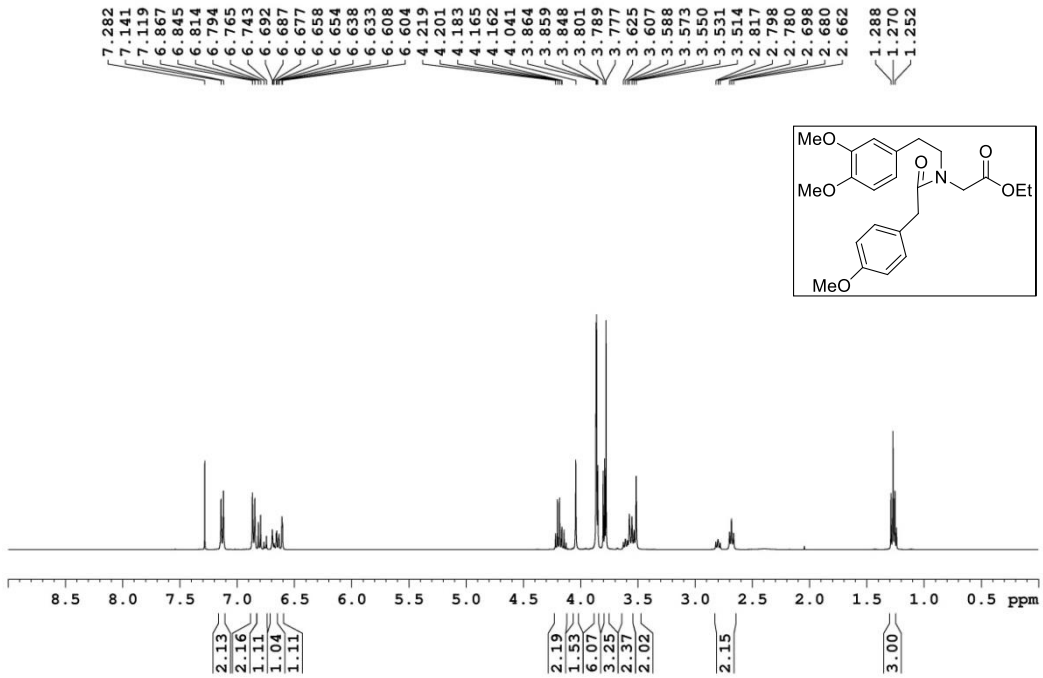

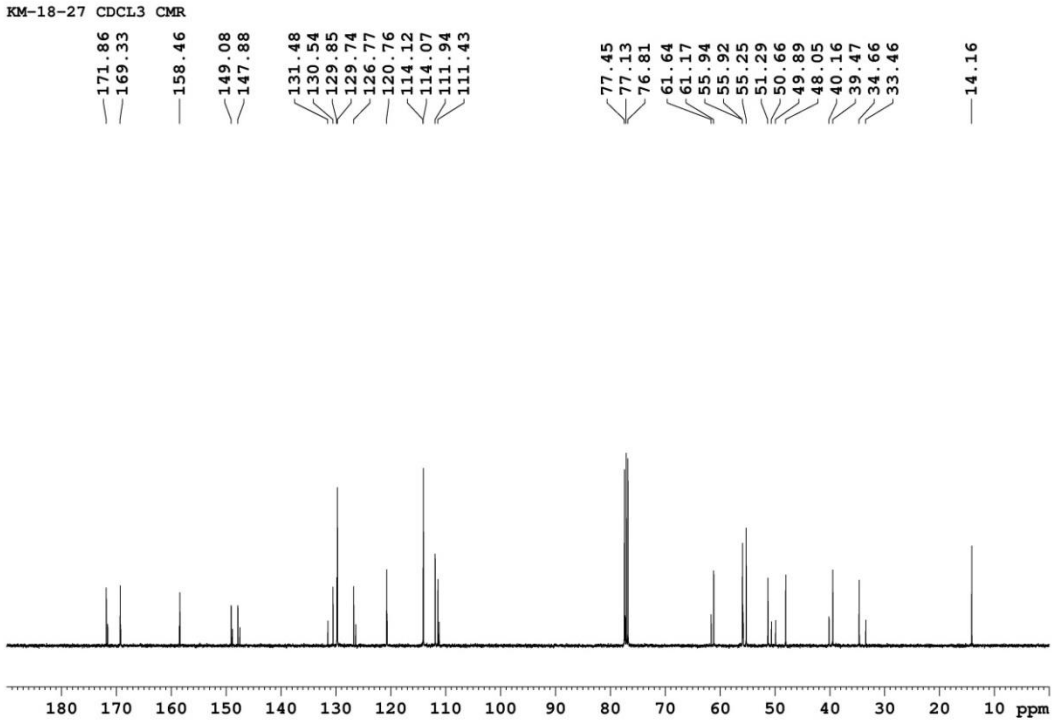
KM-18-27 CDCL3 CMR
171.86
169.33
158.46
149.08
147.88
131.48
130.54
129.85
129.74
126.77
120.76
114.12
114.07
111.94
111.43
77.45
77.13
76.81
61.64
61.17
55.94
55.92
55.25
51.29
50.66
49.89
48.05
40.16
39.47
34.66
33.46
14.16
180 170 160 150 140 130 120 110 100 90 80 70 60 50 40 30 20 10 ppm

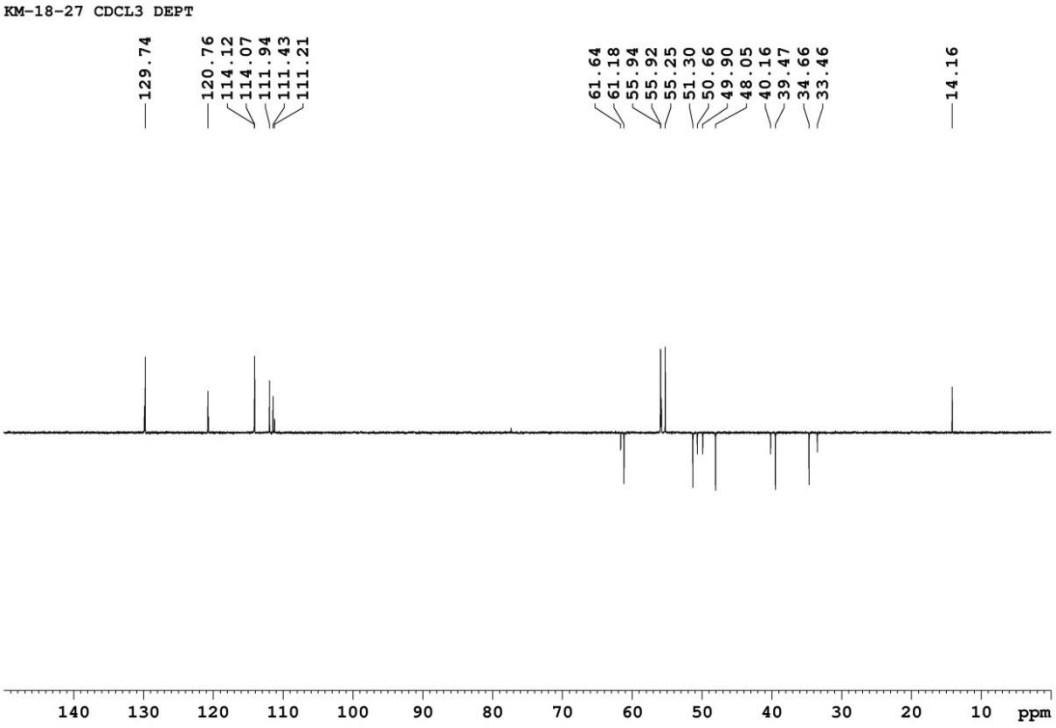
KM-18-27 CDCL3 DEPT
129.74
120.76
114.12
114.07
111.94
111.43
111.21
61.64
61.18
55.94
55.92
55.25
51.30
50.66
49.90
48.05
40.16
39.47
34.66
33.46
14.16
140 130 120 110 100 90 80 70 60 50 40 30 20 10 ppm

KM-17-01 CDCL3 PMR

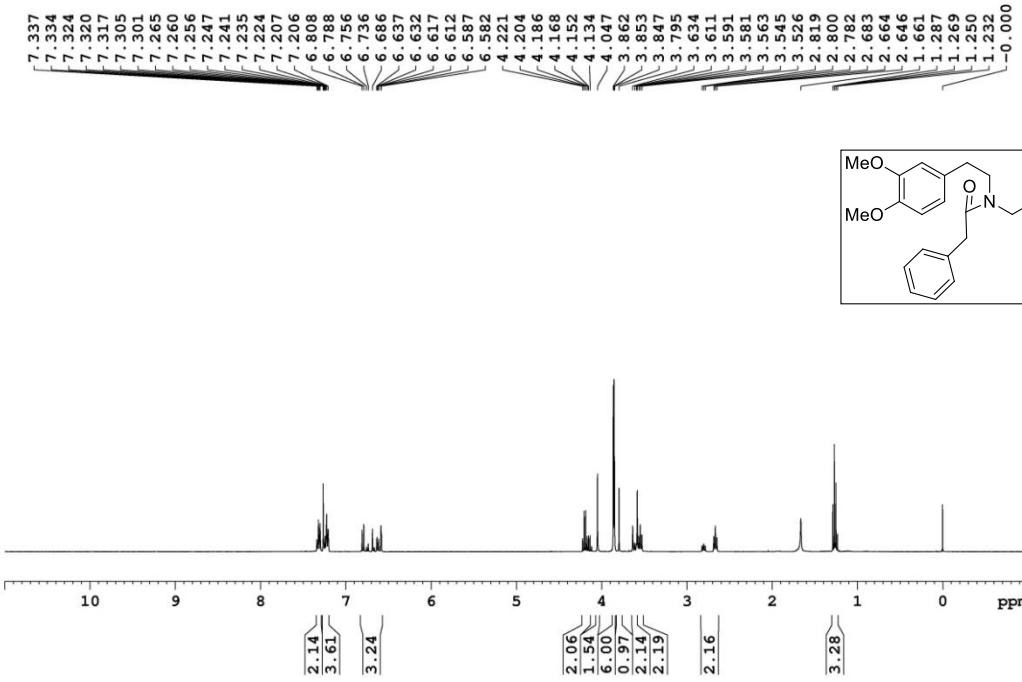

KM-17-01 CDCL3 CMR

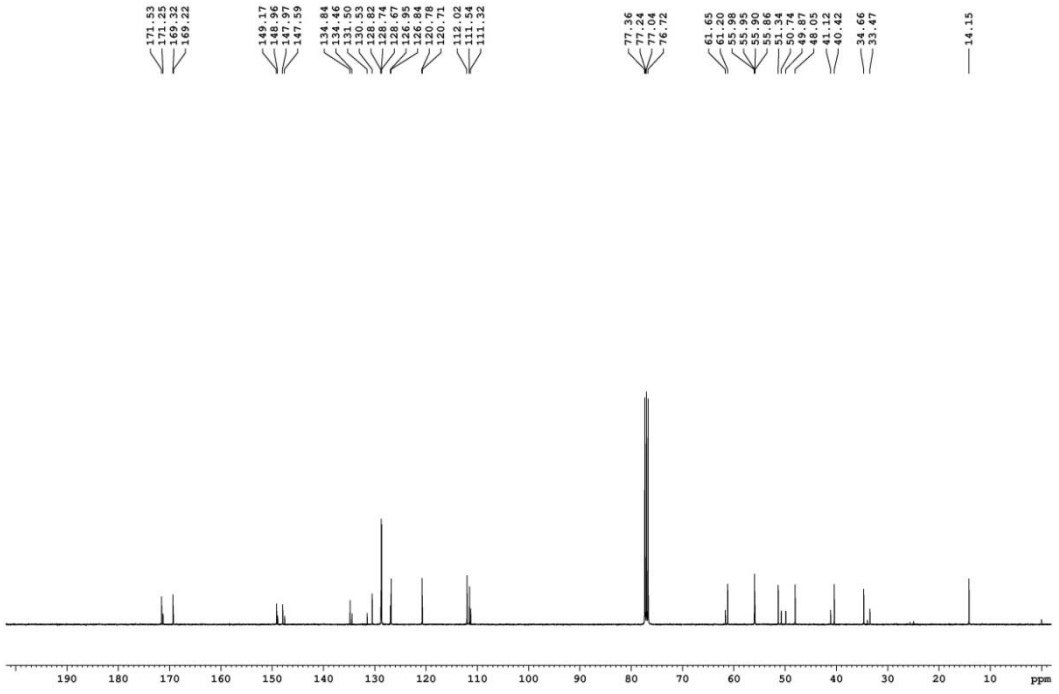

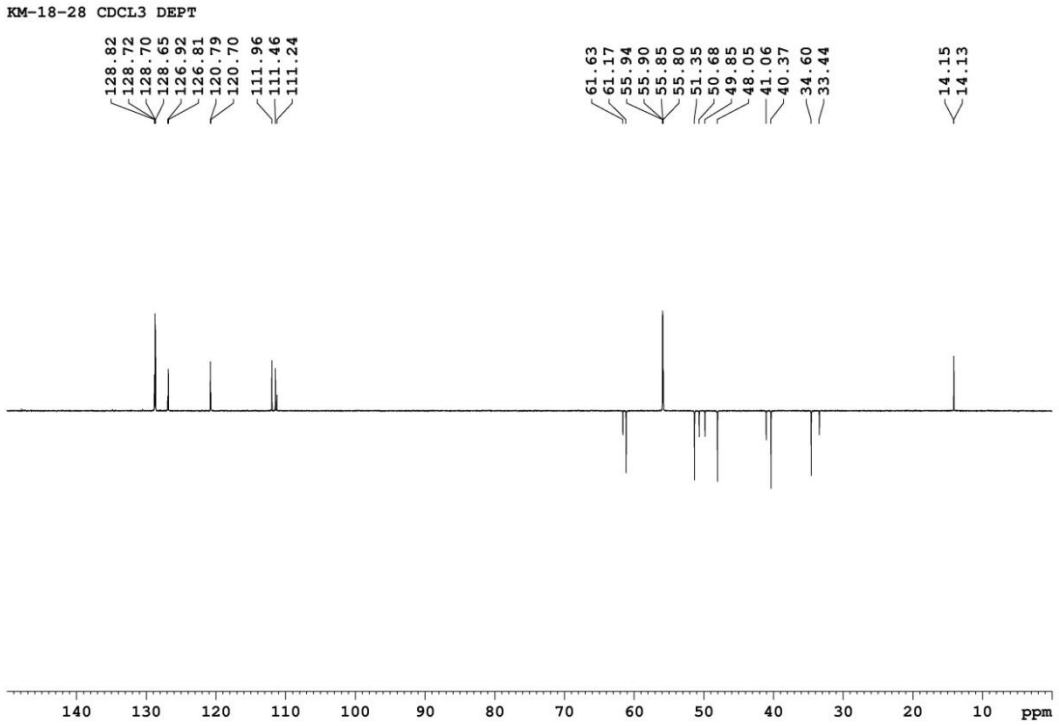
KM-18-28 CDCL3 DEPT
128.82
128.72
128.70
128.65
126.92
126.81
120.79
120.70
111.96
111.46
111.24
61.63
61.17
55.94
55.90
55.85
55.80
51.35
50.68
49.85
48.05
41.06
40.37
34.60
33.44
14.15
14.13
140
130
120
110
100
90
80
70
60
50
40
30
20
10
ppm

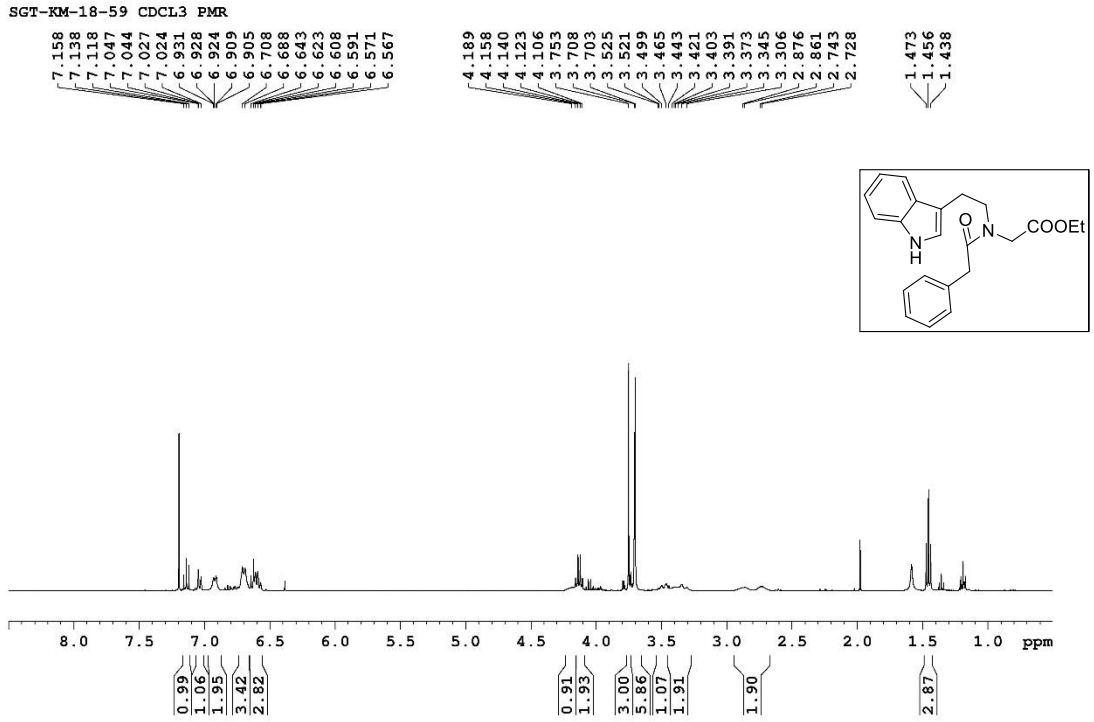
SGT-KM-18-59 CDCL3 PMR
7.158
7.138
7.118
7.047
7.044
7.027
7.024
6.931
6.928
6.924
6.909
6.905
6.708
6.688
6.643
6.623
6.608
6.591
6.571
6.567
4.189
4.158
4.140
4.123
4.106
3.753
3.708
3.703
3.525
3.521
3.499
3.465
3.443
3.421
3.403
3.391
3.373
3.345
3.306
2.876
2.861
2.743
2.728
1.473
1.456
1.438
N
H
O
N
COOEt
8.0
7.5
7.0
6.5
6.0
5.5
5.0
4.5
4.0
3.5
3.0
2.5
2.0
1.5
1.0
ppm
0.99
1.06
1.95
3.42
2.82
0.91
1.93
3.00
5.86
1.07
1.91
1.90
2.87

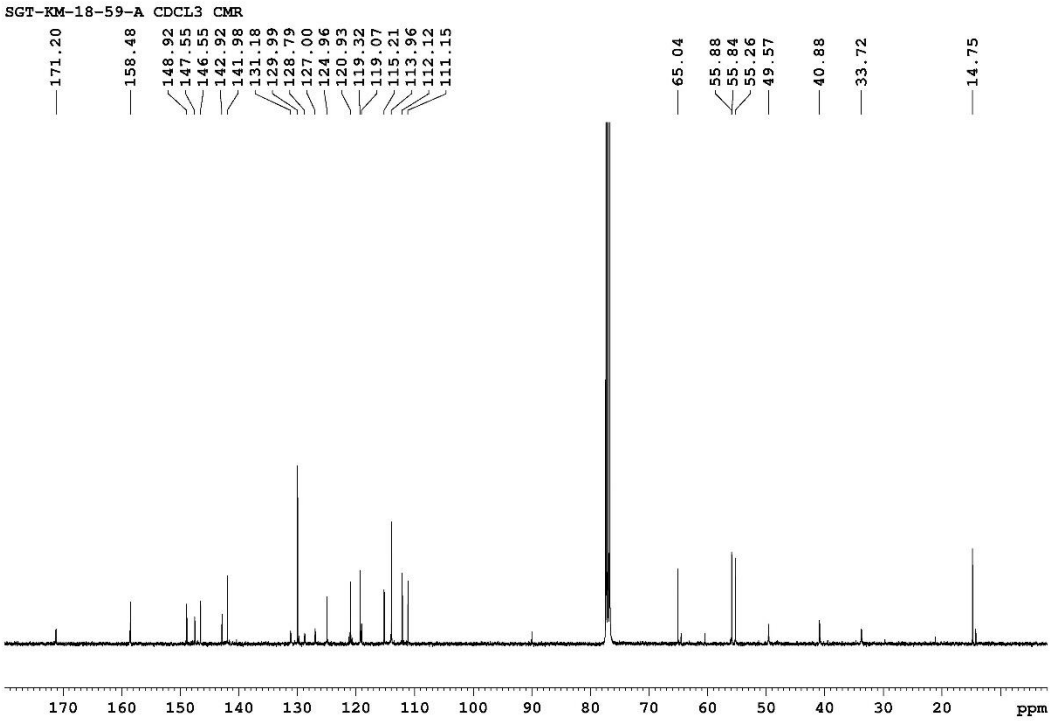
SGT-KM-18-59-A CDCL3 CMR
171.20
158.48
148.92
147.55
146.55
142.92
141.98
131.18
129.99
128.79
127.00
124.96
120.93
119.32
119.07
115.21
113.96
112.12
111.15
65.04
55.88
55.84
55.26
49.57
40.88
33.72
14.75
170 160 150 140 130 120 110 100 90 80 70 60 50 40 30 20 ppm

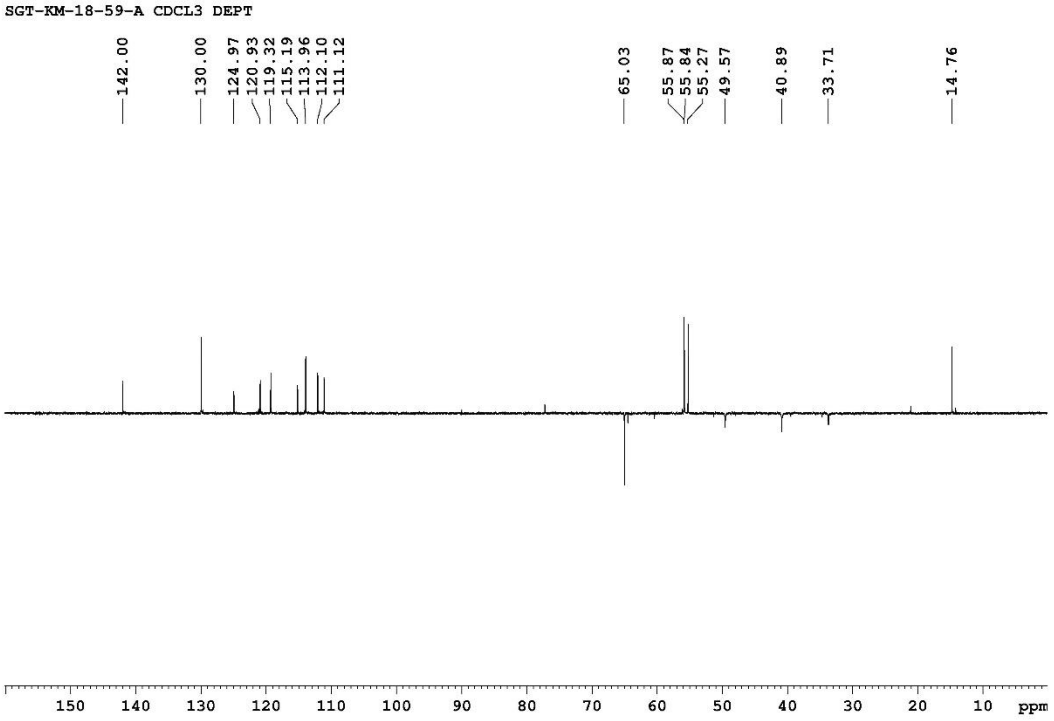
SGT-KM-18-59-A CDCL3 DEPT
142.00
130.00
124.97
120.93
119.32
115.19
113.96
112.10
111.12
65.03
55.87
55.84
55.27
49.57
40.89
33.71
14.76
150 140 130 120 110 100 90 80 70 60 50 40 30 20 10 ppm

HK-12-30 CDCL3 PMR

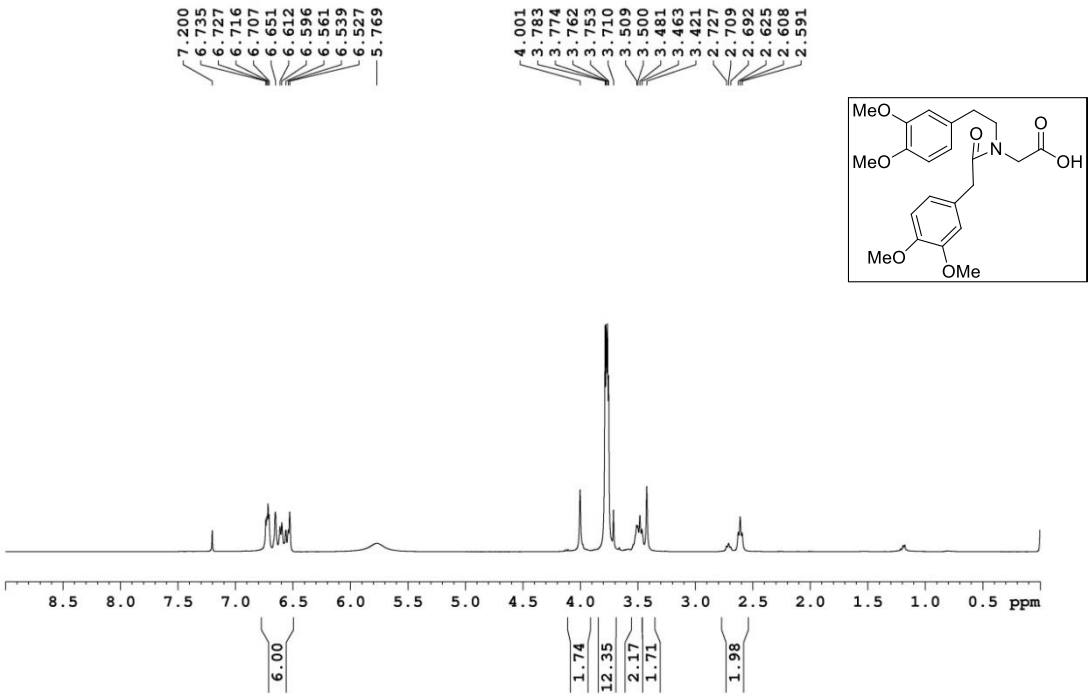

HK-12-30 CDCL3 CMR

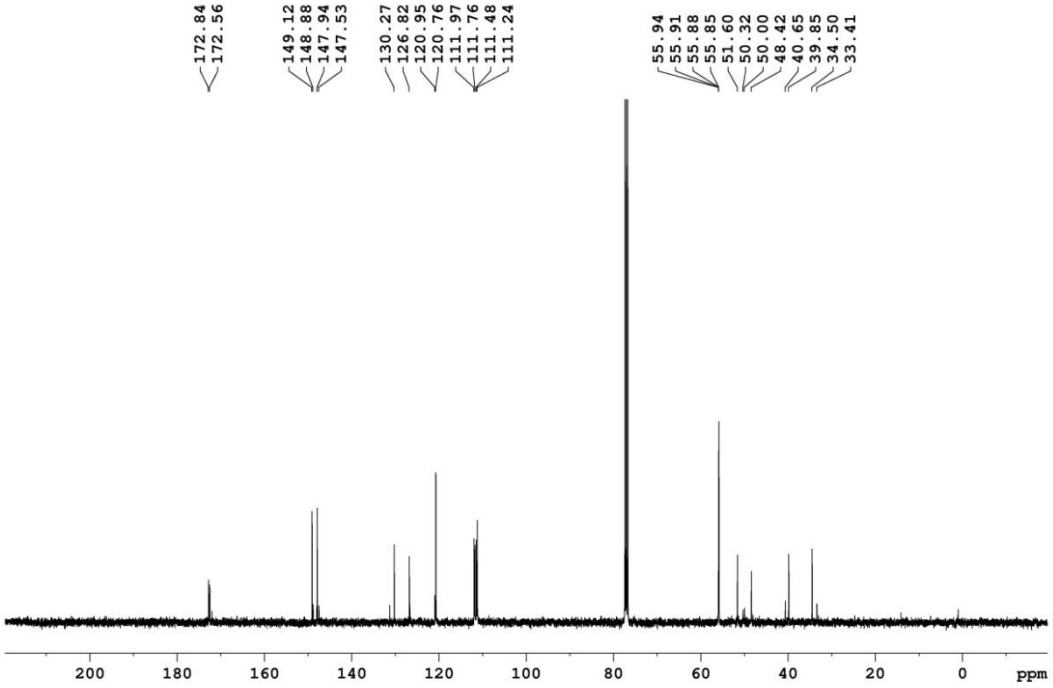

HK-12-30 CDCL3 DEPT

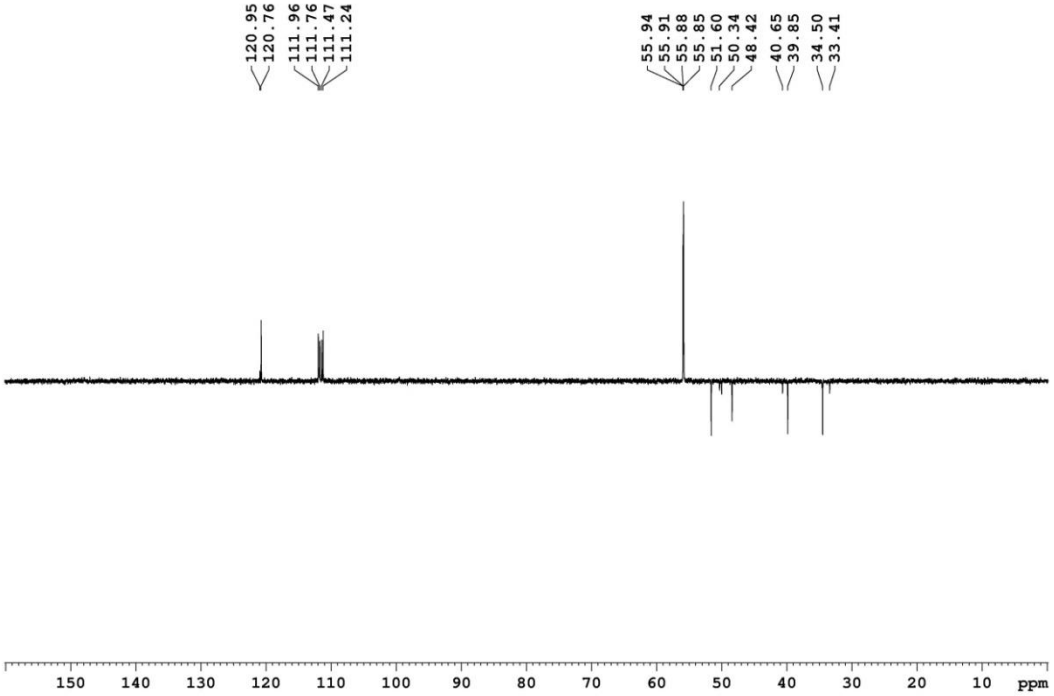

HK-LM-46 CDCL3 PMR

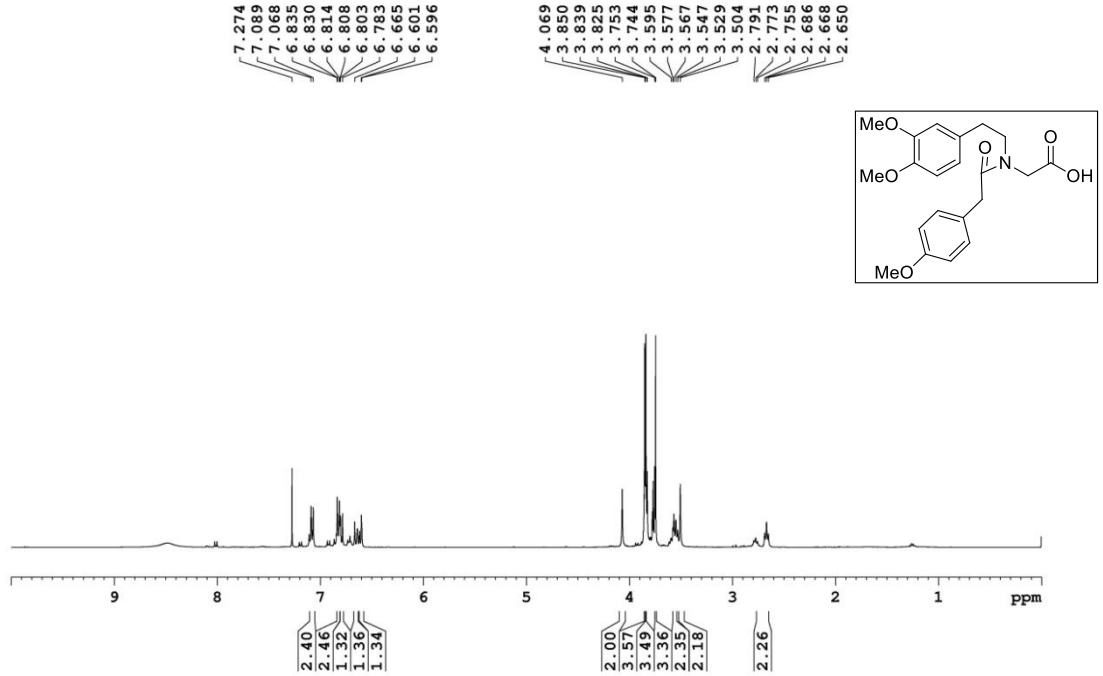

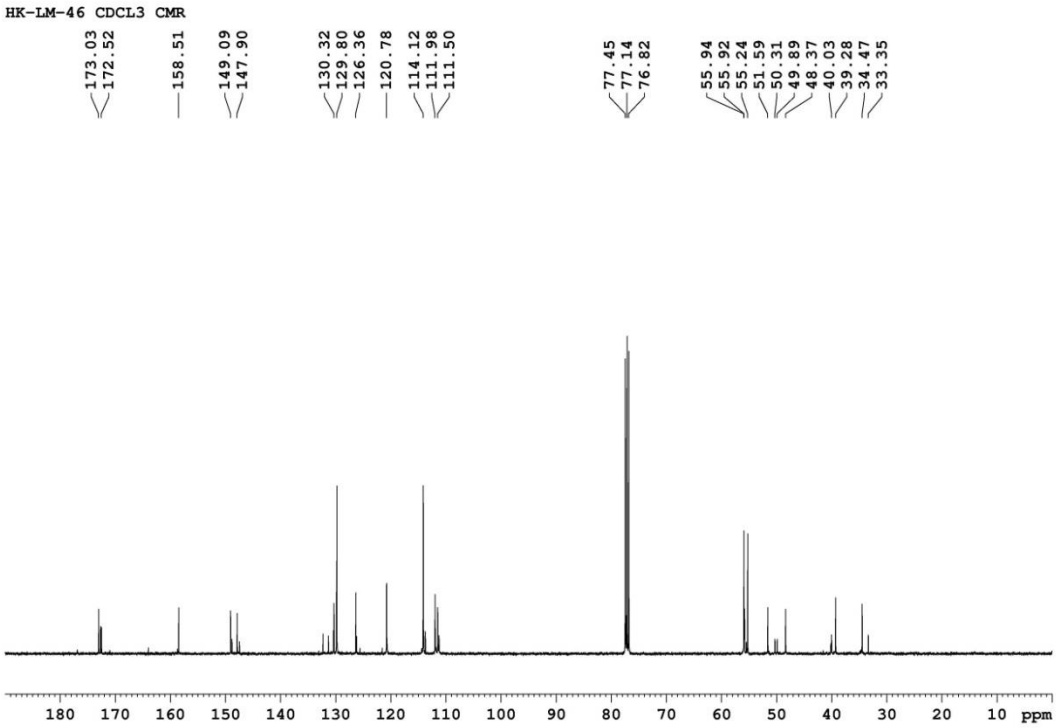
HK-LM-46 CDCL3 CMR
173.03
172.52
158.51
149.09
147.90
130.32
129.80
126.36
120.78
114.12
111.98
111.50
77.45
77.14
76.82
55.94
55.92
55.24
51.59
50.31
49.89
48.37
40.03
39.28
34.47
33.35
180 170 160 150 140 130 120 110 100 90 80 70 60 50 40 30 20 10 ppm

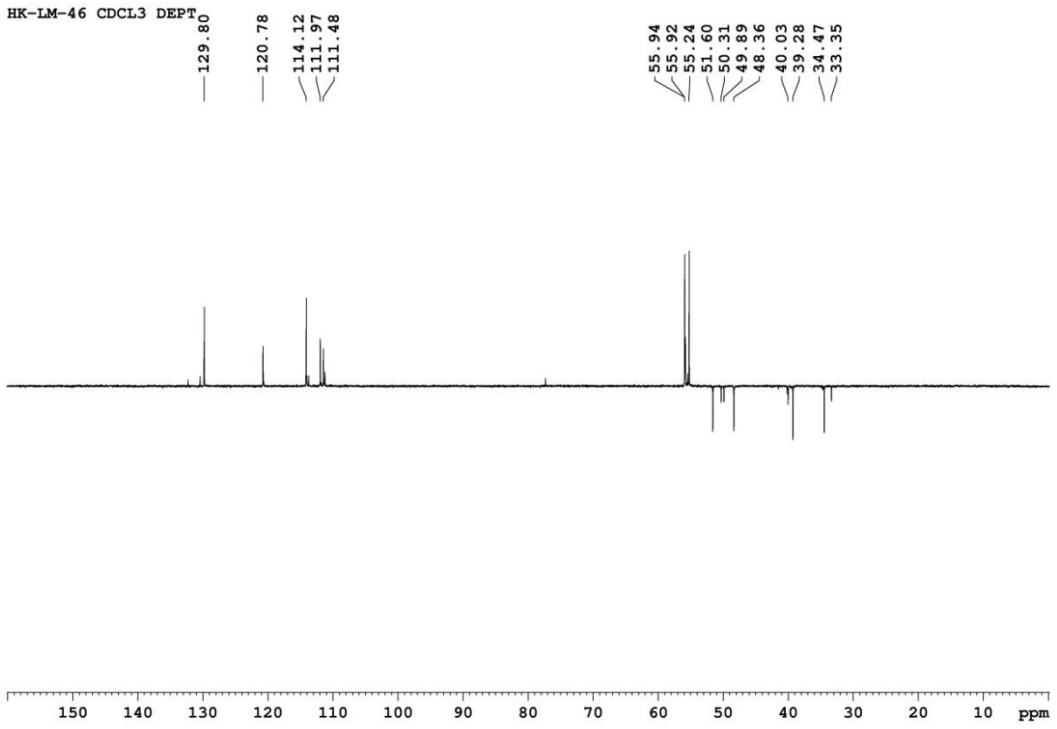
HK-LM-46 CDCL3 DEPT
129.80
120.78
114.12
111.97
111.48
55.94
55.92
55.24
51.60
50.31
49.89
48.36
40.03
39.28
34.47
33.35
150 140 130 120 110 100 90 80 70 60 50 40 30 20 10 ppm

KM-17-02 CDCL3 PMR

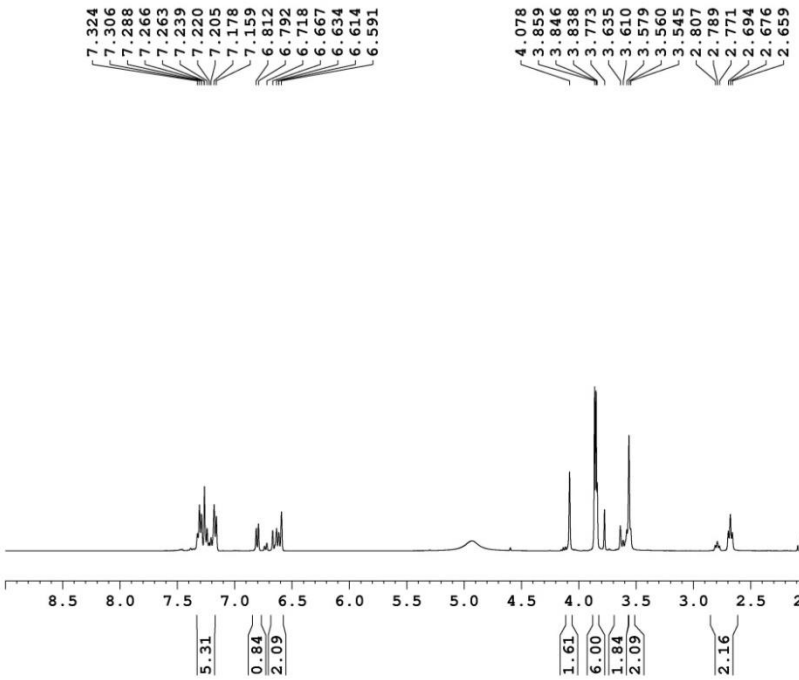

KM-17-02 CDCL3 CMR

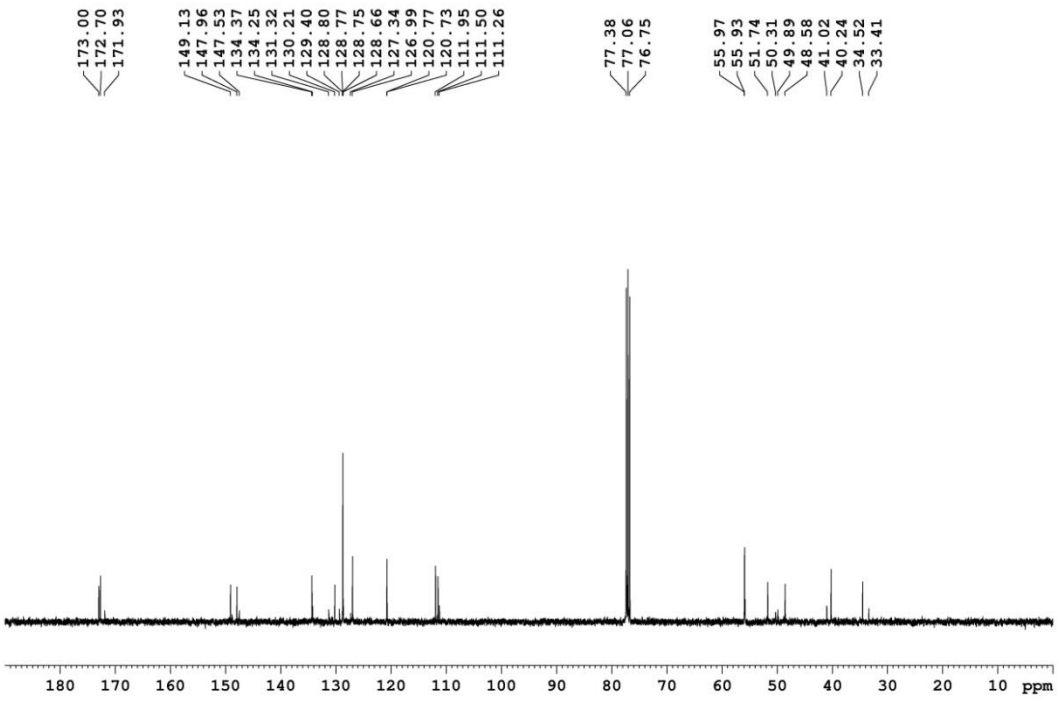

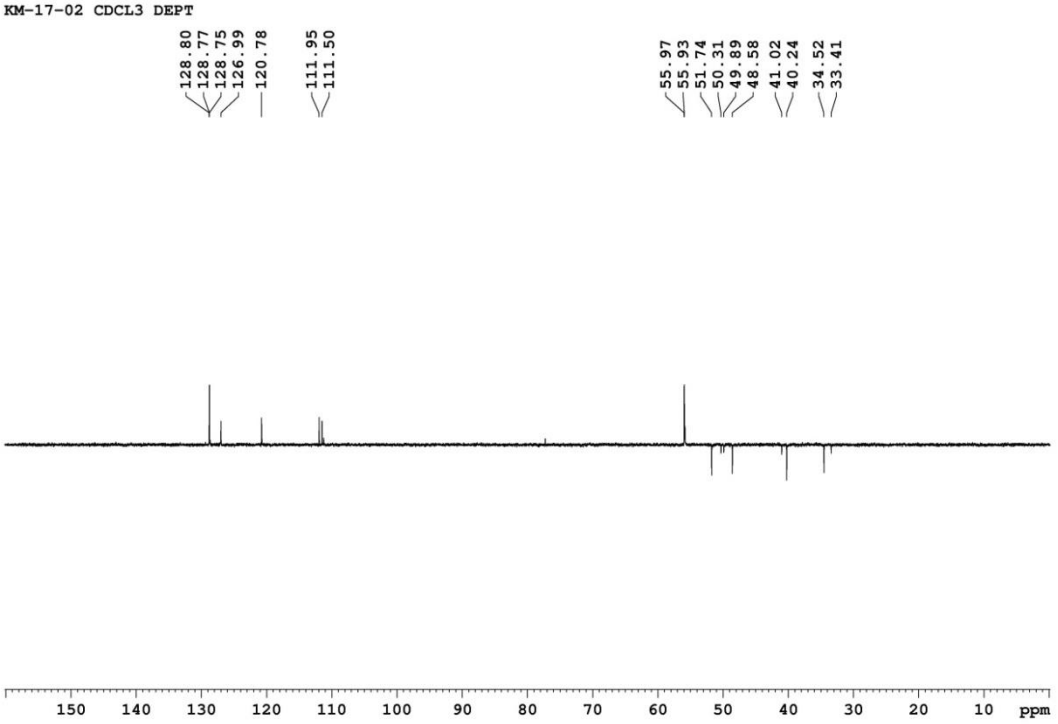
KM-17-02 CDCL3 DEPT
128.80
128.77
128.75
126.99
120.78
111.95
111.50
55.97
55.93
51.74
50.31
49.89
48.58
41.02
40.24
34.52
33.41
150 140 130 120 110 100 90 80 70 60 50 40 30 20 10 ppm

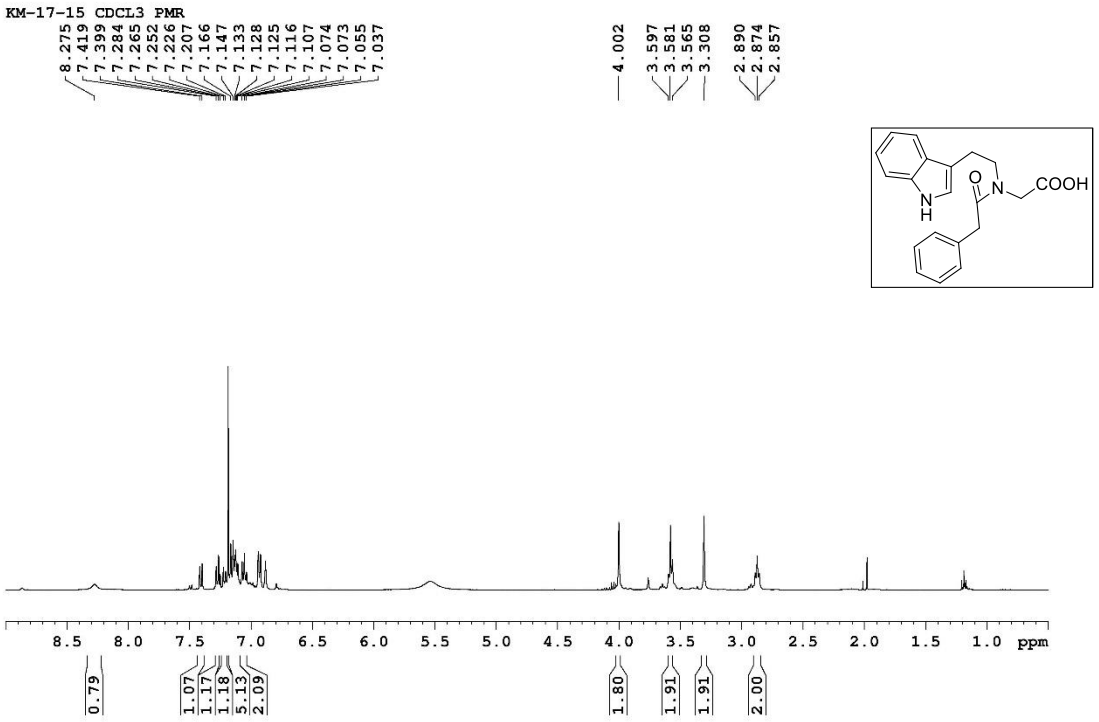
KM-17-15 CDCL3 PMR
8.275
7.419
7.399
7.284
7.265
7.252
7.226
7.207
7.166
7.147
7.133
7.128
7.125
7.116
7.107
7.074
7.073
7.055
7.037
4.002
3.597
3.581
3.565
3.308
2.890
2.874
2.857
O
N
COOH
H
8.5 8.0 7.5 7.0 6.5 6.0 5.5 5.0 4.5 4.0 3.5 3.0 2.5 2.0 1.5 1.0 ppm
0.79
1.07
1.17
1.18
5.13
2.09
1.80
1.91
1.91
2.00

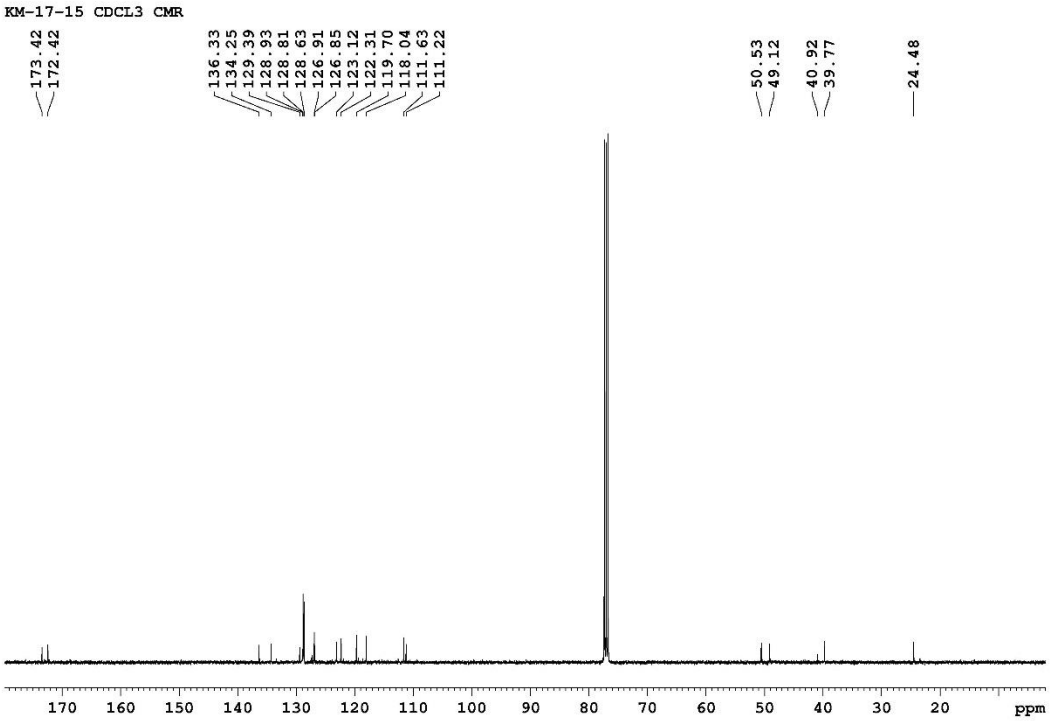
KM-17-15 CDCL3 CMR
173.42
172.42
136.33
134.25
129.39
128.93
128.81
128.63
126.91
126.85
123.12
122.31
119.70
118.04
111.63
111.22
50.53
49.12
40.92
39.77
24.48
170 160 150 140 130 120 110 100 90 80 70 60 50 40 30 20 ppm

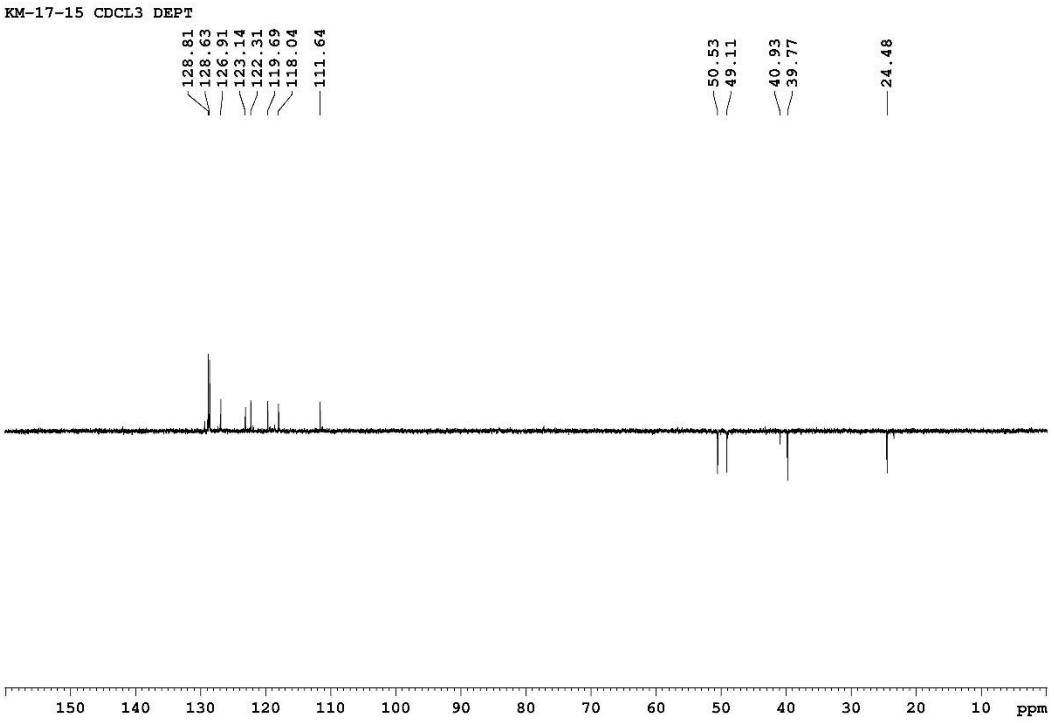
KM-17-15 CDCL3 DEPT
128.81
128.63
126.91
123.14
122.31
119.69
118.04
111.64
50.53
49.11
40.93
39.77
24.48
150 140 130 120 110 100 90 80 70 60 50 40 30 20 10 ppm

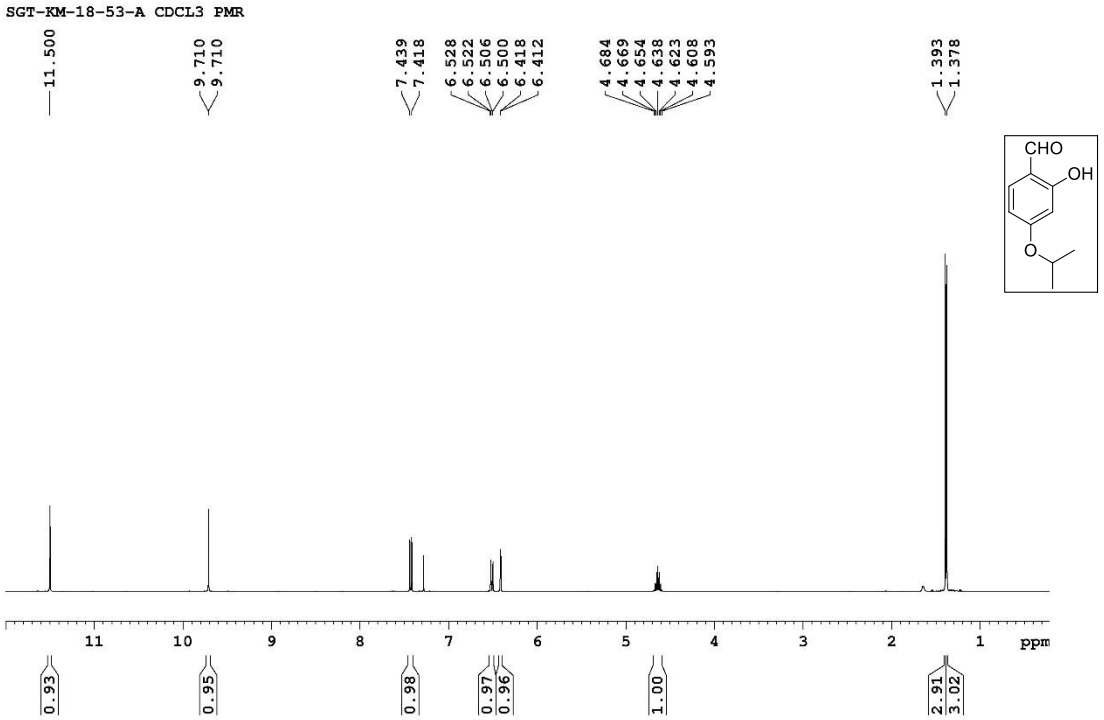
SGT-KM-18-53-A CDCL3 PMR
11.500
9.710
9.710
7.439
7.418
6.528
6.522
6.506
6.500
6.418
6.412
4.684
4.669
4.654
4.638
4.623
4.608
4.593
1.393
1.378
CHO
OH
O
11
10
9
8
7
6
5
4
3
2
1
ppm
0.93
0.95
0.98
0.97
0.96
1.00
2.91
3.02

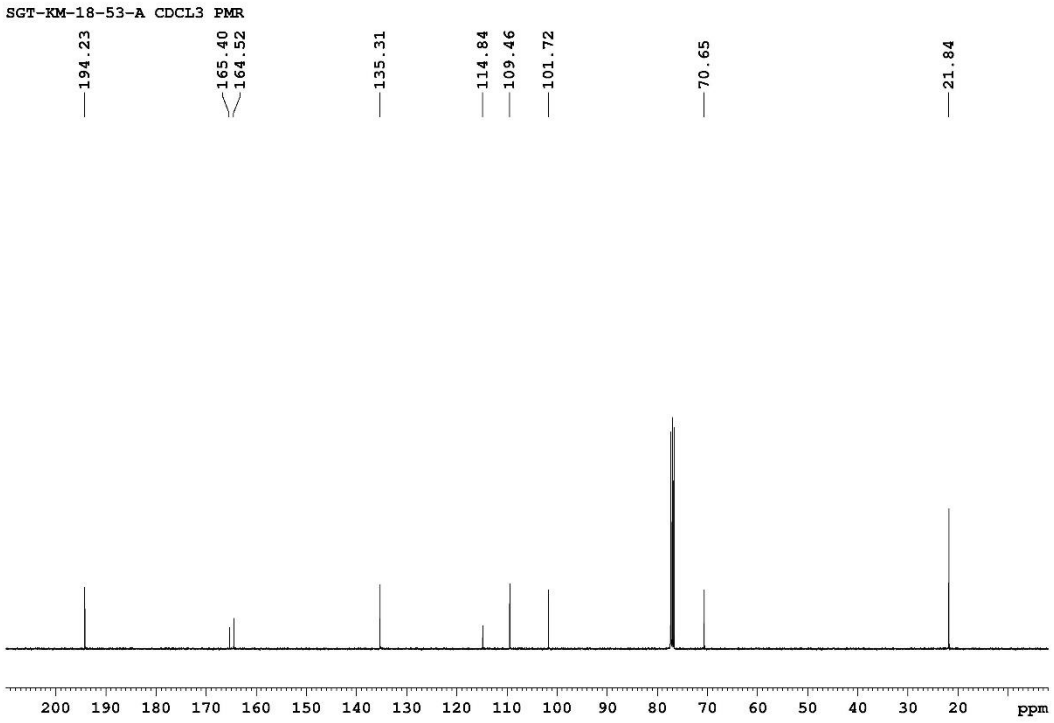
SGT-KM-18-53-A CDCL3 PMR
194.23
165.40
164.52
135.31
114.84
109.46
101.72
70.65
21.84
200
190
180
170
160
150
140
130
120
110
100
90
80
70
60
50
40
30
20
ppm

SGT-KM-18-53-A CDCL3 DEPT

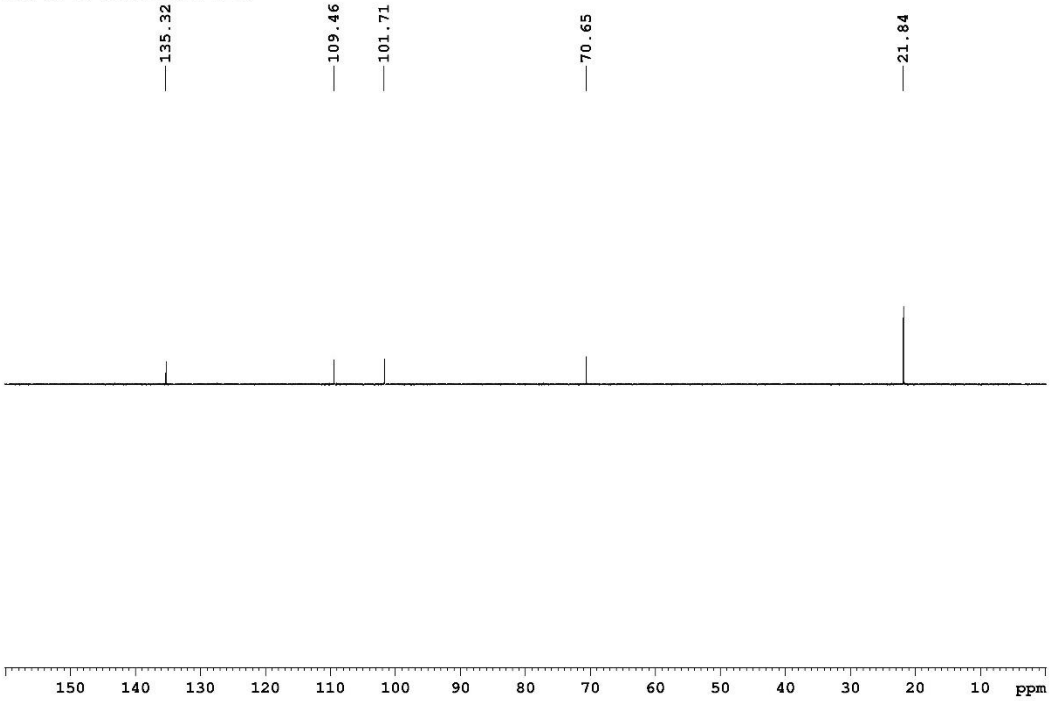

KM-17-20 CDCL3 PMR

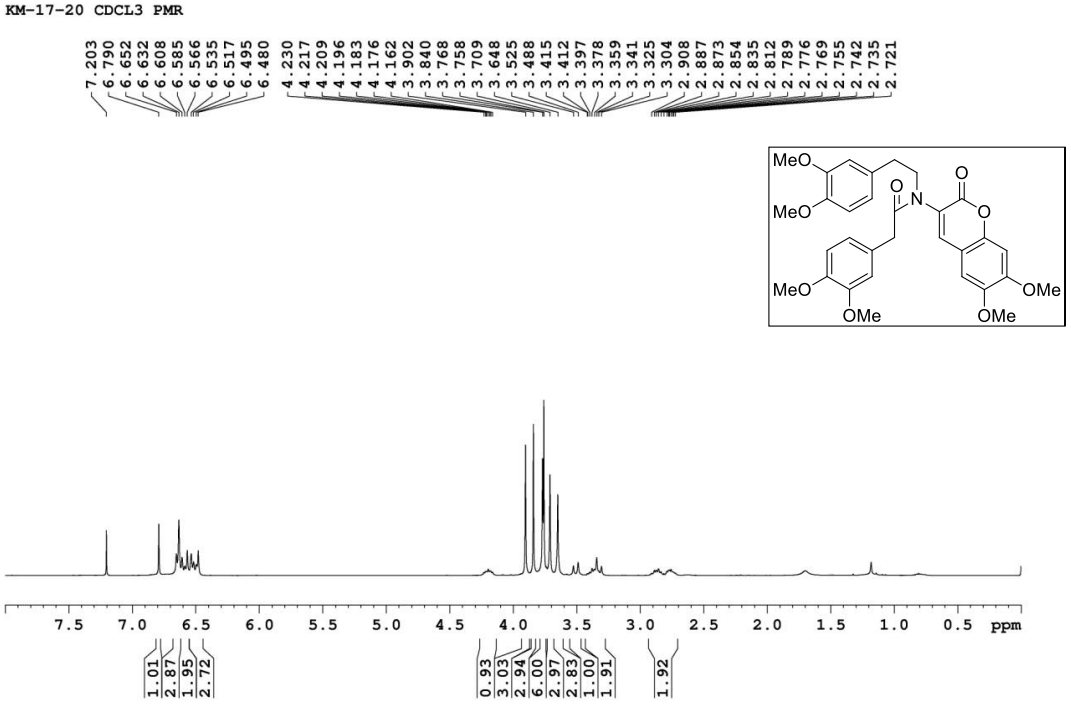

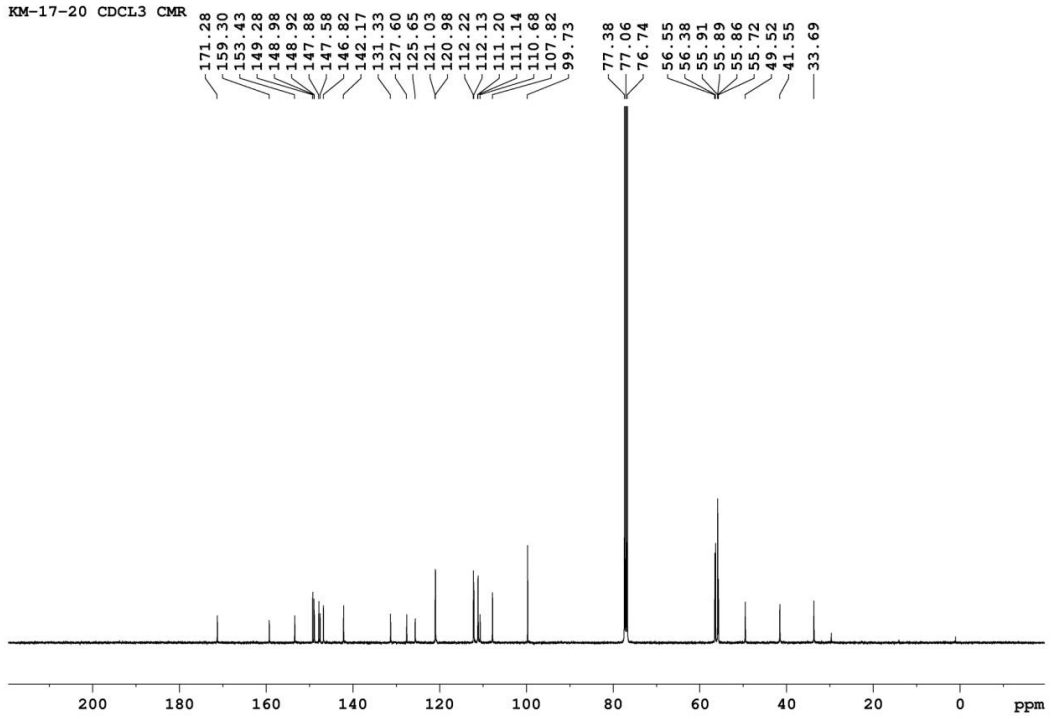
KM-17-20 CDCL3 CMR
171.28
159.30
153.43
149.28
148.98
148.92
147.88
147.58
146.82
142.17
131.33
127.60
125.65
121.03
120.98
112.22
112.13
111.20
111.14
110.68
107.82
99.73
77.38
77.06
76.74
56.55
56.38
55.91
55.89
55.86
55.72
49.52
41.55
33.69
200
180
160
140
120
100
80
60
40
20
0
ppm

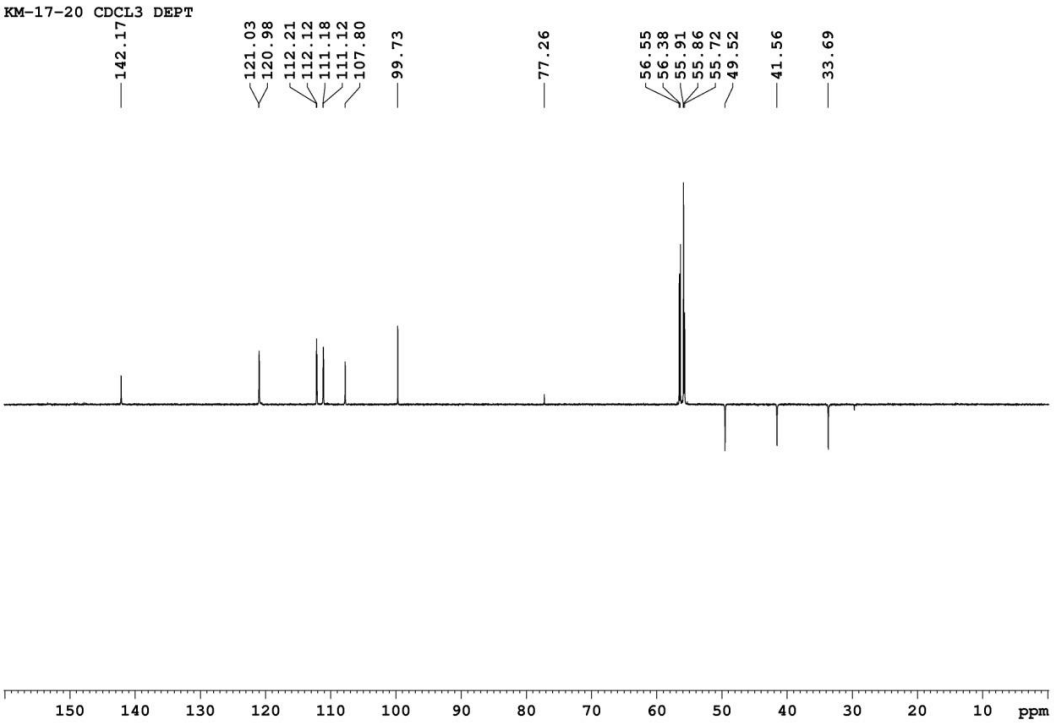
KM-17-20 CDCL3 DEPT
142.17
121.03
120.98
112.21
112.12
111.18
111.12
107.80
99.73
77.26
56.55
56.38
55.91
55.86
55.72
49.52
41.56
33.69
150
140
130
120
110
100
90
80
70
60
50
40
30
20
10
ppm

KM-18-07 CDCL3 PMR

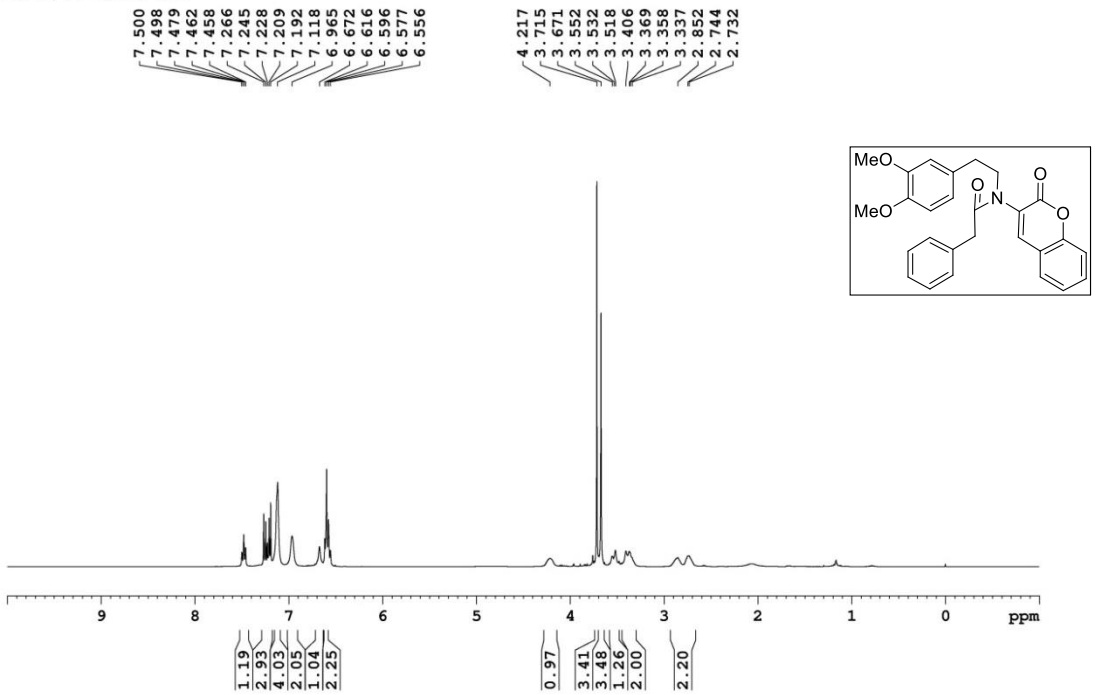

KM-18-07 CDCL3 CMR

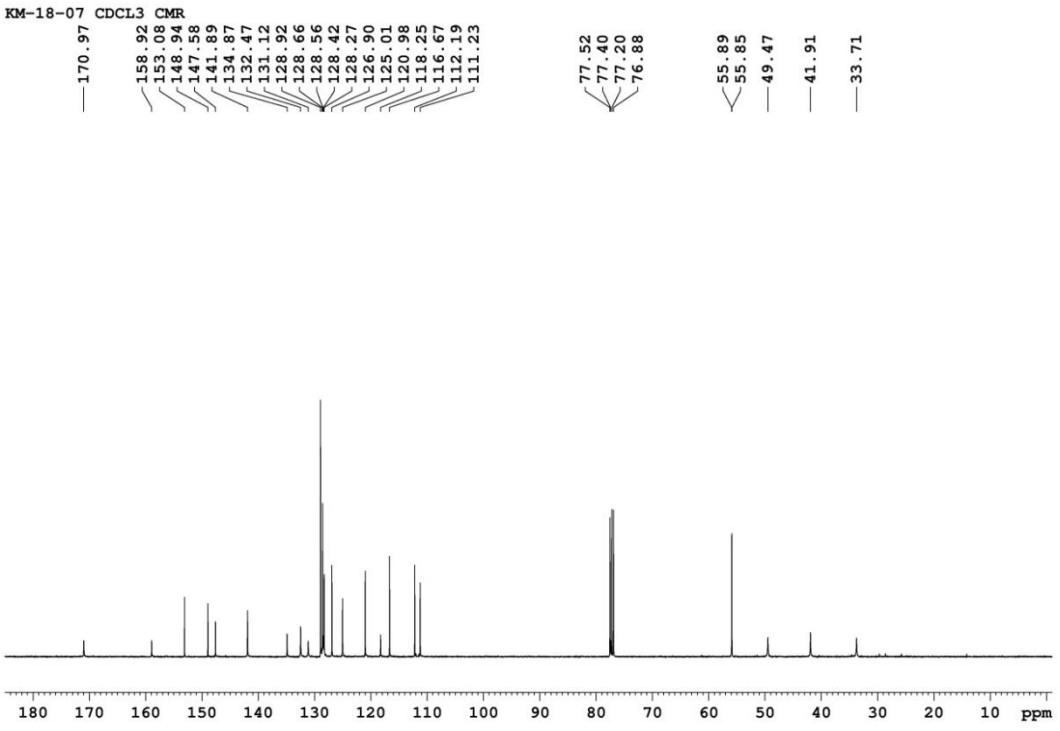

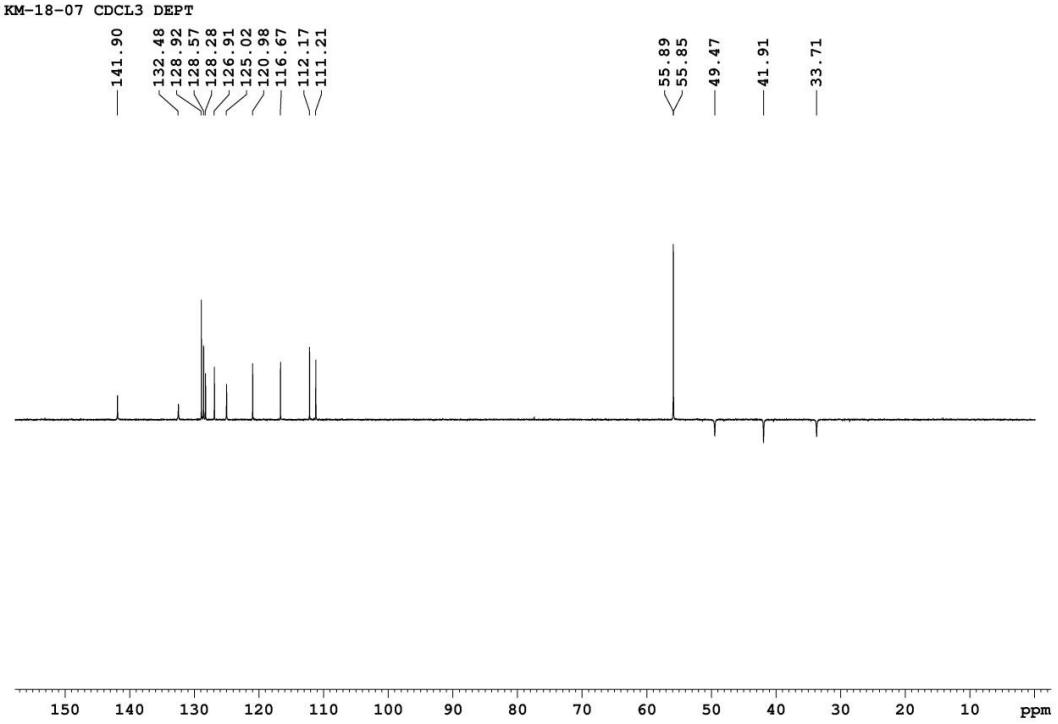
KM-18-07 CDCL3 DEPT
141.90
132.48
128.92
128.57
128.28
126.91
125.02
120.98
116.67
112.17
111.21
55.89
55.85
49.47
41.91
33.71
150
140
130
120
110
100
90
80
70
60
50
40
30
20
10
ppm

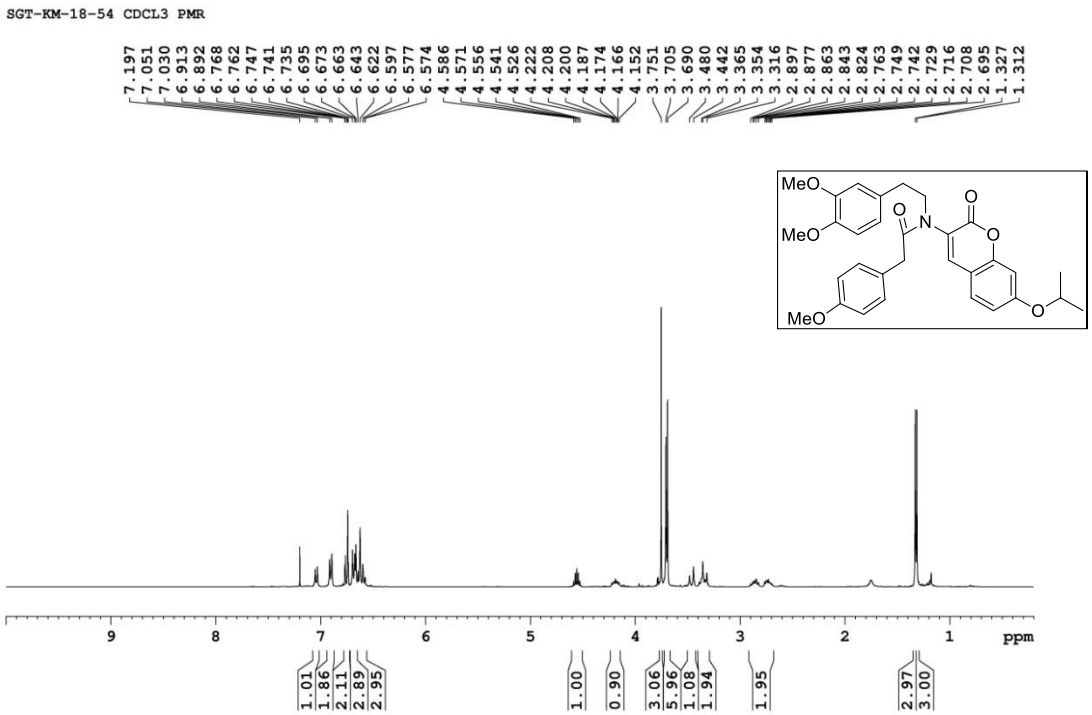
SGT-KM-18-54 CDCL3 PMR
7.197
7.051
7.030
6.913
6.892
6.768
6.762
6.747
6.741
6.735
6.695
6.673
6.663
6.643
6.622
6.597
6.577
6.574
4.586
4.571
4.556
4.541
4.526
4.222
4.208
4.200
4.187
4.174
4.166
4.152
3.751
3.705
3.690
3.480
3.442
3.365
3.354
3.316
2.897
2.877
2.863
2.843
2.824
2.763
2.749
2.742
2.729
2.716
2.708
2.695
1.327
1.312
MeO
MeO
MeO
O
N
O
O
O
9
8
7
6
5
4
3
2
1
ppm
1.01
1.86
2.11
2.89
2.95
1.00
0.90
3.06
5.96
1.08
1.94
1.95
2.97
3.00

SGT-KM-18-54 CDCL3 CMR

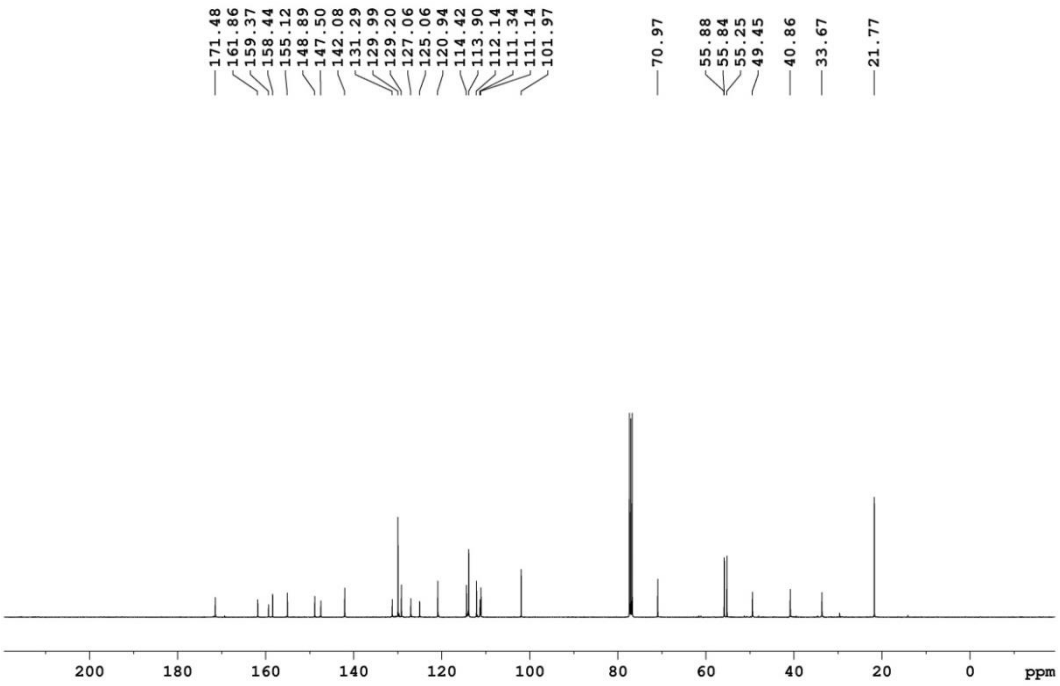

SGT-KM-18-54 CDCL3 DEPT

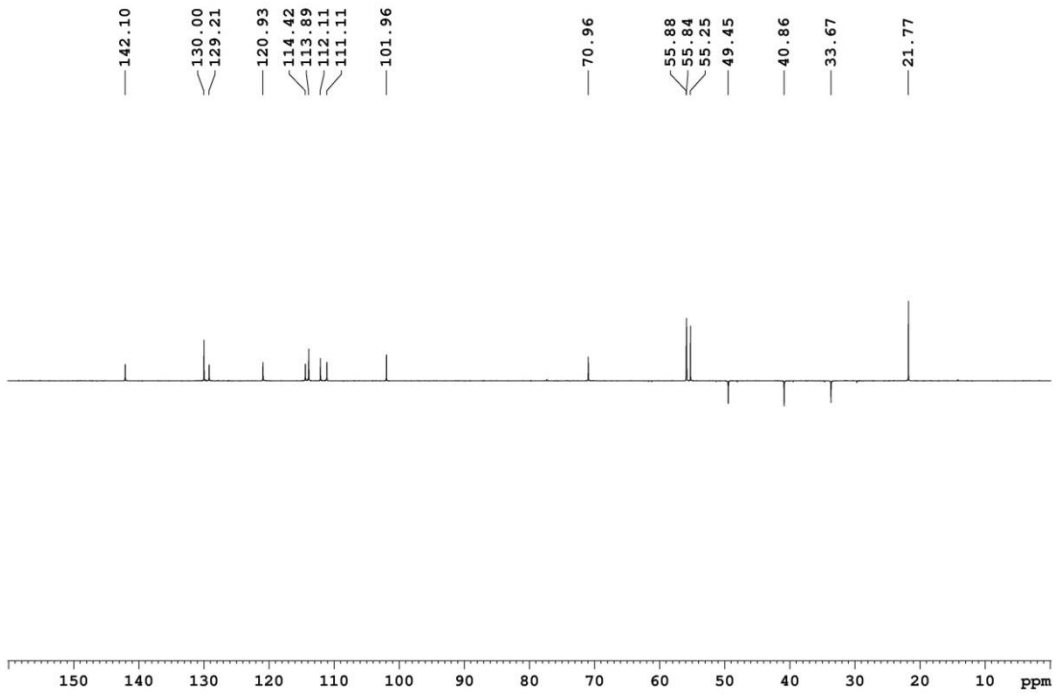

SGT-KM-18-43 CDCL3 PMR

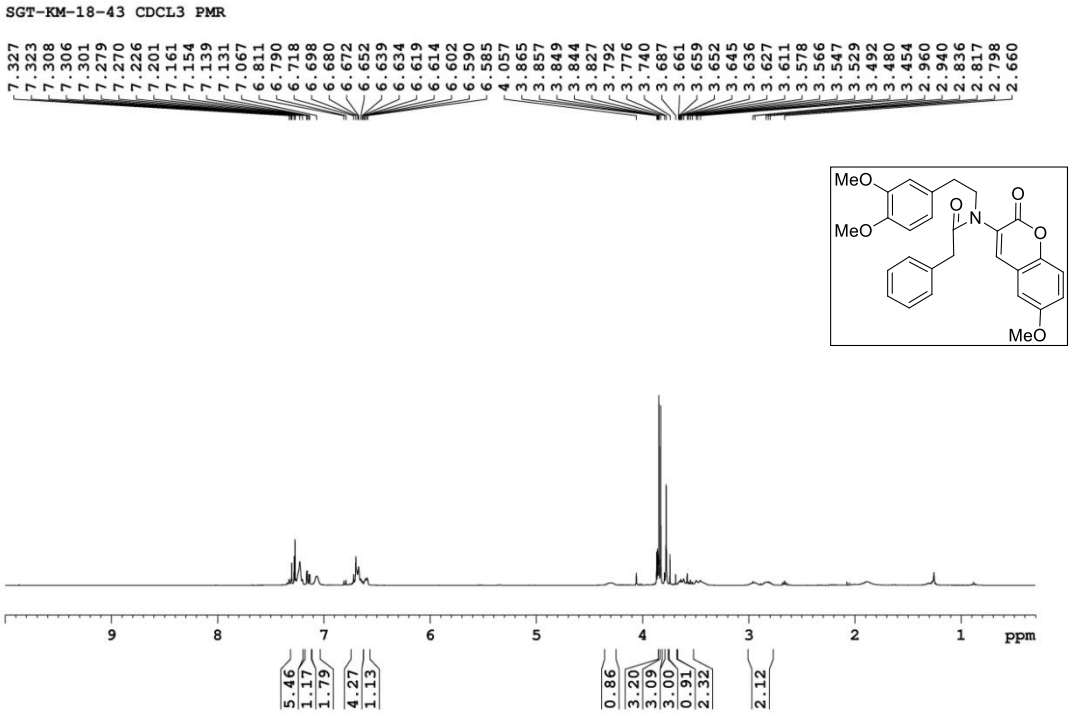

SGT-KM-18-43 CDCL3 CMR

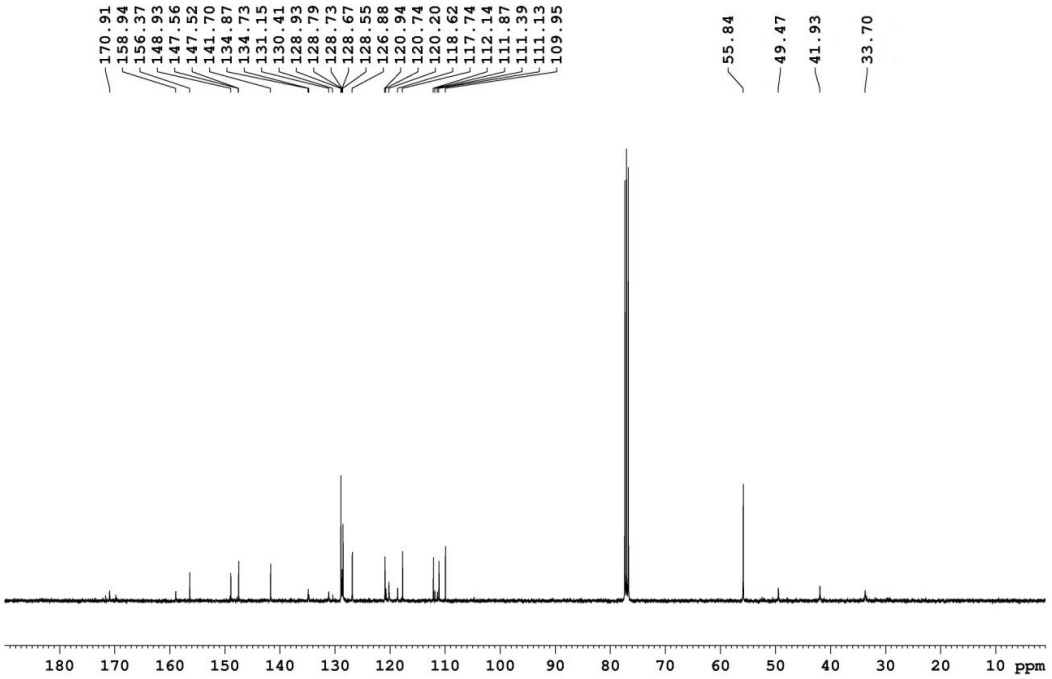

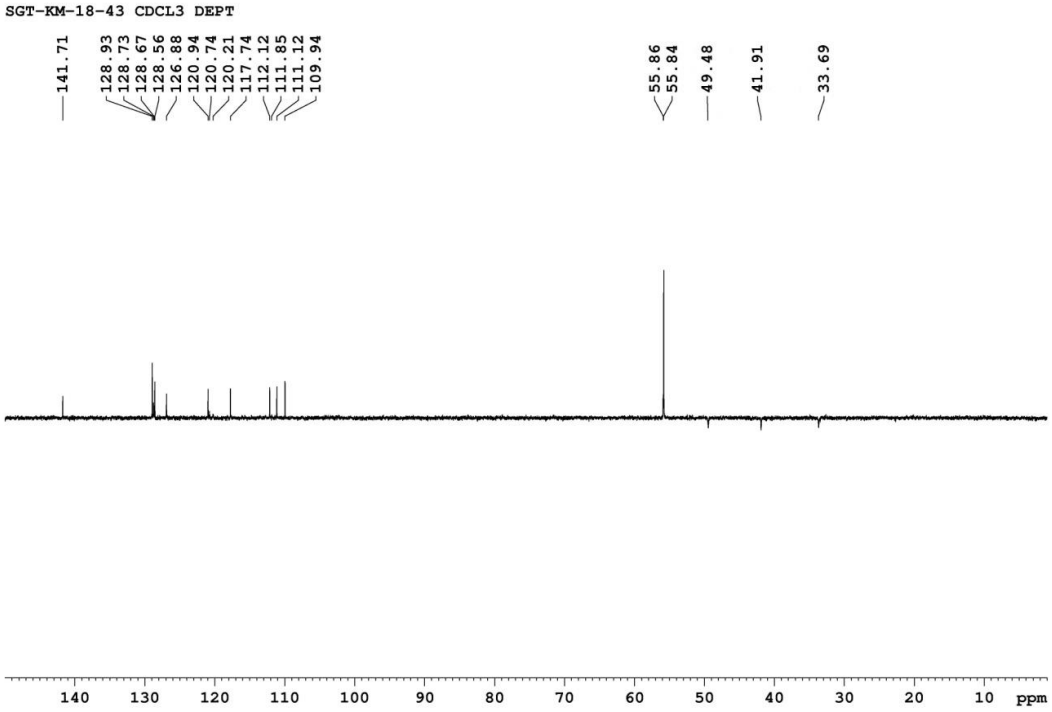
SGT-KM-18-43 CDCL3 DEPT
141.71
128.93
128.73
128.67
128.56
126.88
120.94
120.74
120.21
117.74
112.12
111.85
111.12
109.94
55.86
55.84
49.48
41.91
33.69
140
130
120
110
100
90
80
70
60
50
40
30
20
10
ppm

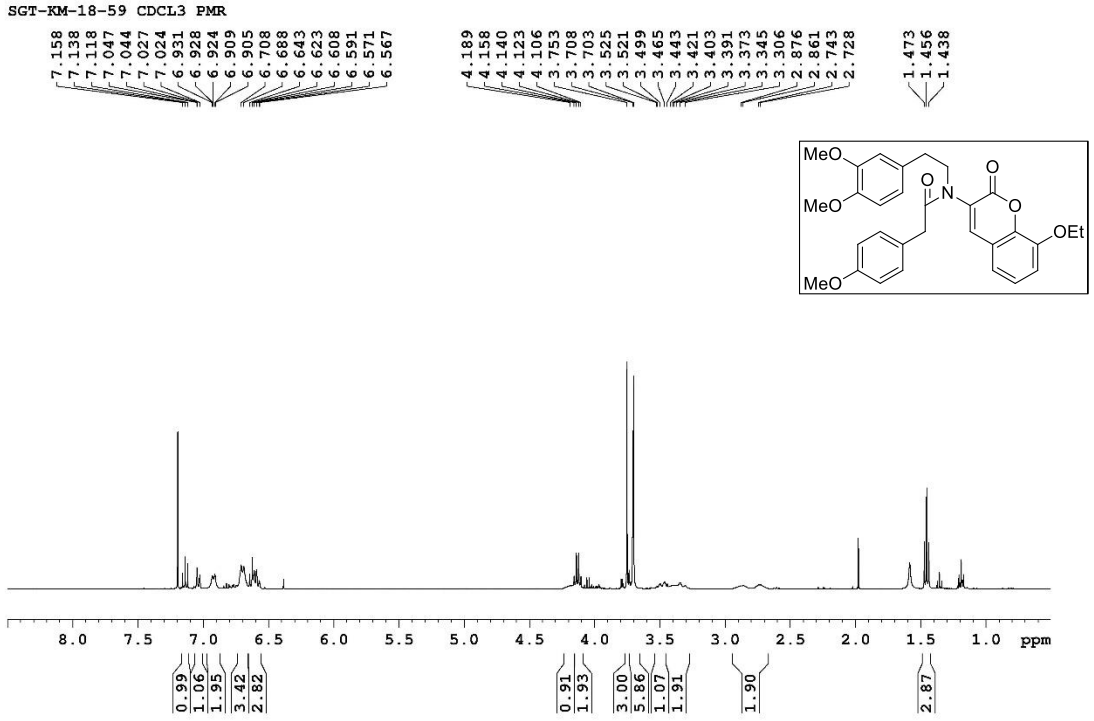
SGT-KM-18-59 CDCL3 PMR
7.158
7.138
7.118
7.047
7.044
7.027
7.024
6.931
6.928
6.924
6.909
6.905
6.708
6.688
6.643
6.623
6.608
6.591
6.571
6.567
4.189
4.158
4.140
4.123
4.106
3.753
3.708
3.703
3.525
3.521
3.499
3.465
3.443
3.421
3.403
3.391
3.373
3.345
3.306
2.876
2.861
2.743
2.728
1.473
1.456
1.438
MeO
MeO
MeO
O
N
O
O
OEt
8.0
7.5
7.0
6.5
6.0
5.5
5.0
4.5
4.0
3.5
3.0
2.5
2.0
1.5
1.0
ppm
0.99
1.06
1.95
3.42
2.82
0.91
1.93
3.00
5.86
1.07
1.91
1.90
2.87

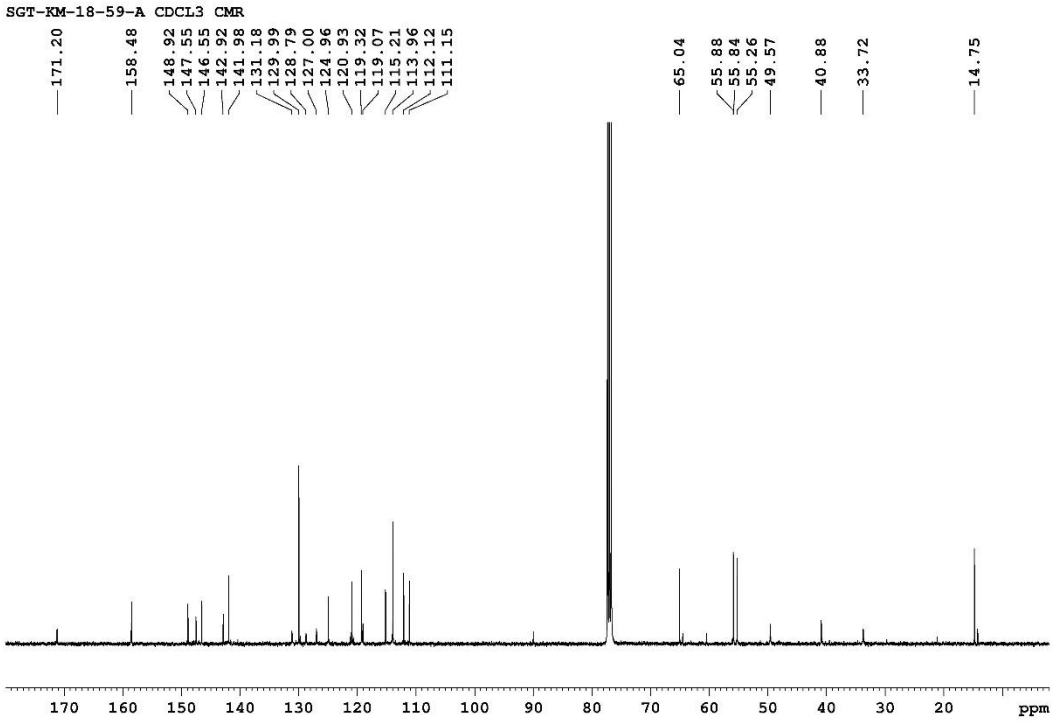
SGT-KM-18-59-A CDCL3 CMR
171.20
158.48
148.92
147.55
146.55
142.92
141.98
131.18
129.99
128.79
127.00
124.96
120.93
119.32
119.07
115.21
113.96
112.12
111.15
65.04
55.88
55.84
55.26
49.57
40.88
33.72
14.75
170 160 150 140 130 120 110 100 90 80 70 60 50 40 30 20 ppm

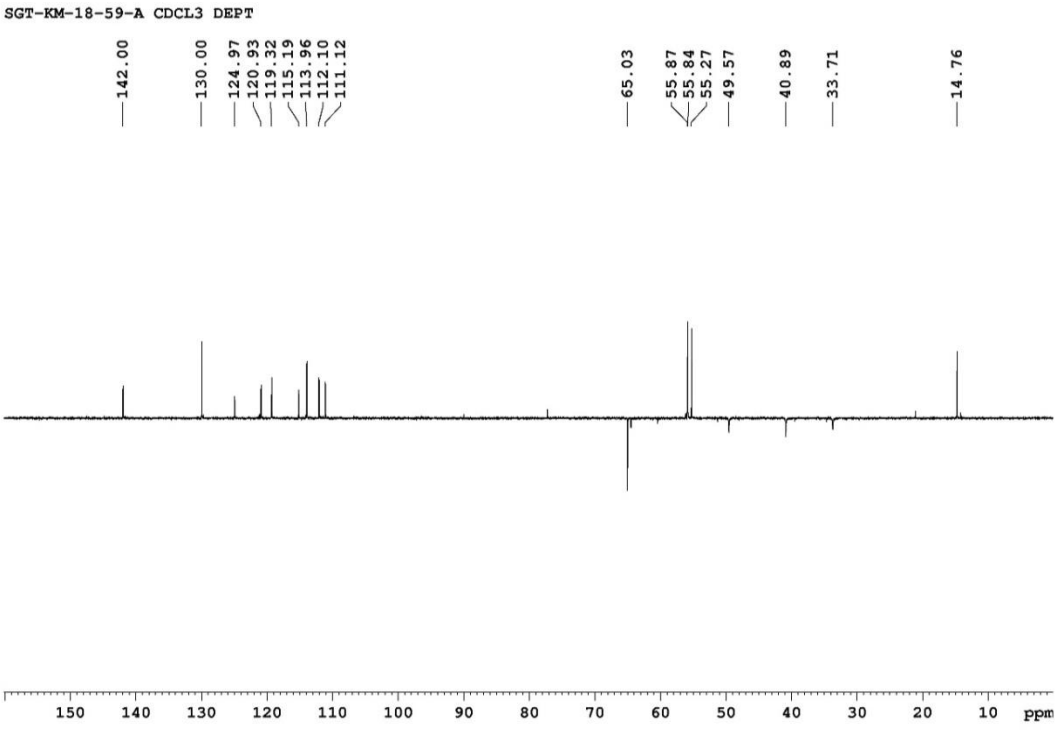
SGT-KM-18-59-A CDCL3 DEPT
142.00
130.00
124.97
120.93
119.32
115.19
113.96
112.10
111.12
65.03
55.87
55.84
55.27
49.57
40.89
33.71
14.76
150 140 130 120 110 100 90 80 70 60 50 40 30 20 10 ppm

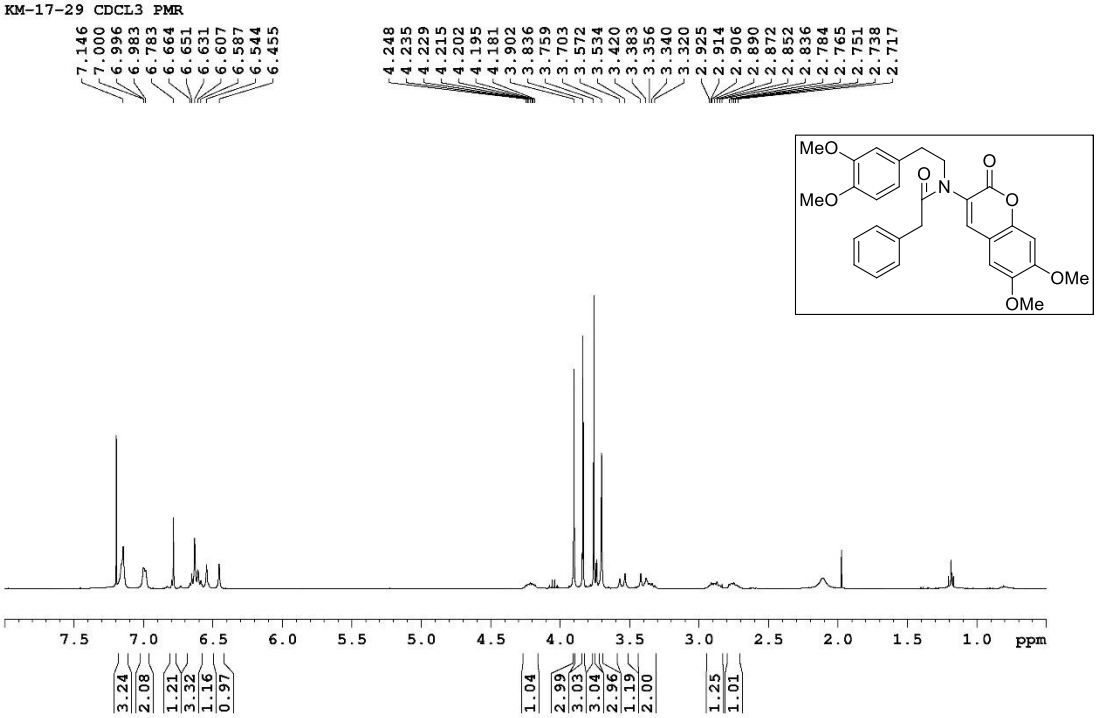
KM-17-29 CDCL3 PMR
7.146
7.000
6.996
6.983
6.783
6.664
6.651
6.631
6.607
6.587
6.544
6.455
4.248
4.235
4.229
4.215
4.202
4.195
4.181
3.902
3.836
3.759
3.703
3.572
3.534
3.420
3.383
3.356
3.340
3.320
2.925
2.914
2.906
2.890
2.872
2.852
2.836
2.784
2.765
2.751
2.738
2.717
MeO
MeO
O
O
N
O
OMe
OMe
7.5
7.0
6.5
6.0
5.5
5.0
4.5
4.0
3.5
3.0
2.5
2.0
1.5
1.0
ppm
3.24
2.08
1.21
3.32
1.16
0.97
1.04
2.99
3.03
3.04
2.96
1.19
2.00
1.25
1.01

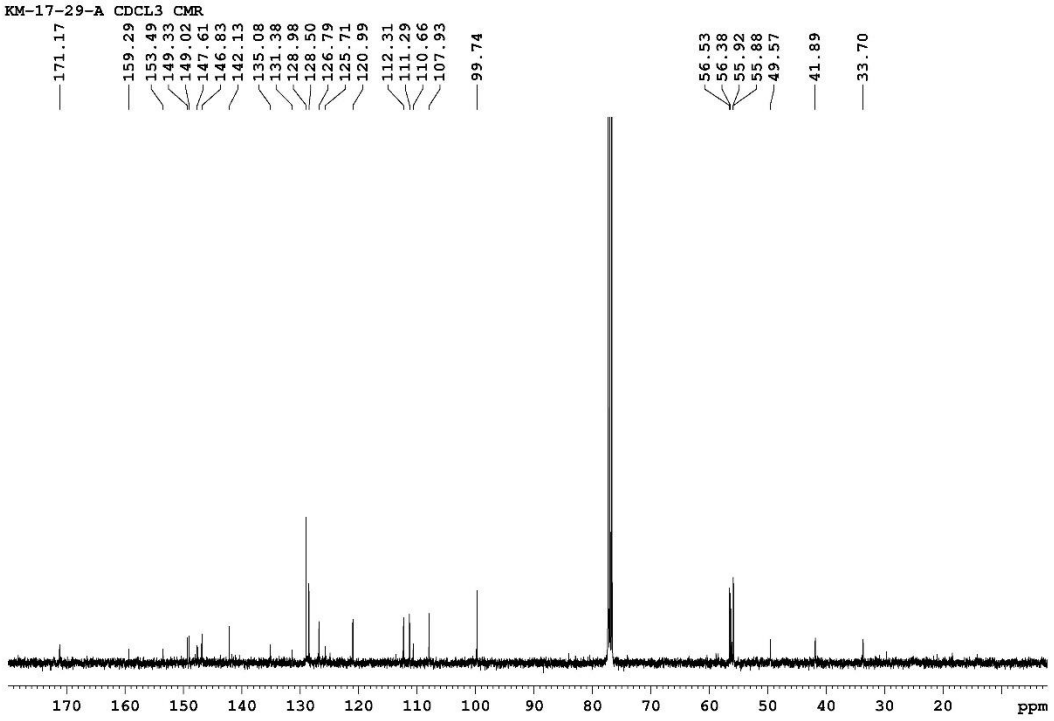
KM-17-29-A CDCL3 CMR
171.17
159.29
153.49
149.33
149.02
147.61
146.83
142.13
135.08
131.38
128.98
128.50
126.79
125.71
120.99
112.31
111.29
110.66
107.93
99.74
56.53
56.38
55.92
55.88
49.57
41.89
33.70
170
160
150
140
130
120
110
100
90
80
70
60
50
40
30
20
ppm

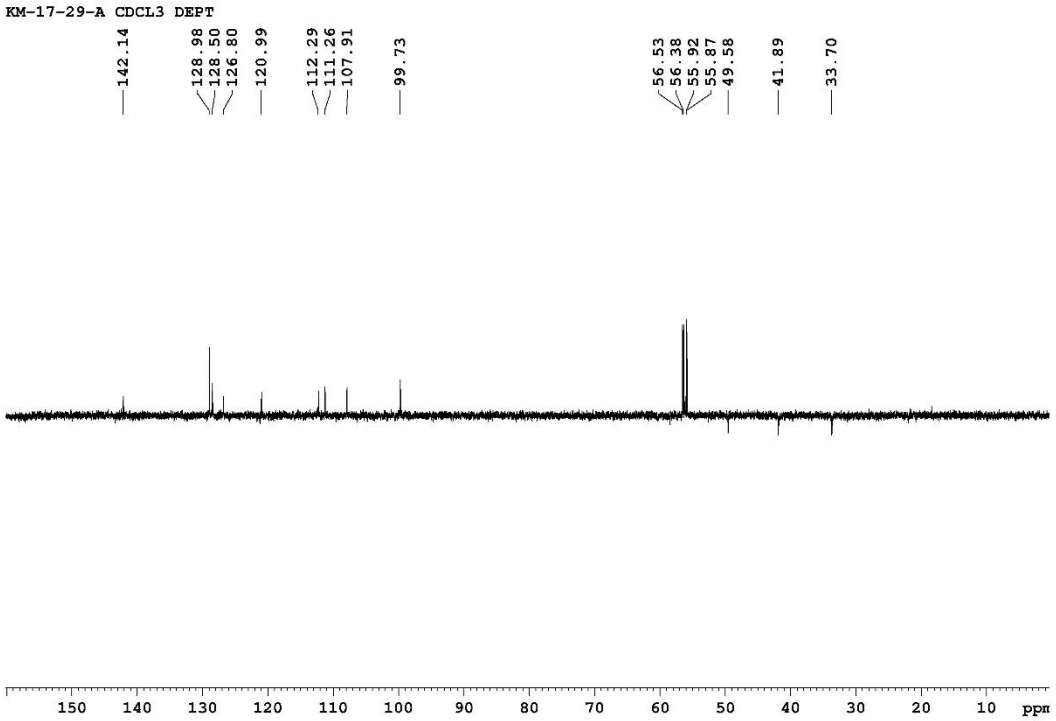
KM-17-29-A CDCL3 DEPT
142.14
128.98
128.50
126.80
120.99
112.29
111.26
107.91
99.73
56.53
56.38
55.92
55.87
49.58
41.89
33.70
150
140
130
120
110
100
90
80
70
60
50
40
30
20
10
ppm

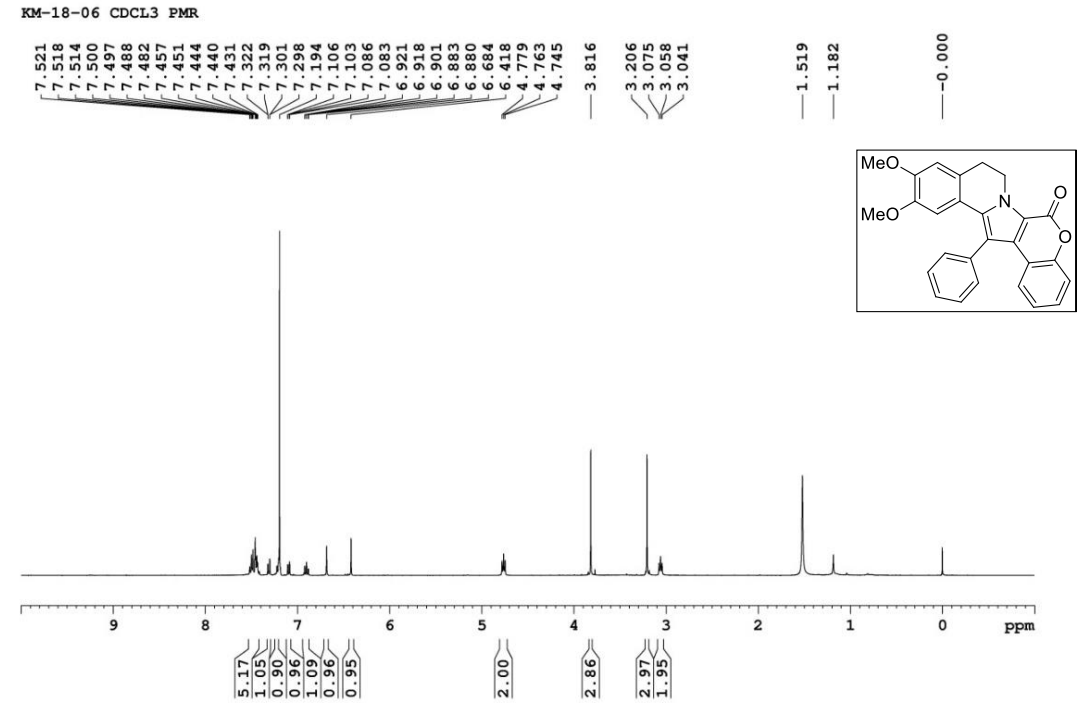
KM-18-06 CDCL3 PMR
7.521
7.518
7.514
7.500
7.497
7.488
7.482
7.457
7.451
7.444
7.440
7.431
7.322
7.319
7.301
7.298
7.194
7.106
7.103
7.086
7.083
6.921
6.918
6.901
6.883
6.880
6.684
6.418
4.779
4.763
4.745
3.816
3.206
3.075
3.058
3.041
1.519
1.182
0.000
MeO
MeO
N
O
O
9
8
7
6
5
4
3
2
1
0
ppm
5.17
1.05
0.90
0.96
1.09
0.96
0.95
2.00
2.86
2.97
1.95

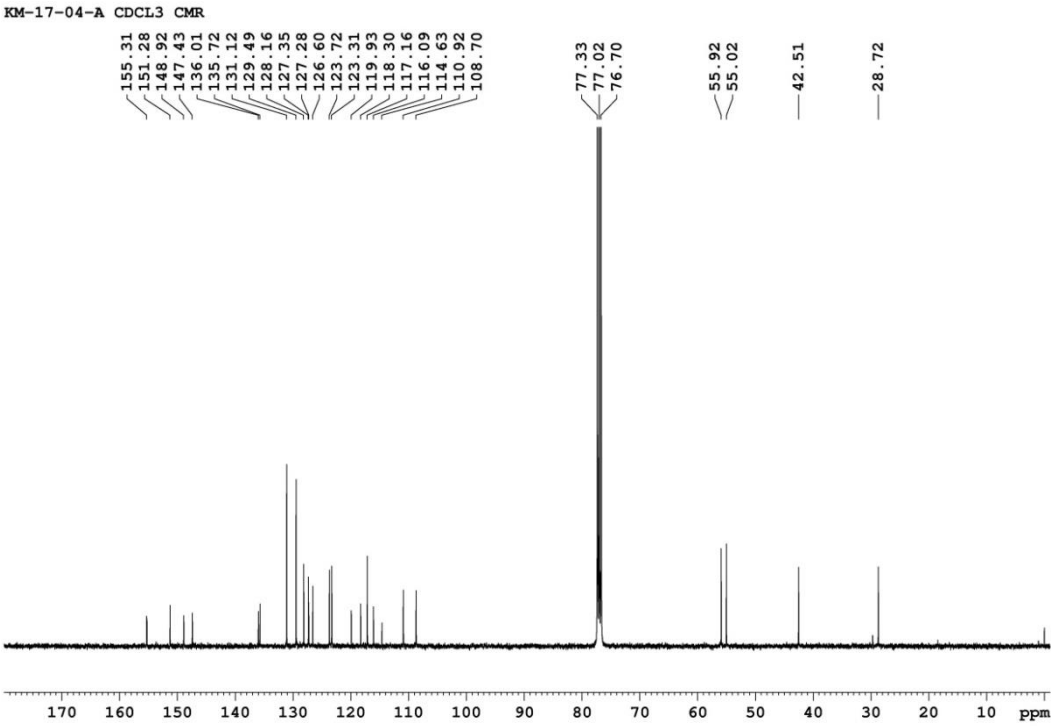
KM-17-04-A CDCL3 CMR
155.31
151.28
148.92
147.43
136.01
135.72
131.12
129.49
128.16
127.35
127.28
126.60
123.72
123.31
119.93
118.30
117.16
116.09
114.63
110.92
108.70
77.33
77.02
76.70
55.92
55.02
42.51
28.72
170 160 150 140 130 120 110 100 90 80 70 60 50 40 30 20 10 ppm

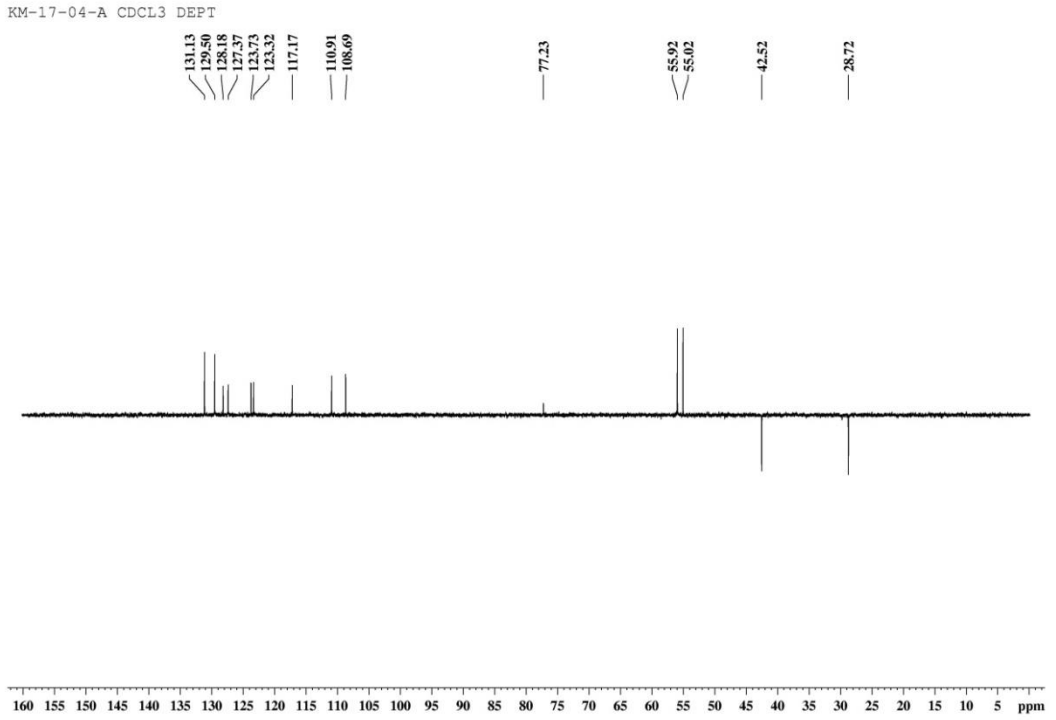
KM-17-04-A CDCL3 DEPT
131.13
129.50
128.18
127.37
123.73
123.32
117.17
110.91
108.69
77.23
55.92
55.02
42.52
28.72
160 155 150 145 140 135 130 125 120 115 110 105 100 95 90 85 80 75 70 65 60 55 50 45 40 35 30 25 20 15 10 5 ppm

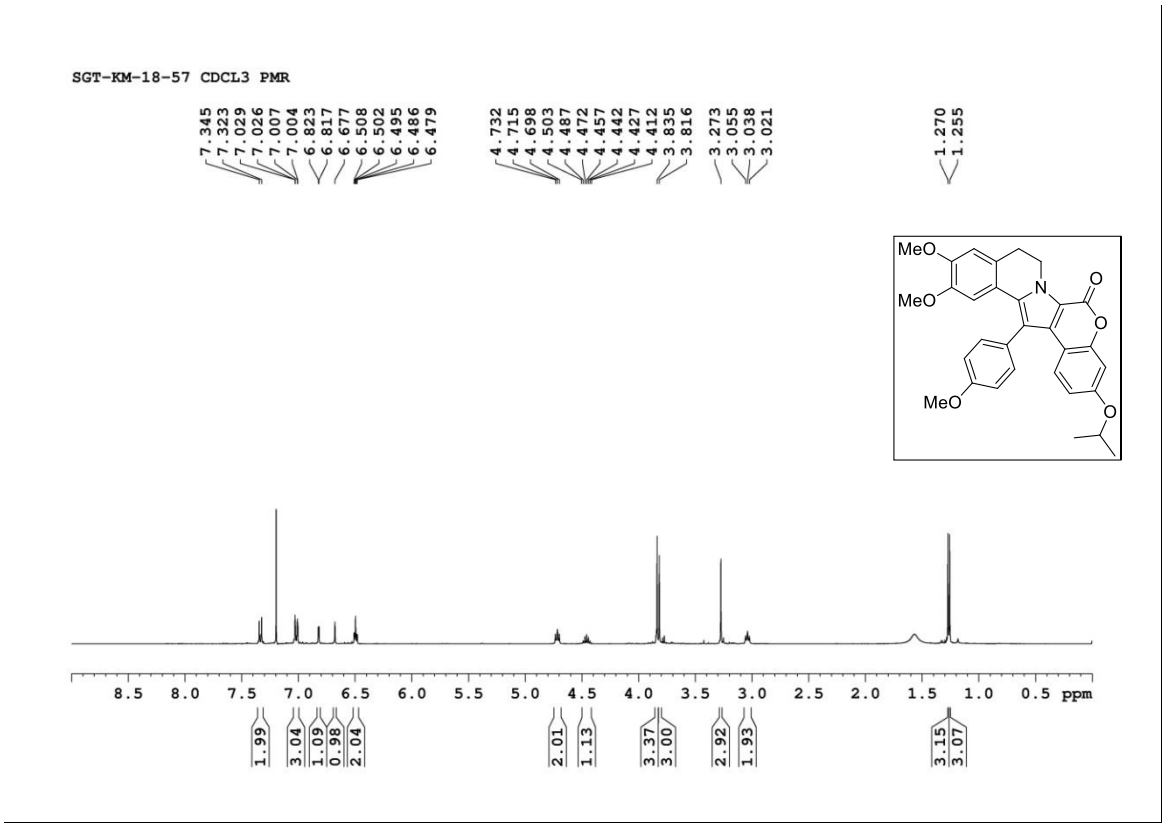
SGT-KM-18-57 CDCL3 PMR
7.345
7.323
7.029
7.026
7.007
7.004
6.823
6.817
6.677
6.508
6.502
6.495
6.486
6.479
4.732
4.715
4.698
4.503
4.487
4.472
4.457
4.442
4.427
4.412
3.835
3.816
3.273
3.055
3.038
3.021
1.270
1.255
MeO
MeO
MeO
N
O
O
O
8.5 8.0 7.5 7.0 6.5 6.0 5.5 5.0 4.5 4.0 3.5 3.0 2.5 2.0 1.5 1.0 0.5 ppm
1.99
3.04
1.09
0.98
2.04
2.01
1.13
3.37
3.00
2.92
1.93
3.15
3.07

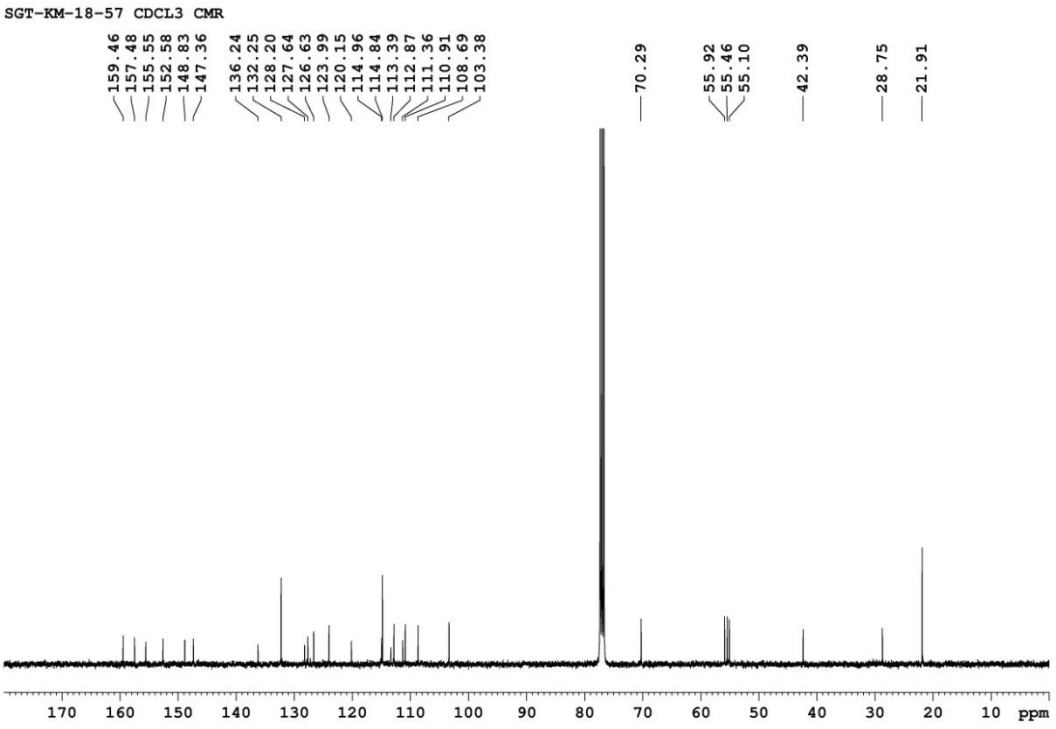
SGT-KM-18-57 CDCL3 CMR
159.46
157.48
155.55
152.58
148.83
147.36
136.24
132.25
128.20
127.64
126.63
123.99
120.15
114.96
114.84
113.39
112.87
111.36
110.91
108.69
103.38
70.29
55.92
55.46
55.10
42.39
28.75
21.91
170 160 150 140 130 120 110 100 90 80 70 60 50 40 30 20 10 ppm

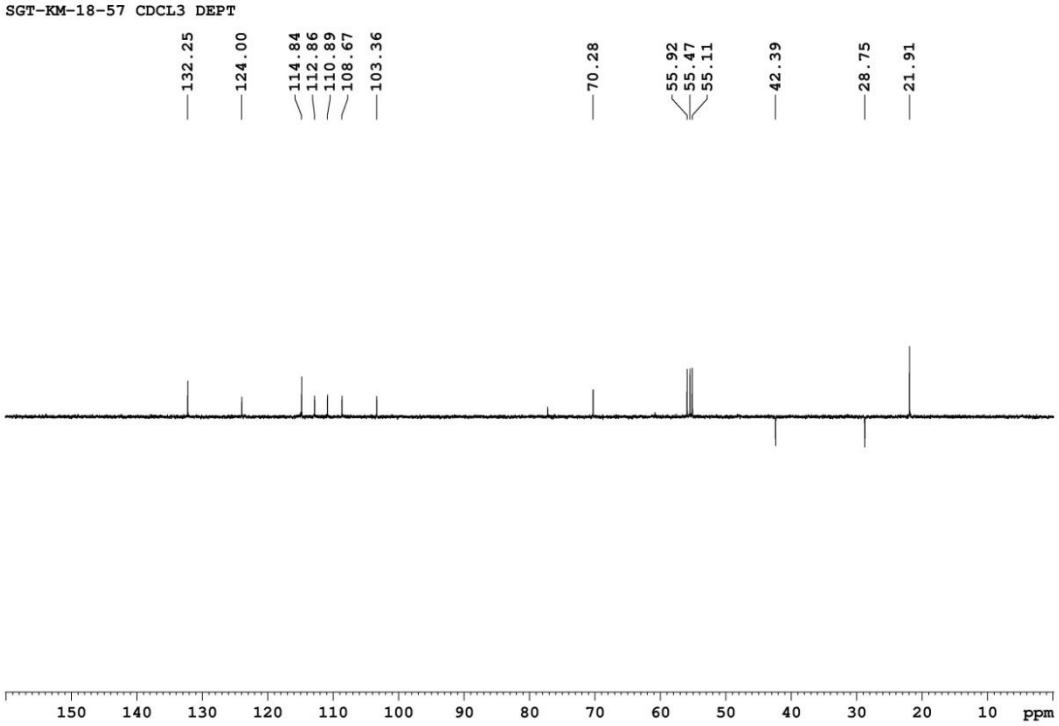
SGT-KM-18-57 CDCL3 DEPT
132.25
124.00
114.84
112.86
110.89
108.67
103.36
70.28
55.92
55.47
55.11
42.39
28.75
21.91
150 140 130 120 110 100 90 80 70 60 50 40 30 20 10 ppm

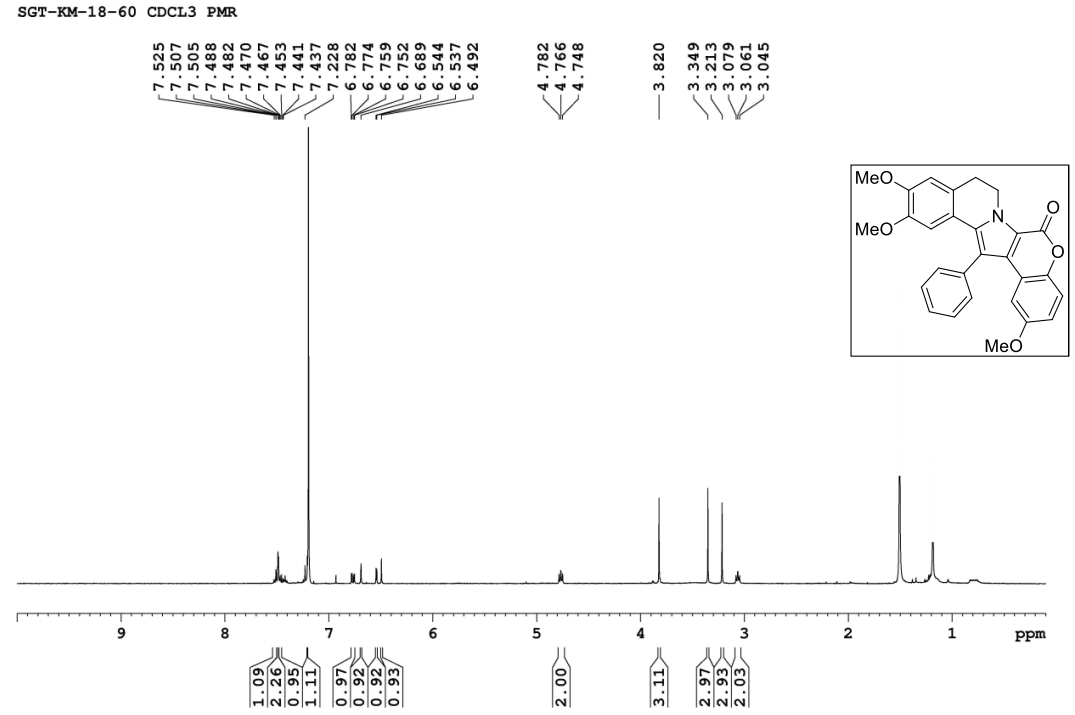
SGT-KM-18-60 CDCL3 PMR
7.525
7.507
7.505
7.488
7.482
7.470
7.467
7.453
7.441
7.437
7.228
6.782
6.774
6.759
6.752
6.689
6.544
6.537
6.492
4.782
4.766
4.748
3.820
3.349
3.213
3.079
3.061
3.045
MeO
MeO
N
O
O
MeO
9 8 7 6 5 4 3 2 1 ppm
1.09
2.26
0.95
1.11
0.97
0.92
0.92
0.93
2.00
3.11
2.97
2.93
2.03

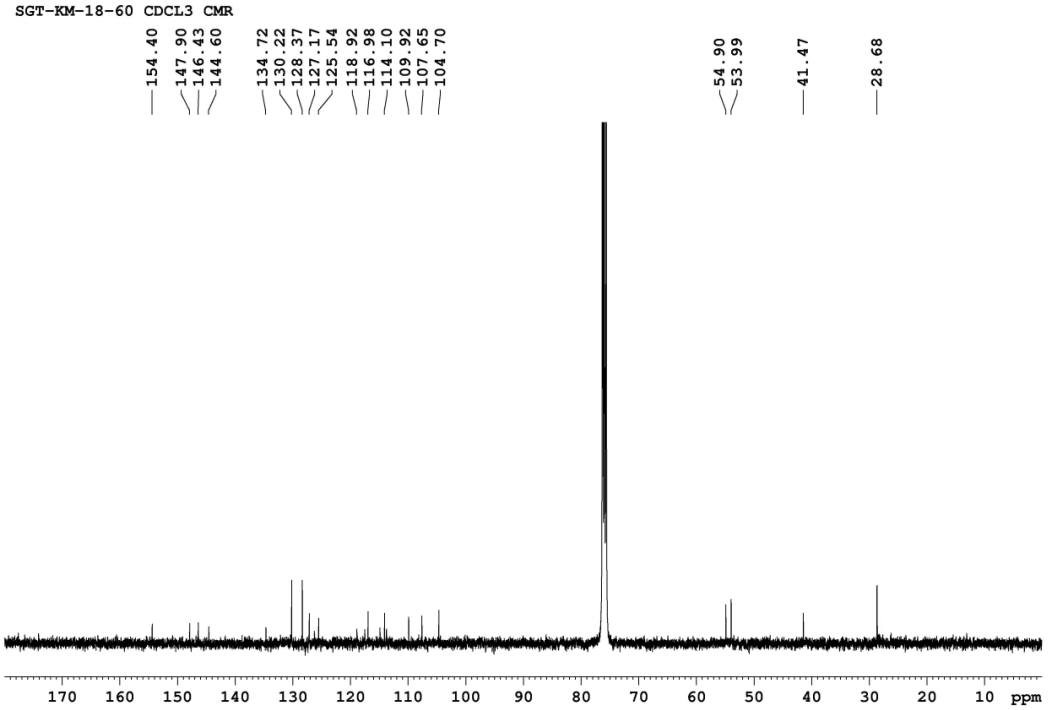
SGT-KM-18-60 CDCL3 CMR
154.40
147.90
146.43
144.60
134.72
130.22
128.37
127.17
125.54
118.92
116.98
114.10
109.92
107.65
104.70
54.90
53.99
41.47
28.68
170 160 150 140 130 120 110 100 90 80 70 60 50 40 30 20 10 ppm

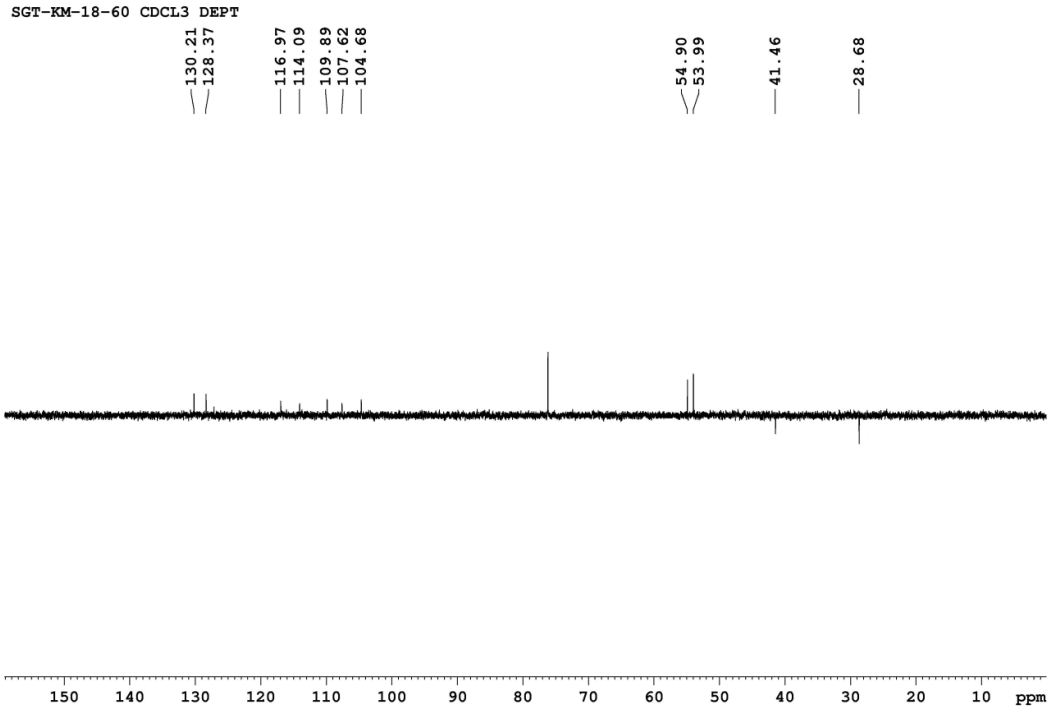
SGT-KM-18-60 CDCL3 DEPT
130.21
128.37
116.97
114.09
109.89
107.62
104.68
54.90
53.99
41.46
28.68
150 140 130 120 110 100 90 80 70 60 50 40 30 20 10 ppm

Chapter 2

Synthetic studies of benzoindolizidine derived alkaloids

Indolizidine alkaloids are an important structural motif that belongs to the broader class of natural products. These indolizidine alkaloids are metabolites derived from lysine and found in various animal and plant sources like higher plants, invertebrates, vertebrates, fungi, and bacteria. The core structure consists of a fused six-five-membered ring system with a bridgehead nitrogen atom. Indolizidine compounds are found in 25-30% of all the alkaloids families. Polyhydroxylated indolizidines like swainsonine, lentiginosine, and castanospermine derived from plants are glycosidase inhibitors. Alkylindolizidine, monomorine is isolated from ants is a trail pheromome. The amphibian's skin has a crucial chemical which has an indolizidine core that helps in their defense against predators. Fig 1. depicts a few naturally occurring indolizidine alkaloids.

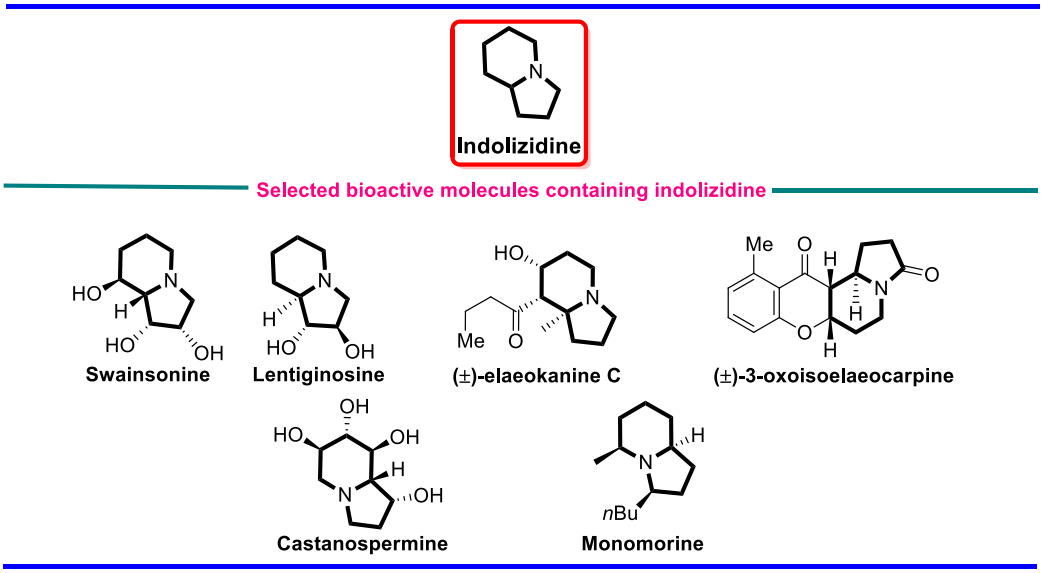

Figure 1: Selected examples of indolizidine alkaloids

Benzoindolizidine alkaloids containing benzene rings fused to one of the rings of indolizine are also known in nature. Few such selected examples are shown in Fig. 2. For instance, crispine contain a benzene ring attached to the piperidine ring. Jamtine and erythraline, in addition, have a cyclohexane ring attached to pyrrolidine. In elaecarpaceae a phenanthrene ring is attached to a piperidine ring. In nuevamine, two benzene rings are attached to the piperidine and pyrrolidine rings.

After developing a convenient method for synthesizing lamellarins containing a partially oxidized indolizidine unit, we thought of synthesizing benzoindolizidine.

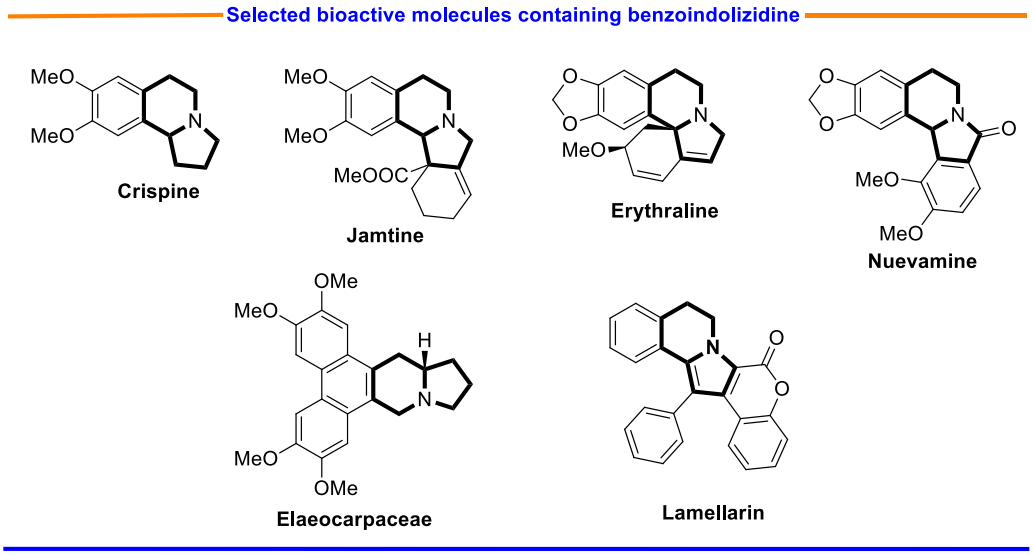

Figure 2. Selected examples of benzoindolizidine alkaloids

Since the benzoindolizidines are of two types where one contains only one benzene ring attached, and the other includes two benzene rings attached, we have divided our synthesis into two sections. Also, the precursors required for these alkaloids require different starting substrates. The first section deals with the synthetic studies towards pyrrolo[2,1-*a*]isoquinoline alkaloids, and the second section deals with synthetic studies of isoindolo[1,2-*a*]isoquinoline compounds. Further, in the third section of this chapter *insilico* molecular docking studies of pyrrolo[2,1-*a*]isoquinoline alkaloids against SARS-CoV-2 viral proteins are described.

Section I: Synthetic studies towards pyrrolo[2,1-*a*]isoquinoline alkaloids

2.I.1 Introduction:

The current section summarizes the isolation, bioactivity, and literature methods developed by researchers across the globe towards pyrrolo-[2,1-*a*]isoquinoline type of natural products followed by a detailed description of our work on the synthesis of it. Many naturally occurring compounds are found to have pyrrolo[2,1-*a*]isoquinoline skeleton in them, for example, crispine A, crispine B, trolline, oleracein E, mescalotam, harmicine**,** MCN-4612-Z, etc. (Figure 1).

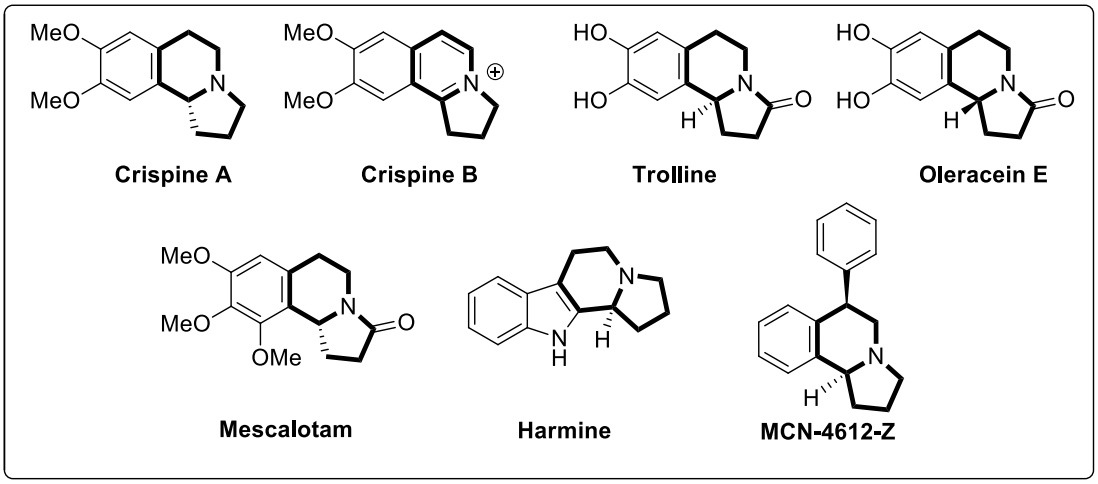

Figure 1: Naturally occurring pyrrolo-[2,1-*a*]isoquinoline compounds

2.I.1.1 Isolation:

1) Crispine A and B: Crispine A and B were isolated by a team of Chinese scientists Zhang et al.[1] in 2002 from the ethanol fraction of *Carduus crispus* L. This plant is a Chinese folk medicine used for the treatment of cold, stomach ache, and rheumatism. Due to the excellent medicinal properties of this plant, scientists worked on the isolation of the main active ingredients. They extracted five compounds from it, out of which two had pyrrolo[2,1-*a*]isoquinoline skeleton and was named crispine A and crispine B.

2) Trolline and Oleracein E: In 2004, Cai[2] and co-workers isolated trolline from the ethanol extracts of the flowers of T. *Chinensis* Bunge. This plant belongs to the family of

ranunculaceae, and it is a common plant found all across China. It is effective against respiratory infections, pharyngitis, tonsillitis, and bronchitis. Also, Zhao and Ding[3] isolated this compound from another plant, *Salsola collina* Pall, and named it Salsoline A which after the analytical study proved to have same the same structure.

On the other hand, another isomer Oleracein E was isolated from *Portulaca oleracea* L. by Du[4] and his team in 2005. Purslane (*Portulaca oleracea*) is an ancient medicine used as diuretic, febrifuge, antiseptic, antispasmodic, and anthelmintic. In 2009, Zhang co-workers[5] isolated the same compound from Meconopsis integrifolia (Maxim.) Franch. Its molecular formula, structure elucidation was done by ^{1}H NMR, HRMS, and optical rotation study showed it is an antipode compound of trolline.

3) Mescalotam: It was isolated well before the isolation of crispine, and trolline, by Kapadia and Fales[6] from the plant *Lophophora williamsii*, generally known as Peyote.

4) Harmicine: It belongs to the class of *β*-carboline indolizidine family. It was isolated in 1997 by Kam and co-workers.[7] It was isolated from the leaves of the Malaysian plant, *Kopsia Griffithii,* in optically pure form. Its structure was confirmed by spectroscopic methods like UV, IR, MS, and NMR.

2.I.1.2 Biological activities:

These compounds show a wide range of biological activities that make them essential molecules in the heterocyclic family. Chinese people used their parent plants for many medicinal uses in ancient times. According to the compounds, some of the biological activity descriptions are given below in the tabular form.

Table 1. Bioactivities of pyrrolo[2,1-*a*]isoquinoline compounds

Naturally occurring indolizine compounds	Bioactivity
Crispine	Cytotoxic activity of the natural products crispine A and crispine B on SKOV3, KB, and HeLa human cancer cell lines have been tested in a sulforhodamine B (SRB) assay. (+) - Crispine A has been tested as a potential ligand for the

	human dopamine receptors D1, D2L, D4, and D5.[8]
Trolline	The antibacterial and antiviral activities of (-)-trolline were tested *in vitro* antibacterial experiments with the Gram-negative bacterial strains *Klebsiella pneumoniae* 02-63, *Pseudomonas aeruginosa* 02-123, and *Haemophilus influenzae* 02-102 and the Gram-positive bacterial strains *Staphylococcus aureus* 01-159, *Streptococcus pneumoniae* 02-19, and *Streptococcus pyogenes* M1371 and showed significant inhibitory activity.[9] Exhibits moderate antiviral activity against influenza virus A (JF 190-15).[9]
Oleracein E	A potent DPPH free radical scavenging activity and a strong inhibitory activity on hydrogen peroxide-induced lipid peroxidation in rat brain. Regarded as an antioxidant.[9]
Mescalotam	No biological activity recorded to date.
Harmicine	In preliminary screening, it showed strong antileishmanial activity. Exhibits antinociceptive activity.[10]
MCN-4612-Z	Shows antidepressant activity.[11]

Due to their wide biological activities and less abundance for advanced studies, scientists have developed many synthetic routes to make these molecules.

2.I.2 Literature review:

Ulrich Pässler and Hans-Joachim Knölker have published a chapter in a book in 2011 wherein the various synthetic routes developed are reviewed.[12] The current section describes the distinct synthetic pathways disclosed after 2010.

An iminium ion cyclization strategy is used by Hurvois and co-workers[13] for the syntheses of both enantiomers of crispine A (Scheme 1). The starting enantiomers of α-amino nitrile derivatives were subjected to nucleophilic substitution reaction in the presence of strong metal alkali base like LDA with 2-(2-iodoethyl)-1,3-dioxolane. Reductive decyanation of

the corresponding addition product using sodium borohydride, followed by catalytic hydrogenation using Pearlman's catalyst, gave the 1,3-dioxolane substituted tetrahydroisoquionoline derivatives. Hydrolysis of acetal with 10% HCl in THF led to the iminium ion cyclized product, which upon reduction using sodium cyanoborohydride gave (-)-crispine A in overall good yields. The same strategy was also used to synthesize the antipode of (-)-crispine A.

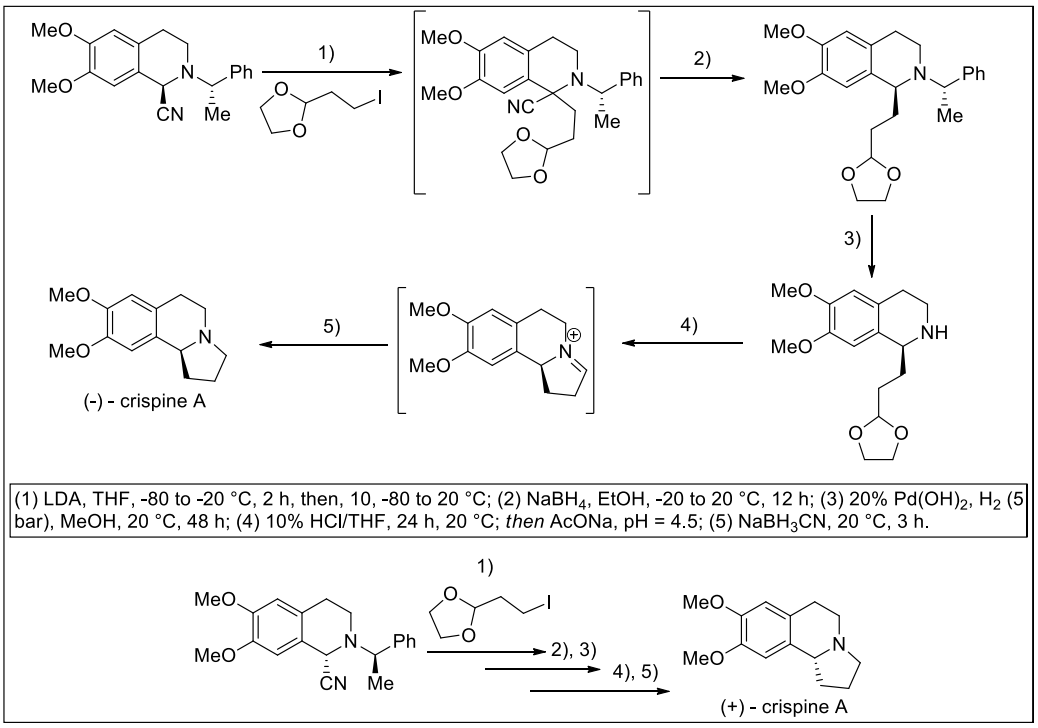

Scheme 1. Iminium ion cyclization reaction strategy to synthesize (+)/(-)-crispine A

Wang and co-workers[14] have shown a systematic construction of indolizidine core using Henry reaction for the synthesis of β-nitroalcohols. They have prepared around 20 derivatives with good enantiomeric ratios bearing various substituents on benzaldehyde. They used their key step to synthesize 2-nitro-1-phenylpropan-1-ol from benzaldehyde and nitromethane. Subsequent catalytic hydrogenation of the nitro group and cyclo-condensation with levulinic acid led to the formation of lactum. The opening of the oxazole ring followed by Pictet-Spengler type cyclization was carried out using titanium tetrachloride. The saturated pyrroloisoquinoline ring structure was obtained by hydrogenation of the double bond. A surreal enantioselective synthesis of 5*R*,10*bR*-dimethyl pyrroloisoquinoline compound is achieved from the anti-selective Henry reaction (Scheme 2).

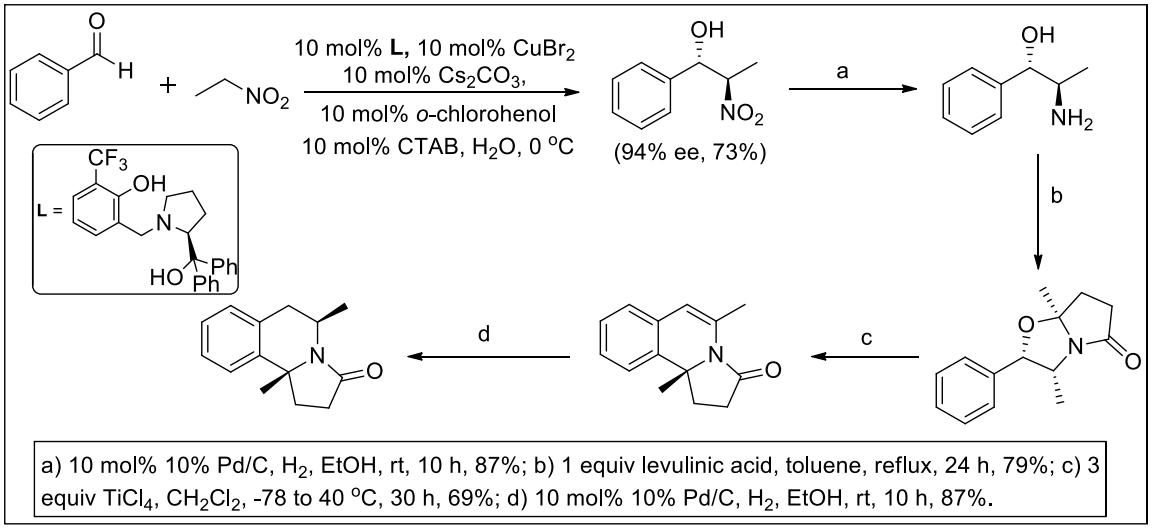

Scheme 2. Depiction of $CuBr_2$ catalyzed Henry reaction and construction of indolizidine core

A multicomponent reaction between α,β-unsaturated aldehyde, dihydroisoquinoline, and bromo methylpropionate surrogates was achieved using organocatalyst to construct optically active annulated indolizidine compounds by Jørgensen and co-workers.[15] (*S*)-2-(Diphenyl(trimethylsilyloxy)methyl)pyrrolidine was used as an organocatalyst in the presence of a mild base like sodium carbonate followed by the addition of phosphorane to give substituted α,β-unsaturated esters of annulated indolizidine compounds. Twelve derivatives with different substitutions on α,β-unsaturated aldehydes were prepared in good yields (Scheme 3).

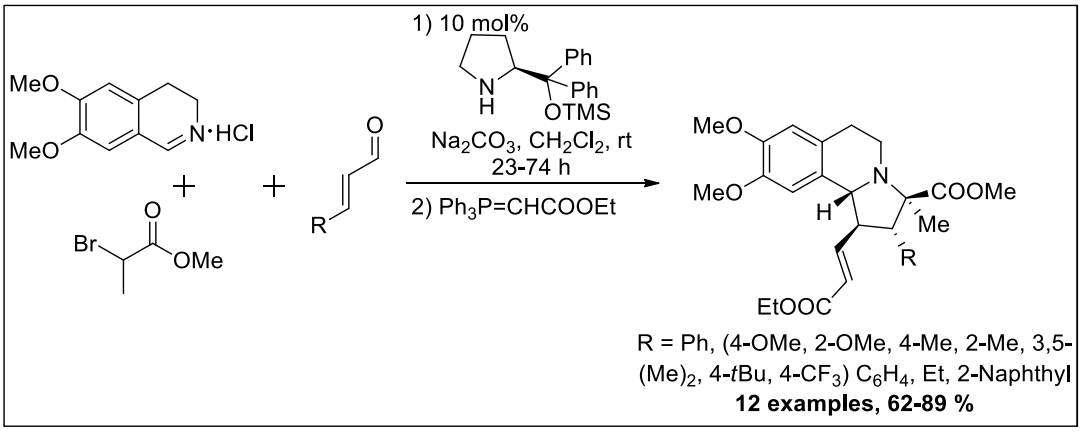

Scheme 3. One-pot construction of pyrrolo-[2,1-*a*]isoquinoline core using organocatalyst

One-pot synthesis of (*R*)–(+)-crispine A from (*R*)-*N*-sulfinyl amine by condensation with 4-chlorobutanal *via* Pictet-Spengler cyclization reaction is processed by Ruano and co-workers.[16] (*R*)-*N*-*p*-Tolylsulfinyl-2-(3,4-dimethoxy)phenylethylamine was prepared from

veratryl amine followed by $BF_3.OEt_2$ mediated Pictet-Spengler cyclization at a very low temperature to get *N*-sulfinyl chloro compound. Easy removal of sulfinyl group with HCl led to the formation of enantiopure (*R*)-(+)-crispine A in overall 55% yield (Scheme 4).

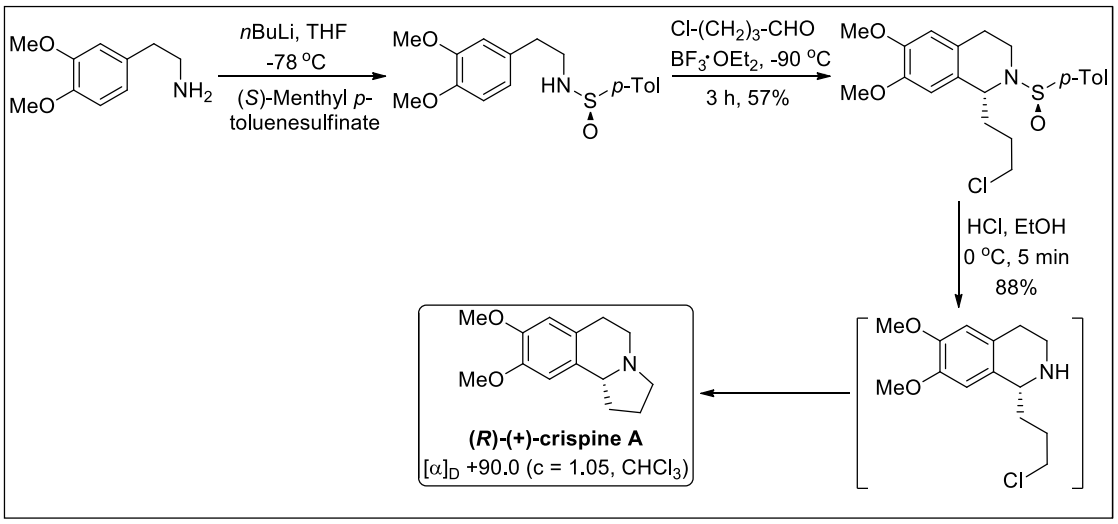

Scheme 4. Total synthesis of (*R*)-(+)-crispine A using Pictet-Spengler cyclization reaction

Knölker and his group[17] showed a very effective silver(I)-promoted oxidative cyclization of α-propalgyl substituted tetrahydroisoquinoline to annulated indolizidines. They have demonstrated the formation of (±)-crispine A by hydrogenation of pyrrole ring. Starting from commercially available homoveratryl amine they prepared 1-propalgyl substituted tetrahydroisoquinoline by first construction of dihydroisoquinoline by refluxing with ethyl formate and then adding (3-(trimethylsilyl)prop-2-yn-1-yl)magnesium bromide at C1 position to get the important synthon for their cyclization step. In this reaction, they got 1-propargyltetrahydroisoquinoline and the 1-allenyltetrahydroisoquinoline (ratio = 61: 2). Further, silver(I) promoted oxidative cyclization of the mixture gave dihydropyrroloisoquinoline moiety. Rh/C catalyzed hydrogenation of pyrrole compound gave (±)-crispine A in good yield (Scheme 5).

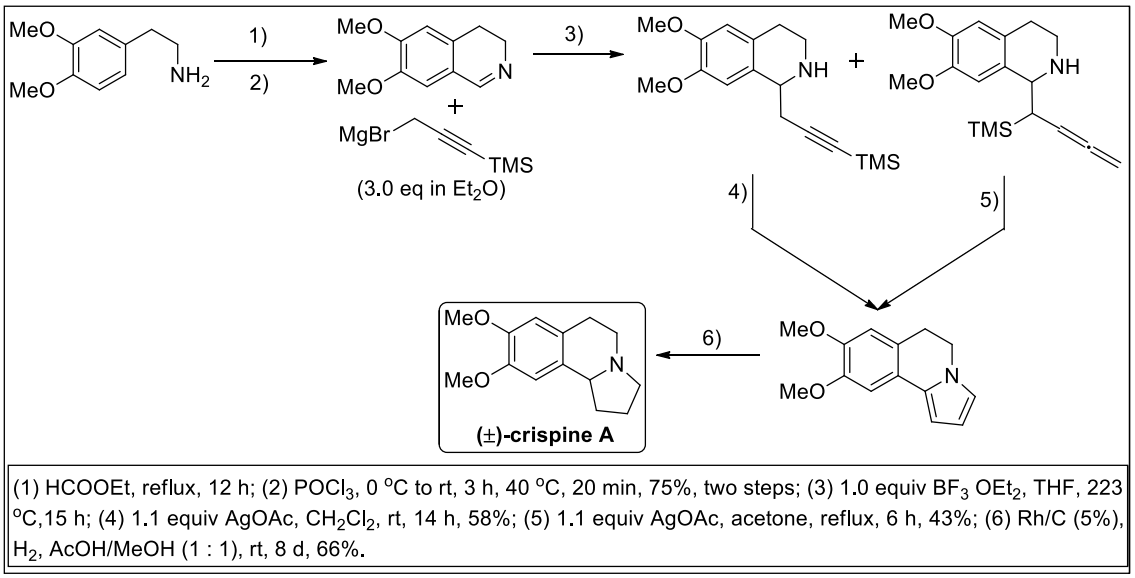

Scheme 5. Total synthesis of (+)-crispine A using silver(I)-promoted oxidative cyclization of α-propalgyl substituted tetrahydroisoquinoline

Subba Reddy et al.[18] have shown the process for the preparation of (-)-crispine A, salsolidine, and benzoquinolizidine with the help of a stereoselective addition of Grignard reagent to chiral *N*-sulfinyl imine. To prepare (-)-crispine A, they begin with a known procedure to convert 2-(3,4-dimethoxyphenyl)ethanol to the corresponding chloroaldehyde and then formed its imine with (*R*)-*tert*-butanesulfinamide. This chloro imine compound led them to diversify their syntheses for (-)-crispine A and (-)-salsolidine. To prepare (-)-crispine A, a stereoselective addition of allyl magnesium bromide was done to get C1-allyl-*N*-sulfinyl tetrahydroisoquinoline product in a 9:1 diastereomeric ratio. This compound was further deprotected by removing the sulfinyl group in ethanolic HCl to get C1-allyl tetrahydroisoquinoline. Protection of free amine with Boc anhydride, followed by hydroboration of allylic double bond and oxidation using hydrogen peroxide gave required *N*-Boc tetrahydro isoquinoline alcohol moiety. The primary alcohol was converted to its mesylate using MsCl and later transformed into (-)-crispine A molecule with the help of TMSOTf in CH_2Cl_2 (Scheme 6).

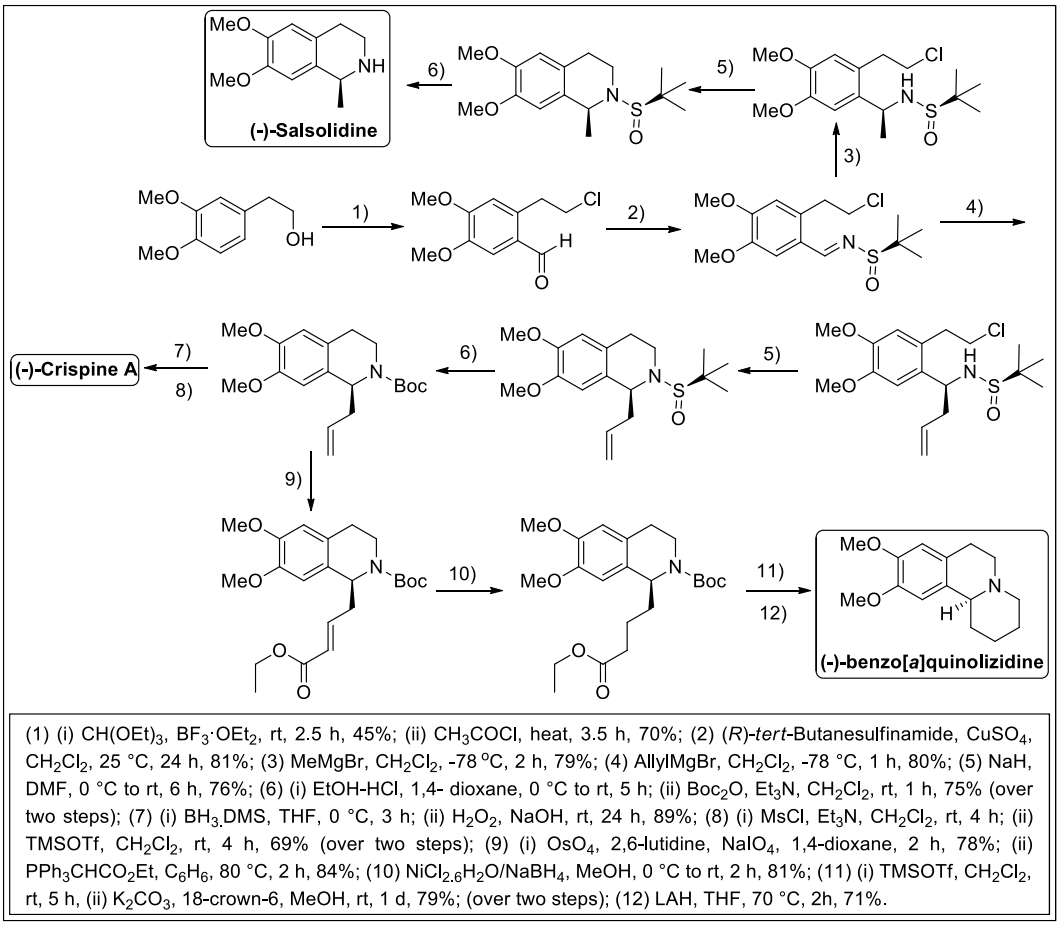

Scheme 6. Total syntheses of (-)-crispine A, (-)-salsolidine, and (-)-benzo[*a*]quinolizidine

An interesting synthetic route is described by Chittiboyina and co-workers[19] for the synthesis of (-)-crispine A. They have carried out a systematic synthesis of (-)-crispine A by implementing asymmetric Keck allylation and Pummerer cyclization as the key steps. Keck allylation of veratraldehyde was successfully used to convert it into homoallyl alcohol. This homoallyl alcohol was subjected to Mitsunobu reaction using diphenylphosphoryl azide and DBU to get a homoallyl azide compound. In one step, they successfully achieved tandem hydroboration–cycloalkylation to get the corresponding pyrrolidine which upon treatment with phenyl vinyl sulfoxide and triethylamine gave *N*-alkylated pyrrolidine compound. Pummerer cyclization of *N*-alkylated pyrrolidine with TFAA (in excess) helped achieve an annulated indolizidine ring in good yield. At last, Bu_3SnH and cat. AIBN in refluxing toluene mediated reductive radical elimination of thiophenyl group furnished (-)crispine A in overall 20% in 6 steps (Scheme 7).

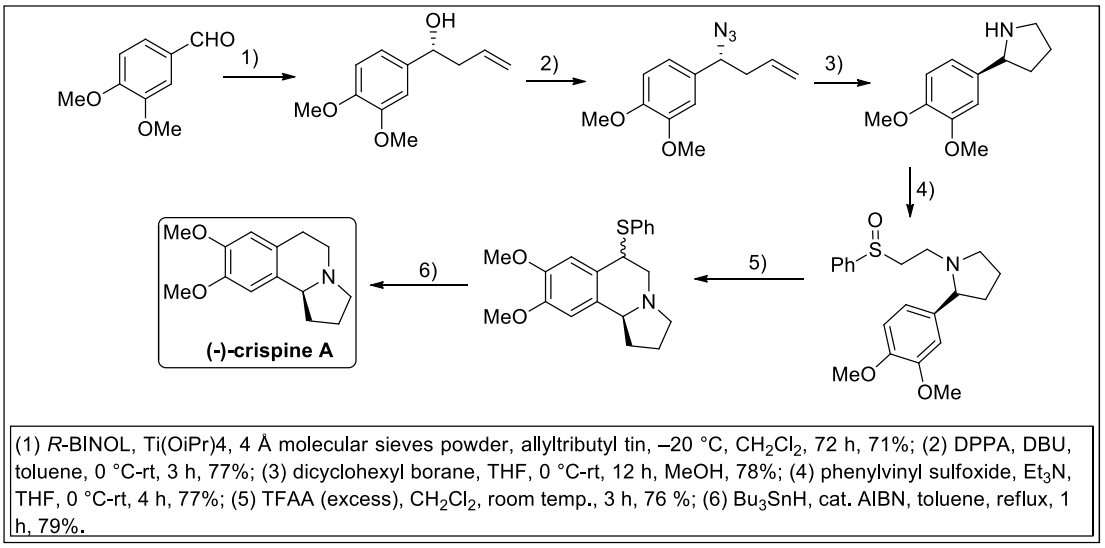

Scheme 7. Total synthsis of (-)-crispine A using asymmetric Keck allylation and Pummerer cyclization reactions

Multicomponent one-pot cascade constructions of C1-allyl tetrahydroisoquinoline and isoindolinones have been achieved by Singh and his group[20] *via* Lewis acid-catalyzed ring-forming reaction. They have demonstrated one C-C and two C-N bond formation events in one pot. This methodology was used for the construction of annulated indolizidine molecules like crispine A.

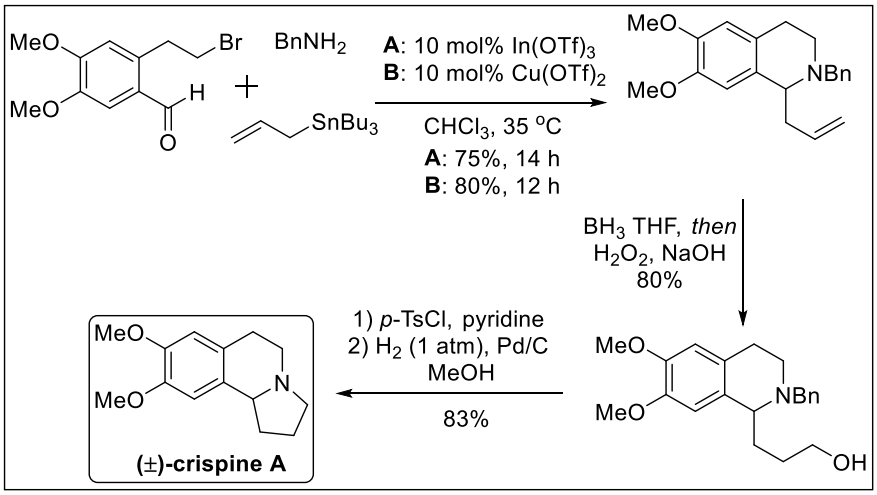

Scheme 8. Total synthesis of (±)-crispine A

They used two Lewis acids $In(OTf)_3$ and $Cu(OTf)_2$ to affect this cyclization. Precursor for the preparation of crispine A was constructed from 2-(2-bromoethyl)-4,5-dimethoxybenzaldehyde, benzylamine, and allyltributylstannane *via* two reagents. One

with $In(OTf)_3$ and the second with $Cu(OTf)_2$ gave C1-allyl-*N*-Bn tetrahydroisoquinoline in 75 and 80% yields, respectively. The allyl compound was converted to primary alcohol using hydroboration-oxidation reaction which was first tosylated and then hydrogenated to form (±)-crispine A in overall 66% yield (Scheme 8).

Weilong Lina and Shengming Ma[21] achieved a practical asymmetric synthesis of (+)-crispine A from commercially available starting materials. CuI catalyzed coupling of propargyl acetate with 6,7-dimethoxy-1,2,3,4-tetrahydroisoquinoline and benzaldehyde furnished 98% enantioselective isomer of C1-propargyl tetrahydroisoquinoline product. The propargyl alcohol obtained from propargyl acetate using KOH was converted to a δ-hydroxy amine by debenzylation and hydrogenation of triple bond using hydrogenation process. Chlorination with thionyl chloride, followed by cyclization, gave enantiopure (+)-crispine A in overall 39% yield in four steps (Scheme 9).

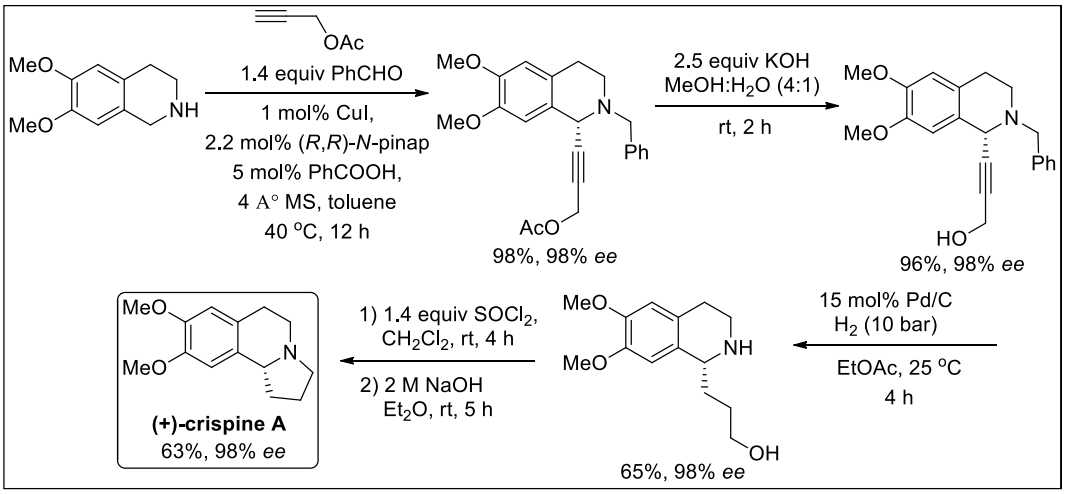

Scheme 9. Total synthesis of (+)-crispine A

Synthesis of trifluoromethylated analogs of harmicine and crispine A is shown by Pandey and Anbarasan[22] using CF_3TMS. One-pot cyclization of tryptamine- and phenethylamine-derived imides were achieved with the insertion of the CF_3 group at C1 position to construct monotrifluoromethylated harmicine and crispine A (Scheme 10).

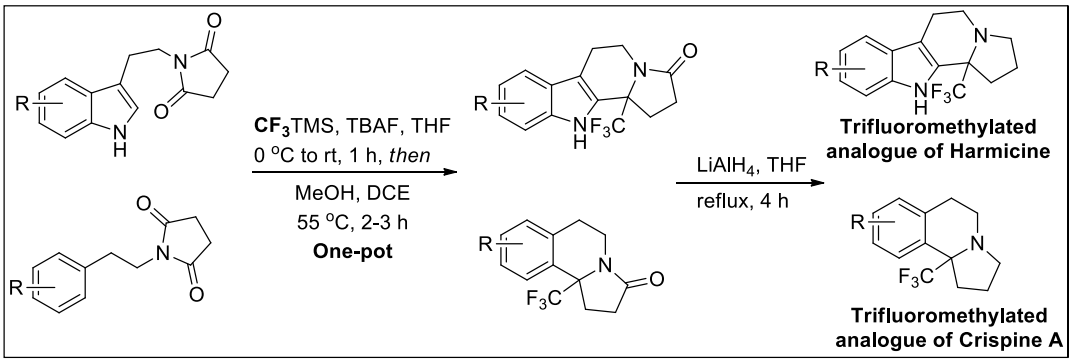

Scheme 10. Synthesis of trifluoromethylated analogs of harmicine and crispine A

Opatz and co-workers[23] reported a highly effective metal-free aerobic photocyanation of tertiary amines using Rose Bengal with TMSCN. They employed their method for the synthesis of (±)-crispine A. *N*-alkylated pyrrolidine was first synthesized from homoveratryl amine and succinic anhydride followed by $LiAlH_4$ reduction. With their developed methodology, they performed α-cyanation on pyrrolidine ring to get α-aminonitrile compound. Subsequently, $AgBF_4$ mediated in situ iminium ion formation followed by cyclization using TFA furnished (±)-crispine A in overall 70% yield in four steps (Scheme 11).

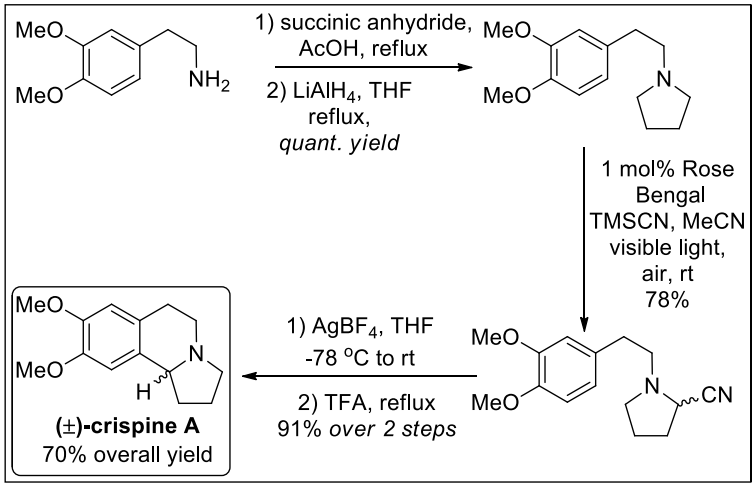

Scheme 11. Total synthesis of (±)-crispine A

Wang's group[24] has performed C-H allylation on *N*-acyl/sulfonyl tetrahydroisoquinolines to get α-allylated tetrahydroisoquinolines. They prepared various α-allylated tetrahydroisoquinoline surrogates and have shown the application to prepare (±)-crispine A.

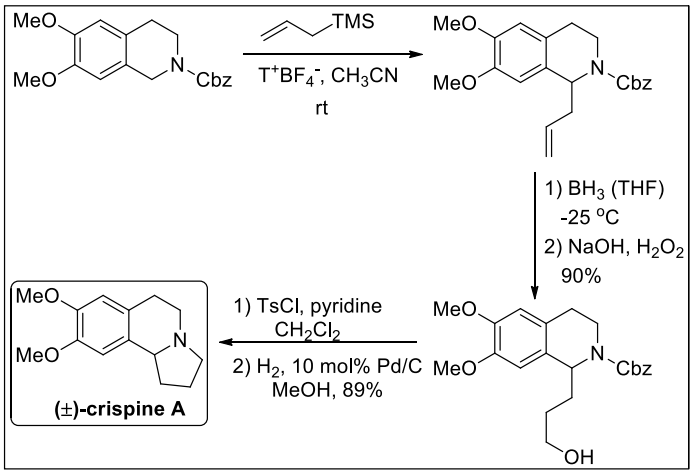

Scheme 12. Total synthesis of (±)-crispine A

N-Cbz protected 6,7-dimethoxy tetrahydroisoqinoline was subjected to direct C−H allylation using 2,2,6,6-tetramethylpiperidine-1-oxoammonium tetrafluoroborate ($T^{+}BF_4^{-}$) in acetonitrile at room temperature. Hydroboration of allylic double bond followed by tosylation of primary alcohol and hydrogenation gave cyclized indolizidine derived product (±)-crispine A (Scheme 12).

Ramanathan et al.[25] elaborated a precise methodological synthesis of isoindoloisoquinolinones, pyrroloisoquinolinones, and benzo[*a*]quinolizinones using TfOH. They have prepared numerous compounds of annulated tetrahydroisoquinolines. Respective imides of phenylethylamine surrogates with succinic anhydrides, phthalic anhydrides, glutaric anhydride were cyclized using excess TfOH and finally reduced with sodium borohydride or adding water to get corresponding pyrroloisoquinolinones, isoindoloisoquinolinones, and benzo[*a*]quinolizinones or hydroxyl derivatives. They synthesized a library of such compounds and even depicted many naturally occurring compound syntheses in their racemic form. They have shown synthesis of (±)-crispine A, (±)-trolline/oleracein E, (±)-erythrabine, (±)-mescalotam from their respective imides in excellent yields (Scheme 13).

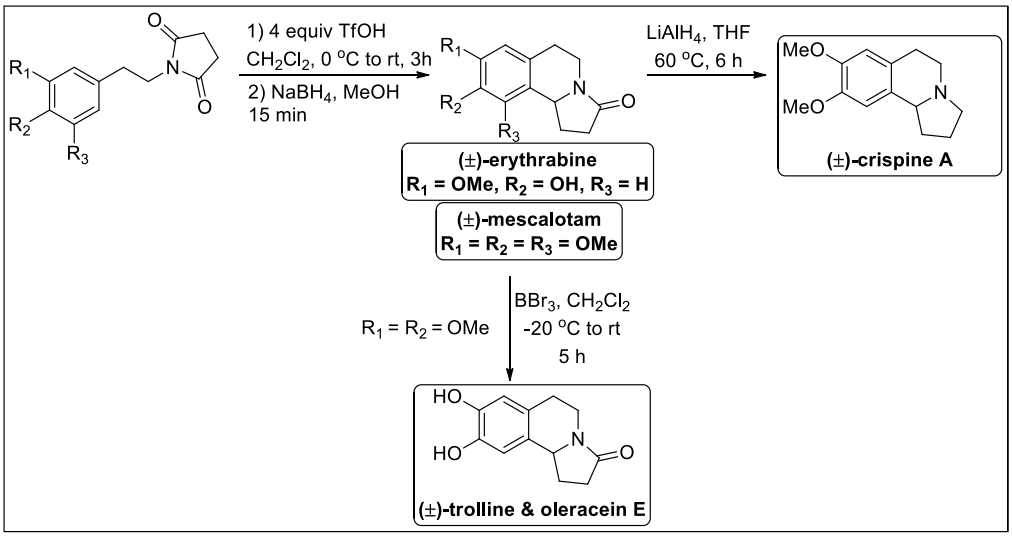

Scheme 13. Total syntheses of (±)-crispine A, (±)-trolline/oleracein E, (±)-erythrabine, (±)-mescalotam

Jebali et al.[26] have described the synthesis of pyrrolo[2,1-*a*]isoquinoline and pyrrolo[2,1-*a*]benzazepine derivatives *via* simple and efficient Bronsted acid-mediated intramolecular Friedel–Crafts cyclization. A cyclization reaction was used to build α,β-unsaturated lactam from phenylethylamine derivatives and ethyl (*Z*)-3-bromomethyl-4-oxo-4-phenylbut-2-enoate or ethyl (*Z*)-3-bromomethyl-4-oxopent-2-enoate which was subsequently further cyclized to pyrrolo[2,1-*a*]isoquinoline and pyrrolo[2,1-*a*]benzazepine moieties.

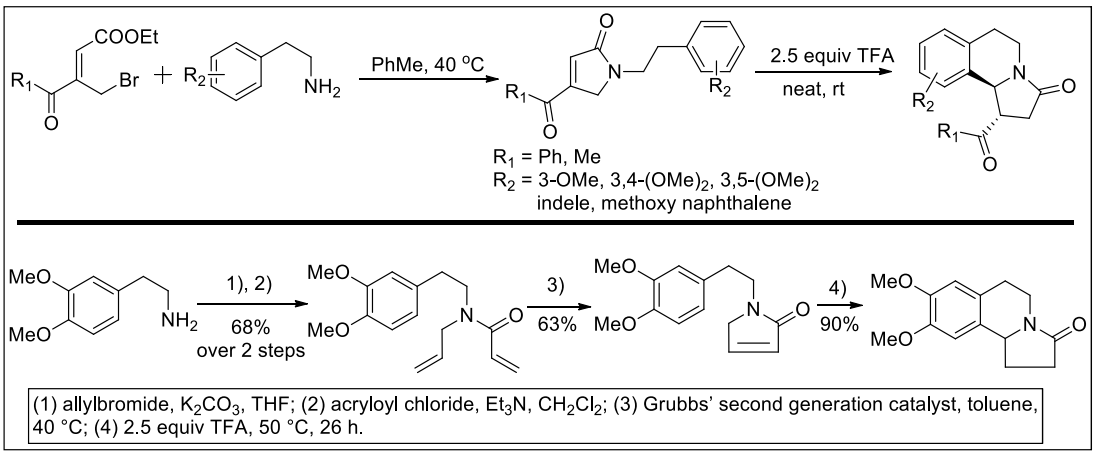

Scheme 14. Construction of pyrrolo[2,1-*a*]isoquinolinone compounds using metathesis reaction

Similarly, they have described the synthesis of oxo-crispine A molecule by starting from alkylation and acylation of homoveratryl amine with allyl bromide and acryloyl chloride to

get a tertiary amide. This amide was cyclized at the internal carbons of both the double bonds to get an α,β-unsaturated lactam, which was cyclized to get annulated indolizidine using excess TFA (Scheme 14). This same compound is a precursor for the synthesis of (±)-crispine A.

A direct α-alkylation to substituted *N*-phenyl tetrahydroisoquinoline reaction is developed by Pandey et al.[27] wherein starting synthon rely on nucleophilic substitution by alkyl selenide compound utilizing photoredox catalysis reaction. They have shown various substitutions at the C1 position of tetrahydroisoquinoline compounds with alkyl selenides proxies. As for the application purpose, they helped themselves with the synthesis of pyrrolo- and pyrido-tetrahydroisoquinoline scaffolds *via* intramolecular Csp^3–Csp^3 coupling as per their strategy. Substituted *N*-alkyl selenide tetrahydroisoquinoline was irradiated at 410 nm in acetonitrile in the presence of catalytic DMA (9,10-dimethoxyanthracene) to produce (±)-crispine A in 65% in one step, along with other tetrahydroisoquinoline compounds (Scheme 15).

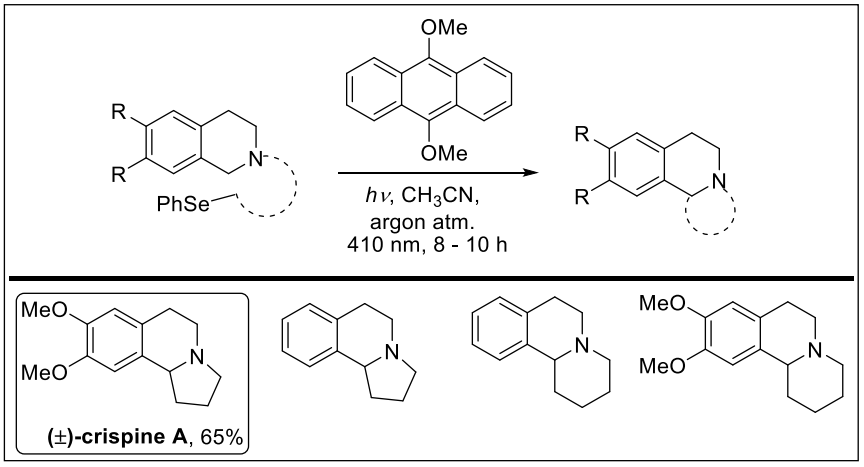

Scheme 15. Total synthesis of (±)-crispine A using α-alkylation to substituted *N*-phenyl tetrahydroisoquinoline

A formal synthesis of (±)-crispine A is described by Basavaiah's group[28] starting from commercially available 6,7-dimethoxy tetrahydroisoquinoline and 3-(acetoxymethyl)-2-methylenepropanoate (Baylis–Hillman acetate). The construction of benzo-fused and indole-fused indolizines was achieved via TBHP/CuBr promoted oxidative intramolecular cyclization strategy. They synthesized (±)-crispine A, by constructing a pyrrole ring from 6,7-dimethoxy tetrahydroisoquinoline by oxidative intramolecular cyclization using a

stoichiometric amount of CuBr and THBP to get 5,6-dihydro-8,9-dimethoxy-2-methoxycarbonylpyrrolo[2,1-*a*]isoquinoline. Further, hydrolysis of the ester with NaOH in refluxing methanol followed by decarboxylation and hydrogenation generated (±)-crispine A (Scheme 16).

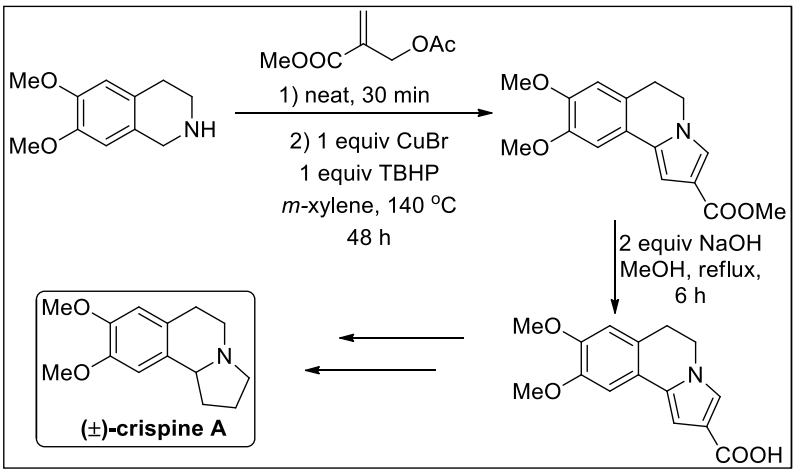

Scheme 16. Total synthesis of (±)-crispine A

Unprecedented asymmetric synthesis of hydroxyl annulated indolizidines is reported by Xu et al.[29] using $Cu(OTf)_2$ as a catalyst from tertiary enamide surrogates as synthons. Around 14 examples of 2-hydroxy-hexahydroindolizi-3-one compounds were prepared with good enantioselectivity (Scheme 17).

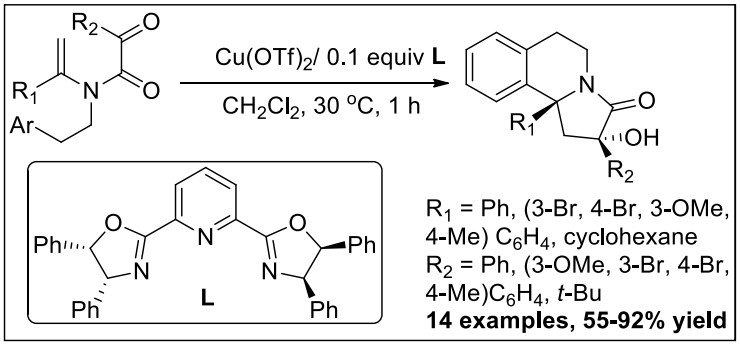

Scheme 17. One-pot construction of 2-hydroxy-hexahydroindolizi-3-one derivatives

Fandrick et al.[30a] have reported a copper-catalyzed asymmetric propargylation of substituted dihydroisoquinoline compounds using propargyl borolane as a propargyl source. With context to this, they have shown the synthesis of naturally occurring (-)-(*S*)-crispine A and (-)-(*S*)-harmicine using their strategy. Respective dihydroisoquinoline

substrates were coupled with propargyl borolane compound showing excellent productivity. The TMS deprotection of corresponding C1-propargylated compounds using a mild base like K_2CO_3 in methanol was performed, which were later cyclized using catalyst reported by Schafer and co-workers[30b] through intramolecular reductive hydroamination cyclization reaction to form indolizidine ring i.e., (-)-(*S*)-crispine A and (-)-(*S*)-harmicine (Scheme 18).

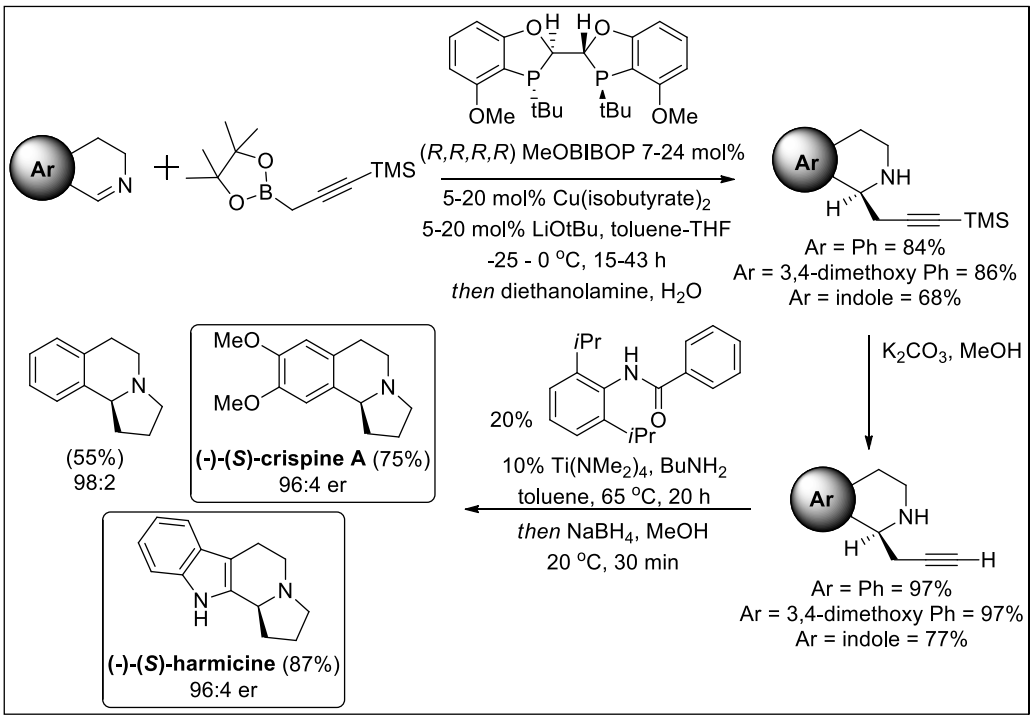

Scheme 18. Total syntheses of (-)-(*S*)-crispine A and (-)-(*S*)-harmicine

Murai et al.[31] have described the oxidative transformation of spiro compounds to fused tricyclic compounds. They have reported the oxidative rearrangement of spiro tetrahydroisoquinolines into fused indolizidine using a simple chlorinating agent like *N*-chlorosuccinimide followed by a nucleophilic attack.

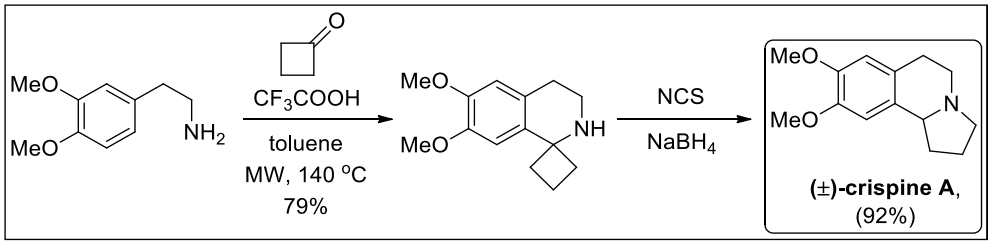

Scheme 19. Total synthesis of (±)-crispine A

Synthesis of (±)-crispine A is shown starting from homoveratryl amine. The corresponding amine was cyclized with cyclobutanone to form the required spiro compound which further upon standard conditions was converted to fused indolizidine (±)-crispine A (Scheme 19). Coldham and co-workers[32] have studied lithiation reaction of *N*-Boc protected substituted tetrahydroisoquinolines followed by electrophilic substitution. They have subjected various bromo-alkyl/alkyne compounds to corresponding lithiated tetrahydroisoquinolines to get C1-substituted tetrahydroisoquinoline compounds. Similarly, they have synthesized the racemic form of crispine A. The required *tert*-butyl 6,7-dimethoxy-3,4-dihydroisoquinoline-2(*1H*)-carboxylate was treated with 1.2 equiv *n*BuLi at -50 ^{o}C, subsequently reacting the corresponding anion with 1,3-dibromopropane gave C1-substituted *tert*-butyl 1-(3-bromopropyl)-6,7-dimethoxy-3,4-dihydroisoquinoline-2(*1H*)-carboxylate. The resultant bromo compound was deprotected then cyclized using CF_3COOH to furnish (±)-crispine A (Scheme 20).

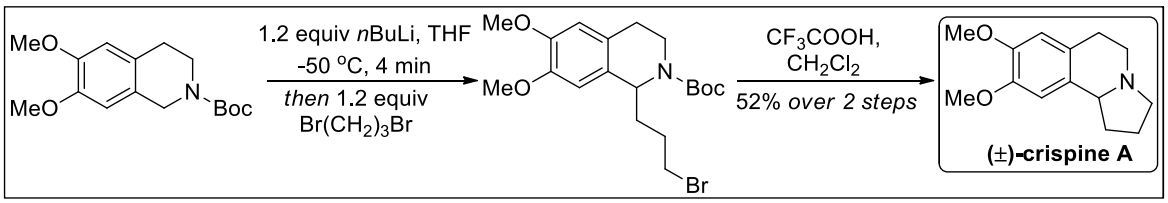

Scheme 20. Total synthesis of (±)-crispine A

Again from the lab of Ramanathan,[33] the iminium ion cyclization strategy is studied on unsymmetrical succinimides to synthesize 1 or 2 alkylsubstituted pyrroloisoquinolinones and indolizinoindolones (Scheme 21).

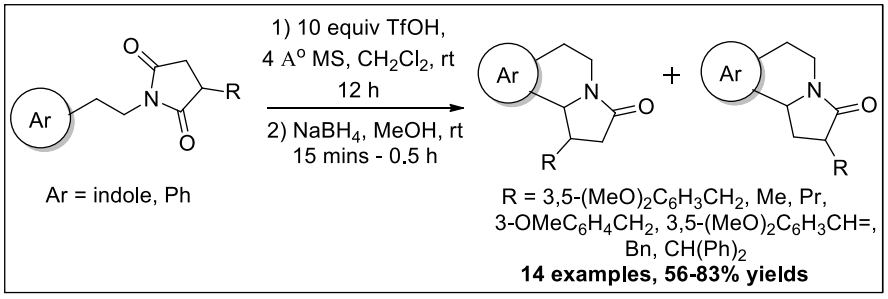

Scheme 21. Iminium ion cyclization strategy to construct pyrrolo[2,1-*a*]isoquinolinone compounds

Carretero and co-workers[34] have reported a highly enantioselective method to synthesize

pyrrolo[2,1-*a*]isoquinoline derivatives using three-step sequential reactions. The key step of their approach is the Cu catalyzed stereoselective pyrrolidine formation from azomethine ylide 1,3-dipolar cycloaddition between *ortho*-alkynylaryl α-iminoester and *N*-methyl melimide or *trans*-bissulfonylethylene substrates. Using this method, they synthesized several pyrrolidine compounds, which were further converted to indolizidines using reduction amination-enamine reduction using a gold catalyst (Scheme 22).

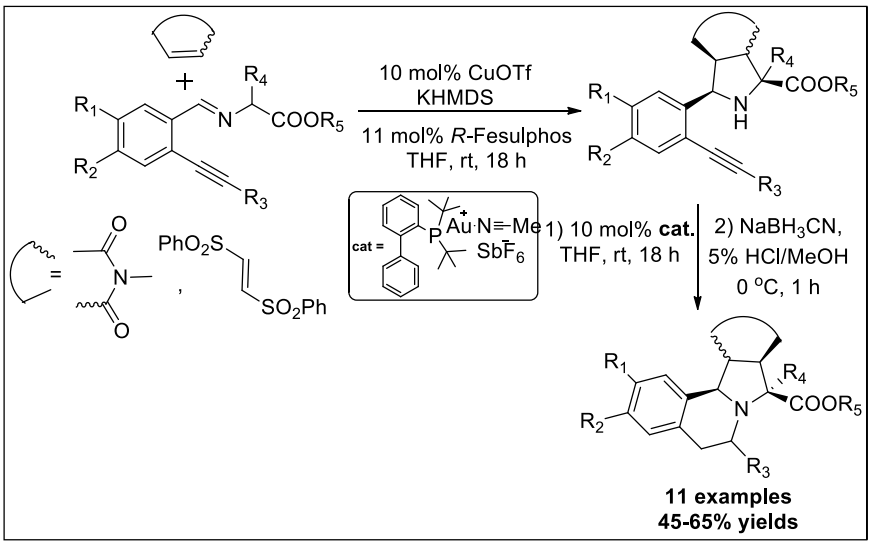

Scheme 22. Enantioselective method to synthesize pyrrolo[2,1-*a*]isoquinoline derivatives

Chiang et al.[35] have developed a method to synthesize asymmetric 1,2-allylation of *N*-Ts- and *N*-Ns-aldimines using Rh (I) catalyst. This methodology was further executed for the synthesis of (-)-crispine A. The enantioselective addition of potassium allyltrifluoroborate with aldimine compound under the optimized condition using Rh (I) catalyst and respective ligand under refluxing toluene afforded corresponding tertiary amine adduct. The tosyl group was later exchanged with the Boc group using *N*-Boc protection and *N*-Ts deprotection reactions. Desilylation of OTBS group with TBAF afforded the hydroxyl compound, which upon mesylation reaction followed by cyclization using sodium hydride gave C1-allyl-*N*-Boc tetrahydroisoquinoline moiety. Hydroboration of allylic double bond then, tosylation of hydroxyl group and deprotection cyclization gave (-)-crispine A in overall 32% yield with 97% *ee* (Scheme 23).

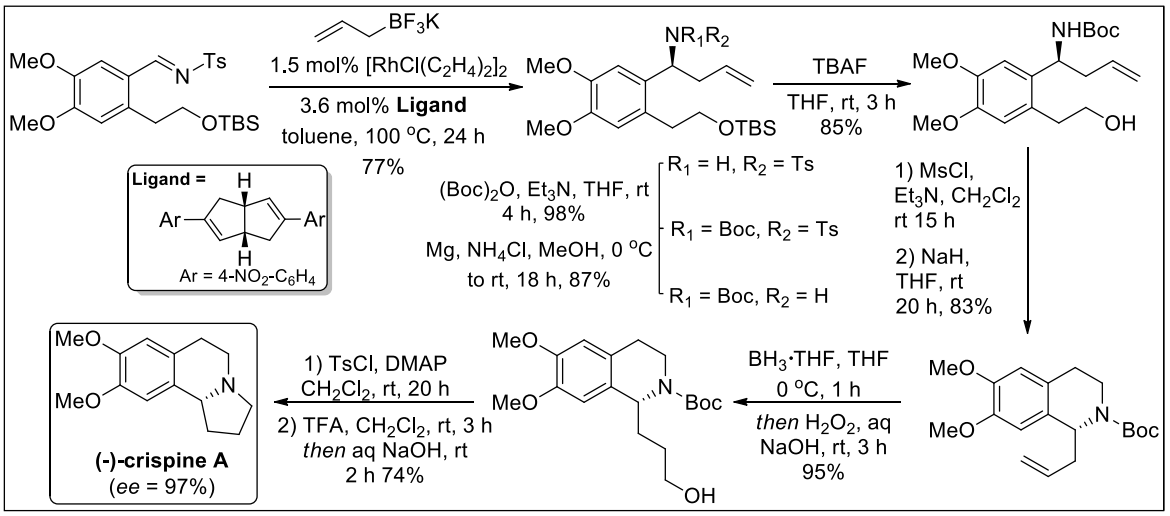

Scheme 23. Total synthesis of (-)-crispine A

Weilong Lina and Shengming Ma[36] have especially focused on constructing enantiopure (-)-trolline and (+)-oleracein E in their work. One-pot construction of *(S)*-propagylic amine from 6,7-dimethoxy tetrahydroisoquinoline, benzaldehyde, and 2-methyl-3-butyn-2-ol using CuI and (*R,Sa*)-*N*-pinap as the chiral catalyst. Later removal of 2-hydroxy-2-propyl group followed by reaction with methyl carbonochloridate and *n*BuLi gave corresponding *(S)*-propagylic ester amine compound. The debenzylation of amine using catalytic hydrogenation followed by cyclization in refluxing toluene gave methyl derivative of (-)-trolline. The (-)-trolline was achieved by demethylating its methyl derivative using BBr_3 in overall 41% yield and 95% *ee*. The same strategy was used to synthesize (+)-oleracein E by changing the chiral catalyst to (*R,Ra*)-*N*-pinap. (+)-Oleracein E was achieved in 39% overall yield and 96% *ee* enantiopurity after demethylation step (Scheme 24).

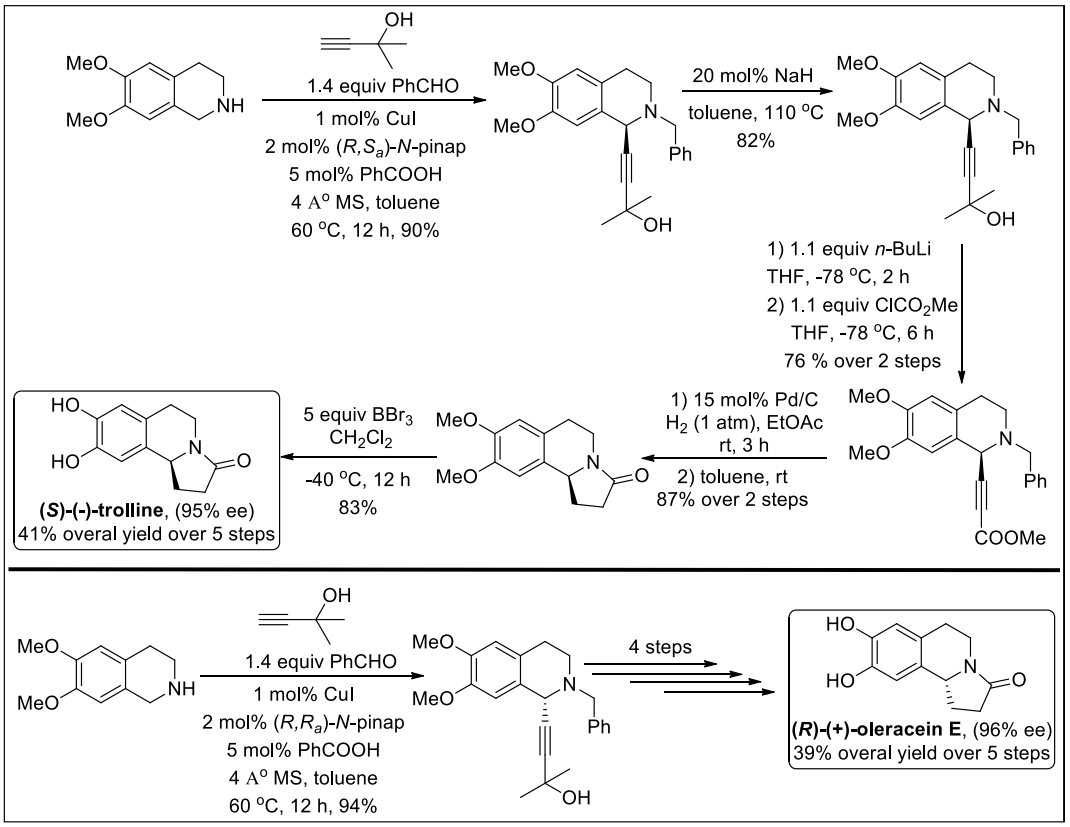

Scheme 24. Total syntheses of (*S*)-(-)-trolline and (*R*)-(+)-oleracein E

Aranzamendi et al.[37] have shown an organolithium addition-chiral intramolecular α-amidoalkylation to *N*-phenethylimides in the presence of 1,1'-bi-2-naphthol (binol)-derived Brønsted acids. They have not demonstrated any synthesis of naturally occurring compounds but have synthesized many pyrroloisoquinolinones and isoindoloisoquinolinones derivatives (Scheme 25).

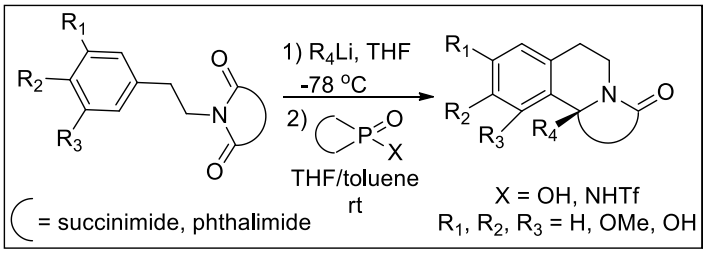

Scheme 25. Construction of pyrrolo[2,1-*a*]isoquinolinone compounds using organolithium addition-chiral intramolecular α-amidoalkylation

Sun and his group[38] have synthesized (+)-crispine A starting from commercially available homoveratryl amine. They have synthesized *N*-*tert*-butanesulfinyl aldimines in water in the presence of Amberlyst-15 catalyst, prompting it as one of the key intermediates in the

synthesis of (+)-crispine A. Homoveratric acid was converted to its methyl ester followed by formylation using dichloromethyl methyl ether in the presence of $AlCl_3$. The resultant aldehyde was condensed with *(S)-N*-tertbutanesulfinamide followed by allylation reaction in one pot to get homoallylic amine. In acidic conditions, homoallylic amine was converted to lactum *via* deprotection cyclization reaction sequence. $LiAlH_4$ reduction of lactum and hydroboration of terminal methylene group of allylic double bond helped to construct the third ring to build (+)-crispine A in overall 32% yield using Appel reaction in the later step (Scheme 26).

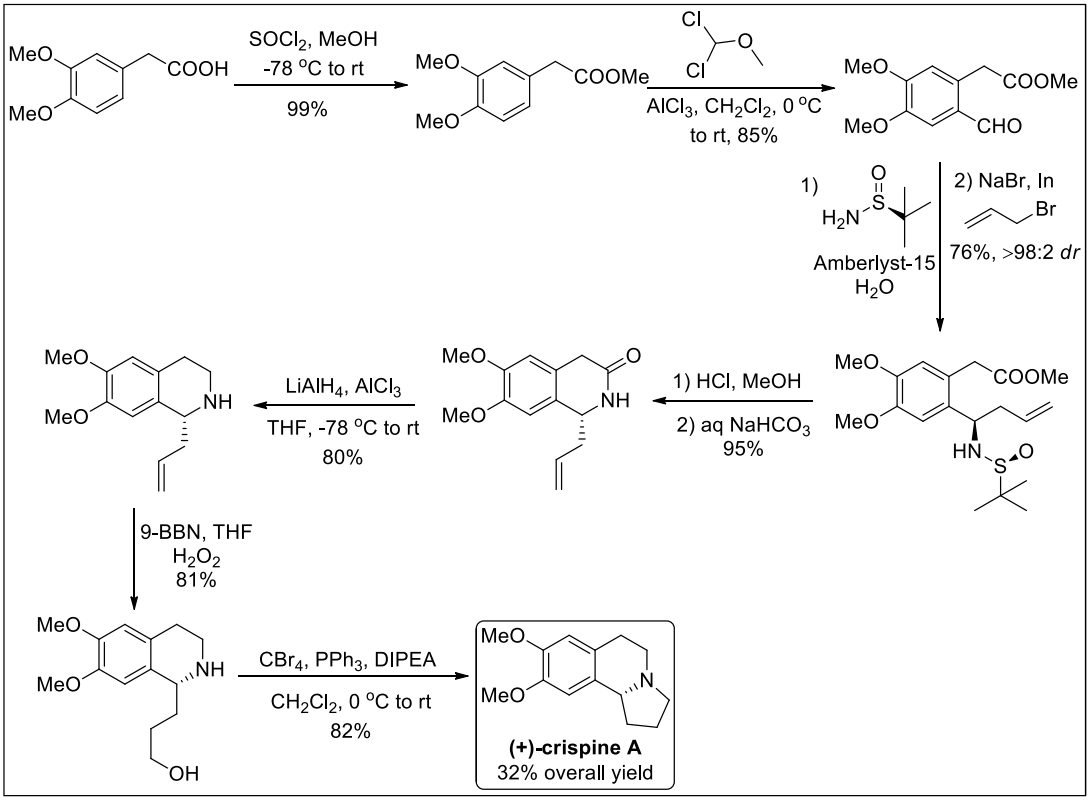

Scheme 26. Total synthesis of (+)-crispine A

Varlamov and co-workers[39] have shown a facile synthesis of 1-oxo-pyrrolo[2,1-*a*]isoquinolines from 1-aroyl-3,4-dihydroisoquinolines and alkynes. From solvent study optimization, toluene was found to be the best solvent, they prepared 11 novel compounds. As per their proposed mechanism, a Michael addition to form a zwitterion type compound followed by aryl group rearrangement led to the formation of 1-oxo-pyrrolo[2,1-*a*]isoquinolines type compounds (Scheme 27).

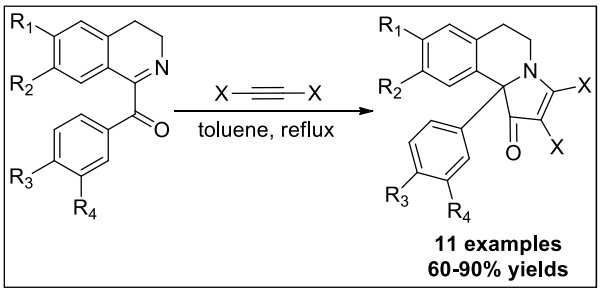

Scheme 27. Synthesis of 1-oxo-pyrrolo[2,1-*a*]isoquinolines

Pohmakotr and co-workers[40] have published a methodology for C1-difluoromethylation of tetrahydroisoquinolines using $TMSCF_2SPh$ as a nucleophile and ($TEMPO^+BF_4^-$) as an oxidant. These compounds were further explored to synthesize *gem*-difluoromethylenated pyrrolo[2,1-*a*]isoquinoline compounds using tributyltin hydride and AIBN. They have synthesized over 11 derivatives of *gem*-difluoromethylenated pyrrolo[2,1-*a*]isoquinoline and 6 of benzo[*a*]quinolizidine compounds (Scheme 28).

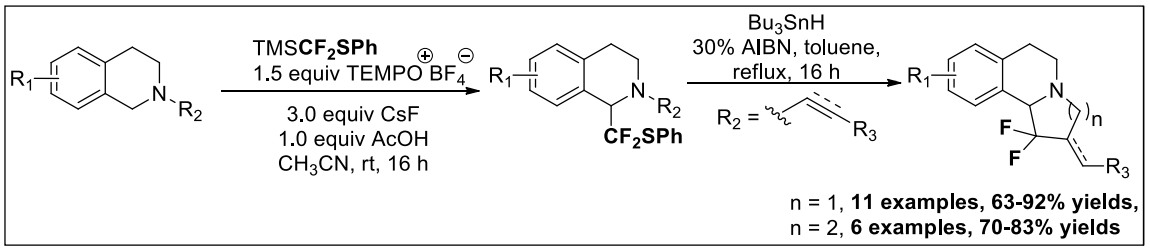

Scheme 28. Syntheses of *gem*-difluoromethylenated pyrrolo[2,1-*a*]isoquinoline derivatives

A multicomponent reaction between homoveratryl amine isocyanide, propylamine, acetic acid, and 4-chlorobenzaldehyde to give Ugi reaction amide adduct was formulated to synthesize benzoindolizidine alkaloids by Zidan *et al*.[41]

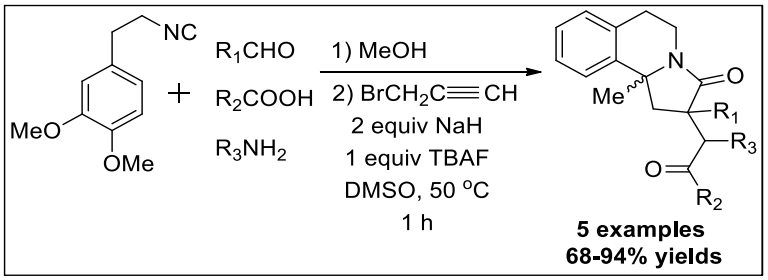

Scheme 29. Syntheses of benzoindolizidine alkaloids using Ugi reaction

This Ugi adduct was treated with propargyl bromide followed by reaction with TsOH gave pyrrolo-isoquinolinones proxies (Scheme 29).

Seidel,[42] with two others, has developed a methodology for the syntheses of pyrrolo[2,1-*a*]isoquinolines derivatives from tetrahydroisoquinolines and 2-(2-oxoethyl)malonates *via* benzoic acid-catalyzed redox-neutral annulation reaction (Scheme 30).

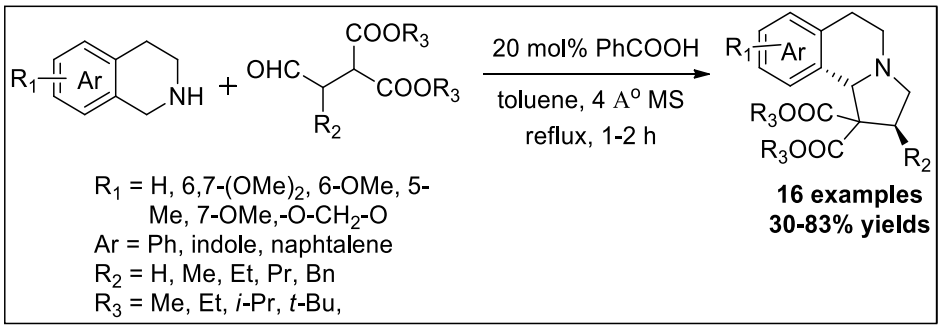

Scheme 30. Syntheses of pyrrolo[2,1-*a*]isoquinolines derivatives *via* benzoic acid-catalyzed redox-neutral annulation reaction

Argade and Kalshetti[43] have developed a synthetic route to synthesize pyrrolo[2,1-*a*]isoquinoline compounds resembling subincanadine alkaloids framework using acyliminium ion cyclization method. Starting from *N*-tosyl tryptamine, its corresponding imide was synthesized by treatment with a succinic anhydride derivative. Grignard reaction using MeMgBr followed by re-acetylation reaction helped them form a core for acyliminium cyclization step. The resulting hydroxyl amide was cyclized using TFA and subsequently reduced to an amino alcohol compound. This amino alcohol was converted to ketoamine using PCC which was further condensed with acetaldehyde in the presence of $TiCl_4$ to get α,β-unsaturated ketoamine compound. The stereoselective framework of subincanadin alkaloids was achieved in an overall 20% yield after 1,4 attack of Grignard reagent on corresponding α,β-unsaturated ketoamine compound (Scheme 31).

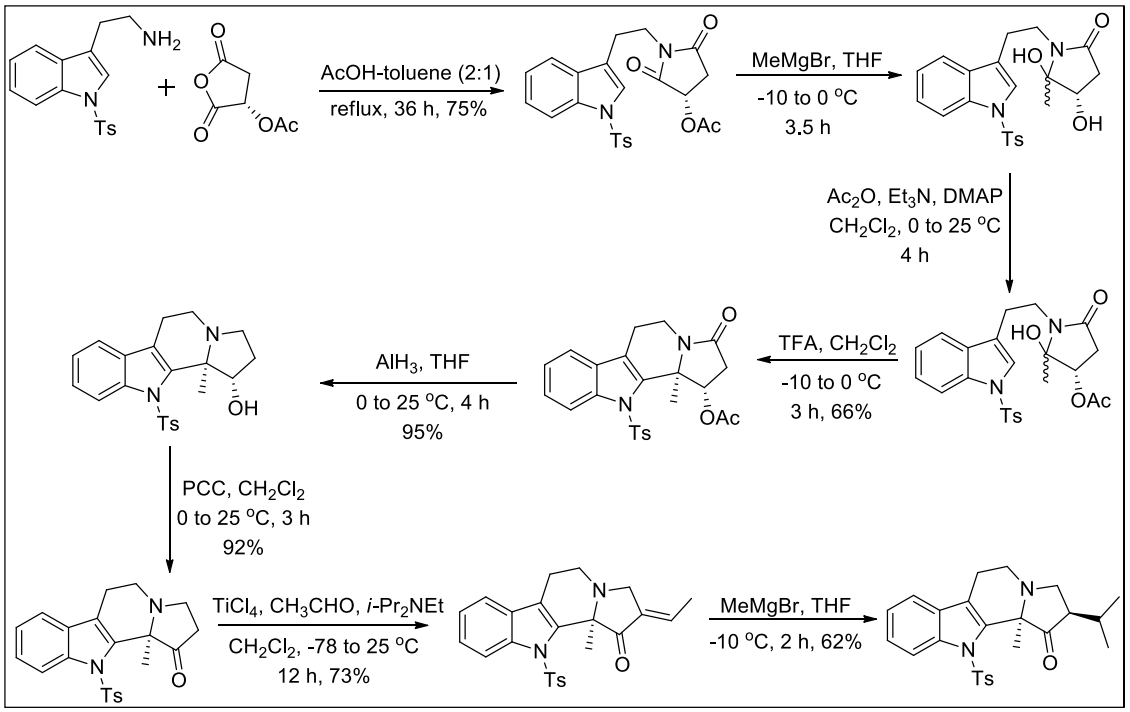

Scheme 31. Syntheses of pyrrolo[2,1-*a*]isoquinoline compounds resembling subincanadine alkaloids

A single diastereomeric aza-Nazarov cyclization reaction between 3,4-dihydroisoquinolines and α,β-unsaturated acyl chlorides has been published by Türkmen and co-workers[44] to construct α-methylene-γ-lactam compounds. Around eight *α*-methylene-γ-lactam compounds were prepared using catalytic silver triflate in refluxing acetonitrile (Scheme 32).

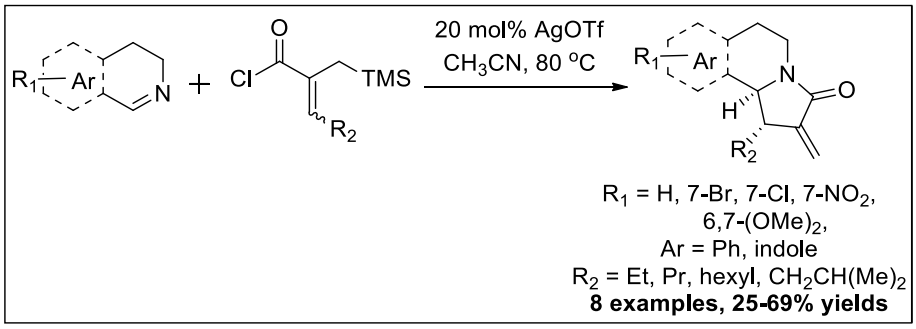

Scheme 32. Syntheses of α-methylene-γ-lactam derivatives *via* diastereomeric aza-Nazarov cyclization reaction

Hailes and co-workers[45] have developed a Pictet-Spengler reaction method to synthesize spiro compounds from various phenethylamine derivatives with unreactive ketones using phosphate buffers. The same strategy was utilized to construct trolline like compound from

dopamine and methyl levulinate using KPi buffer in refluxing methanol solvent (Scheme 33).

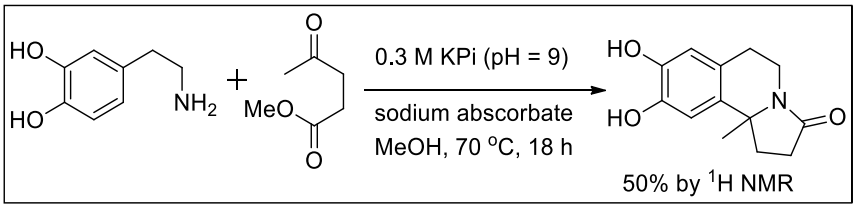

Scheme 33. Elaboration of Pictet-Spengler reaction to construct pyrrolo[2,1-*a*]isoquinoline derivative

A K-PHI photocatalyst catalyzed cyclization reaction was developed by Kurpil et al.[46] to construct pyrrolo[2,1-*a*]isoquinoline type compounds from simple tetrahydroisoquinoline and α,β-unsaturated ketone proxies (Scheme 34).

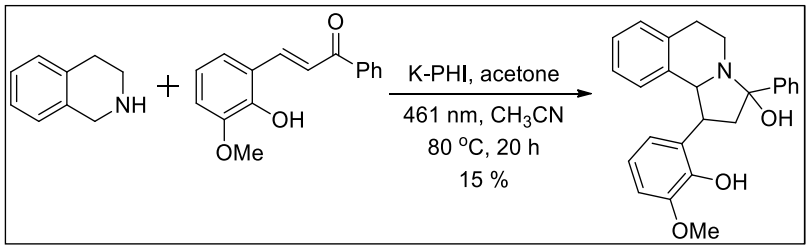

Scheme 34. Construction of pyrrolo[2,1-*a*]isoquinoline type compounds using K-PHI photocatalysts

Zhao and co-workers[47] have shown the construction of pyrrolo[2,1-*a*]isoquinolinone, isoindolo[1,2-*a*]isoquinolinone type compounds *via* cascade reaction between amine nucleophiles alkynoic acids using $AuPPh_3Cl/AgSbF_6$-catalysts in water.

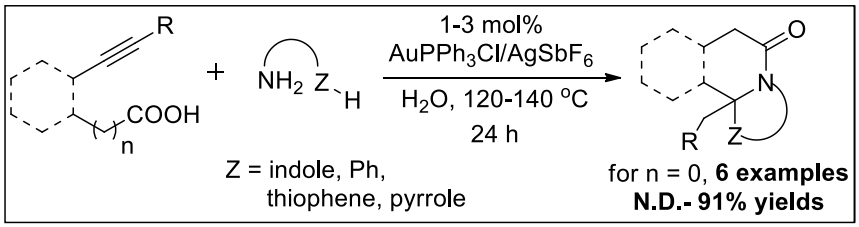

Scheme 35. Construction of pyrrolo[2,1-*a*]isoquinolinone, isoindolo[1,2-*a*]isoquinolinone type derivatives

This high step economic reaction results in the formation of various molecules just by

giving water as a side product. Their method is facile towards functional group tolerance, broad substrate scope, and low catalyst loading using a green solvent like water (Scheme 35).

From Bower's laboratory,[48] an excellent methodology is developed for the syntheses of pyrrolo[2,1-*a*]isoquinolinone and thieno[3,2-*g*]indolizinone compounds from cyclopropane urea compounds using rhodium-catalyzed temporary directing groups carbonylative C-C bond activation followed by Pictet-Spengler cyclization strategy (Scheme 36). For every step, they isolated and studied those compounds that led them to the tricyclic moieties.

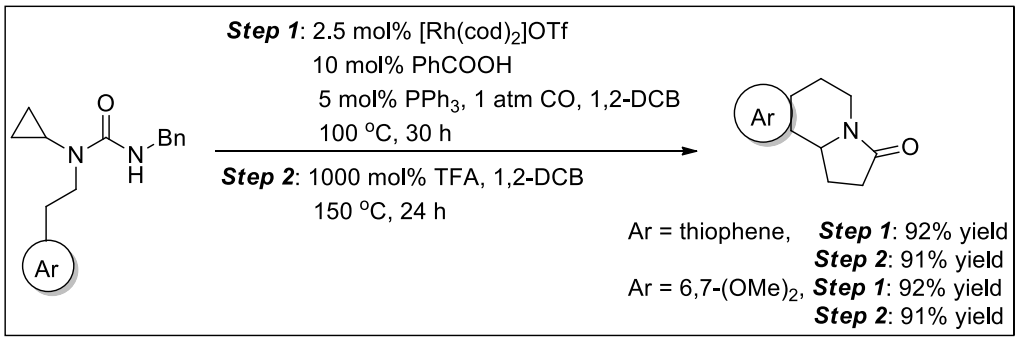

Scheme 36. Syntheses of pyrrolo[2,1-*a*]isoquinolinone and thieno[3,2-*g*]indolizinone derivatives using Pictet-Spengler reaction

Grellepois and co-workers[49] have synthesized cyclic, chiral *α*-trifluoromethylated *N,O*-acetals having a protected *cis*-diol moiety from Weinreb amide product of L-tartaric acid. A two-steps synthesis of tricyclic core was achieved using simple TfOH, 1,1,1,3,3,3-hexafluoro-2-propanol (HFIP) mediated Pictet-Spengler reaction from *O*-acetyl compound of *N,O*-acetal compounds. The methodology was further explored to synthesize various tetrasubstituted derivatives bearing CF_3 group at bridgehead position in the tricyclic ring structure in a *syn* addition manner (Scheme 37).

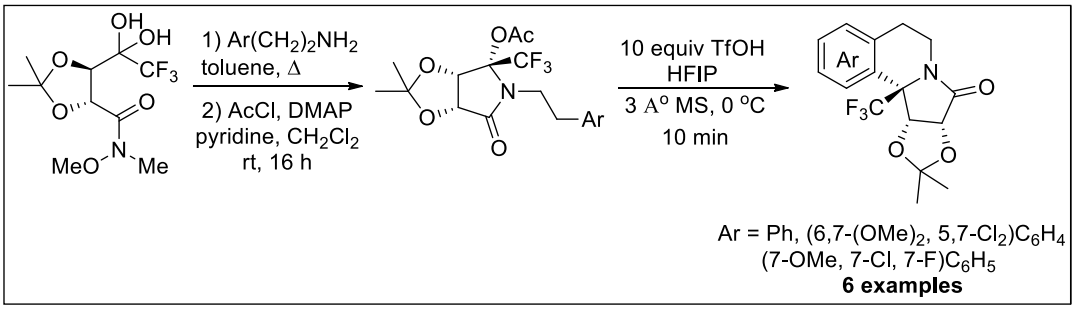

Scheme 37. Syntheses of chiral *α*-trifluoromethylated *N,O*-acetals pyrrolo[2,1-*a*]derivatives

Souquet et al.[50] have synthesized the racemic form of crispine A from 1-(3,4-dimethoxyphenethyl)-1*H*-pyrrol-2(5*H*)-one by treating it with 2 equiv of 12 M HCl in methanol followed by reducing the corresponding pyrrolo[2,1-*a*]isoquinolinone compound using lithium aluminium hydride. They could achieve this simple tricyclic ring molecule just by simple metal-free reaction strategy in less time in overall 45% yield (Scheme 38).

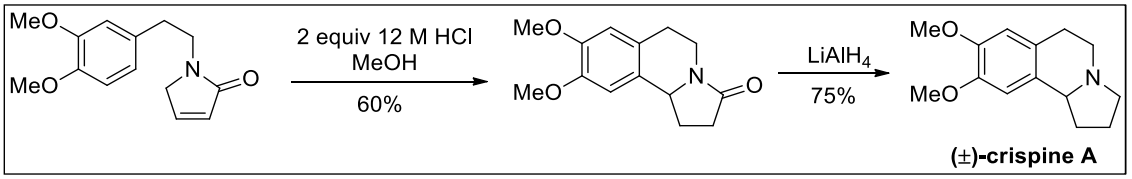

Scheme 38. Total synthesis of (±)-crispine A

The pyrrolo[2,1-*a*]isoquinoline alkaloid and indolizino[8,7-*b*]indole alkaloid synthesis is achieved by Ibnusaud's group[51] from (2*S*,3*R*)-3-hydroxy-5-oxotetrahydrofuran-2,3-dicarboxylic acid methyl esters. These tri and tetracyclic compounds were structurally modified by including trihydroxy chain next to the bridgehead position to convert them to pharmacological skeletons (Scheme 39).

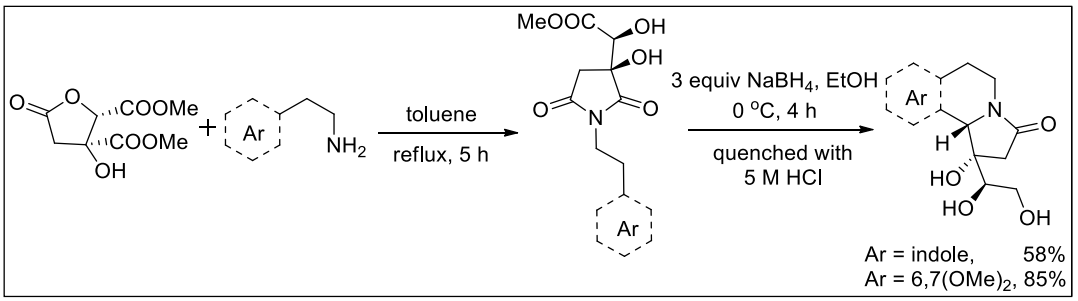

Scheme 39. Syntheses of trihydroxy substituted pyrrolo[2,1-*a*-isoquinoline and indolizino[8,7-*b*]indole alkaloids

Stanoeva and co-workers[52] have employed the Castagnoli–Cushman reaction on dihydroisoquinoline with succinic anhydride to construct pyrrolo[2,1-*a*]isoquinoline system. Further, the structure was elucidated using 1D and 2D NMR techniques (Scheme 40).

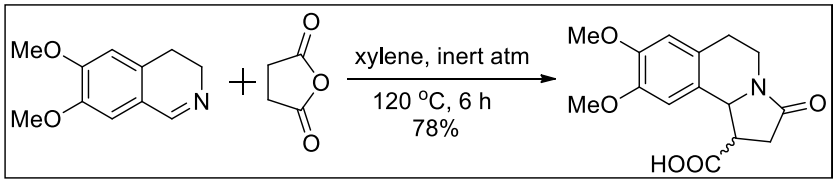

Scheme 40. Synthesis of pyrrolo[2,1-*a*]isoquinoline derivative using Castagnoli–Cushman reaction

Yinying Zheng and two others[53] have synthesized aryl-fused heterocycles from arylethylamines and *α*,*ω*-alkynoic acids using Grubb's ruthenium carbene catalyst followed by subsequent aminolysis and TFA mediated cyclization of *N*-acyl iminium ion with arylethylamines. The strategy was used to construct various pyrrolo-fused heterocycles like indole, furan, thiophene, pyrrole, and benzofuran (Scheme 41).

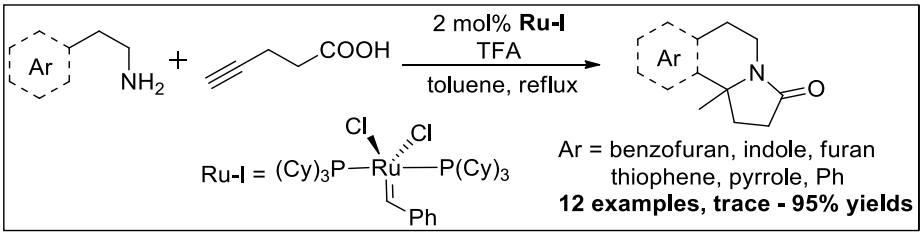

Scheme 41. Syntheses of 10b methylated pyrrolo[2,1-*a*]isoquinoline derivatives

Nalikezhathu et al.[54] have established a methodology for the construction of tetrahydro-*β*-carbolines from alcohols, and tryptamine derivatives using pyridyl-phosphine ruthenium(II) catalyzed tandem alcohol amination/Pictet−Spengler reaction sequence along with the stoichiometric amount of triflic acid. They have applied this methodology to prepare (±)-harmicine molecule from tryptamine and 1,4-butanediol (Scheme 42).

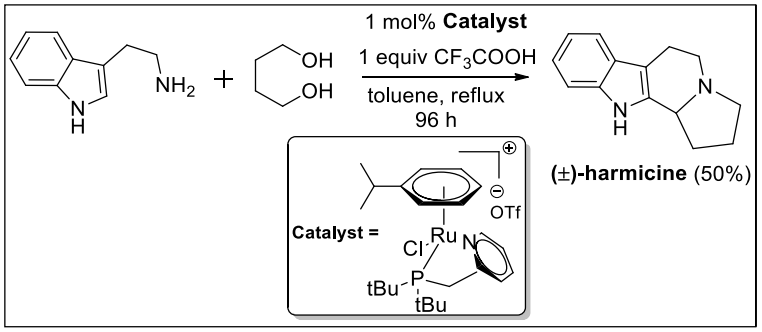

Scheme 42. Total synthesis of (±)-harmicine

Rampanicker's group[55] has reported total syntheses of (+)-crispine A along with other

tetrahydroisoquinoline natural products like, (-)-calycotomine, (-)-salsolidine, (-)-carnegine, (-)-homolaudanosine, (-)-homoprotoberberine. To synthesize (+)-crispine A, they commenced with an aldehyde prepared from 3,4-dimethoxyphenethyl methanesulfonate by formylation, and Wittig reaction, later subjected to another four steps. This aldehyde was further treated with dibenzyl azodicarboxylate in the presence of D-proline and subsequently fused with a Wittig reagent (carbethoxymethylene)triphenylphosphorane to get the corresponding γ-hydrazino-α,β-unsaturated ester. Reduction of γ-hydrazino-α,β-unsaturated ester with Raney-Ni followed by treatment with a mild base like K_2CO_3 in refluxing methanol afforded tricyclic lactum. This lactum upon amide reduction with lithium aluminium hydride ended up giving (+)-crispine A (Scheme 43).

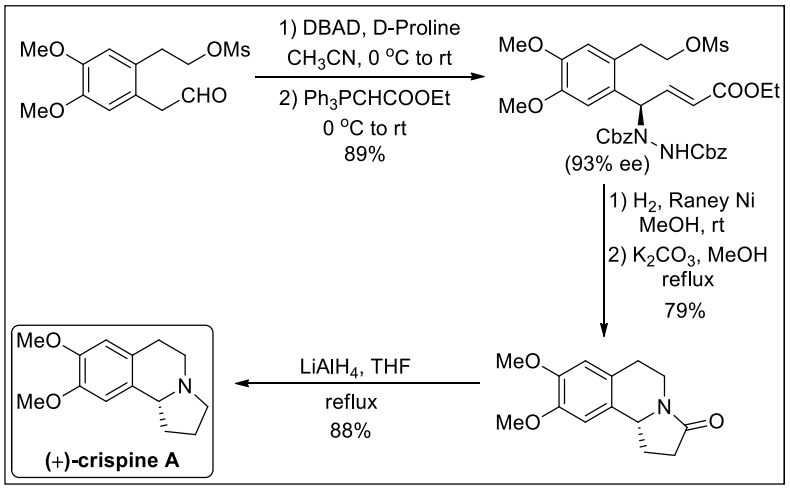

Scheme 43. Total synthesis of (+)-crispine A

Wang and co-workers[56] have established a one-pot methodology for synthesizing tri and tetracyclic ring compounds from 5-chloro-*N*-(phenethyl)pentanamide surrogates in mild conditions at low temperatures. They have exhibited total syntheses of (±)-crispine A, (±)-harmicine along with (±)-xylopinine and (±)-desbromoarborescidine alkaloids. A facile microwave-assisted cyclization was carried out for the syntheses of (±)-crispine A, (±)-harmicine in 86% and 95%, respectively (Scheme 44).

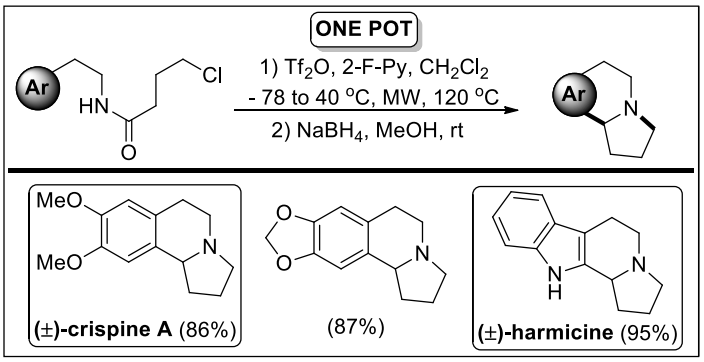

Scheme 44. Total syntheses of (±)-crispine A, and (±)-harmicine

2.I.3 Results and discussion:

Evaluating the reported synthesis revealed that a short and high yielding procedure to synthesize pyrrolo[2,1-*a*]isoquinoline-type molecules is still needed. Relevant to most of the methods, many researchers have prominently focused on building this tricyclic moiety *via* acyliminium ion cyclization, C1 position substitution followed by protection-deprotection-cyclization methods. We proposed a retro-synthesis as depicted in scheme 45.

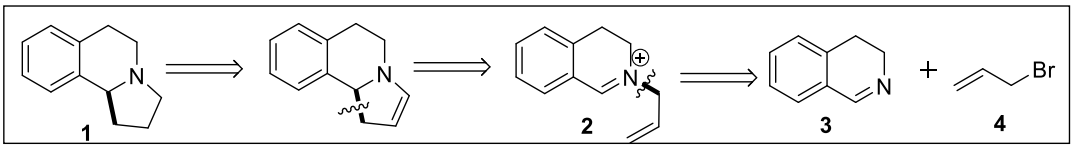

Scheme 45. Retrosynthetic analysis to construct pyrrolo[2,1-*a*]isoquinoline moiety

We thought of achieving pyrrolo[2,1-*a*]isoquinoline from *N*-allyl tetrahydroisoquinoline *via* an intramolecular aza-ene cyclization method.

First, as per reported procedure the synthesis of 3,4-dihydroisoquinoline was carried out using 1,2,3,4-tetrahydroisoquinoline with *N*-bromo succinimide followed by sodium hydroxide treatment.[57] The resultant 3,4-dihydroisoquinoline was obtained in 93% yield after acid-base workup and was used for future reactions without purification (Scheme 46).

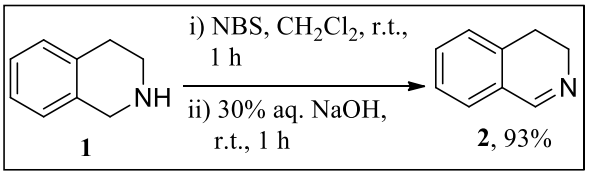

Scheme 46. Synthesis of 3,4-dihydroisoquinoline 3

Further, the formation of *N*-allyl-3,4-dihydroisoquinolin-2-ium bromide was achieved by just reacting 3,4-dihydroisoquinoline with allyl bromide in dry THF under an inert atmosphere (Scheme 47). A fine solid was seen adhered to the walls of the round bottom flask was concentrated on the rotary evaporator to remove THF solvent.

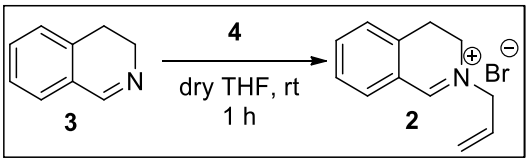

Scheme 47. *N*-allylation of 3,4-dihydroisoquinoline

Upon subjecting the white solid open to the air, it starts forming a sticky mass indicating formation of a hygroscopic salt, its NMR analysis showed the formation of the desired product.

With the desired analytical pure compound **2** in hand, it was subjected to the various reaction conditions for aza-ene reaction. Compound **2** was heated in 1,2-dichlorobenzene at 160 °C and was monitored over the mentioned period on TLC (Table 2, entry 1). Even after heating for 12 h, formations of new spots were not observed on TLC, and the reaction was discarded. Maybe the temperature was not enough to carry out the cyclization, so the sticky mass was heated without any solvent at 200 °C (Table 2, entry 2). After heating for just 15 minutes, it formed various new spots on TLC, and the reaction was subjected to the flash column chromatography, but none of the isolated spots turned out to be our desired product upon NMR analysis. Strong hindered base like sodium bis(trimethylsilyl)amide (NaHMDS) was tried, but that also couldn't do better (Table 2, entry 3). Another organic hindered base, like Hunig's base (*N*,*N*-diisopropylethylamine) was also tried but failed to give the compound **6** (Table 2, entry 4). An attempt with a mild base like K_2CO_3 also failed (Table 2, entry 5). Then, one reported procedure of cyclizing similar compounds was carried out in formic acid[59] at 60 °C, which was also unable to give our product (Table 2, entry 6).

Table 2. Reaction conditions of intramolecular aza-ene reaction

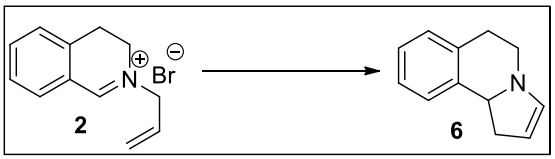

Entry	Reaction condition	Result
1	1,2-dichlorobezene, heat, 160 °C, 12 h	No reaction
2	Neat heating, 200 °C, 15 min – 2 h	Complex mixture
3	NaHMDS in THF, dry THF, -78 °C – rt, 24 h	No reaction
4	Hunig's base, 24 h	No reaction
5	Anhy. K_2CO_3, dry THF, 60 °C, 12 h	No reaction
6	HCOOH, 60 °C, 24 h	No reaction

With various factors disrupting our method to prepare compound **1**, we thought to synthesize our desired molecule in another way. We have proposed the retro-synthesis as depicted in scheme 48.

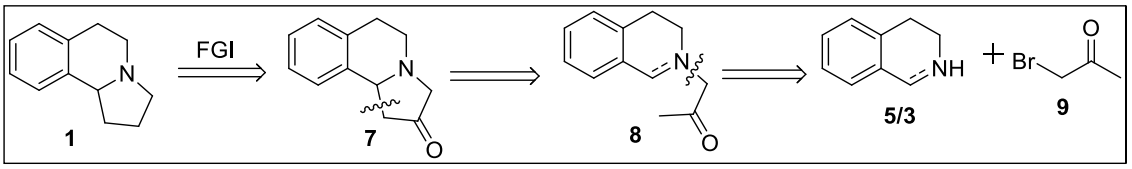

Scheme 48. Retrosynthetic analysis of pyrrolo[2,1-*a*]isoquinoline moiety

Initially, a direct reaction between **3** and **9** was carried in the presence of a stoichiometric amount of L-proline in isopropanol solvent at room temperature (Scheme 49). With no formation of new spots on TLC, the same reaction mixture was then refluxed for more time to observe the disappearance of starting material.

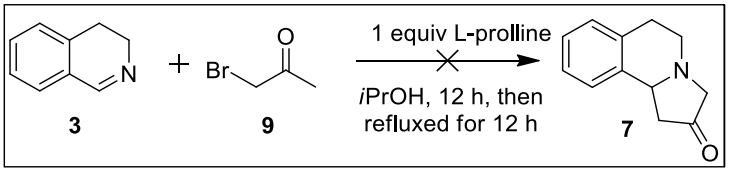

Scheme 49. Attempted synthesis of 1,5,6,10b-tetrahydropyrrolo[2,1-*a*]isoquinolin-2(3*H*)-one 7

After refluxing for 12 hours, its workup was done by 1 N HCl addition and disappointingly recovered the starting material back.

The flaws of the previous reaction conditions made us realize that compound **7** could also be synthesized using a traditional Wacker oxidation reaction followed by in situ cyclization *via* palladium mediated C-H activation. For that, we prepared the required **10** from *N*-allylation reaction between **5** and **4** in dry THF using anhydrous potassium carbonate (Scheme 50). A traditional Wacker oxidation reaction was performed on compound **10** with said reagents as per the reported procedure (Scheme 51). We could isolate the actual Wacker process product **11** in 35% yield but could not get the expected product **7**. The lower yield for compound **11** could be because of bonding between tertiary nitrogen and palladium, inhibiting its formation.

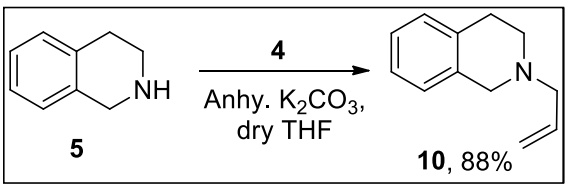

Scheme 50. *N*-allylation of 1,2,3,4-tetrahydroisoquinoline compound

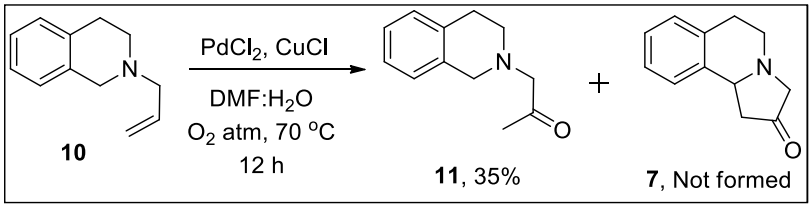

Scheme 51. Attempted Wacker oxidation-cyclization reaction on 2-allyl-1,2,3,4 tetrahydroisoquinoline 10

Then an attempt was made to cyclize compound **11** in other ways. So, *N*-alkylation of **5** with bromoacetone **9** was carried out for the preparation of compound **11** in higher quantities (Scheme 52).

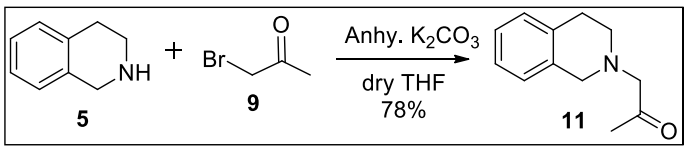

Scheme 52. Synthesis of 1-(3,4-dihydroisoquinolin-2(1*H*)-yl)propan-2-one 11

Areum Jung and Sun-Joon Min[62] have reported DDQ cyclization to construct a six-membered ring around tetrahydroisoquinoline in the presence of excess cesium carbonate in refluxing 1,2-dichloroethane. Using their reported methodology for six-membered ring formation, we attempted to build our molecule using the given procedure (Scheme 53). But that attempt also failed to form a five-membered ring around tetrahydroisoquinoline moiety.

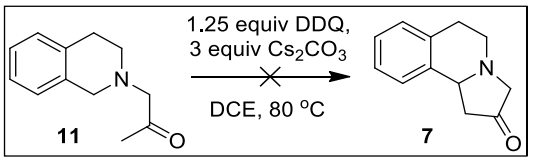

Scheme 53. Attempted synthesis of 1,5,6,10b-tetrahydropyrrolo[2,1-*a*]isoquinolin-2(3*H*)-one 7

An assumption about cyclization reaction using redox photocatalytic reaction was also not bad for the synthesis of **7**. So, we attempted Rose Bengal catalyzed redox photocatalytic reaction in the open air under blue LED (Scheme 54).

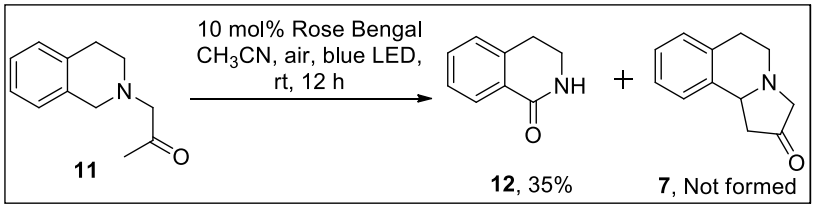

Scheme 54. Photocatalytic cyclization of 1-(3,4-dihydroisoquinolin-2(1*H*)-yl)propan-2-one 11 using Rose Bengal

After stirring it for 12 h at room temperature, a faint spot was observed on TLC, which was confirmed as compound **12** on NMR spectroscopy upon purification over column chromatography. Its analytical data matches that of reported data.

Failure of this strategy prompted us to devise another plan involving a longer route oxidation-cyclization reaction sequence starting from homoveratryl amine and succinic anhydride as depicted in scheme 55. The necessity of this retrosynthetic scheme made us realize that the steps involved in constructing the tricyclic core are simple, and we need to get the final step done. In this method, we tried to formulate both isoquinoline and pyrrole core construction in a single step itself.

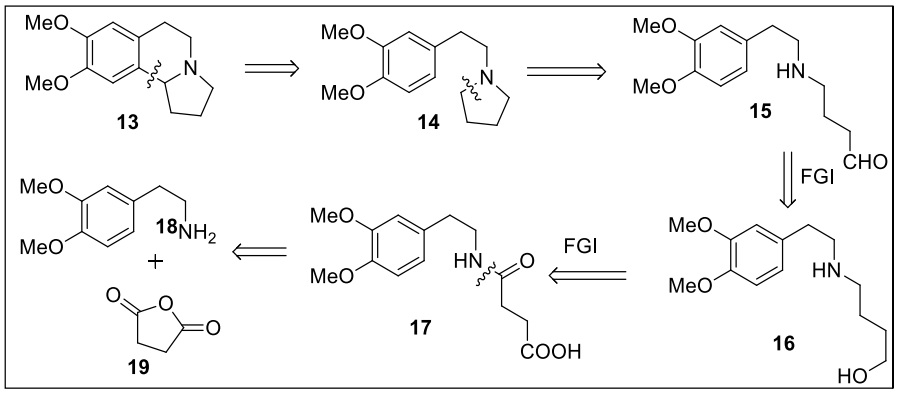

Scheme 55. Retrosynthetic scissoring of (±)-crispine A

The required amide-acid **17** was prepared *via* ring-opening of succinic anhydride by homoveratryl amine in dry CH_2Cl_2 under stirring (Scheme 56). White color solid was precipitated out after filtration gave an analytically pure amide-acid **17**.

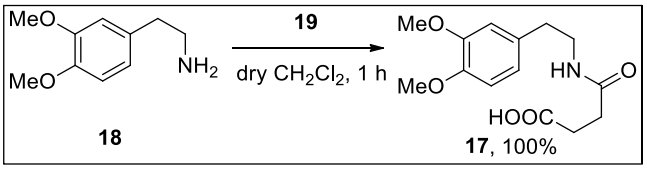

Scheme 56. Synthesis of 4-((3,4-dimethoxyphenethyl)amino)-4-oxobutanoic acid 17

4-((3,4-dimethoxyphenethyl)amino)-4-oxobutanoic acid (17):

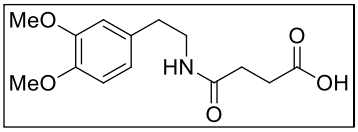

Pale yellow solid, m.p. 122-125°C. IR (KBr) υ_{max}: 3299, 2918, 1693, 1640, 1546, 1231, 734, 660 cm^{-1}. ^1H NMR (400 MHz, $CDCl_3$) δ = 2.46 (t, *J* = 6.4 Hz, 2H), 2.68 (t, *J* = 6.4 Hz, 2H), 2.76 (t, *J* = 7.2 Hz, 2H), 3.47-3.52 (q, 2H), 3.26 & 3.87 (2Xs, 6H), 5.94 (bs, 1H), 6.71-6.73 (d, 2H), 6.80 (d, *J* = 8.4 Hz, 1H) ppm. ^{13}C NMR (100 MHz, $CDCl_3$) δ = 29.7 (CH_2), 30.7 (CH_2), 35.0 (CH_2), 41.0 (CH_2), 55.9 (CH_3), 55.9 (CH_3), 111.4 (CH), 111.9 (CH), 120.7 (CH), 131.1 (Cq), 147.7 (Cq), 149.0 (Cq), 172.3 (Cq), 176.4 (Cq) ppm. LCMS (m/z): $C_{14}H_{19}NO_5H$ $[M+H]^+$: 281.3; Found: 281.6.

Further, complete reduction of both an acid and amide group of compound **17** was made

using $LiAlH_4$ reagent to get the free NH to attack the aldehyde formed in the later step (Scheme 57). The resultant δ-aminoalcohol compound **16** was obtained in 91% yield and was characterized using IR, NMR, and LCMS studies.

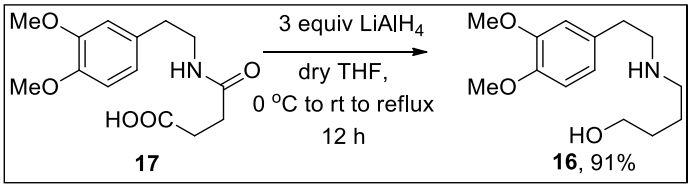

Scheme 57. Reduction of amide-acid 17 to δ-aminoalcohol 16

4-((3,4-dimethoxyphenethyl)amino)butan-1-ol (16):

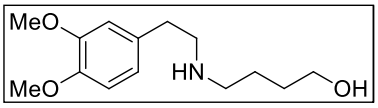

Thick colorless oil. IR (KBr) υ_{max}: 3309, 2919, 1457, 1219, 1053, 761 cm^{-1}. ^1H NMR (400 MHz, $CDCl_3$) δ = 1.35-1.42 (quint, 2H), 1.59-1.71 (m, 3H), 2.60-2.78 (m, 2H), 2.84-2.95 (m, 3H), 3.50-3.54 (m, 2H), 3.57-3.59 (m, 1H), 3.68 (bs, 1H), 3.79 & 3.80 (2Xs, 6H), 6.69-6.76 (m, 3H) ppm. ^{13}C NMR (100 MHz, $CDCl_3$) δ = 22.0 (CH_2), 28.6 (CH_2), 30.9 (CH_2), 54.6 (CH_2), 55.0 ($2XCH_3$), 55.2 (CH_2), 60.9 (CH_2), 110.6 (CH), 110.9 (CH), 119.8 (CH), 129.0 (Cq), 147.0 (Cq), 148.2 (Cq) ppm. LCMS (m/z): $C_{14}H_{23}NO_3H$ $[M+H]^+$: 253.3; Found: 253.4.

The oxidation of alcohol functional group of **16** was carried out using two traditional oxidation reactions like Dess-Martin periodinane and Swern oxidation (Table 3). We anticipated that once the formation of an aldehyde takes place, it would get cyclized with the primary amine NH group and later cyclization could occur under the same reaction conditions or could be performed using some acid. Dess-Martin periodinane reaction was done on **16** as per the reported procedure (Table 3, entry 1). The formation of different spots on TLC other than δ-amino alcohol compound **16** and cyclized iminium ion was not observed, and the remaining starting was isolated in 75% yield. So we attempted Swern oxidation on **16** (Table 3, entry 2). Its low-temperature reaction may not help with the cyclization of NH with the aldehyde group, but we were expecting at least the oxidation of primary alcohol to aldehyde. That also failed to show any change in TLC, and we couldn't

get our desired product, and the remaining starting was isolated in 85% yield.

Table 3. Tandem oxidation-cyclization reaction optimization

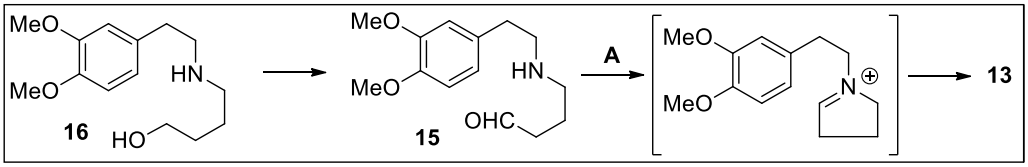

Entry	Reaction condition (A)	Result
1	1.5 equiv DMP, 1.5 equiv $NaHCO_3$, CH_2Cl_2, 0 ^oC to rt, 12 h	Starting recovered (75%)
2	DMSO, $(COCl)_2$, -78 ^oC to -50 ^oC, then 5 equiv Et_3N, rt, 3 h	Starting recovered (85%)

The above methods failed to produce aldehyde in the presence of a free NH group in the molecule, so the protection of the secondary NH group was crucial to make aldehyde from primary alcohol. Protection of NH group with $(Boc)_2$ anhydride went selectively of an amine group with 89% conversion (Scheme 58).

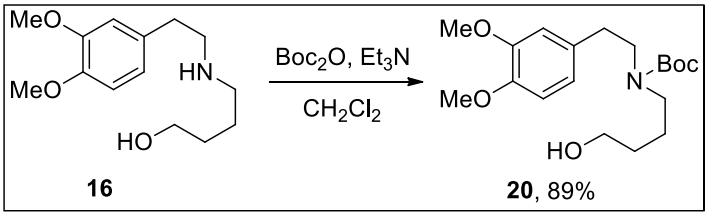

Scheme 58. *N*-Boc protection of *δ*-aminoalcohol 16

***Tert*-butyl 3,4-dimethoxyphenethyl(4-hydroxybutyl)carbamate (20)**:

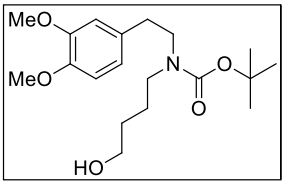

Pale yellow oil. IR (KBr) υ_{max}: 3021, 2944, 2897, 2848, 1626, 1576, 1209, 1005, 879, 752 cm^{-1}. ^1H NMR (400 MHz, $CDCl_3$) δ = 1.39 (s, 9H), 1.99 (m, 4H), 2.69 (t, *J* = 8 Hz, 2H), 3.10 (t, *J* = 6.8 Hz, 2H), 3.29 (t, *J* = 7.6 Hz, 2H), 3.59 (t, *J* = 6 Hz, 2H), 3.79 (s, 3H), 3.80 (s, 3H), 6.64-6.66 (d, 2H), 6.72-6.73 (d, 1H) ppm. ^{13}C NMR (100 MHz, $CDCl_3$) δ = 25.0 (CH_2), 28.5 (3XCH_3), 29.7 (CH_2), 49.4 (CH_2), 55.8 (CH_3), 55.9 (CH_3), 62.6 (3XCH_2), 79.4 (Cq), 111.2 (CH), 112.0 (CH), 120.7 (CH), 131.9 (Cq), 147.5 (Cq), 148.9 (Cq), 155.6 (Cq)

ppm. LCMS (m/z): $C_{19}H_{31}NO_5H$ $[M+H]^+$: 353.4; Found: 353.7.

The Boc-protected δ-amino-alcohol **20** was then subjected to Dess-Martin periodinane reaction, and smoothly primary alcohol group was converted to its corresponding aldehyde in 83% yield (Scheme 59).

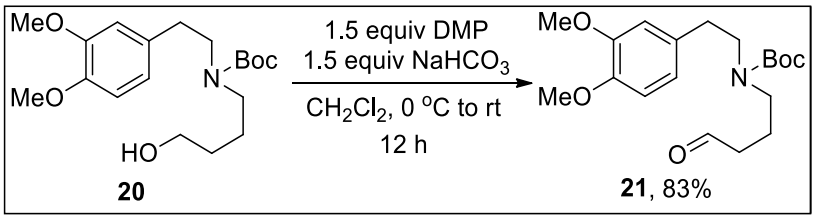

Scheme 59. Oxidation of alcohol to aldehyde using Dess-Martin periodinane reaction

***Tert*-butyl 3,4-dimethoxyphenethyl(4-oxobutyl)carbamate (21)**:

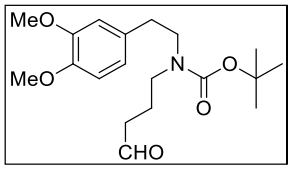

Pale yellow oil. IR (KBr) υ_{max}: 3033, 2953, 2905, 2845, 1629, 1578, 1212, 1145, 1067, 885, 759 cm^{-1}. ^1H NMR (400 MHz, $CDCl_3$) δ = 1.38 (s, 9H), 1.75 (m, 2H), 2.37 (m, 2H), 2.69 (m, 2H), 3.09 (m, 2H), 3.27 (m, 2H), 3.79 & 3.80 (2Xs, 6H), 6.65 (m, 2H), 6.72 (d, *J* = 8 Hz, 1H), 9.69 (s, 1H) ppm. ^{13}C NMR (100 MHz, $CDCl_3$) δ = 28.4 ($3XCH_3$), 29.7 (CH_2), 34.8 (CH_2), 41.1 (CH_2), 46.4 (CH_2), 49.4 (CH_2), 55.8 (CH_3), 55.9 (CH_3), 79.6 (Cq), 111.2 (CH), 112.0 (CH), 120.7 (CH), 131.7 (Cq), 147.5 (Cq), 148.9 (Cq), 155.5 (Cq), 201.9 (O=Cq) ppm. LCMS (m/z): $C_{19}H_{29}NO_5H$ $[M+H]^+$: 351.4; Found: 351.5.

An attempt of one-pot tandem deprotection-cyclization reaction sequence to give us our desired product also failed when a strong acid reaction like TFA with **21** was performed (Scheme 60).

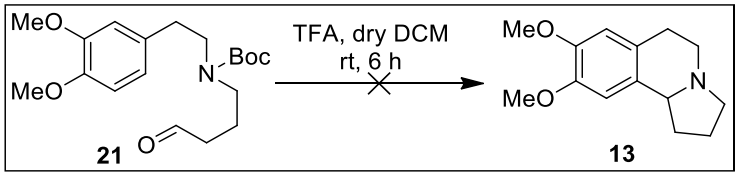

Scheme 60. Attempted synthesis of (±)-crispine A *via* deprotection-cyclization strategy using TfOH

Above failures in getting the final cyclized product suggested that probably the weaker electrophilic nature of the intermediate may be hampering the desired result. Hence, by revisiting all literature reports, we thought of a methodology wherein we can construct pyrrolo[2,1-*a*]isoquinolinone in a single step. The retrosynthesis scissoring of (±)-crispine A molecule suggested two synthons to construct the tricyclic compound (Scheme 61).

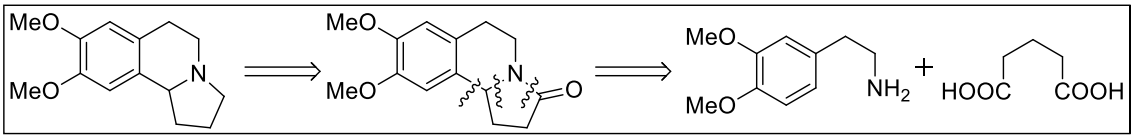

Scheme 61. Retrosynthesis of (±)-crispine A

We inspected the reagents administered to do the reaction between primary amines and dicarboxylic acids and settled for the use of phosphorus pentaoxide (P_4O_{10}) to carry out the reaction. Many reports have focused mainly on the cyclization of 1-phenethylpyrrolidine-2,5-dione *via* acyliminium ion. So, our methodology also depends on forming a one-pot acyliminium ion followed by its cyclization and reduction.

Initially, the model reaction of **18** was carried out with succinic acid **23** in the presence of 2.5 equiv of P_4O_{10} in refluxing toluene (Table 4, entry 1). It didn't cyclize to form tricyclic compound **24** but remained in the form of imide **25**. Although the formation of imide **25** is temperature-dependent, it was further refluxed in dry xylene to check the formation of **24** (Table 4, entry 2). Use of Eaton's reagent (7.5 wt% P_4O_{10} in MsOH) is reported for the cyclization reactions in many journals. So, in freshly prepared Eaton's reagent at room temperature, another reaction was set between **18** and **23** (Table 4, entry 3). It formed tricyclic product **24** in 28% yield but no imide **25** was isolated. The acidity of the reagent or the temperature may be the factors affecting the cyclization, so, with the same 7.5 wt% measurements, we prepared a mixture of P_4O_{10} in TfOH and carried out the reaction at

room temperature (Table 4, entry 4), it facilitated compound **24** in a 45% yield after the reduction process. The same mixture of P_4O_{10} in TfOH at 60 °C, a 20% increase in yield that to the former attempt was seen (Table 4, entry 5). When both the wt% and temperature were increased for P_4O_{10} in TfOH mixture to 8.3 wt% and 100 °C, we could get the compound in 79% in just 2 h followed by reduction using sodium borohydride (Table 4, entry 6).

Table 4. Optimization of reagents

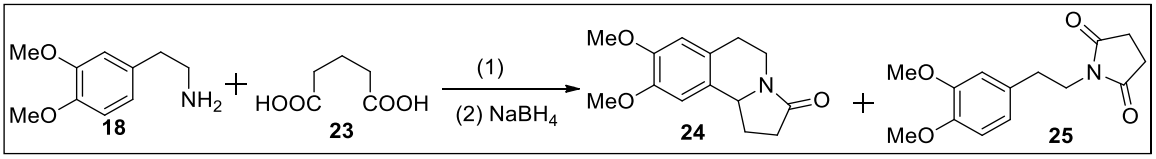

Entry	Reaction condition (1)	Time	%Yield	
			24	**25**
1	P_4O_{10}, dry toluene, Δ	12 h	n.d.	63%
2	P_4O_{10}, dry xylene, Δ	12 h	n.d.	65%
3	Eaton's reagent, rt	8 h	28%	n.d.
4	7.5 wt% P_4O_{10}/TfOH, rt	6 h	45%	n.d.
5	7.5 wt% P_4O_{10}/TfOH, 60 °C	6 h	65%	n.d.
6	**8.3 wt% P_4O_{10}/TfOH, 100 °C**	**2 h**	**79%**	**n.d.**

Once the optimization was successfully done, we prepared a series of compounds using various phenethylamine and dicarboxylic acid derivatives. Compound **24b** was prepared from 3-methoxyphenethylamine **18b** and **23a** using standardized conditions in 74% (Table 5, entry 2). For the synthesis of compound **24c**, its 3,4,5-trimethoxy phenethylamine (mescaline) synthesis was carried out.

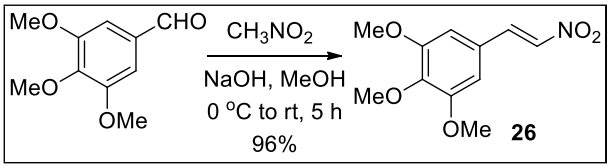

Scheme 62. Synthesis of (*E*)-1,2,3-trimethoxy-5-(2-nitrovinyl)benzene

As mescaline itself is a hallucinating drug and banned by USA and several countries, its production is not done at a large scale. So, we prepared it using the reported condition from 3,4,5-trimethoxybenzaldehyde and nitromethane by condensation reaction using sodium hydroxide (scheme 62).

Further, reduction of (*E*)-1,2,3-trimethoxy-5-(2-nitrovinyl)benzene **26** with lithium aluminium hydride produced mescaline **27** in 83% yield in two steps (Scheme 63).

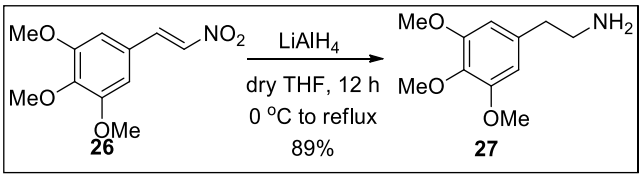

Scheme 63. Synthesis of mescaline

From compound **27** we prepared **24c**, i.e., (±)-mescalotam, by fusing it with **23a** using our optimized condition in 75% yield in one pot (Table 5, entry 3). In arylethylamines, heterocyclic amine like tryptamine **18d** was condensed with **23a** to construct a tetracyclic ring structure **24d** in 81% yield (Table 5, entry 4). Other than succinic acid, we successfully condensed glutaric acid **23b** with substrates like **18a** and **18d** in 74% and 79% respectively to construct compounds **24e** and **24f** (Table 5, entries 5, 6).

Table 5. Syntheses of various pyrrolo[2,1-*a*]isoquinolinone derivatives

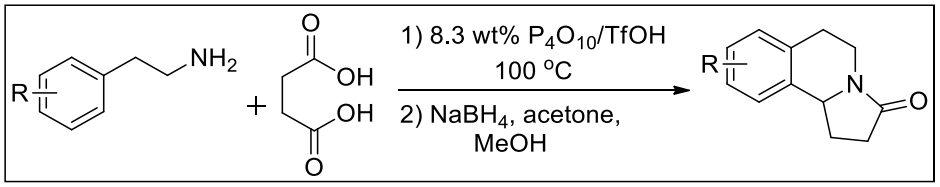

Entry	Phenethylamine	Dibasic acid	Product	Yield
1	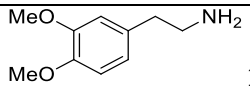 **18a**	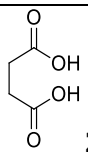 **23a**	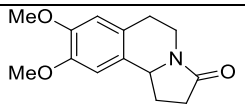 **24a**	79%
2	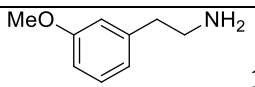 **18b**	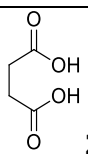 **23a**	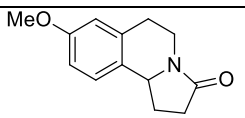 **24b**	74%

3	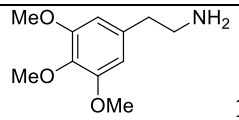 **18c**	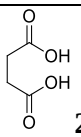 **23a**	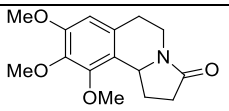 **24c**	75%
4	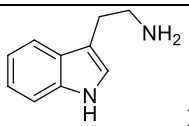 **18d**	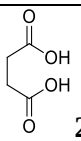 **23a**	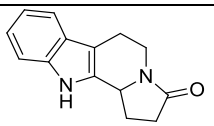 **24d**	81%
5	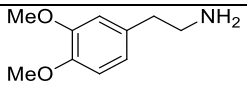 **18a**	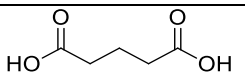 **23b**	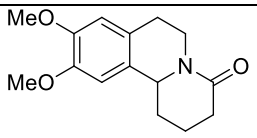 **24e**	74%
6	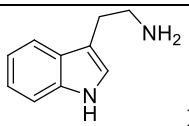 **18d**	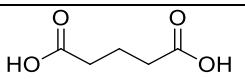 **23b**	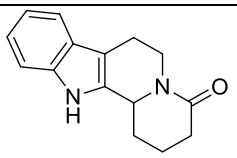 **24f**	79%

The constructed amide derivatives **24a-f** were later defunctionalized to other moieties using various reactions. To prepare (±)-crispine A, compound **24a** was reduced to its respective tertiary amine using reducing reagent like lithium aluminium hydride (Scheme 64). (±)-Crispine A, was prepared in an overall 66% yield starting from **24a** in just two steps.

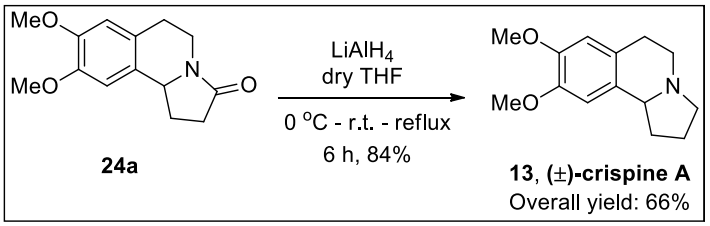

Scheme 64. Synthesis of (±)-crispine A

Similarly, complete demethylation of **24a** using boron tribromide at low temperature yielded (±)-trolline/oleracein E in overall 68% yield (Scheme 65).

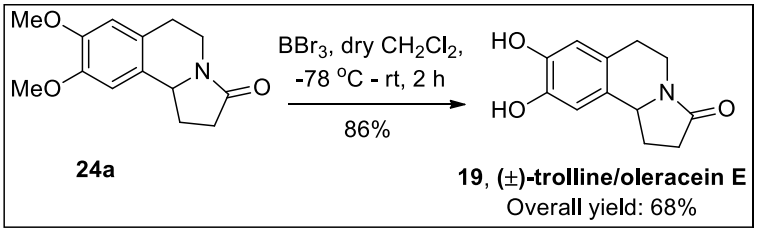

Scheme 65. Synthesis of (±)-trolline/oleracein E

The tetracyclic core of (±)-harmicine was constructed from its precursor **24d** in overall 74% yield (Scheme 66).

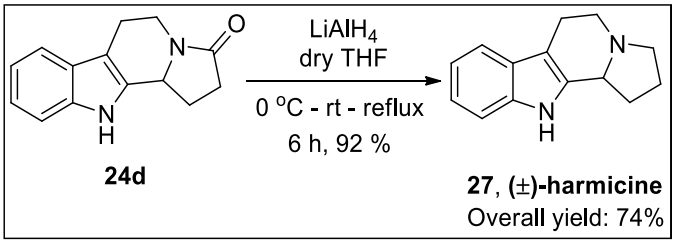

Scheme 66. Synthesis of (±)-harmicine

As discussed in the introduction, mescalotam doesn't exhibit any biological activity in its pure form, so we anticipated synthesizing its trihydroxy derivative. So, compound **24c** was completely demethylated using boron tribromide and successfully analyzed to deduce its exact structure (Scheme 67).

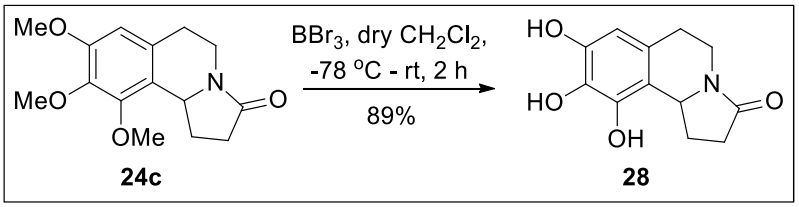

Scheme 67. Synthesis of 8,9,10-trihydroxy-1,5,6,10b-tetrahydropyrrolo[2,1-*a*]isoquinolin-3(2*H*)-one

2.I.4 Conclusion:

In conclusion, we have attempted three methods to develop the tricyclic core of indolizidine compounds. The first method with the aza-ene cyclization step failed to achieve the final core of 1,2,3,5,6,10b-hexahydropyrrolo[2,1-*a*]isoquinoline molecule. The method involving deprotection-cyclization and oxidation-cyclization routes was unable to construct the (±)-crispine A molecule in the final steps. Lastly, the condensation of phenylethylamine and dicarboxylic acid derivatives using 8.3 wt% P_4O_{10}/TfOH methodology was successfully exploited to achieve the (±)-crispine A, (±)-trolline/oleracein E, (±)-harmicine, (±)-mescalotam and trihydroxy derivative of (±)-mescalotam in overall good yields.

2.I.5 Experimental:

2.I.5.1: 3,4-dihydroisoquinoline (3):

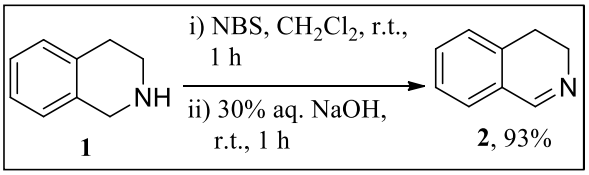

To the 18.8 mmol 1,2,3,4-tetrahydroisoquinoline **5** dissolved in 100 mL of dry CH_2Cl_2, 20.7 mmol of *N*-bromosuccinimide was added portionwise. The reaction was stirred for 1 hour until the starting material is consumed and indicated by TLC. To the reaction mixture, 25 mL of 30% aqueous NaOH solution was added and allowed the reaction to stir for another 1 hour. The organic layer was separated from the reaction mixture and washed with 50 mL of H_2O. Later, extracted with 10% HCl (2 X 50 mL), the aqueous layer was basified using concentrated ammonia (pH = 9). The liberated oil was again extracted using CH_2Cl_2 (3 X 50 mL). Then, the organic layer was dried over anhydrous Na_2SO_4 and concentrated to afford the light yellow oil in a 93% yield. The product was used for the further reaction without any purification.

Pale yellow solid, m.p. 122-125°C. IR (KBr) υ_{max}: 3023, 2947, 2904, 2854, 1630, 1570, 1212, 1010, 879, 757 cm^{-1}. ^1H NMR (400 MHz, $CDCl_3$) δ = 2.75 (t, *J* = 8.4 Hz, 2H), 3.77 (t, *J* = 8 Hz, 2H), 7.16 (d, *J* = 7.2 Hz, 1H), 7.26-7.35 (m, 2H), 7.36-7.38 (q, 1H), 8.33 (s, 1H) ppm. ^{13}C NMR (100 MHz, $CDCl_3$) δ = 25.0 (CH_2), 47.3 (CH_2), 127.1 (CH), 127.3 (CH), 127.4 (CH), 128.5 (CH), 131.1 (Cq), 136.3 (Cq), 160.4 (CH) ppm. Spectral data is in accordance with the literature.[58]

2.I.5.2: 2-allyl-3,4-dihydroisoquinolin-2-ium bromide (2):

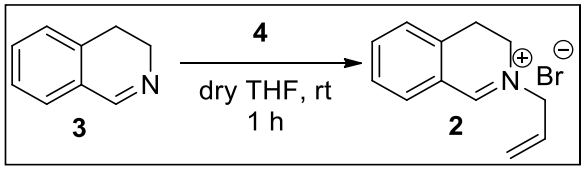

In a two-neck round bottom flask, equipped with a magnetic stirring bar and nitrogen balloon, was taken 10 mmol of 3,4-dihydroisoquinoline **3** and dissolved in 7 mL of dry THF. To that solution, 10 mmol of allyl bromide **4** was added directly and allowed the reaction to stir at room temperature for 1 hour. The formation of white solid on the walls of the round bottom flask indicated the formation of **2**. Then, the THF was evaporated under pressure and immediately its NMR was recorded. The white solid slowly turned to a light brown thick liquid.

Pale yellow solid, m.p. 122-125°C. IR (KBr) υ_{max}: 3423, 3047, 2942, 1631, 1491, 1464, 1426, 1275, 1228, 1001, 956, 775, 716 cm^{-1}. ^1H NMR (400 MHz, $CDCl_3$) δ = 3.33 (t, *J* = 8.4 Hz, 2H), 4.10 (t, *J* = 8 Hz, 2H), 4.72 (d, *J* = 6.4 Hz, 2H), 5.60-5.72 (m, 2H), 6.09-6.19 (m, 1H), 7.50-7.57 (m, 2H), 7.76-7.83 (m, 1H), 7.91 (d, *J* = 7.6 Hz, 1H), 9.28 (s, 1H) ppm. ^{13}C NMR (100 MHz, $CDCl_3$) δ = 24.8 (CH_2), 48.1 (CH_2), 62.5 (CH_2), 123.9 (CH_2), 124.8 (Cq), 128.2 (CH), 128.2 (CH), 128.5 (CH), 133.8 (CH), 136.8 (Cq), 138.0 (CH), 166.8 (CH) ppm. LCMS (m/z): $C_{12}H_{14}BrNH$ $[M+H]^+$: 252.1; Found: 252.4.

2.I.5.3: 2-allyl-1,2,3,4-tetrahydroisoquinoline (10):

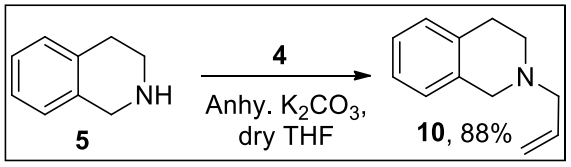

To a 100 mL 2-necked round-bottom flask, was added 10 mmol of 1,2,3,4-tetrahydroisoquinoline **5** dissolved in 10 mL dry THF followed by addition of 20 mmol of anhydrous K_2CO_3. The reaction mixture was cooled to 10°C. Then while stirring, 10 mmol of allyl bromide was added slowly to the amine solution. After the addition, the reaction mixture was stirred at room temperature until the TLC indicated the consumption of starting **5**. The reaction mixture was diluted with 20 mL of CH_2Cl_2 and filtered. The filtrate was evaporated under reduced pressure using a rotary evaporator and purified over flash chromatography on silica gel (Pet. ether and ethyl acetate) to give *N*-allyl 1,2,3,4-tetrahydroisoquinoline **10** as a viscous liquid, in 88% yield.

Pale yellow solid, m.p. 122-125°C. IR (KBr) υ_{max}: 3078, 2972, 2907, 2788, 1642, 1493,

1419, 1100, 972, 757 cm^{-1}. ^1H NMR (400 MHz, $CDCl_3$) δ = 2.74 (t, *J* = 5.6 Hz, 2H), 2.92 (t, *J* = 6 Hz, 2H), 2.17 (d, *J* = 6.4 Hz, 2H), 3.63 (s, 2H), 5.18-5.29 (m, 2H), 5.91-6.01 (m, 1H), 7.00-7.02 (m, 1H), 7.08-7.15 (m, 3H) ppm. ^{13}C NMR (100 MHz, $CDCl_3$) δ = 29.0 (CH_2), 50.6 (CH_2), 56.0 (CH_2), 61.5 (CH_2), 118.0 (CH_2), 125.6 (CH), 126.2 (CH), 126.6 (CH), 128.7 (CH), 134.2 (Cq), 134.7 (Cq), 135.3 (CH) ppm. Spectral data is in accordance with the literature.[60]

2.I.5.4: 1-(3,4-dihydroisoquinolin-2(1*H*)-yl)propan-2-one (11):

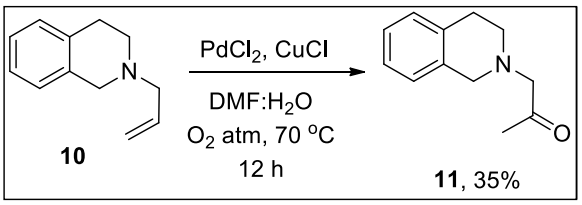

To the stirred solution of 1 mmol of 2-allyl-1,2,3,4-tetrahydroisoquinoline **10** in DMF/ H_2O (7:1) were added 5 mol% of $PdCl_2$ and 10 mol% of CuCl at room temperature. The mixture was heated at 70 °C for the requisite time under an O_2 atmosphere. The reaction mass was then diluted using 10 mL of H_2O after the TLC indicated the consumption of starting compound **10**. After stirring the mixture for 15 mins, it was extracted with ethyl acetate. The organic layer was dried over anhydrous Na_2SO_4 and concentrated under the reduced pressure and subjected to flash chromatography (Pet. ether and ethyl acetate) to give the corresponding compound 1-(3,4-dihydroisoquinolin-2(1H)-yl)propan-2-one **11** as light yellow viscous liquid in 35% yield.

Pale yellow oil. IR (KBr) υ_{max}: 3063, 2977, 2920, 2805, 1681, 1596, 1447, 1388, 1222, 1153, 1107, 971, 922, 710, 699 cm^{-1}. ^1H NMR (400 MHz, $CDCl_3$) δ = 2.21 (s, 3H), 2.79 (t, *J* = 5.6 Hz, 2H), 2.94 (t, *J* = 5.6 Hz, 2H), 3.36 (s, 2H), 3.70 (s, 2H), 6.99-7.10 (m, 1H), 7.11-7.15 (m, 1H) ppm. ^{13}C NMR (100 MHz, $CDCl_3$) δ = 27.7 (CH_3), 28.8 (CH_2), 51.2 (CH_2), 55.9 (CH_2), 68.0 (CH_2), 125.7 (CH), 126.3 (CH), 126.5 (CH), 128.7 (CH), 133.8 (Cq), 134.2 (Cq), 207.2 (O=Cq) ppm. Spectral data is in accordance with the literature.[61]

2.I.5.5: 1-(3,4-dihydroisoquinolin-2(1*H*)-yl)propan-2-one (11):

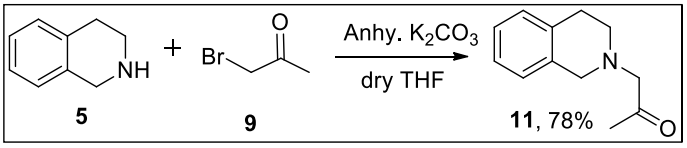

To a 100 mL 2-necked round-bottom flask, was added 10 mmol of 1,2,3,4-

tetrahydroisoquinoline **5** dissolved in 10 mL dry THF followed by addition of 20 mmol of anhydrous K_2CO_3. The reaction mixture was cooled to 10°C. Then while stirring, 10 mmol of bromoacetone was added slowly to the amine solution. After the addition, the reaction mixture was stirred at room temperature until the TLC indicated the consumption of starting **5**. The reaction mixture was diluted with 20 mL of CH_2Cl_2 and filtered. The filtrate was evaporated under reduced pressure using a rotary evaporator and purified over flash chromatography on silica gel (Pet. ether and ethyl acetate) to give 1-(3,4-dihydroisoquinolin-2(1*H*)-yl)propan-2-one **11** as a light yellow viscous liquid, in 78% yield.

2.I.5.6: 3,4-dihydroisoquinolin-1(2*H*)-one (12):

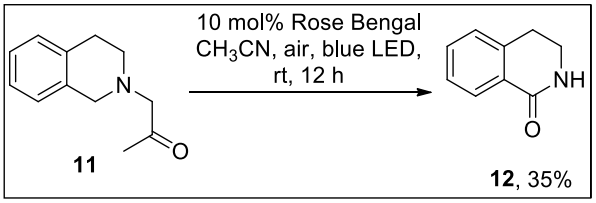

In a 5 mL glass vial, was added 1 mmol of 1-(3,4-dihydroisoquinolin-2(1*H*)-yl)propan-2-one **11** and 10 mol% Rose Bengal dissolved in 2 mL of CH_3CN and allowed to stir at room temperature, open to the air, under the blue LED light for 12 hours. After the completion of the reaction, it was concentrated and the thick mass was purified over flash chromatography on silica gel (Pet. ether and ethyl acetate) to give 3,4-dihydroisoquinolin-1(2H)-one **12** in 35% yield as light yellow viscous liquid.

Brown oil. IR (KBr) υ_{max}: 3258, 3072, 2941, 2868, 1666, 1605, 1576, 1337, 746 cm^{-1}. ^1H NMR (400 MHz, $CDCl_3$) δ = 3.01 (t, *J* = 6.4 Hz, 2H), 3.57 (t, *J* = 9.2 Hz, 2H), 7.22 (d, *J* = 7.6 Hz, 1H), 7.36 (t, *J* = 7.6 Hz, 1H), 7.43-7.47 (m, 1H), 8.06 (d, *J* = 7.6 Hz, 1H) ppm. ^{13}C NMR (100 MHz, $CDCl_3$) δ = 28.4 (CH_2), 40.3 (CH_2), 127.1 (CH), 127.2 (CH), 128.0 (CH), 128.9 (Cq), 132.2 (CH), 138.8 (Cq), 166.4 (Cq) ppm. Spectral data is in accordance with the literature.[63]

2.I.5.7: 4-((3,4-dimethoxyphenethyl)amino)-4-oxobutanoic acid (17):

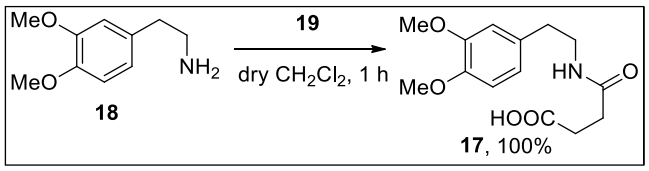

To a stirred solution of 10 mmol of succinic anhydride **19** dissolved in 10 mL dry CH_2Cl_2 was added 10 mmol of homoveratryl amine **18** and stirred the reaction at room temperature for an hour. After the completion of the reaction indicated by TLC, CH_2Cl_2 was evaporated to give 4-((3,4-dimethoxyphenethyl)amino)-4-oxobutanoic acid **17** in 100% yield. The white crude compound was as such used for the next reaction without any purification.

2.I.5.8: 4-((3,4-dimethoxyphenethyl)amino)butan-1-ol (16):

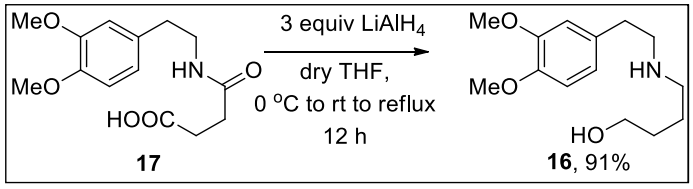

In a 100 mL three-neck round bottom flask equipped with a stirring bar, and condenser was added 90 mmol of $LiAlH_4$ and cooled to 0 °C. To that solid 50 mL of freshly dried THF was added and the reaction was stirred for 5 mins. Then, 30 mmol of 4-((3,4-dimethoxyphenethyl)amino)-4-oxobutanoic acid **17** was dissolved in 10 mL dry THF and slowly added to the above mixture *via* syringe. The reaction was stirred from 0 °C to room temperature for 0.5 hours. Then the reaction was refluxed for another 12 hours before quenching it using the Fieser workup method. The reaction was cooled to 0 °C and diluted with dry diethyl ether. Then, 3.5 mL of H_2O followed by 3.5 mL of 15% NaOH solution and 10.3 mL of H_2O was added sequentially. The reaction mixture was stirred vigorously at room temperature and to that 1 g of anhydrous $MgSO_4$ was added. The resultant solid material was filtered and the filtrate was dried over anhydrous Na_2SO_4 and concentrated over a rotary evaporator to give compound **16** as pale yellow oil in 91% yield. The product was used for the next reaction without any purification.

2.I.5.9: *Tert*-butyl 3,4-dimethoxyphenethyl(4-hydroxybutyl)carbamate (20):

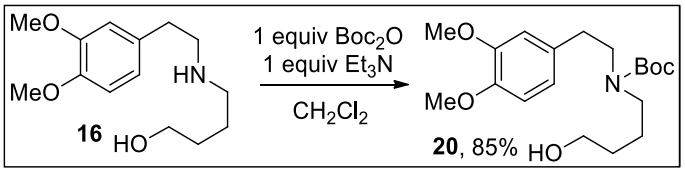

To a solution of 1 mmol of 4-((3,4-dimethoxyphenethyl)amino)butan-1-ol **16** dissolved in 10 mL of CH_2Cl_2 was added 1 equiv of NEt_3 and cooled at 0 °C. To the resulting mixture, 1 equiv of Boc_2O was added slowly and allowed the reaction mixture to stir at room temperature for 3 hours. After the completion of the reaction indicated by TLC, the reaction was quenched with 10 mL H_2O and extracted using CH_2Cl_2. The organic layer was dried over anhydrous Na_2SO_4 and concentrated under reduced pressure over the rotary evaporator to get the crude material. The crude product was purified over flash chromatography on silica gel (Pet. ether and ethyl acetate) to furnish colorless oil in an 85% yield.

2.I.5.10: *Tert*-butyl 3,4-dimethoxyphenethyl(4-oxobutyl)carbamate (21):

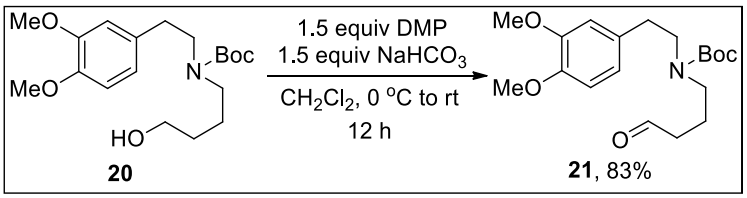

To a stirred mixture of 10 mmol of *tert*-butyl 3,4-dimethoxyphenethyl(4-hydroxybutyl)carbamate **20**, 15 mmol of $NaHCO_3$ in 60 mL CH_2Cl_2 under N_2 atmosphere at 0 °C was added 15 mmol of DMP (Dess-Martin periodinane) and the reaction was allowed to stir for 1 hour. The reaction mixture was then concentrated under vacuum and further extracted with diethyl ether. The organic layer was washed with saturated $NaHCO_3$ solution (5 X 10 mL) and dried over anhydrous Na_2SO_4. The solvent was removed under reduced pressure and purified over flash chromatography on silica gel (Pet. ether and ethyl acetate) to yield crude *tert*-butyl 3,4-dimethoxyphenethyl(4-oxobutyl)carbamate **21** as colorless oil in 83% yield.

2.I.5.11: (*E*)-1,2,3-trimethoxy-5-(2-nitrovinyl)benzene (26):

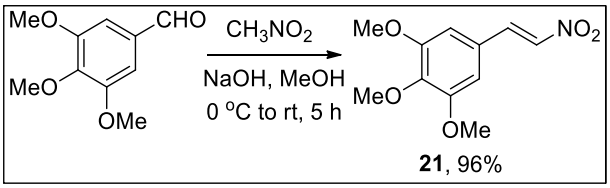

In a 50 mL round bottom flask, 5 mmol of 3,4,5-trimethoxybenzaldehyde and 6 mmol of nitromethane were dissolved in 10 mL methanol. The reaction was stirred at 0 °C and to that solution, 6 mmol of NaOH was added slowly. Then the reaction mixture was warmed to room temperature and stirred for another 1 h. After the disappearance of starting aldehyde on TLC, the reaction was neutralized using 4 N HCl. The resultant precipitate was filtered and the solid residue was washed with cold methanol several times to get the compound **26** in 96% as yellow solid. The compound was used for the next reaction without purification.

Yellow solid, m.p. 118-122 °C. IR (KBr) υ_{max}: 3118, 2931, 1519, 1476, 1389, 1267, 1123, 825, 651 cm^{-1}. ^{1}H NMR (400 MHz, $CDCl_3$) δ = 3.84 & 3.85 (2Xs, 9H), 6.70 (s, 2H), 7.48 (d, *J* = 13.6 Hz, 1H), 7.87 (d, *J* = 13.6 Hz, 1H) ppm. ^{13}C NMR (100 MHz, $CDCl_3$) δ = 56.3 ($3XCH_3$), 61.1 (CH), 106.4 (CH), 125.3 (Cq), 136.4 (CH), 139.4 (CH), 141.7 (Cq), 153.7 (2XCq) ppm. Spectral data is in accordance with the literature.[64]

2.I.5.12: 2-(3,4,5-trimethoxyphenyl)ethanamine (27):

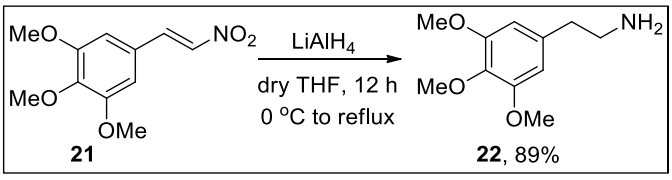

In a 100 mL three-neck round bottom flask equipped with a stirring bar, and condenser was added 90 mmol of $LiAlH_4$ and cooled to 0 °C. To that solid 50 mL of freshly dried THF was added and the reaction was stirred for 5 mins. Then, 30 mmol of (*E*)-1,2,3-trimethoxy-5-(2-nitrovinyl)benzene **26** was dissolved in 10 mL dry THF and slowly added to the above mixture *via* syringe. The reaction was stirred from 0 °C to room temperature for 0.5 hours. Then the reaction was refluxed for another 2 h before quenching it using the Fieser workup

method. The reaction was cooled to 0 °C and diluted with dry diethyl ether. Then, 3.5 mL of H_2O followed by 3.5 mL of 15% NaOH solution and 10.3 mL of H_2O was added sequentially. The reaction mixture was stirred vigorously at room temperature and to that 1 g of anhydrous $MgSO_4$ was added. The resultant solid material was filtered and the filtrate was dried over anhydrous Na_2SO_4 and concentrated over a rotary evaporator to give compound **27** as pale yellow oil in 89% yield. The product was used for the next reaction without any purification.

Pale yellow oil. IR (KBr) υ_{max}: 3415, 1651, 1001, 828 cm^{-1}. ^1H NMR (400 MHz, $CDCl_3$) δ = 2.32 (bs, 2H), 2.71 (t, *J* = 6 Hz, 2H), 2.97 (t, *J* = 6.8 Hz, 2H), 3.76 (s, 3H), 3.79 (s, 6H), 6.34 (s, 2H) ppm. Spectral data is in accordance with the literature.[65]

2.1.5.13: 8,9-dimethoxy-1,5,6,10b-tetrahydropyrrolo[2,1-*a*]isoquinolin-3(2*H*)-one (24a):

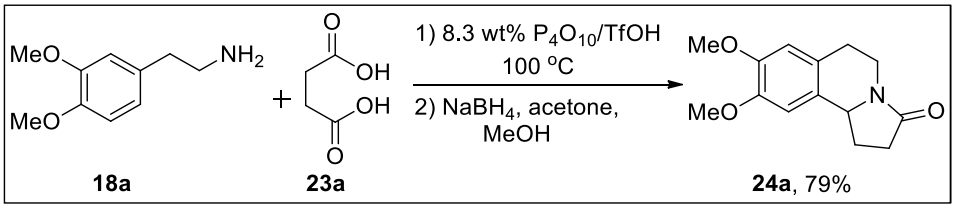

A solution was 8.3 wt% P_4O_{10}/TfOH was prepared by dissolving 0.415 g of P_4O_{10} in 4.585 mL of TfOH by stirring for 30 minutes to get a clear solution. To that solution, 1 mmol of succinic acid **23a** and 1.5 mmol of homoverarylamine **18a** were added and the reaction was heated at 100 °C for 2 h. Then, the reaction was cooled to room temperature and 10 mL of methanol was added. To the stirred mixture, excess $NaBH_4$ was added till the reaction became colorless. After stirring for 30 minutes, acetone was added slowly to quench the excess of $NaBH_4$. The whole solution was evaporated over a rotary evaporator and CH_2Cl_2 was added. The white solid was filtered and the filtrate was dried over anhydrous Na_2SO_4 and concentrated under reduced pressure. The crude product was purified over flash chromatography on silica gel (Pet. ether and ethyl acetate) to get the compound **24a** as colorless oil in 79% yield.

Colourless solid, m.p. 105-108 °C. IR (KBr) υ_{max} = 2929, 2840, 1703, 1614, 1521, 1420, 1256, 1124, 1011 cm^{-1}. ^1H NMR (400 MHz, $CDCl_3$) δ = 2.36-2.63 (m, 4H), 2.76-2.97 (m, 2H), 3.78 (3.79) (2Xs, 6H), 4.1-4.24 (m, 1H), 4.66 (t, *J* = 7.6 Hz, 1H), 6.50 (s, 1H), 6.54 (s, 1H) ppm. ^{13}C NMR (100 MHz, $CDCl_3$) δ = 26.7 (CH_2), 27.1 (CH_2), 30.7 (CH_2), 36.1

(CH_2), 54.9 (CH_3), 55.0 (CH_3), 55.6 (CH), 106.6 (CH), 110.6 (CH), 124.4 (Cq), 128.2 (Cq), 146.8 (Cq), 147.0 (Cq), 172.3 (Cq) ppm. Spectral data is in accordance with the literature.[25]

2.I.5.14: 8-methoxy-1,5,6,10b-tetrahydropyrrolo[2,1-*a*]isoquinolin-3(2*H*)-one (24b):

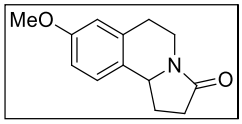

Following the similar protocol described in the 2.I.5.13 with 3-methoxyphenethylamine **18b** gave the product 8-methoxy-1,5,6,10b-tetrahydropyrrolo[2,1-*a*]isoquinolin-3(2*H*)-one **24b** in 74% yield.

Pale yellow solid, m.p 118-120 °C. IR (KBr) υ_{max} = 2929, 1687, 1619, 1509, 1467, 782 cm^{-1}. ^1H NMR (400 MHz, $CDCl_3$) δ = 1.72-1.81 (m, 1H), 2.36-2.42 (m, 1H), 2.46-2.54 (m, 1H), 2.55-2.60 (m, 1H), 2.66-2.70 (m, 1H), 2.81-2.90 (m, 1H), 2.96-3.02 (m, 1H), 3.72 (s, 3H), 4.15-4.20 (m, 1H), 4.66 (t, *J* = 8 Hz, 1H), 6.60 (s, 1H), 6.73 (d, *J* = 8.8 Hz, 1H), 6.96 (d, *J* = 8.4 Hz, 1H) ppm. ^{13}C NMR (100 MHz, $CDCl_3$) δ = 26.7 (CH_2), 27.8 (CH_2), 30.8 (CH_2), 36.0 (CH_2), 54.3 (CH_3), 55.4 (CH), 112.1 (CH), 112.5 (CH), 124.9 (CH), 128.8 (Cq), 133.9 (Cq), 157.3 (Cq), 172.3 (Cq) ppm. Spectral data is in accordance with the literature.[25]

2.I.5.15: 8,9,10-trimethoxy-1,5,6,10b-tetrahydropyrrolo[2,1-*a*]isoquinolin-3(2*H*)-one (24c):

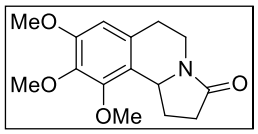

Following the similar protocol described in the 2.I.5.13 with 34,5-trimethoxyphenethylamine **18c** gave the product 8,9,10-trimethoxy-1,5,6,10b-tetrahydropyrrolo[2,1-*a*]isoquinolin-3(2*H*)-one **24c** in 75% yield.

Colourless solid, m.p. 68-71 °C. IR (KBr) υ_{max} = 2931, 2837, 2363, 1690, 1609, 1501, 1457, 1417, 1358, 1310, 1279, 1123, 1099, 1040, 856 cm^{-1}. ^1H NMR (400 MHz, $CDCl_3$) δ

= 1.63-1.74 (m, 1H), 2.42-2.49 (m, 1H), 2.55-2.64 (m, 2H), 2.75-2.88 (m, 3H), 3.77 (s, 6H), 3.87 (s, 3H), 4.30-4.34 (q, 1H), 4.74-4.78 (q, 1H), 6.35 (s, 1H) ppm. ^{13}C NMR (100 MHz, $CDCl_3$) δ = 28.5 (CH_2), 29.1 (CH_2), 31.6 (CH_2), 37.2 (CH_2), 55.7 (CH_3), 56.0 (CH), 60.5 (CH_3), 60.8 (CH_3), 107.4 (CH), 122.6 (Cq), 129.0 (Cq), 140.1 (Cq), 150.7 (Cq), 152.6 (Cq), 174.2 (Cq) ppm. Spectral data is in accordance with the literature.[25]

2.I.5.16: 5,6,11,11b-tetrahydro-1*H*-indolizino[8,7-*b*]indol-3(2*H*)-one (24d):

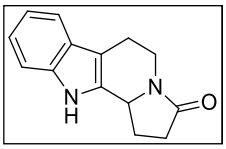

Following the similar protocol described in the 2.I.5.13 with tryptamine **18d** gave the product 5,6,11,11b-tetrahydro-1*H*-indolizino[8,7-*b*]indol-3(2*H*)-one **24d** in 81% yield.

Brown viscous oil. IR (KBr) υ_{max}: 3242, 1660, 1423, 1312, 1094 cm^{-1}. ^{1}H NMR (400 MHz, $CDCl_3$) δ = 1.16-1.23 (m, 1H), 1.86-1.91 (m, 1H), 2.43-2.60 (m, 3H), 2.75-2.81 (m, 2H), 2.80-3.01 (m, 1H), 4.45-4.50 (m, 1H), 4.88-4.90 (m, 1H), 7.06 (t, *J* = 7.2 Hz, 1H), 7.13 (t, *J* = 7.2 Hz, 1H), 7.28 (d, *J* = 8 Hz, 1H), 7.43 (d, *J* = 8 Hz, 1H), 7.99 (bs, 1H) ppm. ^{13}C NMR (100 MHz, $CDCl_3$) δ = 21.0 (CH_2), 25.8 (CH_2), 31.7 (CH_2), 37.7 (CH_2), 54.3 (CH), 108.4 (Cq), 111.0 (CH), 118.5 (CH), 119.9 (CH), 122.3 (CH), 126.8 (Cq), 133.1 (Cq), 136.2 (Cq), 173.3 (Cq) ppm. Spectral data is in accordance with the literature.[66]

2.I.5.17: 9,10-dimethoxy-2,3,6,7-tetrahydro-1*H*-pyrido[2,1-*a*]isoquinolin-4(11b*H*)-one (24e):

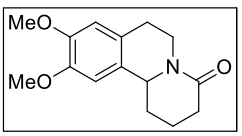

Following the similar protocol described in the 2.I.5.13 with homoveratrylamine **18a** and glutaric acid **23b** gave the product 9,10-dimethoxy-2,3,6,7-tetrahydro-1*H*-pyrido[2,1-*a*]isoquinolin-4(11b*H*)-one **24e** in 74% yield.

Colorless solid, m.p.: 78-79 °C. IR (KBr) υ_{max}: 2939, 2840, 1687, 1623, 1513, 1463, 1355, 1270, 1221, 1019, 872 cm^{-1}. ^{1}H NMR (400 MHz, $CDCl_3$) δ = 1.53-1.63 (m, 1H), 1.73-1.90

(m, 2H), 2.22-2.33 (m, 1H), 2.43-2.57 (m, 3H), 2.69-2.85 (m, 2H), 3.78 (s, 6H), 4.51-4.55 (m, 1H), 4.75-4.79 (m, 1H), 6.54 (s, 1H), 6.60 (s, 1H) ppm. ^{13}C NMR (100 MHz, $CDCl_3$) δ = 19.4 (CH_2), 28.4 (CH_2), 30.8 (CH_2), 32.0 (CH_2), 39.8 (CH_2), 55.9 (OCH_3), 56.1 (OCH_3), 56.7 (CH), 108.2 (CH), 111.5 (CH), 127.2 (Cq), 129.0 (Cq), 147.7 (Cq), 147.8 (Cq), 169.7 (Cq) ppm. Spectral data is in accordance with the literature.[25]

2.I.5.18: 1,2,3,6,7,12b-hexahydroindolo[2,3-*a*]quinolizin-4(12*H*)-one (24f):

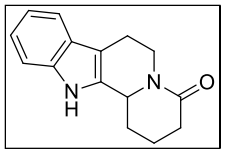

Following the similar protocol described in the 2.I.5.13 with tryptamine **18d** and glutaric acid **23b** gave the product 1,2,3,6,7,12b-hexahydroindolo[2,3-*a*]quinolizin-4(12*H*)-one **24f** in 79% yield.

Off white solid, m.p.: 238-240 °C. IR (KBr) υ_{max}: 3269, 3058, 1602, 1437, 1266 cm^{-1}. ^{1}H NMR (400 MHz, $CDCl_3$) δ = 1.69-1.82 (m, 2H), 1.88-1.93 (m, 1H), 2.32-2.40 (m, 2H), 2.49-2.56 (m, 1H), 2.67-2.74 (m, 1H), 2.77-2.82 (m, 2H), 4.69-4.73 (m, 1H), 5.08-5.12 (m, 1H), 7.05 (t, *J* = 6.8 Hz, 1H), 7.11 (t, *J* = 7 Hz, 1H), 7.27 (d, *J* = 8 Hz, 1H), 7.43 (d, *J* = 7.8 Hz, 1H), 7.88 (bs, 1H) ppm. ^{13}C NMR (100 MHz, $CDCl_3$) δ = 19.4 (CH_2), 21.0 (CH_2), 29.1 (CH_2), 32.4 (CH_2), 40.1 (CH_2), 54.4 (CH), 109.7 (Cq), 110.9 (CH), 118.4 (CH), 119.9 (CH), 122.1 (CH), 126.9 (Cq), 133.3 (Cq), 136.2 (Cq), 169.2 (Cq) ppm. Spectral data is in accordance with the literature.[67]

2.I.5.19: (±)-Crispine A (13):

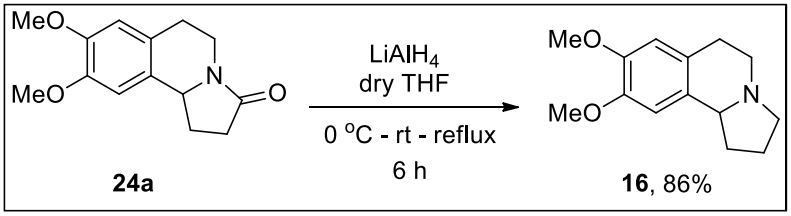

In a 50 mL three-neck round bottom flask equipped with a stirring bar, and condenser was added 40 mmol of $LiAlH_4$ and cooled to 0 °C. To that solid 10 mL of freshly dried THF

was added and the reaction was stirred for 5 mins. Then, 1 mmol of 8,9-dimethoxy-1,5,6,10b-tetrahydropyrrolo[2,1-*a*]isoquinolin-3(2*H*)-one **24a** was dissolved in 5 mL dry THF and slowly added to the above mixture *via* syringe. The reaction was stirred from 0 °C to room temperature for 0.5 hours. Then the reaction was refluxed for another 6 hours before quenching it using the Fieser workup method. The reaction was cooled to 0 °C and diluted with dry diethyl ether. Then, 1.5 mL of H_2O followed by 1.5 mL of 15% NaOH solution and 4.5 mL of H_2O was added sequentially. The reaction mixture was stirred vigorously at room temperature and to that 0.5 g of anhydrous $MgSO_4$ was added. The resultant solid material was filtered and the filtrate was dried over anhydrous Na_2SO_4 and concentrated over a rotary evaporator to give compound **13** as a white solid in 86% yield.

Colorless solid, m.p. 89-92 °C. IR (KBr) υ_{max}: 2939, 2833, 1707, 1609, 1523, 1424, 1248, 1107, 1012, 863, 768 cm^{-1}. ^1H NMR (400 MHz, $CDCl_3$) δ = 1.65-1.72 (m, 1H), 1.79-1.89 (m, 2H), 2.26-2.30 (m, 1H), 2.55-2.73 (m, 3H), 2.91-3.04 (m, 2H), 3.09-3.14 (m, 1H), 3.44 (t, *J* = 8.4 Hz, 1H), 3.78 (s, 6H), 6.50 (s, 1H), 6.54 (s, 1H) ppm. ^{13}C NMR (100 MHz, $CDCl_3$) δ = 22.2 (CH_2), 27.8 (CH_2), 30.6 (CH_2), 48.3 (CH_2), 53.1 (CH_2), 55.9 (CH_3), 56.0 (CH_3), 62.8 (CH), 108.8 (CH), 111.3 (CH), 126.0 (Cq), 130.6 (Cq), 147.3 (Cq), 147.4 (Cq) ppm. Spectral data is in accordance with the literature.[25]

2.I.5.20: (±)-Trolline/oleracein E (19):

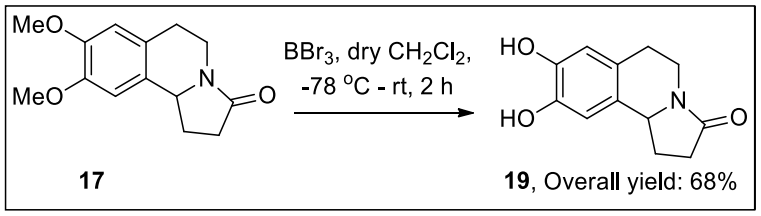

In a two-neck, round bottom flask equipped with stirring bar and nitrogen balloon was added 1 mmol of 8,9-dimethoxy-1,5,6,10b-tetrahydropyrrolo[2,1-*a*]isoquinolin-3(2*H*)-one **24a** and 3 mL of dry CH_2Cl_2 at -78 °C, 0.25 mL of BBr_3 was added and the mixture was stirred for 2 hours till it attained the room temperature. The resulting dark-colored mixture was evaporated under reduced pressure and the crude material was purified over flash chromatography in basic alumina (CH_2Cl_2) to obtain (±)-trolline/oleracein E **19** in 83% yield.

Colorless solid, m.p. 248-252 °C. IR (KBr) υ_{max}: 3334, 3120, 2971, 2968, 2903, 1652,

1615, 1526, 1475, 1446, 1357, 1310, 1278, 1210, 1192, 1163, 1143, 872, 781, 659, 618 cm^{-1}. ^1H NMR (400 MHz, $CDCl_3$) δ = 1.54-1.64 (m, 1H), 2.19-2.25 (m, 1H), 2.36-2.45 (m, 1H), 2.55-2.62 (m, 3H), 2.63-2.95 (m, 1H), 4.58 (t, *J* = 8 Hz, 1H), 6.50 & 6.51 (2Xs, 2H), 8.81 (s, 1H), 8.86 (s, 1H) ppm. ^{13}C NMR (100 MHz, $CDCl_3$) δ = 26.7 (CH_2), 26.8 (CH_2), 30.6 (CH_2), 36.0 (CH_2), 54.9 (CH), 111.0 (CH), 114.7 (CH), 123.0 (Cq), 127.8 (Cq), 143.4 (Cq), 143.5 (Cq), 171.4 (Cq) ppm. Spectral data is in accordance with the literature.[25]

2.I.5.21: (±)-Harmicine:

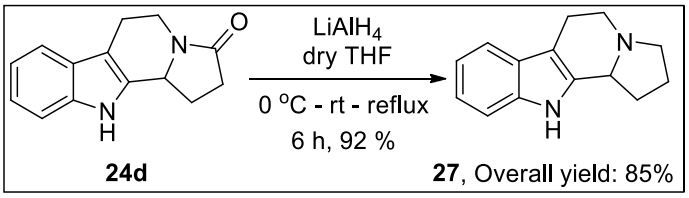

Following the similar protocol described in 2.I.5.19 with compound **24d** gave the product (±)-harmicine **27** in 81% yield.

Colorless solid, m.p. 160-163 °C. IR (KBr) υ_{max}: 3412, 3153, 3058, 2923, 2853, 2748, 2246, 1448, 1352, 1329, 1315, 1284, 1205, 1169, 1144, 1126, 1012, 912, 649 cm^{-1}. ^1H NMR (400 MHz, $CDCl_3$) δ = 1.77-1.84 (m, 3H), 2.19-2.22 (m, 1H), 2.57-2.62 (m, 1H), 2.79-2.90 (m, 3H), 2.98-3.05 (m, 1H), 3.22-3.26 (m, 1H), 4.16-4.18 (m, 1H), 7.00-7.08 (m, 2H), 7.23 (d, *J* = 8 Hz, 1H), 7.40 (*J* = 7.6 Hz, 1H), 8.10 (bs, 1H) ppm. ^{13}C NMR (100 MHz, $CDCl_3$) δ = 17.8 (CH_2), 23.4 (CH_2), 29.5 (CH_2), 46.0 (CH_2), 49.4 (CH_2), 57.1 (CH), 107.6 (Cq), 110.9 (CH), 118.1 (CH), 119.4 (CH), 121.5 (CH), 127.2 (Cq), 135.1 (Cq), 136.0 (Cq) ppm. Spectral data is in accordance with the literature.[68]

2.I.5.22: 8,9,10-trihydroxy-1,5,6,10b-tetrahydropyrrolo[2,1-*a*]isoquinolin-3(2*H*)-one (28):

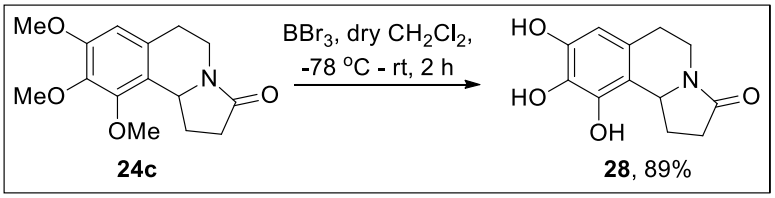

Following the similar protocol described in 2.I.5.20 with 8,9,10-trimethoxy-1,5,6,10b-

tetrahydropyrrolo[2,1-*a*]isoquinolin-3(2*H*)-one **24c** gave the product 8,9,10-trihydroxy-1,5,6,10b-tetrahydropyrrolo[2,1-*a*]isoquinolin-3(2*H*)-one **28** in 89% yield.

Colourless solid, m.p. 278-283 °C. IR (KBr) υ_{max}: 3345, 3127, 2967, 2945, 1652, 1623, 1524, 1480, 1451, 1363, 1306, 1281, 1207, 1148, 874, 784, 659, 617 cm^{-1}. ^{1}H NMR (400 MHz, $CDCl_3$) δ = 1.44-1.55 (m, 1H), 2.13-2.19 (m, 1H), 2.36-2.57 (m, 3H), 2.72-2.78 (m, 2H), 4.05-4.09 (m, 1H), 4.62-4.66 (q, 1H), 6.07 (s, 1H), 8.19 (s, 1H), 8.40 (s, 1H), 9.03 (s, 1H) ppm. ^{13}C NMR (100 MHz, $CDCl_3$) δ = 28.5 (CH_2), 28.8 (CH_2), 31.6 (CH_2), 36.9 (CH_2), 54.8 (CH), 106.9 (CH), 116.5 (Cq), 124.3 (Cq), 131.7 (Cq), 143.9 (Cq), 145.1 (Cq), 172.6 (Cq) ppm. HRMS (m/z): calculated for $C_{12}H_{13}NO_4Na$ $[M+Na]^+$: 258.0742; found 258.0739.

2.I.6 References:

1) Zhang, Q.; Tu, G.; Zhao, Y.; Cheng, T. *Tetrahedron* **2002**, *58*, 6795.
2) Wang, R. F.; Yang, X. W.; Ma, C. M.; Cai, S. Q.; Li, J. N.; Shoyama, Y. *Heterocycles* **2004**, *63*, 1443.
3) Zhao, Y.-X.; Ding, X.-B. *Yaoxue Xuebao* **2004**, *39*, 598.
4) Xiang, L.; Xing, D.; Wang, W.; Wang, R.; Ding Y.; Du, L. *Phytochemistry* **2005**, *66*, 2595.
5) Wu, H.-F.; Shen, J.-W.; Song, Z.-J.; Ge-Sang, S.-L.; Zhu, H.-J.; Peng, S.-L.; Zhang, X.-F. *Nat. Prod. R&D* **2009**, *21*, 430.
6) Kapadia, G. J.; Fales, H. M. *Chem. Commun*. **1968**, 1688.
7) Kam, T. S.; Sim K. M. *Phytochemistry* **1998**, *47*, 145.
8) El-Subbagh, H.; Wittig, T.; Decker, M.; Elz, S.; Nieger, M.; Lehmann, J. *Arch. Pharm.* **2002**, *335*, 443.
9) Yang, Z.; Liu, C.; Xiang L.; Zheng, Y. *Phytother. Res*. **2009**, *23*, 1032.
10) Spindola, H. M.; Vendramini-Costa, D. B.; Rodrigues, M. T.; Jr Foglio, M. A.; Pilli, R. A.; Carvalho, J. E. *Pharmacol Biochem Behav.* **2012**, *102*, 133.
11) Maryanoff, B. E.; McComsey, D. F.; Costanzo, M. J.; Setler, P. E.; Gardocki, J. F.; Shank, R. P.; Schneider, C. R. *J. Med. Chem.* **1984**, *27*, 8, 943.
12) Pässler, U.; Knölker, H.-J. *The Pyrrolo[2,1-a]isoquinoline Alkaloids*, Hans-Joachim Knölker, The Alkaloids: Chemistry and Biology, Academic Press, **2011**, 70, 79.
13) Louafi, F.; Moreau, J.; Shahane, S.; Golhen, S.; Roisnel, T.; Sinbandhit, S.; Hurvois, J. P. *J. Org. Chem.* **2011**, *76*, 9720.
14) Xu, K.; Lai, G.; Zha, Z.; Pan, S.; Chen, H.; Wang, Z. *Chem. - A Eur. J.* **2012**, *18*, 12357.
15) Fraile, A.; Scarpino Schietroma, D. M.; Albrecht, A.; Davis, R. L.; Jørgensen, K. A. *Chem. - A Eur. J.* **2012**, *18*, 2773.
16) Sánchez-Obregón, R.; Ortiz, B.; Mastranzo, V. M.; Yuste, F.; Ruano, J. L. G. *Tetrahedron Lett.* **2013**, *54*, 1893.
17) Agarwal, S.; Kataeva, O.; Schmidt, U.; Knölker, H. J. *RSC Adv.* **2013**, *3*, 1089.
18) Reddy, N. S. S.; Reddy, B. J. M.; Reddy, B. V. S. *Tetrahedron Lett.* **2013**, *54*, 4228.
19) Rotte, S. C. K.; Chittiboyina, A. G.; Khan, I. A. *Eur. J. Org. Chem.* **2013**, *28*, 6355.
20) Dhanasekaran, S.; Bisai, V.; Unhale, R. A.; Suneja, A.; Singh, V. K. *Org. Lett.* **2014**, *16*, 6068.

21) Lin, W.; Ma, S. *Org. Chem. Front.* **2014**, *1*, 338.

22) Pandey, V. K.; Anbarasan, P. *J. Org. Chem.* **2014**, *79*, 4154.

23) Orejarena Pacheco, J. C.; Lipp, A.; Nauth, A. M.; Acke, F.; Dietz, J. P.; Opatz, T. *Chem. - A Eur. J.* **2016**, *22*, 5409.

24) Yan, C.; Liu, Y.; Wang, Q. *Org. Lett.* **2015**, *17*, 5714.

25) Selvakumar, J.; Rao, R. S.; Srinivasapriyan, V.; Marutheeswaran, S.; Ramanathan, C. R. *Eur. J. Org. Chem.* **2015**, *2015*, 2175.

26) Jebali, K.; Planchat, A.; Amri, H.; Mathé-Allainmat, M.; Lebreton, J. *Synthesis* **2016**, *48*, 1502.

27) Pandey, G.; Tiwari, S. K.; Singh, B. *Tetrahedron Lett.* **2016**, *57*, 4480.

28) Basavaiah, D.; Lingaiah, B.; Reddy, G. C.; Sahu, B. C. *Eur. J. Org. Chem.* **2016**, *2016*, 2398.

29) Xu, X. M.; Zhao, L.; Zhu, J.; Wang, M. X. *Angew. Chemie - Int. Ed.* **2016**, *55*, 3799.

30) (a) Fandrick, D. R.; Hart, C. A.; Okafor, I. S.; Mercadante, M. A.; Sanyal, S.; Masters, J. T.; Sarvestani, M.; Fandrick, K. R.; Stockdill, J. L.; Grinberg, N.; Gonnella, N.; Lee, H.; Senanayake, C. H. *Org. Lett.* **2016**, *18*, 6192. (b) Yim, J. C-H.; Bexrud, J. A.; Ayinla, R. O.; Leitch, D. C.; Schafer, L. L. *J. Org. Chem.* **2014**, *79*, 2015.

31) Murai, K.; Matsuura, K.; Aoyama, H.; Fujioka, H. *Org. Lett.* **2016**, *18*, 1314.

32) Talk, R. A.; Duperray, A.; Li, X.; Coldham, I. *Org. Biomol. Chem.* **2016**, *14*, 4908.

33) Selvakumar, J.; Mangalaraj, S.; Achari, K. M. M.; Mukund, K.; Ramanathan, C. R. *Synthesis* **2017**, *49*, 1053.

34) Molina, A.; Pascual-Escudero, A.; Adrio, J.; Carretero, J. C. *J. Org. Chem.* **2017**, *82*, 11238.

35) Chiang, P. F.; Li, W. S.; Jian, J. H.; Kuo, T. S.; Wu, P. Y.; Wu, H. L. *Org. Lett.* **2018**, *20*, 158.

36) Lin, W.; Ma, S. *Org. Chem. Front.* **2017**, *4*, 958.

37) Aranzamendi, E.; Sotomayor, N.; Lete, E. *ACS Omega* **2017**, *2*, 2706.

38) Sun, K.; Yuan, B. H.; Hu, Y.; Sun, X. W.; Lin, G. Q. *J. Saudi Chem. Soc.* **2018**, *22*, 654.

39) Voskressensky, L. G.; Borisova, T. N.; Matveeva, M. D.; Khrustalev, V. N.; Titov, A. A.; Aksenov, A. V.; Dyachenko, S. V.; Varlamov, A. V. *Tetrahedron Lett.* **2017**, *58*, 877.

40) Punirun, T.; Soorukram, D.; Kuhakarn, C.; Reutrakul, V.; Pohmakotr, M. *J. Org. Chem.* **2018**, *83*, 765.

41) Zidan, A.; Cordier, M.; El-Naggar, A. M.; Abd El-Sattar, N. E. A.; Hassan, M. A.; Khalil, A. K.; El Kaïm, L. *Org. Lett.* **2018**, *20*, 2568.

42) Zhu, Z.; Chandak, H. S.; Seidel, D. *Org. Lett.* **2018**, *20*, 4090.

43) Kalshetti, M. G.; Argade, N. P. *Indian J. Chem., Sec. B* **2019**, *58*, 669.

44) Donmez, S. E.; Soydaş, E.; Aydln, G.; Şahin, O.; Bozkaya, U.; Türkmen, Y. E. *Org. Lett.* **2019**, *21*, 554.

45) Zhao, J.; Méndez-Sánchez, D.; Ward, J. M.; Hailes H. C. *J. Org. Chem.* **2019**, *84*, 7702.

46) Kurpil, B.; Otte, K.; Mishchenko, A.; Lamagni, P.; Lipiński, W.; Lock, N.; Antonietti, M.; Savateev, A. *Nat. Commun.* **2019**, *10*, 945.

47) Jia, X.; Li, P.; Liu, X.; Lin, J.; Chu, Y.; Yu, J.; Wang, J.; Liu, H.; Zhao, F. *Molecules* **2019**, *24*, 988.

48) Wang, G.-W.; Sokolova, O. O.; Young, T. A.; Christodoulou, E. M. S.; Butts, C. P.; Bower, J. F. *J. Am. Chem. Soc.* **2020**, *142*, 19006.

49) Ben Jamaa, A.; Latrache, M.; Riguet, E.; Grellepois, F. *J. Org. Chem.* **2020**, *85*, 9585.

50) Souquet, F.; Drici, W.; Fayssal, S. A.; Lazouni, I.; Thueillon, S.; Pérard-Viret, J. A. *Synthesis* **2020**, *52*, 2970.

51) Habel, D.; Nair, D. S.; Kallingathodi, Z.; Mohan, C.; Pillai, S. M.; Nair, R. R.; Thomas, G.; Haleema, S.; Gopinath, C.; Abdul, R. V.; Fritz, M.; Puente, A. R.; Johnson, J. L.; Polavarapu, P. L.; Ibnusaud, I. *J. Nat. Prod.* **2020**, *83*, 2178.

52) Pashev, A.; Burdzhiev, N.; Stanoeva, E. *Beilstein J. Org. Chem.* **2020**, *16*, 1456.

53) Zheng, Y.; Liu, J.; Lei, X. *Org. Chem. Front.* **2020**, *7*, 660.

54) Nalikezhathu, A.; Cherepakhin, V.; Williams, T. *J. Org. Lett.* **2020**, *22*, 4979.

55) Ansari, A.; Gorde, A. B.; Ramapanicker, R. *Tetrahedron* **2021**, *88*, 132121.

56) Song, Q.; Liu, Y.; Cai, L.; Cao, X.; Qian, S.; Wang, Z. *Chinese Chem. Lett.* **2021**, *32*, 1713.

57) Patrick, U.; Schlamkow, M. A.; Choi, C.-Y.; Kerkenpass, H.; Henssen, B.; Pietruszka, J. *Eur. J. Org. Chem.* **2021**, *2021*, 6254.

58) Jawale, D. V.; Gravel, E.; Shah, N.; Dauvois, V.; Li, H.; Namboothiri, I. N. N.; Doris, E. *Chem. - A Eur. J.* **2015**, *21*, 7039.

59) Karthikeyan, I.; Arunprasatha, D.; Sekar, G. *Chem. Commun.* **2015**, *51*, 1701.

60) Vuillaume, P. Y.; Jonas, A. M.; Laschewsky, A. *Macromolecules* **2002**, *35*, 5004.

61) Dai, X.; Rabeah, J.; Yuan, H.; Brueckner, A.; Cui, X.; Shi, F. *ChemSusChem* **2016**, *9*, 3133.

62) Jung, A.; Min, S.-J. *Asian J. Org. Chem.* **2019**, *8*, 1617.

63) Hiroaki, K.; Akinari, S.; Yuko, O.; Tomohiko, O. *Chem. Eur. J.* **2014**, *20*, 8682.

64) Changge, Z.; Shuai, H.; Yang, L.; Chao, J.; Wei, Z.; Ge, F.; Jianquan, H. *Org. Lett.* **2020**, *22*, 4868.

65) Wangke, Q.; Weijian, L.; Haifeng, S.; Zeng, L.; Liyuan, Z.; Rui, Z.; Lei, Z.; Shengbin, Z.; Yu, Z.; Hualiang, J.; Xuechu, Z.; Hong, L. *Bioorg. Med. Chem.* **2012**, *20*, 4862.

66) da Silva, W. A.; Rodrigues, M. T.; Shankaraiah, N.; Ferreira, R. B.; Kleber, Z. A. C.; Pilli, R.A.; Santos, L. S. *Org. Lett.* **2009**, 11, 3238.

67) Selvaraj, M.; Ramanathan, C. R. *RSC Adv.* **2012**, 2, 12665.

68) Pressnitz, D.; Fischereder, E.-M.; Pletz, J.; Kofler, C.; Hammerer, L.; Hiebler, K.; Lechner, H.; Richter, N.; Eger, E.; Kroutil, W. *Angew. Chem. Int. Ed.* **2018**, *57*, 10683.

NMR Spectra

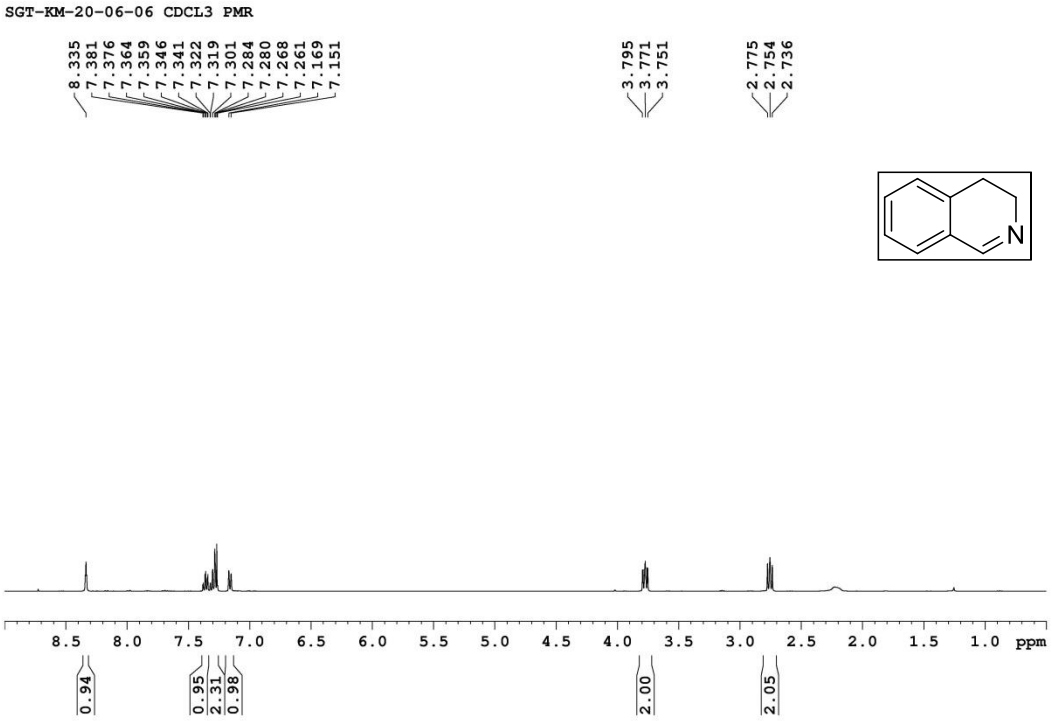
SGT-KM-20-06-06 CDCL3 PMR
8.335
7.381
7.376
7.364
7.359
7.346
7.341
7.322
7.319
7.301
7.284
7.280
7.268
7.261
7.169
7.151
3.795
3.771
3.751
2.775
2.754
2.736
N
8.5 8.0 7.5 7.0 6.5 6.0 5.5 5.0 4.5 4.0 3.5 3.0 2.5 2.0 1.5 1.0 ppm
0.94
0.95
2.31
0.98
2.00
2.05

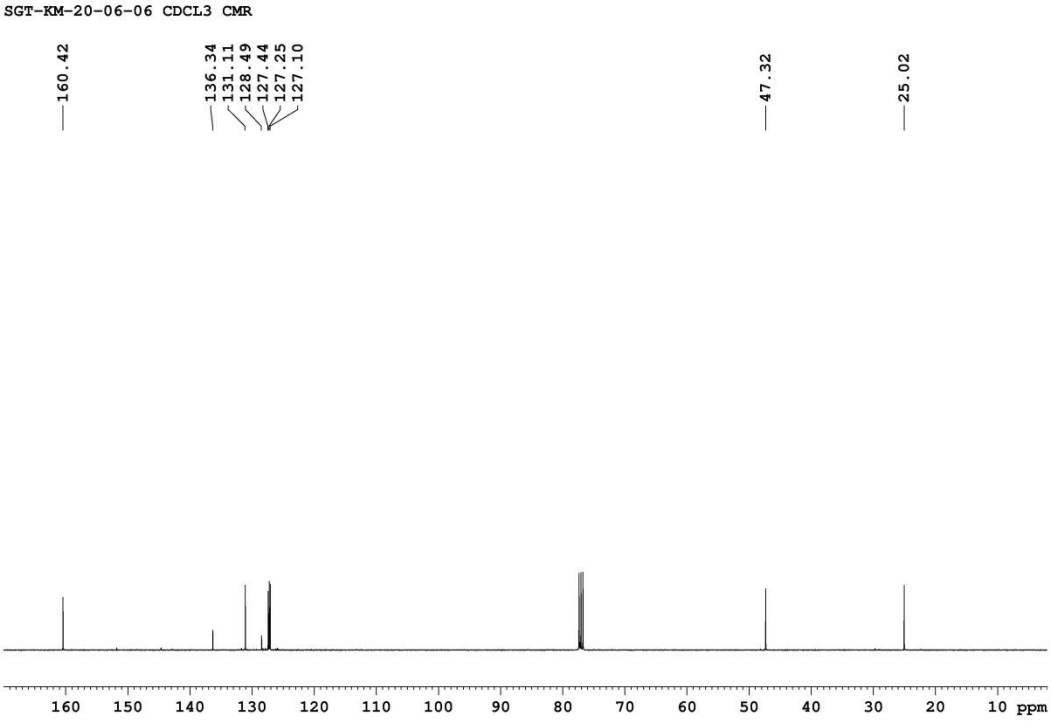
SGT-KM-20-06-06 CDCL3 CMR
160.42
136.34
131.11
128.49
127.44
127.25
127.10
47.32
25.02
160 150 140 130 120 110 100 90 80 70 60 50 40 30 20 10 ppm

SGT-KM-20-06-06 CDCL3 DEPT

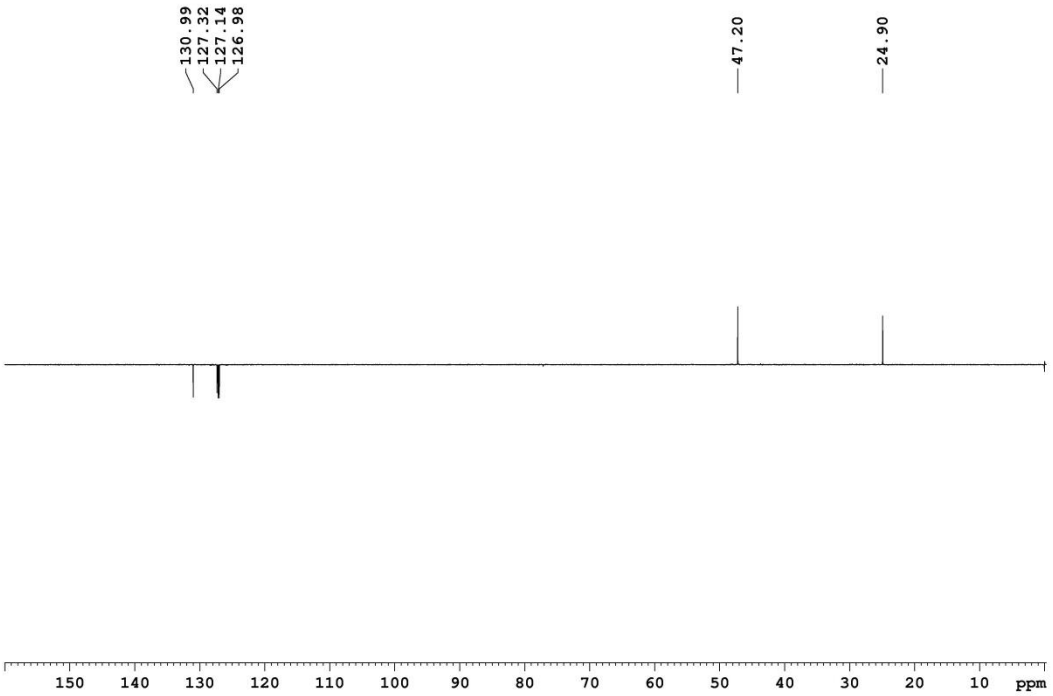

SGT-KM-20-06-11 MEOD PMR

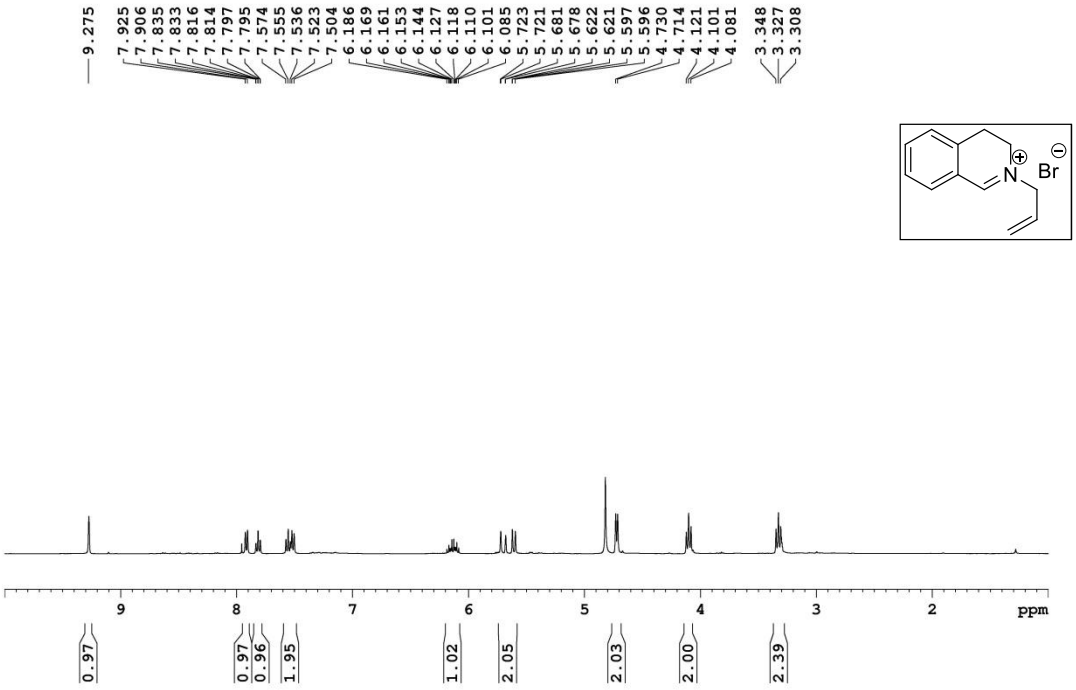

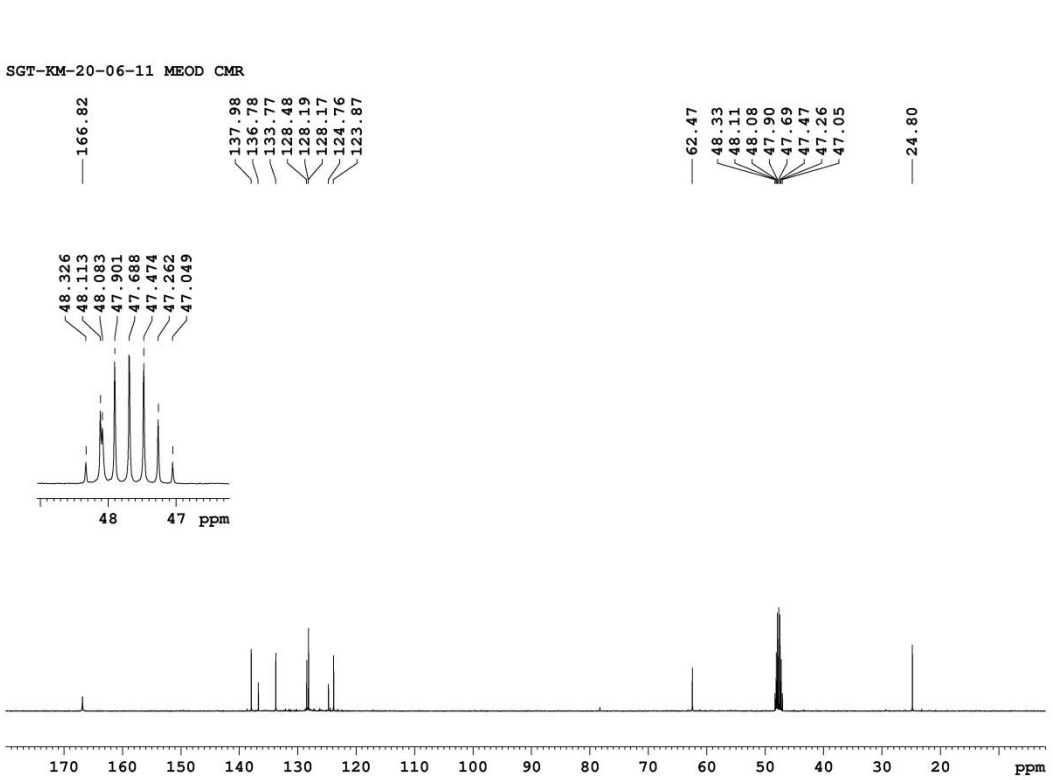
SGT-KM-20-06-11 MEOD CMR
166.82
137.98
136.78
133.77
128.48
128.19
128.17
124.76
123.87
62.47
48.33
48.11
48.08
47.90
47.69
47.47
47.26
47.05
24.80
48.326
48.113
48.083
47.901
47.688
47.474
47.262
47.049
48
47 ppm
170 160 150 140 130 120 110 100 90 80 70 60 50 40 30 20 ppm

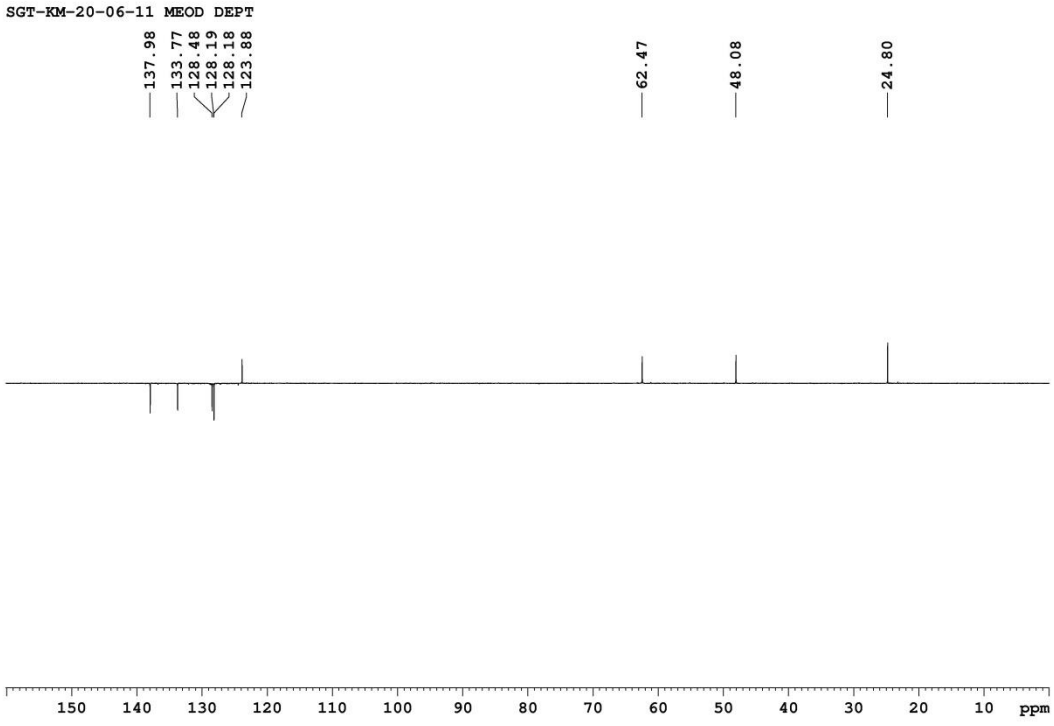
SGT-KM-20-06-11 MEOD DEPT
137.98
133.77
128.48
128.19
128.18
123.88
62.47
48.08
24.80
150 140 130 120 110 100 90 80 70 60 50 40 30 20 10 ppm

SGT-KM-20-09-06 CDCL3 PMR

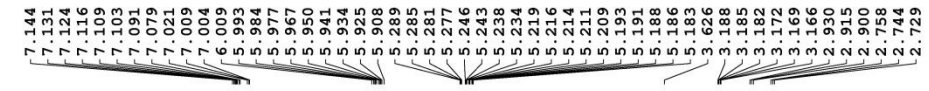

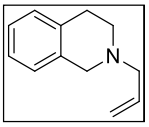

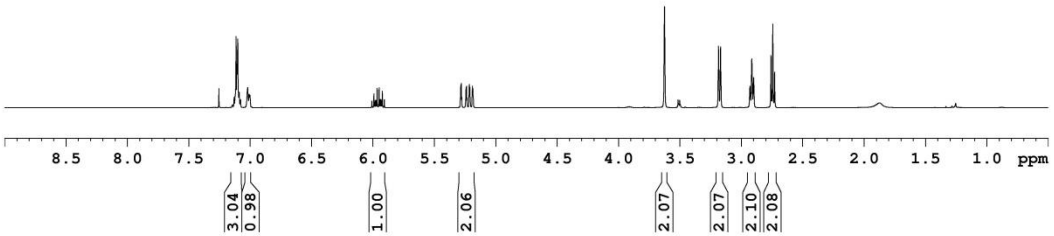

SGT-KM-20-09-06 CDCL3 CMR

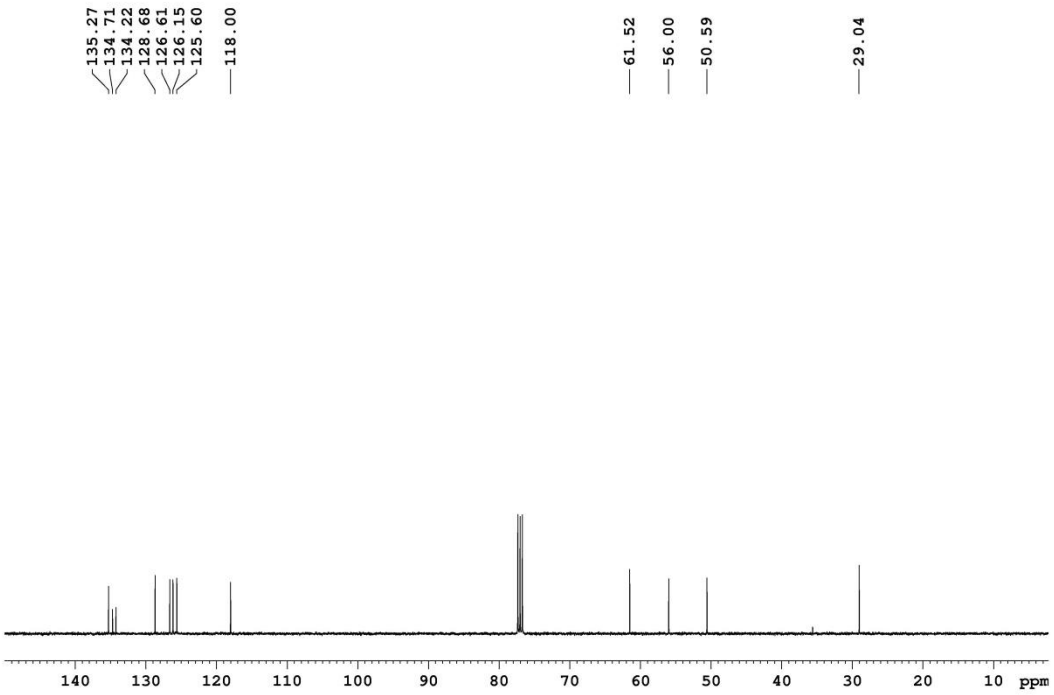

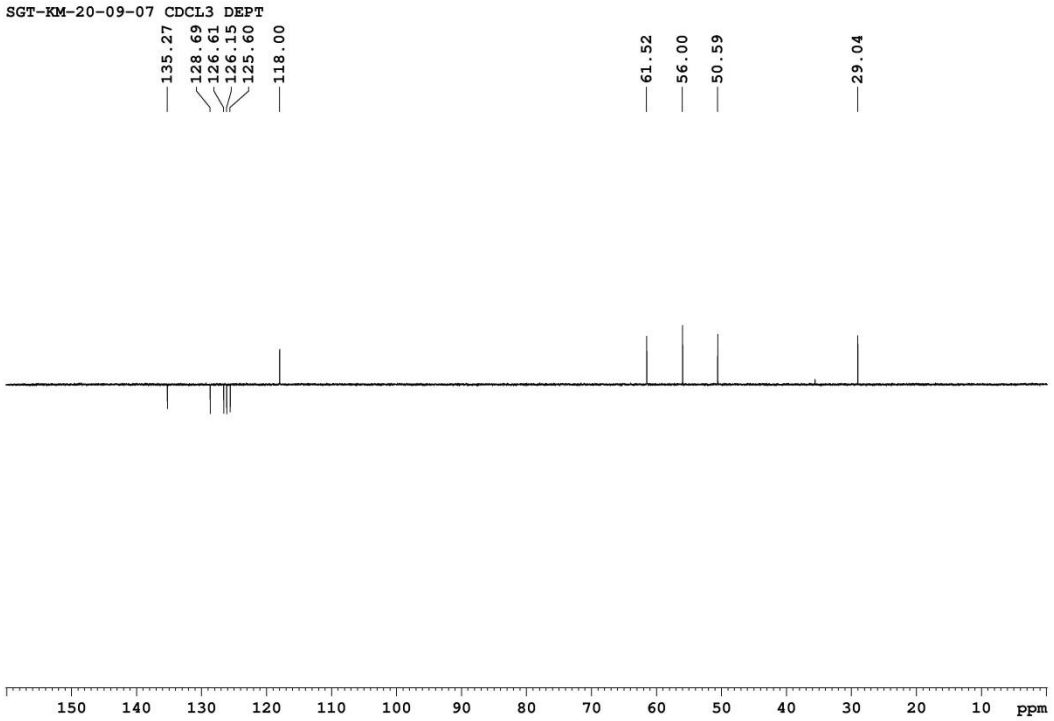
SGT-KM-20-09-07 CDCL3 DEPT
135.27
128.69
126.61
126.15
125.60
118.00
61.52
56.00
50.59
29.04
150 140 130 120 110 100 90 80 70 60 50 40 30 20 10 ppm

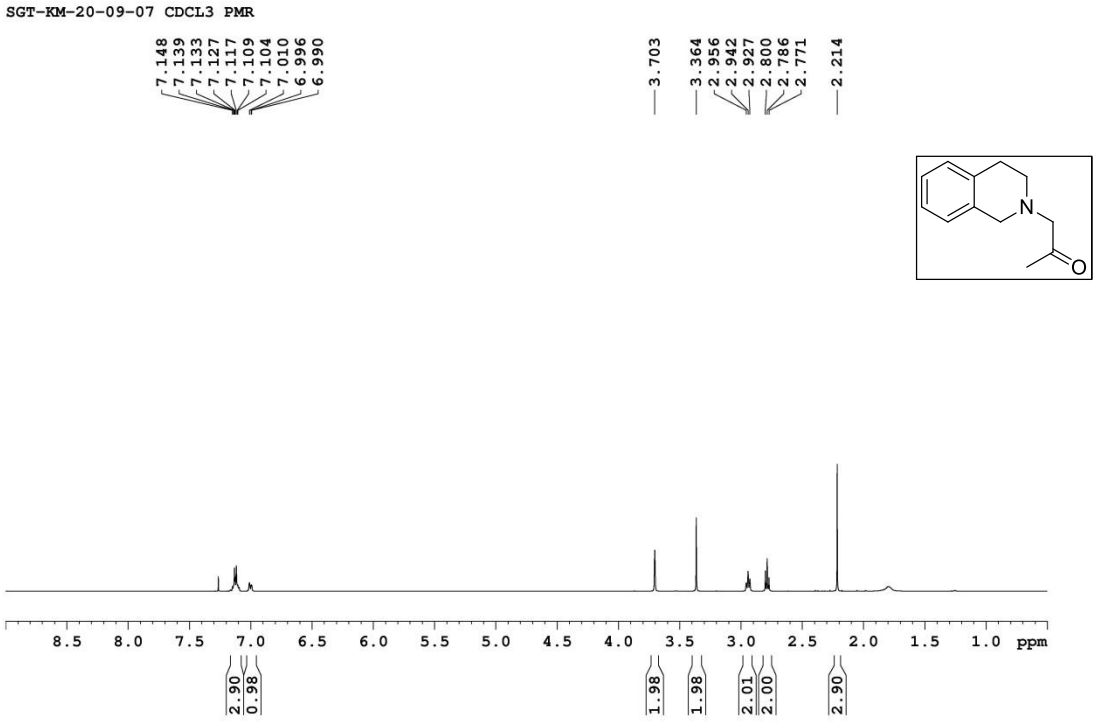
SGT-KM-20-09-07 CDCL3 PMR
7.148
7.139
7.133
7.127
7.117
7.109
7.104
7.010
6.996
6.990
3.703
3.364
2.956
2.942
2.927
2.800
2.786
2.771
2.214
N
O
8.5 8.0 7.5 7.0 6.5 6.0 5.5 5.0 4.5 4.0 3.5 3.0 2.5 2.0 1.5 1.0 ppm
2.90
0.98
1.98
1.98
2.01
2.00
2.90

SGT-KM-20-09-07 CDCL3 CMR

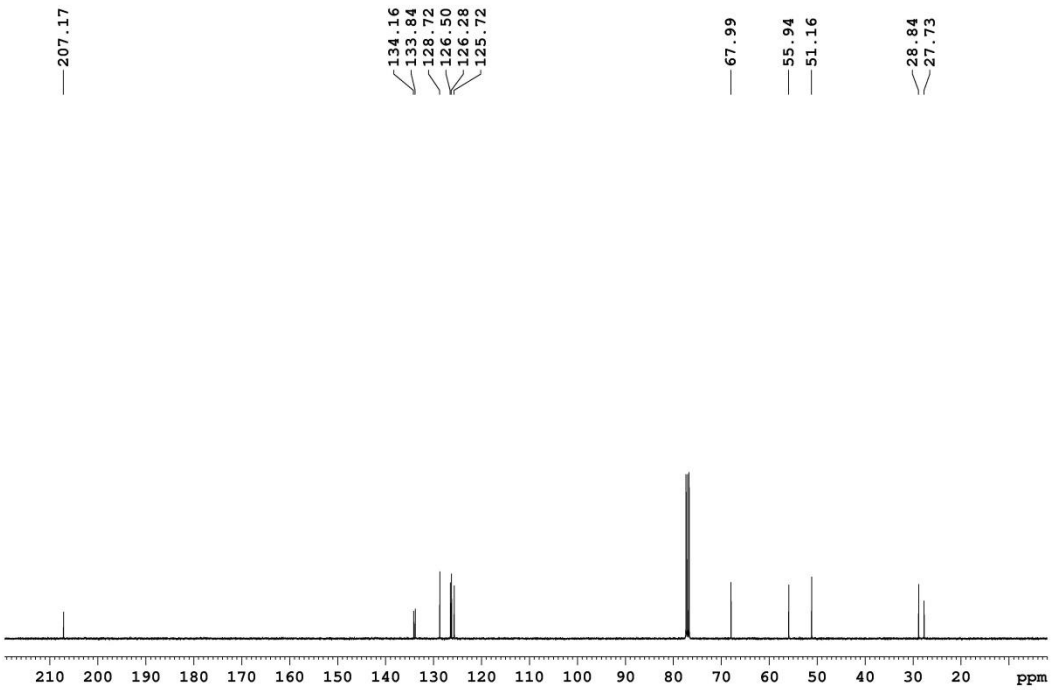

SGT-KM-20-09-07 CDCL3 DEPT

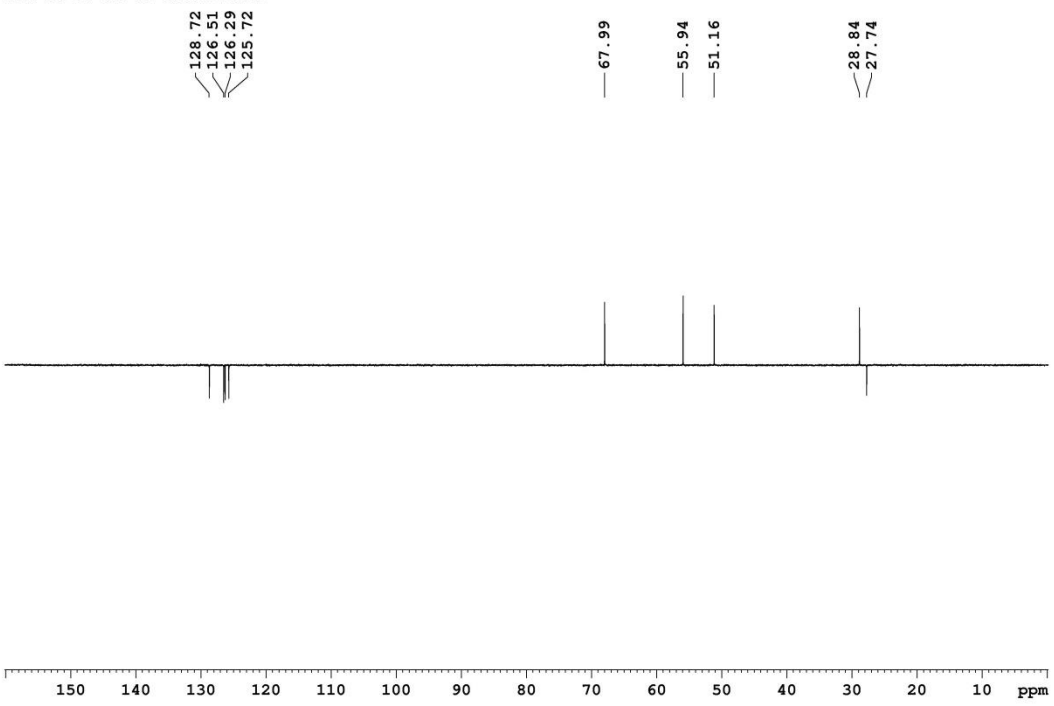

SGT-KM-20-10-01 CDCL3 PMR

8.074
8.055
7.472
7.469
7.454
7.450
7.435
7.431
7.374
7.355
7.336
7.230
7.211
6.323
3.593
3.570
3.553
3.022
3.006
2.989

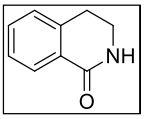

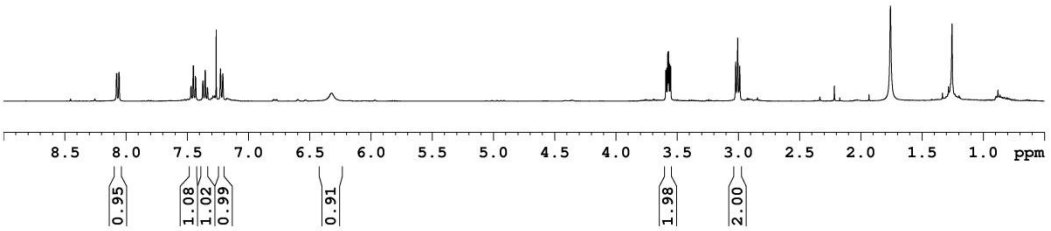

SGT-KM-20-10-01 CDCL3 CMR

166.36
138.83
132.21
128.87
128.03
127.25
127.11
40.26
28.35

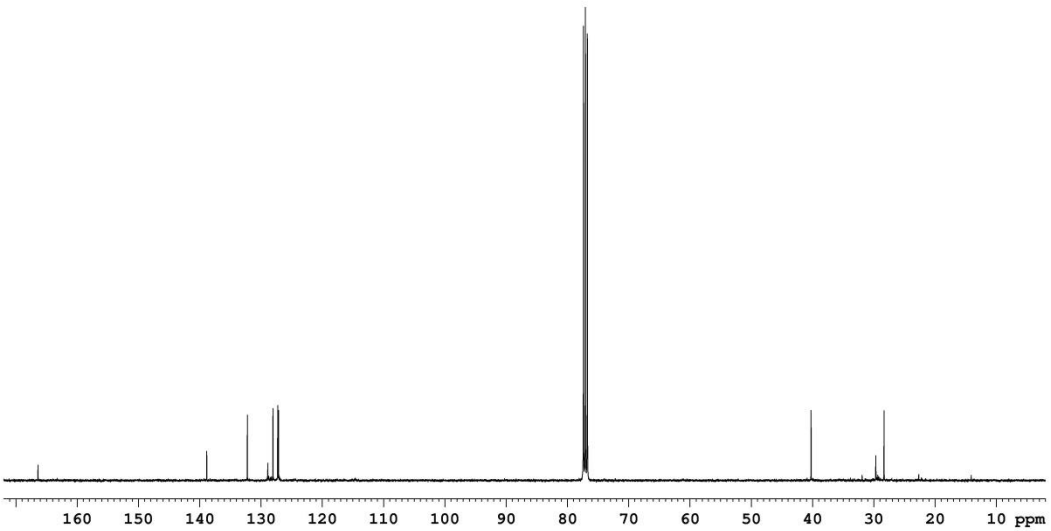

SGT-KM-20-10-01 CDCL3 DEPT

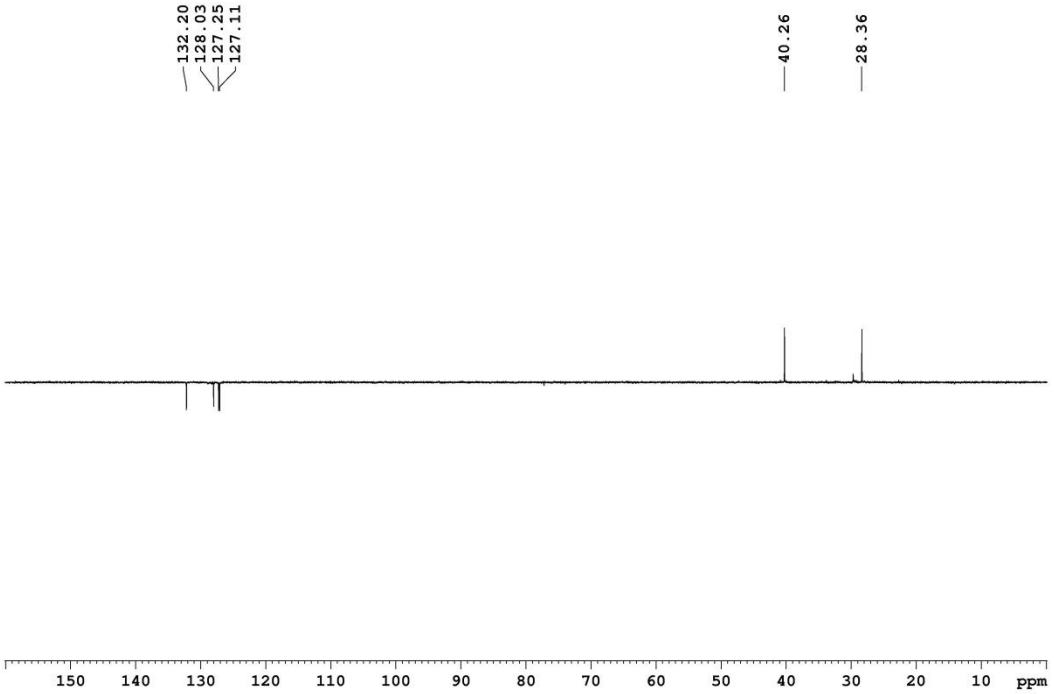

SGT-KM-20-11-07 CDCL3 PMR

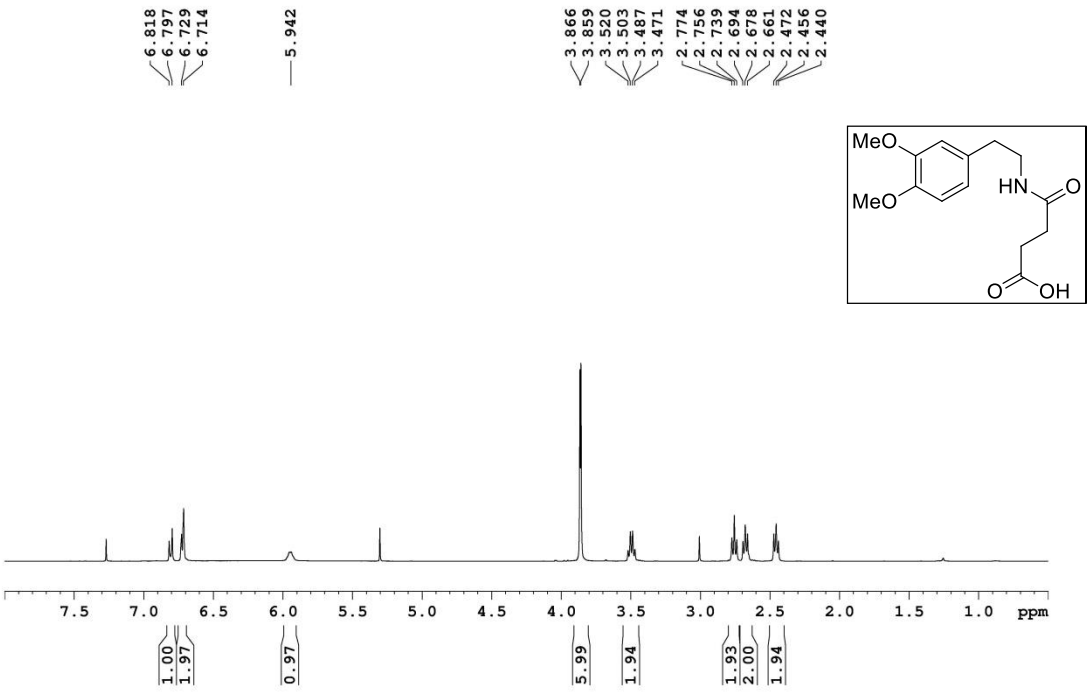

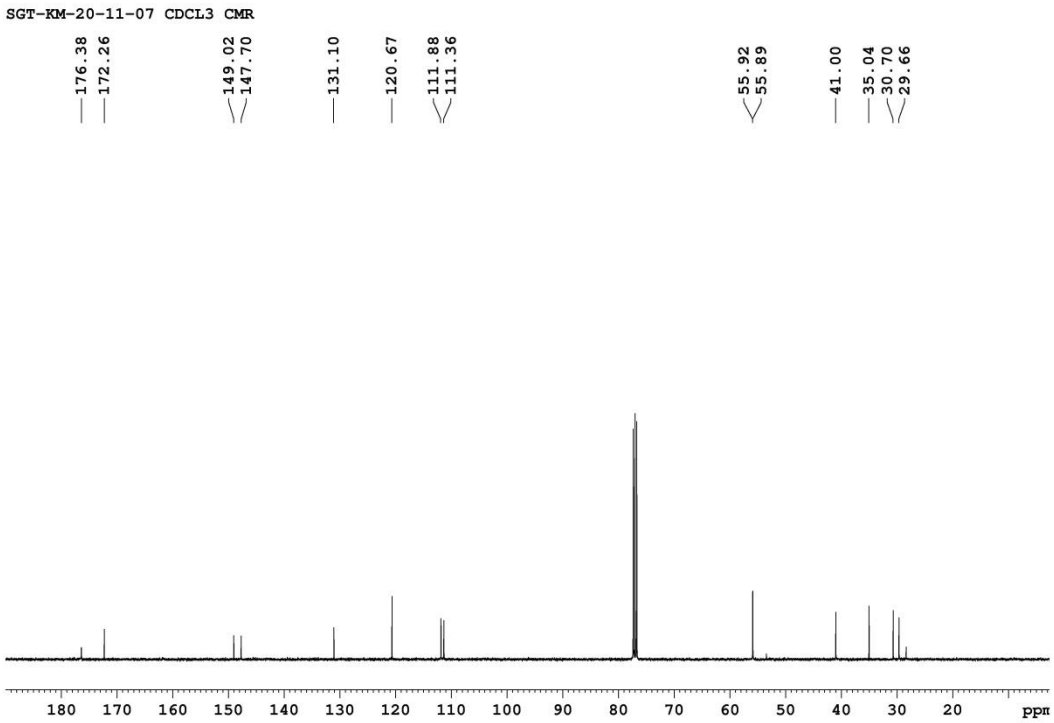
SGT-KM-20-11-07 CDCL3 CMR
176.38
172.26
149.02
147.70
131.10
120.67
111.88
111.36
55.92
55.89
41.00
35.04
30.70
29.66
180 170 160 150 140 130 120 110 100 90 80 70 60 50 40 30 20 ppm

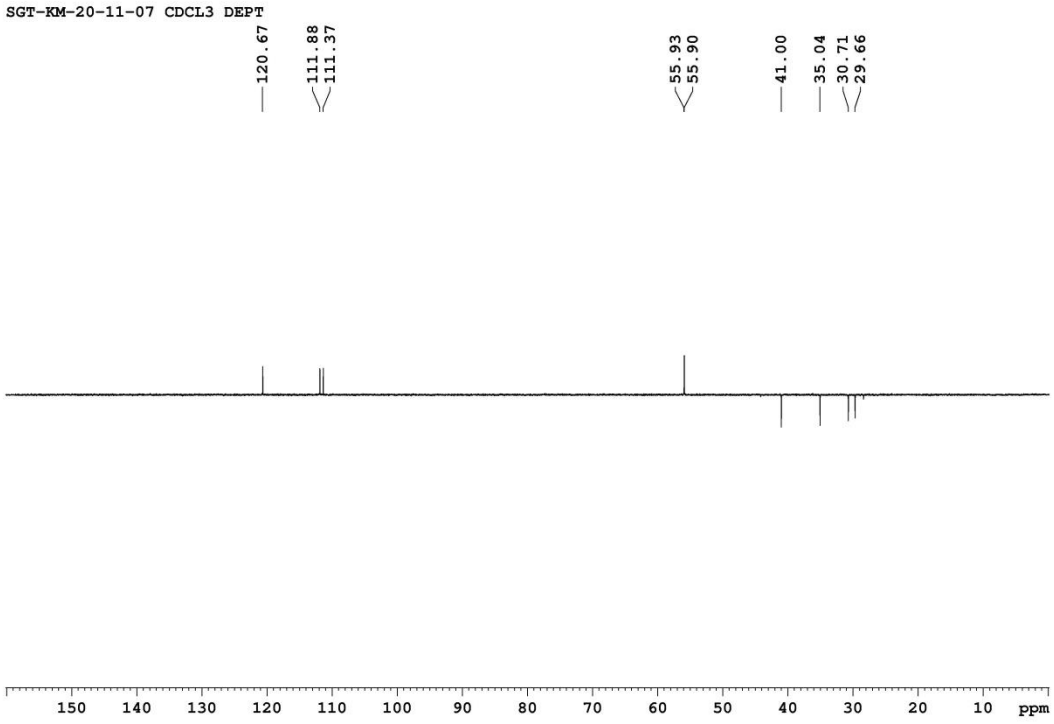
SGT-KM-20-11-07 CDCL3 DEPT
120.67
111.88
111.37
55.93
55.90
41.00
35.04
30.71
29.66
150 140 130 120 110 100 90 80 70 60 50 40 30 20 10 ppm

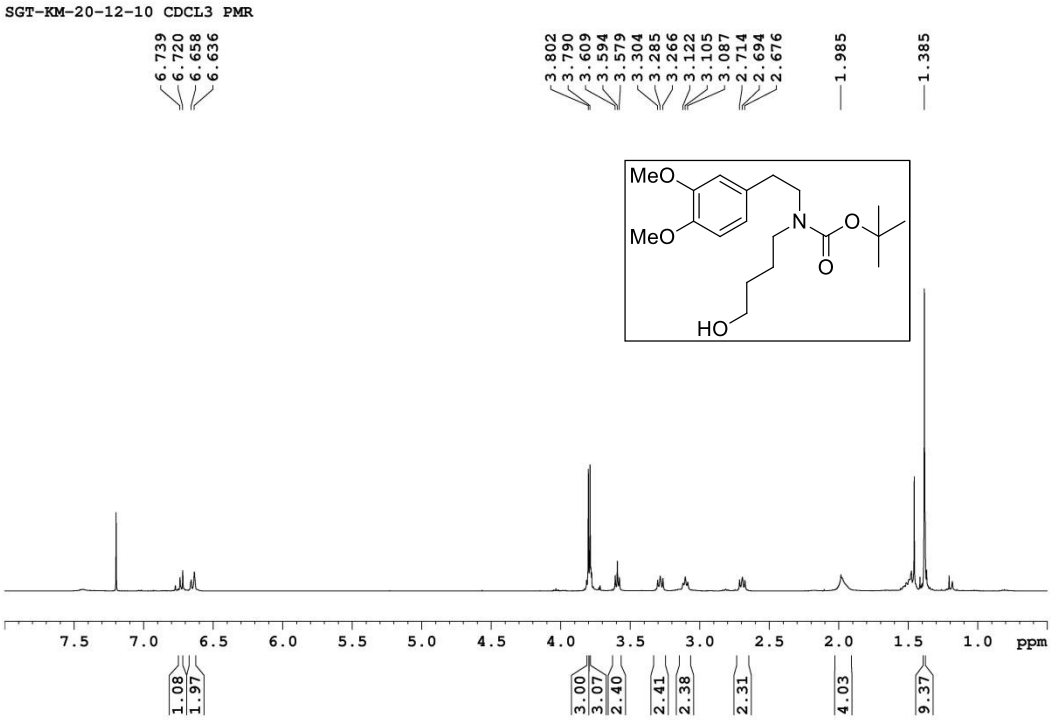
SGT-KM-20-12-10 CDCL3 PMR
6.739
6.720
6.658
6.636
3.802
3.790
3.609
3.594
3.579
3.304
3.285
3.266
3.122
3.105
3.087
2.714
2.694
2.676
1.985
1.385
MeO
MeO
N
O
O
HO
7.5
7.0
6.5
6.0
5.5
5.0
4.5
4.0
3.5
3.0
2.5
2.0
1.5
1.0
ppm
1.08
1.97
3.00
3.07
2.40
2.41
2.38
2.31
4.03
9.37

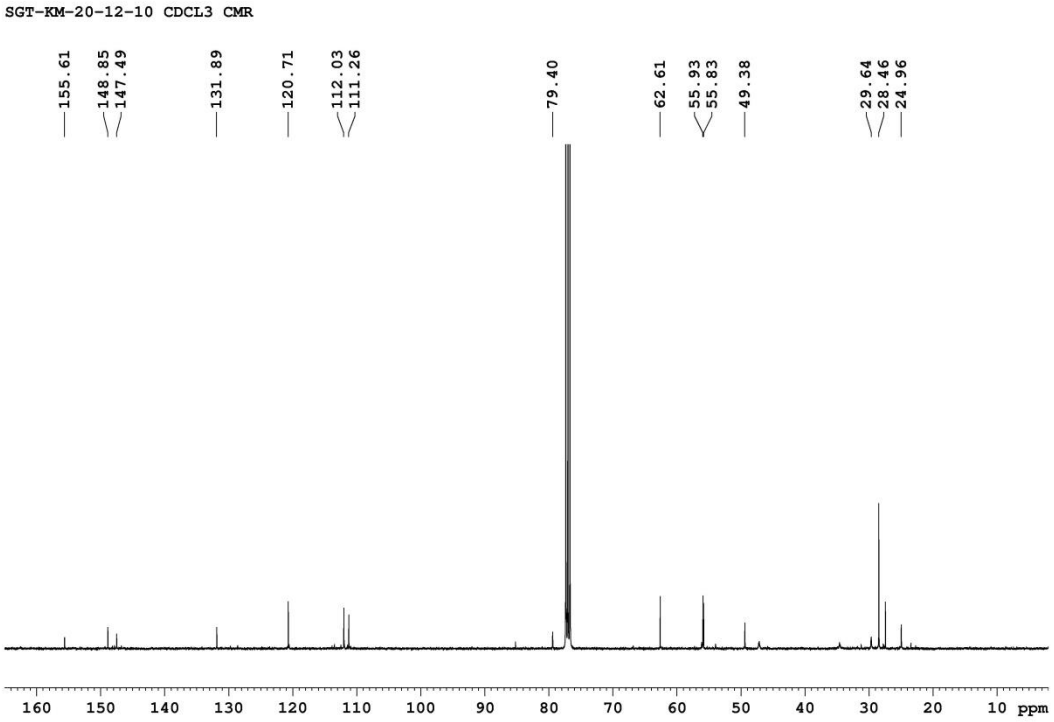
SGT-KM-20-12-10 CDCL3 CMR
155.61
148.85
147.49
131.89
120.71
112.03
111.26
79.40
62.61
55.93
55.83
49.38
29.64
28.46
24.96
160
150
140
130
120
110
100
90
80
70
60
50
40
30
20
10 ppm

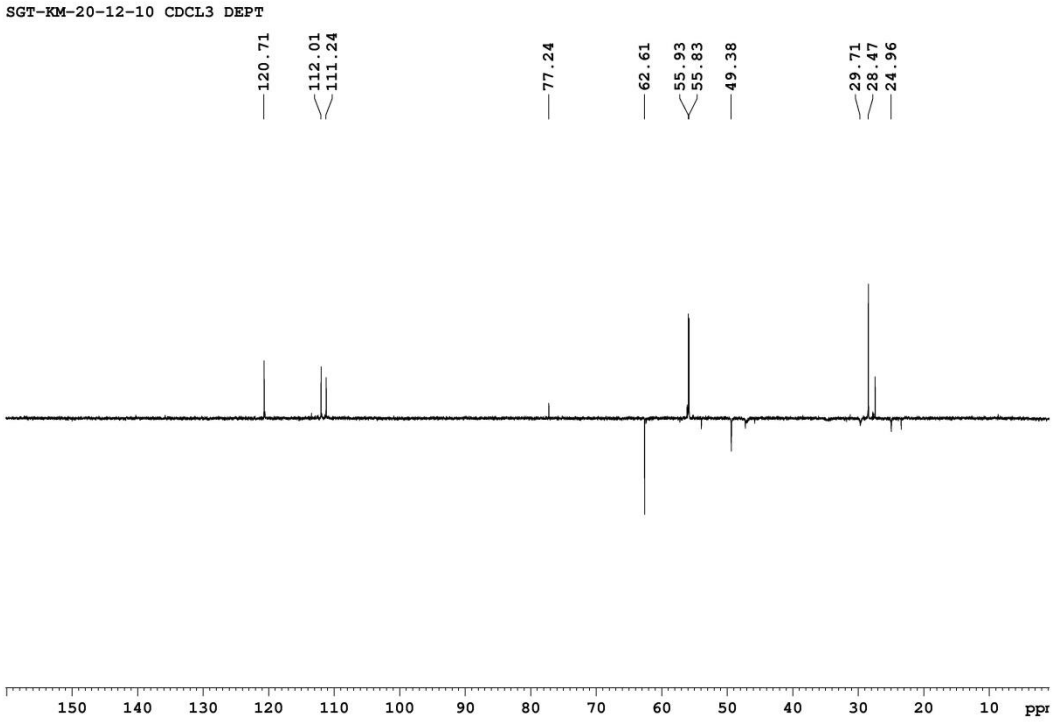
SGT-KM-20-12-10 CDCL3 DEPT
120.71
112.01
111.24
77.24
62.61
55.93
55.83
49.38
29.71
28.47
24.96
150 140 130 120 110 100 90 80 70 60 50 40 30 20 10 ppm

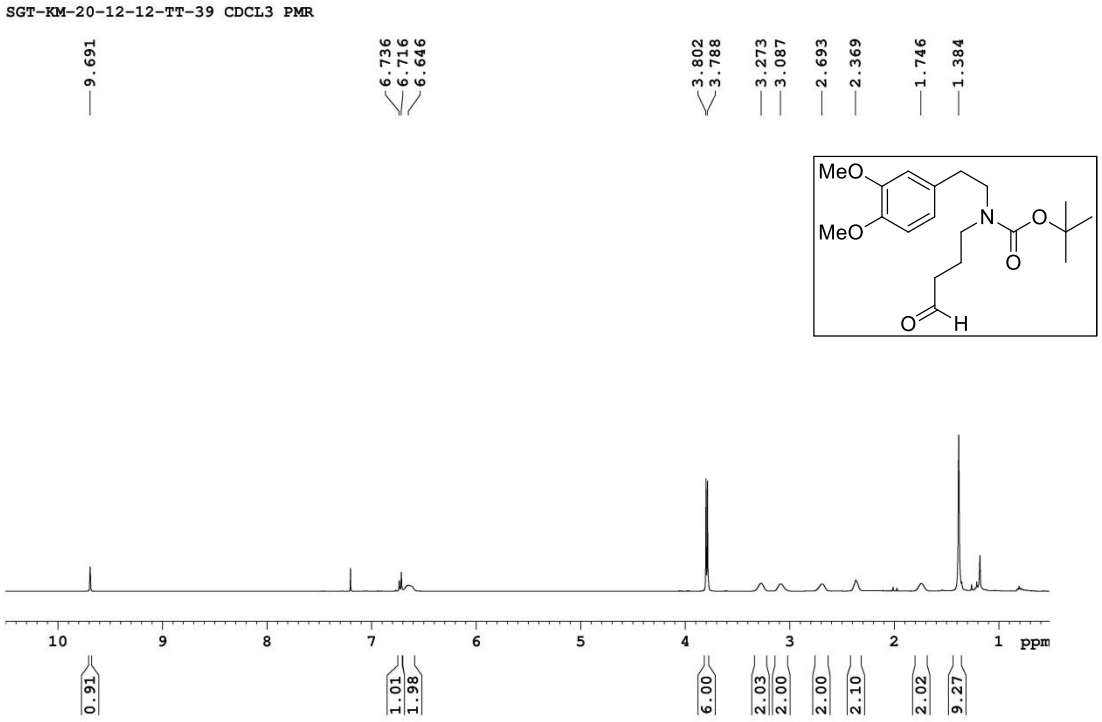
SGT-KM-20-12-12-TT-39 CDCL3 PMR
9.691
6.736
6.716
6.646
3.802
3.788
3.273
3.087
2.693
2.369
1.746
1.384
MeO
MeO
N
O
O
O
H
10 9 8 7 6 5 4 3 2 1 ppm
0.91
1.01
1.98
6.00
2.03
2.00
2.00
2.10
2.02
9.27

SGT-KM-20-12-12-TT-39 CDCL3 CMR

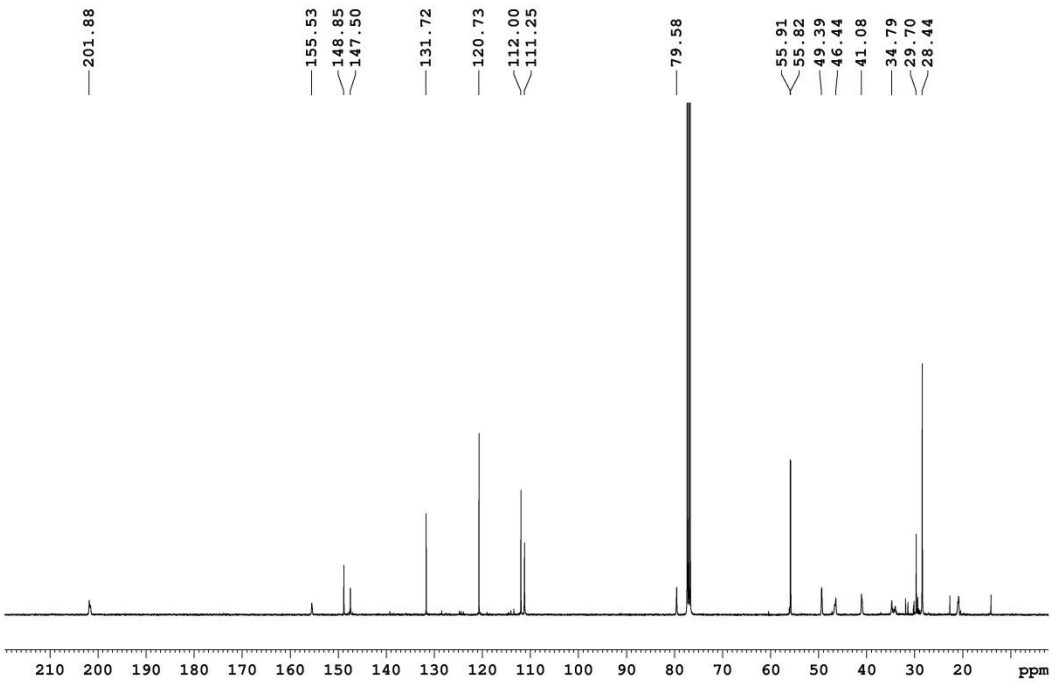

SGT-KM-20-12-12-TT-39 CDCL3 DEPT

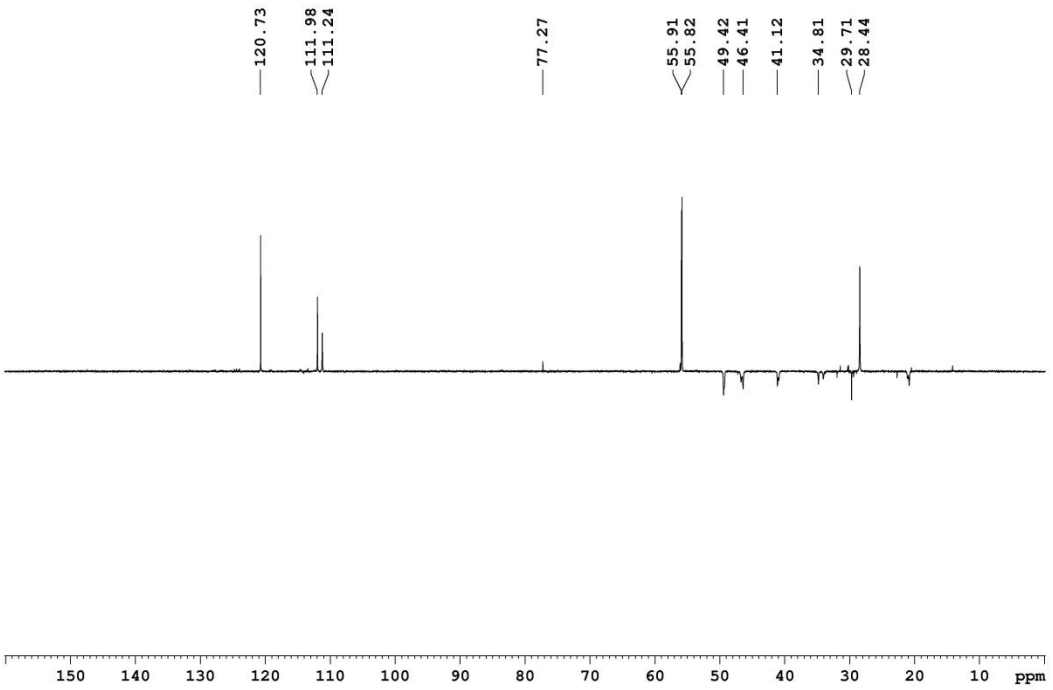

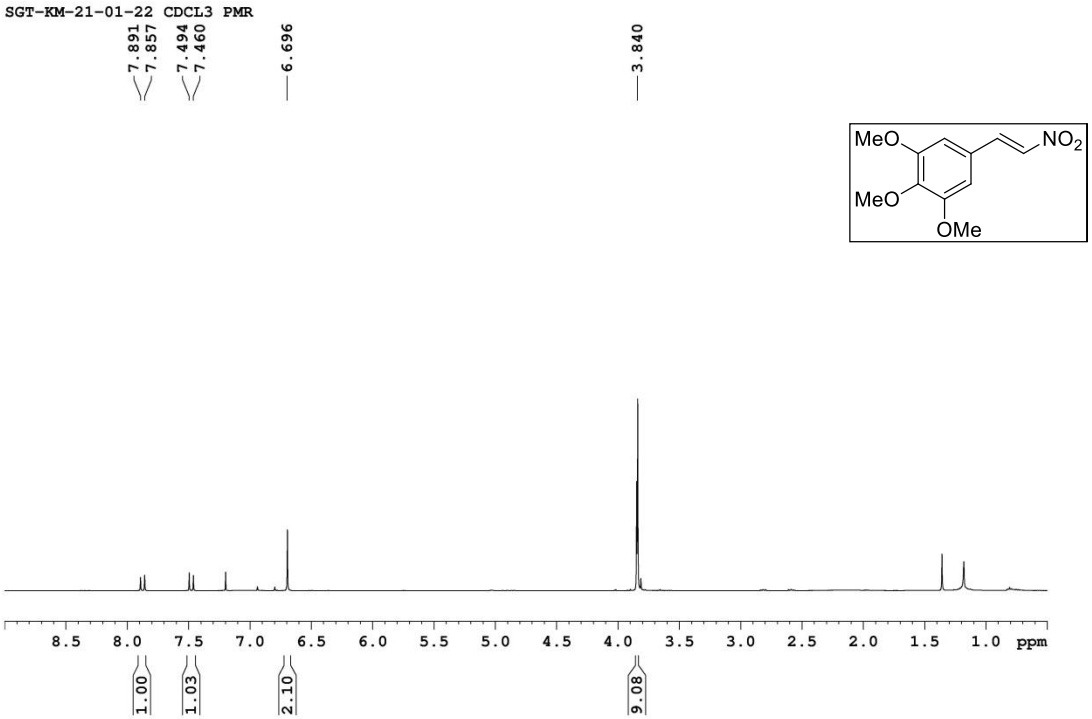
SGT-KM-21-01-22 CDCL3 PMR
7.891
7.857
7.494
7.460
6.696
3.840
MeO
NO2
MeO
OMe
8.5 8.0 7.5 7.0 6.5 6.0 5.5 5.0 4.5 4.0 3.5 3.0 2.5 2.0 1.5 1.0 ppm
1.00
1.03
2.10
9.08

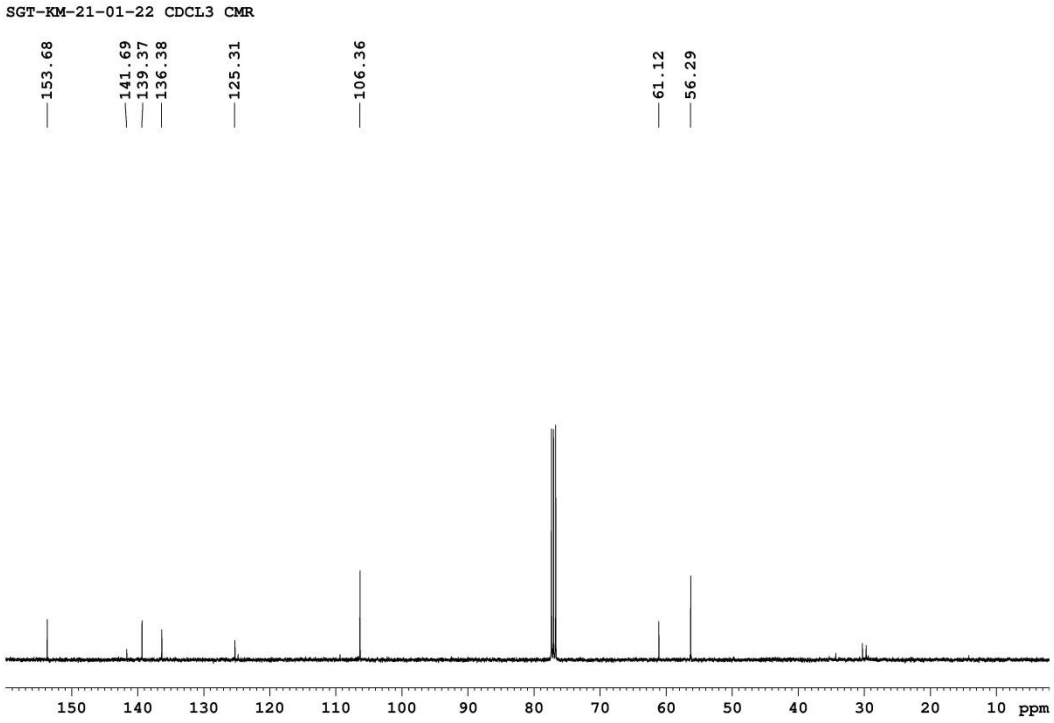
SGT-KM-21-01-22 CDCL3 CMR
153.68
141.69
139.37
136.38
125.31
106.36
61.12
56.29
150 140 130 120 110 100 90 80 70 60 50 40 30 20 10 ppm

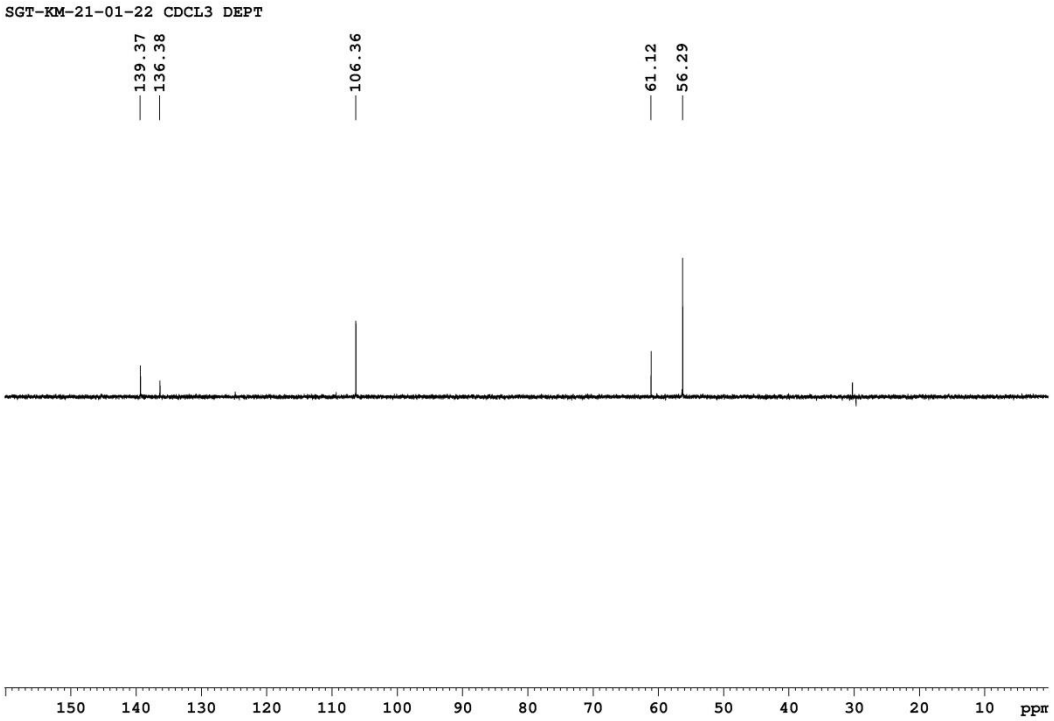
SGT-KM-21-01-22 CDCL3 DEPT
139.37
136.38
106.36
61.12
56.29
150 140 130 120 110 100 90 80 70 60 50 40 30 20 10 ppm

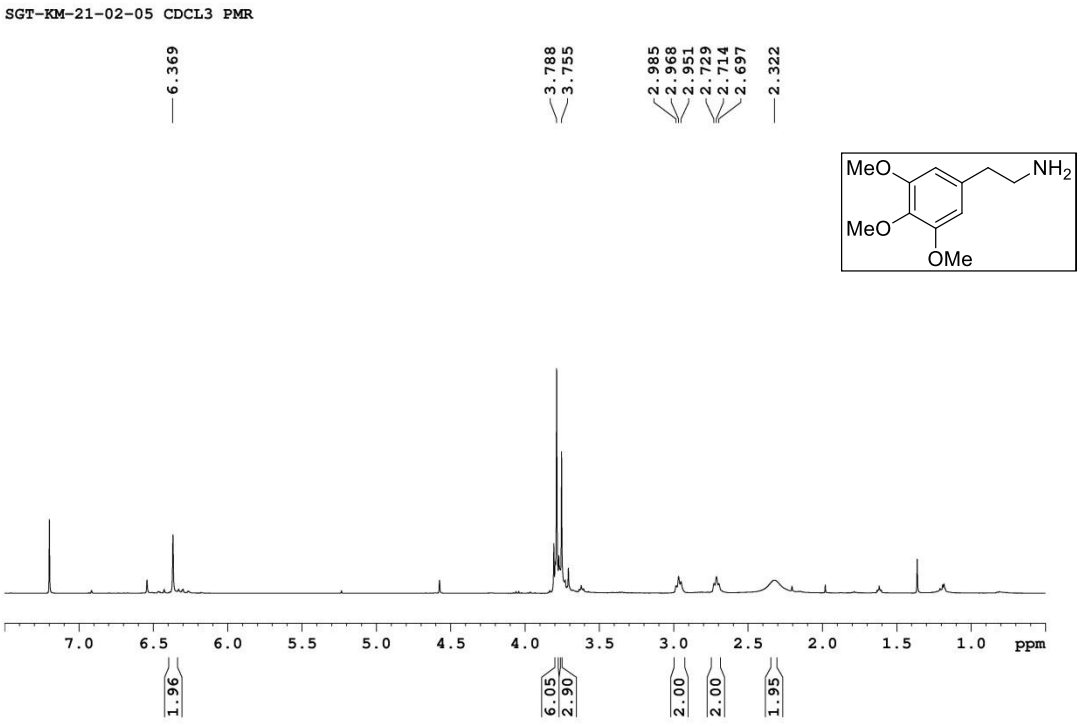
SGT-KM-21-02-05 CDCL3 PMR
6.369
3.788
3.755
2.985
2.968
2.951
2.729
2.714
2.697
2.322
MeO
NH2
MeO
OMe
7.0 6.5 6.0 5.5 5.0 4.5 4.0 3.5 3.0 2.5 2.0 1.5 1.0 ppm
1.96
6.05
2.90
2.00
2.00
1.95

SGT-KM-21-01-15-3 CDCL3 PMR

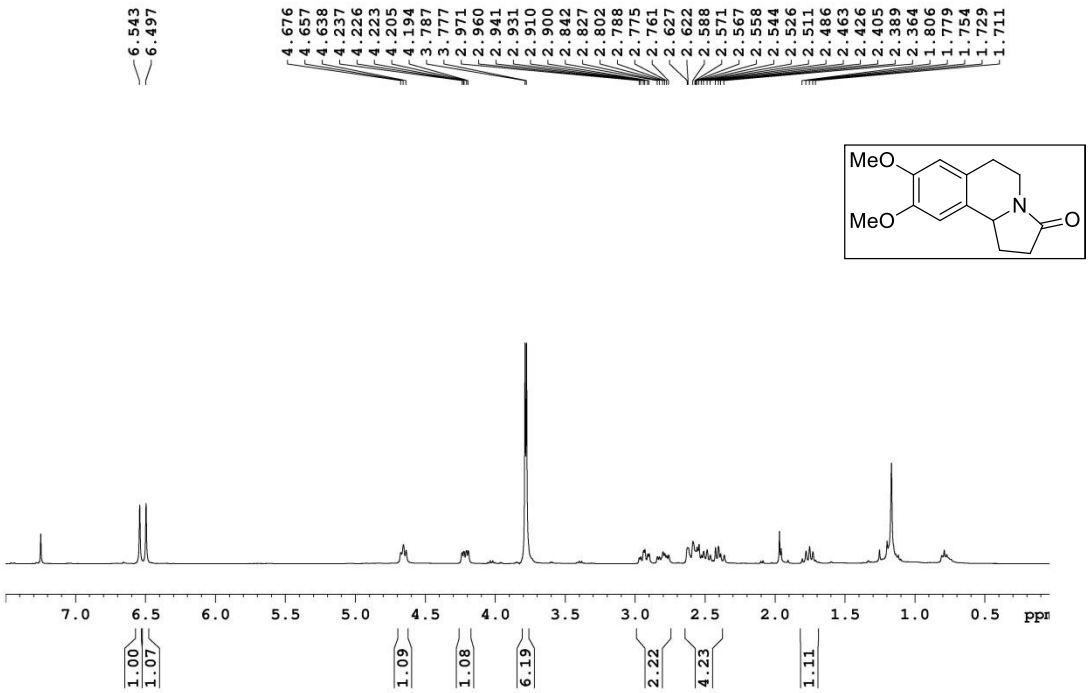

SGT-KM-21-01-15-3 CDCL3 CMR

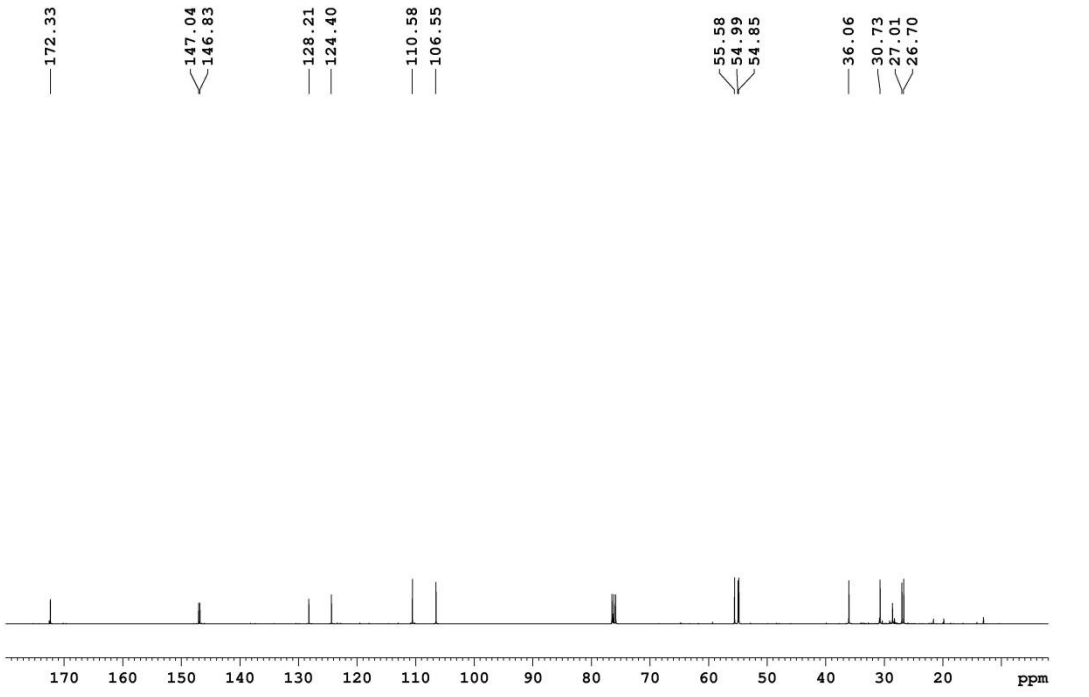

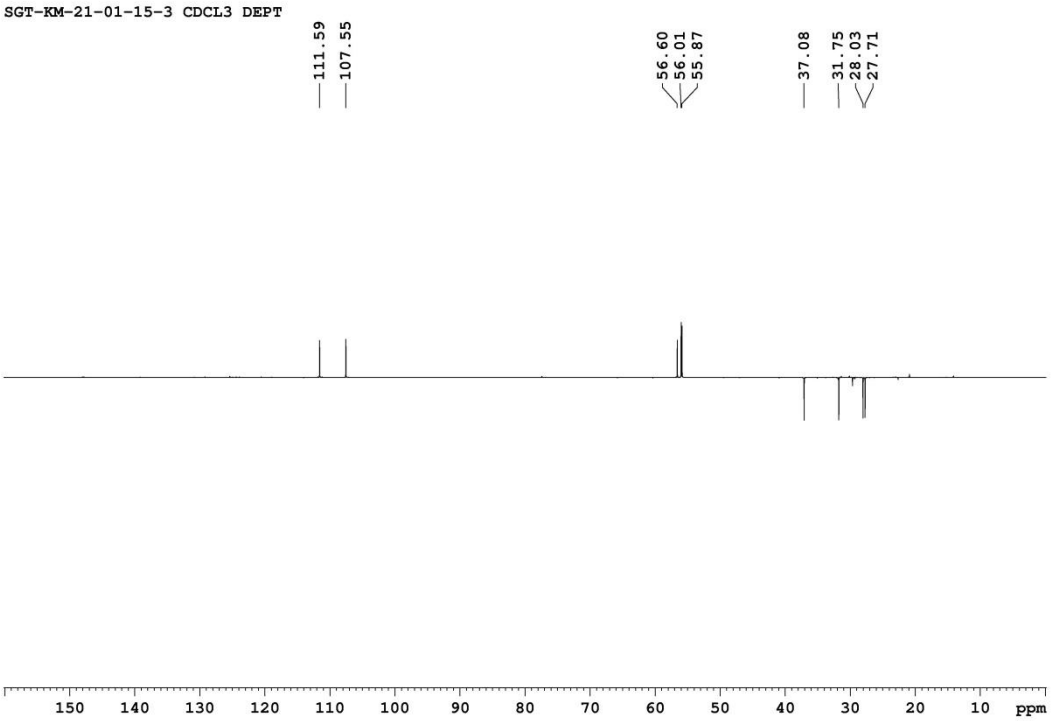
SGT-KM-21-01-15-3 CDCL3 DEPT
111.59
107.55
56.60
56.01
55.87
37.08
31.75
28.03
27.71
150 140 130 120 110 100 90 80 70 60 50 40 30 20 10 ppm

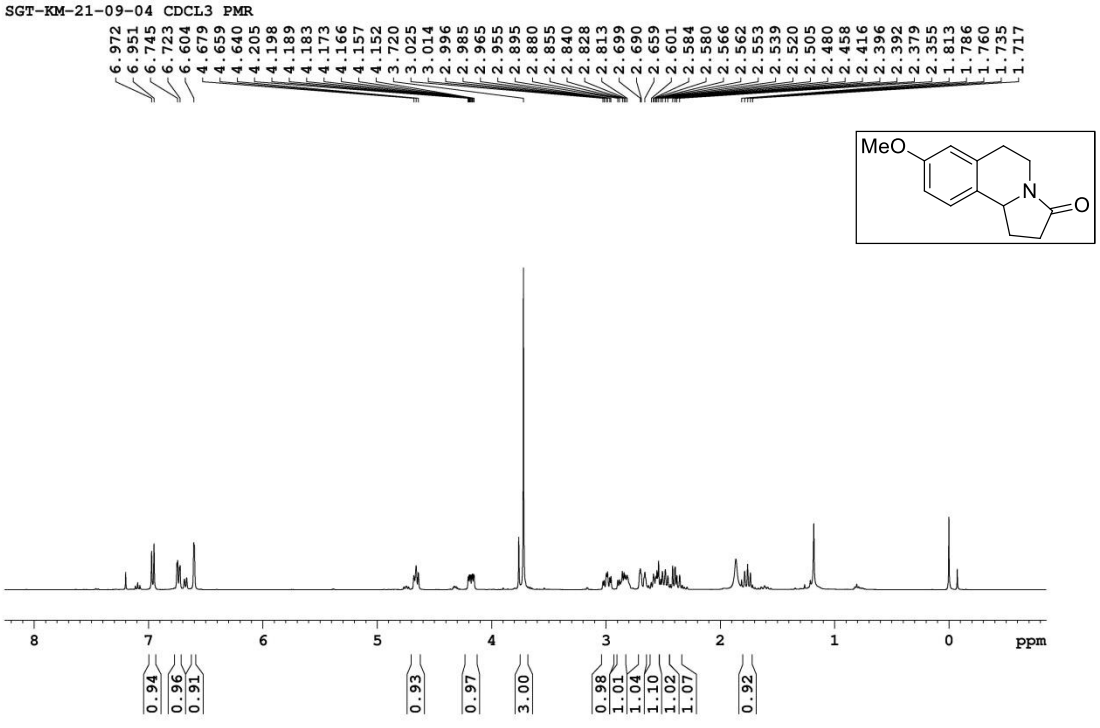
SGT-KM-21-09-04 CDCL3 PMR
6.972
6.951
6.745
6.723
6.604
4.679
4.659
4.640
4.205
4.198
4.189
4.183
4.173
4.166
4.157
4.152
3.720
3.025
3.014
2.996
2.985
2.965
2.955
2.895
2.880
2.855
2.840
2.828
2.813
2.699
2.690
2.659
2.601
2.584
2.580
2.566
2.562
2.553
2.539
2.520
2.505
2.480
2.458
2.416
2.396
2.392
2.379
2.355
1.813
1.786
1.760
1.735
1.717
MeO
N
O
8 7 6 5 4 3 2 1 0 ppm
0.94
0.96
0.91
0.93
0.97
3.00
0.98
1.01
1.04
1.10
1.02
1.07
0.92

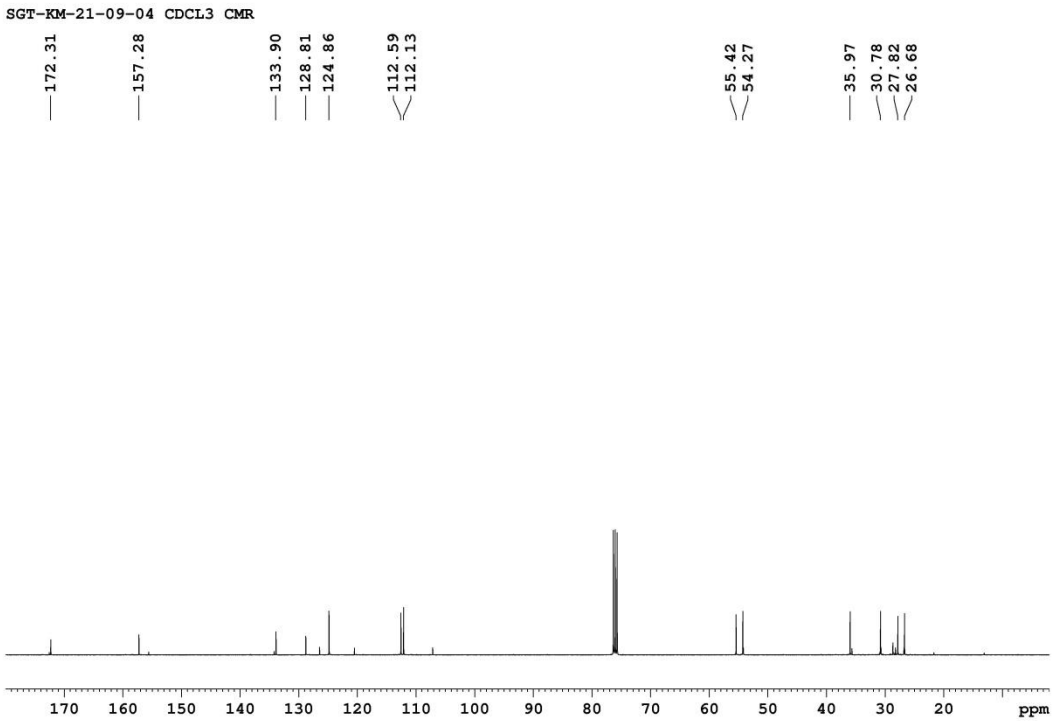
SGT-KM-21-09-04 CDCL3 CMR
172.31
157.28
133.90
128.81
124.86
112.59
112.13
55.42
54.27
35.97
30.78
27.82
26.68
170 160 150 140 130 120 110 100 90 80 70 60 50 40 30 20 ppm

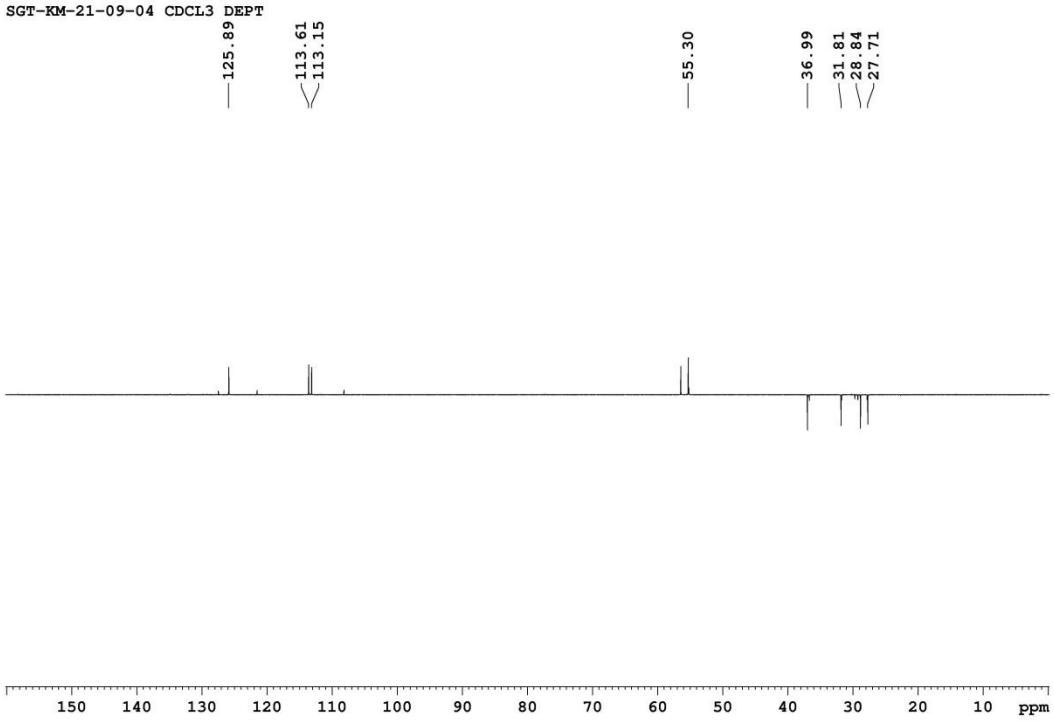
SGT-KM-21-09-04 CDCL3 DEPT
125.89
113.61
113.15
55.30
36.99
31.81
28.84
27.71
150 140 130 120 110 100 90 80 70 60 50 40 30 20 10 ppm

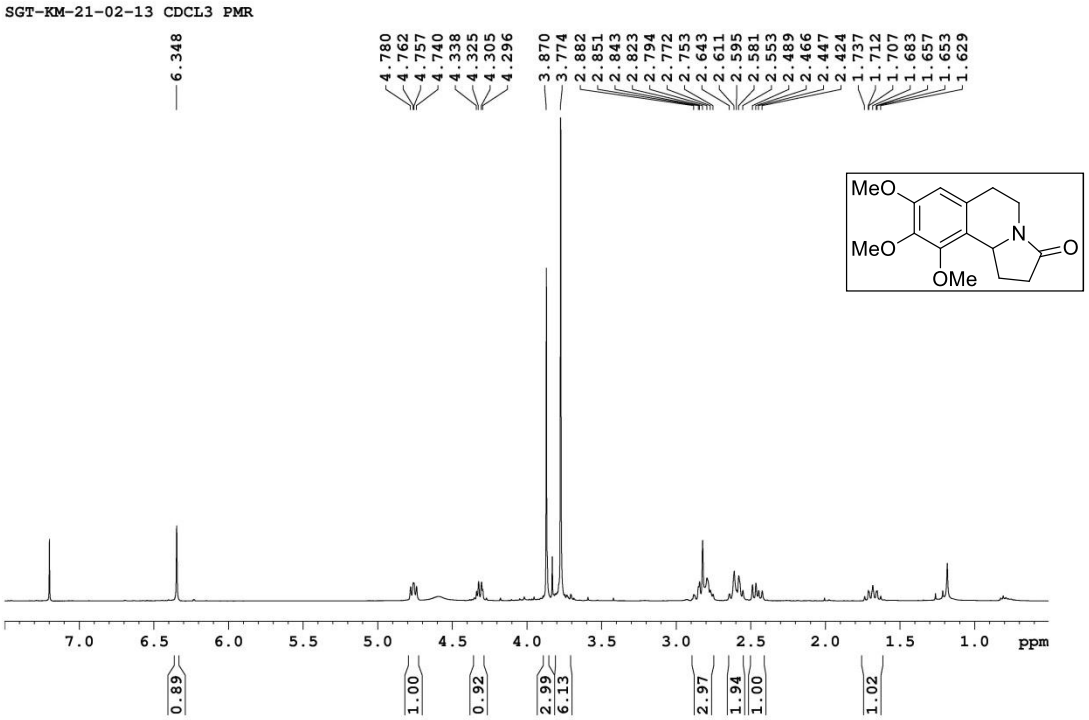
SGT-KM-21-02-13 CDCL3 PMR
6.348
4.780
4.762
4.757
4.740
4.338
4.325
4.305
4.296
3.870
3.774
2.882
2.851
2.843
2.823
2.794
2.772
2.753
2.643
2.611
2.595
2.581
2.553
2.489
2.466
2.447
2.424
1.737
1.712
1.707
1.683
1.657
1.653
1.629
MeO
MeO
OMe
N
O
7.0
6.5
6.0
5.5
5.0
4.5
4.0
3.5
3.0
2.5
2.0
1.5
1.0
ppm
0.89
1.00
0.92
2.99
6.13
2.97
1.94
1.00
1.02

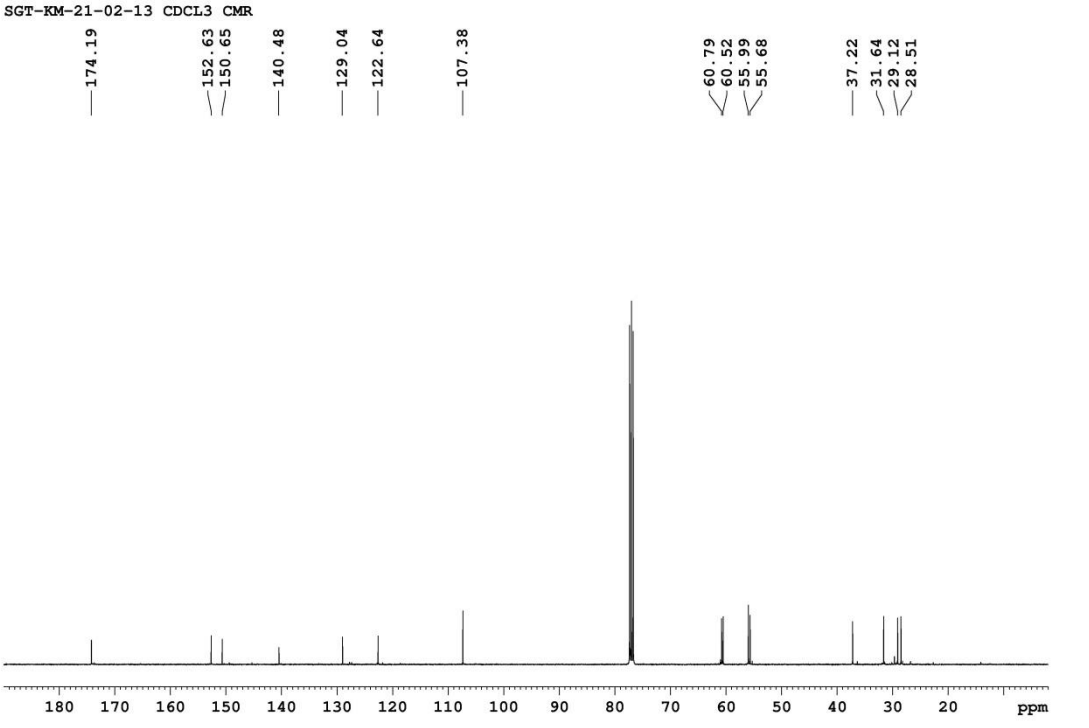
SGT-KM-21-02-13 CDCL3 CMR
174.19
152.63
150.65
140.48
129.04
122.64
107.38
60.79
60.52
55.99
55.68
37.22
31.64
29.12
28.51
180
170
160
150
140
130
120
110
100
90
80
70
60
50
40
30
20
ppm

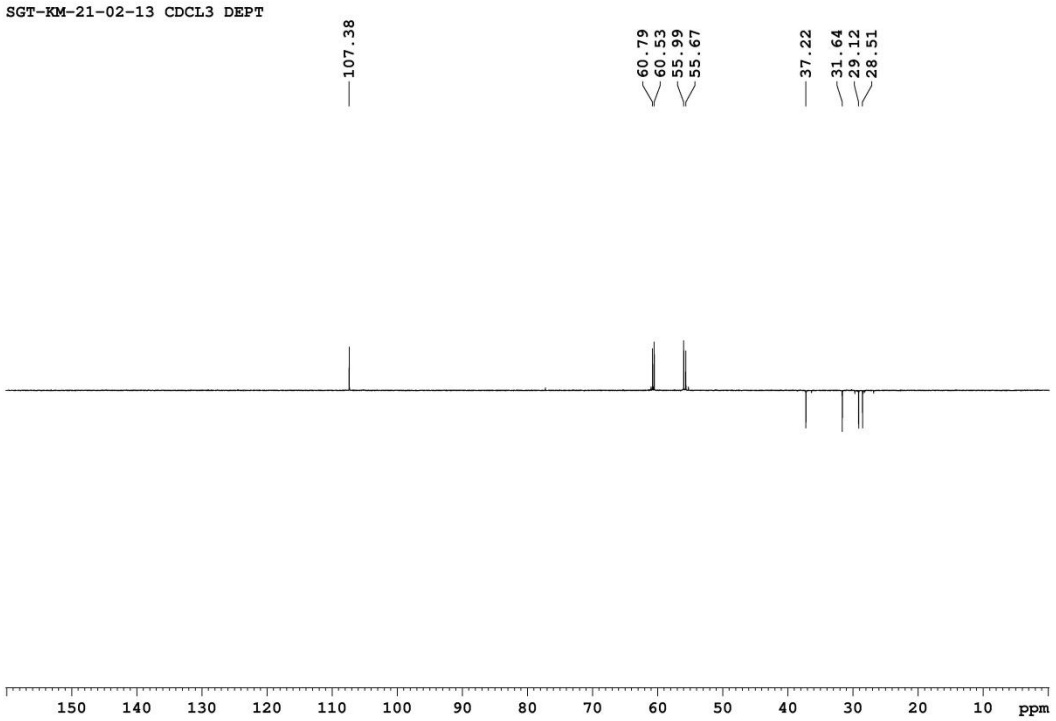
SGT-KM-21-02-13 CDCL3 DEPT
107.38
60.79
60.53
55.99
55.67
37.22
31.64
29.12
28.51
150 140 130 120 110 100 90 80 70 60 50 40 30 20 10 ppm

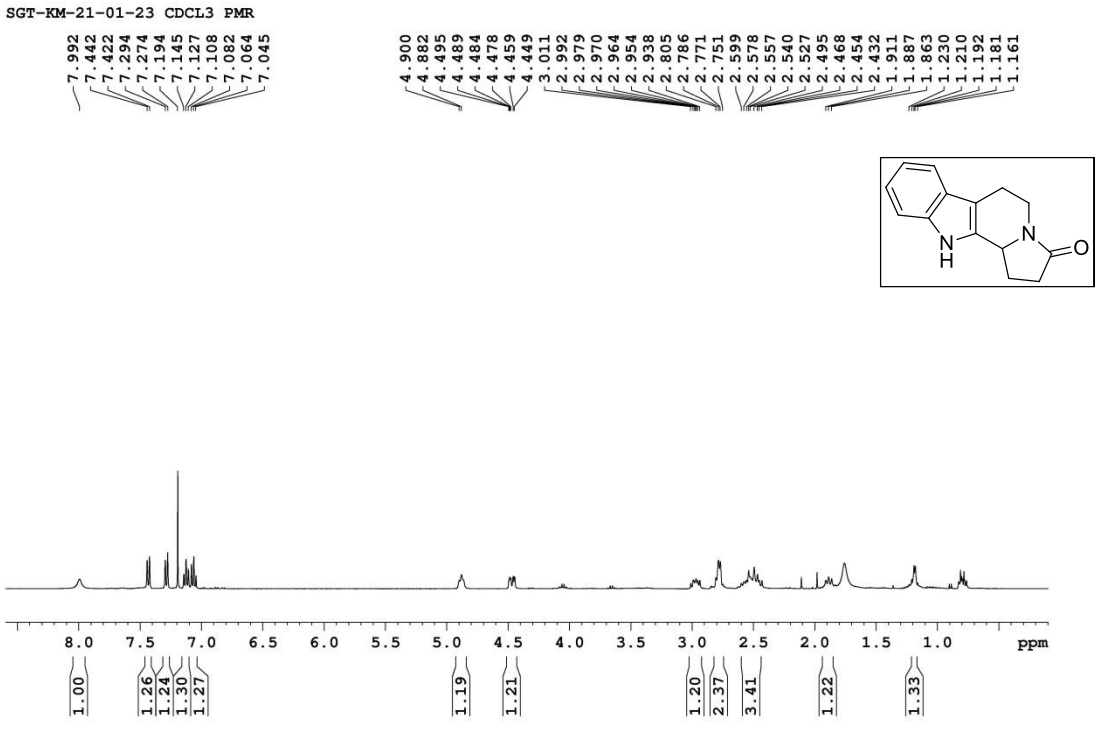
SGT-KM-21-01-23 CDCL3 PMR
7.992
7.442
7.422
7.294
7.274
7.194
7.145
7.127
7.108
7.082
7.064
7.045
4.900
4.882
4.495
4.489
4.484
4.478
4.459
4.449
3.011
2.992
2.979
2.970
2.964
2.954
2.938
2.805
2.786
2.771
2.751
2.599
2.578
2.557
2.540
2.527
2.495
2.468
2.454
2.432
1.911
1.887
1.863
1.230
1.210
1.192
1.181
1.161
N
H
N
O
8.0 7.5 7.0 6.5 6.0 5.5 5.0 4.5 4.0 3.5 3.0 2.5 2.0 1.5 1.0 ppm
1.00
1.26
1.24
1.30
1.27
1.19
1.21
1.20
2.37
3.41
1.22
1.33

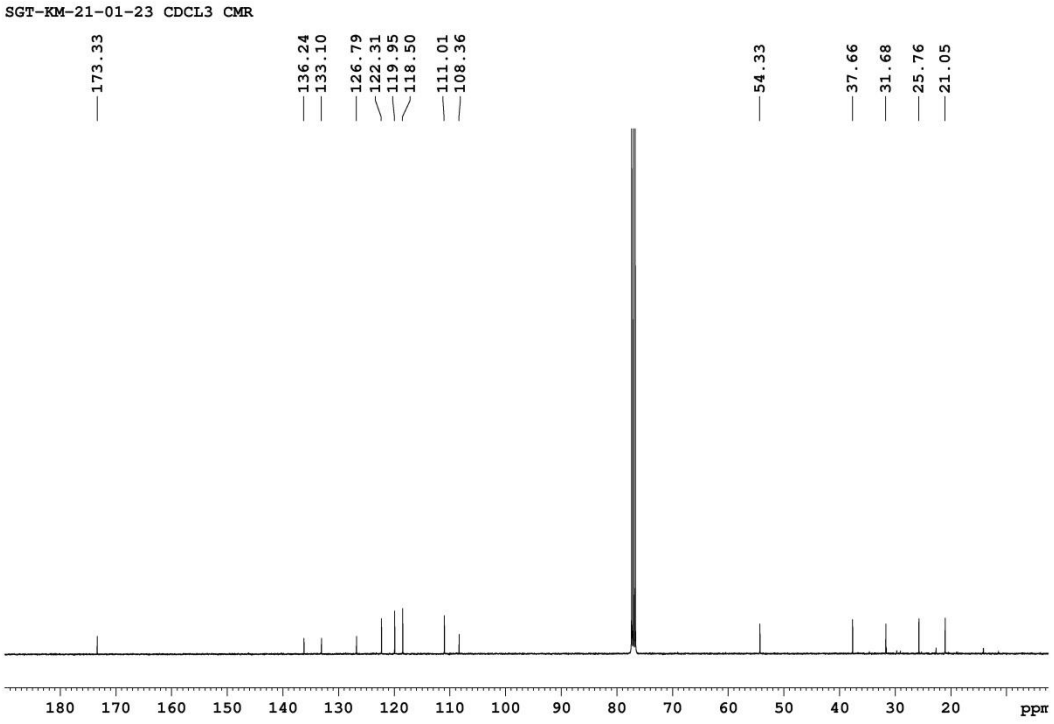
SGT-KM-21-01-23 CDCL3 CMR
173.33
136.24
133.10
126.79
122.31
119.95
118.50
111.01
108.36
54.33
37.66
31.68
25.76
21.05
180 170 160 150 140 130 120 110 100 90 80 70 60 50 40 30 20 ppm

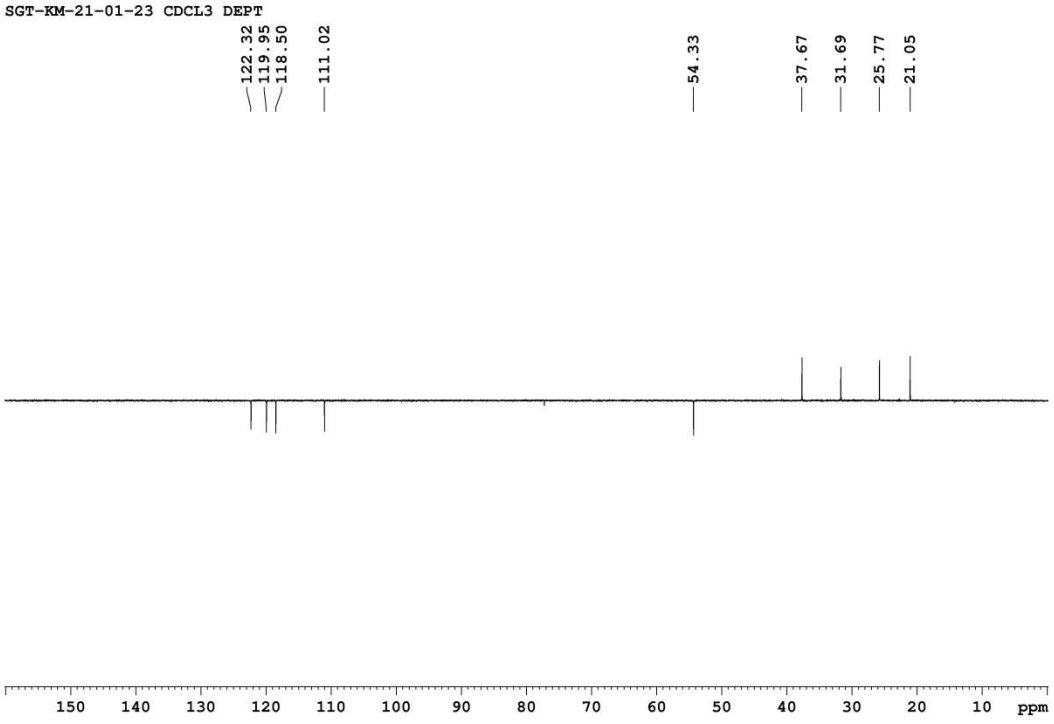
SGT-KM-21-01-23 CDCL3 DEPT
122.32
119.95
118.50
111.02
54.33
37.67
31.69
25.77
21.05
150 140 130 120 110 100 90 80 70 60 50 40 30 20 10 ppm

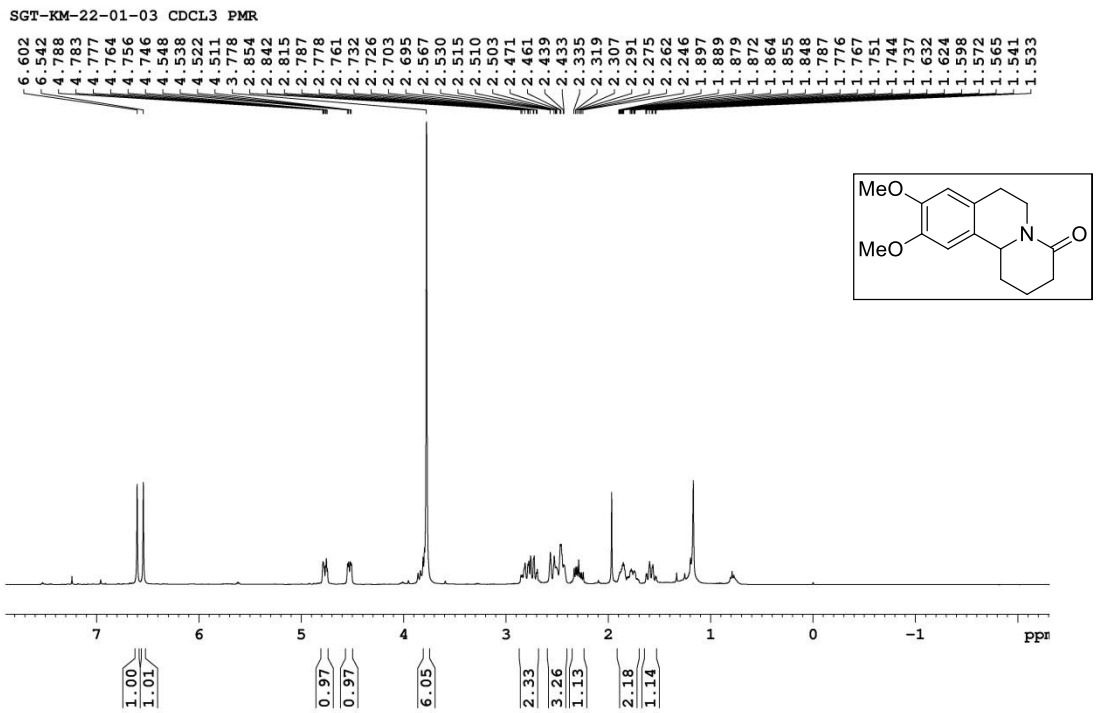
SGT-KM-22-01-03 CDCL3 PMR
6.602 6.542 4.788 4.783 4.777 4.764 4.756 4.746 4.548 4.538 4.522 4.511 3.778 2.854 2.842 2.815 2.787 2.778 2.761 2.732 2.726 2.703 2.695 2.567 2.530 2.515 2.510 2.503 2.471 2.461 2.439 2.433 2.335 2.319 2.307 2.291 2.275 2.262 2.246 1.897 1.889 1.879 1.872 1.864 1.855 1.848 1.787 1.776 1.767 1.751 1.744 1.737 1.632 1.624 1.598 1.572 1.565 1.541 1.533
MeO
MeO
N
O
7 6 5 4 3 2 1 0 −1 ppm
1.00 1.01 0.97 0.97 6.05 2.33 3.26 1.13 2.18 1.14

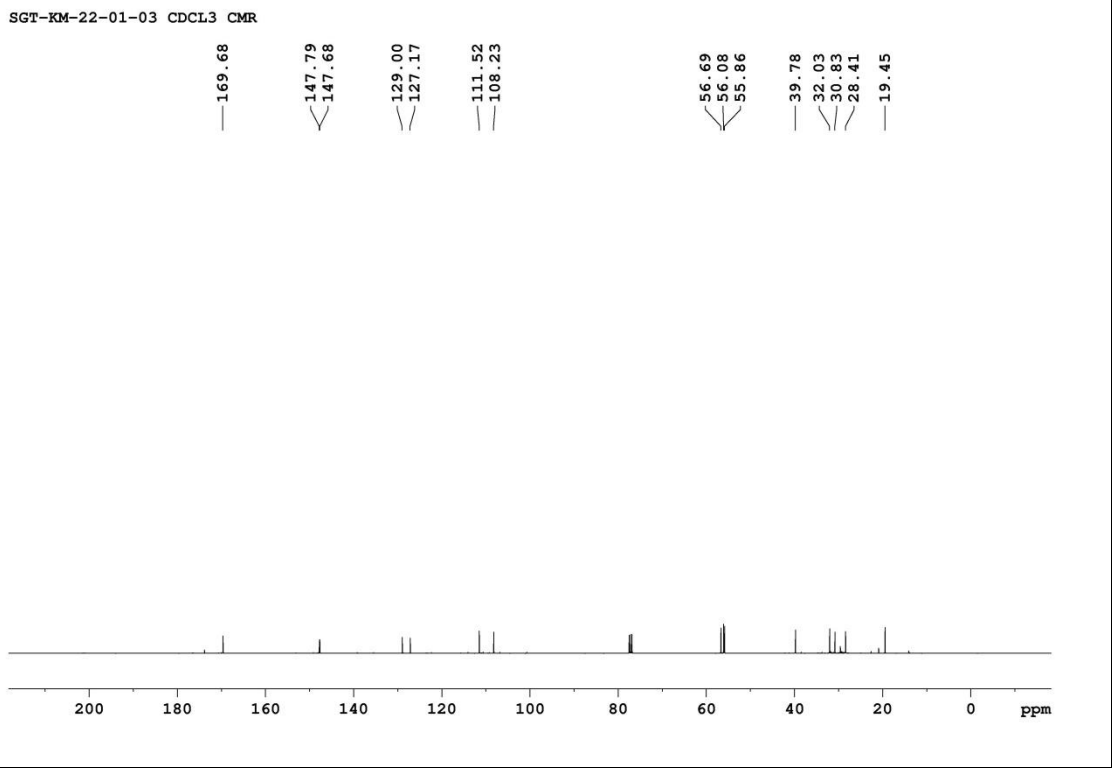
SGT-KM-22-01-03 CDCL3 CMR
169.68
147.79 147.68
129.00 127.17
111.52 108.23
56.69 56.08 55.86
39.78 32.03 30.83 28.41 19.45
200 180 160 140 120 100 80 60 40 20 0 ppm

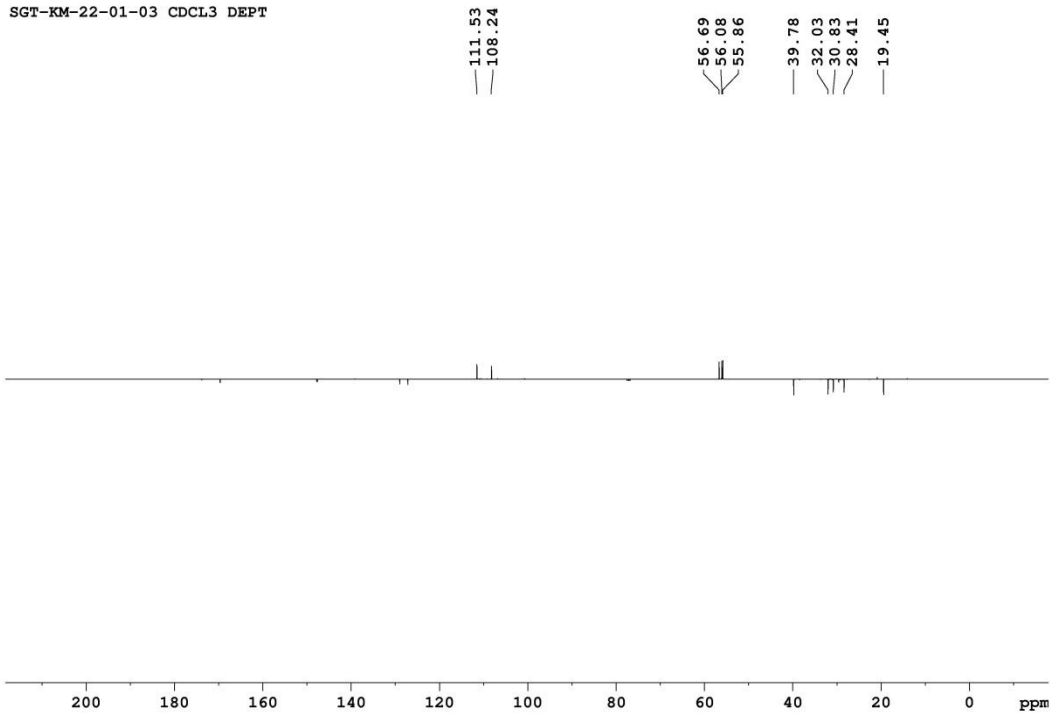
SGT-KM-22-01-03 CDCL3 DEPT
111.53
108.24
56.69
56.08
55.86
39.78
32.03
30.83
28.41
19.45
200
180
160
140
120
100
80
60
40
20
0
ppm

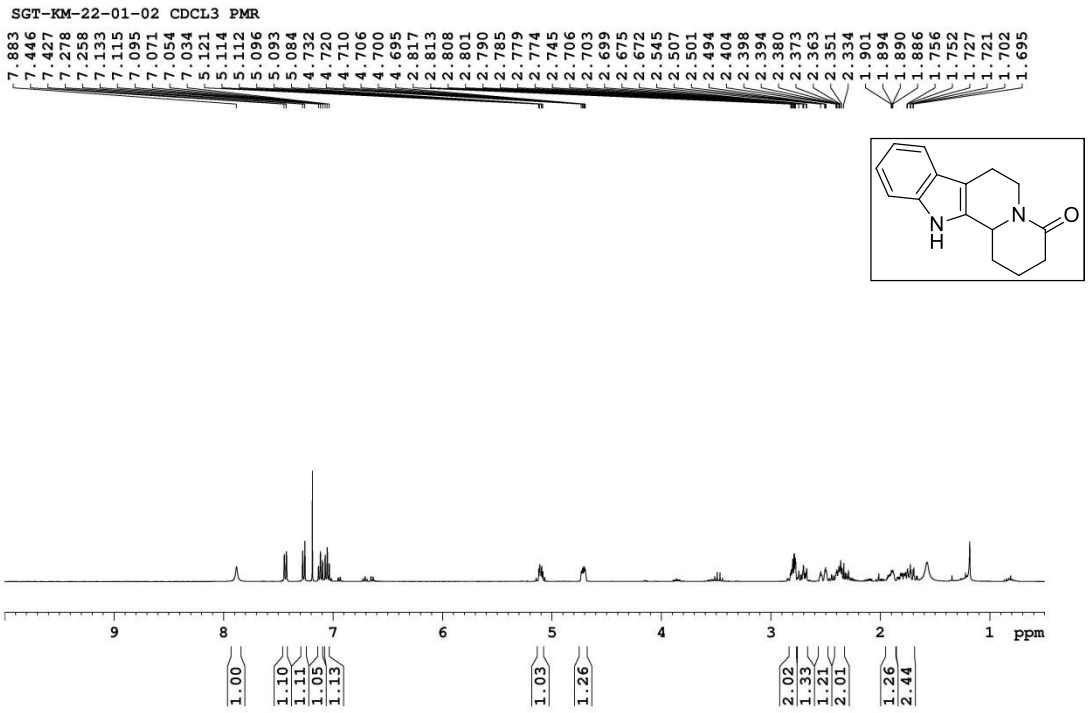
SGT-KM-22-01-02 CDCL3 PMR
7.883
7.446
7.427
7.278
7.258
7.133
7.115
7.095
7.071
7.054
7.034
5.121
5.114
5.112
5.096
5.093
5.084
4.732
4.720
4.710
4.706
4.700
4.695
2.817
2.813
2.808
2.801
2.790
2.785
2.779
2.774
2.745
2.706
2.703
2.699
2.675
2.672
2.545
2.507
2.501
2.494
2.404
2.398
2.394
2.380
2.373
2.363
2.351
2.334
1.901
1.894
1.890
1.886
1.756
1.752
1.727
1.721
1.702
1.695
N
H
N
O
9
8
7
6
5
4
3
2
1
ppm
1.00
1.10
1.11
1.05
1.13
1.03
1.26
2.02
1.33
1.21
2.01
1.26
2.44

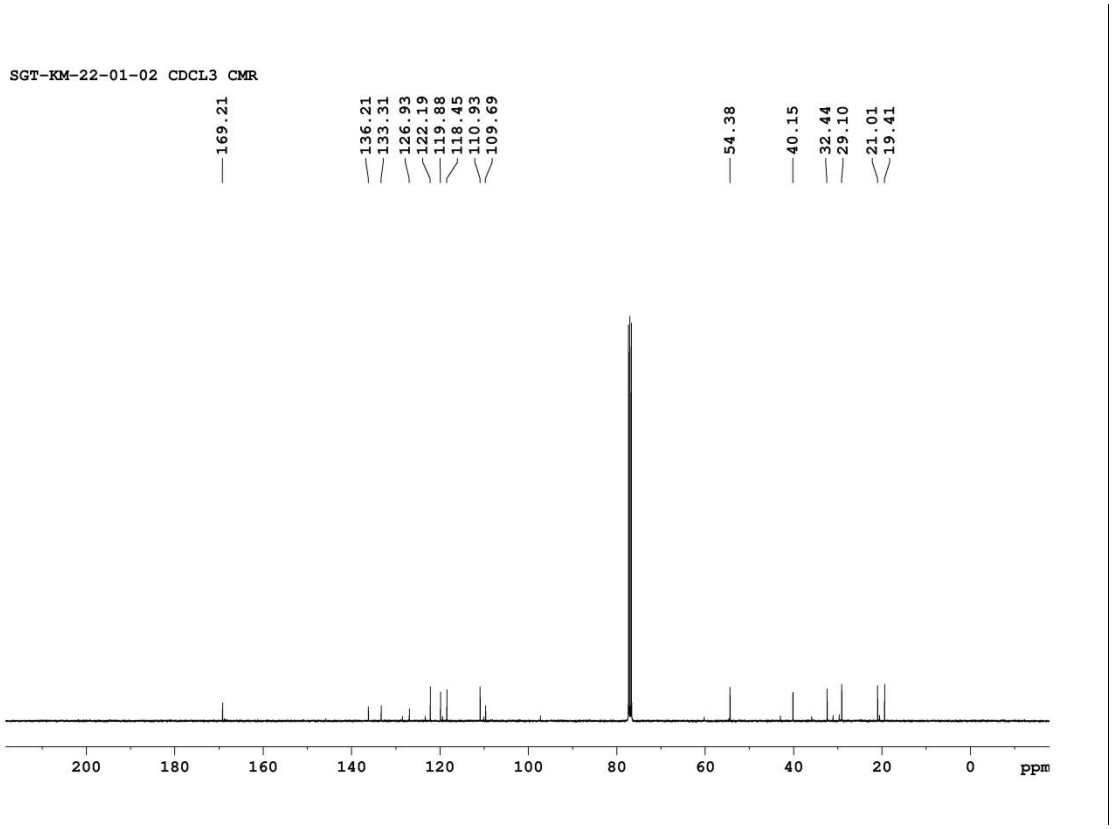
SGT-KM-22-01-02 CDCL3 CMR
169.21
136.21
133.31
126.93
122.19
119.88
118.45
110.93
109.69
54.38
40.15
32.44
29.10
21.01
19.41
200
180
160
140
120
100
80
60
40
20
0
ppm

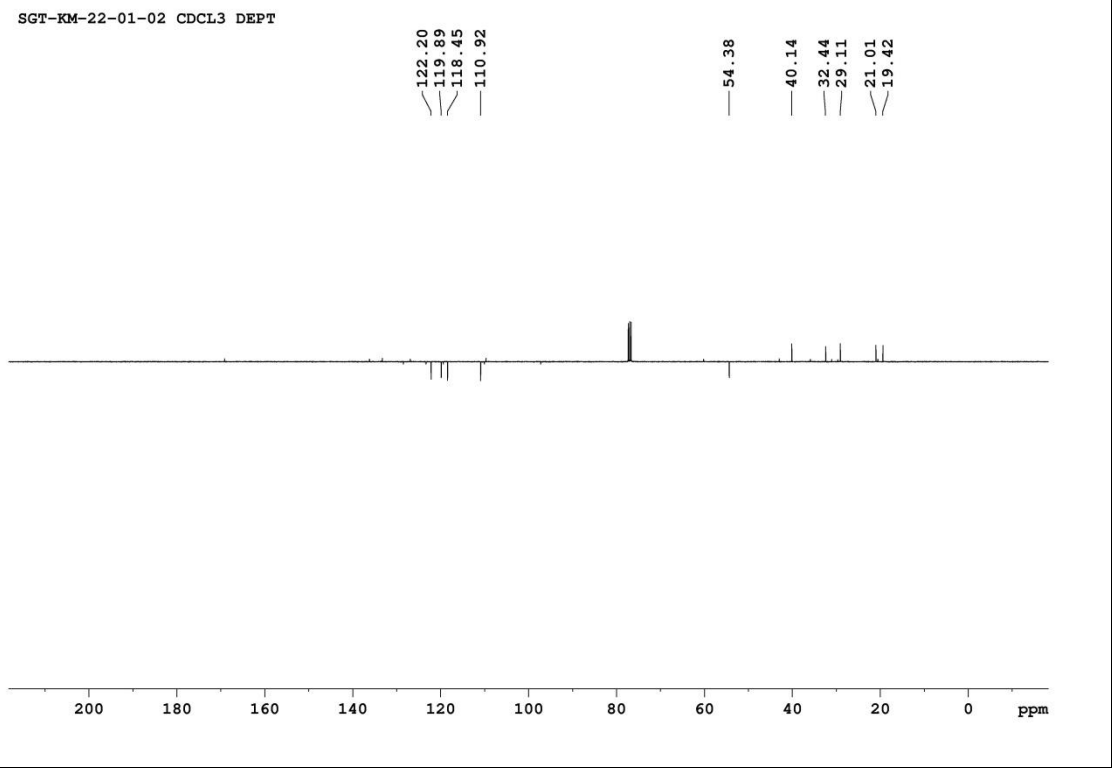
SGT-KM-22-01-02 CDCL3 DEPT
122.20
119.89
118.45
110.92
54.38
40.14
32.44
29.11
21.01
19.42
200
180
160
140
120
100
80
60
40
20
0
ppm

SGT-KM-21-01-18 CDCL3 PMR

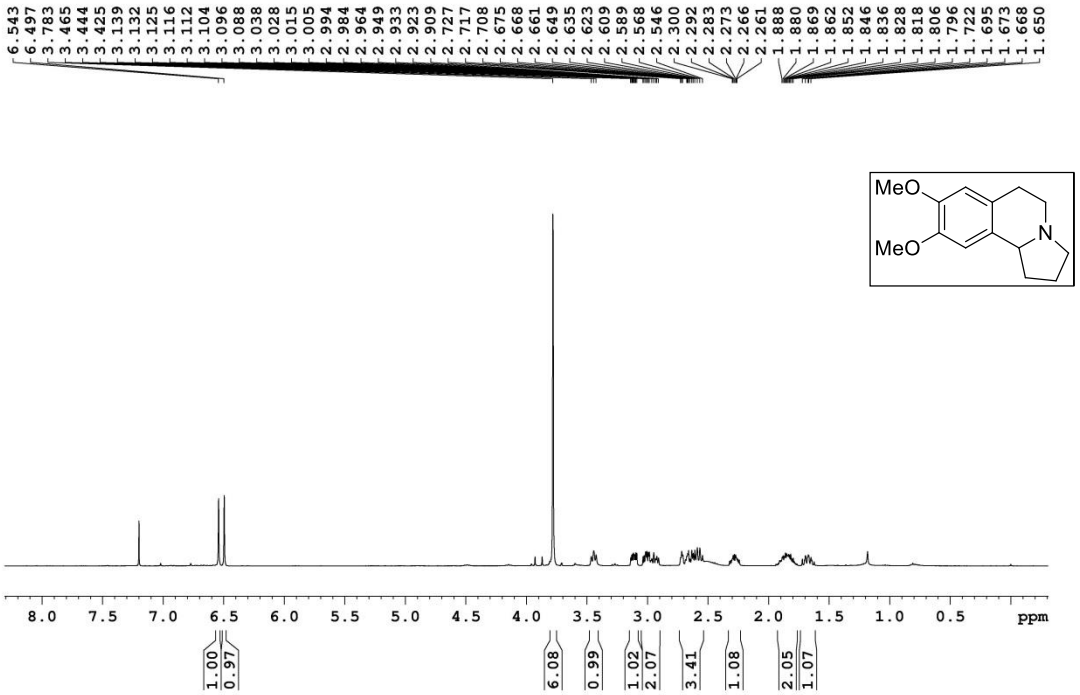

SGT-KM-21-01-18 CDCL3 CMR

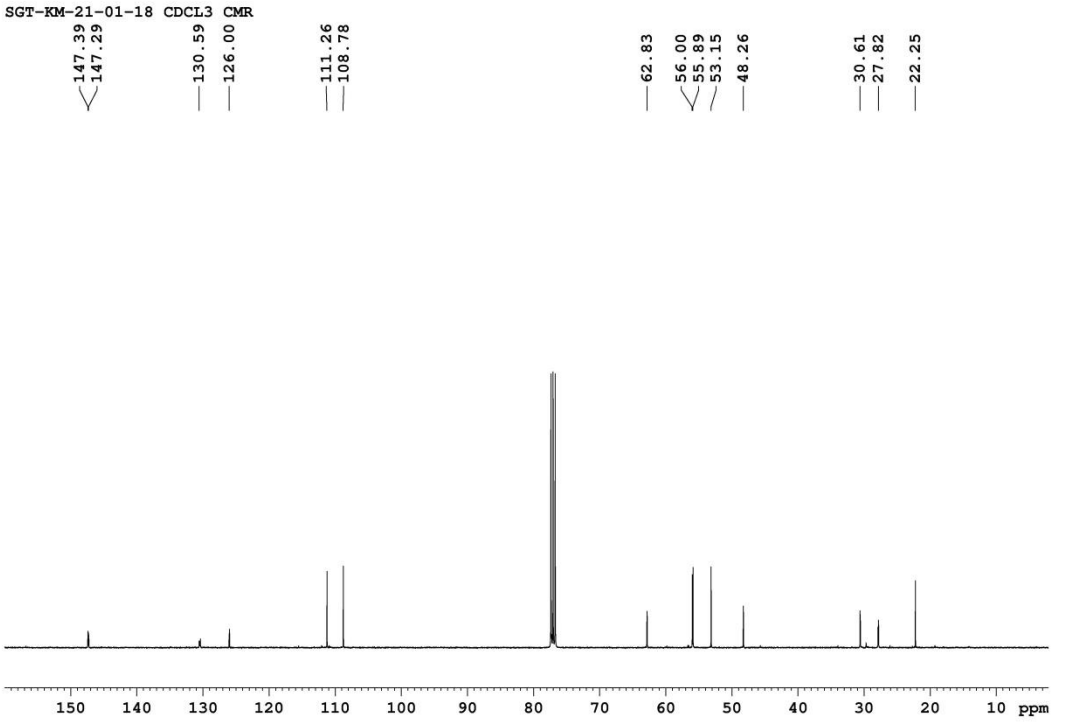

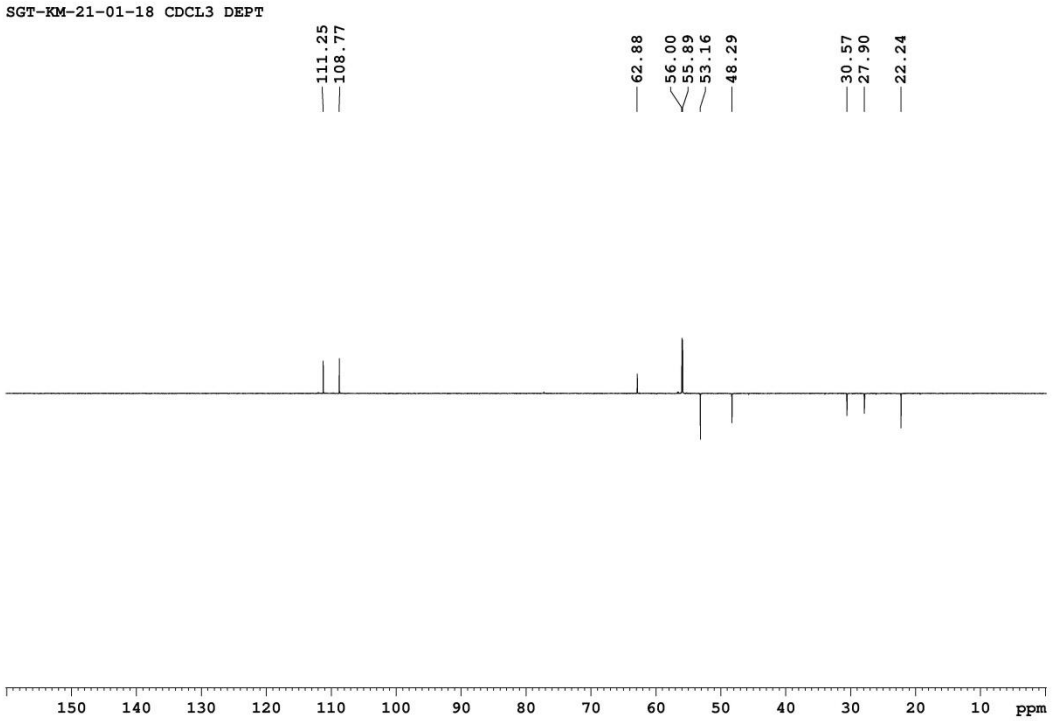
SGT-KM-21-01-18 CDCL3 DEPT
111.25
108.77
62.88
56.00
55.89
53.16
48.29
30.57
27.90
22.24
150 140 130 120 110 100 90 80 70 60 50 40 30 20 10 ppm

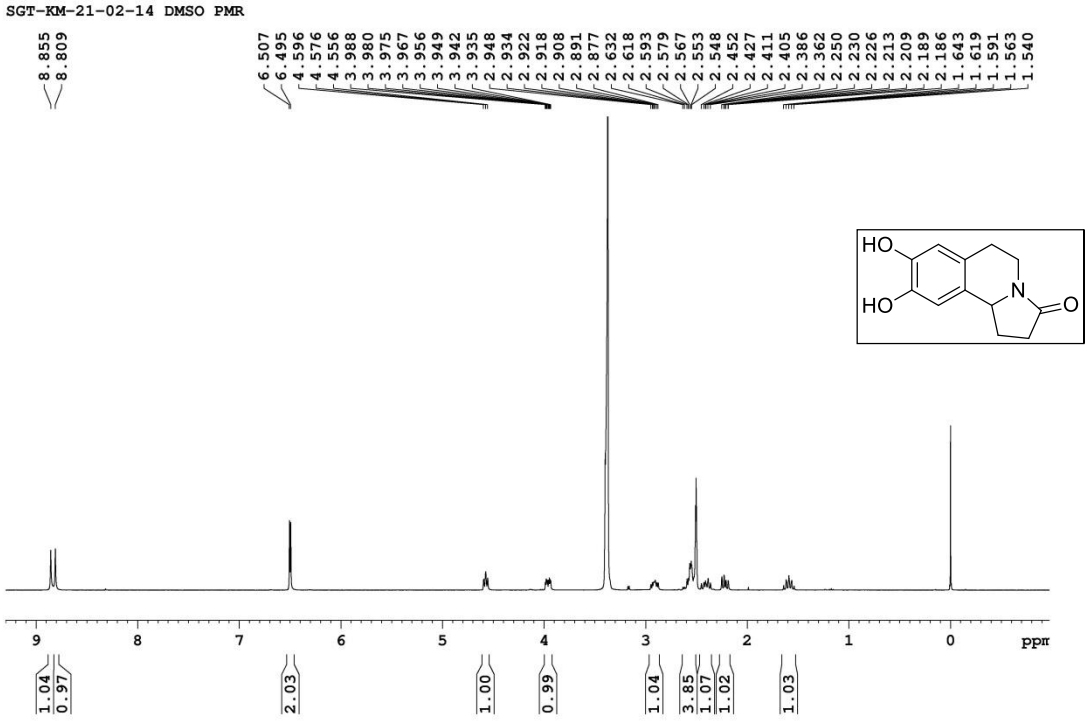
SGT-KM-21-02-14 DMSO PMR
8.855
8.809
6.507
6.495
4.596
4.576
4.556
3.988
3.980
3.975
3.967
3.956
3.949
3.942
3.935
2.948
2.934
2.922
2.918
2.908
2.891
2.877
2.632
2.618
2.593
2.579
2.567
2.553
2.548
2.452
2.427
2.411
2.405
2.386
2.362
2.250
2.230
2.226
2.213
2.209
2.189
2.186
1.643
1.619
1.591
1.563
1.540
HO
HO
N
O
9 8 7 6 5 4 3 2 1 0 ppm
1.04
0.97
2.03
1.00
0.99
1.04
3.85
1.07
1.02
1.03

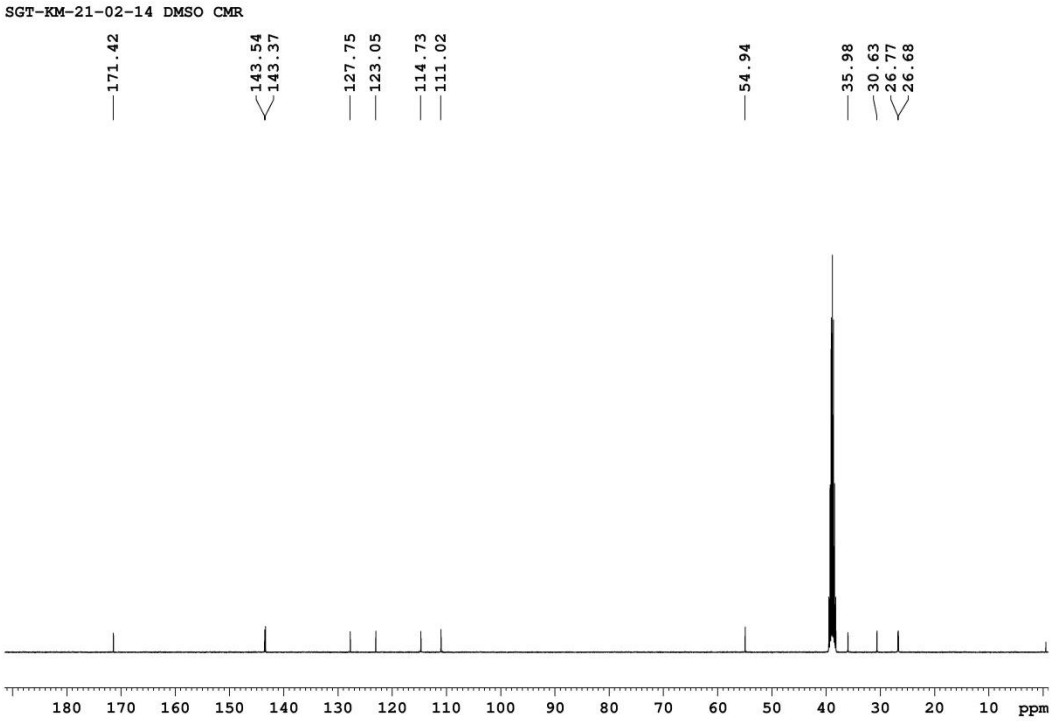
SGT-KM-21-02-14 DMSO CMR
171.42
143.54
143.37
127.75
123.05
114.73
111.02
54.94
35.98
30.63
26.77
26.68
180 170 160 150 140 130 120 110 100 90 80 70 60 50 40 30 20 10 ppm

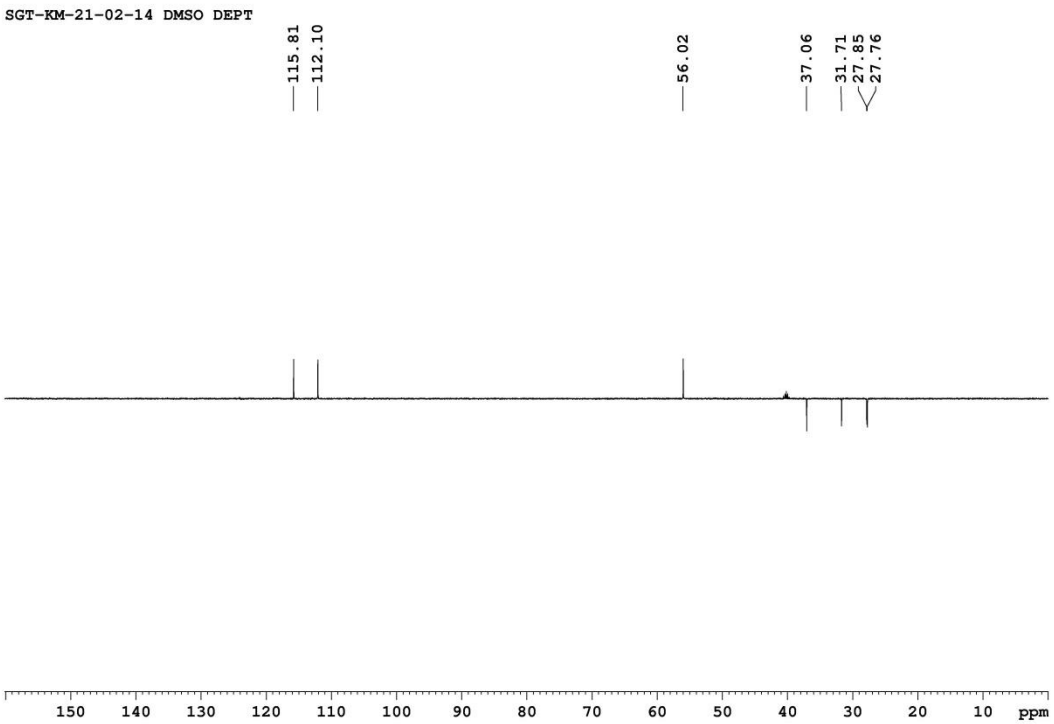
SGT-KM-21-02-14 DMSO DEPT
115.81
112.10
56.02
37.06
31.71
27.85
27.76
150 140 130 120 110 100 90 80 70 60 50 40 30 20 10 ppm

SGT-KM-21-01-21 CDCL3 PMR

8.101 7.418 7.399 7.240 7.220 7.081 7.064 7.046 7.042 7.035 7.018 7.000 4.180 4.175 4.169 4.162 3.268 3.262 3.255 3.249 3.236 3.230 3.223 3.217 3.046 3.034 3.020 3.013 3.008 3.002 2.988 2.976 2.896 2.884 2.875 2.870 2.861 2.843 2.830 2.811 2.788 2.623 2.617 2.612 2.584 2.579 2.573 2.219 2.208 2.200 2.191 1.840 1.829 1.811 1.800 1.790 1.782 1.773 1.766

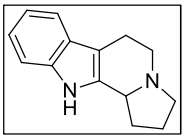

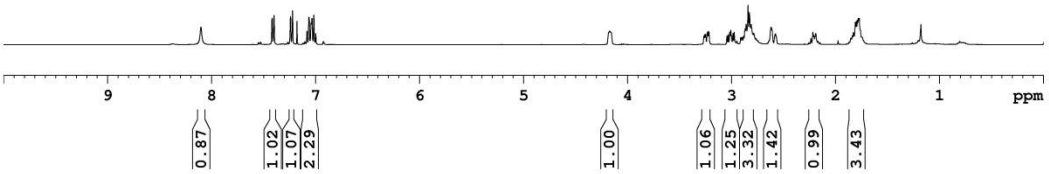

0.87 1.02 1.07 2.29 1.00 1.06 1.25 3.32 1.42 0.99 3.43

SGT-KM-21-01-21-A CDCL3 CMR

136.04 135.07 127.23 121.48 119.40 118.12 110.85 107.61 57.07 49.39 45.98 29.48 23.39 17.80

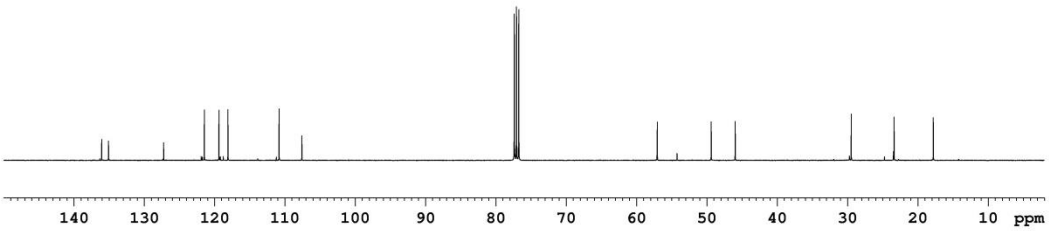

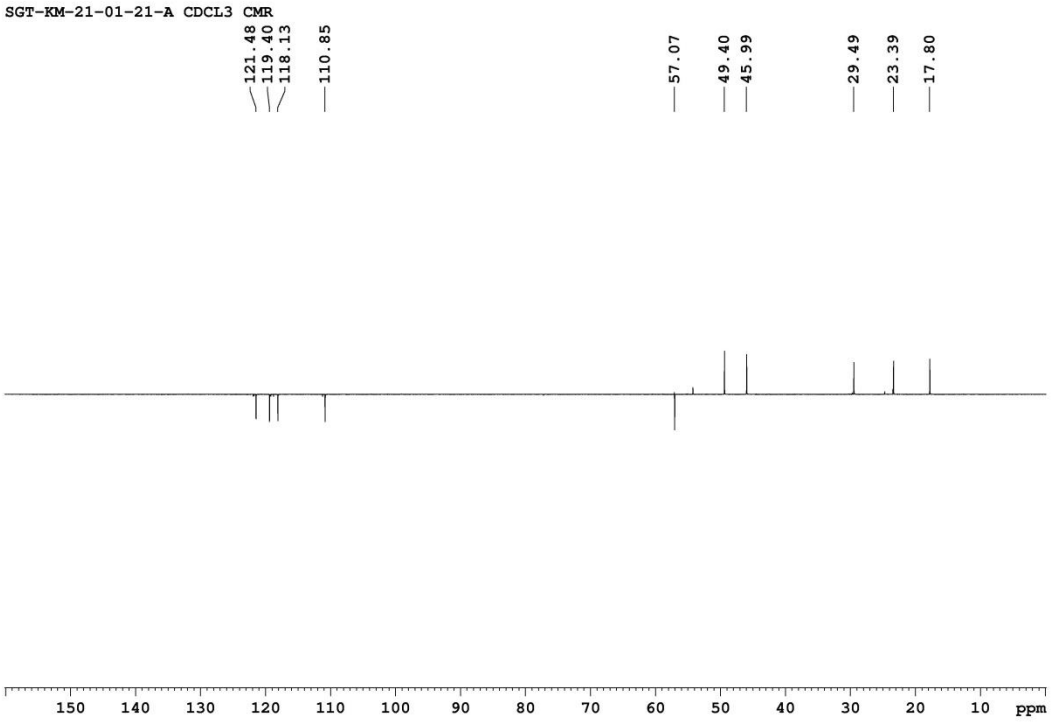
SGT-KM-21-01-21-A CDCL3 CMR
121.48
119.40
118.13
110.85
57.07
49.40
45.99
29.49
23.39
17.80
150 140 130 120 110 100 90 80 70 60 50 40 30 20 10 ppm

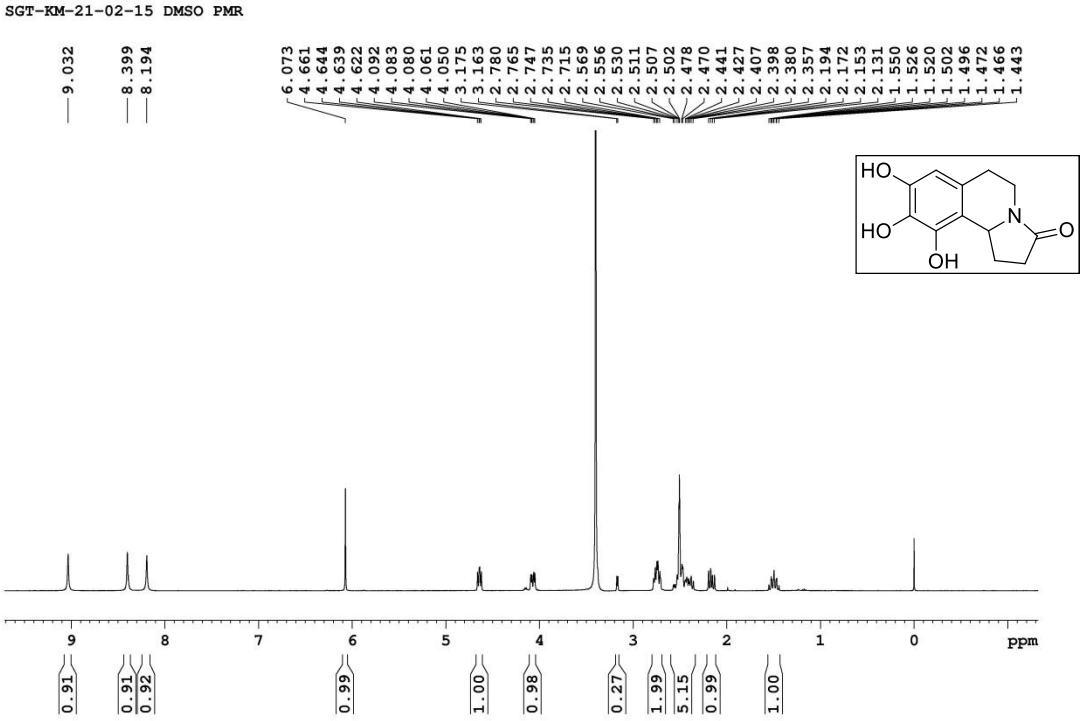
SGT-KM-21-02-15 DMSO PMR
9.032
8.399
8.194
6.073
4.661
4.644
4.639
4.622
4.092
4.083
4.080
4.061
4.050
3.175
3.163
2.780
2.765
2.747
2.735
2.715
2.569
2.556
2.530
2.511
2.507
2.502
2.478
2.470
2.441
2.427
2.407
2.398
2.380
2.357
2.194
2.172
2.153
2.131
1.550
1.526
1.520
1.502
1.496
1.472
1.466
1.443
HO
HO
OH
N
O
9 8 7 6 5 4 3 2 1 0 ppm
0.91
0.91
0.92
0.99
1.00
0.98
0.27
1.99
5.15
0.99
1.00

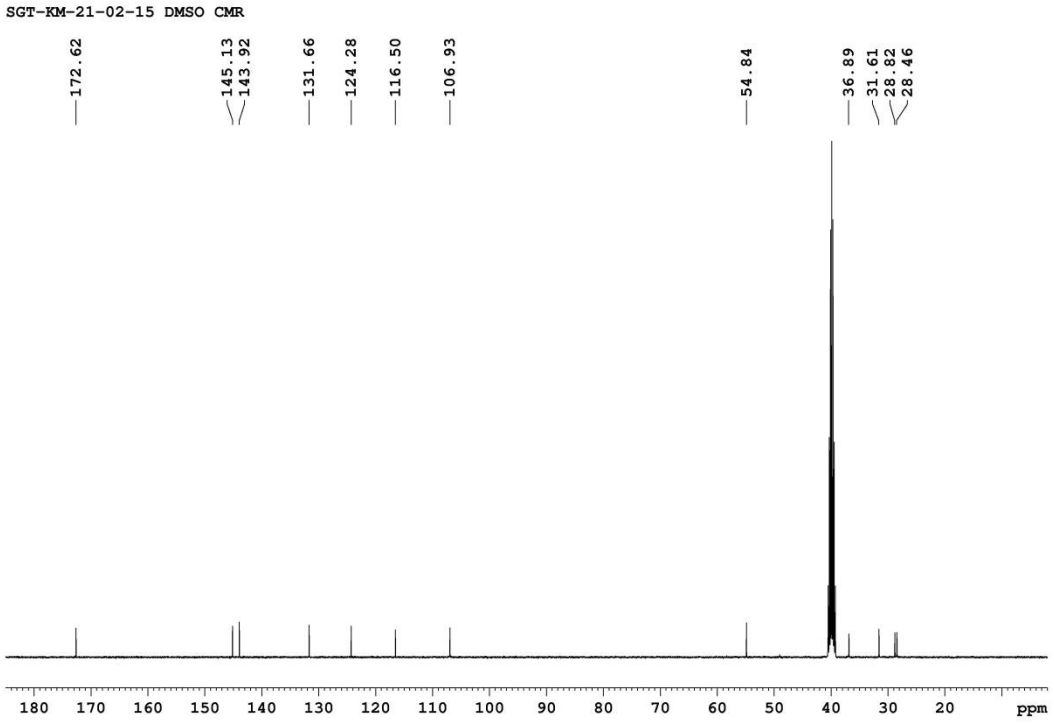
SGT-KM-21-02-15 DMSO CMR
172.62
145.13
143.92
131.66
124.28
116.50
106.93
54.84
36.89
31.61
28.82
28.46
180 170 160 150 140 130 120 110 100 90 80 70 60 50 40 30 20 ppm

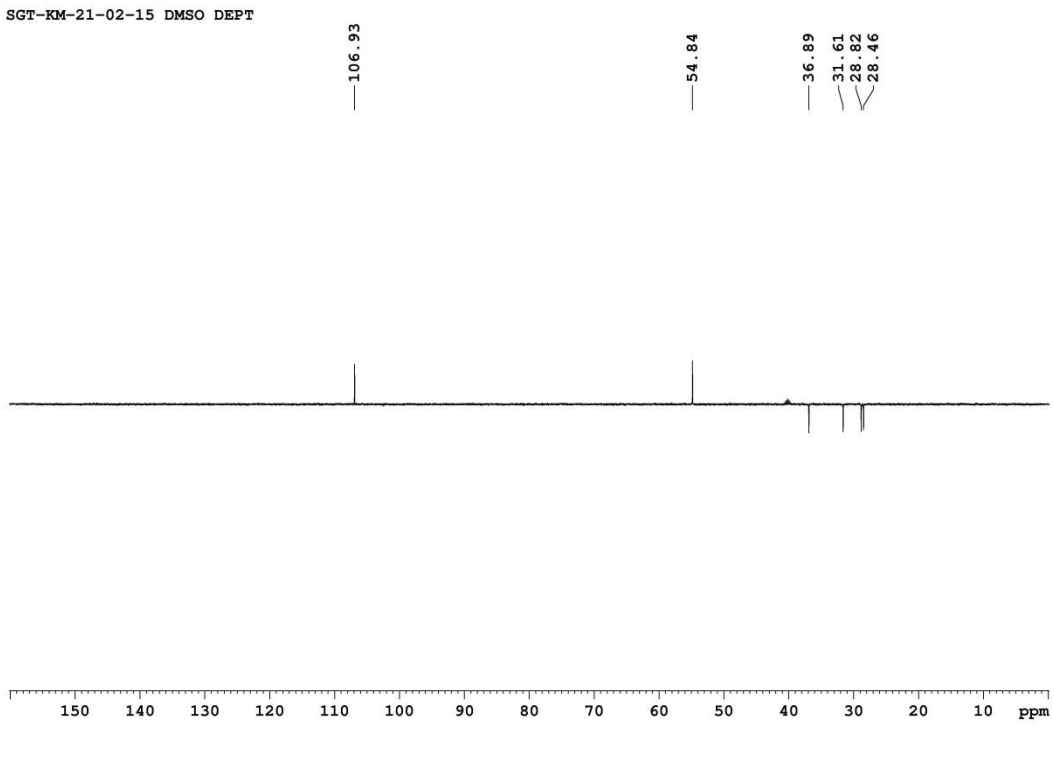
SGT-KM-21-02-15 DMSO DEPT
106.93
54.84
36.89
31.61
28.82
28.46
150 140 130 120 110 100 90 80 70 60 50 40 30 20 10 ppm

Section II: Synthetic studies of isoindolo[1,2-*a*]isoquinoline compounds

2.II.1 Introduction:

The isoindolo[1,2-*a*]isoquinoline structural motif belonging to the indolizidine class of the family is widely distributed in nature. The naturally occurring (±)-nuevamine[1] from the *Berberies darwini* Hook species is the first eminent member of the isoindolo-[1,2-*a*]isoquinoline family, also hirsutine and jamtine, isolated from *Cocculus Hirustus* belongs to the same family[2] (Fig. 1). These natural products and their synthetic analogs have been reported to display a wide spectrum of biological and pharmacological activities.[3] For instance, CRR-271 can act as a poly(ADP-ribose) polymerase-1 inhibitor.[4] Similarly, molecules containing isoindolo[2,1-*a*]quinoline scaffolds have shown bioactivities like antipsychotic,[5] antihypertensive,[6] and antiulcer,[7] even shown protective effects against N_2-induced hypoxia,[8] as well as inhibitory actions against DNA gyrase[9] and topoisomerase.[10]

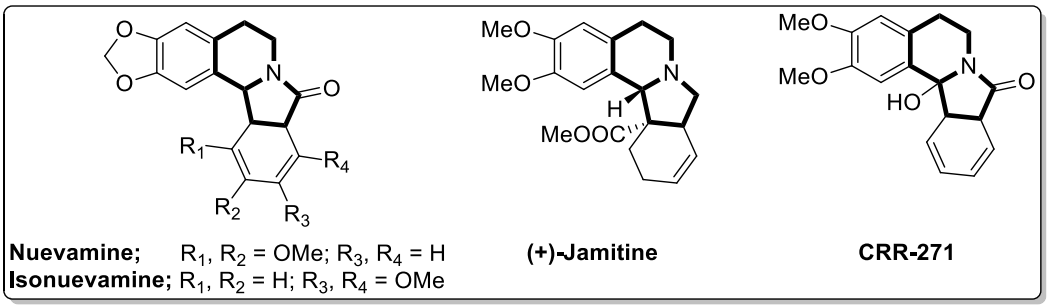

Figure 1. Selected tetracyclic natural products with indolizidine core

The demand for readily access to natural products and natural products like molecular systems has been always on the increasing trend. Hence synthetic organic chemist task is always well defined to synthesize the molecules on demand. Atom economy and selectivity are the real keys for synthetic efficiencies.

2.II.2 Literature review:

Although more or less similar to pyrrolo[2,1-*a*]isoquinoline compounds, isoindolo[1,2-*a*]isoquinoline compounds were synthesized emphatically by various research groups. The

construction of tetracyclic core from simple synthons along with high atom economy and fewer steps is challenging for the researchers. Scientists have revealed many distinct routes to develop isoindolo[1,2-*a*]isoquinoline compounds efficiently along with synthesizing a variety of variably substituted moieties placing them among different classes of chemicals. Here we have discussed a few research papers deriving their purpose of synthesizing isoindolo[1,2-*a*]isoquinoline compounds in the past decade.

Daïch et al.[11] have developed a short and efficient synthesis of mainly enantiopure fused pyrroloimidazolones and pyrroloisoquinolinones along with isoindoloisoquinolinones *via* intramolecular electrophilic cyclization of an *N*-acyliminium ion precursor (Scheme 1). To construct the tetracyclic core of isoindoloisoquinolinone, (*R*)-phenylglycinol was converted to α-hydroxy lactam in three steps, i.e., protection of primary amine with Boc group, coupling with phthalimide by Mitsunobu reaction using DIAD.

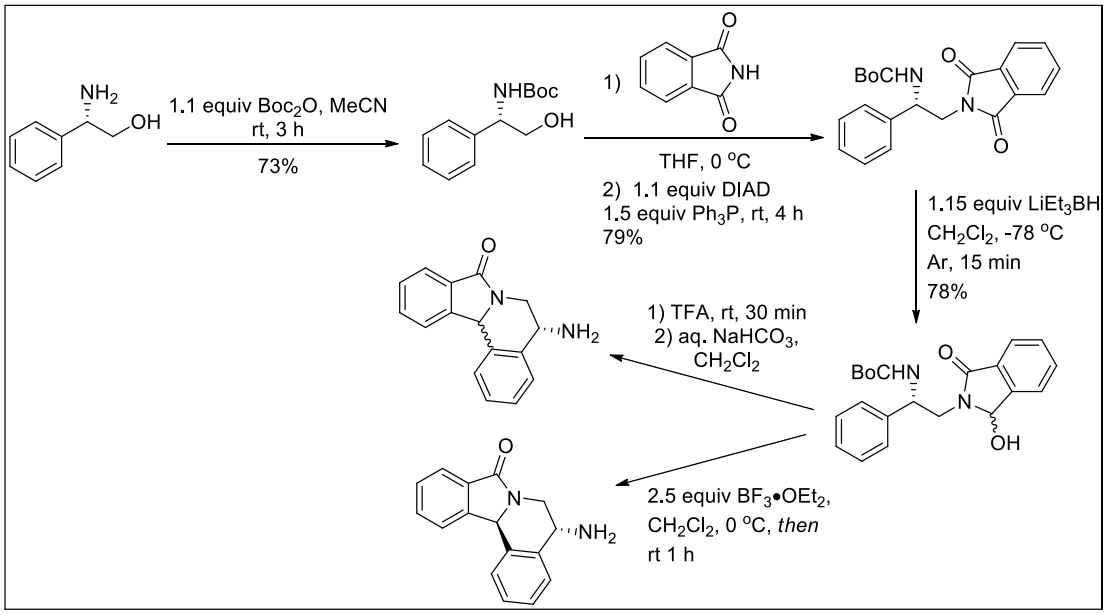

Scheme 1. Syntheses of fused pyrroloimidazolones and pyrroloisoquinolinones

Chemoselective reduction of imide was carried out using slightly excess of $LiEt_3BH$ to get α-hydroxy lactam in 78%, which was later subjected to two different reaction conditions. The normal acid-mediated *N*-acyliminium ion cyclization was performed using TFA and found the formation of both diastereoisomers in equal ratio. Whereas, reaction with $BF_3{\cdot}OEt_2$ delivered only one diastereomer exclusively. Using the Felkin-Ahn model they could explain the formation of respective diastereomers.

Selvakumar and Ramanathan[12] have reported the synthesis of fused isoindoloisoquinolinone skeleton from phenethylphthalimides using trifluoromethanesulfonic acid Bronsted acid (Scheme 2). A library of heavily substituted tetracyclic compounds has been exhibited utilizing intramolecular cyclization of corresponding phenethylphthalimides. They have optimized the required stoichiometry of TfOH for the cyclization and found that with 4 equiv of TfOH and at 0 °C to room temperature, one can synthesize these compounds with good yields. Even, a hydroxy model substrate of (±)-nuevamine is synthesized in 85% yield from its respective phenethylphthalimide.

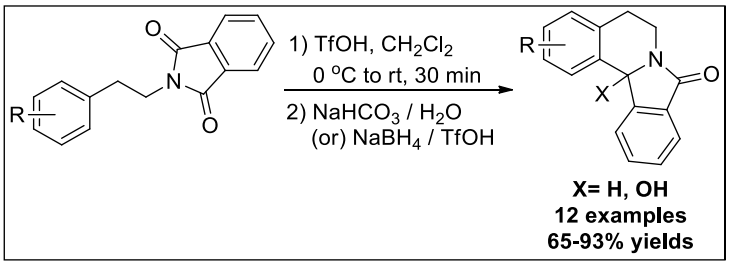

Scheme 2. Synthesis of isoindolo[1,2-*a*]isoquinolinone derivatives using Bronsted acid

Argade and co-workers[13] succinctly described the regioselective formation of isonuevamine moiety over nuevamine *via* regioselective reduction of 3,4-dimethoxyhomopiperonylphthalimide using sodium borohydride and DIBAL-H (Scheme 3). 3,4-Dimethoxyphthalic anhydride was coupled with homopiperonyl amine in refluxing *o*-dichlorobenzene to furnish 3,4-dimethoxyhomopiperonylphthalimide. Taking as a challenge, they regioselectively reduced one of the carbonyl groups of 3,4-dimethoxyhomopiperonylphthalimide using $NaBH_4$ and DIBAL-H reducing agents in various solvents and at different temperatures. The reduction of imide 3,4-dimethoxyhomopiperonylphthalimide with $NaBH_4$ in dry THF at room temperature exclusively reduced C3 carbonyl to furnish lactamol. With syntheses of C1 and C3 lactamols, they later converted C3 lactamol to C1 lactamol using NaOMe. Then Bronsted acid TFA mediated cyclization followed by reduction furnished them both (±)-nuevamine and (±)-isonuevamine.

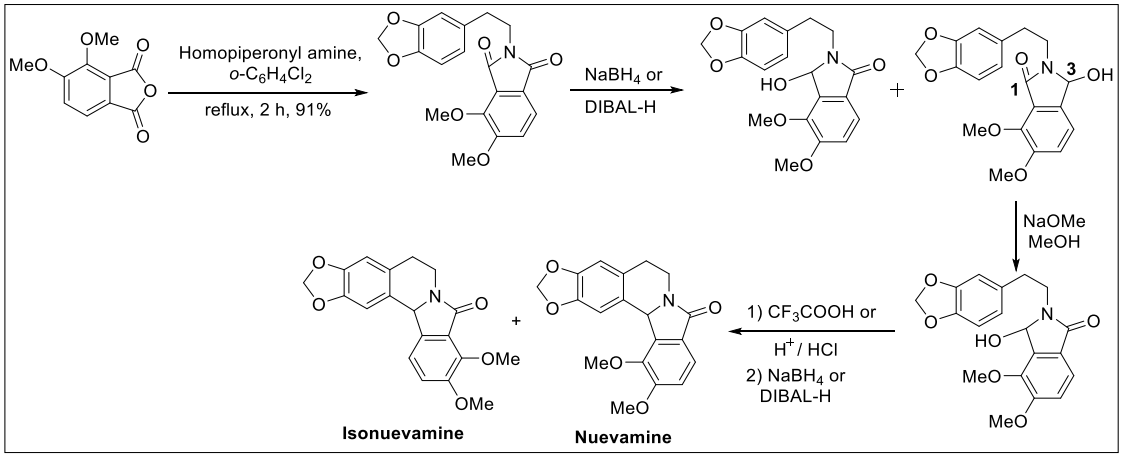

Scheme 3. Total syntheses of nuevamine and isonuevamine

Aranzamendi et al.[14] have demonstrated BINOL-derived Brønsted acid-catalyzed conversion of 12b-hydroxy isoindoloisoquinolines to 12b-indole isoindoloisoquinolines *via* Parham cyclization−intermolecular α-amidoalkylation by indole surrogates (Scheme 4). Using Parham cyclization reaction preparation of 12b-hydroxy isoindoloisoquinolines were carried out in the presence of *n*BuLi and it was further subjected to α-amidoalkylation using catalytic chiral Brønsted acids (mainly BINOL derived phosphoric acids) with indole derivatives. The chiral catalyst facilitated the reaction of indoles *via N*-acyliminium ion formation giving average enantiomeric excess for the 12b-indole isoindoloisoquinoline compounds.

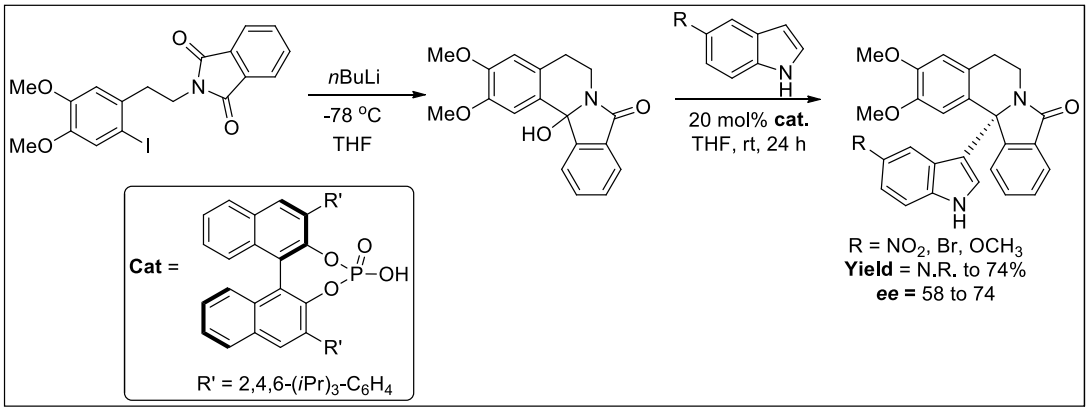

Scheme 4. BINOL-derived Brønsted acid-catalyzed conversion of 12b-hydroxy isoindoloisoquinolines to 12b-indole isoindoloisoquinolines

Wang and his team[15] have reported the construction of an unorthodox kind of isoindoloisoquinoline compounds using L-proline catalyzed asymmetric Michael reaction

starting from 1-butanal and nitrostyrene (Scheme 5). First, an asymmetric Michael reaction between 1-butanal and nitrostyrene was carried out using 10 mol% of L-proline and methyl *tert*-butyl ether to get nitroaldehyde (*2R,3S*)-2-ethyl-4-nitro-3-phenylbutanal. This nitroaldehyde compound was reduced, and fused with phthlandione to get imide compound. Reduction followed the conversion of the resultant ω-carbinol-lactam (lactamol) to its ethyl ether, furnished isoindoloisoquinolinone compound mixture in 49% yield after cyclizing with $TiCl_4$.

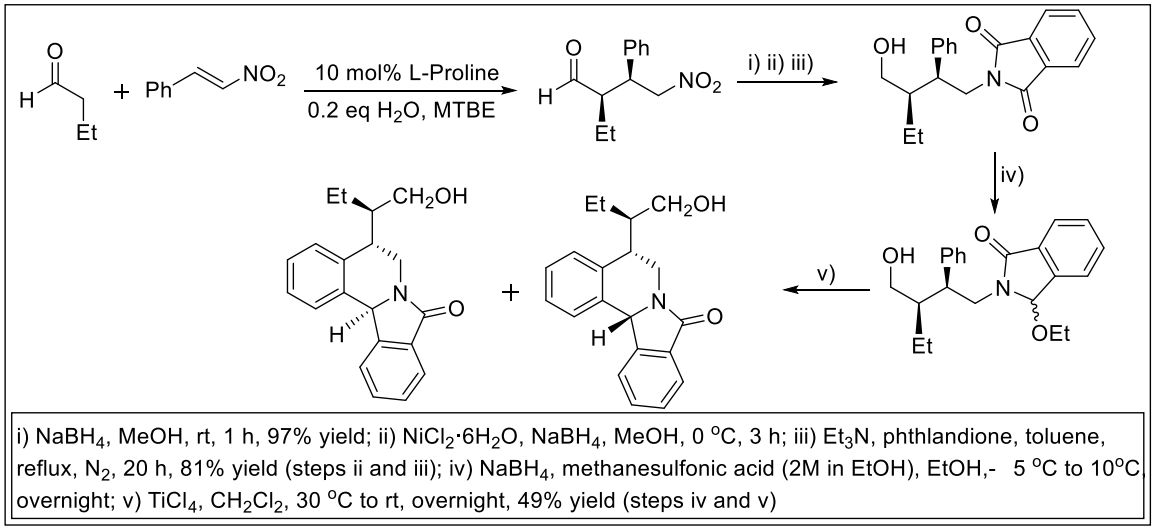

Scheme 5. Syntheses of isoindolo[1,2-*a*]isoquinolinone derivatives using L-proline catalyzed asymmetric Michael reaction

Kim and Min[16] have published the construction of isoindoloisoquinoline compounds from oxazolidinediones using simple $TiCl_4$ mediated intramolecular Friedel−Crafts reaction (Scheme 6). Various derivatives of isoindoloisoquinolinone were synthesized along with racemic nuevamine alkaloid.

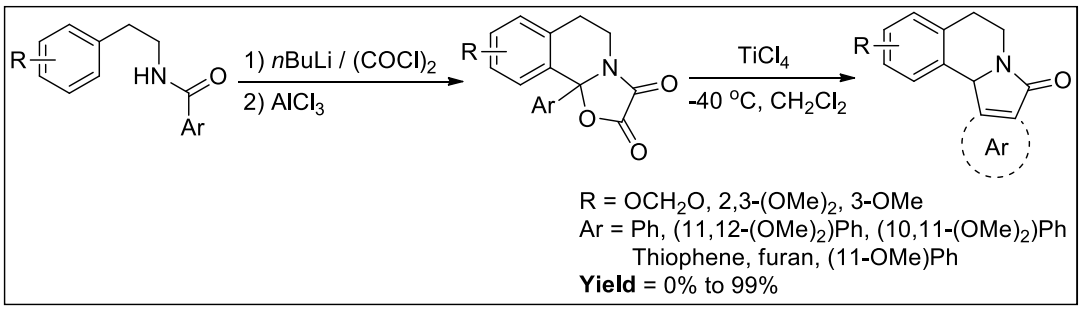

Scheme 6. Construction of isoindolo[1,2-*a*]isoquinolinone substrates *via* $TiCl_4$ mediated intramolecular Friedel−Crafts reaction

Dalla and his team[17] has developed a methodology for the construction of isoindoloisoquinolinone compounds along with pyrroloisoquinolinone also by carrying out the reaction in refluxing 1,1,2,2-tetrachloroethane (TCE), which gave them an advantage of releasing a small amount of HCl by thermolytic elimination (Scheme 7). Likewise, they have synthesized various compounds using different aryl groups and bearing different substituents on the aryl ring.

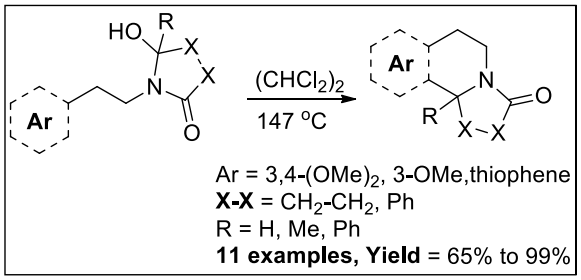

Scheme 7. Syntheses of indolizidine compounds in 1,1,2,2-tetrachloroethane (TCE)

Roy and Maity[18] collaboratively reported synthesis of a variety of indolizidine compounds using iridium tin complex *via N*-acyliminium ion cyclization strategy (Scheme 8). Phthalic anhydride-derived γ-hydroxylactams containing arylethyl chain was reacted in the presence of 1 mol% of $[Cp^{*}Ir(SnCl_3)_2\{SnCl_2(H_2O)_2\}]$ in DCE to provide the tetracyclic ring products in excellent yields.

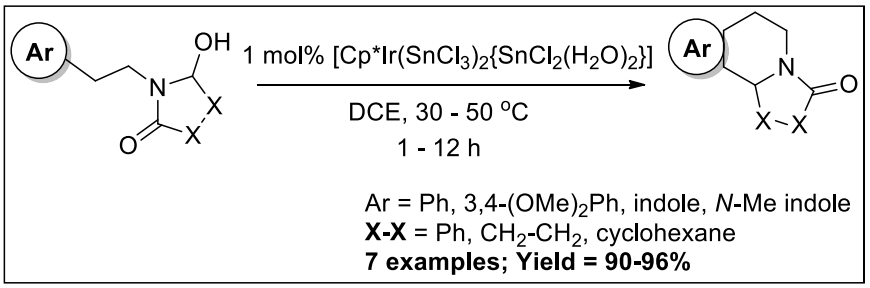

Scheme 8. Syntheses of indolizidine compounds using iridium tin complex *via N*-acyliminium ion cyclization strategy

Pandey and Anbarasan[19] have shown syntheses of monotrifluoromethylated isoindoloisoquinolinones and pyrroloisoquinolinones using CF_3TMS in the presence of methanesulfonic acid (MsOH). A one-pot cyclization of trifluoromethylated acyliminium ions *via* MsOH mediated heminal intermediate was used for the synthesis of α-

trifluoromethylated amine derivatives (Scheme 9).

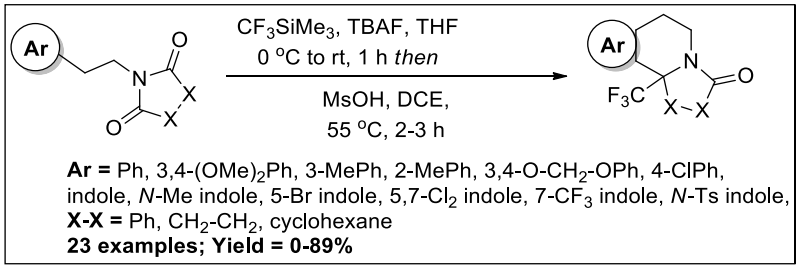

Scheme 9. Syntheses of monotrifluoromethylated isoindoloisoquinolinones and pyrroloisoquinolinones

Seo and Kim[20] have shown a cyclization of benzamidoacrylate intermediate to magallanesine using Heck reaction followed by Friedel–Crafts reaction sequences. During this they have also shown the synthesis of ethyl 2-(2,3-dimethoxy-8-oxo-5,6,8,12b tetrahydroisoindolo[1,2-*a*]isoquinolin-12b-yl)acetate starting from commercially available homoveratryl amine and 2-iodo benzoic acid (Scheme 10). Thus, homoveratryl amine and acid were converted to the corresponding iodoarylamide using an EDCl coupling agent. Then it was reacted with ethylpropiolate in the presence of cesium carbonate to obtain amidoacrylate, which was then cyclized to form a five-membered ring using Heck reaction and later converted to isoindoloisoquinolinone moiety using $AlCl_3$ mediated Friedel-Crafts reaction.

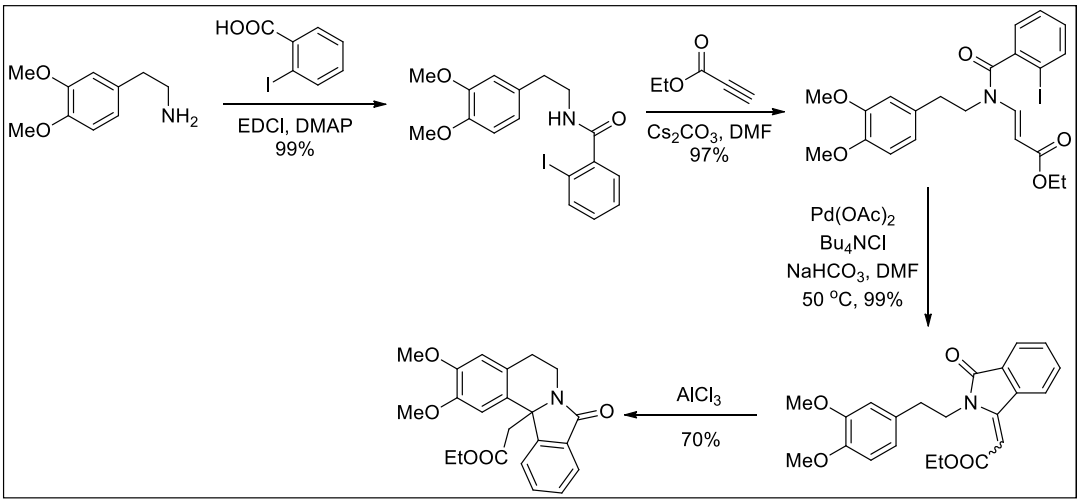

Scheme 10. Synthesis of indolizidine compound using Heck and Friedel-Craft's reactions

Rao et al.[21] have constructed a C-C bond between various 3-hydoxyisoindolinones and a

variety of aryl-, heteroaryl-, and alkenylboronic acids using $Cu(OTf)_2$ catalyst to build C3 aryl-, heteroaryl-, and alkenyl-substituted isoindolinones (Scheme 11). For the basic utility of the methodology, they have successfully synthesized the tetracyclic ring motif of the alkaloid nuevamine.

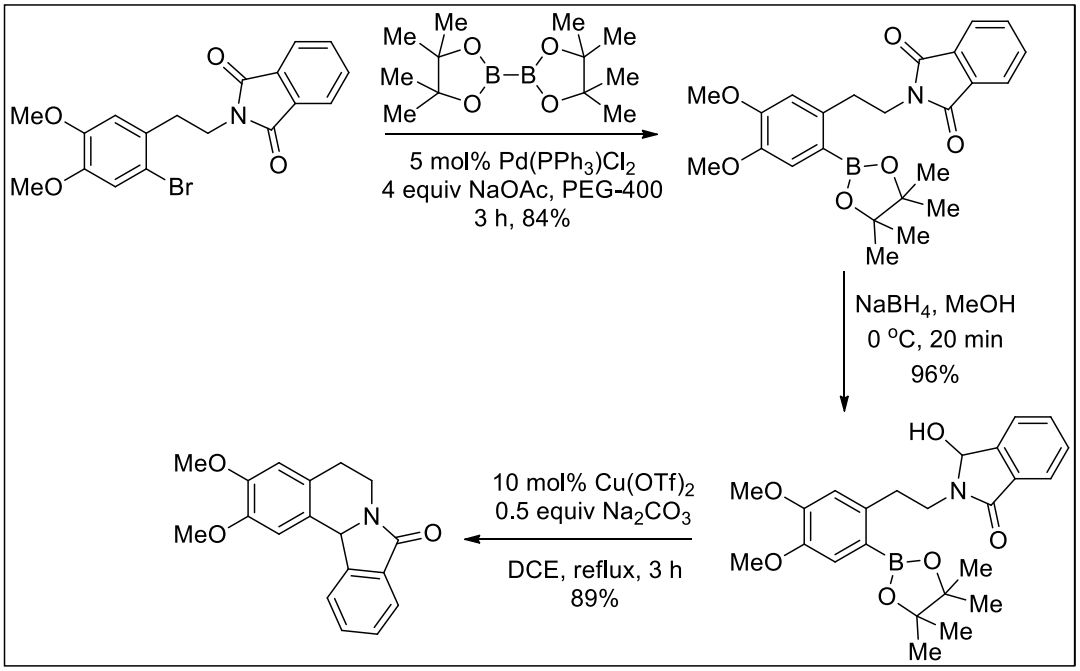

Scheme 11. Intramolecular cyclization of 3-hydoxyisoindolinones aryl boronic acid using $Cu(OTf)_2$ catalyst

For the synthesis of nuevamine, the starting phthalimide was converted to its boronic acid derivative using a Pd-catalyzed reaction with hindered bis(pinacolato)diboron compound. Reduction of imide to lactamol and then using their developed method by $Cu(OTf)_2$ catalyzed cyclization furnished racemic nuevamine.

Ramanathan and co-workers[22] have explored the *N*-acyliminium cyclization of phthalimides *via* Lewis acid like boron tribromide mediated cyclization to isoindoloisoquinolinones and pyrroloisoquinolinones (Scheme 12). They have synthesized various indolizidine compounds using an excess of boron tribromide to demonstrate the imide carbonyl activation reaction of phenethylphthalimide.

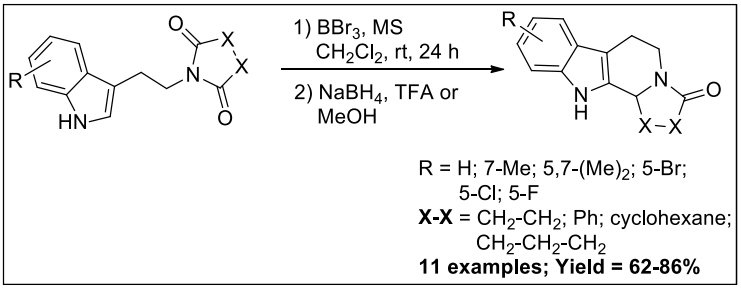

Scheme 12. Syntheses of indolizidine compounds *via N*-acyliminium cyclization reaction using BBr_3

The same group[23] has synthesized various isoindoloisoquinolinones and hydroxyl isoindoloisoquinolinones from corresponding phthalimides using triflic acid cyclization followed by sodium borohydride reduction and basic workup respectively (Scheme 13).

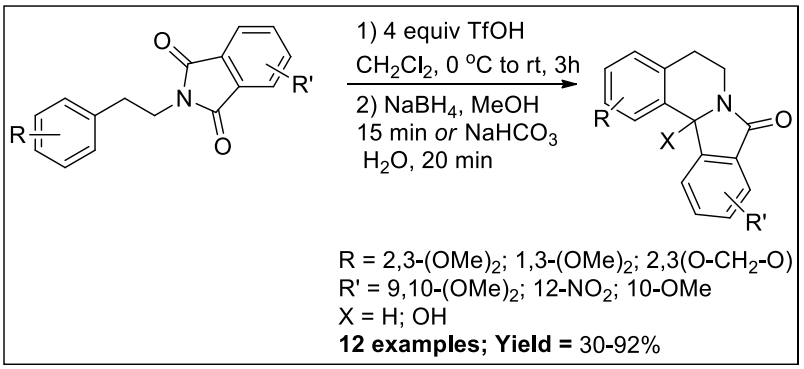

Scheme 13. Syntheses of isoindoloisoquinolinones and hydroxyl isoindoloisoquinolinones using TfOH

In the same year, the same group[4] established syntheses of a series of compounds named CRR using their reaction methodology mentioned above (Scheme 14). These CRR compounds are useful towards inhibition of poly(ADP-ribose) polymerase 1 and are widely studied in recent times. The library of 12b-hydroxy-substituted isoindoloisoquinoline compounds synthesized was named CRR-203, CRR-204, CRR-211, CRR-222, CRR-224, CRR-227, CRR-228, CRR-271 depending upon the different substituents groups at different positions as mentioned below. Further, authors have studied the compounds for the antioxidant activity for lipid peroxidation at cellular and genomic DNA damage protection at the nuclear level, and to protect chicken enthrocytes against H_2O_2 induced damage at 100 µM concentration as evident from the cell viability.

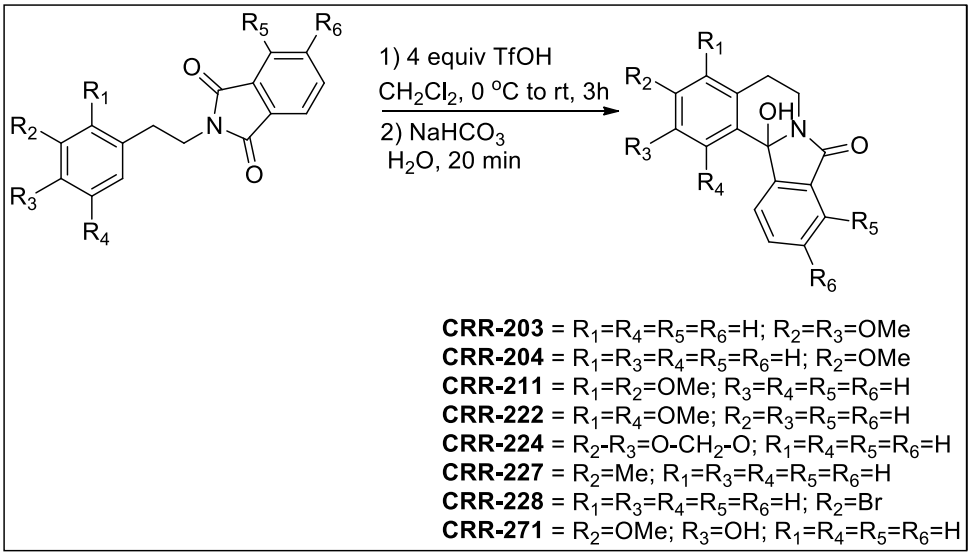

Scheme 14. Syntheses of 12b-hydroxy-substituted isoindoloisoquinoline derivatives

Sharma and co-workers[24] have reported a C-C bond-forming reaction between *N*-protected tetrahydroisoquinoline compounds with in situ generated arynes (Scheme 15). *n*BuLi mediated synthesis of α-carbanion derived from *N*-Boc tetrahydroisoquinoline was coupled with in situ generated aryne moiety of chlorobenzene at low temperature. The temperature rise furnished the isoindoloisoquinolinone compound by knocking off *t*-butoxide group. Also, they have shown the synthesis of the drug (±)-FR115427 by using their strategy.

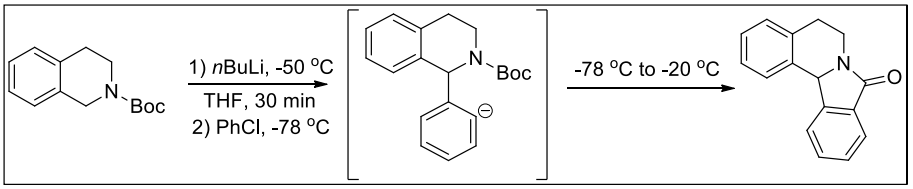

Scheme 15. Synthesis of 5,6-dihydroisoindolo[1,2-*a*]isoquinolin-8(12b*H*)-one by in situ generation of aryne using nBuLi

Varga et al.[25] have shown a one-pot Ugi four-center, three-component reaction (Ugi-4C-3CR) to construct isoindolinone compounds from various amines, 2-formylbenzoic acids, and *tert*-butyl isocyanide using propylphosphonic anhydride (T3P®) in microwave condition (Scheme 16). Along with the synthesis of isoindolinones they have used their strategy to synthesize nuevamine alkaloid. The syntheses of isoindoloisoquinolinone type compounds were carried out from arylethylamines and 2-formylbenzoic acid derivatives using T3P in solvent ethyl acetate in the microwave.

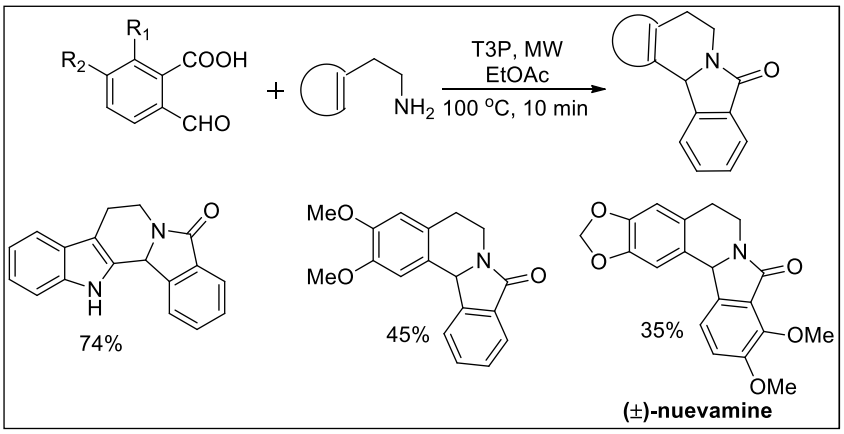

Scheme 16. One-pot syntheses of (±)-nuevamine and isoindolo[1,2-*a*]isoquinolinone derivatives using T3P

Zhao's group[26] has shown the reaction between 1,3-unsubstituted 2-(1*H*-indol-2-yl)ethanamines and alkynoic acids for the first time to achieve gold-catalyzed highly selective cascade reactions to furnish fused systems of methyl-substituted aryl and heteroaryl moieties of pyrroloisoquinoline, isoindoisoquinoline skeletons (Scheme 17). A catalytic amount of gold catalyst $Au(PPh_3)Cl$ along with triflic acid was employed to synthesize tetracyclic fused compounds.

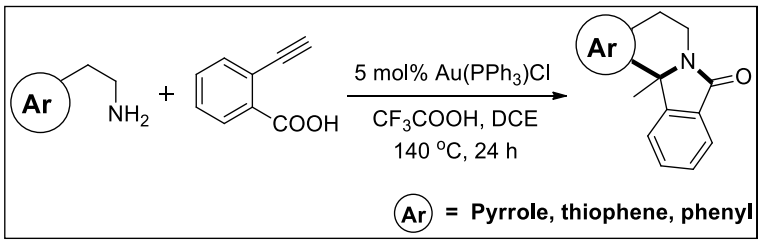

Scheme 17. One-pot syntheses of indolizidine derivatives using $Au(PPh_3)Cl$ as catalyst

Zhao's team[27] has published an intermolecular amidoalkylation reaction of γ-hydroxy lactams with various C, O, N, S nucleophiles, catalyzed by $NiCl_4 \cdot 6H_2O$ in refluxing 1,2-dichloroethane (Scheme 18). They have synthesized a variety of nucleophile attached isoindolinone compounds in very high yields. Also, they could successfully carry out intramolecular cyclization of *N*-phenethyl-γ-hydroxy phthalamide compounds using their optimized condition as mentioned below. They have synthesized five such isoindoloisoquinolinone compounds with very high yields but failed to produce CF_3 substituted compounds.

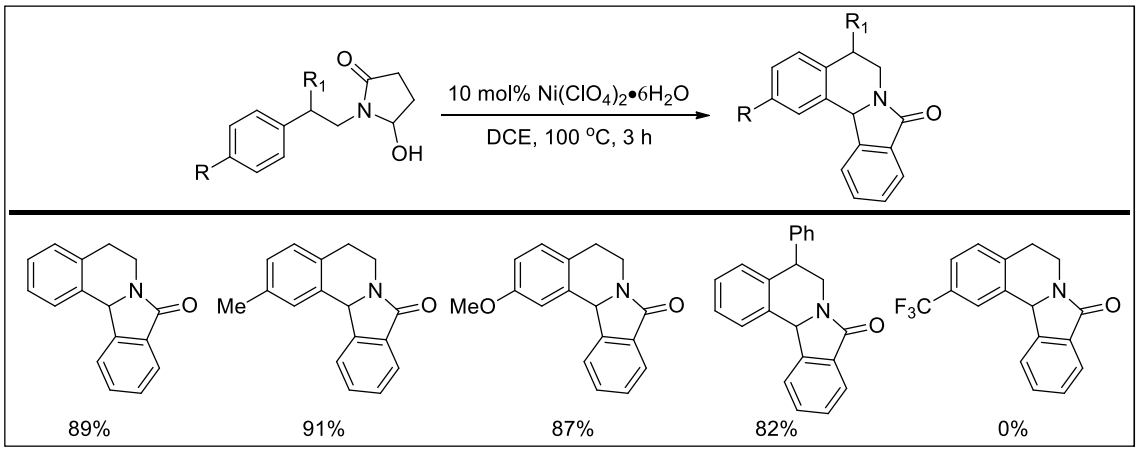

Scheme 18. Construction of isoindolo[1,2-*a*]isoquinolinone derivatives using catalytic $NiCl_4 \cdot 6H_2O$

Kurva et al.[28] have established syntheses of isoindolinones from 2-nitrobenzoic acid derivatives using Ugi reaction *via* S_NAr reaction. A strong base potassium *tert*-butylate was used to trigger the cyclization followed by S_NAr reaction, deamidification/oxidation sequence to furnish 2- hydroxyisoindolinones (Scheme 19).

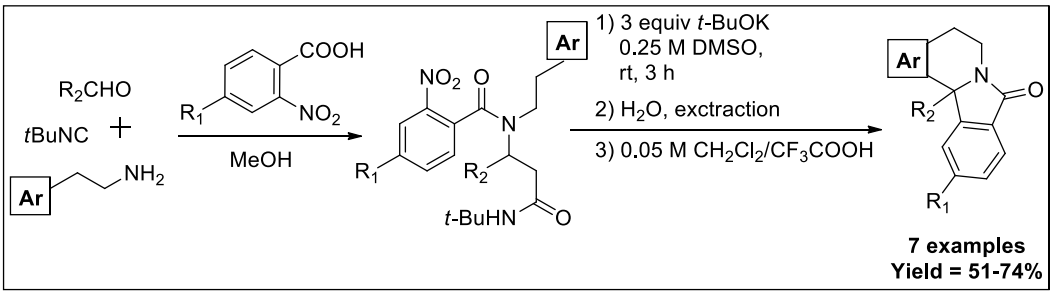

Scheme 19. Syntheses of isoindolo[1,2-*a*]isoquinolinone derivatives using Ugi reaction *via* S_NAr reaction

Tetracyclic compounds like isoindoloisoquinolinones were also synthesized *via* Pictet-Spengler cyclization reaction using TfOH.

Chang and co-workers[29] have reported the construction of isoindolo[1,2-*a*]isoquinoline and isoindolo[2,1-*a*]quinoline derivatives by condensation of methyl 2-acylbenzoates with 2-arylethanamines or 2-acylanilines in the presence of trifluoroacetic acid *via N*-acyliminium ion cyclization method (Scheme 20).

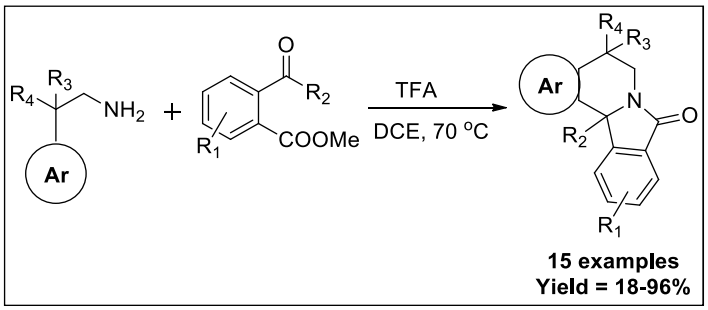

Scheme 20. Construction of isoindolo[1,2-*a*]isoquinolinone derivatives using TFA

2.II.3 Results and discussion:

Retrosynthetically the pyrrolidone ring of the isoindoloisoquinolinone can be constructed from benzenoids (two aryl substrates) in four ways as shown in fig. 2 during the crucial tetracyclization.

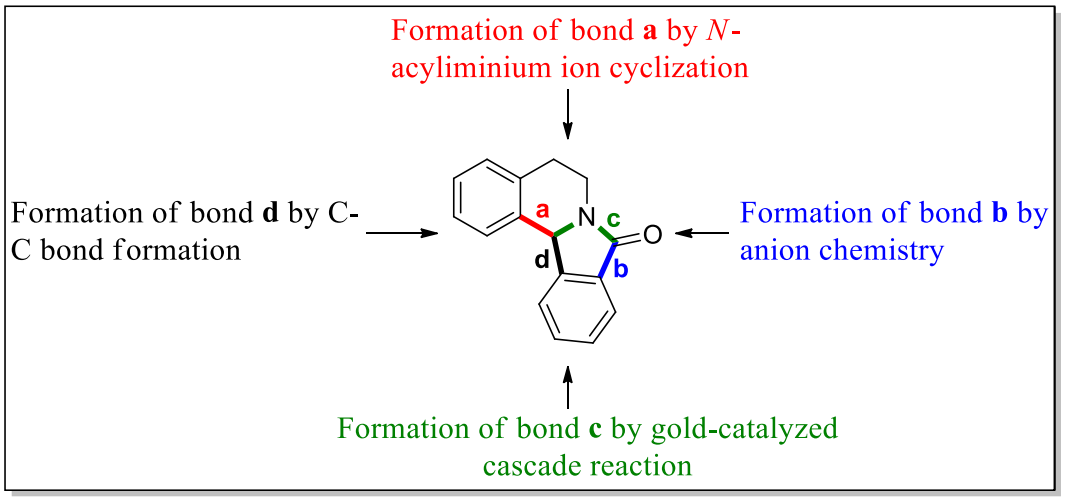

Figure 2. Depiction of constructions of different bonds to synthesize isoindoloisoquinolinone core

As evident from the enormous literature work, researchers have worked on building the isoindoloisoquinolinone moiety mostly *via* bond **a** formation (*N*-acyliminium ion cyclization strategy) as the last step. Only one report each is available via bond **b** and **c** construction (using benzyne strategy), however, there are no reports *via* bond **d** construction as the last step. Hence we thought of venturing into the construction of isoinoloqiolinoline *via* the construction of bond **d** as the crucial step.

There are a lot of reports on Csp^3-Csp^3 coupling of C1 carbon of *N*-protected-1,2,3,4-

tetrahydroisoquinoline with various nucleophiles implying that C1 carbon is reactive towards many coupling reagents. To interpret the construction of isoindoloisoquinoline compounds by forming a **d** bond, one can imagine only intramolecular dehydrogenative C-C coupling reactions. The retrosynthesis of compound **1** suggested simple moieties to make C-C bond formation facile (Scheme 21). The required *N*-benzyl-1,2,3,4-tetrahydroisoquinoline **2** further disconnected into benzyl bromide **3** and 1,2,3,4-tetrahydrosioquinoline **4** which is an even simpler synthon.

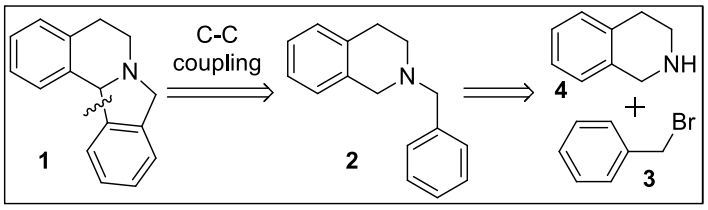

Scheme 21. Retrosynthetic pathway

Using the reported procedure for *N*-alkylation, we synthesized compounds **2** from **3** and **4** using a mild base like K_2CO_3 in acetonitrile (Scheme 22). Although the benzene ring of the benzyl moiety is not activated to facile this reaction, we gave it a try to see the efficacy of our idea.

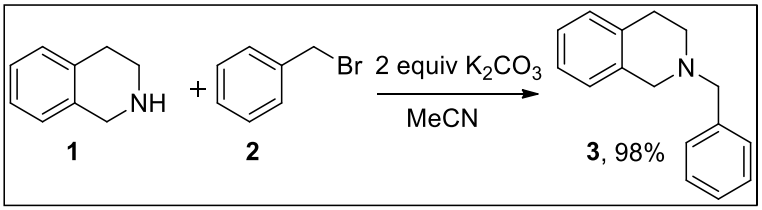

Scheme 22. Synthesis of 2-benzyl-1,2,3,4-tetrahydroisoquinoline

Various expensive catalysts have been employed for most of the intra/intermolecular dehydrogenative coupling reactions, but we thought of using simple, inexpensive catalysts for our methodology. Our lab has shown the extensive importance of the molecular iodine reagent by carrying out simple to complex transformations till now.[30]

N-benzyl-1,2,3,4-tetrahydroisoquinoline compound **3** was subjected to various reaction conditions to construct a tetracyclic ring core. Initially, compound **3** with molecular iodine was stirred in dry toluene for 1 d (Table 1, entry 1). But there was no change seen in TLC

for that reaction. So, the same reaction was refluxed under an oxygen atmosphere for another 6 h (Table 1, entry 2) and noticed a formation of a new bright spot on TLC. Upon column purification and characterization it turned out to be the amide analog of the starting amine **3**. Then, instead of molecular iodine, we thought of using metal salts for the same reaction. A stoichiometric amount of copper bromide ($CuBr_2$) was refluxed in dry toluene with **3** in open-air condition (Table 1, entry 3). But it turned out to be ineffective towards cyclization and even the α-amidation process. So the necessity of polar solvent was assumed and the following same reaction was refluxed in acetonitrile, which furnished amide analog in 45% yield (Table 1, entry 4).

Table 1. Optimization of reagents

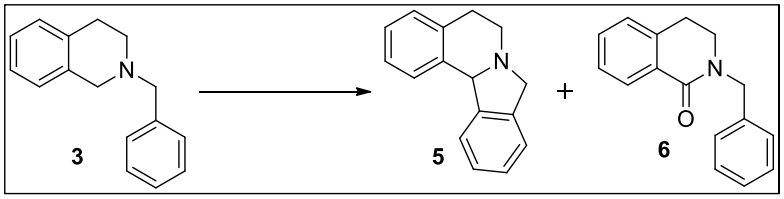

Entry	Reaction conditions	Results	%Yield
1	1 equiv I_2, dry toluene, rt, 24 h	No reaction	N.A.
2	1 equiv I_2, dry toluene, reflux, O_2 atm, 6 h	Formation of amide **6**	35%
3	1 equiv $CuBr_2$, dry toluene, reflux, 6–12 h	No reaction	N.A.
4	1 equiv $CuBr_2$, MeCN, reflux, 6–12 h	Formation of amide **6**	45%

As we understood that, compound **3** is more prone to its oxidation process under the above conditions, we thought of preparing its amide and then later cyclizing it *via* Bischler-Napieralski reaction. By slightly modifying table 1, entry 4 reaction condition by adding water in the reaction we could synthesize its amide **6** in 60% yield (Scheme 23).

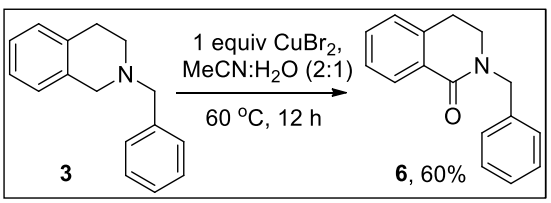

Scheme 23. Synthesis of 2-benzyl-3,4-dihydroisoquinolin-1(2*H*)-one 5

Later, compound **6** was then heated in freshly distilled phosphorus oxychloride in an inert atmosphere at 80 °C (Scheme 24). The disappearance of the starting material was checked

on the TLC every 15 minutes time span for confirming that the reaction is going as planned. But even after heating for 3 h, there was no change in the TLC observed, so, it was then concentrated over the rotary evaporator and then subjected to reduction using $NaBH_4$ in ethanol thinking that we may not be observing the intermediate salt on TLC. But unfortunately, the purpose of the reaction was not served and this attempt also failed.

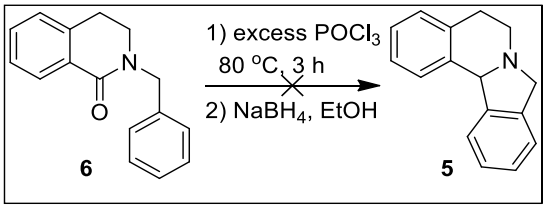

Scheme 24. Attempted synthesis of 5,6,8,12b-tetrahydroisoindolo[1,2-*a*]isoquinoline

From the above failures, we proceeded with an electron-rich benzene compound to prepare our expected tetracyclic compound. A direct reaction between **4** and veratraldehyde **7** was performed in the presence of catalytic *p*-TSA in refluxing dry toluene (Scheme 25). Even after the constant heating for 6 hours, a highly polar spot on TLC was not seen converting to any other new spots, so it was refluxed for another 24 hours. Even after prolonged heating, no change in TLC was observed, so, we added a stoichiometric amount of molecular iodine to it to make the reaction possible. But unfortunately, that attempt also remained unsuccessful.

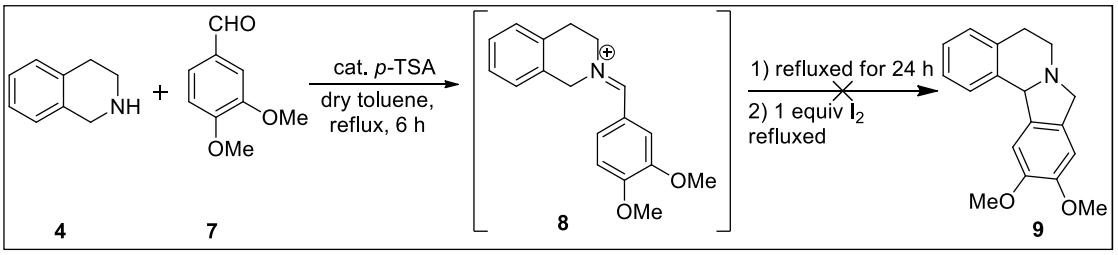

Scheme 25. Attempted one-pot cyclization reaction

An attempt was made to cyclize **4** with **6** in formic acid-xylene mixture under reflux condition (Scheme 26). Continuous heating for straight 2 days also failed to give expected tetracyclic product, which upon removal of solvent and aqueous workup furnished both the starting **4** and **6** back.

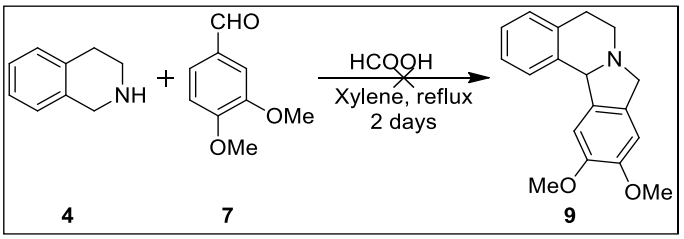

Scheme 26. Attempted synthesis of 10,11-dimethoxy-5,6,8,12b-tetrahydroisoindolo[1,2-*a*]isoquinoline 8

With several failed attempts, we charted the methodology developed for the syntheses of pyrrolo[2,1-*a*]isoquinoline compounds and carried out the preparation of isoindolo[1,2-*a*]isoquinoline compounds. Similarly, like the previous section's retrosynthesis, the 3 bonds and 2 components method applies here. So phenethylamine along with phthalic acid was the main components figured out from the retrosynthesis (Scheme 27).

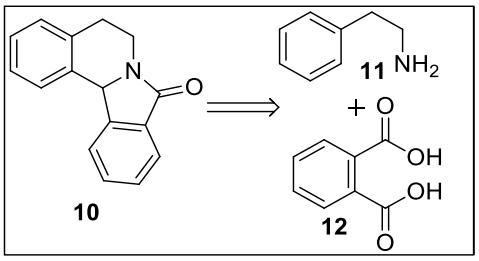

Scheme 27. Retrosynthetic pathway

A one-pot cyclization reaction of phenethylamines **11** and phthalic acid derivatives **12** was subjected to previously optimized reaction conditions of P_4O_{10} in TfOH at 100 °C to obtain various derivatives of simple isoindoloisoquinolinone and γ-hydroxy isoindoloisoquinolinone after reduction and addition reactions respectively (Scheme 28).

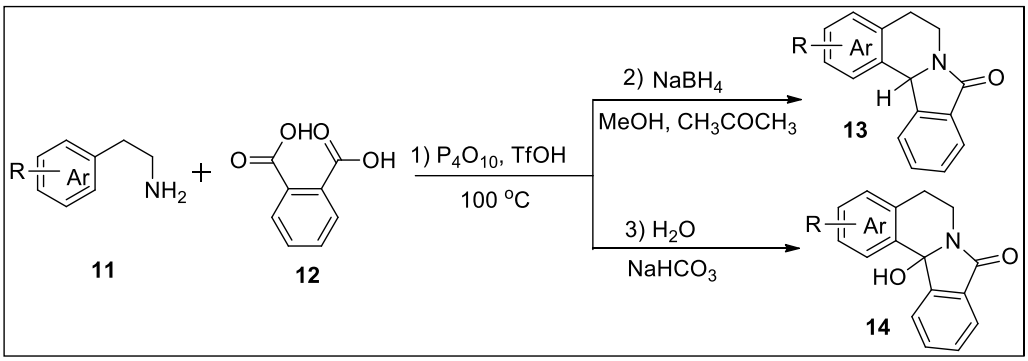

Scheme 28. Condensation-cyclization of phenylethylamine with phthalic acid derivatives

Four various aryl/heteroaryl ethylamines were treated with phthalic acid in heating with 8.3 wt% P_4O_{10}/TfOH mixture at 100 °C followed by reduction of the subsequent iminium ion to produce the final adducts. Compound **13a** was prepared from homoveratryl amine **11a** and phthalic acid **12a** in 89% yield (Table 2, entry 1).

Table 2. Syntheses of isoindoloisoquinolinones

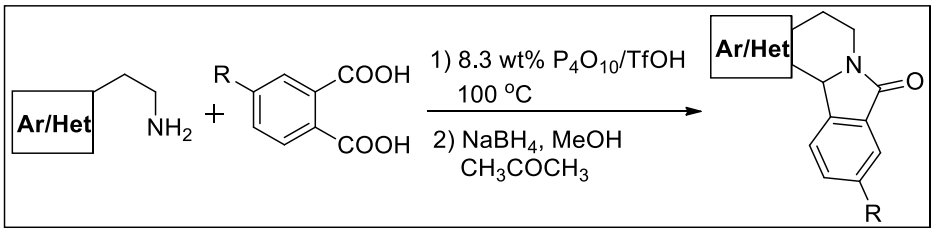

Entry	Phenethylamine	Dibasic acid	Product	Yield
1	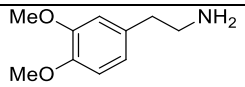 **11a**	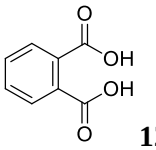 **12a**	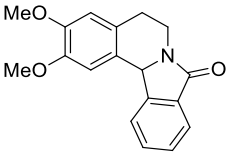 **13a**	89%
2	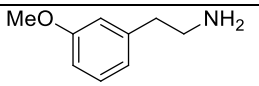 **11b**	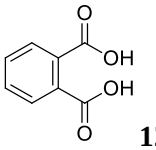 **12a**	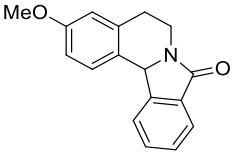 **13b**	85%
3	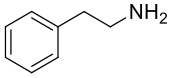 **11c**	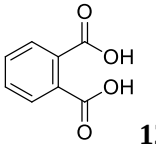 **12a**	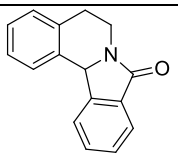 **13c**	84%
4	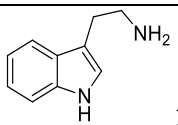 **11d**	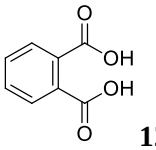 **12a**	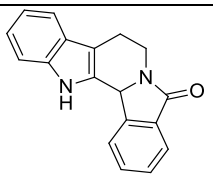 **13d**	87%

Whereas its mono methoxy **13b**, and unsubstituted **13c** analogs were prepared successfully from their respective amines **11b**, **11c** in 85% and 84% respectively (Table 2, entries 2, 3). Other than simple aryl compounds, a heteroaryl derivative of pentacyclic ring structure **13d** from tryptamine **11d** and phthalic acid **12a** in 87% yield was obtained (Table 2, entry 4). Successful incorporation of hydride ion using $NaBH_4$ at γ-position furnished all desired isoindoloisoquinolinone compounds successfully.

After accomplishing the target molecules, we synthesized their γ-hydroxy analogs by doing

workup using saturated sodium bicarbonate. The respective aryl/heteroaryl ethylamines **11a**, **11b**, **11c** were condensed with two phthalic acid derivatives. With simple phthalic acid **12a** four derivatives of γ-hydroxy isoindoloisoquinolinones **14a**, **14b**, **14c**, **14d** were prepared from their corresponding amines by just using a simple basic workup (Table 3, entries 1, 2, 3, 4). Novel analogs like **14e**, **14f**, and **14g** were prepared using 4-nitrophthalic acid **12b**. It was fused with homoveratryl amine **11a** to get **14e** in 91% yield (Table 3, entry 5). The reaction of 3-methoxyphenethyl amine **11b** went smoothly to form **14f** in 89% yield (Table 3, entry 6). Also, tryptamine-derived γ-hydroxy analog **14g** was synthesized, which gave a slightly higher yield than the former amines (Table 3, entry 7).

Table 3. Syntheses of γ-hydroxy isoindoloisoquinolinones

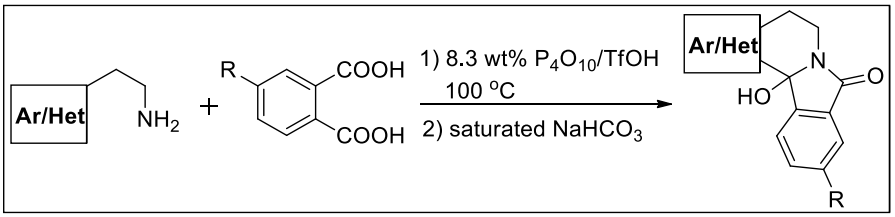

Entry	Phenethylamine	Dibasic acid	Product	Yield
1	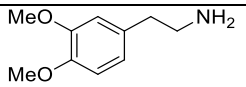 **11a**	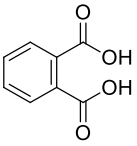 **12a**	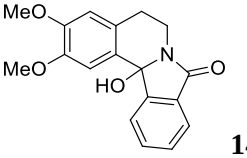 **14a**	87%
2	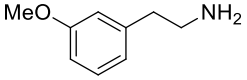 **11b**	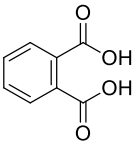 **12a**	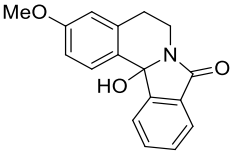 **14b**	86%
3	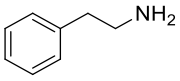 **11c**	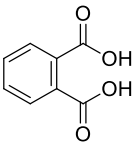 **12a**	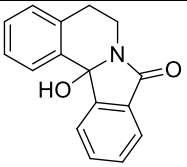 **14c**	83%
4	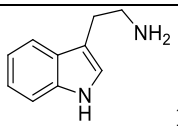 **11d**	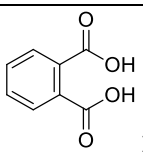 **12a**	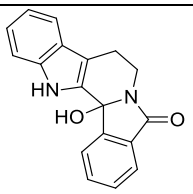 **14d**	88%

5	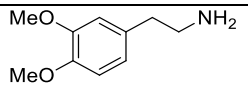 **11a**	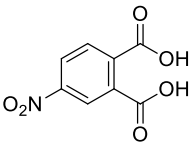 **12b**	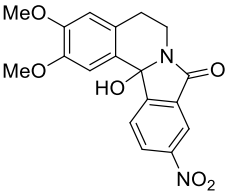 **14e**	91%
6	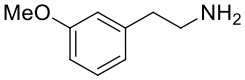 **11b**	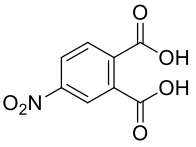 **12b**	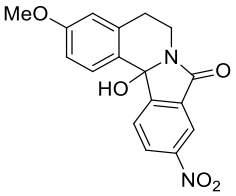 **14f**	89%
7	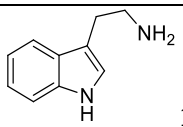 **11d**	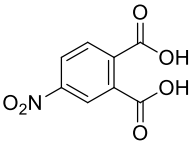 **12b**	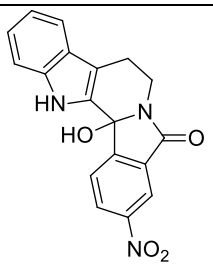 **14g**	92%

2.II.4 Conclusion:

An attempt was made to synthesize isoindolo-[1,2-*a*]isoquinoline compounds via C-C coupling strategy using molecular iodine as a reagent. Several one-pot reactions were also carried out to facile the reaction towards success.

A useful one-pot syntheses method of isoindolo-[1,2-*a*]isoquinoline compounds was developed using cheap, and readily available reactants and reagents. Various derivatives of isoindolo-[1,2-*a*]isoquinoline compounds were synthesized possessing different substituents on different rings in high yields.

2.II.5 Experimental:

2.II.5.1: 2-benzyl-1,2,3,4-tetrahydroisoquinoline (3):

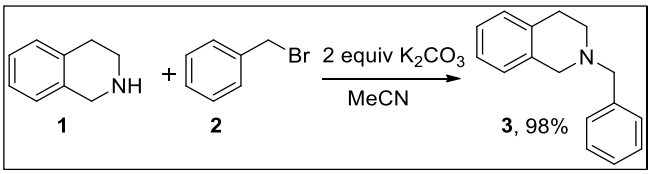

To a solution of 20 mmol of K_2CO_3 in 15 mL of acetonitrile, 10 mmol of 1,2,3,4-tetrahydroisoquinoline **1** was added. To this mixture, 10 mmol of benzyl bromide was added. The reaction mixture was then refluxed overnight. After the disappearance of both the starting materials on TLC, the reaction was filtered and the filtrate was concentrated under the reduced pressure. The resultant crude was purified over flash chromatography on silica gel (Pet. ether and ethyl acetate) as an eluent.

Pale yellow oil. IR (KBr) υ_{max}: 3021, 2903, 2797, 1905, 1655, 1601, 1472, 1361, 1283, 1133, 1084, 1011, 939, 866, 655 cm^{-1}. ^1H NMR (400 MHz, $CDCl_3$) δ = 2.65 (t, *J* = 5.6 Hz, 2H), 2.80 (t, *J* = 5.6 Hz, 2H), 3.54 (s, 3H), 3.59 (s, 3H), 6.87-6.89 (m, 1H), 6.99-7.03 (m, 3H), 7.18-7.20 (m, 1H), 7.22-7.26 (m, 2H), 7.20-7.32 (m, 2H) ppm. ^{13}C NMR (100 MHz, $CDCl_3$) δ = 29.2 (CH_2), 50.7 (CH_2), 56.2 (CH_2), 62.9 (CH_2), 125.7 (CH), 126.2 (CH), 126.7 (CH), 127.2 (CH), 128.4 (2XCH), 128.8 (CH), 129.2 (2XCH), 134.4 (Cq), 135.0 (Cq), 138.4 (Cq) ppm. Spectral data is in accordance with the literature.[31]

2.II.5.2: 2-benzyl-3,4-dihydroisoquinolin-1(2*H*)-one (6):

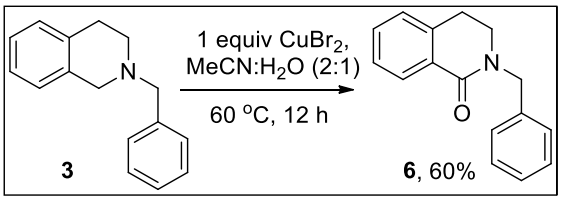

In a single neck round bottom flask equipped with refluxing condenser and the magnetic stirring bar was added 1 mmol of 2-benzyl-1,2,3,4-tetrahydroisoquinoline **3** in 5 mL acetonitrile-water mixture. 1 equiv $CuBr_2$ was added to the reaction mixture and heated at 60 °C for 12 hours. After the completion of the reaction, it was concentrated under reduced pressure. The crude mixture was diluted using 5 mL CH_2Cl_2 and to that 5 mL of H_2O was

added. The two layers were separated and the organic layer was dried over anhydrous Na_2SO_4 and evaporated over a rotary evaporator. The purification of the crude mixture over flash chromatography on silica gel using (Pet. ether and ethyl acetate) provided colorless oil in 60% yield.

Colourless oil. IR (KBr) υ_{max}: 3026, 2901, 1650, 1602 cm^{-1}. ^1H NMR (400 MHz, $CDCl_3$) δ = 2.87 (t, *J* = 6.8 Hz, 2H), 3.42 (t, *J* = 6.4 Hz, 2H), 4.74 (s, 2H), 7.08 & 7.09 (d, 1H), 7.19-7.24 (m, 1H), 7.24-7.26 (m, 4H), 7.29-7.37 (m, 2H), 8.09 (m, 1H) ppm. Spectral data is in accordance with the literature.[32]

2.II.5.3: 2,3-dimethoxy-5,6-dihydroisoindolo[1,2-*a*]isoquinolin-8(12b*H*)-one (13a):

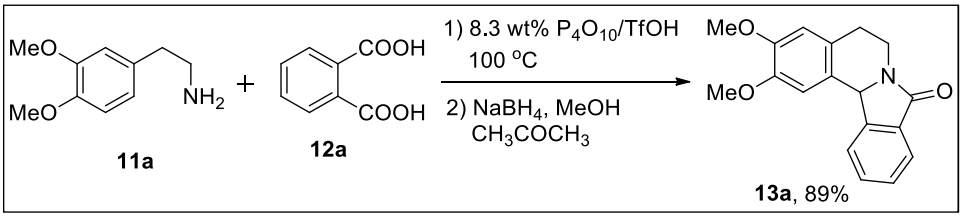

A solution was 8.3 wt% P_4O_{10}/TfOH was prepared by dissolving 0.415 g of P_4O_{10} in 4.585 mL of TfOH and the reaction was stirred for 30 minutes to get the clear solution. To that solution, 1 mmol of phthalic acid **12a** and 1.5 mmol of homoverarylamine **11a** were added and the reaction was heated at 100 °C for 2 hours. Then, the reaction was cooled to room temperature and 10 mL of methanol was added. To the stirred mixture, excess $NaBH_4$ was added till the reaction becomes colorless. After stirring for 30 minutes, acetone was added slowly to quench the excess of $NaBH_4$. The whole solution was evaporated over a rotary evaporator and CH_2Cl_2 was added. The white solid was filtered and the filtrate was dried over anhydrous Na_2SO_4 and concentrated under reduced pressure. The crude product was purified over flash chromatography on silica gel (Pet. ether and ethyl acetate) to get the compound **13a** as a colorless solid in 89% yield.

Colourless solid, m.p. 177-179 °C. IR (KBr) υ_{max}: 3348, 2992, 2923, 2892, 1681, 1608, 1497, 1372, 1162 cm^{-1}.^1H NMR (400 MHz, $CDCl_3$) δ = 2.73-2.79 (m, 1H), 2.94-3.02 (m, 1H), 3.36-3.43 (m, 1H), 3.84 (s, 3H), 3.93 (s, 3H), 4.46-4.51 (m, 1H), 5.59 (s, 1H), 6.66 (s, 1H), 7.12 (s, 1H), 7.47 (t, *J* = 6.8 Hz, 1H), 7.601 (t, *J* = 7.2 Hz, 1H), 7.82-7.87 (m, 2H) ppm. ^{13}C NMR (100 MHz, $CDCl_3$) δ = 29.0 (CH_2), 38.2 (CH_2), 55.9 (CH_3), 56.2 (CH_3), 59.0 (CH), 108.7 (CH), 112.0 (CH), 123.1 (CH), 123.9 (CH), 126.0 (Cq), 126.9 (Cq),

128.4 (CH), 131.6 (CH), 132.7 (Cq), 144.6 (Cq), 147.8 (Cq), 148.3 (Cq), 167.9 (Cq) ppm. Spectral data is in accordance with the literature.[33]

2.II.5.4: 3-methoxy-5,6-dihydroisoindolo[1,2-*a*]isoquinolin-8(12b*H*)-one (13b):

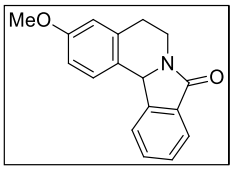

Following the similar protocol described in section 2.II.5.3 with 3-methoxyphenethylamine **11b** gave the product 3-methoxy-5,6-dihydroisoindolo[1,2-*a*]isoquinolin-8(12b*H*)-one **13b** in a 85% yield.

Pale yellow oil. IR (KBr) υ_{max}: 3349, 2923, 2891, 1656, 1609 1501, 1373, 1162 cm^{-1}. ^{1}H NMR (400 MHz, $CDCl_3$) δ = 2.78-2.85 (m, 1H), 2.95-3.04 (m, 1H), 3.40-3.47 (m, 1H), 3.75 (s, 3H), 4.37-4.42 (m, 1H), 5.56 (s, 1H), 6.70 (s, 1H), 6.80-6.82 (m, 1H), 7.43-7.51 (m, 2H), 7.57 (t, *J* = 7.2 Hz, 1H), 7.79-7.86 (m, 2H) ppm. ^{13}C NMR (100 MHz, $CDCl_3$) δ = 29.7 (CH_2), 38.1 (CH_2), 55.3 (CH_3), 58.8 (CH), 112.8 (CH), 114.0 (CH), 123.4 (CH), 123.8 (CH), 126.3 (CH), 126.5 (Cq), 128.4 (CH), 131.5 (CH), 132.7 (Cq), 136.1 (Cq), 144.6 (Cq), 158.7 (Cq), 167.9 (Cq) ppm.

2.II.5.4: 5,6-dihydroisoindolo[1,2-*a*]isoquinolin-8(12b*H*)-one (13c):

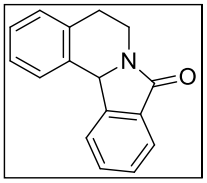

Following the similar protocol described in section 2.II.5.3 with phenethylamine **11c** gave the product 5,6-dihydroisoindolo[1,2-*a*]isoquinolin-8(12b*H*)-one **13c** in an 84% yield.

Colourless oil. IR (KBr) υ_{max}: 2923, 2891, 1685, 1597, 1499, 1371, 1163 cm^{-1}. ^{1}H NMR (400 MHz, $CDCl_3$) δ = 2.86-2.92 (m, 1H), 3.03-3.11 (m, 1H), 3.46-3.53 (m, 1H), 4.40-4.46 (m, 1H), 5.67 (s, 1H), 7.18-7.30 (m, 3H), 7.49 (t, *J* = 7.6 Hz, 1H), 7.49 (t, *J* = 9.2 Hz, 2H), 7.86-7.89 (m, 2H) ppm. ^{13}C NMR (100 MHz, $CDCl_3$) δ = 29.4 (CH_2), 38.2 (CH_2), 59.2 (CH), 123.5 (CH), 123.9 (CH), 125.2 (CH), 126.7 (CH), 127.5 (CH), 128.5 (CH), 129.3

(CH), 131.6 (CH), 132.8 (Cq), 134.3 (Cq), 134.8 (Cq), 144.2 (Cq), 168.0 (Cq) ppm.

2.II.5.5: 7,8,13,13b-tetrahydro-5*H*-benzo[1,2]indolizino[8,7-*b*]indol-5-one (13d):

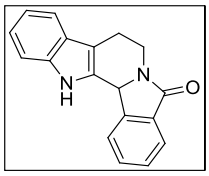

Following the similar protocol described in section 2.II.5.3 with tryptamine **11d** gave the product 3-methoxy-5,6-dihydroisoindolo[1,2-*a*]isoquinolin-8(12b*H*)-one **13b** in an 85% yield.

White solid, m.p. 259-262 °C. IR (KBr) υ_{max}: 1670, 1462, 1417, 1297, 725 cm^{-1}. ^{1}H NMR (400 MHz, $CDCl_3$) δ = 2.66-2.75 (m, 1H), 2.80-2.84 (m, 1H), 3.32-3.39 (m, 1H), 4.59-4.63 (q, 1H), 6.04 (s, 1H), 6.99 (t, *J* = 7.6 Hz, 1H), 7.16 (t, *J* = 8 Hz, 1H), 7.41 (d, *J* = 8.5 Hz, 2H), 7.54 (t, *J* = 7.4 Hz, 1H), 7.69-7.77 (m, 2H), 8.31 (d, *J* = 7.6 Hz, 1H), 11.37 (s, 1H) ppm. ^{13}C NMR (100 MHz, $CDCl_3$) δ = 21.9 (CH_2), 38.2 (CH_2), 57.1 (CH), 107.7 (Cq), 111.8 (CH), 118.6 (CH), 119.3 (CH), 122.0 (CH), 123.6 (CH), 124.3 (CH), 126.7 (Cq), 129.1 (Cq), 131.4 (CH), 132.2 (Cq), 132.3 (CH),137.0 (Cq), 144.1 (Cq), 167.6 (Cq) ppm.

2.II.5.6: 12b-hydroxy-2,3-dimethoxy-5,6-dihydroisoindolo[1,2-*a*]isoquinolin-8(12b*H*)-one (14a):

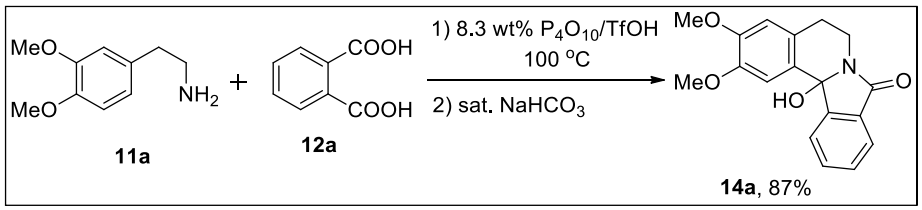

A solution was 8.3 wt% P_4O_{10}/TfOH was prepared by dissolving 0.415 g of P_4O_{10} in 4.585 mL of TfOH and stirred for 30 minutes to get the clear solution. To that solution, 1 mmol of phthalic acid **12a** and 1.5 mmol of homoverarylamine **11a** were added and the reaction was heated at 100 °C for 2 hours. Then, the reaction was cooled to room temperature and the reaction was diluted using CH_2Cl_2. Then, 15 mL saturated $NaHCO_3$ solution was added and stirred for 30 minutes. The two layers were separated and the organic layer was dried

over anhydrous Na_2SO_4 and concentrated under reduced pressure. The crude product was purified over flash chromatography on silica gel (Pet. ether and ethyl acetate) to get the compound **14a** as a colorless solid in an 87% yield.

Colorless solid, m.p. 157-160 °C. IR (KBr) υ_{max}: 3239, 2989, 2940, 2844, 1681, 1615, 1498, 1338, 1138, 958 cm^{-1}. ^1H NMR (400 MHz, DMSO-d_6) δ = 2.67-2.81 (m, 2H), 3.37-3.45 (m, 1H), 3.71 (s, 3H), 3.83 (s, 3H), 4.22-4.27 (m, 1H), 6.72 (s, 1H), 7.00 (s, 1H), 7.46 (s, 1H), 7.53 (t, *J* = 7.2 Hz, 1H), 7.66-7.71 (m, 2H), 8.21 (d, *J* = 8 Hz, 1H) ppm. ^{13}C NMR (100 MHz, DMSO-d_6) δ = 29.0 (CH_2), 34.9 (CH_2), 55.9 (CH_3), 56.3 (CH_3), 86.0 (Cq), 111.5 (CH), 112.1 (CH), 123.0 (CH), 124.3 (CH), 127.4 (Cq), 129.5 (Cq), 129.7 (CH), 130.7 (Cq), 133.0 (CH), 147.9 (Cq), 149.1 (Cq), 149.3 (Cq), 166.6 (Cq) ppm. Spectral data is in accordance with the literature.[34]

2.II.5.7: 12b-hydroxy-3-methoxy-5,6-dihydroisoindolo[1,2-*a*]isoquinolin-8(12b*H*)-one (14b):

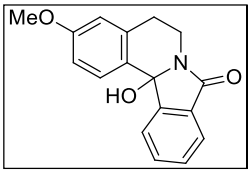

Following the similar protocol described in section 2.II.5.6 with 3-methoxyphenethylaime **11b** and **12a** gave the product 12b-hydroxy-3-methoxy-5,6-dihydroisoindolo[1,2-*a*]isoquinolin-8(12b*H*)-one **14b** upon workup with saturated $NaHCO_3$ in a 86% yield.

Colourless solid, m.p. 165-168 °C. IR (KBr) υ_{max}: 3249, 2991, 2931, 2829, 1689, 1619, 1499, 1329, 1127, 959 cm^{-1}. ^1H NMR (400 MHz, DMSO-d_6) δ = 2.80-2.83 (m, 2H), 3.40-3.48 (m, 1H), 3.71 (s, 3H), 4.20-4.25 (m, 1H), 6.73 (s, 1H), 6.85-6.88 (m, 1H), 6.97 (s, 1H), 7.52 (t, *J* = 7.2 Hz, 1H), 7.66 (d, *J* = 7.2 Hz, 2H), 7.91 (d, *J* = 8 Hz, 1H), 8.13 (d, *J* = 7.2 Hz, 1H) ppm. ^{13}C NMR (100 MHz, DMSO-d_6) δ = 29.6 (CH_2), 34.7 (CH_2), 55.6 (CH), 86.0 (Cq), 113.4 (CH), 113.6 (CH), 122.9 (CH), 124.3 (CH), 129.7 (CH), 129.8 (CH), 130.1 (Cq), 130.7 (Cq), 132.9 (CH), 136.5 (Cq), 149.2 (Cq), 159.0 (Cq), 166.5 (Cq) ppm.

2.II.5.8: 12b-hydroxy-5,6-dihydroisoindolo[1,2-*a*]isoquinolin-8(12b*H*)-one (14c):

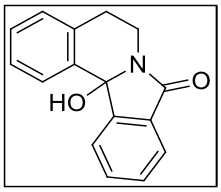

Following the similar protocol described in section 2.II.5.6 with phenethylamine **11c** and **12a** gave the product 12b-hydroxy-5,6-dihydroisoindolo[1,2-*a*]isoquinolin-8(12b*H*)-one **14c** in an 83% yield.

White solid, m.p. 139-141 °C. IR (KBr) υ_{max}: 3238, 2998, 2926, 2840, 1689, 1617, 1499, 1339, 1139, 968 cm^{-1}. ^{1}H NMR (400 MHz, DMSO-d_6) δ = 2.83-2.86 (m, 2H), 3.47 (bs, 1H), 4.20-4.25 (m, 1H), 7.07 (s, 1H), 7.17-7.19 (m, 1H), 7.23-7.31 (m, 2H), 7.54 (t, *J* = 7.4 Hz, 1H), 7.66-7.71 (m, 2H), 8.00 (d, *J* = 7.4 Hz, 1H), 8.17 (d, *J* = 7.6 Hz, 1H) ppm. ^{13}C NMR (100 MHz, DMSO-d_6) δ = 29.2 (CH_2), 34.8 (CH_2), 86.1 (Cq), 123.0 (CH), 124.4 (CH), 126.9 (CH), 128.4 (CH), 128.5 (CH), 129.5 (CH), 129.8 (CH), 130.9 (Cq), 132.9 (CH), 134.8 (Cq), 137.8 (Cq), 148.9 (Cq), 166.5 (Cq) ppm.

2.II.5.9: 13b-hydroxy-7,8,13,13b-tetrahydro-5*H*-benzo[1,2]indolizino[8,7-*b*]indol-5-one (14d):

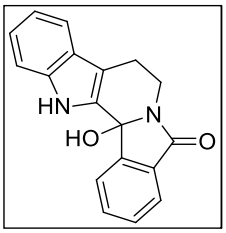

Following the similar protocol described in section 2.II.5.6 with tryptamine **11d** and **12a** gave the product 13b-hydroxy-7,8,13,13b-tetrahydro-5*H*-benzo[1,2]indolizino[8,7-*b*]indol-5-one **14d** in a 88% yield.

Colourless solid, m.p. 158-162 °C. IR (KBr) υ_{max}: 3246, 3002, 2939, 2842, 1689, 1604, 1498, 1330, 1139, 973 cm^{-1}. ^{1}H NMR (400 MHz, DMSO-d_6) δ = 2.66-2.74 (m, 1H), 2.80-2.84 (m, 1H), 4.40-4.45 (m, 1H), 7.00 (t, *J* = 7.6 Hz, 1H), 7.13 (t, *J* = 7.6 Hz, 1H), 7.32 (bs, 1H), 7.38 (d, *J* = 8.4 Hz, 1H), 7.44 (d, *J* = 8 Hz, 1H), 7.56 (t, *J* = 7.2 Hz, 1H), 7.69-7.75

(m, 2H), 8.32 (d, *J* = 7.6 Hz, 1H), 11.53 (s, 1H) ppm. ^{13}C NMR (100 MHz, DMSO-d_6) δ = 21.9 (CH_2), 35.4 (CH_2), 84.5 (Cq), 109.3 (Cq), 112.0 (CH), 119.3 (CH), 119.4 (CH), 122.7 (CH), 123.2 (CH), 124.1 (CH), 125.9 (Cq), 130.0 (CH), 130.7 (Cq), 132.9 (CH), 133.4 (Cq), 136.8 (Cq), 147.4 (Cq), 166.9 (Cq) ppm.

2.II.5.10: 12b-hydroxy-2,3-dimethoxy-10-nitro-5,6-dihydroisoindolo[1,2-*a*]isoquinolin-8(12b*H*)-one (14e):

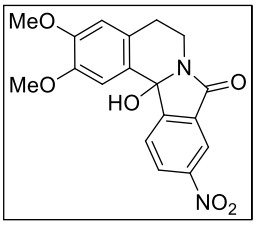

Following the similar protocol described in section 2.II.5.6 with homoveratrylamine **11a** and **12b** gave the product 12b-hydroxy-2,3-dimethoxy-10-nitro-5,6-dihydroisoindolo[1,2-*a*]isoquinolin-8(12b*H*)-one **14e** in a 91% yield.

Yellow solid, m.p. 165-168 °C. IR (KBr) υ_{max}: 3348, 2993, 2931, 2808, 1676, 1609, 1554, 1494, 1329, 1133 cm^{-1}. ^{1}H NMR (400 MHz, DMSO-d_6) δ = 2.74-2.86 (m, 2H), 3.45-3.50 (m, 1H), 3.73 (s, 3H), 3.85 (s, 3H), 4.26-4.30 (m, 1H), 6.77 (s, 1H), 7.35 (s, 1H), 7.46 & 7.52 (2Xs, 1H), 8.32-8.38 (m, 1H), 8.49-8.57 (m, 1H) ppm. ^{13}C NMR (100 MHz, DMSO-d_6) δ = 28.9 (CH_2), 35.2 (CH_2), 56.0 (CH_3), 56.4 (CH_3), 86.1 (Cq), 111.4 (CH), 112.3 (CH), 118.0 (CH), 126.1 (CH), 127.7 (Cq), 128.0 (CH), 132.1 (Cq), 135.8 (Cq), 148.1 (Cq), 150.1 (Cq), 151.0 (Cq), 154.5 (Cq), 164.3 (Cq) ppm. HRMS (m/z): calculated for $C_{18}H_{16}N_2O_6Na$ $[M+Na]^+$: 379.0906; found 379.0903.

2.II.5.11: 12b-hydroxy-3-methoxy-10-nitro-5,6-dihydroisoindolo[1,2-*a*]isoquinolin-8(12b*H*)-one (14f):

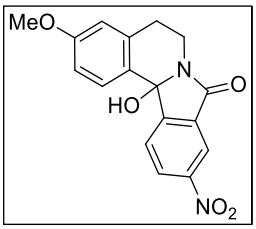

Following the similar protocol described in section 2.II.5.6 with 3-methoxyphenethylamine **11b** and **12b** gave the product 12b-hydroxy-3-methoxy-10-nitro-5,6-dihydroisoindolo[1,2-*a*]isoquinolin-8(12b*H*)-one **14f** in a 89% yield.

Pale yellow solid, m.p. 154-156 °C. IR (KBr) υ_{max}: 3345, 2981, 2926, 2818, 1664, 1602, 1545, 1488, 1339, 1137 cm^{-1}. ^{1}H NMR (400 MHz, DMSO-d_6) δ = 2.85-2.88 (m, 2H), 3.48-3.53 (m, 1H), 3.74 (s, 3H), 4.23-4.28 (m, 1H), 6.77 (s, 1H), 6.90-6.93 (m, 1H), 7.32 (s, 1H), 7.92-8.01 (m, 2H), 8.36-8.39 (m, 1H), 8.87 (s, 1H). ^{13}C NMR (100 MHz, DMSO-d_6) δ = 29.6 (CH_2), 35.1 (CH_2), 55.6 (CH_3), 85.9 (Cq), 113.7 (CH), 113.9 (CH), 119.3 (CH), 124.6 (CH), 125.6 (CH), 128.8 (Cq), 129.8 (CH), 135.7 (Cq), 136.6 (Cq), 150.1 (Cq), 150.9 (Cq), 159.3 (Cq), 164.2 (Cq) ppm. HRMS (m/z): calculated for $C_{17}H_{14}N_2O_5Na$ $[M+Na]^+$: 349.0800; found 349.0873.

2.II.5.12: 13b-hydroxy-3-nitro-7,8,13,13b-tetrahydro-5*H*-benzo[1,2]indolizino[8,7-*b*]indol-5-one (14g):

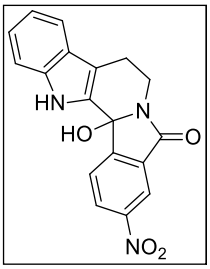

Following the similar protocol described in section 2.II.5.6 with tryptamine **11c** and **12b** gave the product 13b-hydroxy-3-nitro-7,8,13,13b-tetrahydro-5*H*-benzo[1,2]indolizino[8,7-*b*]indol-5-one **14g** in a 92% yield.

Colourless solid, m.p. 176-179 °C. IR (KBr) υ_{max}: 3345, 2992, 2927, 2818, 1664, 1603, 1543, 1488, 1335, 1132 cm^{-1}. ^{1}H NMR (400 MHz, DMSO-d_6) δ = 2.72-2.80 (m, 1H), 2.85-2.90 (m, 1H), 3.54-3.58 (m, 1H), 4.46-4.50 (m, 1H), 7.02 (t, *J* = 7.6 Hz, 1H), 7.16 (t, *J* = 7.6 Hz, 1H), 7.40 (d, *J* = 8.4 Hz, 1H), 7.46 (d, *J* = 8 Hz, 1H), 7.69 & 7.68 (2Xs, 1H), 8.38-8.43 (m, 1H), 8.62 (s, 1H), 11.68 (s, 1H) ppm. ^{13}C NMR (100 MHz, DMSO-d_6) δ = 21.9 (CH_2), 35.7 (CH_2), 84.5 (Cq), 110.2 (Cq), 112.0 (CH), 118.3 (CH), 119.4 (CH), 119.6 (CH), 123.0 (CH), 125.6 (CH), 125.9 (Cq), 128.2 (CH), 131.9 (Cq), 132.1 (Cq), 137.0 (Cq), 149.3 (Cq), 152.6 (Cq), 164.7 (Cq) ppm. HRMS (m/z): calculated for $C_{18}H_{13}N_3O_4H$ $[M+H]^+$: 336.0984; found 336.0985.

2.II.6 References:

1) Valencia, E.; Freyer, A. J.; Shamma, M.; Fajardo, V. *Tetrahedron Lett.* **1984**, *25*, 599.

2) Chopra, R. N.; Chopra, I. C.; Handa, K. L.; Kapoor, L. D. "Indigenous Drugs of India," U.N. Dhar and Sons, Calcutta, **1958**, *501*.

3) Logesh, R.; Das, N.; Adhikari, D. A.; Devkota, H. P. *Medicine* **2020**, *7*, 1069.

4) Suyavaran, A.; Ramamurthy, C.; Mareeswaran, R.; Shanthi, Y. V.; Selvakumar, J.; Mangalaraj, S.; Kumar, M. S.; Ramanathan, C. R.; Thirunavukkarasu, C. *Bioorg. Med. Chem.* **2015**, *23*, 488.

5) (a) Zhuang, Z.; Kung, M.; Mu, M.; Kung, H. F. *J. Med. Chem.* **1998**, *41*, 157. (b) Norman, M. H.; Minick, D. J.; Rigdon, G. C. *J. Med. Chem.* **1996**, *39*, 149.

6) Ferland, J. M.; Demerson, C. A.; Humber, L. G. *Can. J. Chem.* **1985**, *63*, 361.

7) Lippmann, W. U.S. Patent 4, 267, 1891981; *Chem. Abstr.* **1981**, *95*, 61988m.

8) Ishihara, Y.; Kiyota, Y.; Goto, G. *Chem. Pharm. Bull.* **1990**, *38*, 3024.

9) Lübbers, T.; Angehrn, P.; Gmünder, H.; Herzig, S. *Bioorg. Med. Chem. Lett* **2007**, *17*, 4708.

10) Sui, Z.; Altom, J.; Nguyen, V. N.; Fernandez, J.; Bernstein, J. I.; Hiliard, J. J.; Barrett, J. F.; Podlogar, B. L.; Ohemeng, K. A. *Bioorg. Med. Chem. 6*, 735.

11) Fleury, J. F.; Netchitaïlo, P.; Daïch, A. *Synlett* **2011**, *13*, 1821.

12) Selvakumar, J.; Ramanathan, C. R. *Org. Biomol. Chem.* **2011**, *9*, 7643.

13) Wakchaure, P. B.; Kunte, S. S.; Argade, N. P. *Indian J. Chem. - Sect. B Org. Med. Chem.* **2011**, *50*, 868.

14) Aranzamendi, E.; Sotomayor, N.; Lete, E. *J. Org. Chem.* **2012**, *77*, 2986.

15) Xu, K.; Zhang, S.; Hu, Y.; Zha, Z.; Wang, Z. *Chem. - A Eur. J.* **2013**, *19*, 3573.

16) Min, J. Y.; Kim, G. *J. Org. Chem.* **2014**, *79*, 1444.

17) Hamon, M.; Dickinson, N.; Devineau, A.; Bolien, D.; Tranchant, M. J.; Taillier, C.; Jabin, I.; Harrowven, D. C.; Whitby, R. J.; Ganesan, A.; Dalla, V. *J. Org. Chem.* **2014**, *79*, 1900.

18) Maity, A. K.; Roy, S. *Adv. Synth. Catal.* **2014**, *356*, 2627.

19) Pandey, V. K.; Anbarasan, P. *J. Org. Chem.* **2014**, *3*, 9.

20) Seo, S. Y.; Kim, G. *Tetrahedron Lett.* **2015**, *56*, 3835.

21) Rao, H. S. P.; Rao, A. V. B. *J. Org. Chem.* **2015**, *80*, 1506.

22) Mangalaraj, S.; Selvakumar, J.; Ramanathan, C. R. *J. Chem. Sci*. **2015**, *2015*, 811.

23) Selvakumar, J.; Rao, R. S.; Srinivasapriyan, V.; Marutheeswaran, S.; Ramanathan, C. R. *Eur. J. Org. Chem.* **2015**, *2015*, 2175.

24) Singh, K. N.; Singh, P.; Kaur, M.; Sharma, E. *ChemistrySelect* **2017**, *2*, 2213.

25) Varga, V.; Milen, M.; Ábrányi-Balogh, P. *Tetrahedron Lett.* **2018**, *59*, 3683.

26) Qiao, J.; Jia, X.; Li, P.; Liu, X.; Zhao, J.; Zhou, Y.; Wang, J.; Liu, H.; Zhao, F. *Adv. Synth. Catal.* **2019**, *361*, 1419.

27) Zhang, S.; Shi, X.; Li, J.; Hou, Z.; Song, Z.; Su, X.; Peng, D.; Wang, F.; Yu, Y.; Zhao, G. *ACS Omega* **2019**, *4*, 19420.

28) Kurva, M.; Dolé Kerim, M.; Gàmez-Montaño, R.; El Kaim, L. *Org. Biomol. Chem.* **2019**, *17*, 9655.

29) Huang, Z.; Meng, Y.; Wu, Y.; Song, C.; Chang, J. *Tetrahedron* **2021**, *93*, 132280.

30) (a) Parvatkar, P. T.; Parameswaran, P. S.; Tilve, S. G. *Chem. Eur. J.* **2012**, *18*, 5460. (b) Parvatkar, P. T.; Parameswaran, P. S.; Tilve, S. G. *J. Org. Chem.* **2009**, *74*, 8369. (c) Volvoikar, P. S.; Tilve, S. G. *Org. Lett.* **2016**, *18*, 892. (d) Naik, M. M.; Kamat, D.P.; Tilve, S. G.; Kamat, V.P. *Tetrahedron* **2014**, *70*, 5221. (e) Parvatkar, P. T.; Ajay, A. K.; Bhat, M. K.; Parameswaran, P. S.; Tilve, S. G. *Med.*

Chem. Res. **2013**, *22*, 88. (f) Mandrekar, K. S.; Tilve, S. G. *New J. Chem.* **2021**, *45*, 4152.

31) Alshammari, A. S.; Natte, K.; Kalevaru, N. V.; Bagabas, A.; Jagadeesh, R. V. *J. Catal.* **2020**, 382, 141.

32) Kurouchi, H.; Ohwada, T. *J. Org. Chem.* **2020**, *85*, 876.

33) Saidov, A. S.; Levkovich, M. G.; Alimova, M.; Vinogradova, V. I. *Chem. Nat. Comp.* **2014**, *49*, 1099.

34) Suyavaran, A.; Ramamurthy, C.; Mareeswaran, R.; Shanthi, Y. V.; Selvakumar, J.; Mangalaraj, S.; Kumar, M. S.; Ramanathan, C. R.; Thirunavukkarasu, C. *Bioorg. Med. Chem.* **2015**, *23*, 488.

NMR Spectra

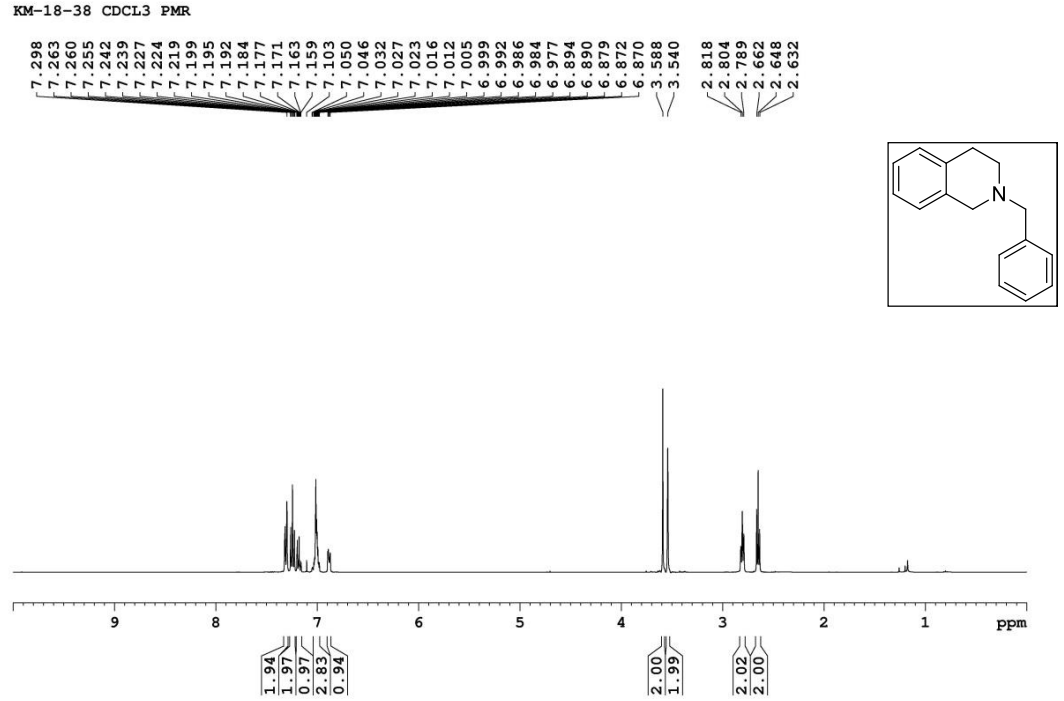
KM-18-38 CDCL3 PMR
7.298
7.263
7.260
7.255
7.242
7.239
7.227
7.224
7.219
7.199
7.195
7.192
7.184
7.177
7.171
7.163
7.159
7.103
7.050
7.046
7.032
7.027
7.023
7.016
7.012
7.005
6.999
6.992
6.986
6.984
6.977
6.894
6.890
6.879
6.872
6.870
3.588
3.540
2.818
2.804
2.789
2.662
2.648
2.632
N
9
8
7
6
5
4
3
2
1
ppm
1.94
1.97
0.97
2.83
0.94
2.00
1.99
2.02
2.00

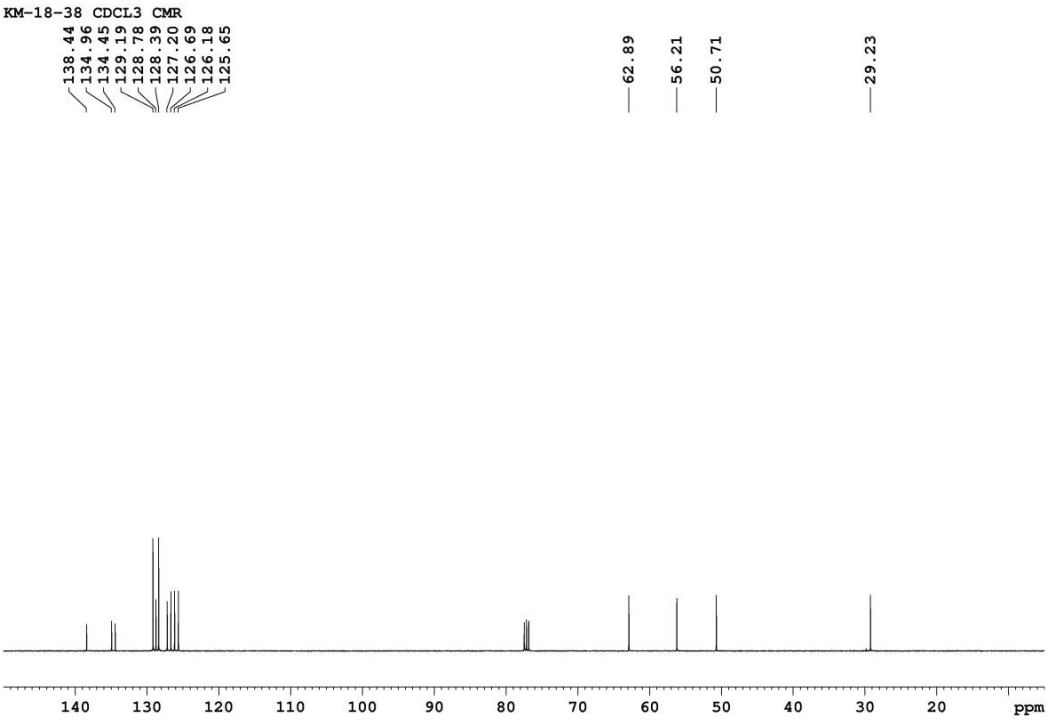
KM-18-38 CDCL3 CMR
138.44
134.96
134.45
129.19
128.78
128.39
127.20
126.69
126.18
125.65
62.89
56.21
50.71
29.23
140
130
120
110
100
90
80
70
60
50
40
30
20
ppm

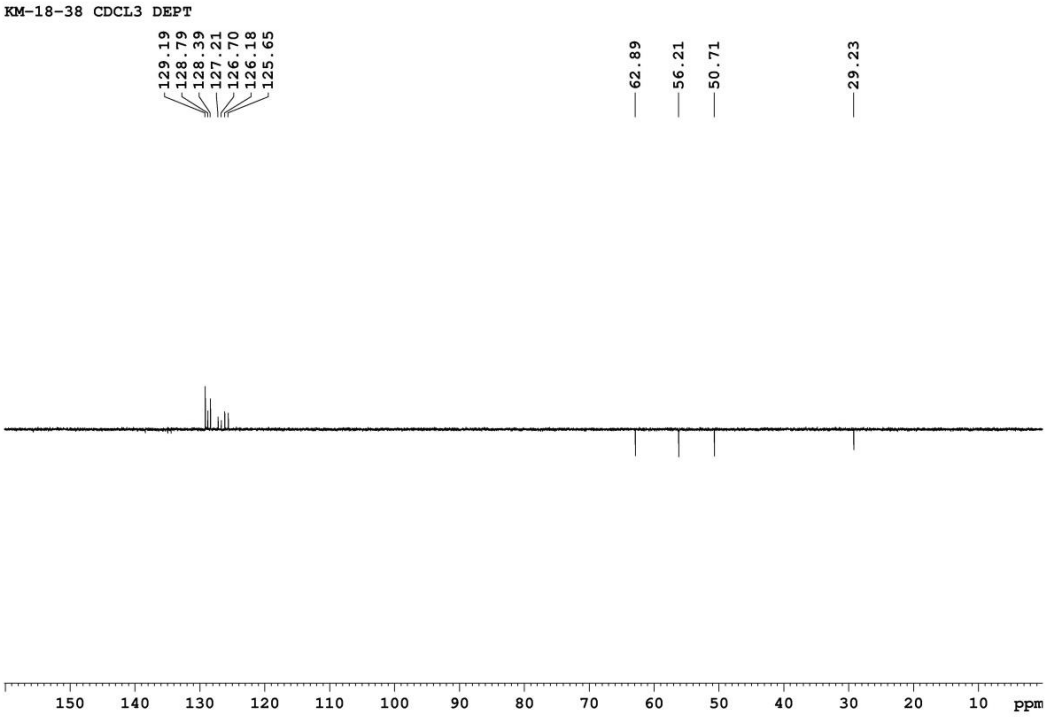
KM-18-38 CDCL3 DEPT
129.19
128.79
128.39
127.21
126.70
126.18
125.65
62.89
56.21
50.71
29.23
150 140 130 120 110 100 90 80 70 60 50 40 30 20 10 ppm

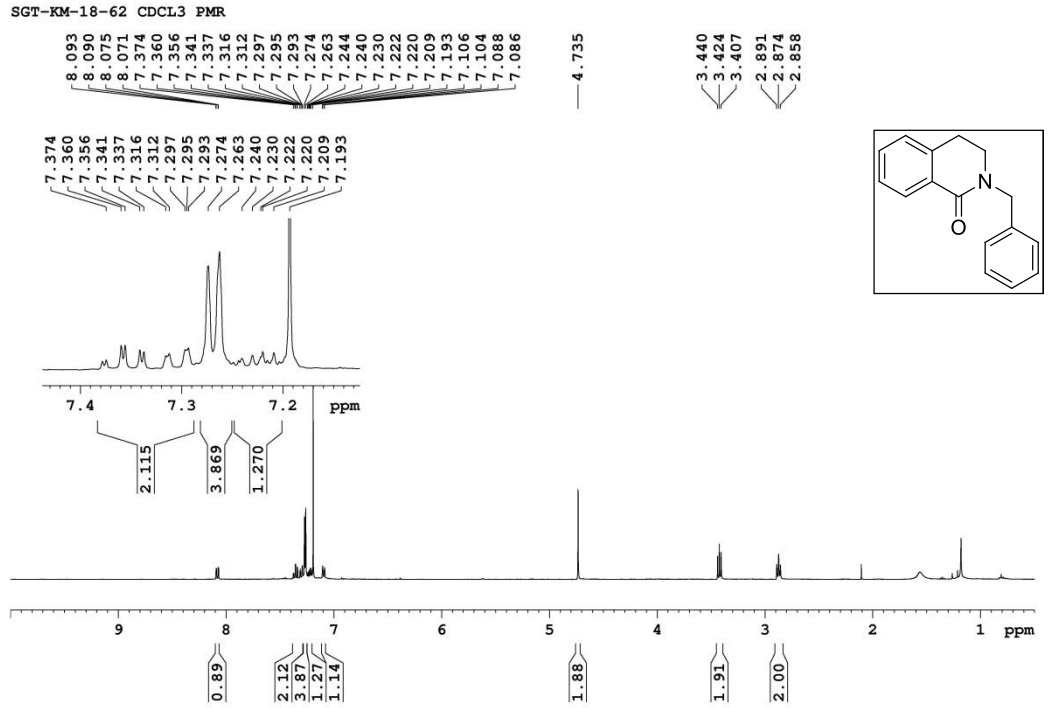
SGT-KM-18-62 CDCL3 PMR
8.093
8.090
8.075
8.071
7.374
7.360
7.356
7.341
7.337
7.316
7.312
7.297
7.295
7.293
7.274
7.263
7.244
7.240
7.230
7.222
7.220
7.209
7.193
7.106
7.104
7.088
7.086
4.735
3.440
3.424
3.407
2.891
2.874
2.858
7.4 7.3 7.2 ppm
2.115
3.869
1.270
9 8 7 6 5 4 3 2 1 ppm
0.89
2.12
3.87
1.27
1.14
1.88
1.91
2.00
N
O

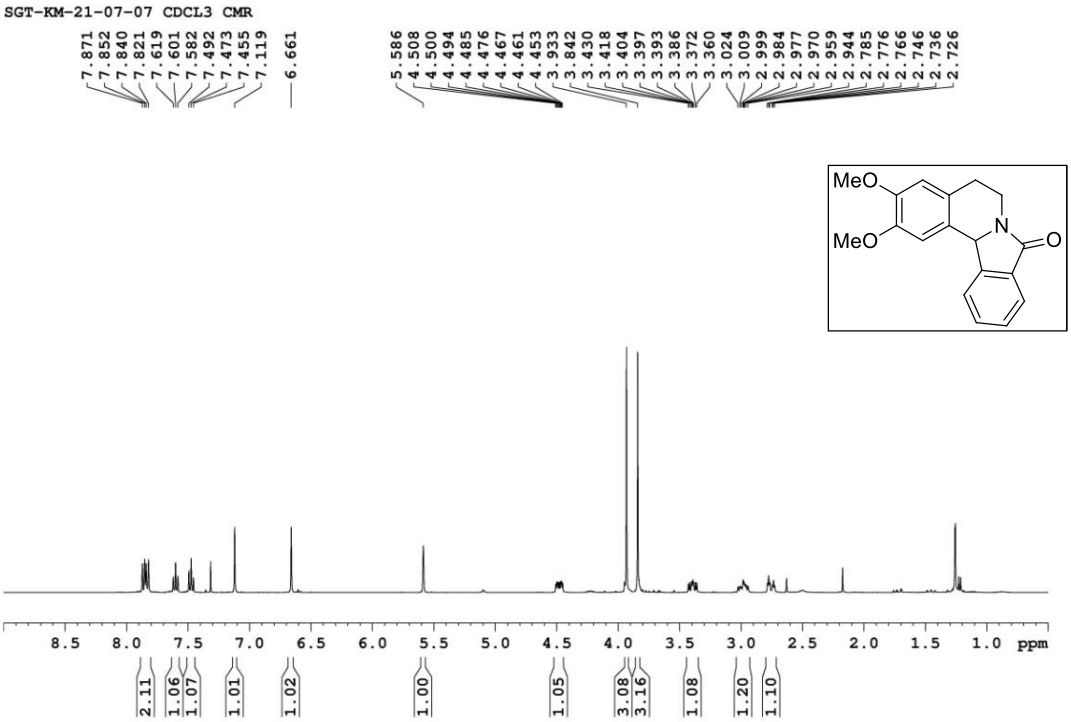
SGT-KM-21-07-07 CDCL3 CMR
7.871
7.852
7.840
7.821
7.619
7.601
7.582
7.492
7.473
7.455
7.119
6.661
5.586
4.508
4.500
4.494
4.485
4.476
4.467
4.461
4.453
3.933
3.842
3.430
3.418
3.404
3.397
3.393
3.386
3.372
3.360
3.024
3.009
2.999
2.984
2.977
2.970
2.959
2.944
2.785
2.776
2.766
2.746
2.736
2.726
MeO
MeO
N
O
8.5 8.0 7.5 7.0 6.5 6.0 5.5 5.0 4.5 4.0 3.5 3.0 2.5 2.0 1.5 1.0 ppm
2.11
1.06
1.07
1.01
1.02
1.00
1.05
3.08
3.16
1.08
1.20
1.10

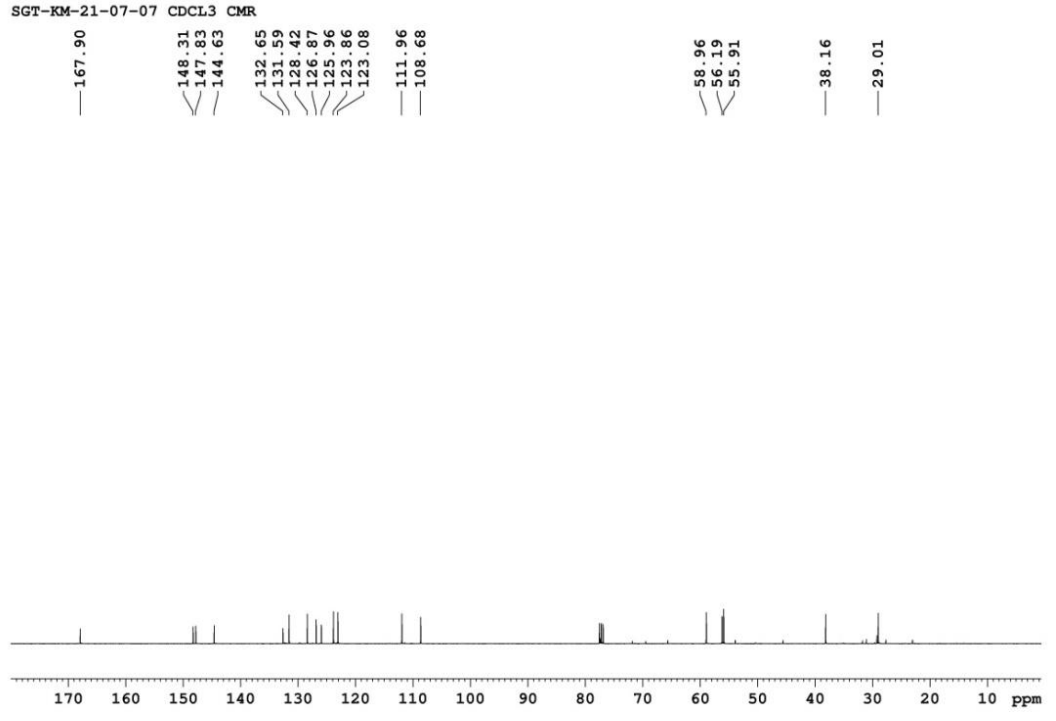
SGT-KM-21-07-07 CDCL3 CMR
167.90
148.31
147.83
144.63
132.65
131.59
128.42
126.87
125.96
123.86
123.08
111.96
108.68
58.96
56.19
55.91
38.16
29.01
170 160 150 140 130 120 110 100 90 80 70 60 50 40 30 20 10 ppm

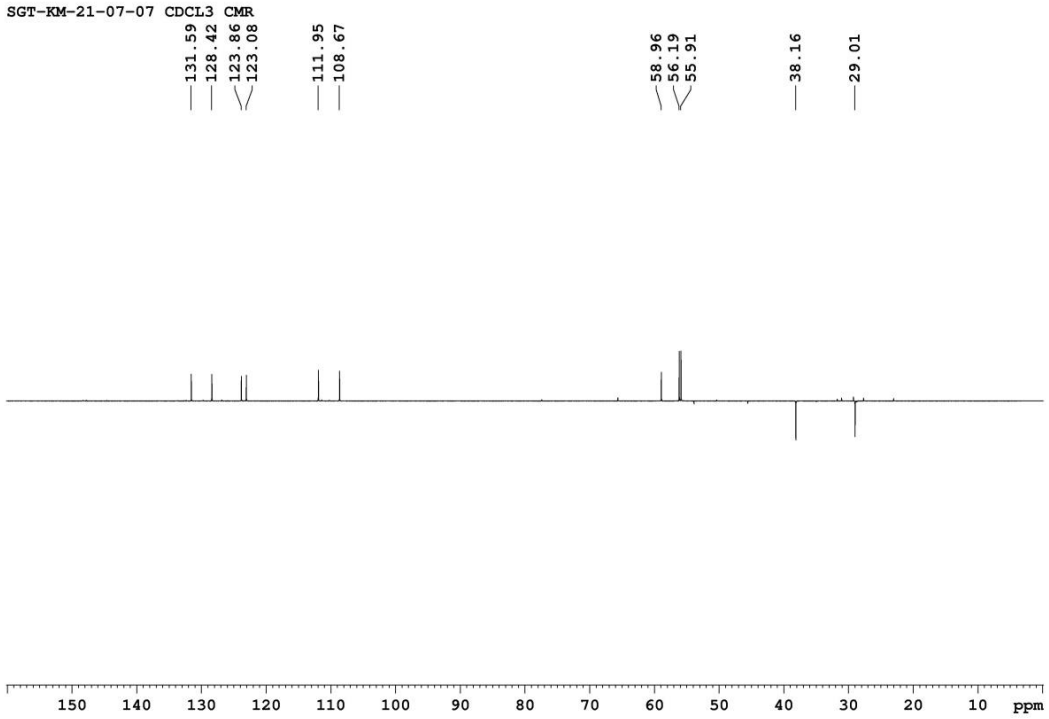
SGT-KM-21-07-07 CDCL3 CMR
131.59
128.42
123.86
123.08
111.95
108.67
58.96
56.19
55.91
38.16
29.01
150 140 130 120 110 100 90 80 70 60 50 40 30 20 10 ppm

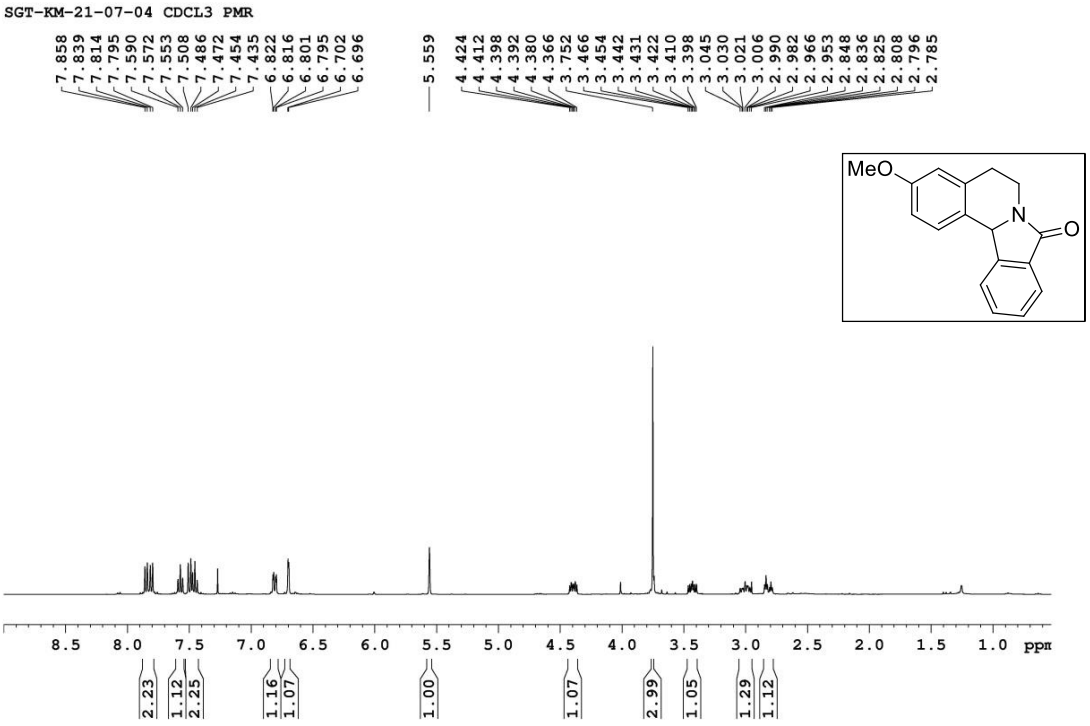
SGT-KM-21-07-04 CDCL3 PMR
7.858
7.839
7.814
7.795
7.590
7.572
7.553
7.508
7.486
7.472
7.454
7.435
6.822
6.816
6.801
6.795
6.702
6.696
5.559
4.424
4.412
4.398
4.392
4.380
4.366
3.752
3.466
3.454
3.442
3.431
3.422
3.410
3.398
3.045
3.030
3.021
3.006
2.990
2.982
2.966
2.953
2.848
2.836
2.825
2.808
2.796
2.785
MeO
N
O
8.5 8.0 7.5 7.0 6.5 6.0 5.5 5.0 4.5 4.0 3.5 3.0 2.5 2.0 1.5 1.0 ppm
2.23
1.12
2.25
1.16
1.07
1.00
1.07
2.99
1.05
1.29
1.12

SGT-KM-21-07-04-A CDCL3 CMR

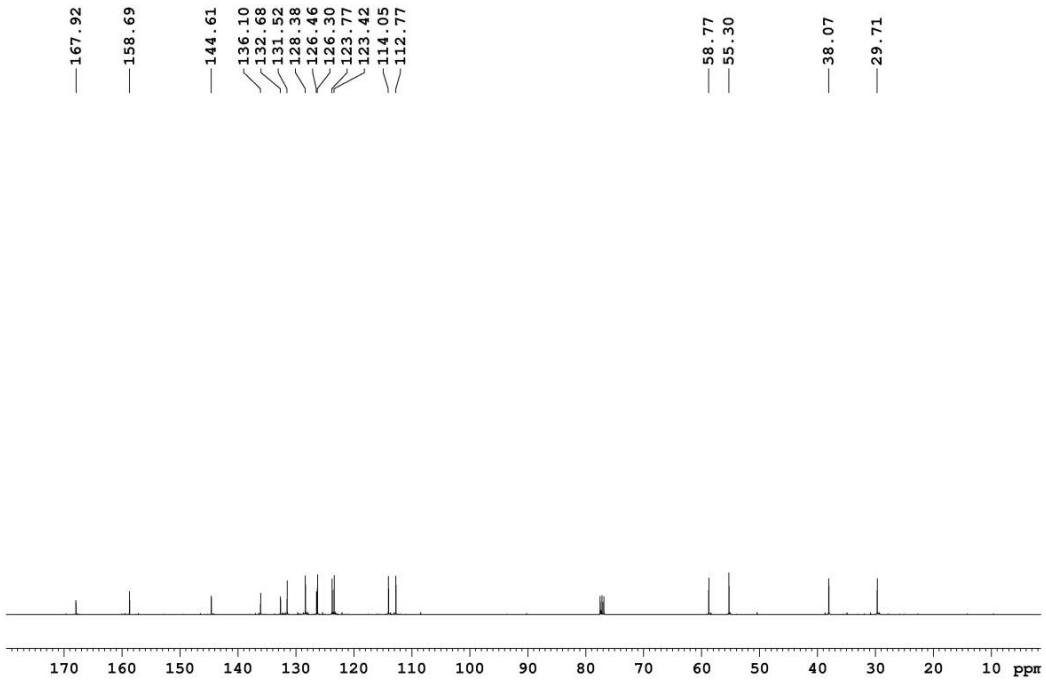

SGT-KM-21-07-04-A CDCL3 DEPT

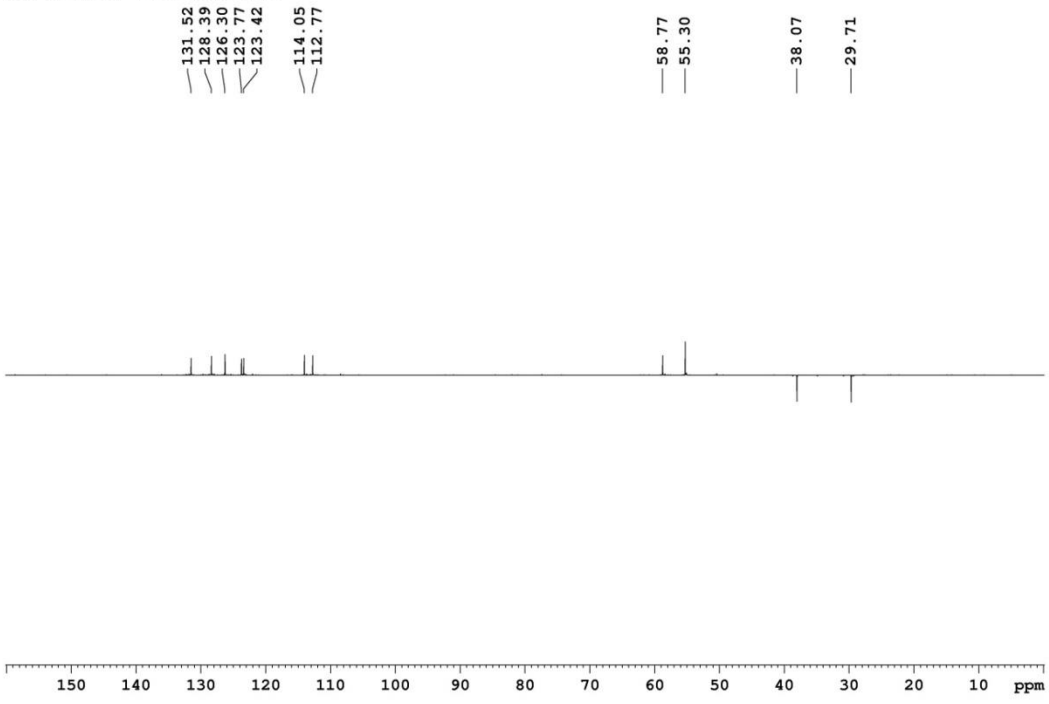

SGT-KM-21-07-02 CDCL3 PMR

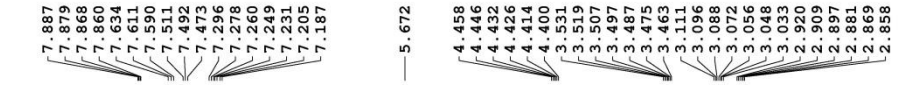

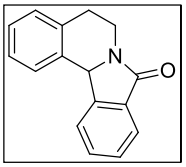

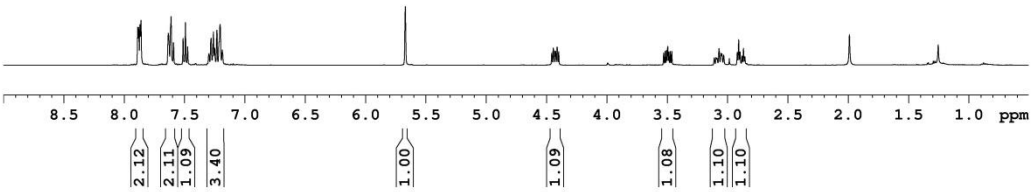

SGT-KM-21-07-02 CDCL3 CMR

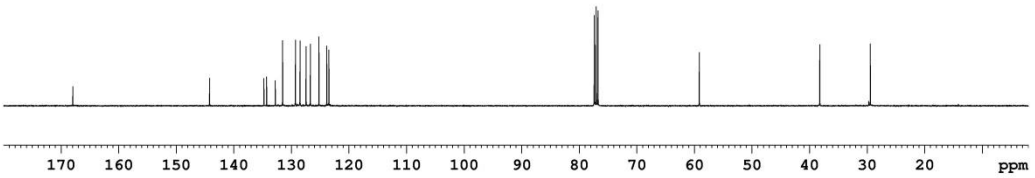

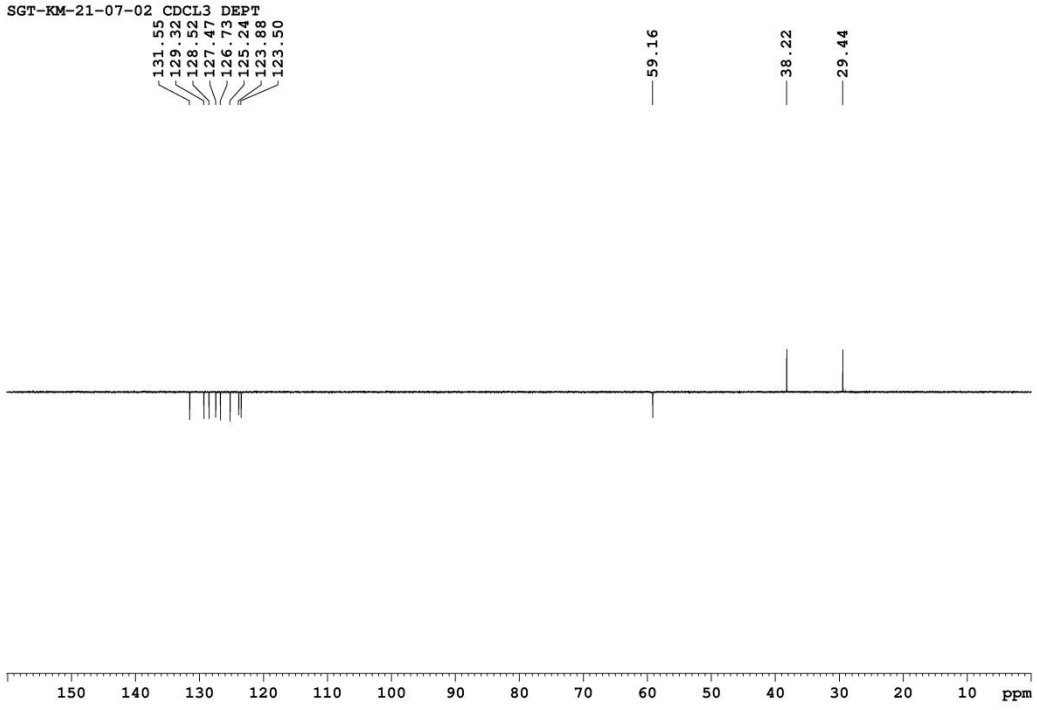
SGT-KM-21-07-02 CDCL3 DEPT
131.55
129.32
128.52
127.47
126.73
125.24
123.88
123.50
59.16
38.22
29.44
150 140 130 120 110 100 90 80 70 60 50 40 30 20 10 ppm

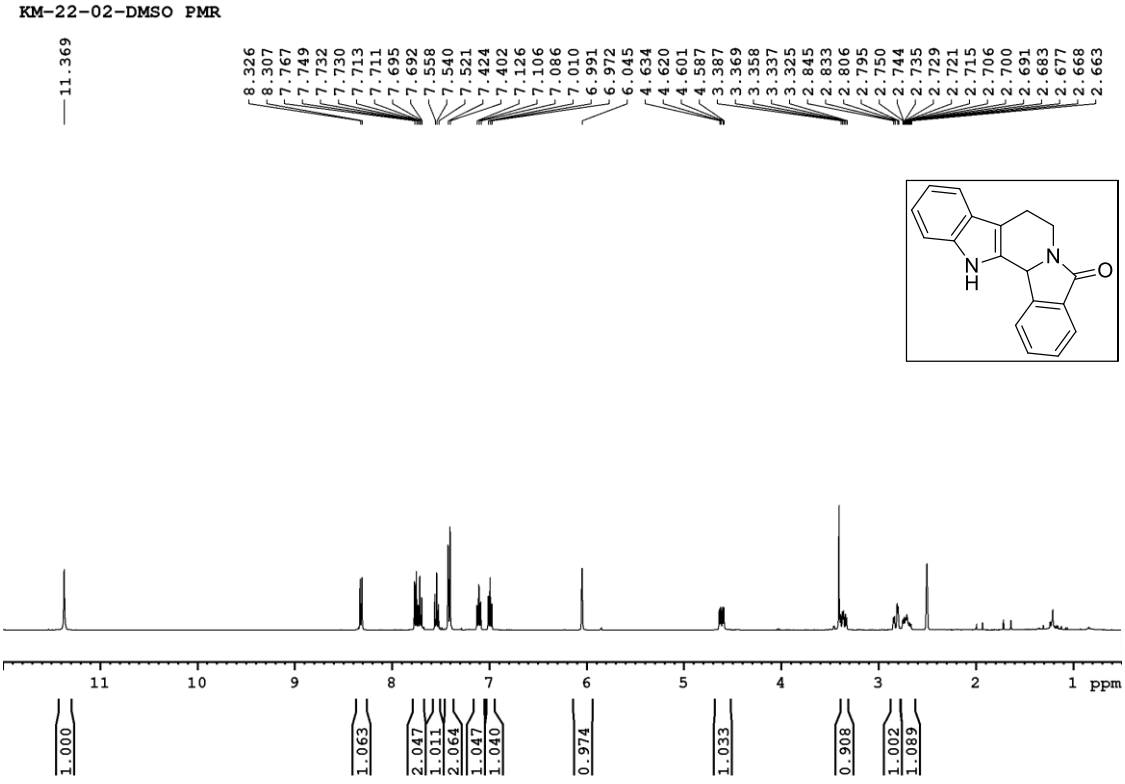
KM-22-02-DMSO PMR
11.369
8.326
8.307
7.767
7.749
7.732
7.730
7.713
7.711
7.695
7.692
7.558
7.540
7.521
7.424
7.402
7.126
7.106
7.086
7.010
6.991
6.972
6.045
4.634
4.620
4.601
4.587
3.387
3.369
3.358
3.337
3.325
2.845
2.833
2.806
2.795
2.750
2.744
2.735
2.729
2.721
2.715
2.706
2.700
2.691
2.683
2.677
2.668
2.663
N
H
N
O
11 10 9 8 7 6 5 4 3 2 1 ppm
1.000
1.063
2.047
1.011
2.064
1.047
1.040
0.974
1.033
0.908
1.002
1.089

KM-22-02 DMSO CMR

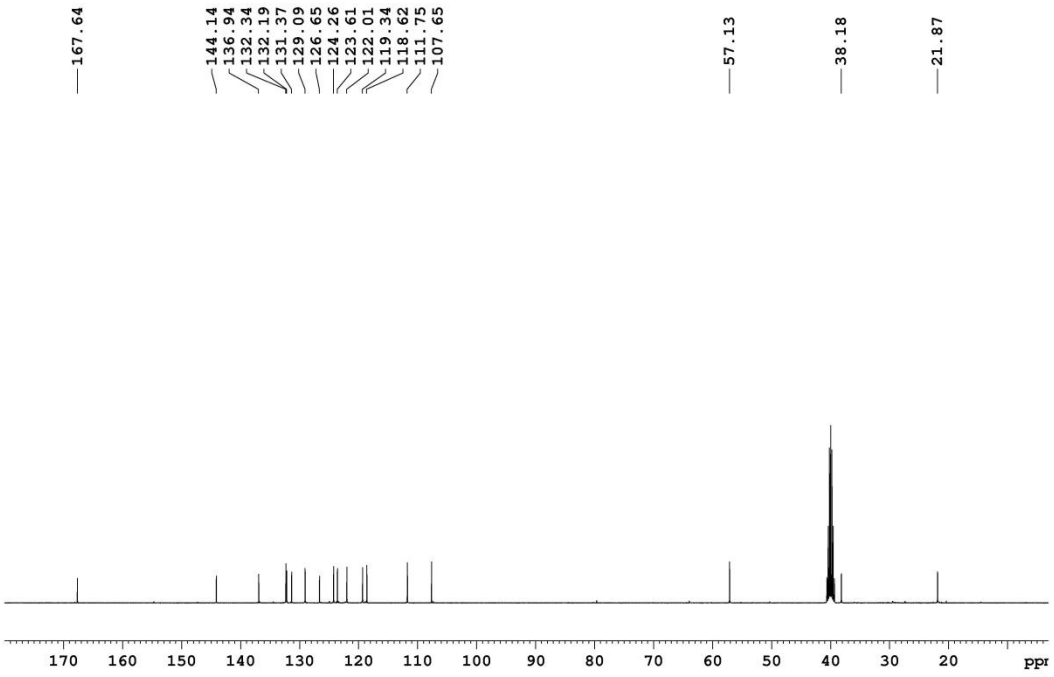

KM-22-02 DMSO DEPT

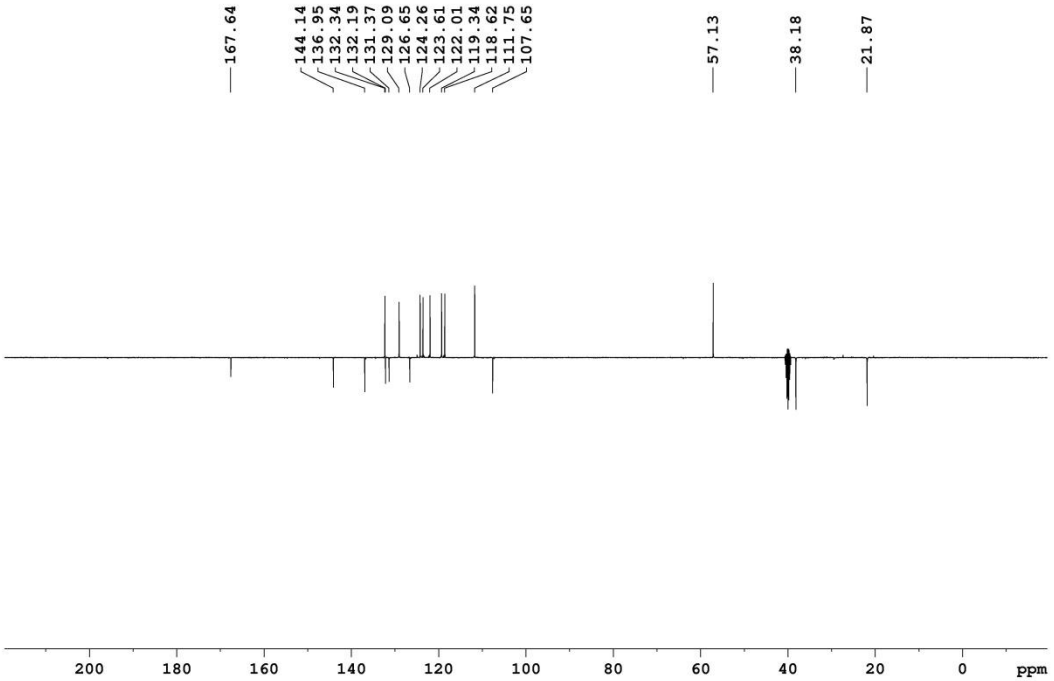

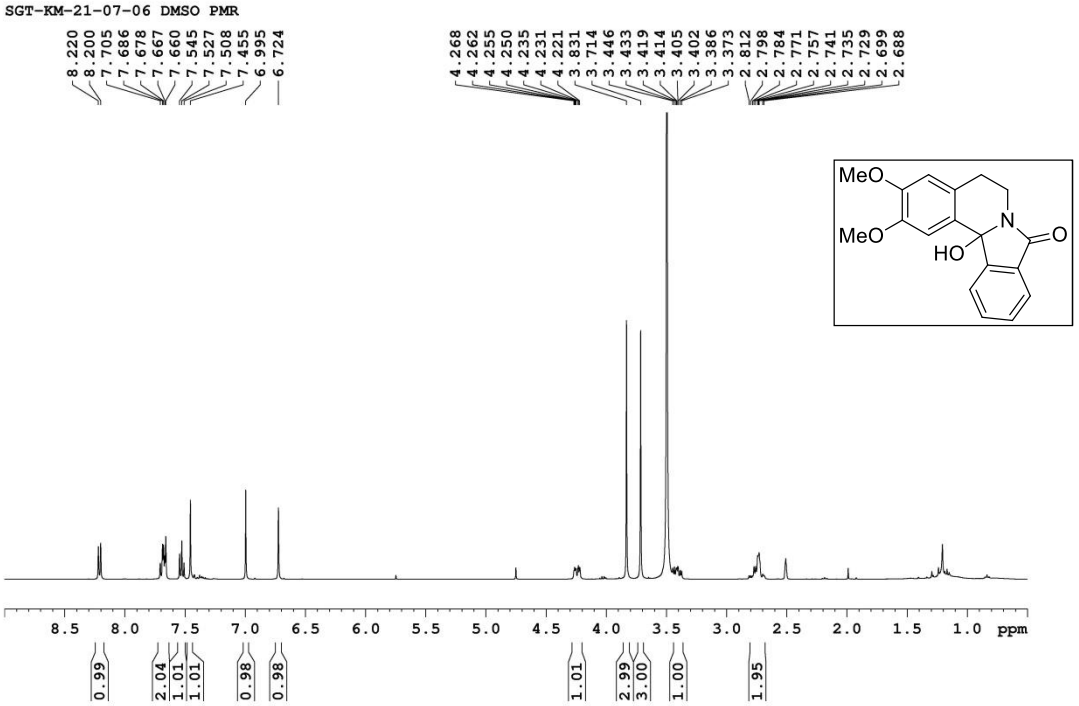
SGT-KM-21-07-06 DMSO PMR
8.220
8.200
7.705
7.686
7.678
7.667
7.660
7.545
7.527
7.508
7.455
6.995
6.724
4.268
4.262
4.255
4.250
4.235
4.231
4.221
3.831
3.714
3.446
3.433
3.419
3.414
3.405
3.402
3.386
3.373
2.812
2.798
2.784
2.771
2.757
2.741
2.735
2.729
2.699
2.688
MeO
MeO
HO
N
O
8.5 8.0 7.5 7.0 6.5 6.0 5.5 5.0 4.5 4.0 3.5 3.0 2.5 2.0 1.5 1.0 ppm
0.99
2.04
1.01
1.01
0.98
0.98
1.01
2.99
3.00
1.00
1.95

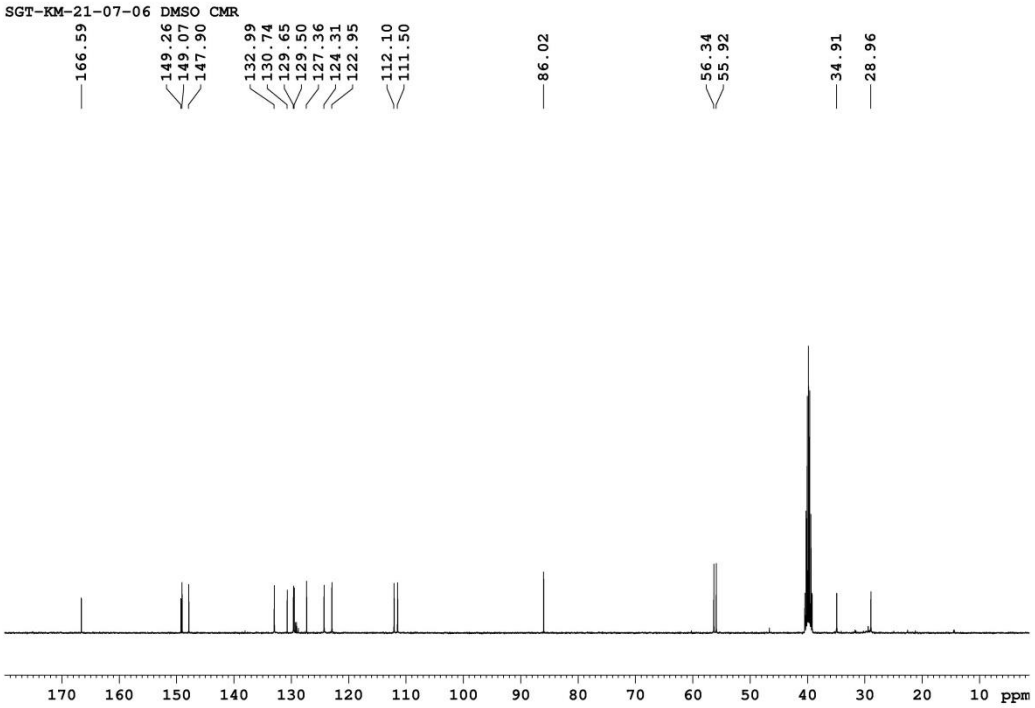
SGT-KM-21-07-06 DMSO CMR
166.59
149.26
149.07
147.90
132.99
130.74
129.65
129.50
127.36
124.31
122.95
112.10
111.50
86.02
56.34
55.92
34.91
28.96
170 160 150 140 130 120 110 100 90 80 70 60 50 40 30 20 10 ppm

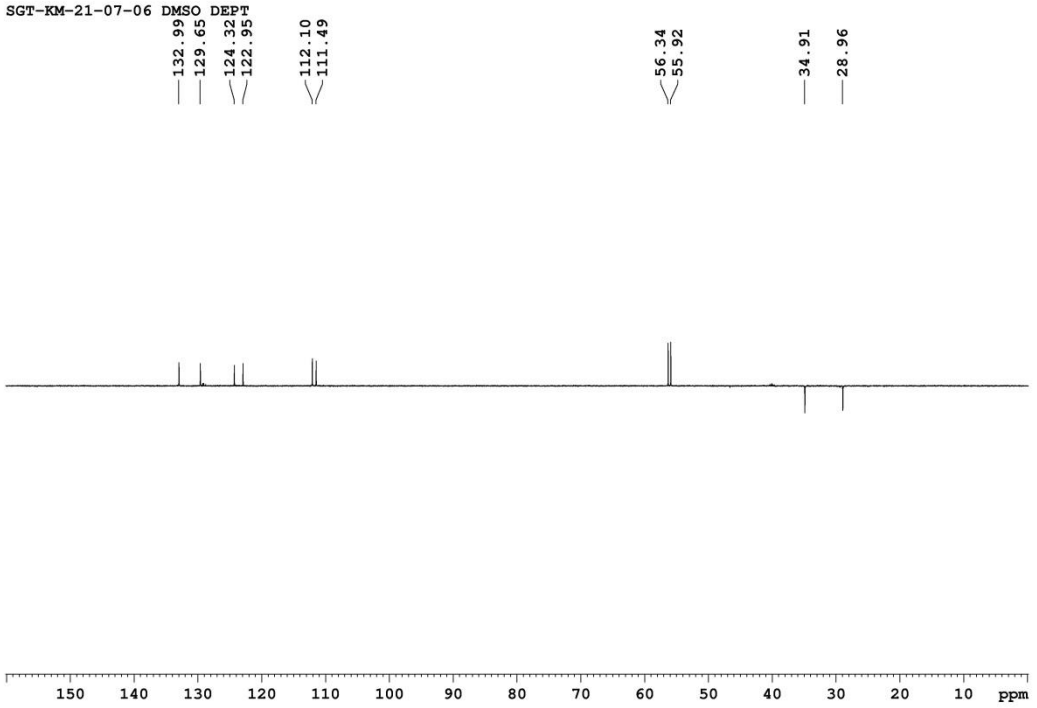
SGT-KM-21-07-06 DMSO DEPT
132.99
129.65
124.32
122.95
112.10
111.49
56.34
55.92
34.91
28.96
150 140 130 120 110 100 90 80 70 60 50 40 30 20 10 ppm

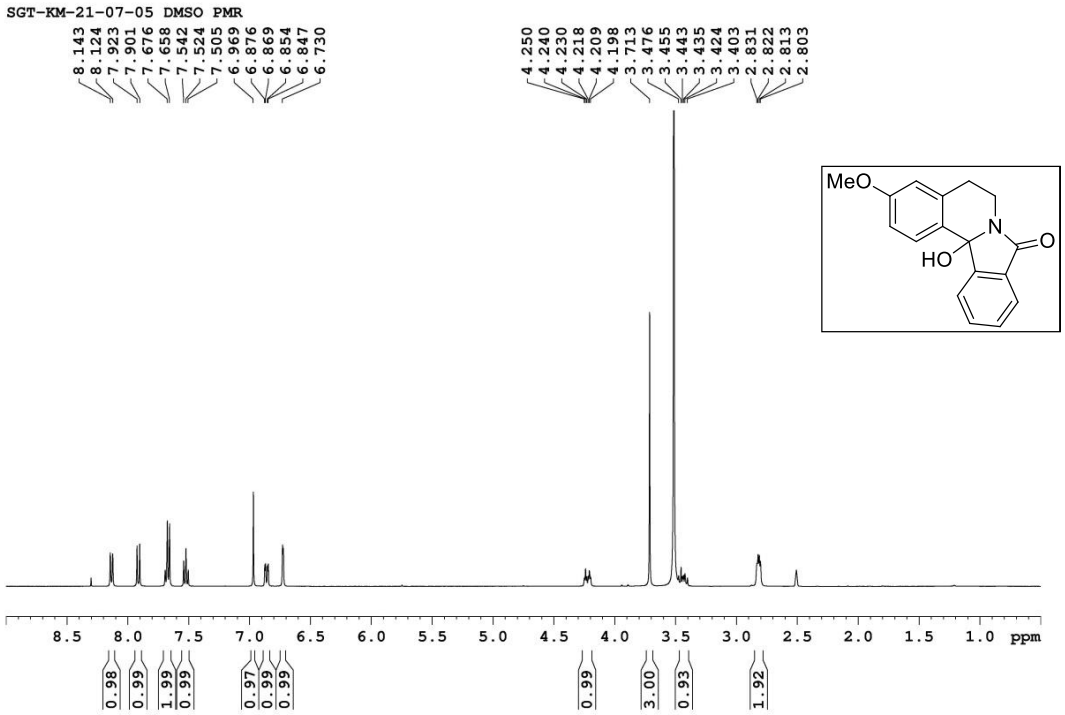
SGT-KM-21-07-05 DMSO PMR
8.143
8.124
7.923
7.901
7.676
7.658
7.542
7.524
7.505
6.969
6.876
6.869
6.854
6.847
6.730
4.250
4.240
4.230
4.218
4.209
4.198
3.713
3.476
3.455
3.443
3.435
3.424
3.403
2.831
2.822
2.813
2.803
MeO
N
O
HO
8.5 8.0 7.5 7.0 6.5 6.0 5.5 5.0 4.5 4.0 3.5 3.0 2.5 2.0 1.5 1.0 ppm
0.98
0.99
1.99
0.99
0.97
0.99
0.99
0.99
3.00
0.93
1.92

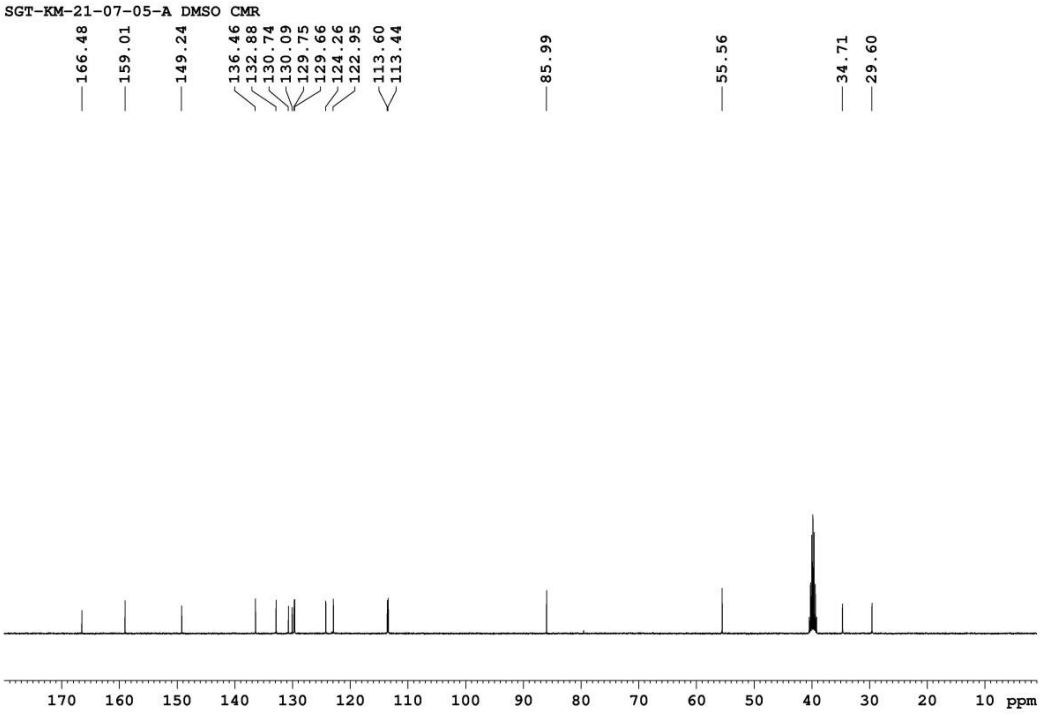
SGT-KM-21-07-05-A DMSO CMR
166.48
159.01
149.24
136.46
132.88
130.74
130.09
129.75
129.66
124.26
122.95
113.60
113.44
85.99
55.56
34.71
29.60
170 160 150 140 130 120 110 100 90 80 70 60 50 40 30 20 10 ppm

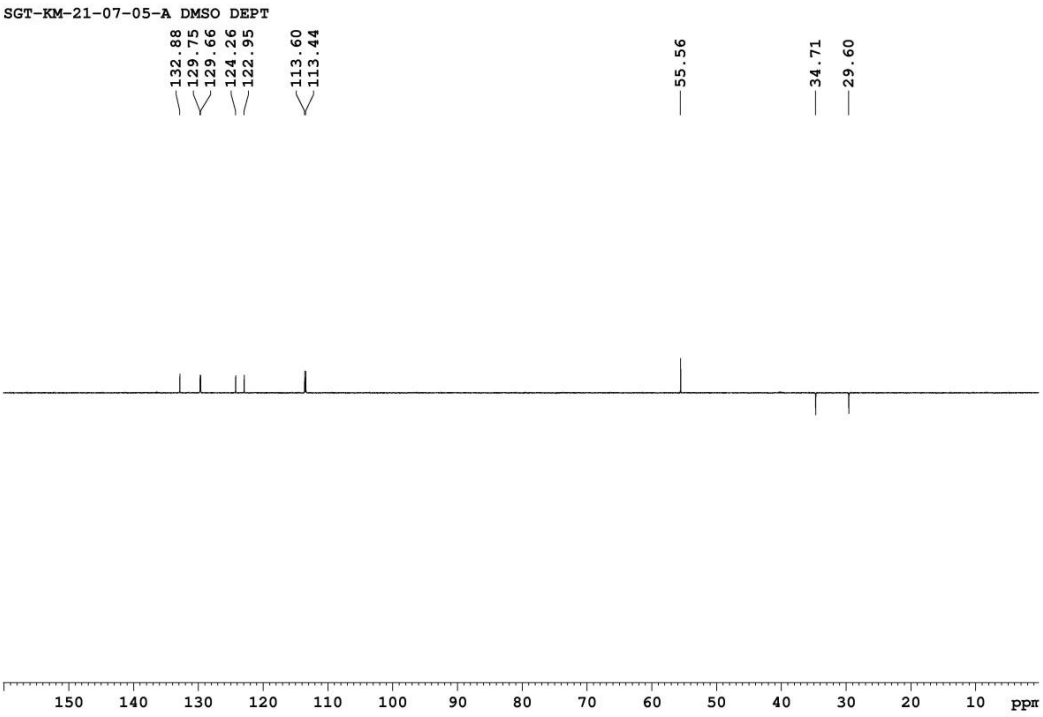
SGT-KM-21-07-05-A DMSO DEPT
132.88
129.75
129.66
124.26
122.95
113.60
113.44
55.56
34.71
29.60
150 140 130 120 110 100 90 80 70 60 50 40 30 20 10 ppm

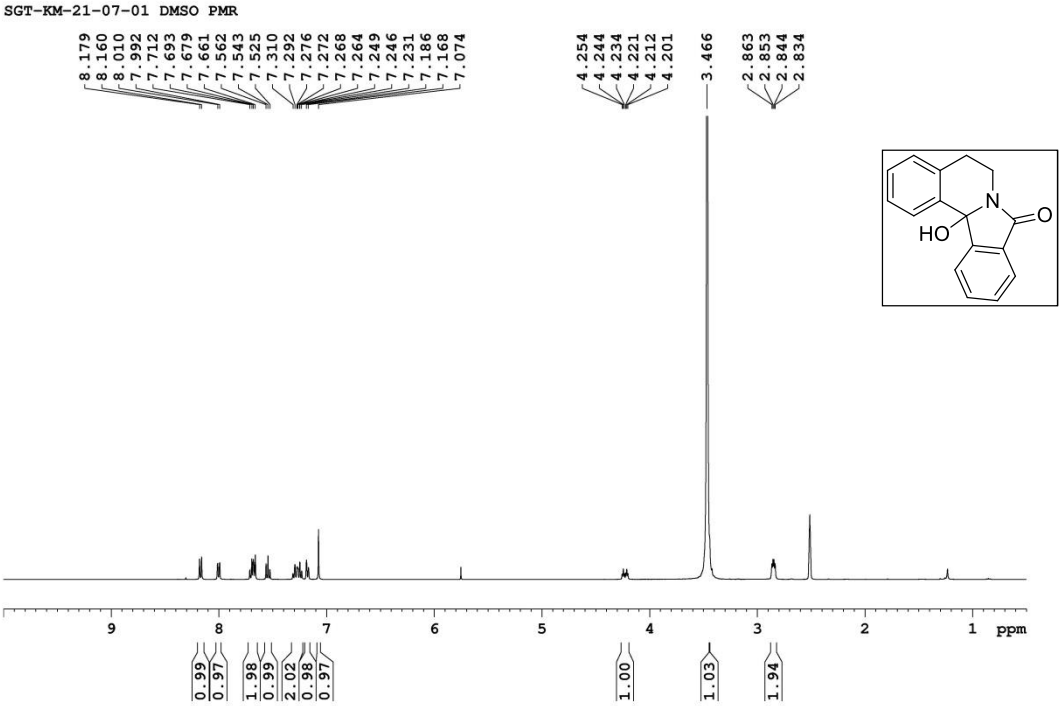
SGT-KM-21-07-01 DMSO PMR
8.179
8.160
8.010
7.992
7.712
7.693
7.679
7.661
7.562
7.543
7.525
7.310
7.292
7.276
7.272
7.268
7.264
7.249
7.246
7.231
7.186
7.168
7.074
4.254
4.244
4.234
4.221
4.212
4.201
3.466
2.863
2.853
2.844
2.834
N
O
HO
9
8
7
6
5
4
3
2
1
ppm
0.99
0.97
1.98
0.99
2.02
0.98
0.97
1.00
1.03
1.94

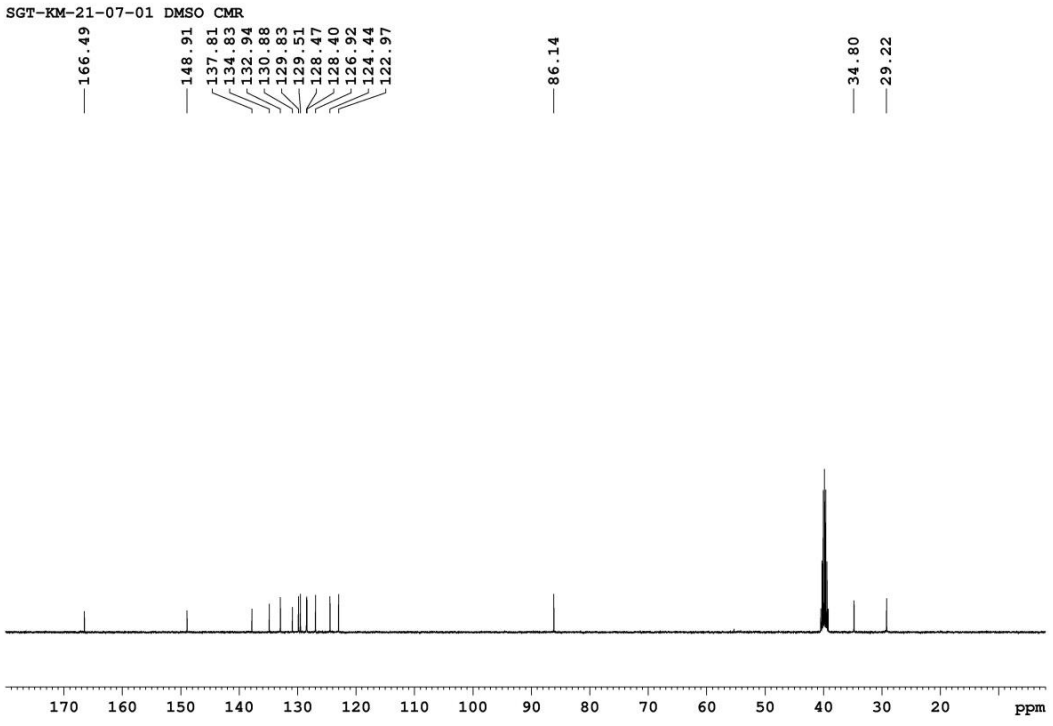
SGT-KM-21-07-01 DMSO CMR
166.49
148.91
137.81
134.83
132.94
130.88
129.83
129.51
128.47
128.40
126.92
124.44
122.97
86.14
34.80
29.22
170
160
150
140
130
120
110
100
90
80
70
60
50
40
30
20
ppm

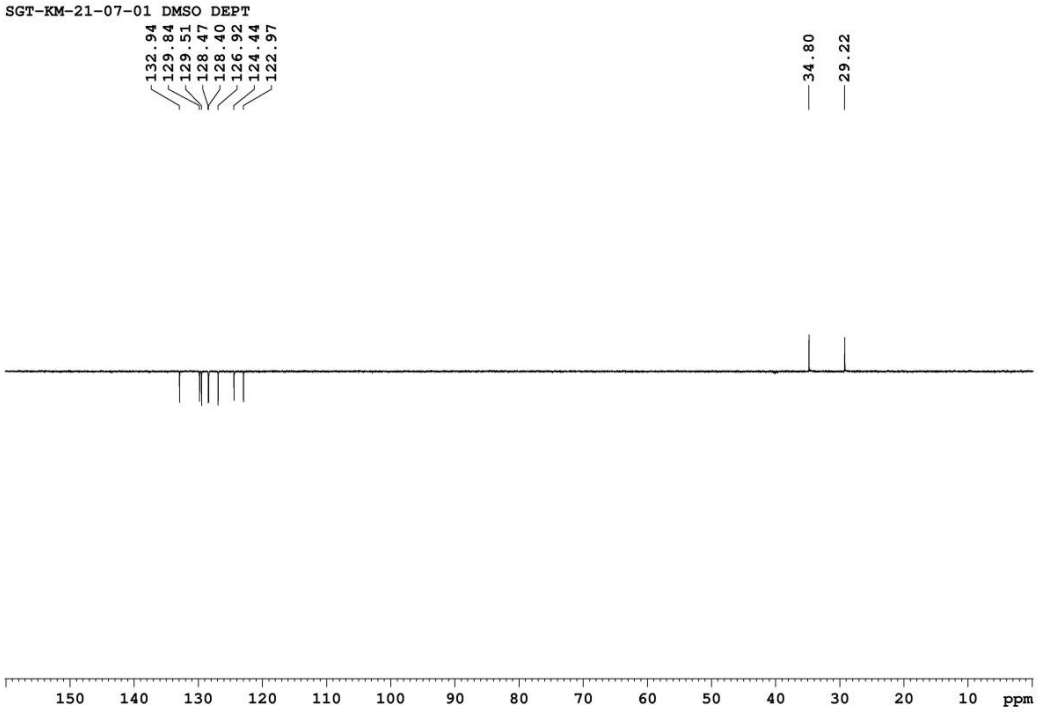
SGT-KM-21-07-01 DMSO DEPT
132.94
129.84
129.51
128.47
128.40
126.92
124.44
122.97
34.80
29.22
150 140 130 120 110 100 90 80 70 60 50 40 30 20 10 ppm

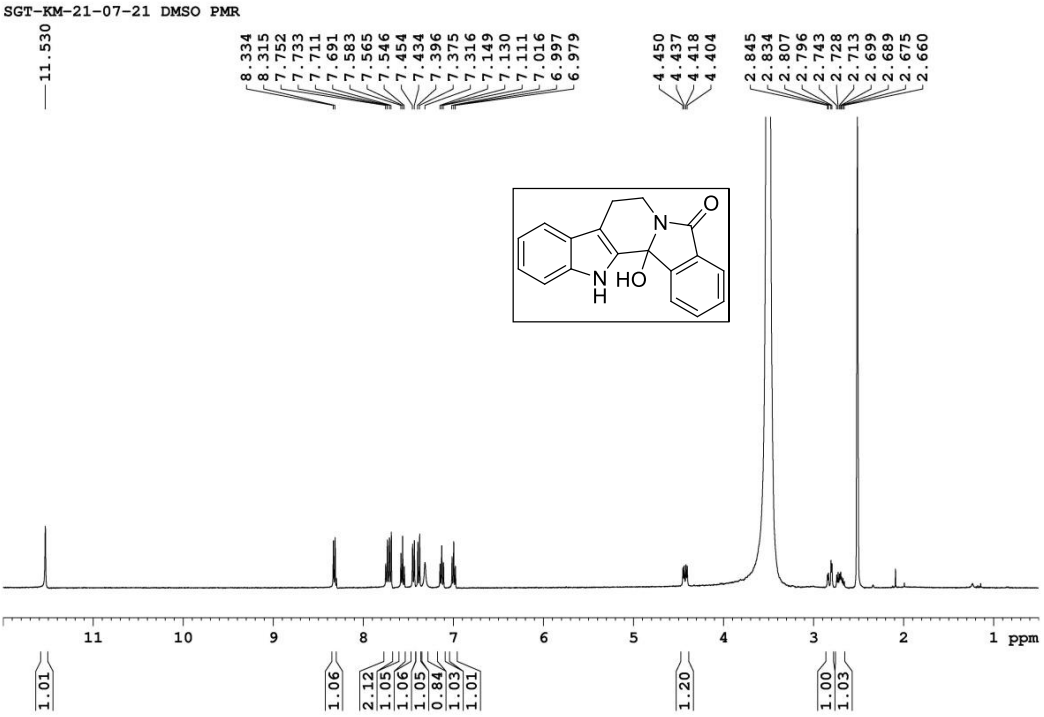
SGT-KM-21-07-21 DMSO PMR
11.530
8.334
8.315
7.752
7.733
7.711
7.691
7.583
7.565
7.546
7.454
7.434
7.396
7.375
7.316
7.149
7.130
7.111
7.016
6.997
6.979
4.450
4.437
4.418
4.404
2.845
2.834
2.807
2.796
2.743
2.728
2.713
2.699
2.689
2.675
2.660
O
N
N
H
HO
11 10 9 8 7 6 5 4 3 2 1 ppm
1.01
1.06
2.12
1.05
1.06
1.05
0.84
1.03
1.01
1.20
1.00
1.03

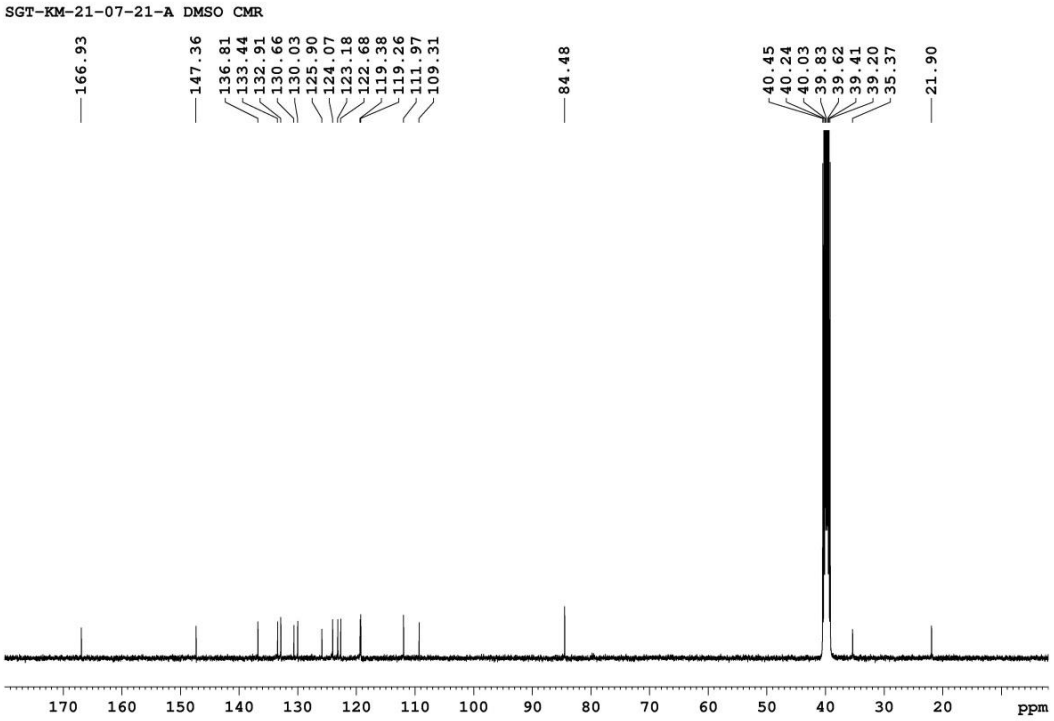
SGT-KM-21-07-21-A DMSO CMR
166.93
147.36
136.81
133.44
132.91
130.66
130.03
125.90
124.07
123.18
122.68
119.38
119.26
111.97
109.31
84.48
40.45
40.24
40.03
39.83
39.62
39.41
39.20
35.37
21.90
170 160 150 140 130 120 110 100 90 80 70 60 50 40 30 20 ppm

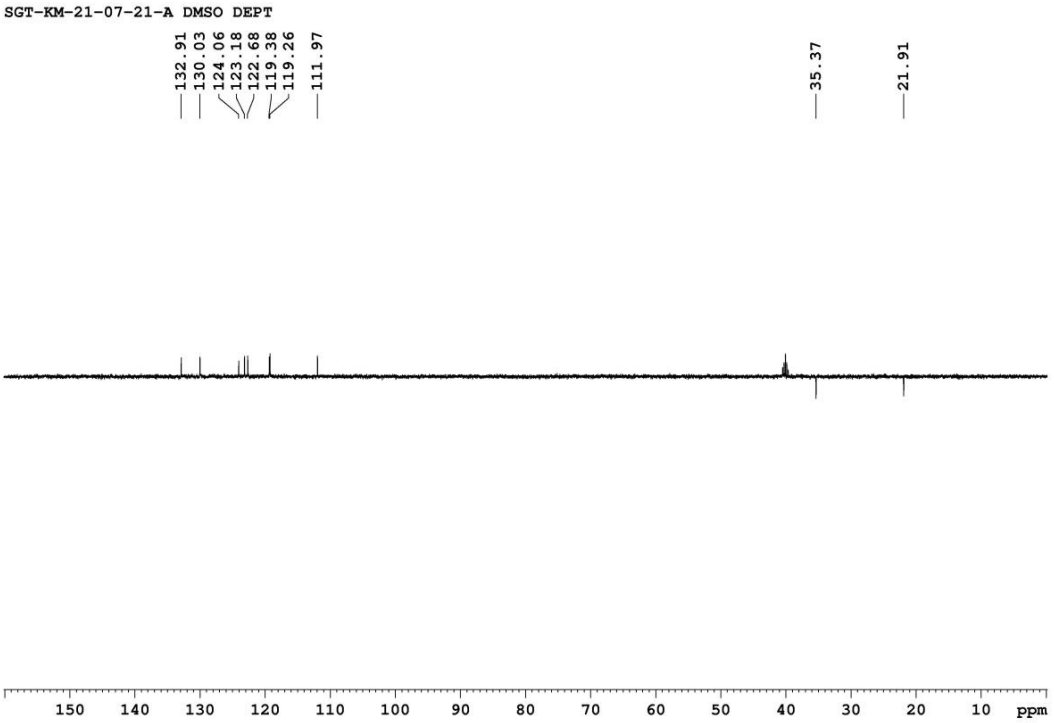
SGT-KM-21-07-21-A DMSO DEPT
132.91
130.03
124.06
123.18
122.68
119.38
119.26
111.97
35.37
21.91
150 140 130 120 110 100 90 80 70 60 50 40 30 20 10 ppm

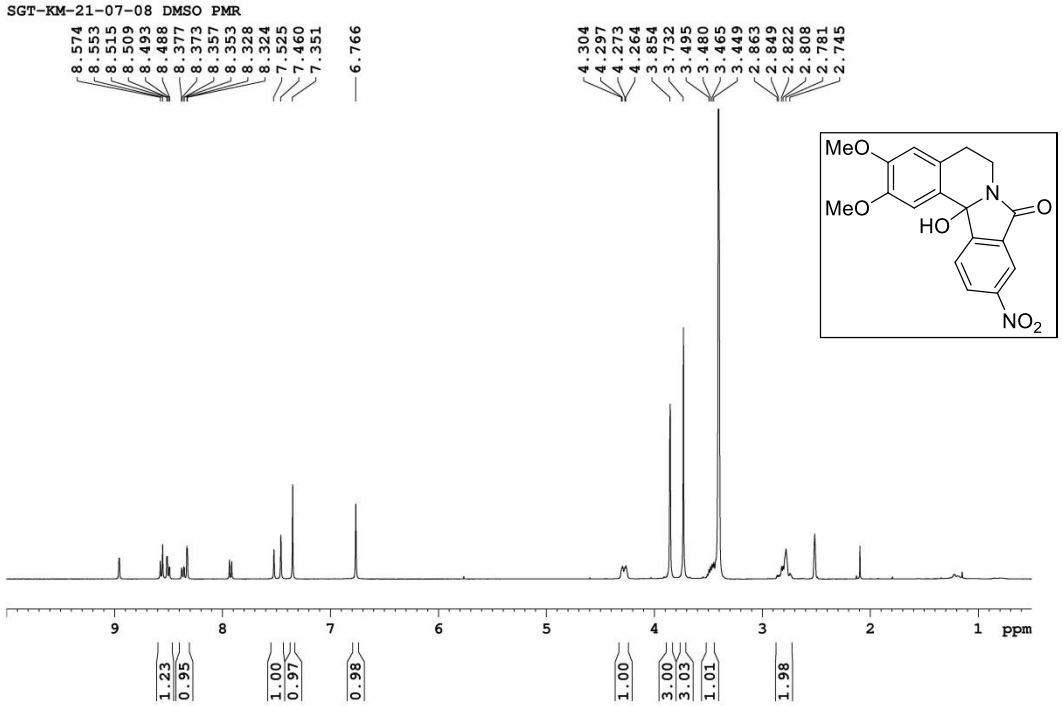
SGT-KM-21-07-08 DMSO PMR
8.574
8.553
8.515
8.509
8.493
8.488
8.377
8.373
8.357
8.353
8.328
8.324
7.525
7.460
7.351
6.766
4.304
4.297
4.273
4.264
3.854
3.732
3.495
3.480
3.465
3.449
2.863
2.849
2.822
2.808
2.781
2.745
MeO
MeO
N
O
HO
NO2
9
8
7
6
5
4
3
2
1
ppm
1.23
0.95
1.00
0.97
0.98
1.00
3.00
3.03
1.01
1.98

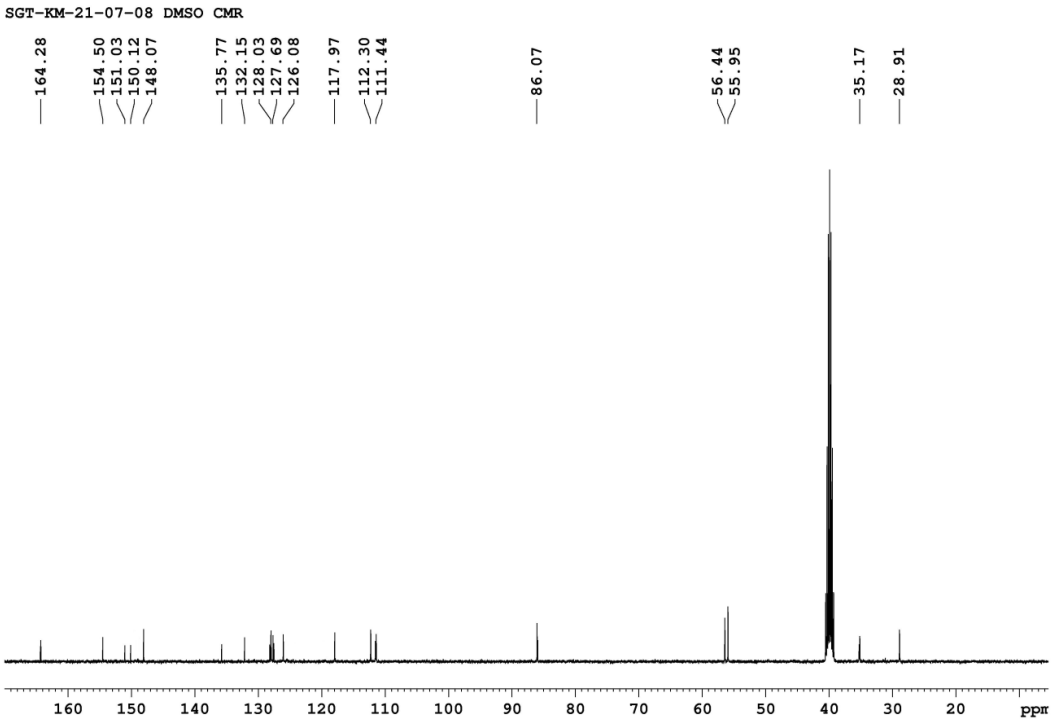
SGT-KM-21-07-08 DMSO CMR
164.28
154.50
151.03
150.12
148.07
135.77
132.15
128.03
127.69
126.08
117.97
112.30
111.44
86.07
56.44
55.95
35.17
28.91
160
150
140
130
120
110
100
90
80
70
60
50
40
30
20
ppm

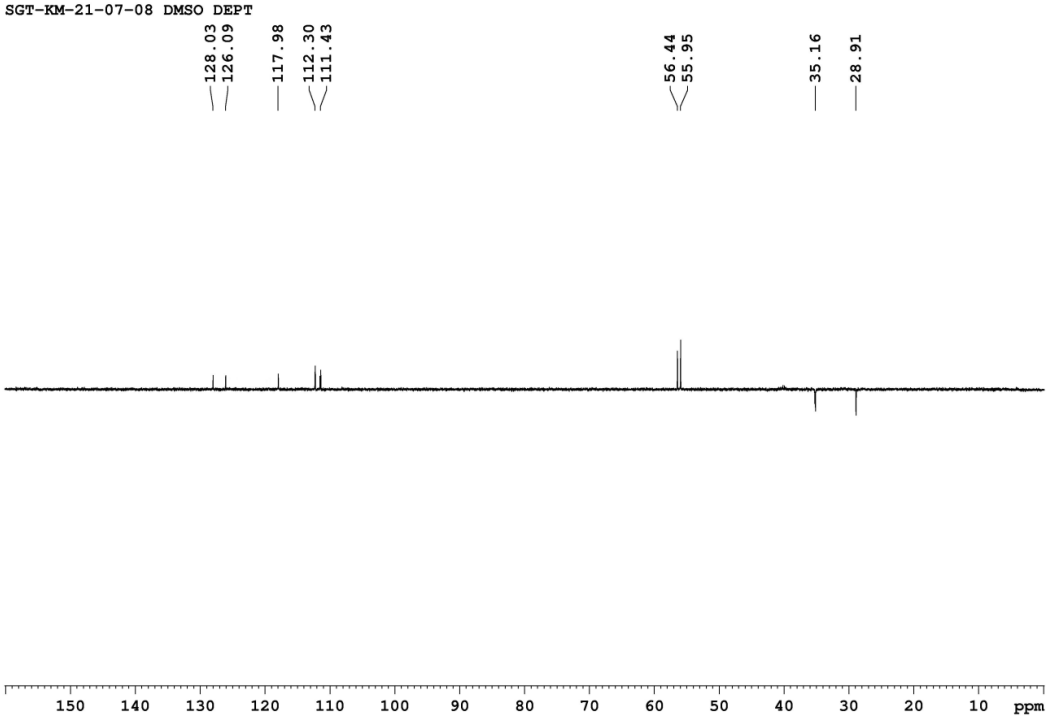
SGT-KM-21-07-08 DMSO DEPT
128.03
126.09
117.98
112.30
111.43
56.44
55.95
35.16
28.91
150 140 130 120 110 100 90 80 70 60 50 40 30 20 10 ppm

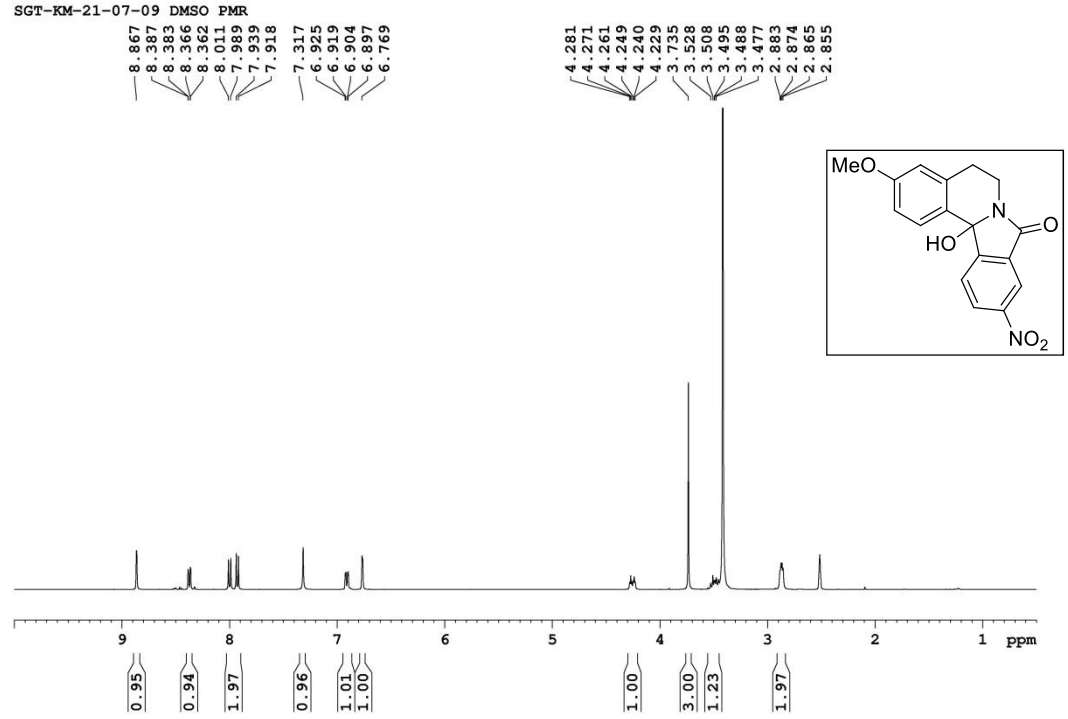
SGT-KM-21-07-09 DMSO PMR
8.867
8.387
8.383
8.366
8.362
8.011
7.989
7.939
7.918
7.317
6.925
6.919
6.904
6.897
6.769
4.281
4.271
4.261
4.249
4.240
4.229
3.735
3.528
3.508
3.495
3.488
3.477
2.883
2.874
2.865
2.855
MeO
N
O
HO
NO2
9 8 7 6 5 4 3 2 1 ppm
0.95
0.94
1.97
0.96
1.01
1.00
1.00
3.00
1.23
1.97

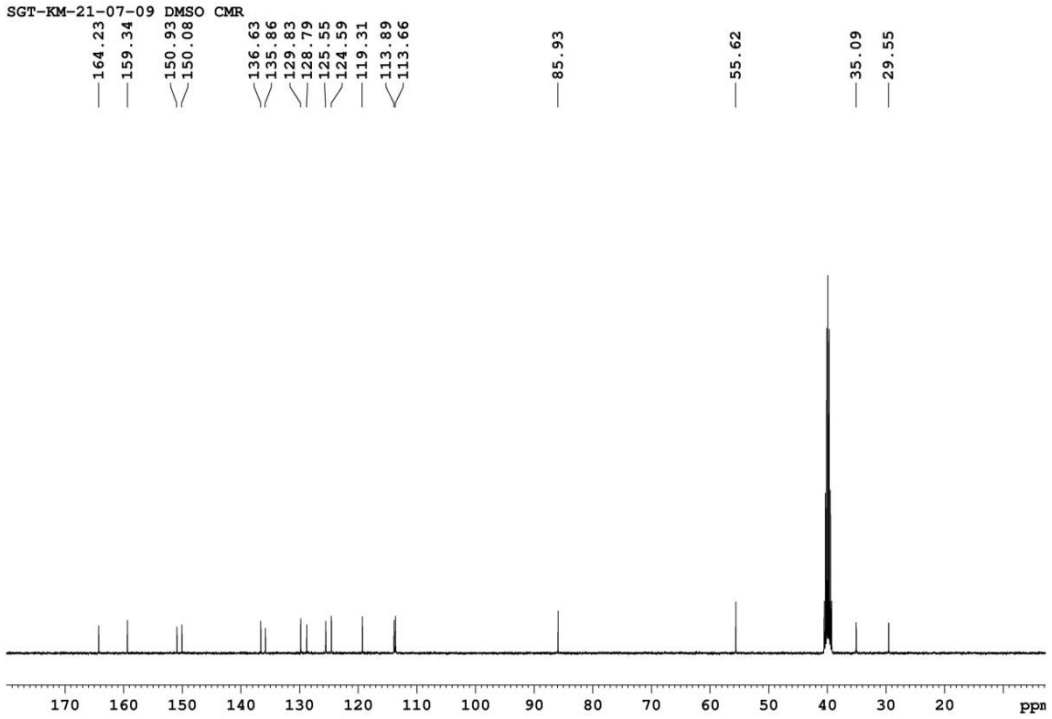
SGT-KM-21-07-09 DMSO CMR
164.23
159.34
150.93
150.08
136.63
135.86
129.83
128.79
125.55
124.59
119.31
113.89
113.66
85.93
55.62
35.09
29.55
170 160 150 140 130 120 110 100 90 80 70 60 50 40 30 20 ppm

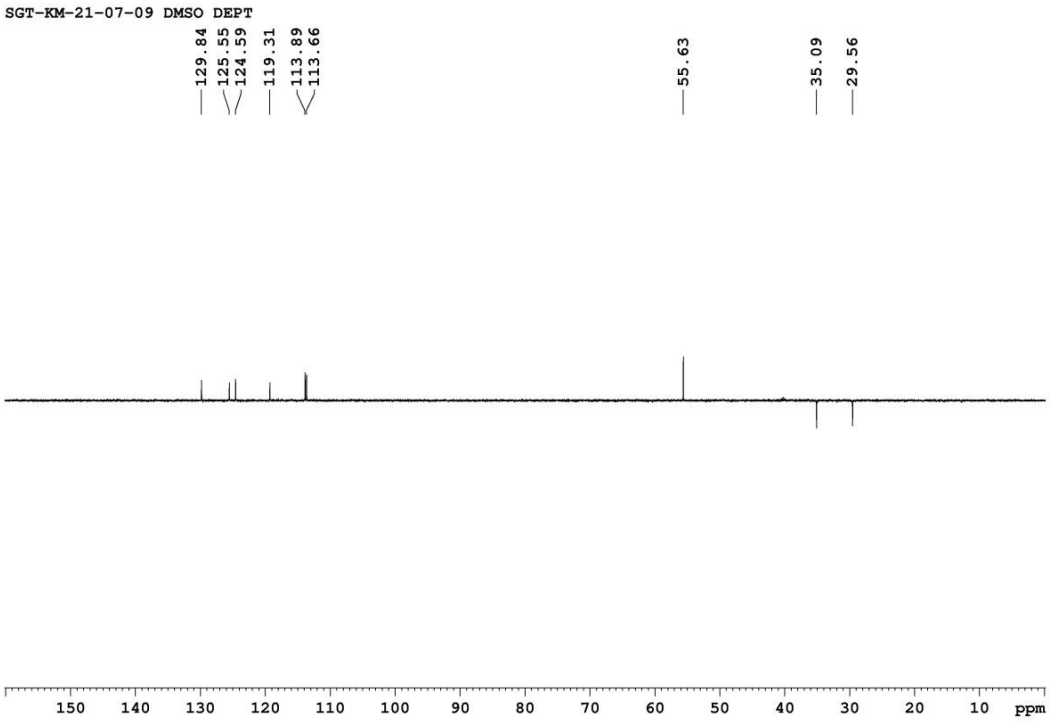
SGT-KM-21-07-09 DMSO DEPT
129.84
125.55
124.59
119.31
113.89
113.66
55.63
35.09
29.56
150 140 130 120 110 100 90 80 70 60 50 40 30 20 10 ppm

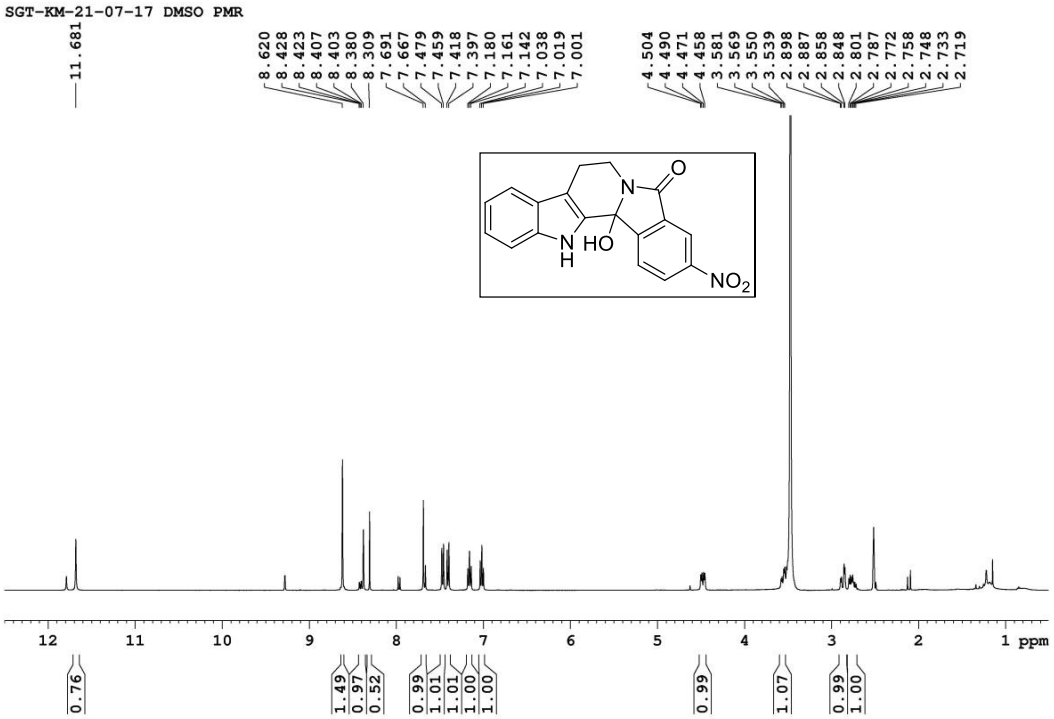
SGT-KM-21-07-17 DMSO PMR
11.681
8.620
8.428
8.423
8.407
8.403
8.380
8.309
7.691
7.667
7.479
7.459
7.418
7.397
7.180
7.161
7.142
7.038
7.019
7.001
4.504
4.490
4.471
4.458
3.581
3.569
3.550
3.539
2.898
2.887
2.858
2.848
2.801
2.787
2.772
2.758
2.748
2.733
2.719
O
N
N
H
HO
NO2
12
11
10
9
8
7
6
5
4
3
2
1 ppm
0.76
1.49
0.97
0.52
0.99
1.01
1.01
1.00
1.00
0.99
1.07
0.99
1.00

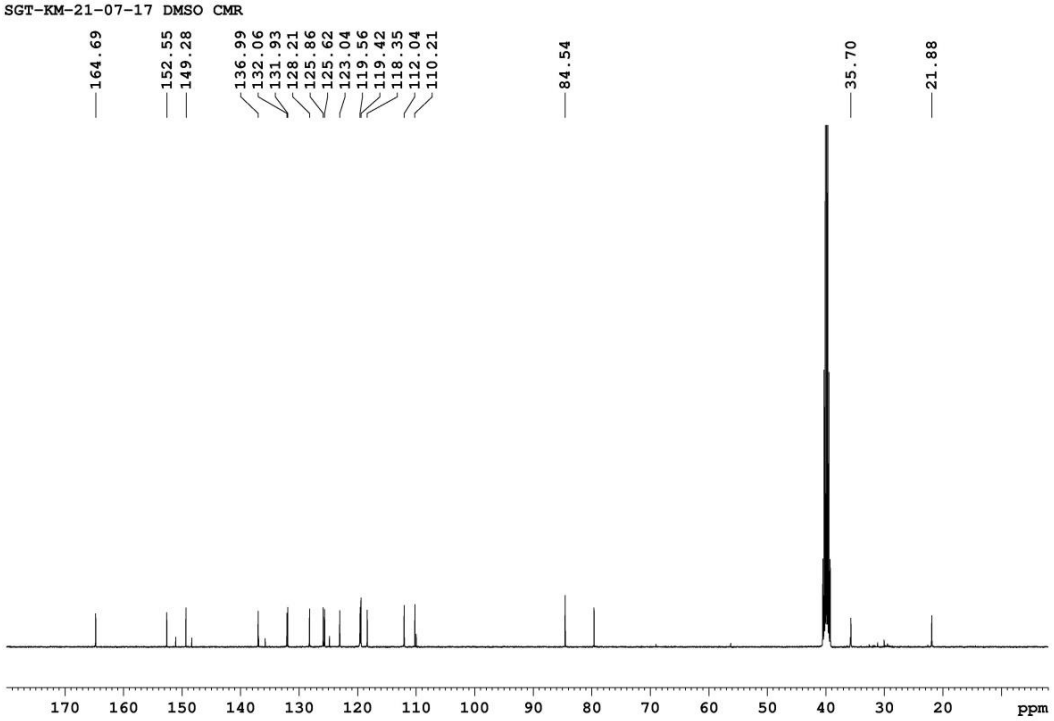
SGT-KM-21-07-17 DMSO CMR
164.69
152.55
149.28
136.99
132.06
131.93
128.21
125.86
125.62
123.04
119.56
119.42
118.35
112.04
110.21
84.54
35.70
21.88
170
160
150
140
130
120
110
100
90
80
70
60
50
40
30
20
ppm

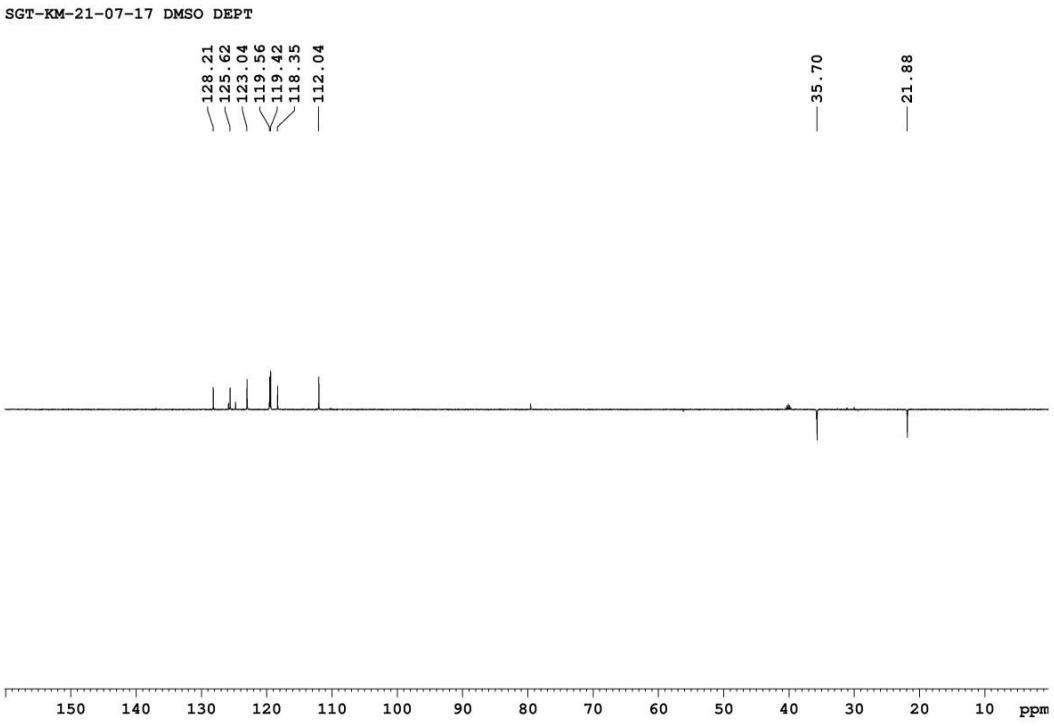
SGT-KM-21-07-17 DMSO DEPT
128.21
125.62
123.04
119.56
119.42
118.35
112.04
35.70
21.88
150
140
130
120
110
100
90
80
70
60
50
40
30
20
10
ppm

Section III: *In Silico* Molecular Docking study of Pyrrolo[2,1-*a*]isoquinoline moieties with SARS-CoV-2 proteins

2.III.1 Introduction:

There are natural disasters and man-made havoc, killing millions to billions of people worldwide. Nature takes care of its cataclysm quickly, but it is challenging to handle the human-made holocaust. The outbreak of covid-19 in late 2019 has shaken the entire human community. First identified from the Wuhan Institute of Virology, Wuhan, China, is considered a major lab leak case by many scientists; whereas others believe it to have a natural origin.[1] The debate regarding its origin is still raging on the internet. In history, such a pandemic situation had arisen in the world about 100 years before.

Since it is already active from late 2019 till now, it is highly crucial to understand what covid-19 is. Covid-19 is caused by severe acute respiratory syndrome coronavirus 2 (SARS-CoV-2). It is a highly pathogenic human coronavirus (CoV) attacking mainly the respiratory system, causing pneumonia. This virus is considered from the *coronaviridae* family, accompanying the Middle East respiratory syndrome coronavirus (MERSCoV) and SARS-CoV. Unlike other CoV's like HCoV-NL63, HCoV-229E, HCoV-OC43, and HCoVHKU1 which cause mild respiratory tract infections, these three viruses are zoonotic and are responsible for severe infections in humans, leading to death in some cases.[2] The SARS-CoV-2 virus is enveloped, single-stranded RNA betacoronaviruses, positive polarity, and their genomes encode nonstructural proteins (nsps), and several accessory, and structural proteins.[3,4]

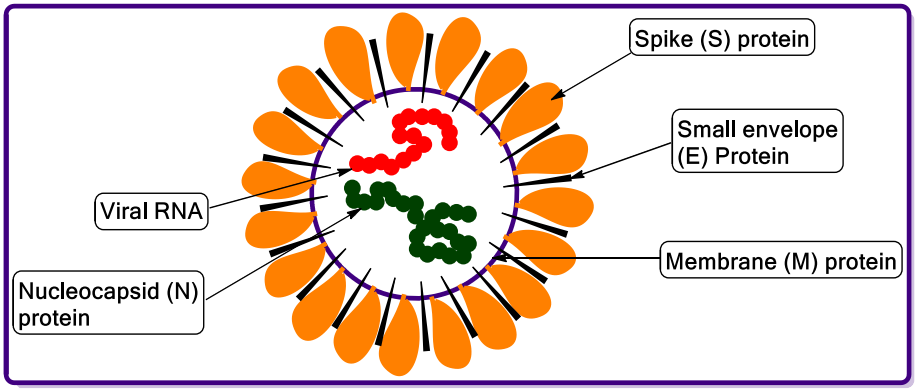

Figure 1. Schematic diagram of SARS-CoV-2 virus

The constitution of biological bodies of coronavirus is spike (S) glycoprotein, envelope (E) protein, membrane (M) protein, and nucleocapsid (N) protein (Fig. 1).[5]

These proteins play more important functions in the viral life cycle. A crucial role in virus pathogenesis and organ tropism is played by spike (S) protein being responsible for the viral entry through receptor recognition and membrane fusion.[6] The smallest of the structural proteins is envelope (E) protein playing a major role in assembly, budding, envelope formation, and virulence.[7] The membrane (M) protein has membrane-binding properties which promote viral assembly.[8] There is also present a multifunctional protein named nucleocapsid (N) protein that protects the genome by packaging the viral RNA genome into a ribonucleoprotein complex called a nucleocapsid.[9] Some computational studies were carried out to identify the structure and function of the E protein[10] and the other structural proteins[11] for the search of new therapeutics based on structural proteins of SARS-CoV-2.

Although scientists have figured out the molecular anatomy of the CoV, it is also important to understand its attack on the host cell and its behavior inside the host cell. For the past 15 years, a controversial debate is fuming regarding the coronavirus entry in the host cell, wherein non-endosomal pathways were regarded as a means of CoV entry into the host cell. Until 2004, Jingqiang *et al.*[12] showed the fusion of SAR-CoV's with the cellular surface after attacking the host cell membrane. After the loss of envelopes by virions, the disappearance of the nucleocapsid showed no further endocytic events. Ng *et al.*[13] remarkably, observed a fusion of CoV with the plasma membrane and the inclusion of spherical viral cores into the cytoplasm inside the large cellular vacuoles when studied on a

patient having SAR-CoV in Singapore. However, this study points towards the endosomal pathway as an entry of CoV in the host cell.

Wang and co-workers,[14] based on their observation on SAR-CoV, have established an alternative pathway for the virus entry into the host cell, apart from the virion fusion with the plasma membrane. Their astonishing study showed that the entry of the virus is an endocytosis-dependent manner mediated by pH and receptors of the host cell. Internalization of SARS-CoV receptor angiotensin-converting enzyme (ACE2) is induced from the cell surface to cytoplasmic compartments by the spike (S) protein itself or a pseudovirus bearing S protein. Besides this, the ACE2 receptor in vesicles is blocked by lysosomotropic a drug which leads to impairing their recycling to the plasma membrane. SARS-CoV exploits the endocytic pathway to infect the cells as indicated by the effect on pseudoviruses by inhibition of pH acidification, as they found, in a clathrin- and caveolin-independent manner.

Now, as the importance of studying the new SAR-CoV-2 variant is surfaced, scientists are relentlessly examining the entry and behavior of SAR-CoV-2 in the host cell. A few years ago, two viruses belonging to the *coronaviridae* family, SARS-CoV[15,16] and MERS-CoV[17] attacked the human species causing pneumonia-like illness worldwide. Elucidation of the similarities of their entry pathways is essential.

The entry of Coronavirus depends majorly on the spike (S) protein, and then according to the viral strain and cell type studied, the S protein is cleaved by several different cellular proteases.[18−24] SARS-CoV-2 shows similar entry requirements to those of SARS-CoV as both viruses are coincident in the cellular receptor ACE2. Lysosomotropic drugs profoundly inhibit infection by SARS-CoV-2 similar to SARS-CoV in cells transduced with pseudovirus.[25] Therefore, the preferred route for SARS-CoV-2 entry into the host cell is through the endocytic pathway as suggested by these results.

Furthermore, entry of SARS-CoV and SARS-CoV-2 pseudovirions' based on their dependence on endosomal acidification relies on late endosomal compartments. Thus, for the impairment of SARS-CoV-2 infection, the inhibition of endosomal maturation is necessary. Impairment of pseudovirions' entry can be done by treating cells with chemical inhibitors (YM201636 and apilimod) of the PIKfyve enzyme which is involved in the

phosphoinositides metabolism regulating endosomal maturation. Ebola virus (EBOV) and African swine fever virus are a few other viruses which depend on PIKfyve enzyme described and both dependent on the late endosome for entry.[26−28] Ruination of SARS-CoV-2 infection is carried out by blocking other proteins characteristic of the late endosomal compartments, like two-pore channel 2 (TPC2) (but not transient receptor potential cation channel mucolipin TRMPL1), indicating that TPC2 is important for SARS-CoV-2 pseudovirions' entry.[25] Protease activation of S glycoprotein plays an important role for coronavirus entry.

A crucial part is cooperated by lysosomal cathepsins for SARS- and MERS-CoV entry via endocytosis. Cathepsin L is also critically required by SARS-CoV-2 for a thriving infection priming into lysosomes to enter the cells since its inhibition decreased by 76% the entry of SARS-CoV-2 S pseudovirions. Contrary to this, cathepsin B inhibition showed an insignificant effect.[25]

The encounter of the host cell with the virus leads to disassembling of the virus to release the nucleocapsid and the viral genome. Translation of the open reading frame (ORF) 1a/b then takes place by the host ribosomes into two polyproteins (pp1a and pp1ab) which encodes 16 nsps and other structural and accessory proteins are encoded by the remaining ORFs. Cleavage of the polyproteins takes place by the participation of two proteases, the main protease (3CLpro, nsp5) and the papain-like protease (PLpro, nsp3), to procreate nsp2−16 involved in the replication−transcription complex (RTC).[29] Some of the proteases are RNA-dependent RNA polymerase (RdRp, nsp12) and helicase (nsp13). In coronavirus, an assembly of the virion components into the endoplasmic reticulum Golgi intermediate compartment complex is then followed finally getting released from the infected cells by exocytosis.[30]

It is the need of the hour to search for therapeutic options for SARS-CoV-2 which are potentially druggable targets because all CoV enzymes and proteins are involved in viral replication and the control of host cellular machineries. It takes around 1 to 3 years to develop a new drug or vaccine and get it in the market for the consumers.

Chloroquine and hydroxychloroquine:

Back in the seventeenth century, the indigenous people in Peru extracted the bark of the Cinchona tree (*Cinchona officinalis*) and used it to fight chills and fever.[31] This herbal medicine was introduced in Europe in the year 1633, where it was used for the same purpose and also began to be used against malaria. In 1820, the quinine was isolated from the extract which is a quinoline antimalarial drug.[32] The German government after World War I, sought alternatives to quinine. Hans Andersag and co-workers at the Bayer laboratories discovered Chloroquine in 1934 which is a synthetic analog with the same mechanism of action and named it Resochin.[33] Chloroquine proved to be a significant therapeutic value as an antimalarial drug found out after many clinical trials conducted by United States government-sponsored for antimalarial drug development. Early in the pandemic, it was studied to treat COVID-19 but these studies were largely discontinued in the summer of 2020 and were not recommended for this purpose.

In 1955, the United States approved the hydroxy analog of chloroquine for medical use and it's on the World Health Organization's List of Essential Medicines. For prevention and treating coronavirus disease 2019 (COVID 19), hydroxychloroquine had been studied but was found ineffective for this purpose after the clinical trials and showed the possible risk of dangerous side effects. The notional use of hydroxychloroquine for COVID 19 intimidates its availability for people with established manifestation.

Favipiravir:

Japan has approved Favipiravir to treat influenza but it is only indicated for novel influenza (strains that cause more severe disease) rather than seasonal influenza.[34] The probability of resistance developing appears low as of the year 2020. Favipiravir is under study to treat several viral infections, including SARS-CoV-2. It is a pyrazinecarboxamide derivative similar to the other antiviral drugs like T-1105 and T-1106.[35] Selective inhibition of viral RNA-dependent RNA polymerase is probably taken as the mechanism of its action. Favipiravir is available in both oral and intravenous formulations as a prodrug that is metabolized to its active form, favipiravir-ribofuranosyl-5'-triphosphate (favipiravir-RTP). Favipiravir-RTP is a nucleoside analog and it mimics both adenosine and guanosine for the viral RdRP.[36]

Molnupiravir:

A prodrug of the synthetic nucleoside derivative N^4-hydroxycytidine.[37] Molnupiravir makes use of its antiviral action through the introduction of copying errors during viral RNA replication.[38] In March 2020, this drug was efficiently used to treat human cells infected with the novel coronavirus by the researchers who were studying SARS-CoV-2. The first demonstration was published in the journal Nature Microbiology by Plemper's group.[39] They established proof-of-concept that treatment with molnupiravir taken orally completely suppresses virus transmission to untreated contacts within 24 hours against SARS-CoV-2 in an animal model.

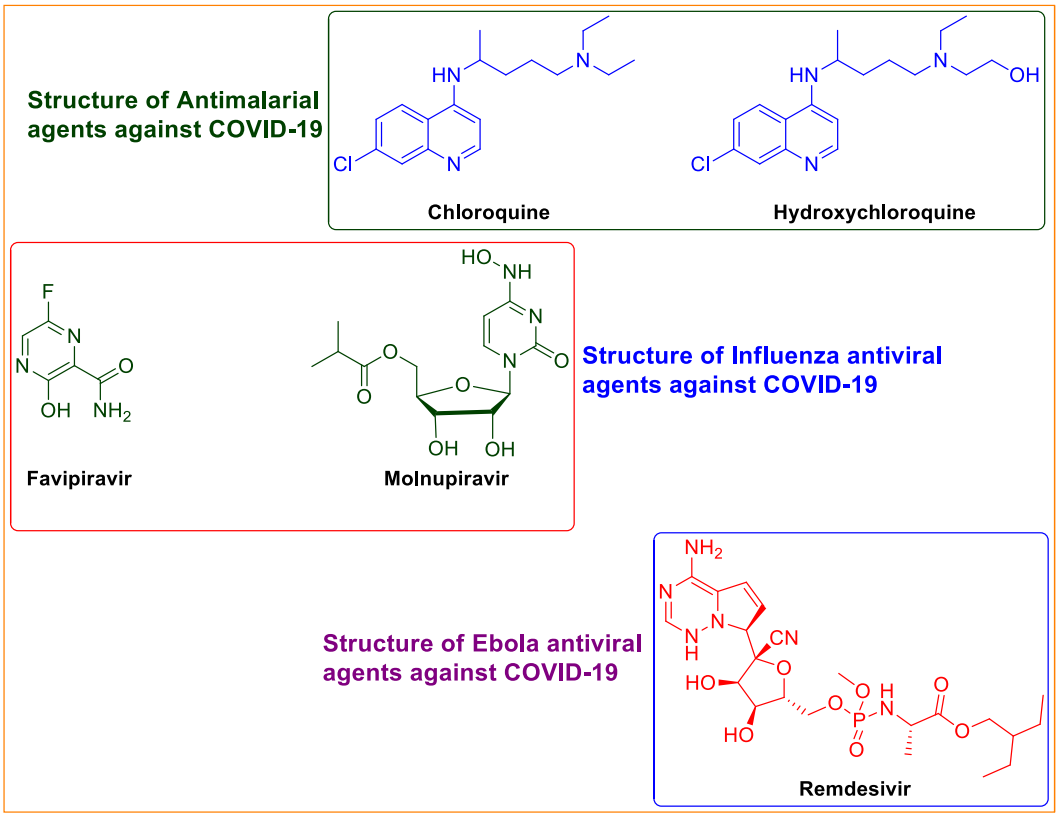

Figure 2. Selected drug molecules with activity against COVID-19

Remdesivir:

Before being studied as a post-infection treatment for COVID-19, Remdesivir was originally developed to treat hepatitis C and was subsequently scrutinized for Ebola virus disease and Marburg virus infections.[40] Remdesivir was developed by the biopharmaceutical company Gilead Sciences as a broad-spectrum antiviral medication and was sold under the brand name Veklury. The United States approved Remdesivir for medical use in October 2020. It was accepted by the U.S. Food and Drug Administration

(FDA) based on the agency's analysis of data from three randomized, controlled clinical trials that included participants hospitalized with mild-to-severe COVID 19.

Of the above drugs approved for covid treatment, Favipiravir is a small molecule and also has an amide linkage. If one sees the search for anti-covid agents in the initial phase it is mainly concentrated on the repurposing of old molecules. As mentioned in the previous section, the pyrrolo[2,1-*a*]isoquinolines demonstrate various interesting biological activities including antiviral activity. So, we thought of evaluating some of pyrrolo[2,1-*a*]isoquinolines in *insilico* studies.

2.III.2 Molecular docking studies of favipiravir against various SARS-CoV-2 proteins:

Table 1. Binding potential of favipiravir drug with drug targets of SARS-CoVs-2 proteins[41]

Entry	Protein name	PDB ID	B. E. (kcal/mol)	Cluster RMSD (Å)	Interacting residues	Hydrogen bonds
1	ADP ribose phosphate of NSP3	6VXS	-4.5	0.0	Lys31, Pro32, His86, Ala89, Lys90	2: intra hydrogen bonds within the drug molecule
2	C-terminal dimerization domain of Nucleocapsid Phosphoprotein	6WJI	-4.6	0.0	Val270, Arg277	1: Val270
3	HR2 domain	6LVN	-4.0	0.0	Glu21, Lys24	1: Glu21
4	Main protease	6Y2E	-4.7	0.0	Glu14, Gly15, Met17, Ala70	0

5	NSP10	6W75-B	-4.6	0.0	Thy4292, Cys4294, Asn4358	1: Cys4294
6	NSP15 Endoribonuclease	6VWW	-4.7	0.0	Gln202, Glu203, Phe204, Ala256, Phe259	1: Ala256
7	NSP16	6W75-A	-5.0	0.0	Thr6934, Phe6948, Phe6947	0
8	Nsp9 RNA binding protein	6W4B	-4.6	0.0	Ser14, Asn26, Asp27, Ala29, Asp48	1: Ser14
9	Nucleocapsid protein N-terminal RNA binding domain	6M3M	-4.3	0.0	Gly115, Ala120, Gly121, Tyr124, Asn141, Pro143	1: Tyr124
10	ORF7A encoded accessory protein	6W37	-4.3	0.0	Glu18, Ser22, Gly23, Thr24, Tyr25, Phe31	1:Ser22
11	Papain-like preotease	6W9C	-4.7	0.0	Asp76, Arg82, Tyr154, Asn156	0
12	Post fusion core of S2 subunit	6LXT	-4.5	0.0	Ser967, Gly971, Leu1166	1:Leu1166
13	Prefusion of the	6VSB	-4.6	0.0	Tyr38,	1:Asp40

	spike glycoprotein with a single receptor binding domain				Asp40, Gly283	
14	RNA-dependent RNA polymerase NSP12	6M71.A	-4.9	0.0	Trp800	1:Trp800
15	RNA-dependent RNA polymerase NSP7	6M71.C	-4.1	0.0	Asp38, Ala42, Lys43, Asp44	0
16	RNA-dependent RNA polymerase NSP8	6M71.B.D	-4.4	0.0	Tyr135, Ser177,	2: Tyr135, Ser177
17	Spike ectodomain structure (open state)	6VYB	-4.8	0.0	Met740, Tyr741, Gly744, Leu977, Arg1000	0
18	Spike glycoprotein (closed stated)	6VXX	-5.1	0.0	Tyr741, Gly744, Leu966, Leu977, Arg1000	1: Gly744
19	Main protease NSP5	6LU7	-4.4	0.0	His164, Met165, Asn142, Ser144, Gly143, Cys145, His41	5: His164, Asn142, Cys145, Gly143, Ser144

2.III.3 Molecular docking analysis:

2.III.3.1 Preparation of the protein:

Molecular docking is a reliable tool that serves the purpose of finding energy minimization and binding affinity between ligand and protein. Windows 10 Home Single Language operating system (64-bit), installed on a home-built DELL desktop computer, equipped with Intel Core i3-7100 CPU @ 3.90 GHz processor and 4.00 GB memory, was utilized for all computational work. In the current study, SAR-CoVs-2 protein (PDB ID: 6LU7)-ligand interaction is studied by using free AutoDock 4.2 software used for molecular docking studies. First, we chose protein used for favipiravir **L1** ligand studied by Chowdhury et al.[42] and downloaded its pdb file from the main database i.e., Research Collaboratory for Structural Bioinformatics Protein Data Bank (RCSB PDB). The actual pdb file of the protein 6LU7 comes with its co-crystallized inhibitor shown in figure 3, so we removed its inhibitor from the 3D structure of the protein at the starting stage of our docking study. The reason to detach the inhibitor ligand is that it should not block the active site for the next ligand which we are going to incorporate and to result in inaccurate docking results. In order to have an accurate binding site for the protein-ligand interaction, we removed all the Hetatoms (Heteroatoms) present on the protein. The additional polar hydrogens and Kollman charges were added to the protein. The output of the protein structure was later saved as pdbqt format in the folder created for the molecular docking.

Referring to Chowdhurry et al. work, we considered the following parameters used by them in our docking studies such as Grid box coordinate x = -10.729204, y = 12.417653, z = 68.816122 along with grid box parameters 40 X 40 X 40 of the position of the target protein.

Structure of the inhibitor: (*3S,6S,9S,12S,E*)-benzyl 9-isobutyl-6-isopropyl-3-methyl-1-(5-methylisoxazol-3-yl)-1,4,7,10-tetraoxo-12-(((*S*)-2-oxopyrrolidin-3-yl)methyl)-2,5,8,11-tetraazapentadec-13-en-15-oate:

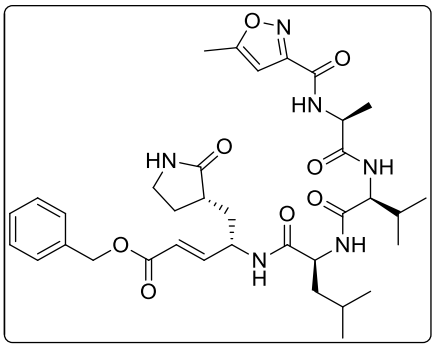

Figure 3. Structure of the inhibitor of 6LU7 protein

2.III.3.2 Interaction of ligands with protein:

The structure of the standard ligand **L1** was taken from PubChem and the pyrrolo[2,1-*a*]isoquinoline compounds (**L2** – **L8)** under considerations were drawn in ChemDraw Ultra 12.0 and were converted to pdb file. Next, the pdb files of the ligand **L1, L2, L3, L4, L5, L6, L7,** and **L8** have been individually converted to pdbqt files in AutoDock 4.2 software. The structure of the ligand **L1** – **L8** is depicted below in figure 4.

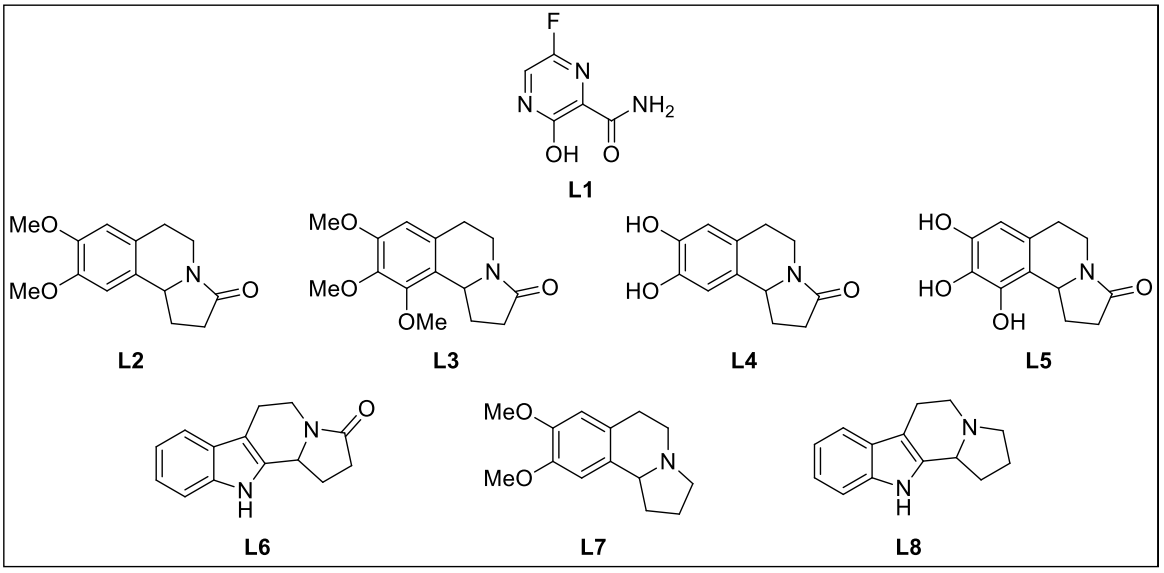

Figure 4. Structures of various ligands used for molecular docking

L1:

With 4 conventional hydrogen bonds and 1 non-conventional hydrogen bond, favipiravir showed favorable activity with the Mpro NSP5 (PDB ID: 6LU7) of COVID-19, with an affinity of -4.35 kcal/mol at 66.11 A° RMSD. It showed strong interaction with the protease in a binding pocket of chain A in the above-mentioned grid box (Fig. 5).

Consequently, this binding interaction results in four conventional hydrogen bonds with the nitrogen of the amide functional group (attached to the pyrazine ring), oxygen (attached to the pyrazine ring), and a nitrogen of the amide functional group within the pyrazine ring with ALA81 (2.11 A°), THR84 (1.92 A°), HIS96 (1.75 A°), and ILE86 (2.03 A°). On the other hand, Fluorine attached to the pyrazine ring showed non-conventional hydrogen bonding with HIS96 (3.08 A°), whereas, no Van der Waal's interaction was observed for **L1** during docking. All the respective interactions is been tabulated in table 2. Since the binding interactions were characterized by 4 conventional hydrogen bonds and 1 non-conventional hydrogen bond these interactions can be considered as a possible mode of binding of ligand **L1** with the Mpro NSP5s of COVID-19.

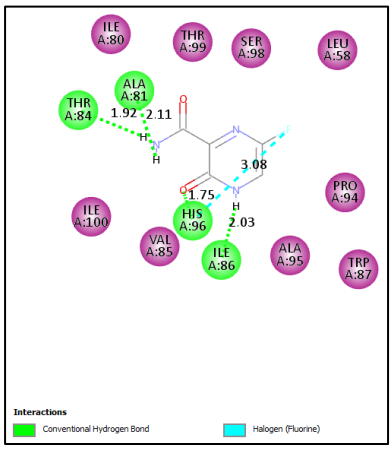

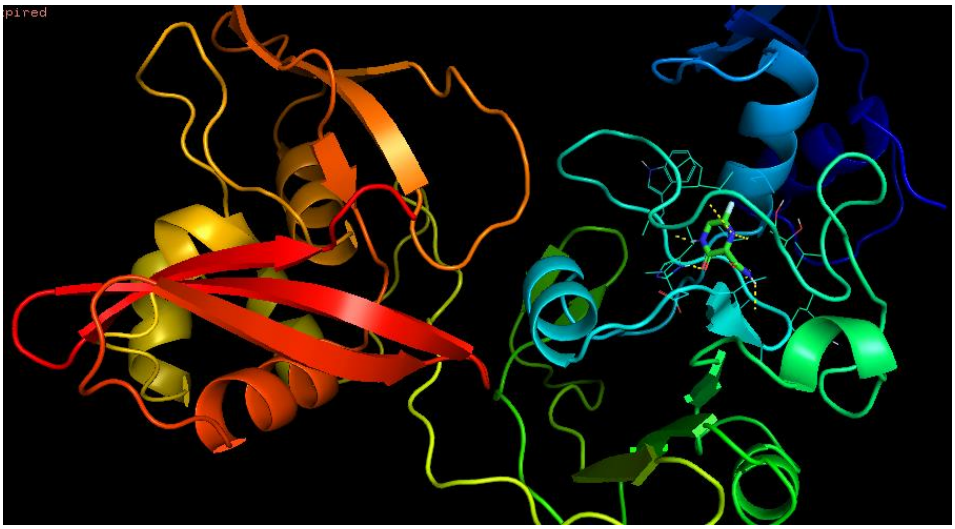

Figure 5. Interaction of L1 with Mpro NSP5 (PDB ID: 6LU7)

L2:

With two conventional hydrogen bonds and one non-conventional hydrogen bonds each, ligand **L2** showed the favorable activity with the Mpro NSP5 (PDB ID: 6LU7) of COVID-

19, with an affinity of -6.20 kcal/mol at 72.33 A° RMSD. It showed strong interaction than **L1** with the protease in a binding pocket of chain A in the above-mentioned grid box (Fig. 6). Consequently, this binding interaction results in two conventional hydrogen bonds with the oxygen of the amide functional group of the pyrrolidone ring, and one of the oxygen of the methoxy group attached to the isoquinoline benzene ring with TYR54 (2.90 A°), GLU166 (2.10 A°), respectively. On the other hand, methyl of the other methoxy group attached to the isoquinoline benzene ring and oxygen of the amide group of pyrrole ring showed non-conventional hydrogen bonding with HIS164 (3.49 A°) and ARG188 (3.18 A°), whereas, it also favored Van der Waal's interaction with PRO52 during docking. All the respective interactions are mentioned in table 2.

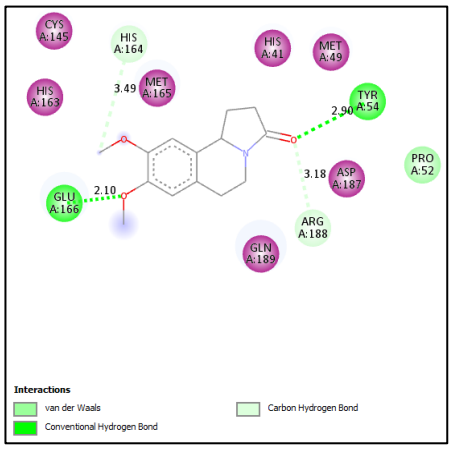

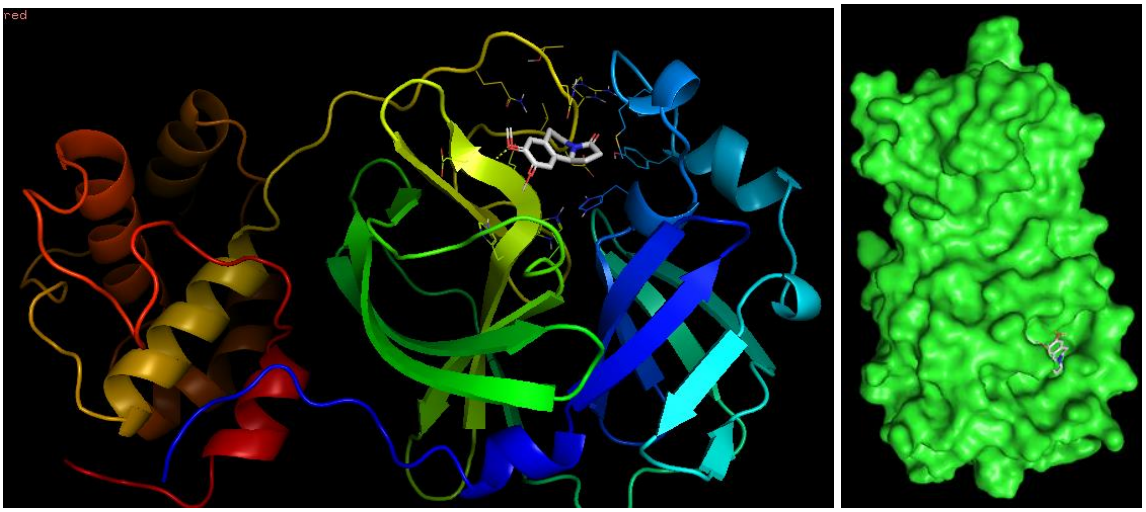

Figure 6. Interaction of L2 with Mpro NSP5 (PDB ID: 6LU7)

L3:

With 3 conventional hydrogen bonds, 2 non-conventional hydrogen bonds, and 1 Van der Waal bonding ligand **L3** showed the favorable activity with the Mpro NSP5 (PDB ID:

6LU7) of COVID-19, with an affinity of -6.20 kcal/mol at 72.00 A° RMSD. It showed strong interaction than **L1** and more or less the same as that to **L2** with the protease in a binding pocket of chain A in the above-mentioned grid box (Fig. 7). Consequently, this binding interaction results in three conventional hydrogen bonds with the oxygen of the amide functional group of the pyrrolidone ring, and two of the oxygen of the methoxy group attached to the isoquinoline benzene ring with TYR54 (3.40 A°), GLU166 (2.10 A°), and CYS145 (3.48 A°) respectively. On the other hand, methyl of the other methoxy group attached to the isoquinoline benzene ring and oxygen of the amide group of pyrrole ring showed non-conventional hydrogen bonding with HIS164 (3.76 A°) and ARG188 (3.00 A°), whereas, it also favored Van der Waal's interaction with PRO52 during docking. All the respective interactions are mentioned in table 2.

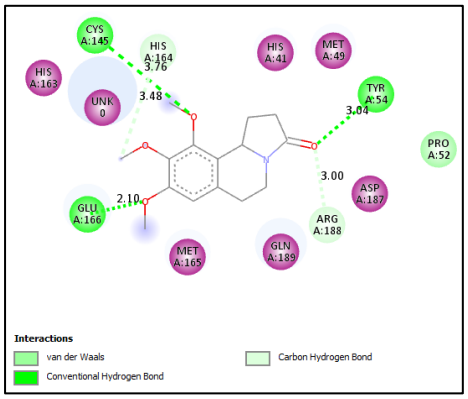

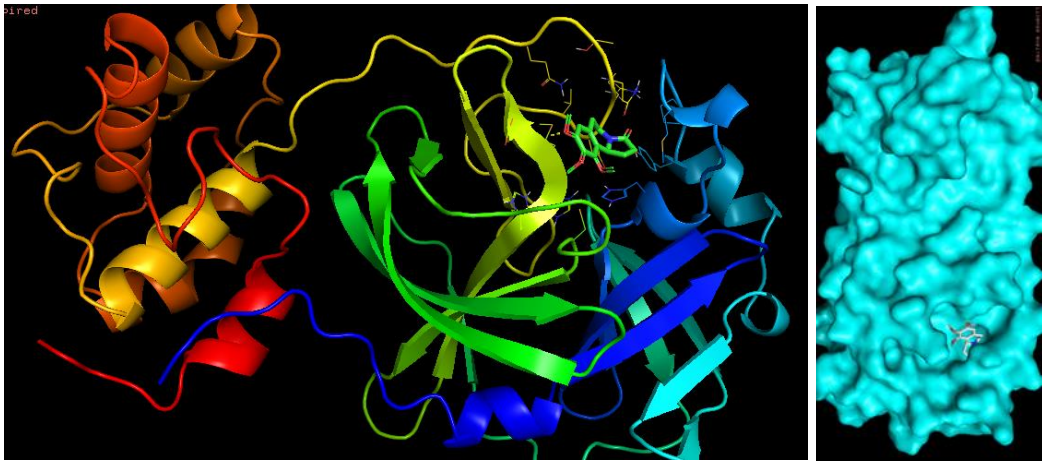

Figure 7. Interaction of L3 with Mpro NSP5 (PDB ID: 6LU7)

L4:

With two conventional hydrogen bonds, one non-conventional hydrogen bond, and one Van der Waal bonding ligand **L4** showed the favorable activity with the Mpro NSP5 (PDB ID: 6LU7) of COVID-19, with an affinity of -6.33 kcal/mol at 72.38 A° RMSD. It showed

strong interaction than **L1**, **L2**, and **L3** with the protease in a binding pocket of chain A in the above-mentioned grid box (Fig. 8). Consequently, this binding interaction results in two conventional hydrogen bonds, both with the hydrogens of the separate hydroxyl groups attached to the isoquinoline benzene ring with GLU166 (1.86 A°), GLU166 (2.10 A°), respectively. On the other hand, methylene group carbon attaching the isoquinoline and pyrrolidone ring along with the amide nitrogen showed non-conventional hydrogen bonding with HIS164 (3.64 A°), whereas, it also favored Van der Waal's interaction with LEU167 during docking. All the respective interactions is been mentioned in table 2.

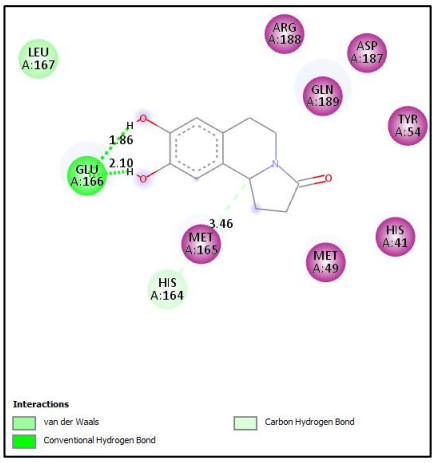

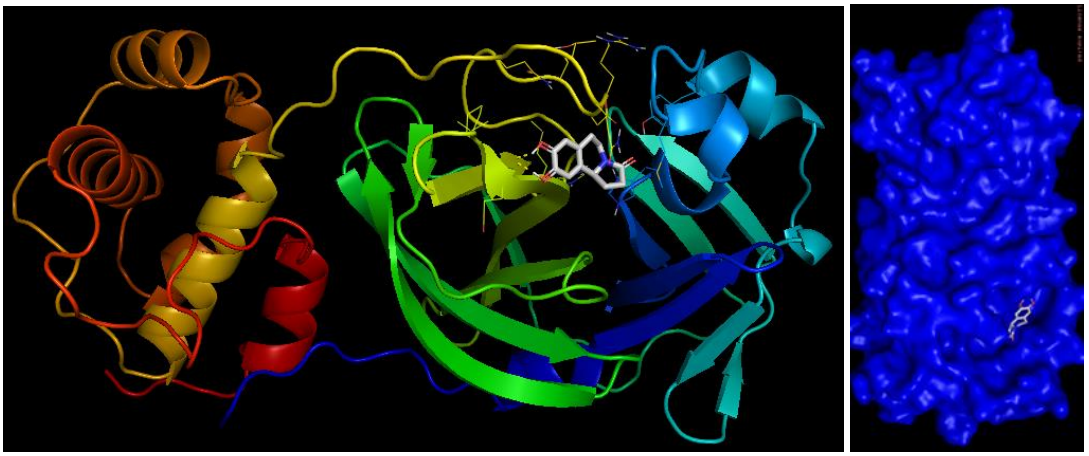

Figure 8. Interaction of L4 with Mpro NSP5 (PDB ID: 6LU7)

L5:

With three conventional hydrogen bonds, one non-conventional hydrogen bond, and one Van der Waal bonding ligand **L5** showed the favorable activity with the Mpro NSP5 (PDB ID: 6LU7) of COVID-19, with an affinity of -6.03 kcal/mol at 72.01 A° RMSD. It showed strong interaction than **L1**, **L2**, and **L3** but a little less than **L4** with the protease in a binding pocket of chain A in the above-mentioned grid box (Fig. 9). Consequently, this

binding interaction results in two conventional hydrogen bonds, all three hydrogens of hydroxyl groups attached to the isoquinoline benzene ring with ARG188 (1.80 A°), ARG188 (2.00 A°), and THR190 (1.97 A°). On the other hand, oxygen of one of the hydroxyl groups attached to isoquinoline benzene showed non-conventional hydrogen bonding with PRO168 (3.33 A°), whereas, it also favored Van der Waal's interaction with LEU167 during docking. All the respective interactions is been mentioned in table 2.

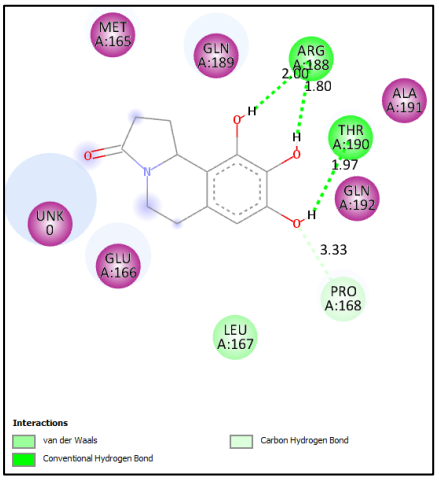

Figure 9. Interaction of L5 with Mpro NSP5 (PDB ID: 6LU7)

L6:

With only one conventional hydrogen bond, and no non-conventional hydrogen bond or Van der Waal bonding ligand, **L6** showed the favorable activity with the Mpro NSP5 (PDB ID: 6LU7) of COVID-19, with an affinity of -7.04 kcal/mol at 72.90 A° RMSD. It showed strong interaction than all other ligands mentioned above with the protease in a binding pocket of chain A in the above-mentioned grid box (Fig. 10). Consequently, this binding

interaction results in one conventional hydrogen bond, with the nitrogen of indole amine group showed with ARG188 (2.04 A^{o}). All the respective interactions is been mentioned in table 2.

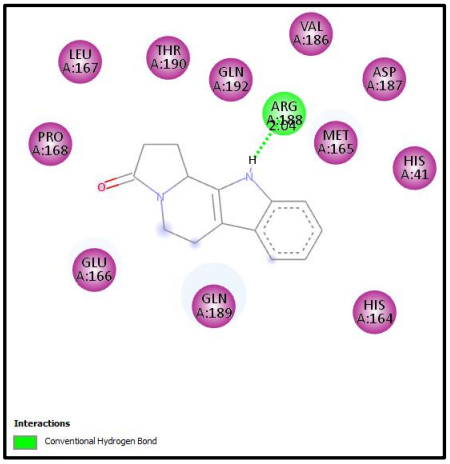

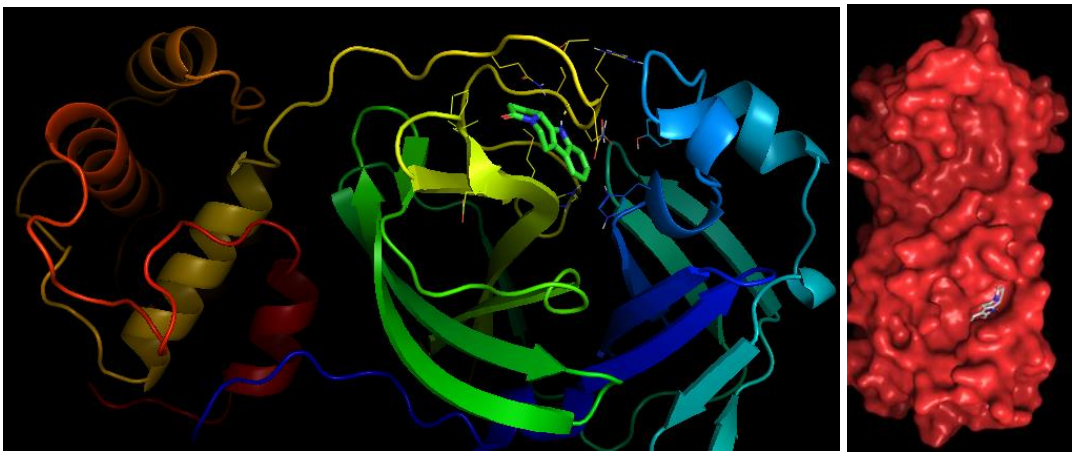

Figure 10. Interaction of L6 with Mpro NSP5 (PDB ID: 6LU7)

L7:

With no conventional hydrogen bonds, non-conventional hydrogen bonds, and three Van der Waal bonding ligand **L7** showed less activity with the Mpro NSP5 (PDB ID: 6LU7) of COVID-19, with an affinity of -3.42 kcal/mol at 73.04 A° RMSD which is lesser than the ligand **L1**. It showed less strong interaction than all other ligands mentioned above with the protease in a binding pocket of chain A in the above-mentioned grid box (Fig. 11). Consequently, this binding interaction results in Van der Waals interaction with GLN189 (4.88 A°), GLU166 (3.02 A°), and GLU166 (3.23 A°) from the whole structure. All the ligand interactions are summarized in table 2.

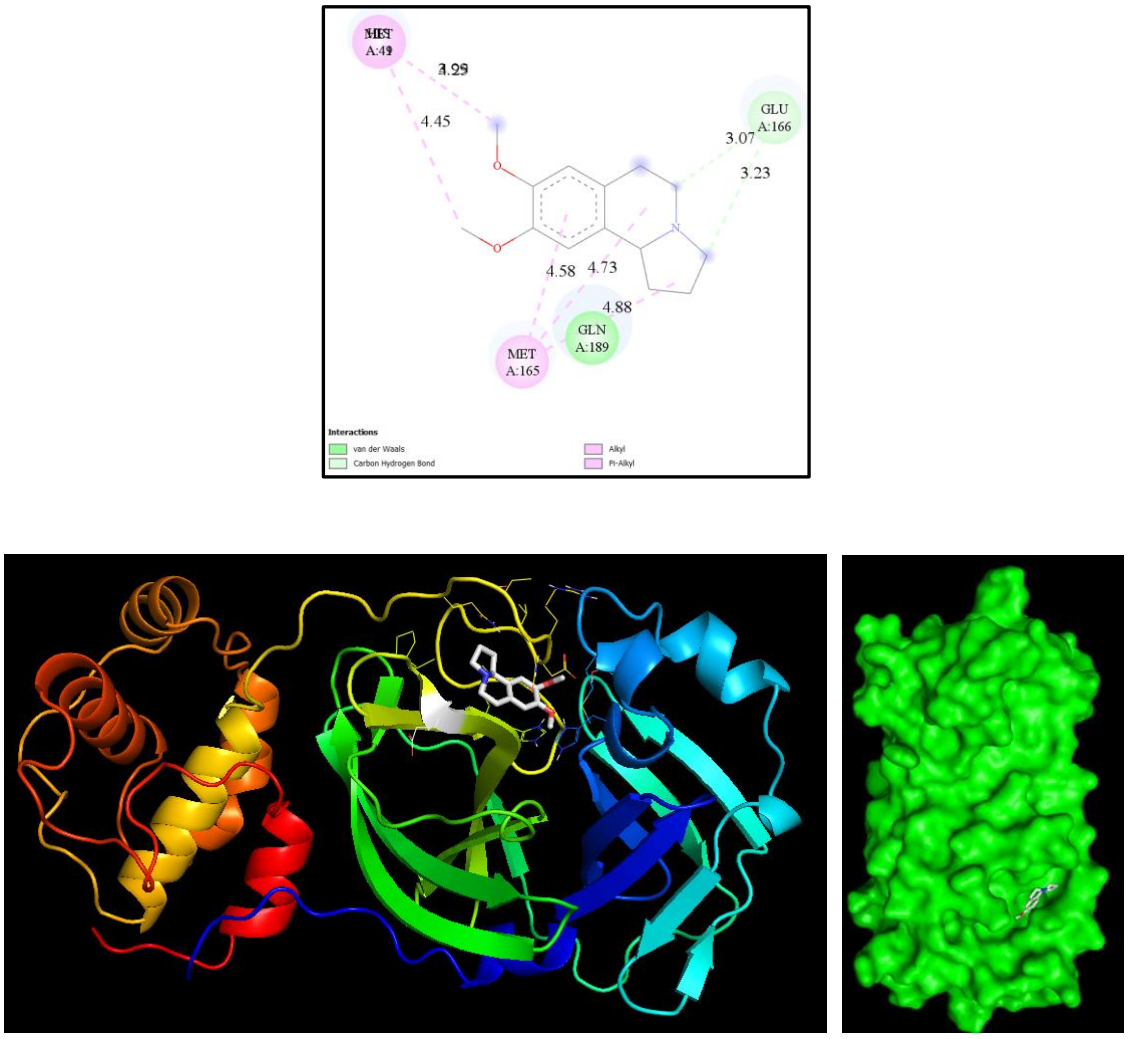

Figure 11. Interaction of L7 with Mpro NSP5 (PDB ID: 6LU7)

L8:

With only one conventional hydrogen bond, five Van der Waal bonding, and no non-conventional hydrogen bonds, ligand **L8** showed the favorable activity with the Mpro NSP5 (PDB ID: 6LU7) of COVID-19, with an affinity of -6.92 kcal/mol at 73.18 A° RMSD. It showed strong interaction than all other ligands except ligand **L6** mentioned above with the protease in a binding pocket of chain A in the above-mentioned grid box (Fig. 12). Consequently, this binding interaction results in one conventional hydrogen bond, with the nitrogen of indole amine group showed with ARG188 (1.94 A^{o}).

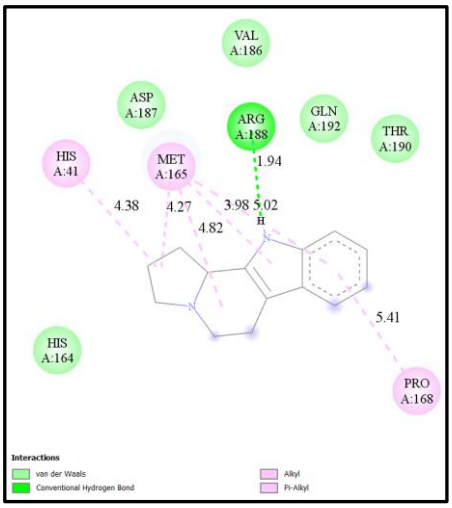

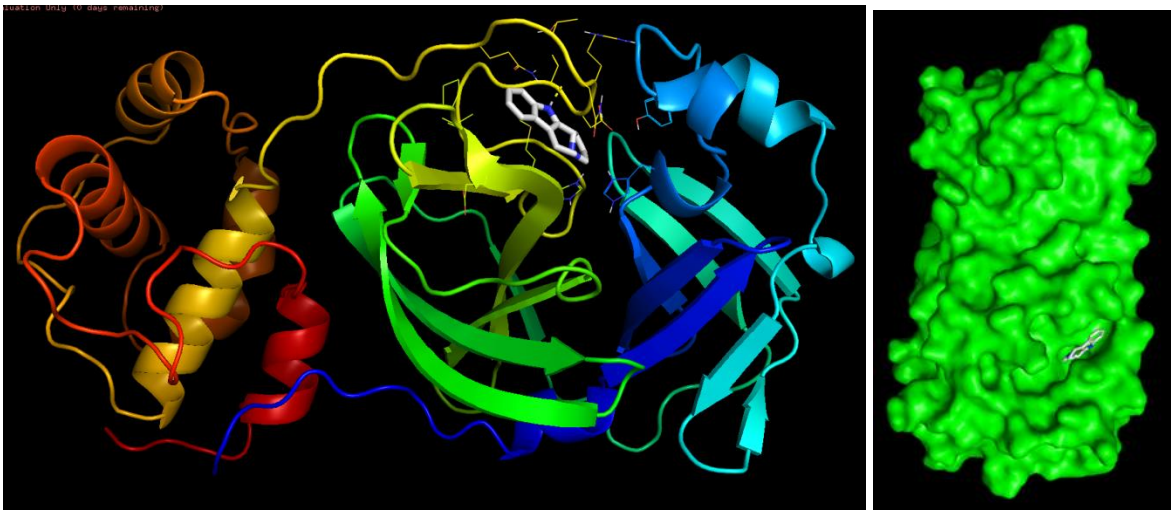

Figure 12. Interaction of L8 with Mpro NSP5 (PDB ID: 6LU7)

Table 2. Molecular docking results of ligands L1-L8 against Mpro NSP5 (PDB ID: 6LU7)

Structure	Docking Score	Reference RMSD (A^o)	Ki (µM)	Interactions		
				Conventional Hydrogen Bonding	Non-Conventional Hydrogen Bonding	Van der Waal Bonding
L1	-4.35	66.11	648.68	ALA81 (2.11 A°)	HIS96 (3.08 A^o)	-
				THR84 (1.92 A^o)		
				HIS96 (1.75 A^o)		
				ILE86 (2.03 A^o)		

L2	-6.20	72.33	28.77	GLU166 (2.10 A^o) TYR54 (2.90 A^o)	HIS164 (3.49A^o) ARG188 (3.18A^o)	PRO52
L3	-6.20	72.00	28.66	CYS145 (3.48 A^o) GLU166 (2.10 A^o) TYR54 (3.40 A^o)	HIS164 (3.76 A^o) ARG188 (3.00 A^o)	PRO52
L4	-6.33	72.38	23.03	GLU166 (1.86 A^o) GLU166 (2.10 A^o)	HIS164 (3.64 A^o)	LEU167
L5	-6.03	72.01	28.66	ARG188 (2.00 A^o) ARG188 (1.80 A^o) THR190 (1.97 A^o)	PRO168 (3.33 A^o)	LEU167
L6	-7.04	72.90	6.86	ARG188 (2.04 A^o)	-	-
L7	-3.42	73.04	3.22 mM	-	-	GLN189 GLU166 GLU166
L8	-6.92	73.18	8.40	ARG188 (1.94 A^o)	-	ASP187 VAL186 GLN 192 THR190 HIS164

2.III.4 Conclusion:

Our present work represents the *insilico* molecular docking studies of pyrrolo[2,1-*a*]isoquinoline compounds against the Main protease NSP5 (PDB ID: 6LU7) of SARS-CoV-2 virus. A repurposed drug like favipiravir, which shows greater activity for influenza has gathered too much attention recently against COVID-19. It has shown binding energy of 4.35 Kcal/mol against 6LU7 which matches with the previously published works. Our compounds mentioned as **L2-L8** have shown excellent activities against 6LU7 in molecular docking studies. Further, in vitro and in vivo studies are needed to establish the efficacy of these products.

2.III.5 References:

1) Maxmen, A.; Mallapaty, S. *Nature* **2021**, *594*, 313.
2) Cui, J.; Li, F.; Shi, Z. L. *Nat. Rev. Microbiol.* **2019**, *17*, 181.
3) Stadler, K.; Masignani, V.; Eickmann, M.; Becker, S.; Abrignani, S.; Klenk, H. D.; Rappuoli, R. *Nat. Rev. Microbiol.* **2003**, *1*, 209.
4) Zhou, Y.; Yang, Y.; Huang, J.; Jiang, S.; Du, L. *Viruses* **2019**, *11*, E60.
5) Gil, C.; Ginex, T.; Maestro, I.; Nozal, V.; Barrado-Gil, L.; Cuesta-Geijo, M. Á.; Urquiza, J.; Ramírez, D.; Alonso, C.; Campillo, N. E.; Martinez, A. *J. Med. Chem.* **2020**, *63*, 12359.
6) Gallagher, T. M.; Buchmeier, M. J. *Virology* **2001**, *279*, 371.
7) Castaño-Rodriguez, C.; Honrubia, J. M.; Gutierrez-Alvarez, J.; DeDiego, M. L.; Nieto-Torres, J. L.; Jimenez-Guardeno, J. M.; Regla- Nava, J. A.; Fernandez-Delgado, R.; Verdia-Baguena, C.; Queralt-Martin, M.; Kochan, G.; Perlman, S.; Aguilella, V. M.; Sola, I.; Enjuanes, L. *mBio* **2018**, *9*, e02325.
8) Neuman, B. W.; Kiss, G.; Kunding, A. H.; Bhella, D.; Baksh, M. F.; Connelly, S.; Droese, B.; Klaus, J. P.; Makino, S.; Sawicki, S. G.; Siddell, S. G.; Stamou, D. G.; Wilson, I. A.; Kuhn, P.; Buchmeier, M. J. *J. Struct. Biol.* **2011**, *174*, 11.
9) McBride, R.; van Zyl, M.; Fielding, B. C. *Viruses* **2014**, *6*, 2991.
10) Gupta, M. K.; Vemula, S.; Donde, R.; Gouda, G.; Behera, L.; Vadde, R. *J. Biomol. Struct. Dyn.* **2021**, *39*, 2617.
11) Dong, S.; Sun, J.; Mao, Z.; Wang, L.; Lu, Y. L.; Li, J. *J. Med. Virol.* **2020**.
12) Qinfen, Z.; Jinming, C.; Xiaojun, H.; Huanying, Z.; Jicheng, H.; Ling, F.; Kunpeng, L.; Jingqiang, Z. *J. Med. Virol.* **2004**, *73*, 332.
13) Ng, M. L.; Tan, S. H.; See, E. E.; Ooi, E. E.; Ling, A. E. *J. Med. Virol.* **2003**, *71*, 323.
14) Wang, H.; Yang, P.; Liu, K.; Guo, F.; Zhang, Y.; Zhang, G.; Jiang, C. *Cell Res.* **2008**, *18*, 290.
15) Drosten, C.; Gunther, S.; Preiser, W.; van der Werf, S.; Brodt, H. R.; Becker, S.; Rabenau, H.; Panning, M.; Kolesnikova, L.; Fouchier, R. A.; Berger, A.; Burguiere, A. M.; Cinatl, J.; Eickmann, M.; Escriou, N.; Grywna, K.; Kramme, S.; Manuguerra, J. C.; Muller, S.; Rickerts, V.; Sturmer, M.; Vieth, S.; Klenk, H. D.; Osterhaus, A. D.; Schmitz, H.; Doerr, H. W. *N. Engl. J. Med.* **2003**, *348*, 1967.

16) Ksiazek, T. G.; Erdman, D.; Goldsmith, C. S.; Zaki, S. R.; Peret, T.; Emery, S.; Tong, S.; Urbani, C.; Comer, J. A.; Lim, W.; Rollin, P. E.; Dowell, S. F.; Ling, A.-E.; Humphrey, C. D.; Shieh, W.-J.; Guarner, J.; Paddock, C. D.; Rota, P.; Fields, B.; DeRisi, J.; Yang, J.-Y.; Cox, N.; Hughes, J. M.; LeDuc, J. W.; Bellini, W. J.; Anderson, L. J. *N. Engl. J. Med.* **2003**, *348*, 1953.

17) Zaki, A. M.; van Boheemen, S.; Bestebroer, T. M.; Osterhaus, A. D.; Fouchier, R. A. *N. Engl. J. Med.* **2012**, *367*, 1814.

18) Millet, J. K.; Whittaker, G. R. *Proc. Natl. Acad. Sci. U. S. A.* **2014**, *111*, 15214.

19) Bertram, S.; Dijkman, R.; Habjan, M.; Heurich, A.; Gierer, S.; Glowacka, I.; Welsch, K.; Winkler, M.; Schneider, H.; Hofmann-Winkler, H.; Thiel, V.; Pohlmann, S. *J. Virol* **2013**, *87*, 6150.

20) Bertram, S.; Glowacka, I.; Muller, M. A.; Lavender, H.; Gnirss, K.; Nehlmeier, I.; Niemeyer, D.; He, Y.; Simmons, G.; Drosten, C.; Soilleux, E. J.; Jahn, O.; Steffen, I.; Pohlmann, S. *J. Virol* **2011**, *85*, 13363.

21) Gierer, S.; Bertram, S.; Kaup, F.; Wrensch, F.; Heurich, A.; Kramer-Kuhl, A.; Welsch, K.; Winkler, M.; Meyer, B.; Drosten, C.; Dittmer, U.; von Hahn, T.; Simmons, G.; Hofmann, H.; Pohlmann, S. *J. Virol* **2013**, *87*, 5502.

22) Shirato, K.; Kawase, M.; Matsuyama, S. *J. Virol.* **2013**, *87*, 12552.

23) Shirogane, Y.; Takeda, M.; Iwasaki, M.; Ishiguro, N.; Takeuchi, H.; Nakatsu, Y.; Tahara, M.; Kikuta, H.; Yanagi, Y. *J. Virol.* **2008**, *82*, 8942.

24) Park, J. E.; Li, K.; Barlan, A.; Fehr, A. R.; Perlman, S.; McCray, P. B., Jr.; Gallagher, T. *Proc. Natl. Acad. Sci. U. S. A.* **2016**, *113*, 12262.

25) Ou, X.; Liu, Y.; Lei, X.; Li, P.; Mi, D.; Ren, L.; Guo, L.; Guo, R.; Chen, T.; Hu, J.; Xiang, Z.; Mu, Z.; Chen, X.; Chen, J.; Hu, K.; Jin, Q.; Wang, J.; Qian, Z. *Nat. Commun.* **2020**, *11*, 1620.

26) Nelson, E. A.; Dyall, J.; Hoenen, T.; Barnes, A. B.; Zhou, H.; Liang, J. Y.; Michelotti, J.; Dewey, W. H.; DeWald, L. E.; Bennett, R. S.; Morris, P. J.; Guha, R.; Klumpp-Thomas, C.; McKnight, C.; Chen, Y. C.; Xu, X.; Wang, A.; Hughes, E.; Martin, S.; Thomas, C.; Jahrling, P. B.; Hensley, L. E.; Olinger, G. G., Jr.; White, J. M. *PLoS Neglected Trop. Dis.* **2017**, *11*, e0005540.

27) Cuesta-Geijo, M. A.; Galindo, I.; Hernaez, B.; Quetglas, J. I.; Dalmau-Mena, I.; Alonso, C. *PLoS One* **2012**, *7*, e48853.

28) Qiu, S.; Leung, A.; Bo, Y.; Kozak, R. A.; Anand, S. P.; Warkentin, C.; Salambanga, F. D. R.; Cui, J.; Kobinger, G.; Kobasa, D.; Cote, M. *Virology* **2018**, *513*, 17.

29) V'Kovski, P.; Gerber, M.; Kelly, J.; Pfaender, S.; Ebert, N.; Braga Lagache, S.; Simillion, C.; Portmann, J.; Stalder, H.; Gaschen, V.; Bruggmann, R.; Stoffel, M. H.; Heller, M.; Dijkman, R.; Thiel, V. *eLife* **2019**, *8*, e42037.

30) McBride, C. E.; Li, J.; Machamer, C. E. J. *Virol.* **2007**, *81*, 2418.

31) Brown, D. *Encyclopedia of herbs and their uses*, 1st ed.; Houghton Mifflin, **1995**.

32) Furuta, Y.; Takahashi, K.; Shiraki, K.; Sakamoto, K.; Smee, D. F.; Barnard, D. L.; Gowen, B. B.; Julander, J. G.; Morrey, J. D. *Antiviral. Res.* **2009**, *82*, 95.

33) Krafts, K.; Hempelmann, E.; Stania, A. S. *Parasitol. Res.* **2012**, *111*, 1.

34) Shiraki, K.; Daikoku, T. *Pharmacol. Ther*. **2020**, *209*, 107512.

35) Furuta, Y.; Takahashi, K.; Shiraki, K.; Sakamoto, K.; Smee, D. F.; Barnard, D. L.; Gowen, B. B.; Julander, J. G.; Morrey, J. D. *Antivir. Res*. **2009**, *82*, 95.

36) Jin, Z.; Smith, L. K.; Rajwanshi, V. K.; Kim, B.; Deval, J. *PLoS ONE* **2013**, *8*, e68347.

37) Toots, M.; Yoon, J. J.; Cox, R. M.; Hart, M.; Sticher, Z. M.; Makhsous, N. *Sci. Transl. Med*. **2019**, *11*, eaax5866.

38) Toots, M.; Yoon, J. J.; Hart, M.; Natchus, M. G.; Painter, G. R.; Plemper, R. K. *Transl. Res.* **2020**, *218*, 16.

39) Cox, R. M.; Wolf J. D.; Plemper, R. K. *Nat. Microbiol.* **2021**, *6***,** 11.

40) Warren, T. K.; Jordan, R.; Lo, M. K.; Ray, A. S.; Mackman, R. L.; Soloveva, V. *Nature*. **2016**, *531*, 381.

41) Skariyachan, S.; Gopal, D.; Chakrabarti, S.; Kempanna, P.; Uttarkar, A.; Muddebihalkar, A. G.; Niranjan, V. *Comput. Biol. Med.* **2020**, *126*, 104054.

42) Yadav, P.; Rana, M.; Chowdhury, P. *J. Mol. Struct*. **2021**, *1246*, 131253.

Chapter 3

Oxidative cleavage of the C–N bond of aryl and heteroaryl (dimethylamino)methyl groups into aldehydes

3.1 Introduction:

Carbonyl compounds are precursors for a wide range of agrochemicals, pharmaceuticals, fine chemicals, vitamins, and fragrances.

Indole scaffolds are widely distributed in nature. Parent indole is a naturally occurring compound prepared mainly by a variety of bacteria.[1] Also, some plants have yielded indole, usually in small amounts, mainly as a byproduct of its substituted derivatives upon extraction. Robinia pseudocacia,[2] the jasmines,[3] certain citrus plants,[4] and orange blossoms[5] produce indole. In the animal body, indole is found wherever puss formation occurs,[6] in the liver,[7] brain,[8] and bile.[9] Production of the handful of indole from natural resources is harrowing without harming nature. Scientist across the globe has evolved with many strategies for the large-scale production of indole surrogates from easily accessible chemicals. Baeyer[10] first achieved laboratory preparation of indole from indigo in 1868. Over the decades, many researchers came up with many indole syntheses, until in 1883, Fischer and Jourden[11] showed an efficient large scalable synthesis of (2-phenyl)indole from phenylhydrazine and acetophenone. Carbonyl functionalization of indole compounds is critical for synthesizing naturally occurring bioactive molecules. Amongst the carbonyl compounds of indole, indole-3-carboxaldehyde can be distinguished as a vital synthon for the above purpose. Indole-3-carboxaldehyde is a naturally occurring compound found in tomato seedling, pea seedling, barley, lupine, cabbage, and cotton.[12] It is an essential building block for the synthesis of many natural and synthetic biologically active compounds, especially antitumor (camalexin,[13] coscinamide,[14] hyrtiosin B,[15] topsentin B1-B2,[16] convolutamydine A,[17] isoaplysin A[18]), antidepressant (α-methyltryptamine),[19] antimicrobial (phytoalexins: brassinin and cyclobrassinin),[20] antiviral (chondramide A),[21] anthelmintic (chondramide C),[22] monoamine oxidase inhibitor (aplysinopin),[23] antiplasmodial (isocryptolepine),[24] antifungal (phytoalexins: caulilexins A–C),[25] DNA replication and transcription inhibitor (cryptosanginolentine),[26] and muscle relaxant (α,β-cyclopiazonic acid)[27] agents (Figure 1).

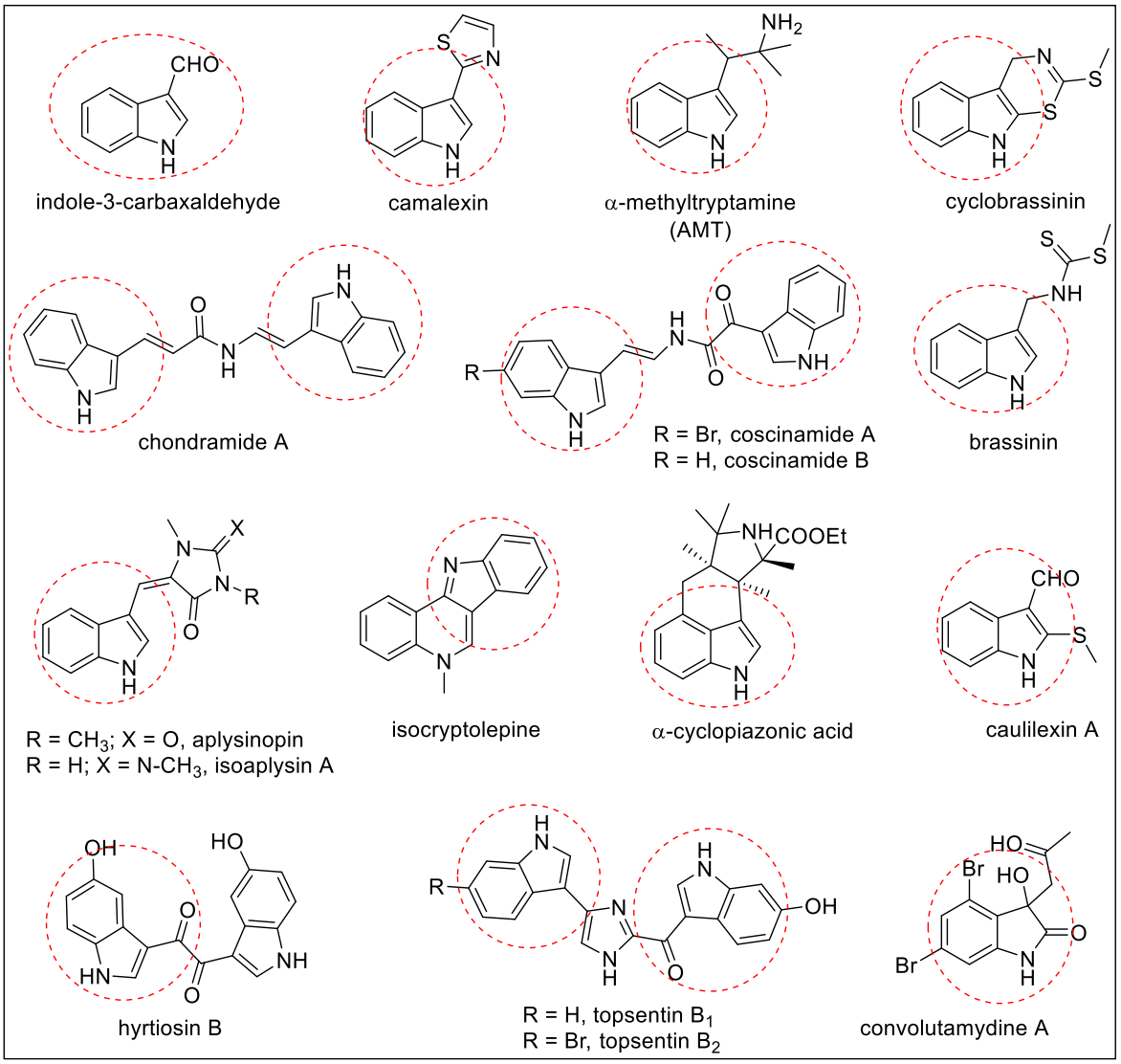

Figure 1. Essential bioactive natural products having indole core

3.2 Literature review:

Over the years, scientists have developed many strategies to introduce carbonyl groups to indole bearing different substituents. The conventional ways involve the reaction of indoles with phosphorous oxychloride/dimethylformamide mixture (Vilsmeier–Haack reaction),[28] dichloromethyl methyl ether/titanium tetrachloride (Rieche's reaction),[29] hexamine/mild acid (Duff's reaction),[30] and chloroform/sodium hydroxide mixture (Reimer–Tiemann reaction).[31] Due to their harsh reaction conditions, low selectivity, and poor functional group compatibility, chemists have developed mild, effective, and regioselective carbonylation of indoles.

The following literature survey is sectioned depending upon the types of synthons used to

construct the aldehyde group.

3.2.1 Oxidation of alcohols to aldehydes:

Many strategies have emerged in past years to synthesize aryl and heteroaryl aldehydes using hitherto developed catalysts. Scientists have shown synthesis and applicative studies of various transition metal catalysts to transform alcohol functional groups to aldehydes (Table 1, entries 1, 2, 3, 5, 6, 7, 8, 10, 11). Even simple hypervalent iodine reagents with strong acid have been employed (Table 1, entry 13). Photocatalytic reagents like 9-fluorenone (Table 1, entry 9) and Rose Bengal (Table 1, entry 12) have also been utilized to construct the aldehyde group from alcohols.

Table 1. Transformation of alcohols to aldehydes using unconventional methods

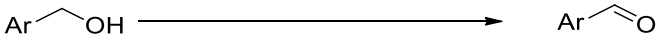

Entry	Reaction conditons	Examples	Yields	Reference
1	2 mol% Cu(BPYDCE)$(OAc)_2$, TEMPO, base free, air, 30 ^oC Cu(BPYDCE)$(OAc)_2$= 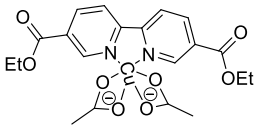	20 examples	>99%	Mei et al. [32]
2	20 mol% cellulose-Cu-nano catalyst, H_2O (3.5 mL)/CH_3CN (1.5 mL), microwave	19 examples	0 – 94%	Baruah et al. [33]
3	5 mol% $Cu(MeCN)_4OTf$, 5 mol% ^{OMe}bpy, 1 mol% ABN, 10 mol% NMI, MeCN, air, rt, 1 h	37 examples	30 – 98%	Steve et al. [34]
4	$FeCl_3$, ligand, H_2O_2, H_2O, rt, Ligand = 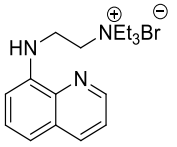	22 examples	Trace to 94%	Yan et al. [35]
5	1 mol% $Cu(OAc)_2$, 1 mol% TEMPO, CH_3CN/H_2O, air, rt	38 examples	81-96%	Jiang et al. [36]
6	*Condition 1*: 0.25 mol% $Co_2Mn_3O_8$, toluene, air, 130 ^oC *Condition 2*: 0.05 mol% $Co_2Mn_3O_8$, toluene, H_2O_2, 130 ^oC	15 examples 9 examples	30-88% 72-95%	Sarmah et al. [37]

7	1 mol% $K_2OsO_4.2H_2O$, 3 equiv $K_3[Fe(CN)_6]$, 3 equiv K_2CO_3, $CH_3CN:H_2O$ (1:1), 60 ^oC	45 examples	Trace to 98%	Fernandes et al. [38]
8	9-Fluorenone, air/O_2, DMSO, rt, blue LED	23 examples 33 examples	61-95% 59-99%	Zhang et al. [39] Schilling et al. [40]
9	5 mol% CuBr, 5 mol% ligand, 5 mol% TEMPO, H_2O, air, rt Ligand= 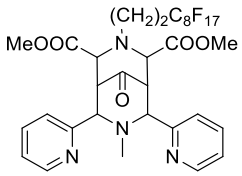	21 examples	59-96%	Ang et al. [41]
10	*Condition 1*: Fe_3O4-LD-Cu nanocatalyst, air, 25-30 ^oC, 5 h *Condition 2*: Fe_3O_4-LD-Cu nanocatalyst, 30% H_2O_2, 70 ^oC, 5 h Fe_3O_4-LD-Cu= 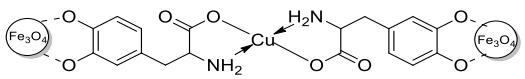	13 examples	50-55% 87-90%	Rathore et al. [42]
11	5 mol% Rose Bengal, 3 equiv NH_4SCN, O_2, CH_3CN, *hv* (23WCFL lamp), 20 h	24 examples	100%	Sheriff et al. [43]
12	1.1 equiv IBX, 5 mol% TfOH, dioxane, rt	21 examples	75-99%	Kumar et al. [44]
13	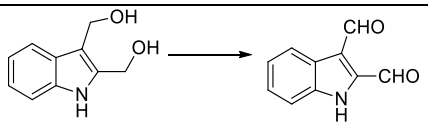 MnO_2/C, THF, 48 h	1 example	20%	Misztal et al. [45]

3.2.2 Preparation of aldehydes from *α*-oxo carboxylic acids:

Chuang and co-workers[46] have developed a simple method for synthesizing aldehydes from *α*-oxocarboxylic acids *via* decarboxylation using PPh_3 and Et_3N in heating conditions (Scheme 1). *α*-Oxocarboxylic acids containing electron-donating and withdrawing groups on aryl and heteroaryl and alkyl moieties have been transformed into corresponding aldehydes. The one-pot synthesis of deuterated aldehydes using D_2O as a deuterium source is also utilized to synthesize 11 examples in good yields.

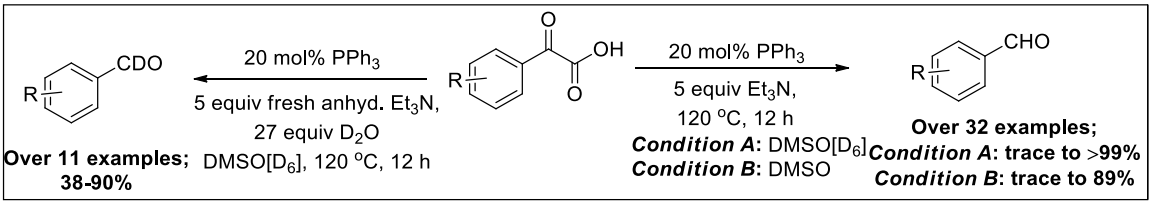

Scheme 1. Conversion of *α*-oxocarboxylic acids into aldehydes

Wu and co-workers[47] have shown intermolecular dehydrogenative–decarboxylative coupling of indoles with glyoxylic acid to form aldehydes without forming *N*-formylation product (Scheme 2). They have employed Cu, Ni, and Fe catalysts in the presence of sodium acetate and silver carbonate bases in heating DMSO conditions. A library of indoles was converted into the corresponding 3-formylindoles in moderate to good yields with excellent functional group tolerance.

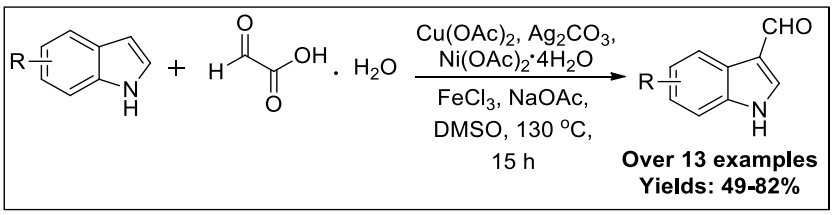

Scheme 2. Synthesis of indole-3-carobxaldehyde using intermolecular dehydrogenative–decarboxylative coupling of indoles with glyoxylic acid

Wang's team[48] has reported a novel organocatalytic strategy for the formylation of aryl and heteroaryl boronic acids (Scheme 3). An engineering between aryl boronic acids, amines, and glyoxylic acid to form α-amino acid forming *via* Petasis reaction helped to synthesize aldehydes.

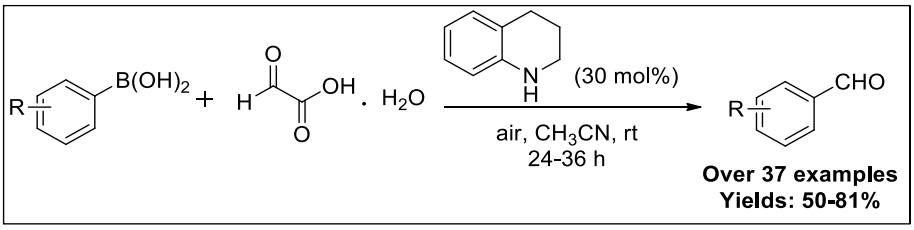

Scheme 3. Formylation of aryl and heteroaryl boronic acids using organocatalyst

3.2.3 Preparation of aldehydes by C-S bond cleavage:

Bonesi et al.[49] have developed a mild synthesis of aldehydes and ketones from the

corresponding benzyl ethyl sulfides in aprotic solvents *via* photosensitized oxidation using sensitizer-like triphenylporphine and Rose Bengal (Scheme 4).

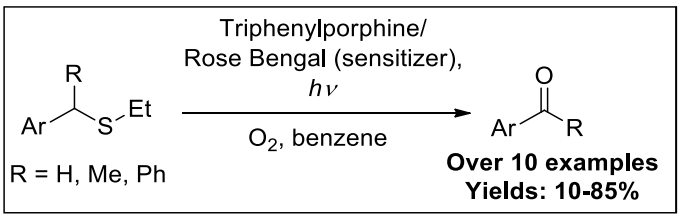

Scheme 4. Photosentisitized oxidative synthesis of aldehydes and ketones from the benzyl ethyl sulfides

Cheng et al.[50] have reported NH_4OAc promoted formylation of indole in DMSO:H_2O solvent mixture, wherein DMSO act as a carbon source for the formylation reaction (Scheme 5). The involvement of the Pummerer reaction is proposed by doing a mechanistic study with the employment of a series of reactions.

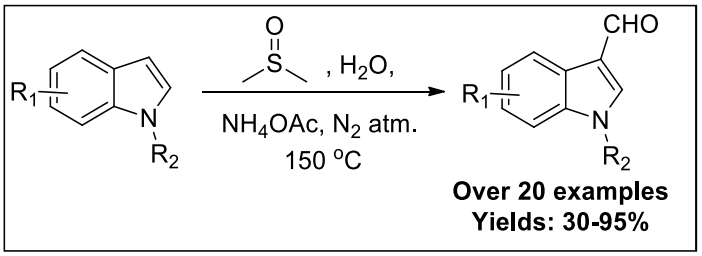

Scheme 5. Formylation of indole derivatives using DMSO as carbon source

Kuhkarna's team[51] has shown the surreal use of difluoro(phenylsulfanyl)methane ($PhSCF_2H$) to undergo $SnCl_4$ mediated reaction with aromatic compounds leading to the formation of the aromatic aldehydes in good to excellent yields (Scheme 6). They have provided the analytical evidence for the formation of a thionium intermediate through NMR and TD-DFT studies. The reaction is even suitable for the synthesis of aromatic aldehydes containing electron-withdrawing groups like esters.

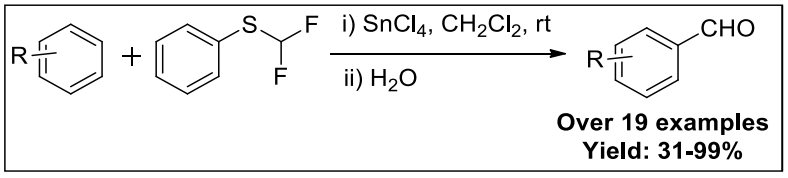

Scheme 6. Synthesis of aromatic aldehydes using $SnCl_4$ and difluoro(phenylsulfanyl)methane

Cui and co-workers[52] have developed an efficient method for the formylation of pyrroloisoquinolines using bromoisobutyrate and dimethyl sulfoxide as carbonyl reagents. Numerous pyrroloisoquinoline aldehydes have been prepared in good yields with excellent functional group tolerance.

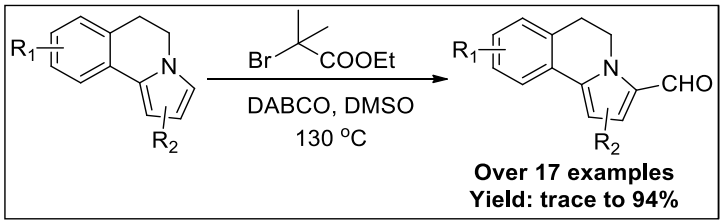

Scheme 7. Formylation of pyrroloisoquinolines using bromoisobutyrate and dimethyl sulfoxide

3.2.4 Synthesis of aldehyde from various amine and amides:

3.2.4.1 Use of HMTA as carbonyl source:

Wang et al.[53a] has developed efficient iodine catalyzed chemoselective formylation of indole moieties using HMTA as a carbonyl source in the presence of activated carbon (Scheme 8). Whereas, Sakee and co-workers[53b] have shown the use of HMTA and silica-supported ceric ammonium nitrate (CAN–SiO_2) for the formylation of indole compounds (Scheme 8).

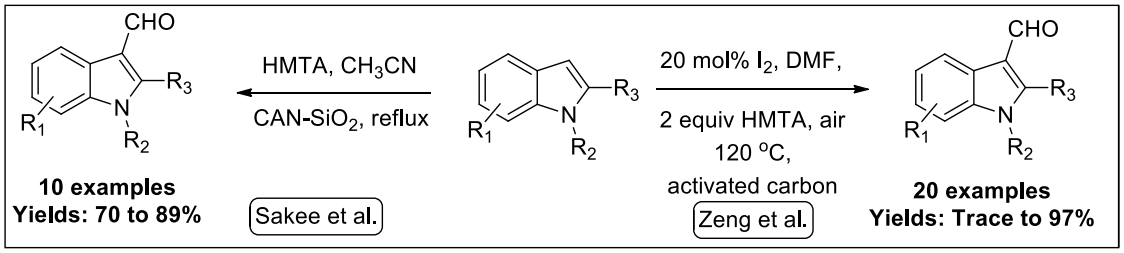

Scheme 8. Iodine catalyzed chemoselective formylation of indole moieties using HMTA

3.2.4.2 Use of TMEDA as carbonyl source:

This group of literature methods focuses on using TMEDA (tetramethylethylenediamine) as a carbon source for formylation reaction.

Xiang Li et al.[54] have developed an aerobic visible-light-mediated C-3 formylation reaction of indole catalyzed by Rose Bengal in the presence of potassium iodide (Scheme 9). The

one-pot synthesis of C3-formyl indole derivatives *via* C-N bond cleavage under visible light gave access to synthesize a variety of derivatives. The reaction shows excellent functional group tolerance.

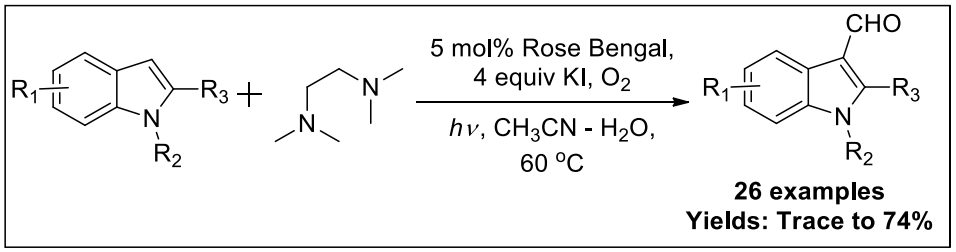

Scheme 9. Rose Bengal catalyzed C-3 formylation reaction of indole derivatives

Zhang and co-workers[55] have achieved an aerobic $CuCl_2$ catalyzed formylation of indole derivatives having various aryl groups under mild conditions (Scheme 10). Syntheses of indole-3-carboxaldehyde derivatives are achieved with excellent regioselectivity and good yield.

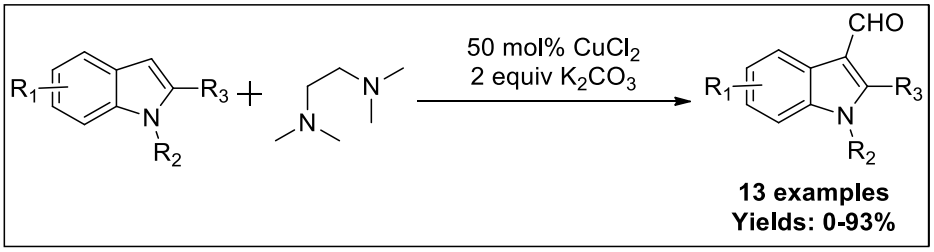

Scheme 10. $CuCl_2$ catalyzed formylation of indole

Two groups from China province have worked on the construction of C-C bonds to form indole-3-carboxaldehyde derivatives using iodine reagent. Liu's group[56] has developed a method for the C3-formylation reaction of indoles with TMEDA as carbon source using an excess of molecular iodine and base, under an oxygen atmosphere in 1,4-dioxane at 100 °C temperature. They have introduced a formyl group on around 28 various indoles derivatives in moderate to good yields. On the other hand, Cai's group[57] has worked on molecular iodine catalyzed aerobic formylation reaction of indoles with TMEDA in DMF at 100 °C. They have achieved the synthesis of 19 indole-3-carboxaldehyde derivatives in good yields. Moreover, the effect of solvent in both the transformation indicates the in situ generations of iminium ion source generated from TMEDA with and without base (Scheme 11).

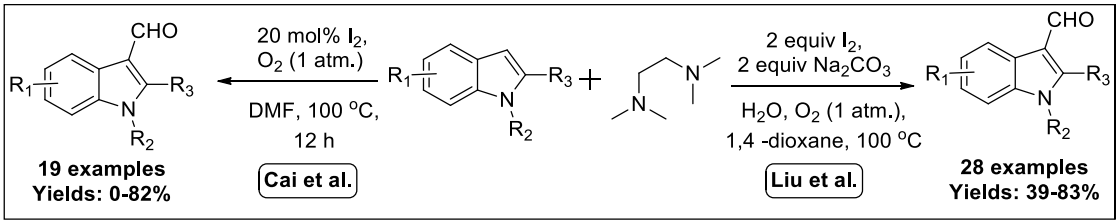

Scheme 11. Molecular iodine mediated construction of C-C bonds to form indole-3-carboxaldehyde derivatives

Cheng et al.[58] have reported a copper-catalyzed formylation reaction on indole derivatives by employing molecular oxygen as the suitable oxidant (Scheme 12).

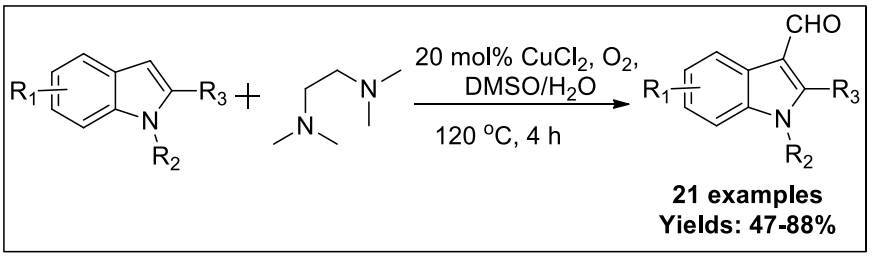

Scheme 12. Copper chloride catalyzed formylation reaction on indole derivatives

Indoles were formylated at the C-3 position with an iminium ion source generated from TMEDA and later with the attack of water to furnish the carbonyl entity. Their method shows good functional group tolerance along with overall moderate to good yields of the derivatives.

An organic photocatalyst is employed by Yu et al.[59] to carry out the transition metal-free, formylation of indoles (Scheme 13). A series of carbazole-derived highly conjugated microporous polymers (CMPs) with tunable redox potentials have been studied and their photocatalytic activity for the C-3 formylation and thiocyanation of indoles have been explored using TMEDA as carbon source and KSCN as cyanide source, respectively. Likewise, 16 such substituted indole-3-carboxaldehyde derivatives have been prepared.

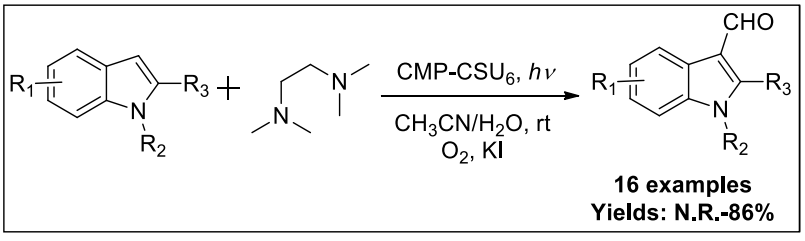

Scheme 13. C-3 formylation of indoles using carbazole-derived microporous photocatalyst

A temperature-dependent new domino trifluoromethylation-cyclization method for the preparation of 2-(trifluoromethyl) indoles and 3-formyl-2-(trifluoromethyl)-indoles using easily accessible 2-alkynylanilines and $CuCF_3$/TMEDA reagent is been established by Tsui et al. (Scheme 14).[60] The domino trifluoromethlaytion-cyclization-formylation reaction favors at a higher temperature of 80 °C, whereas the trifluoromethylation-cyclization is achieved at room temperature. The method provides a variety of trifluoromethylated indoles and indole-3-carboxaldehyde proxies in excellent yields.

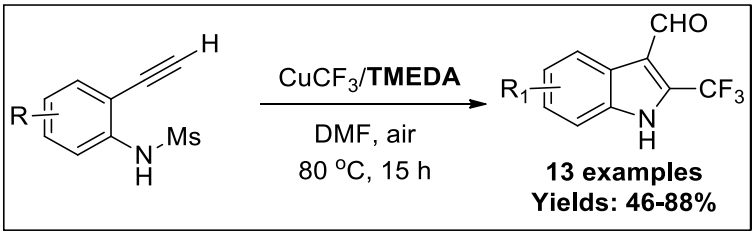

Scheme 14. Preparation of 3-formyl-2-(trifluoromethyl)-indoles using $CuCF_3$/TMEDA reagent

3.2.4.3 Use of 2-(dimethylamino)ethanol as carbonyl source:

Ma et al.[61] have reported the selective syntheses of bisindolyl methane and 3-formylindole derivatives using an *N*,*N*-dimethylethanolamine as a new carbon source, catalyzed by $CuCl_2$ and $CoCl_2$, respectively under mildly acidic conditions (Scheme 15).

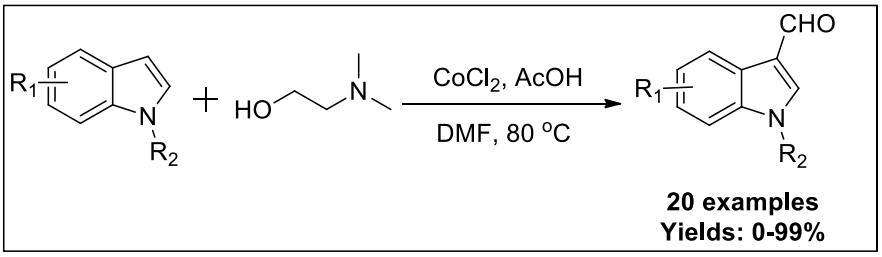

Scheme 15. $CoCl_2$ catalyzed C3-formylation of indoles

The oxygen atmosphere favored the formation of 3-formylindoles than bisindolyl methanes.

Su's and Wang's groups[62,63] have worked on formylation of indoles using methyl aniline as a carbon source (Scheme 16). Transition metal-catalyzed in situ generations of iminium ion source for the formylation reaction by employing TBHP as an oxidant in PivOH and *N*-

methyl acetamide as solvents at room temperature is employed by Su's group. In contrast, Wang's group achieved the same target without using any transition metal catalyst and by just employing *n*-butylammonium iodide (nBu$_4$NI) in DMSO at 80 °C. Both the groups have displayed excellent use of methyl aniline for the formylation reaction by synthesizing 16 to 17 derivatives in good yields.

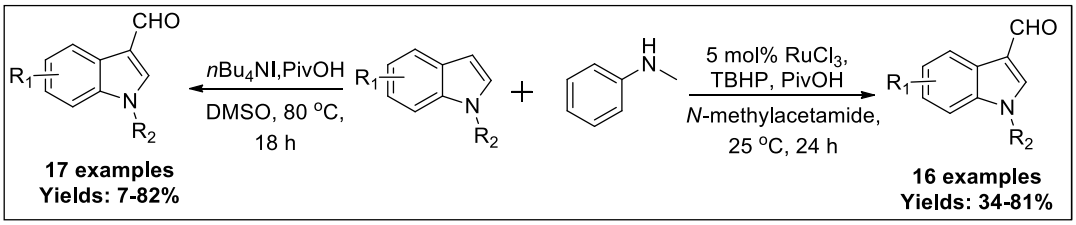

Scheme 16. Formylation of indoles using methyl aniline as a carbon source

Lei et al.[64] have described the selective formylation indole using 4-methoxy *N*,*N*-substituted aniline as a carbon source, employing DDQ reagent in the presence of pivalic acid (PivOH) (Scheme 17). Synthesis of around six formylated indoles in moderate to good yields is achieved.

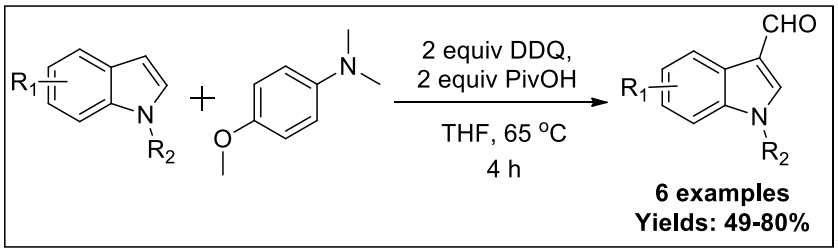

Scheme 17. Formylation of indole derivatives using DDQ and PivOH

Wang and co-workers[65] have developed a one-pot dual functionalization method of C3-formylation and *N*-aminomethylation indoles with 4-substituted-*N*, *N*-dimethylaniline using potassium iodide as a catalyst and *t*-butyl peroxy benzoate as a co-oxidant (Scheme 18). Over 20 derivatives with dual functionalization are prepared in good to excellent yields.

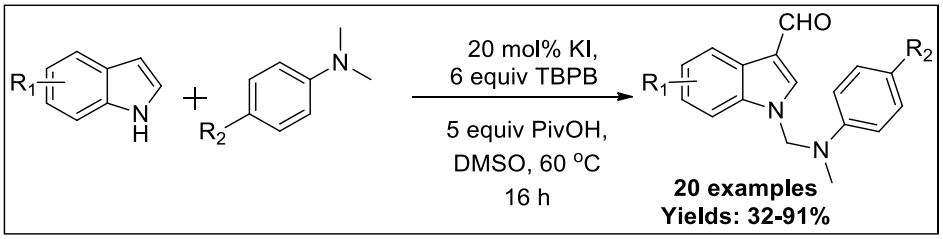

Scheme 18. C3-formylation on *N*-substituted indole derivatives using potassium iodide

3.2.4.4 Syntheses of aldehydes using formaldehyde:

Zeng's group[66] has developed an efficient intermolecular iron-catalyzed C3- formylation of indoles surrogates under aerobic conditions by employing formaldehyde and aqueous ammonia (Scheme 19). They have prepared various substituted indole-3-carboxaldehyde compounds in moderate to excellent yields.

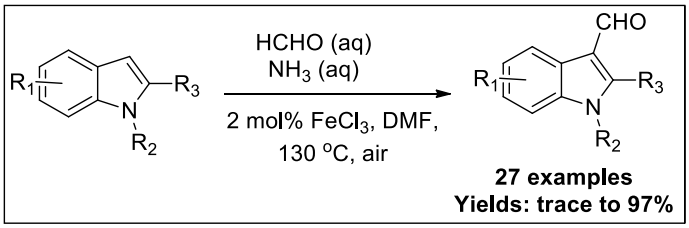

Scheme 19. Iron-catalyzed C3- formylation of indole surrogates

Zheng et al.[67] have reported an effective method for the oxidative cross-coupling of indoles with various aldehydes to construct C3-aldehydes and ketones (Scheme 20). They have employed formaldehyde and synthesized over 22 compounds *via* a Mannich-type reaction and a C−N bond cleavage enabled by electrochemistry for the carbonyl introduction.

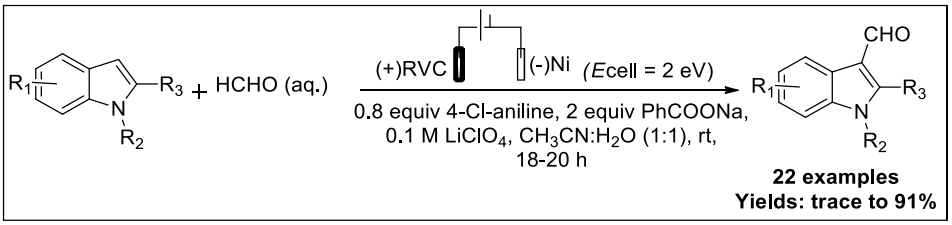

Scheme 20. Development of electrochemical process for the syntheses of indole-3-carboxaldehyde derivatives *via* C-N bond cleavage

3.2.4.5 Use of amide proxies as carbonyl source:

Han et al.[68] have shown copper iodide mediated cyanation of indoles using

dimethylformamide as a cyanide carbon source in the presence of trifluroacetic acid. Instead of dimethylformamide, the use of dimethylacetamide exclusively furnishes indole-3-carboxaldehyde instead of 3-cyano indole (Scheme 21). Over 12 examples of various substituted indoles have been formylated in good yields.

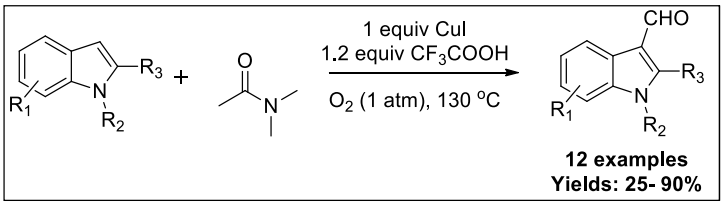

Scheme 21. Syntheses of indole-3-carboxaldehyde using dimethylacetamide as a carbon source

Efran and co-workers[69] have shown an introduction of WCl_6 in dimethylformamide (DMF) as a new reagent system for amide formation of aryl halides in the presence of $PdCl_2$. Using this protocol, they carried out a reaction on indole using WCl_6 and DMF separately, showing the formation of a Vilsmeyer iminium type intermediate responsible for carbonylation of aryl halides (Scheme 22).

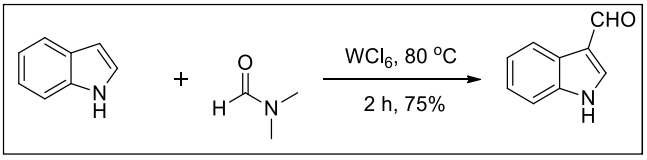

Scheme 22. Synthesis of indole-3-carboxaldehyde using WCl_6 in dimethylformamide

Liang et al.[70] have reported a cesium fluoride and triflic anhydride mediated selective Friedel–Crafts acylation of indoles *via* the cleavage of the amide C–N bond in the presence of cesium carbonate as a base at a very low temperature (Scheme 23). This method illustrates the C-C bond formation between amides with indoles to form ketones and aldehydes without transition metal catalysts.

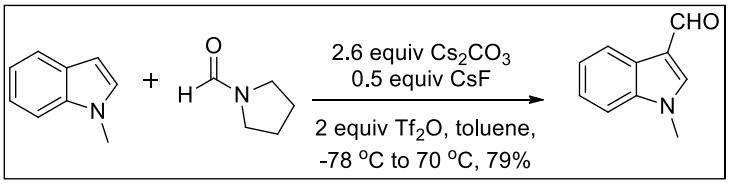

Scheme 23. Synthesis of *N*-methylindole-3-carboxaldehyde *via* Friedel–Crafts acylation of indoles

Jiao and Ding[71] have described the direct cyanation of indoles and benzofurans employing *N*,*N*-dimethylformamide (DMF) as both reagent and solvent (Scheme 24). The method prescribed for the cyanation process can generate the substituted indole-3-carboxaldehyde in a 48% yield when the base K_2CO_3 is replaced with KOAc. Although it was not targeted to do the formylation reaction on indoles, it is one of the methods that show the use of DMF as a carbonyl source.

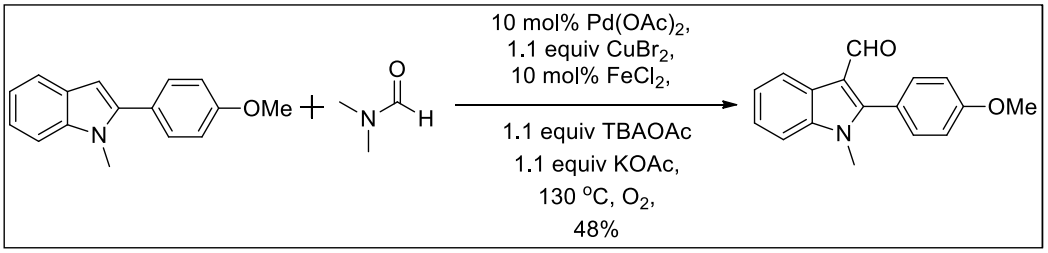

Scheme 24. Synthesis of 2-(4-methoxyphenyl)-1-methyl-1*H*-indole-3-carbaldehyde

Roozbin et al.[72] have introduced the mixture of *N*,*N*-dimethylformamide, and 2,4,6-trichloro-1,3,5-triazine (cyanuric chloride) as an easy handling formylating agent for the selective formylation of indoles and pyrroles at the positions of C(3) and C(2), respectively in an efficient manner (Scheme 25). They have synthesized a library of C(2)-formylated pyrrole and C(3)-formylated indole compounds using their method.

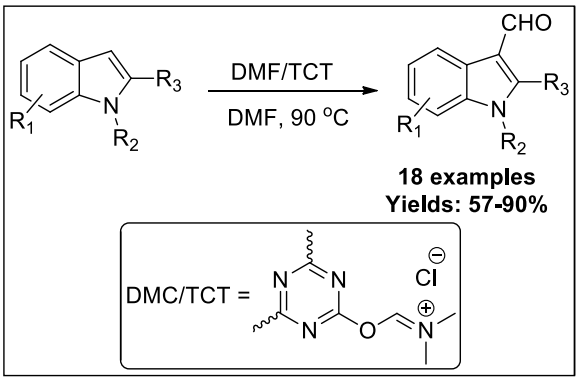

Scheme 25. Syntheses of indole-3-carboxaldehyde derivatives using DMF/TCT mixture

Wang et al.[73] have reported a copper iodide-mediated cyanation of indoles using benzyl cyanide as a cyanide source under aerobic conditions (Scheme 26). Although, without the use of benzyl cyanide, they could synthesize indole-3-carboxaldehyde in 16% along with an indolo[2,1-*b*]quinazoline-6,12-dione in 46% yields.

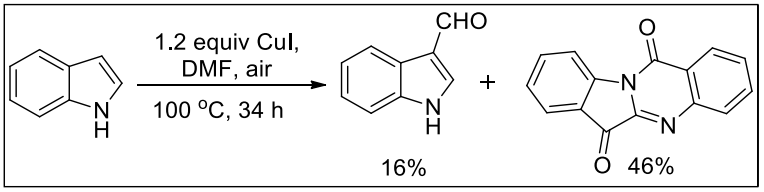

Scheme 26. Copper iodide mediated synthesis of indole-3-carboxaldehyde

Lin et al.[74] have shown a one-pot reaction of *o*-alkynylanilines with dimethylformamide (DMF) catalyzed by copper triflate under an oxygen atmosphere to multisubstituted 3-formyl indole scaffolds where DMF serves as the caron source for the formylation of indole compounds as well as solvent (Scheme 27). The reaction mechanism proceeds through a domino 5-endo-dig cyclization reaction followed by formylation to give multisubstituted indole derivatives.

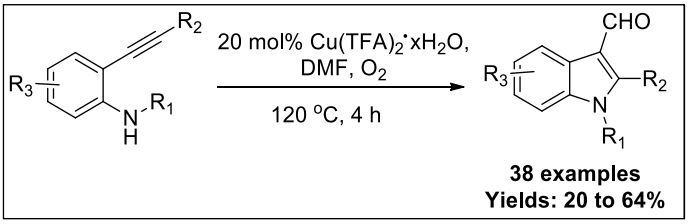

Scheme 27. Copper triflate catalyzed syntheses of indole-3-carboxaldehyde derivatives

3.2.4.6 Syntheses of aldehyde by C-N bond cleavage:

Here distinct methods describing the oxidative C-N bond cleavage are highlighted, resembling our methodology described in the next section.

Ishikura and co-workers[75] using slightly excess of PCC in DMF solvent at 100 °C obtained indole-3-carboxaldehyde compounds in moderate to good yields from gramines (Scheme 28).

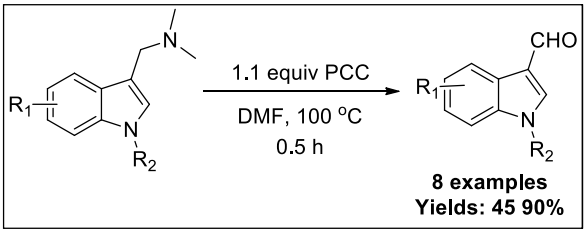

Scheme 28. Syntheses of indole-3-carboxaldehyde derivatives from gramine compounds using PCC

Desjardins et al.[76] have developed hypervalent iodine reagent mediated chemoselective oxidative conversion of benzylic amines into aldehydes (Scheme 29). They have exclusively worked on formylating only aryl moieties where the mild oxidation of tertiary amine corresponds to Polonovski reaction shows excellent functional group tolerance even for the hydroxyl groups.

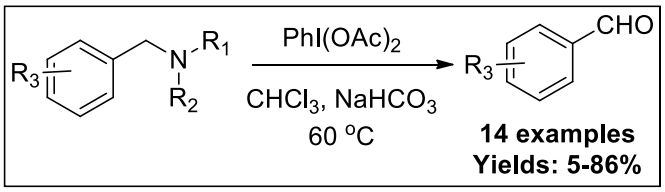

Scheme 29. Hypervalent iodine reagent mediated chemoselective oxidative conversion of benzylic amines into aldehydes

Studolski and co-workers[77] have accomplished the synthesis of a series of indole-3-carboxaldehyde derivatives *via* visible-light-mediated oxygenation of 3-*N*,*N*-(dimethylaminomethyl)-indoles bearing different substituents by using ruthenium catalyst (Scheme 30). They have successfully deduced the plausible mechanism and have shown the practical application of this method by doing a formal synthesis of (-)- Vincorine.

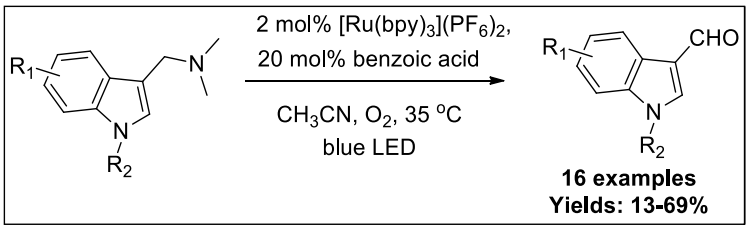

Scheme 30. Syntheses of indole-3-carboxaldehyde derivatives using ruthenium catalyst

3.3 Results and discussion:

We envisaged synthesizing an azepine ring fused to an indole ring as an extension to the previously published work from our laboratory on intramolecular cross-dehydrogenative coupling reaction for the synthesis of 5,11-dialkylindolo[3,2-*c*]quinoline salts and 5,7-dimethylindolo[2,3-*c*]quinoline salts using molecular iodine and TBHP as an oxidant.[78] We applied the same condition to cyclize *N*,*N*-dimethyl-1-(2-phenyl-1*H*-indol-3-yl)methanamine at the terminal methyl carbon with the neighboring phenyl ring, but it gave us complex mixtures upon $Na_2S_2O_3$ workup (Table 2, entry 1). Later, without any oxidants,

we attempted the synthesis of 6-methyl-5,6,7,12-tetrahydrobenzo[5,6]azepino[4,3-*b*]indole by employing 2 equiv of I_2, in $CHCl_3$ under inert condition (Table 2, entry 2). As it didn't furnish any new spots on TLC, we then heated the reaction in neat condition at 160 °C to see any cyclized product (Table 2, entry 3). But that also ended up in a complex mixture. Refluxing the *N*,*N*-dimethyl-1-(2-phenyl-1*H*-indol-3-yl)methanamine in acetonitrile in the presence of iodine, serendipitously, resulted in the spontaneous C-N bond breaking of the starting substrate forming an aldehyde after aqueous workup in 15% yield (Table 2, entry 4). Then we thought of the addition of a base to further the reaction. Addition of an excess of sodium carbonate in the presence of 1.2 equiv I_2 in non-polar solvent chloroform gave 2-phenyl-indole-3-carboxaldehyde in 53% yield (Table 2, entry 5).

Table 2. Attempted synthesis of 6-methyl-5,6,7,12-tetrahydrobenzo[5,6]azepino[4,3-*b*]indole

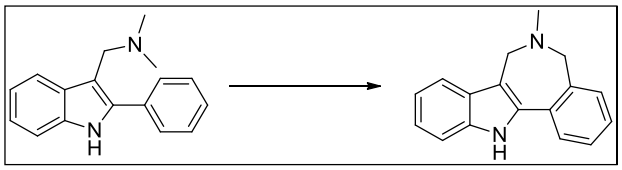

Entry	Reaction condition	Results
1	1 equiv I_2, 70% TBHP in decan, Ar atm., rt, 2-12 h	Complex mixture
2	2 equiv I_2, Ar atm., $CHCl_3$, rt, 6 h	No reaction
3	1.2 equiv I_2, neat heating 160 °C, Ar atm., 1 h	Complex mixture
4	1 equiv I_2, CH_3CN, 80 °C, 3-12 h	Formation of aldehyde (15%)
5	**1 equiv I_2, 2 equiv Na_2CO_3, $CHCl_3$, rt, 12 h**	**Formation of aldehyde (53%)**

2-Phenyl-1*H*-indole-3-carbaldehyde (3h):

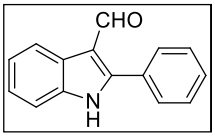

White solid, m.p. 252°C. IR (KBr) υ_{max}: 3138, 2937, 1631, 1581 cm^{-1}. ^1H NMR (400 MHz, DMSO-d_6) δ = 7.32 – 7.24 (m, 2H), 7.52 (d, *J* = 7.8 Hz, 1H), 7.62 – 7.53 (m, 3H), 7.78 (d, *J* = 7.2, 2H), 8.21 (d, *J* = 7.6 Hz, 1H), 9.96 (s, 1H), 12.44 (s, 1H). ^{13}C NMR (100 MHz, DMSO-d_6) δ = 112.5 (CH), 113.9 (Cq), 121.5 (CH), 123.0 (CH), 124.2 (CH), 126.2, 129.5 (2XCH), 130.2 (Cq), 130.3 (3XCH), 135.4 (Cq), 149.6 (Cq), 186.0 (Cq) ppm. Spectral data is in accordance with the literature.[79]

Understanding the importance of the reaction, we gave a thought about producing indole-3-carboxaldehyde molecules using this strategy. We prepared gramine using the standard Mannich reaction procedure in 89% yield (Scheme 31) and subjected it to the above reaction condition. The reaction of gramine with slightly excess molecular iodine and sodium carbonate gave the expected indole-3-carboxaldehyde in 41% yield (Scheme 32).

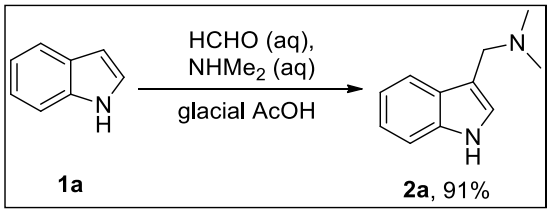

Scheme 31. Synthesis of gramine

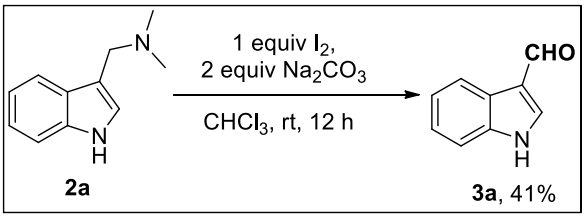

Scheme 32. Oxidative cleavage of C-N bond using molecular iodine

1*H*-Indole-3-carbaldehyde (3a):

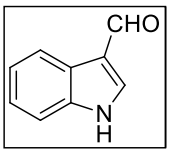

Pale yellow solid, m.p. 189 °C. IR (KBr) υ_{max}: 3225, 2889, 1635, 1226 cm^{-1}. ^{1}H NMR (400 MHz, DMSO-d_6) δ = 7.29 – 7.21 (m, 2H), 7.54 (d, *J* = 8.0 Hz, 1H), 8.14 (d, *J* = 8.0 Hz, 1H), 8.28 (s, 1H), 9.96 (s, 1H). ^{13}C NMR (100 MHz, DMSO-d_6) δ = 112.9 (CH), 118.7 (Cq), 121.3 (CH), 122.6 (CH), 124.0 (CH), 137.5 (Cq), 138.9 (CH), 185.5 (O=Cq) ppm. Spectral data is in accordance with the literature.[79]

The unexpected approach gave us the platform to show the use of molecular iodine in breaking the C-N bond in a very effective manner. But there was still the necessity to see how to improve the yield of the carbonyl compound; we performed a set of reactions by

playing with the stoichiometries of the reagents and solvents (Table 3).

To begin with, we treated parent gramine **1** with 1 equiv of molecular iodine in chloroform, followed by workup with aq $Na_2S_2O_3$ gave 12% of aldehyde **2a** along with most of the unreacted gramine (Table 3, entry 1). We reasoned that the iodide ion liberated in the reaction may not act as a better conjugate base to abstract the methylene proton. Hence, we thought of performing the reaction under basic conditions. The reaction of **1** with 1 equiv. of iodine and 1 equiv of Na_2CO_3 as a base increased the yield to 35% (Table 3, entry 2). Increase in iodine and base loading to 1.1 equiv and 1.5 equiv respectively, furnished **2a** in 65% (Table 3, entry 3). Alternatives for Na_2CO_3 examined were $NaHCO_3$ and Cs_2CO_3, but no substantial change was seen in the yields (Table3, entries 4 and 5). Reaction with a stoichiometric amount of NaOH failed to give the product (Table 3, entry 6). On the other hand, the use of NIS failed as an alternative for iodine in deamination of **1** (Table 3, entry 7). Furthermore, other solvents were studied as a means to increase productivity. Thus, we tried 1,2-dichloroethane as an alternative for $CHCl_3$ (Table 3, entry 8), but chloroform remained the best. Polar solvents like ethanol, tetrahydrofuran, 1,4-dioxane, and acetonitrile were tried (Table 3, entries 9–12), from which 1,4-dioxane served our purpose, giving **2a** in 81% yield. To reduce the aqueous workup step in the reaction and achieve spontaneous oxidative cleavage, we studied aqueous–organic solvent mixtures. The screening was carried out in THF:H_2O, ACN:H_2O, $CHCl_3$:H_2O, and 1,4-dioxane:H_2O solvent mixtures to observe any increase in yield (Table 3, entries 13–16). But unfortunately, none of the solvent combinations achieved this goal. The use of a co-oxidant like aq. TBHP in ethanol was examined, which did not result in any product formation (Table 3, entry 17).

Table 3. Optimization of reaction conditions

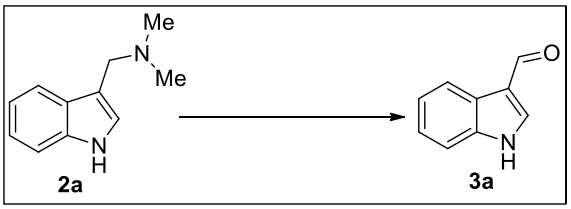

Entry	Reagent	Oxidant	Base	Solvent	% Yield
1	I_2 (1 equiv)	-	-	$CHCl_3$	12
2	I_2 (1 equiv)	-	Na_2CO_3 (1 equiv)	$CHCl_3$	35

3	I_2 (1.1 equiv)	-	Na_2CO_3 (1.5 equiv)	$CHCl_3$	65
4	I_2 (1.1 equiv	-	$NaHCO_3$ (1.5 equiv)	$CHCl_3$	45
5	I_2 (1.1 equiv)	-	Cs_2CO_3 (1.5 equiv)	$CHCl_3$	49
6	I_2 (1.1 equiv)	-	NaOH (1 equiv)	Ethanol	N. R.
7	NIS(1.1 equiv)	-	Na_2CO_3 (1.5 equiv)	$CHCl_3$	25
8	I_2 (1.1 equiv)	-	Na_2CO_3 (1.5 equiv)	DCE	53
9	I_2 (1.1 equiv)	-	Na_2CO_3 (1.5 equiv)	Ethanol	45
10	I_2 (1.1 equiv)	-	Na_2CO_3 (1.5 equiv)	THF	69
11	**I_2 (1.1 equiv)**	**-**	**Na_2CO_3 (1.5 equiv)**	**1,4-dioxane**	**81**
12	I_2 (1.1 equiv)	-	Na_2CO_3 (1.5 equiv)	Acetonitrile	46
13	I_2 (1.1 equiv)	-	Na_2CO_3 (1.5 equiv)	THF:H_2O	46
14	I_2 (1.1 equiv)	-	Na_2CO_3 (1.5 equiv)	ACN : H_2O	37
15	I_2 (1.1 equiv)	-	Na_2CO_3 (1.5 equiv)	$CHCl_3$:H_2O	29
16	I_2 (1.1 equiv)	-	Na_2CO_3 (1.5 equiv)	1,4-dioxane: H_2O	62
17	I_2 (1.1 equiv)	TBHP	-	THF	N. R.

The need for the exact stoichiometries of reagents and the solvent were set, but we studied other alternatives in place of dimethyl Mannich bases. Because with any other amines, it would be a wholesome best strategy to prepare carbonyl compounds if we could oxidize the C-N bond more effectively.

We synthesized various Mannich bases of indole using different secondary amines like dimethylamine, diethylamine, pyrrolidine. The reaction with diethylamine and pyrrolidine gave the corresponding Mannich bases in 78% and 85% yields (Scheme 33). But the same reaction with diisopropylamine failed to form a Mannich base of indole.

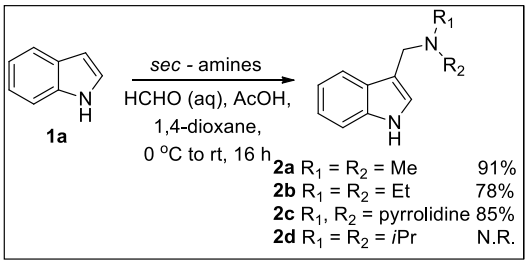

Scheme 33. Syntheses of various Mannich bases of indole

These Mannich bases were then subjected to the optimized reaction condition to compare their ability to depart the amine after the oxidative C-N bond cleavage. As tested, gramine resulted in 81% conversion in the corresponding indole-3-carboxaldehyde but, diethylamine and pyrrolidine Mannich bases couldn't do much better (Scheme 34).

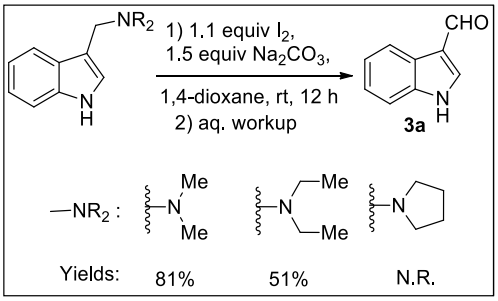

Scheme 34. Screening of various Mannich bases for the synthesis of indole-3-carboxaldehyde

We prepared various Mannich bases of indole, aryl, and heteroaryl compounds with the set optimized condition. The Mannich bases of indoles were designed using their respective indole derivatives (Table 2). Compounds like **1b** and **1c** were prepared using standard NaH mediated *N*-alkylation of indole with methyl iodide and benzyl bromide (Scheme 35). Compound **1b** was prepared in 95% yield whereas; **1c** was prepared in 92% yield.

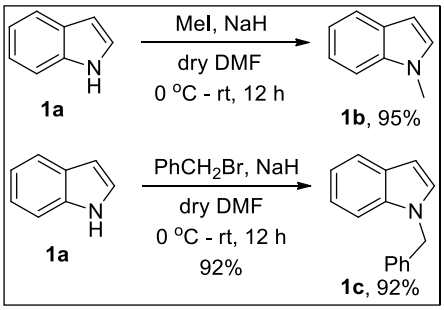

Scheme 35. *N*-methylation and *N*-benzylation of indole

Later, **1b** was converted to its Mannich base of dimethylamine and formaldehyde in 91% (Table 4, entry 1). Likewise, **1c** was also coupled with dimethylamine and formaldehyde to form **2c** in 87% yield (Table 4, entry 2). Indole bearing electron-donating group like methoxy group **1d** was transformed into its corresponding Mannich base **2d** in 78% yield (Table 4, entry 3). Indoles bearing chloro **1e**, NO_2 **1f**, CN **1g** groups, were also converted to their corresponding Mannich bases **2e, 2f, 2g** in 71%, 68%, 71% yields, respectively (Table 4, entries 4, 5, 6). However, various substituents at the C2 position of indole were also employed to synthesize gramine derivatives. Like, Mannich bases of 2-phenyl indole **1h**, 2-methyl indole **1i** and ethyl indole-2-carboxylate **1j** were prepared in 75%, 85%, 78% respectively (Table 4, entries 7, 8, 9).

Table 4. Syntheses of gramine derivatives

Entry	Starting indole	Mannich bases	% Yield
1	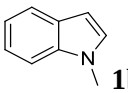 **1b**	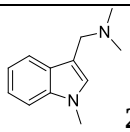 **2e**	91%
2	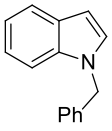 **1c**	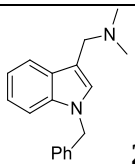 **2f**	87%
3	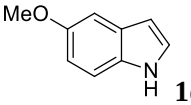 **1d**	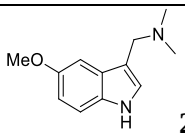 **2g**	78%
4	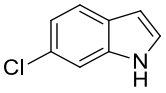 **1e**	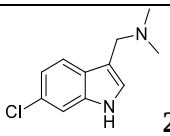 **2h**	71%
5	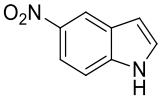 **1f**	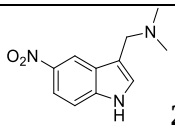 **2i**	68%
6	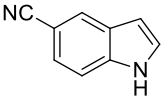 **1g**	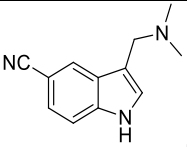 **2j**	71%
7	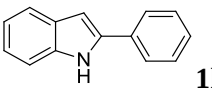 **1h**	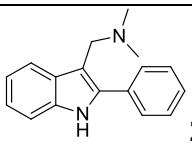 **2k**	75%

8	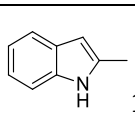 **1i**	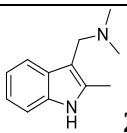 **2l**	85%
9	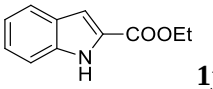 **1j**	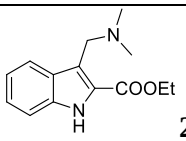 **2m**	78%

Along with indole, heterocycles like 4-hydroxycoumarin **1k** were subjected to Mannich reaction using a reported procedure to form **2k** in 67% yield (Scheme 36). It was interesting to see how **2k** would undergo our optimized strategy to convert into its carbonyl moiety.

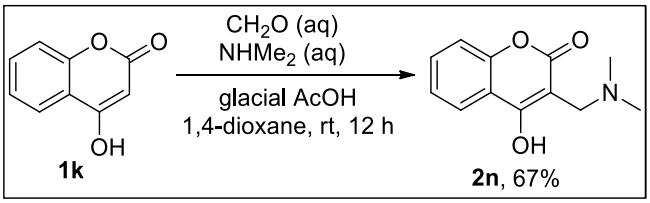

Scheme 36. Synthesis of Mannich base of 4-hydroxycoumarin

Even the Mannich base of thiophene **2l** was prepared from its aldehyde **3l** (as we did not have thiophene) by heating in Monowave 50 at 150 °C in excess of aqueous dimethylamine in the presence of catalytic acetic acid and anhydrous magnesium sulfate followed by reducing it with sodium borohydride (Scheme 37). After the column purification on basic alumina, we could isolate **2o** in a 73% yield.

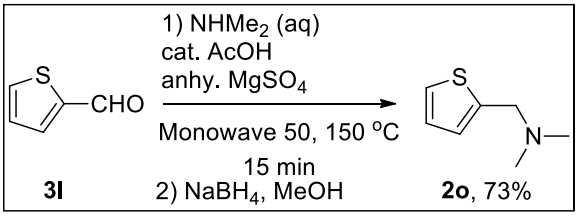

Scheme 37. Synthesis of Mannich base of thiophene

We have also prepared Mannich bases of aryl rings with direct Mannich reaction or from their corresponding bases. Mannich base of β-naphthol **2m** was prepared using a reported procedure wherein β-naphthol **1l** was reacted with aqueous formaldehyde and aqueous dimethylamine and stirred at room temperature in the presence of anhydrous magnesium

sulphate (Scheme 38). We could obtain **2m** in 95% yield as a white solid.

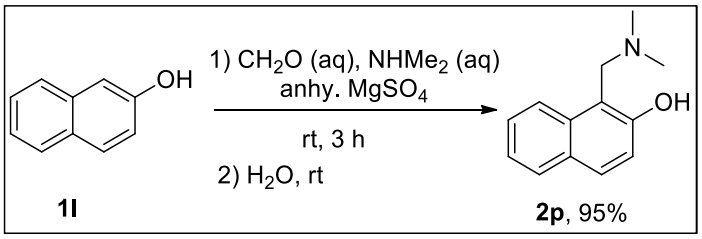

Scheme 38. Synthesis of Mannich base of β-naphthol

Mannich bases **2q-s** were prepared from their corresponding aldehydes as done in the case of thiophene-2-aldehyde just to check the generality of the reaction on aryl amines.

With a handful of Mannich bases of various aryl and heteroaryl systems, we then transformed them into their carbonyl compounds using our optimum reaction condition (Table 3, entry11). We prepared *N*-methyl **3b** and *N*-benzyl **3c** indole-3-carboxaldehydes. Aldehydes bearing substituents like 5-OMe **3d**, 6- Cl **3e**, 5-NO_2 **3f**, 5-CN **3g,** 2-phenyl **3h**, 2-methyl **3i**, and 2-COOEt **3j**, were obtained from their respective gramines in excellent to good yields. Heterocyclic amines, 3-((dimethylamino)methyl)-4- hydroxy-2*H*-chromen-2-one and *N*,*N*-dimethyl-1-(thiophen-2-yl) methanamine were also converted to 4-hydroxy-2-oxo-2*H*chromene- 3-carboxaldehyde **3k** and thiophene-2-carboxaldehyde **3l**, respectively, in moderate yields. Furthermore, to exploit the feasibility of the reaction methodology, aryl compounds were also subjected to this oxidative cleavage reaction. Mannich adducts 1-((dimethylamino)methyl)naphthalen-2-ol, *N*,*N*-dimethyl veratrylamine, 2,3,4-trimethoxy-*N*,*N*-dimethylbenzenemethanamine and 1-(3-methoxyphenyl)-*N*,*N*-dimethylmethanamine were transformed into their aldehydes **3m**, **3n**, **3o,** and **3p**, respectively, in good yields.

Table 5. Oxidative cleavage of the C–N bond of (dimethylamino)-methyl derivatives to aldehydes

Entry	Product	%Yield	Entry	Product	%Yield
1	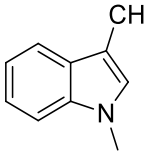 **3b**	83%	9	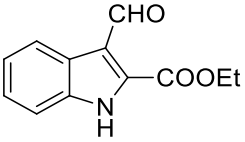 **3j**	68%

2	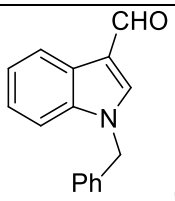 **3c**	78%	10	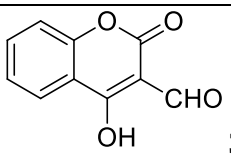 **3k**	35%
3	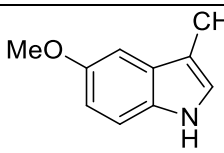 **3d**	71%	11	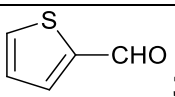 **3l**	59%
4	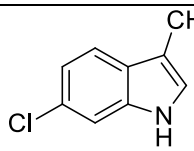 **3e**	75%	12	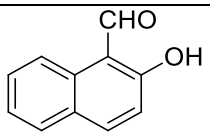 **3m**	56%
5	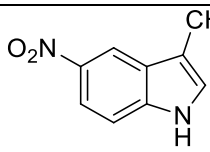 **3f**	79%	13	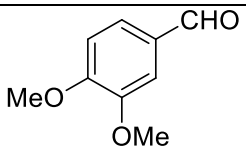 **3n**	67%
6	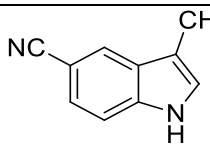 **3g**	43%	14	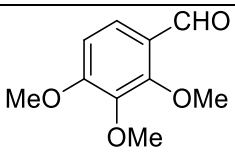 **3o**	64%
7	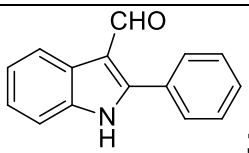 **3h**	63%	15	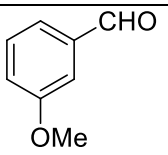 **3p**	59%
8	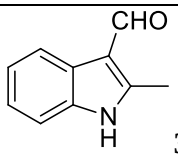 **3i**	61%			

With the successful conversion of aryl and heteroaryl (dimethylamino)-methyl derivatives to aldehydes, we thought of giving it a try to prepare aliphatic aldehydes using our strategy. We chose to carry out this transformation on 3-(dimethylamino)-1-phenylpropan-1-one **2q** to convert it into 1,3-ketoaldehyde. We synthesized **2q** using a reported procedure from acetophenone (Scheme 39).

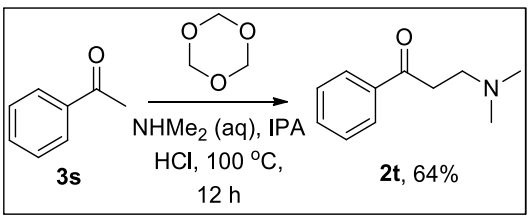

Scheme 39. Synthesis of 3-(dimethylamino)-1-phenylpropan-1-one 2t from acetophenone 3s using Mannich reaction

With our optimized condition, we then attempted to oxidatively cleave the C-N bond of **2t** to furnish **3q** (Scheme 40). But the reaction didn't go as planned and the strategy remained restricted to the aromatic aldehyde preparations only.

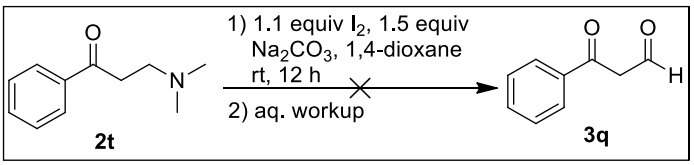

Scheme 40. Attempted synthesis of 3-oxo-3-phenylpropanal 3q

Next, we thought to synthesize ketones from the corresponding (dimethylamino)-methyl derivatives to elaborate our strategy more. We prepared a phenyl substituted (dimethylamino)-methyl derivative of indole **2u** by employing indole, benzaldehyde, and dimethylamine (Scheme 41).

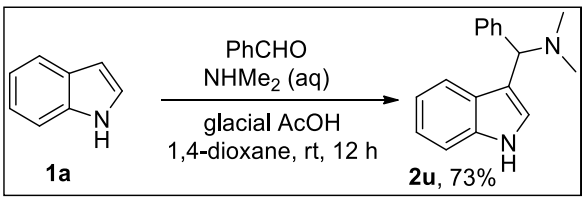

Scheme 41. Synthesis of 1-(1*H*-indol-3-yl)-*N*,*N*-dimethyl-1-phenylmethanamine 2u

The reaction of **2u** was put as per our procedure, but unfortunately, the reaction didn't go as planned (Scheme 42). Repetitive attempts also failed in other solvents like chloroform, acetonitrile, and dimethylformamide to furnish **3r** even in trace amounts.

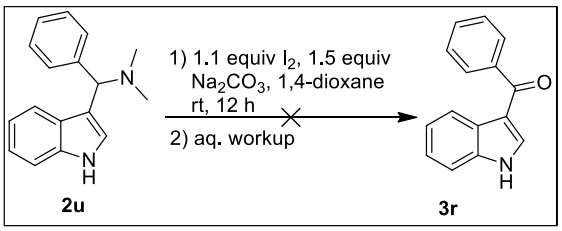

Scheme 42. Attempted synthesis of (1*H*-indol-3-yl)(phenyl)methanone 3r

We synthesized **2v** from acetophenone **3s** as same that of **2o**, by reducing the enamine

formed using sodium borohydride in methanolic HCl in the later stage (Scheme 43). As expected, we couldn't isolate **2v** more than 43%, but it was enough for us to give it a try for our strategy.

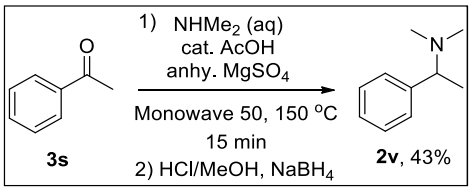

Scheme 43. Monowave synthesis of Mannich base of acetophenone

When **2v** was treated with molecular iodine and sodium carbonate, it furnished **3s** in 53% yield (Scheme 44).

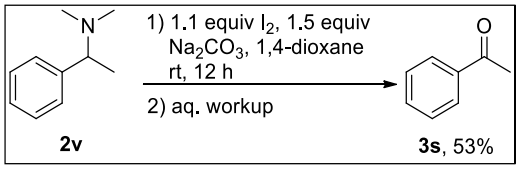

Scheme 44. Synthesis of acetophenone 3s *via* oxidative cleavage of C-N bond

With this success, we prepared (dimethylamino)-methyl derivative of benzophenone **2w** from readily available benzophenone **3t** using the same procedure that to **2o** and **2v** (Scheme 45). It was not hectic as that of acetophenone derivative **2v**, with normal reduction with sodium borohydride we could synthesize **2w** in a 95% yield. The conversion from **2w** to **3t** went smoothly to furnish **3t** in 89% yield (Scheme 46).

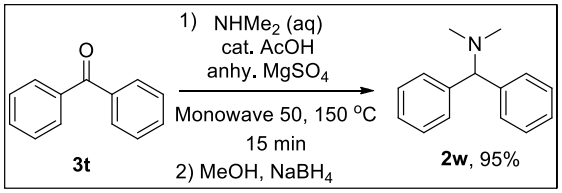

Scheme 45. Monowave synthesis of Mannich base of benzophenone

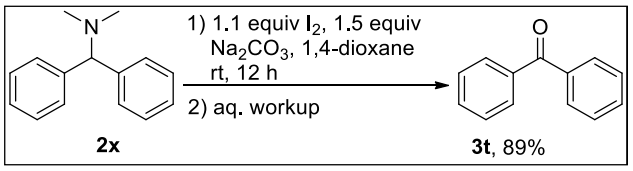

Scheme 46. Synthesis of benzophenone 3t *via* oxidative cleavage of C-N bond

A three-component reaction was carried out between indole, formaldehyde, and dimethylamine; however, it gave **3a** in only 53% yield. Using an excess of iodine and base did not improve the reaction yield substantially for the one-pot procedure (Scheme 47).

Gram scale synthesis for the conversion of gramine **2a** to indole-3-carboxaldehyde **3a** provided **3a** in 71% yield (Scheme 48).

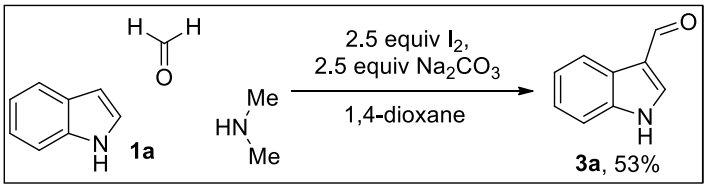

Scheme 47. One-pot synthesis of indole-3-carboxaldehyde

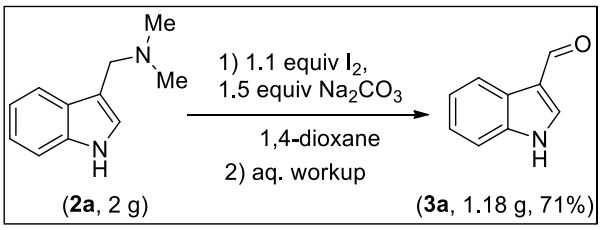

Scheme 48. Gram-scale synthesis of indole-3-carboxaldehyde

The plausible mechanistic pathway for the product is depicted in (Scheme 49). We speculated that iodine might be acting as a mild Lewis acid that coordinates with the nitrogen of the dimethylamine. The base then might deprotonate the coordinated amine to generate the iminium salt, which then hydrolyses during the workup to deliver the aldehyde group.

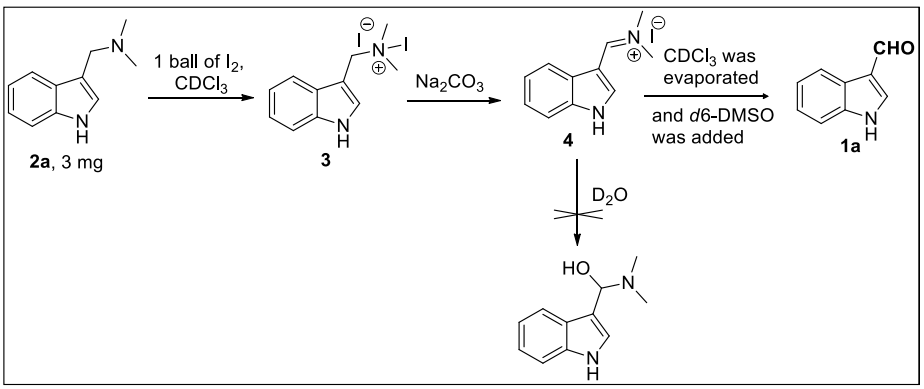

Scheme 49. Representation of mechanistic aspects of our methodology using NMR spectroscopy

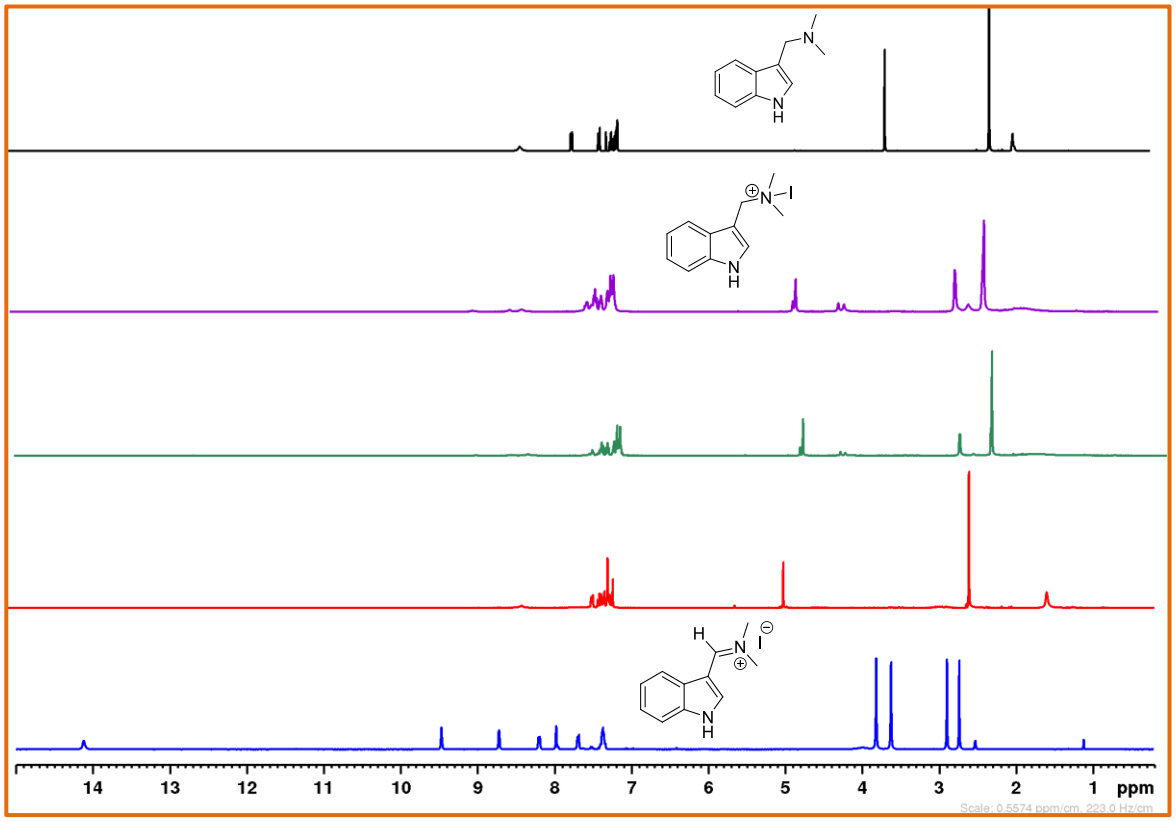

Figure 2. Depiction of series of transformation of gramine into indole-3-carboxaldehyde using NMR spectroscopy

We carried out the reaction in an NMR tube in $CDCl_3$ as the solvent to confirm the mechanism. As speculated, the coordination of iodine shifted the methylene protons downfield initially. After a while, the signal due to the methylene protons disappeared, and salt was seen precipitated out in $CDCl_3$ due to its insolubility in the solvent. After removal of $CDCl_3$, DMSO-d_6 was added, and the NMR was recorded, in which the iminium salt proton was seen clearly (Figure 2).

We also tried the reaction in the presence of 1 equiv of dioxane to check whether the solvent has any role in the reaction (Scheme 50). However, no change in the spectrum was observed to suggest its participation. Also, no bis-indole formation was seen, ruling out the possibility of forming (1*H*-indol-3-yl)methanol and subsequent oxidation.

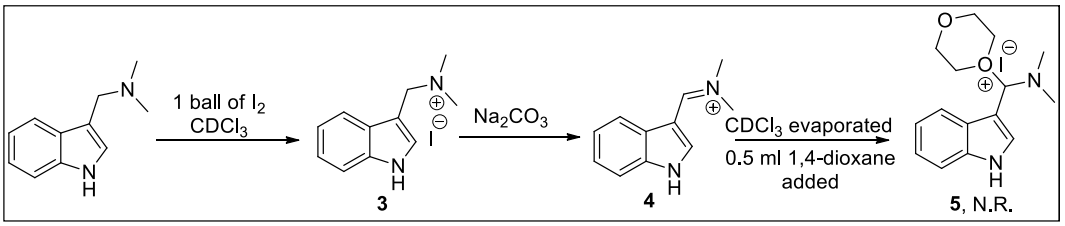

Scheme 50. Solvent participation study using NMR spectroscopy

3.4 Conclusion:

A cheap, environmentally benign methodology was developed to carry out oxidative cleavage of the C-N bond of (dimethylamino)methyl group of indoles and aryl compounds. *N*-deprotected indoles were also successively α-oxygenated to give their carboxaldehydes moieties in good yields. The feasibility of the method failed to convert the aliphatic (dimethylamino)methyl group into its corresponding keto aldehyde compound. The methodology proved applicable to other heterocyclic compounds. The conversion of the Mannich base of 1-(1*H*-indol-3-yl)-*N*,*N*-dimethyl-1-phenylmethanamine to the ketone functional group failed, which further instilled the curiosity to contemplate such reactions. The one-pot conversion of the aryl and heteroaryl systems to their corresponding aldehyde derivatives was also feasible in moderate yield. We have successfully demonstrated the mechanistic study of our methodology by using NMR spectroscopy, which helped us rule out the other prominent side reactions.

3.5 Experimental:

3.5.1: 1-methyl-1*H*-indole (1b):

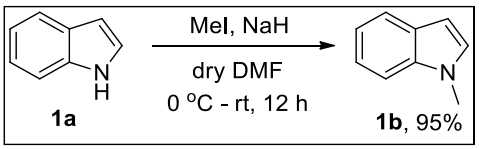

A solution of 10 mmol of indole in dry THF (25 mL) was cooled at 0 °C and 30 mmol of NaH was added slowly under vigorous stirring. The resulting mixture was stirred for 30 minutes at 0 °C. Later, 30 mmol of methyl iodide was added dropwise to the above mixture and allowed to warm up to room temperature, and stirred overnight. Upon the disappearance of indole on TLC, 30 mL of saturated ammonium chloride was added and the mixture was extracted in ethyl acetate (3 X 30 mL). The resulting organic layer was dried over anhydrous sodium sulphate and concentrated under vacuum to give light brown color liquid. The crude liquid was purified over flash chromatography on silica gel (Pet. ether and ethyl acetate) to obtain the product in a 95% yield.

Pale yellow oil. IR (KBr) υ_{max}: 3063, 2921, 1512, 1468, 1332, 1252, 743 cm^{-1}. ^{1}H NMR (400 MHz, $CDCl_3$) δ = 3.78 (s, 3H), 6.48 (s, 1H), 7.04 (s, 1H), 7.09-7.12 (m, 1H), 7.20-7.24 (m, 1H), 7.27 (d, *J* = 8 Hz, 1H), 7.63 (d, *J* = 7.6 Hz, 1H) ppm. ^{13}C NMR (100 MHz, $CDCl_3$) δ = 32.8 (CH_3), 100.9 (CH), 109.2 (CH), 119.3 (CH), 120.9 (CH), 121.5 (CH), 128.5 (Cq), 128.8 (CH), 136.7 (Cq) ppm.

3.5.2: 1-benzyl-1*H*-indole (1c):

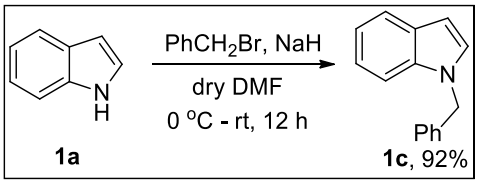

Following the similar procedure as described in experiment 3.5.1 with benzyl bromide gave the white solid product in 92% yield.

White solid, m.p. 48-52 °C. IR (KBr) υ_{max}: 3033, 1744, 1518, 1497, 1469, 1463, 1363, 1323, 1180, 1089, 773, 727 cm^{-1}. ^{1}H NMR (400 MHz, $CDCl_3$) δ = 5.33 (s, 2H), 6.54 (s,

1H), 6.56-7.19 (m, 5H), 7.23-7.31 (m, 4H), 7.64 (d, *J* = 7.6 Hz, 1H) ppm. ^{13}C NMR (100 MHz, $CDCl_3$) δ = 50.1 (CH_2), 101.7 (CH), 109.7 (CH), 119.5 (CH), 121.0 (CH), 121.7 (CH), 126.8 (2XCH), 127.6 (CH), 128.3 (CH), 128.8 (2XCH), 128.8 (Cq), 136.3 (Cq), 137.6 (Cq) ppm.

3.5.3: 1-(1*H*-indol-3-yl)-*N*,*N*-dimethylmethanamine (2a):

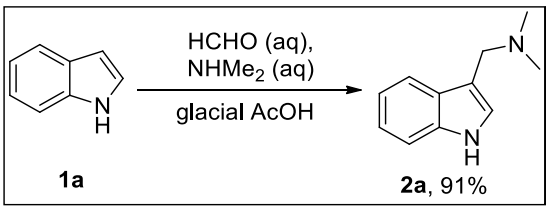

In a round bottom flask, equipped with magnetic stirring, an aqueous solution of dimethylamine was poured at 0 °C followed by the addition of glacial acetic acid. Till the fumes settle, the aqueous solution of formaldehyde was added slowly at the same temperature under vigorous stirring. The following mixture was allowed to stir for 15 minutes and then it was poured in a prechilled beaker with a magnetic stirring bar containing indole. Allowed the mixture to attain room temperature and then it was warmed to 60 °C for another 6 hours. The disappearance of indole on TLC suggested the completion of the reaction and it was poured in cold aqueous KOH solution with vigorous stirring. The resulting white crystals were filtered and washed with cold water and dried. The following dried solid was recrystallized in an acetone-hexane (1:4) mixture and analyzed using NMR to give corresponding dimethylaminomethyl indole compounds in the respective yields.

Pale yellow solid, m.p. 122-125 °C. IR (KBr) υ_{max}: 3060, 2987, 1498, 1250, 1065, 1057, 748 cm^{-1}. ^{1}H NMR (400 MHz, $CDCl_3$) δ = 2.28 (s, 6H), 3.64 (s, 2H), 7.10-7.17 (m, 2H), 7.18-7.20 (m, 1H), 7.37 (d, *J* = 8 Hz, 1H), 7.69 (d, *J* = 8 Hz, 1H), 8.33 (bs, 1H) ppm. ^{13}C NMR (100 MHz, $CDCl_3$) δ = 45.2 ($2XCH_3$), 54.6 (CH_2), 111.1 (CH), 113.0 (Cq), 119.2 (CH), 119.6 (CH), 122.0 (CH), 123.8 (CH), 127.9 (Cq), 136.2 (Cq) ppm.

3.5.4: *N,N*-dimethyl-1-(1-methyl-1*H*-indol-3-yl)methanamine (2e):

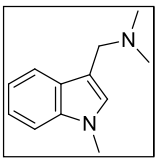

Following the similar procedure as described in experiment 3.5.3 gave the pale brown oil product in 91% yield.

Pale brown oil. IR (KBr) υ_{max}: 3078, 2928, 1513, 1466, 1327, 1240, 1257, 1069, 1059, 743 cm^{-1}. ^{1}H NMR (400 MHz, $CDCl_3$) δ = 2.58 (s, 6H), 3.81 (s, 3H), 4.08 (s, 2H), 7.16-7.20 (m, 1H), 7.25-7.34 (m, 1H), 7.35 (d, *J* = 8 Hz, 1H), 7.39 (s, 1H), 7.60 (d, *J* = 8 Hz, 1H) ppm. ^{13}C NMR (100 MHz, $CDCl_3$) δ = 33.0 (CH_3), 42.8 ($2XCH_3$), 52.7 (CH_2), 105.0 (Cq), 109.8 (CH), 118.3 (CH), 120.1 (CH), 122.1 (CH), 128.1 (Cq), 131.1 (CH), 136.8 (Cq) ppm.

3.5.5: 1-(1-benzyl-1*H*-indol-3-yl)-*N,N*-dimethylmethanamine (2f):

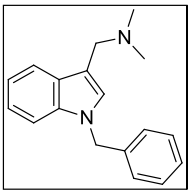

Following the similar procedure as described in experiment 3.5.3 gave the off-white solid product an 87% yield.

Off white solid, m.p. 54-59 °C. IR (KBr) υ_{max}: 3028, 1743, 1513, 1488, 1469, 1460, 1443, 1357, 1339, 1320, 1254, 1183, 1084, 1068, 1057, 759, 740, 695 cm^{-1}. ^{1}H NMR (400 MHz, $CDCl_3$) δ = 2.37 (s, 6H), 3.78 (s, 2H), 5.28 (s, 2H), 7.09-7.19 (m, 5H), 7.23-7.29 (m, 4H), 7.67 (d, *J* = 7.6 Hz, 1H) ppm. ^{13}C NMR (100 MHz, $CDCl_3$) δ = 44.5 (CH_3), 51.0 (CH_2), 53.8 (CH_2), 109.9 (CH), 110.2 (Cq), 119.2 (CH), 119.7 (CH), 122.0 (CH), 126.9 (2XCH), 127.7 (CH), 128.6 (Cq), 128.7 (CH), 128.8 (2XCH), 136.6 (Cq), 137.4 (Cq) ppm.

3.5.6: 1-(5-methoxy-1*H*-indol-3-yl)-*N,N*-dimethylmethanamine (2g):

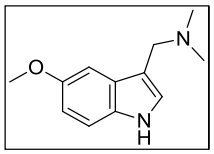

Following the similar procedure as described in experiment 3.5.3 gave the brown solid product in 78% yield.

Brown solid, m.p. 130-134 °C. IR (KBr) υ_{max}: 3363, 2849, 2612, 1449, 1210, 760 cm^{-1}. ^{1}H NMR (400 MHz, $CDCl_3$) δ = 2.33 (s, 6H), 3.64 (s, 2H), 3.86 (s, 3H), 6.86 (d, *J* = 6.8, 1H), 7.07 (s, 1H), 7.15 (s, 1H), 7.22 (d, *J* = 8.8 Hz, 1H), 8.65 (bs, 1H) ppm. ^{13}C NMR (100 MHz, $CDCl_3$) δ = 45.3 ($2XCH_3$), 54.5 (CH_2), 55.9 (OCH_3), 100.9 (CH), 111.9 (CH), 112.1 (CH), 112.6 (Cq), 124.7 (CH), 128.3 (Cq), 131.4 (Cq), 154.0 (Cq) ppm.

3.5.7: 1-(6-chloro-1*H*-indol-3-yl)-*N*,*N*-dimethylmethanamine (2h):

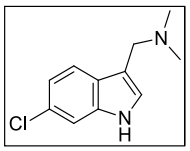

Following the similar procedure as described in experiment 3.5.3 gave the off-white solid product in 71% yield.

Off white solid, m.p. 132-135 °C. IR (KBr) υ_{max}: 1623, 1544, 1513, 1208, 745 cm^{-1}. ^{1}H NMR (400 MHz, $CDCl_3$) δ = 2.31 (s, 6H), 3.63 (s, 2H), 7.00-7.11 (m, 2H), 7.23-7.29 (m, 1H), 7.59-7.62 (m, 1H) ppm. ^{13}C NMR (100 MHz, $CDCl_3$) δ = 45.3 ($2XCH_3$), 54.4 (CH_2), 110.1 (CH), 111.0 (CH), 113.3 (Cq), 120.1 (CH), 120.2 (Cq), 124.4 (CH), 126.4 (Cq), 136.6 (Cq) ppm.

3.5.8: *N*,*N*-dimethyl-1-(5-nitro-1*H*-indol-3-yl)methanamine (2i):

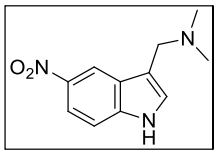

Following the similar procedure as described in experiment 3.5.3 gave the yellow solid

product in 68% yield.

Yellow solid, m.p. 172-175 °C. IR (KBr) υ_{max}: 3412, 2918, 2803, 1520, 1471, 1330, 1097, 753 cm^{-1}. ^{1}H NMR (400 MHz, $CDCl_3$) δ = 2.40 (s, 6H), 3.80 (s, 2H), 7.33 (s, 2H), 8.03-8.06 (m, 1H), 8.63 (s, 1H) ppm. ^{13}C NMR (100 MHz, $CDCl_3$) δ = 44.4 ($2XCH_3$), 53.4 (CH_2), 111.4 (CH), 113.6 (Cq), 116.3 (CH), 117.7 (CH), 127.1 (Cq), 128.0 (CH), 139.4 (Cq), 141.7 (Cq) ppm.

3.5.9: 3-((dimethylamino)methyl)-1*H*-indole-5-carbonitrile (2j):

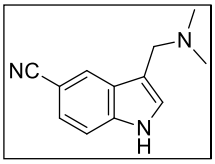

Following the similar procedure as described in experiment 3.5.3 gave the white solid product in 71% yield.

White solid, m.p. 98-102 °C. IR (KBr) υ_{max}: 3054, 2925, 1518, 1469, 1329, 1244, 745 cm^{-1}. ^{1}H NMR (400 MHz, DMSO-d_6) δ = 2.43 (s, 6H), 4.09 (s, 2H), 7.45-7.48 (m, 1H), 7.58 (d, *J* = 8.4 Hz, 1H), 7.73 (d, *J* = 2.4 Hz, 1H), 8.30 (d, *J* = 7.6 Hz, 1H), 11.89 9 (s, 1H) ppm. ^{13}C NMR (100 MHz, DMSO-d_6) δ = 54.8 ($2XCH_3$), 62.2 (CH_2), 106.8 (Cq), 111.7 (CH), 118.2 (CH), 125.9 (CH), 129.1 (Cq), 130.1 (Cq), 133.2 (CH), 136.7 (Cq), 142.9 (Cq) ppm.

3.5.10: *N*,*N*-dimethyl-1-(2-phenyl-1*H*-indol-3-yl)methanamine (2k):

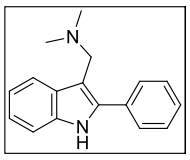

Following the similar procedure as described in experiment 3.5.3 gave the pale white solid product in 75% yield.

Pale white solid, m.p. 130-133 °C. IR (KBr) υ_{max}: 3146, 2974, 2935, 1498, 1460, 1425, 1317, 1277, 1238, 1123, 1051, 748, 703 cm^{-1}. ^{1}H NMR (400 MHz, $CDCl_3$) δ = 2.28 (s, 6H), 3.63 (s, 2H), 7.13-7.24 (m, 2H), 7.34-7.30 (m, 2H), 7.44-7.48 (m, 2H), 7.37-7.77 (m, 3H), 8.26 (bs, 1H) ppm. ^{13}C NMR (100 MHz, $CDCl_3$) δ = 45.5 ($2XCH_3$), 53.5 (CH), 110.7

(CH), 119.6 (CH), 120.0 (CH), 122.2 (CH), 127.7 (CH), 128.3 (CH), 128.8 (3XCH), 130.0 (2XCq), 132.9 (Cq), 135.6 (Cq) ppm.

3.5.11: *N*,*N*-dimethyl-1-(2-methyl-1*H*-indol-3-yl)methanamine (2l):

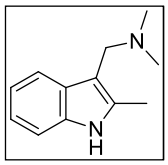

Following the similar procedure as described in experiment 3.5.3 gave the pale white solid product an 85% yield.

Pale white solid, m.p. 120-125 °C. IR (KBr) υ_{max}: 1243, 1149, 1061, 1018, 789 cm^{-1}. ^{1}H NMR (400 MHz, $CDCl_3$) δ = 2.27 (s, 6H), 2.33 (s, 3H), 3.55 (s, 2H), 7.08 (s, 2H), 7.21 (s, 1H), 7.58 (s, 1H), 8.19 (bs, 1H) ppm. ^{13}C NMR (100 MHz, $CDCl_3$) δ = 11.8 (CH_3), 45.3 ($2XCH_3$), 53.2 (CH_2), 110.1 (CH), 118.4 (CH), 119.42 (CH), 120.9 (CH), 129.4 (Cq), 133.6 (Cq), 135.1 (2XCq) ppm.

3.5.12: Ethyl 3-((dimethylamino)methyl)-1*H*-indole-2-carboxylate (2m):

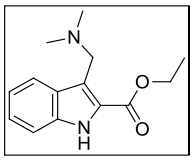

Following the similar procedure as described in experiment 3.5.3 gave the white solid product in 78% yield.

White solid, m.p. 77-80 °C. IR (KBr) υ_{max}: 3300, 1700, 1198, 989, 768 cm^{-1}. ^{1}H NMR (400 MHz, $CDCl_3$) δ = 1.44 (t, *J* = 7.2 Hz, 3H), 2.37 (s, 6H), 4.05 (s, 2H), 4.40-4.45 (q, 2H), 7.15 (t, *J* =7.6 Hz, 1H), 7.31 (t, *J* = 7.2 Hz, 1H), 7.38 (d, *J* = 8 Hz, 1H), 7.83 (d, *J* = 8 Hz, 1H), 9.12 (bs, 1H) ppm. ^{13}C NMR (100 MHz, $CDCl_3$) δ = 14.4 (CH_3), 45.2 ($2XCH_3$), 52.3 (CH_2), 61.0 (CH_2), 111.8 (CH), 119.2 (Cq), 120.6 (CH), 121.5 (CH), 125.0 (Cq), 125.6 (CH), 128.6 (Cq), 135.7 (Cq), 162.2 (Cq) ppm.

3.5.13: 3-(pyrrolidin-1-ylmethyl)-1*H*-indole (2c):

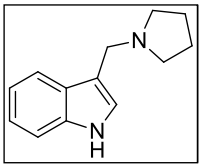

Following the similar procedure as described in experiment 3.5.3 gave the white solid product an 85% yield.

White solid, m.p. 127-129 °C. IR (KBr) υ_{max}: 3416, 2967, 2828, 1605, 1492, 1457, 1095, 747 cm^{-1}. ^{1}H NMR (400 MHz, $CDCl_3$) δ = 1.76-1.79 (m, 4H), 2.6 (bs, 4H), 3.84 (s, 2H), 7.09-7.19 (m, 3H), 7.31 (d, *J* = 8Hz, 1H), 7.70 (d, *J* = 7.6 Hz, 1H), 8.56 (bs, 1H) ppm. ^{13}C NMR (100 MHz, $CDCl_3$) δ = 23.5 ($2XCH_2$), 50.3 (CH_2), 54.1 ($2XCH_2$), 111.1 (CH), 113.6 (Cq), 119.1 (CH), 119.4 (CH), 121.8 (CH), 123.4 (CH), 127.8 (Cq), 136.1 (Cq) ppm.

3.5.14: *N*-((1*H*-indol-3-yl)methyl)-*N*-ethylethanamine (2b):

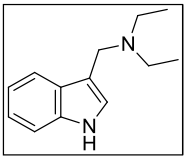

Following the similar procedure as described in experiment 3.5.3 gave the brown solid product in 78% yield.

Brown solid, m.p. 103-105 °C. IR (KBr) υ_{max}: 3057, 2976, 1623, 1539, 1506, 1458 cm^{-1}. ^{1}H NMR (400 MHz, $CDCl_3$) δ = 1.09 (t, *J* = 7 Hz, 6H), 2.54-2.60 (q, 4H), 3.79 (s, 2H), 7.09-7.13 (m, 2H), 7.16-7.19 (m, 2H), 7.71 (d, *J* = 7.8 Hz, 1H), 8.18 (bs, 1H) ppm. ^{13}C NMR (100 MHz, $CDCl_3$) δ = 11.6 (CH_3), 46.4 ($2XCH_2$), 47.6 (CH_2), 111.3 (CH), 112.3 (Cq), 119.2 (CH), 119.4 (CH), 121.8 (CH), 124.2 (CH), 128.2 (Cq), 136.2 (Cq) ppm.

3.5.15: 3-((dimethylamino)methyl)-4-hydroxy-2*H*-chromen-2-one (2n):

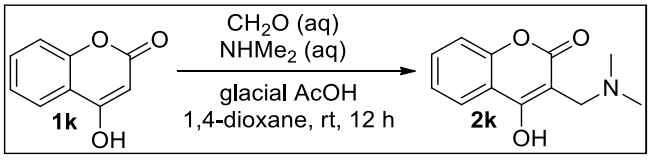

In a three-neck round bottom flask equipped with a guard tube and a dropping funnel, 2.8 mmol of aqueous formaldehyde was mixed in 2.4 mL of 1,4-dioxane along with 0.2 mL of H_2O and 2.6 mL of glacial acetic acid. The resulting mixture was cooled at 0 °C and at once 2.8 mmol of the aqueous solution of dimethylamine was added. After stirring for 15-20 minutes, 2.6 mmol of 4-hydroxycoumarin **1k** dissolved in 2.4 mL of 1,4-dioxane was added dropwise to the above mixture. After the addition of **1k**, the mixture was allowed to stir at 0 °C for another 2 hours and then for 12 hours at room temperature. After the disappearance of **2k** in TLC, 3.2 mL of H_2O was added along with 150 mg of celite and stirred for 20 minutes. The resulting mixture was filtered off over celite bed and the filtrate was cooled and treated with 2N NaOH slowly. The resultant precipitate was filtered and dried under vacuum to give compound **2k** in 67% yield as white solid.

White solid, m.p. 142-146 °C. IR (KBr) υ_{max}: 3078, 2859, 1648, 1606, 15431, 1465, 1408, 1352, 1290, 1223, 1039, 978, 761 cm^{-1}. ^1H NMR (400 MHz, $CDCl_3$) δ = 2.89 (s, 6H), 4.21 (s, 2H), 7.19-7.23 (m, 2H), 7.43-7.48 (m, 1H), 7.91-7.93 (m, 1H) ppm. ^{13}C NMR (100 MHz, $CDCl_3$) δ = 42.7 ($2XCH_3$), 55.6 (CH_2), 88.8 (Cq), 116.5 (CH), 121.6, 123.1 (CH), 124.6 (CH), 124.8 (Cq), 131.5 (CH), 154.1 (Cq), 166.4 (Cq), 176.1 (Cq) ppm.

3.5.16: *N,N*-dimethyl-1-(thiophen-2-yl)methanamine (2o):

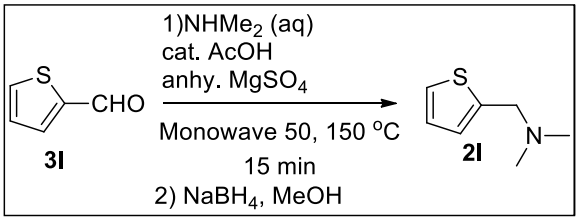

A 1 mmol of thiophene-2-carboxaldehyde **3l** was mixed with an aqueous solution of dimethylamine and glacial acetic acid in a Monowave 50 standard vial equipped with its stirring bar. To that 350 mg of anhydrous magnesium sulphate was added and the vial was fixed in the Monowave 50. Then, using the Monowave 50 program, a temperature was set to 150 °C for 15 min using the RAMP method, and the reaction was allowed to heat. After the completion of reaction time, the disappearance of **3l** was observed on TLC and later the reaction mixture was diluted using methanol and cooled to 0 °C. A 4 mmol of $NaBH_4$ was then added slowly to the cooled reaction mixture followed by methanol and let the mixture get warm while stirring for another 30 minutes. After the completion of the reaction, it was

quenched using cold water and extracted using ethyl acetate (3 X 10 mL). the resultant organic layer was dried over anhydrous Na_2SO_4 and concentrated under a vacuum. The thick liquid was then purified over flash chromatography on basic alumina (Pet. ether and ethyl acetate) to give compound **2l** in 73% yield as a colorless liquid.

Off white solid, m.p. 157-159 °C. IR (KBr) υ_{max}: 2509, 2811 cm^{-1}. ^1H NMR (400 MHz, $CDCl_3$) δ = 2.30 (s, 6H), 3.72 (s, 2H), 6.90-6.94 (m, 2H), 7.16 (t, *J* = 4 Hz, 1H) ppm.

3.5.16: 1-((dimethylamino)methyl)naphthalen-2-ol (2p):

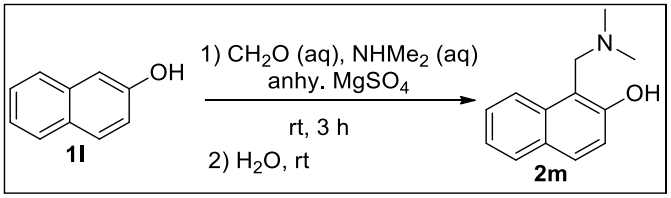

To a mixture of 1 mmol of β-naphthol **1l**, 60 mg anhydrous magnesium sulphate, and 1.5 mmol of an aqueous solution of dimethylamine in the round bottom flask, 1.5 mmol of an aqueous solution of formaldehyde was added and the resulting mixture was further allowed to stir at room temperature for 3 hours. After the completion of the reaction, it was quenched with 5 mL of water and it was extracted using ethyl acetate (3 X 5 mL). Then, the organic layer was washed with water, brine and it was dried over anhydrous Na_2SO_4 and concentrated on the rotary evaporator to give compound **2m** in 95% yield as white solid.

White solid, m.p. 73-76 °C. IR (KBr) υ_{max}: 3387, 3011, 2956, 1627, 1442, 1331, 1248 cm^{-1}. ^1H NMR (400 MHz, $CDCl_3$) δ = 2.35 (s, 6H), 4.04 (s, 2H), 7.10 (d, *J* = 8.8 Hz, 1H), 7.22-7.27 (m, 1H), 7.36-7.42 (m, 1H), 7.64-7.77 (m, 3H), 10.2 (s, 1H) ppm. ^{13}C NMR (100 MHz, $CDCl_3$) δ = 44.6 ($2XCH_3$), 57.9 (CH_2), 111.4 (Cq), 119.3 (CH), 121.0 (CH), 122.5 (CH), 126.4 (CH), 128.5 (CH), 129.0 (CH), 129.3 (CH), 132.6 (Cq), 133.8 (Cq), 156.8 (Cq) ppm.

3.5.17: 1-(3,4-dimethoxyphenyl)-*N*,*N*-dimethylmethanamine (2q):

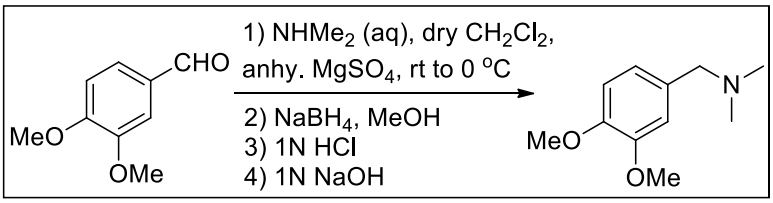

In 0.5 mol of aqueous dimethylamine solution was dissolved 6 mmol of 3,4-dimethoxybenzaldehyde and stirred the mixture at room temperature until the solution becomes clear. To that solution, 0.22 mol of $NaBH_4$ was added and stirred for 30 minutes. The resultant mixture was acidified using 1N HCl and it was washed using ether (2 X 5 mL). The aqueous solution was then basified using 1N NaOH solution to adjust the pH at 12 followed by extraction using ether (2 X 10 mL). The organic layer was dried over anhydrous sodium Na_2SO_4 and concentrated over a rotary evaporator to furnish compound **2n** in 96% yield as a colorless viscous oil.

Colorless viscous oil. IR (KBr) υ_{max}: 3077, 2948, 1593, 1458, 1131, 1018 cm^{-1}. ^1H NMR (400 MHz, $CDCl_3$) δ = 2.23 (s, 6H), 3.37 (s, 2H), 3.87 (s, 3H), 3.89 (s, 3H), 6.80 (s, 2H), 6.89 (s, 1H) ppm. ^{13}C NMR (100 MHz, $CDCl_3$) δ = 45.2 (CH_3), 55.8 (OCH_3), 55.9 (OCH_3), 64.1 (CH_2), 110.6 (CH), 112.1 (CH), 121.3 (CH), 131.2 (Cq), 148.1 (Cq), 148.9 (Cq) ppm.

3.5.18: *N*,*N*-dimethyl-1-(2,3,4-trimethoxyphenyl)methanamine (2r):

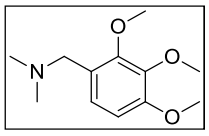

Following the similar procedure as described in experiment 3.5.17 with 2,3,4-trimethoxybenzaldehyde gave the white solid product in 94% yield.

Colorless viscous oil. IR (KBr) υ_{max}: 3074, 2944, 1596, 1459, 1122, 1009 cm^{-1}. ^1H NMR (400 MHz, $CDCl_3$) δ = 2.23 (s, 6H), 3.38 (s, 2H), 3.87 (s, 3H), 3.88 (s, 3H), 3.89 (s, 3H), 6.64 (d, J = 8.4 Hz, 1H), 6.98 (d, J = 8.8 Hz, 1H) ppm. ^{13}C NMR (100 MHz, $CDCl_3$) δ = 45.2 (2XCH_3), 56.0 (OCH_3), 57.6 (CH_2), 60.8 (OCH_3), 61.0 (OCH_3), 107.0 (CH), 124.3 (Cq), 125.2 (CH), 142.1 (Cq), 152.5 (Cq), 152.9 (Cq) ppm.

3.5.19: 1-(3-methoxyphenyl)-*N*,*N*-dimethylmethanamine (2s):

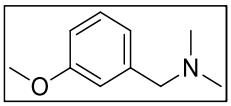

Following the similar procedure as described in experiment 3.5.17 with 3-methoxybenzaldehyde gave the pale yellow viscous oil product in 90% yield.

Pale yellow viscous oil. IR (KBr) υ_{max}: 2947, 1611, 1494, 1271, 1046 cm^{-1}. ^{1}H NMR (400 MHz, $CDCl_3$) δ = 2.23 (s, 6H), 3.40 (s, 2H), 3.80 (s, 3H), 6.79-6.81 (m, 1H), 6.88-6.89 (m, 2H), 7.22 (t, *J* = 8 Hz, 1H) ppm. ^{13}C NMR (100 MHz, $CDCl_3$) δ = 45.4 ($2XCH_3$), 55.2 (OCH_3), 64.4 (CH_2), 112.8 (CH), 114.3 (CH), 121.5 (CH), 129.2 (CH), 140.4 (Cq), 159.6 (Cq) ppm.

3.5.20: 3-(dimethylamino)-1-phenylpropan-1-one (2t):

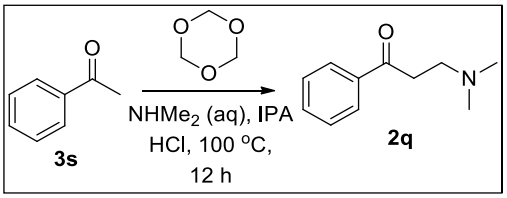

A mixture of 10 mmol of acetophenone, 12 mmol of an aqueous solution of dimethylamine, 15 mmol of 1,3,5-trioxane, and 1.2 mL of HCl was stirred in isopropyl alcohol and heated at 100 °C in a sealed tube for 12 hours. After the complete disappearance of acetophenone on TLC, isopropyl alcohol was evaporated completely on the rotary evaporator and 15 mL ethyl acetate was added to the reaction mixture and allowed to stir vigorously at room temperature for another 3 hours. The solid material precipitated out was filtered and washed with acetone to afford to obtain *N*,*N*-dimethyl-3-oxo-3-phenylpropan-1-aminium chloride, which was later basified with 1 N NaOH to give compound **2q** in 67% yield as a colorless liquid.

Colorless liquid. IR (KBr) υ_{max}: 3459, 2951, 2655, 2467, 1596, 1383, 1226, 1136, 959 cm^{-1}. ^{1}H NMR (400 MHz, $CDCl_3$) δ = 2.29 (s, 6H), 2.76 (t, *J* = 7.2 Hz, 2H), 3.16 (t, *J* = 7.2 Hz, 2H), 7.45-7.48 (m, 2H), 7.54-7.58 (m, 1H), 7.96-7.98 (m, 2H) ppm.

3.5.21: 1-(1*H*-indol-3-yl)-*N*,*N*-dimethyl-1-phenylmethanamine (2u):

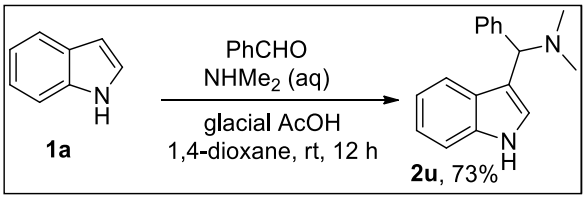

Following the similar procedure as described in experiment 3.5.16 with benzaldehyde instead of formaldehyde, gave the white solid product in 73% yield.

White solid, m.p. 198-203 °C. IR (KBr) υ_{max}: 3059, 2941, 1627, 1478, 1333, 747 cm^{-1}. ^{1}H NMR (400 MHz, $CDCl_3$) δ = 2.28 (s, 6H), 4.55 (s, 1H), 7.08 (t, *J* = 7.2 Hz, 1H), 7.10-7.20 (m, 3H), 7.25-7.32 (m, 3H), 7.50 (d, *J* = 7.6 Hz, 2H), 7.73 (d, *J* = 8 Hz, 1H), 8.13 (bs, 1H) ppm. ^{13}C NMR (100 MHz, $CDCl_3$) δ = 44.5 ($2XCH_3$), 69.3 (CH), 111.0 (CH), 118.2 (Cq), 119.4 (CH), 120.0 (CH), 122.0 (CH), 122.4 (CH), 126.7 (CH), 126.9 (2XCH), 128.0 (2XCH), 128.2 (Cq), 136.2 (Cq), 143.1 (Cq) ppm.

3.5.22: *N*,*N*-dimethyl-1-phenylethanamine (2v):

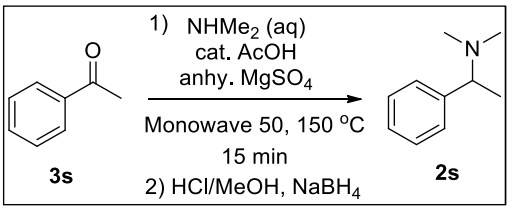

A solution of 3 mmol aqueous dimethylamine, 5 drops glacial acetic acid, 350 mg anhydrous magnesium sulphate, and 1 mmol of benzophenone were packed in Monowave 50 vial equipped with stirring bar and heated at 150 °C for 15 mins. After 15 mins, TLC was checked for the disappearance of the starting benzophenone and later the reaction mixture was diluted using 2N HCl/methanol maintaining the pH of ~3, and stirred the reaction for 2 hours. A 4 mmol of $NaBH_4$ was then added slowly to the cooled reaction mixture and let the mixture to get warm while stirring for another 30 minutes. After the completion of the reaction, it was quenched using cold water and extracted using ethyl acetate (3 X 10 mL). The resultant organic layer was dried over anhydrous Na_2SO_4 and concentrated under a vacuum. The thick liquid was then purified over flash chromatography on basic alumina (Pet. ether and ethyl acetate) to give compound **2s** in

43% yield.

Pale yellow oil. IR (KBr) υ_{max}: 2981, 2818, 2769, 1450, 1377, 1353, 1249, 1158, 1077, 959, 757 cm^{-1}. ^1H NMR (400 MHz, $CDCl_3$) δ = 1.37 & 1.38 (2Xs, 3H), 2.19 (s, 6H), 3.22-3.28 (q, 1H), 7.22-7.38 (m, 5H) ppm.

3.5.23: *N*,*N*-dimethyl-1,1-diphenylmethanamine (2w):

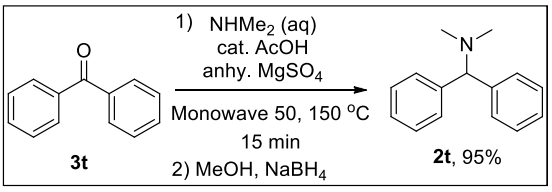

A solution of 3 mmol aqueous dimethylamine, 5 drops glacial acetic acid, 350 mg anhydrous magnesium sulphate, and 1 mmol of benzophenone were packed in Monowave 50 vial equipped with stirring bar and heated at 150 °C for 15 mins. After 15 mins, TLC was checked for the disappearance of the starting benzophenone and later the reaction mixture was diluted using methanol and cooled to 0 °C. A 4 mmol of $NaBH_4$ was then added slowly to the cooled reaction mixture and let the mixture to get warm while stirring for another 30 minutes. After the completion of the reaction, it was quenched using cold water and extracted using ethyl acetate (3 X 10 mL). The resultant organic layer was dried over anhydrous Na_2SO_4 and concentrated under a vacuum. The thick liquid was then purified over flash chromatography on basic alumina (Pet. ether and ethyl acetate) to give compound **2t** in 95% yield as pale yellow solid.

Pale yellow solid, m.p. 66-69 °C. IR (KBr) υ_{max}: 3067, 3028, 2962, 2814, 1503, 1458, 1188, 1023, 768, 747 cm^{-1}. ^1H NMR (400 MHz, $CDCl_3$) δ = 2.20 (s, 6H), 4.06 (s, 1H), 7.17 (t, *J* = 7.2 Hz, 2H), 7.27 (t, *J* = 7.4 Hz, 4H), 7.42 (d, *J* = 7.5 Hz, 4H) ppm. ^{13}C NMR (100 MHz, $CDCl_3$) δ = 44.8 ($2XCH_3$), 78.1 (CH), 126.9 (2XCH), 127.7 (4XCH), 128.5 (4XCH), 143.4 (2XCq) ppm.

3.5.24: General procedure for preparation of aldehydes and ketones (3a – 3t):

To the solution of 1 mmol indole dissolved in 2 mL of 1,4-dioxane was added 1.5 equiv sodium carbonate and 1.1 equiv iodine and was stirred for 12 h at room temperature. After the completion of the reaction (checked on TLC), 5 mL water was added and stirred for another 3 h. The aqueous layer was extracted using ethyl acetate. The organic layer was

dried over sodium sulfate and concentrated on a rotary evaporator. The crude sample was purified over flash chromatography (CH_2Cl_2 and MeOH).

3.5.25: 1-Methyl-1*H*-indole-3-carboxaldehyde (3b):

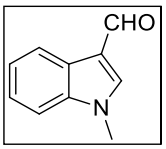

Following the similar procedure as described in experiment 3.5.24 gave the pale brown solid product an 83% yield.

Pale brown solid, m.p. 72°C. IR (KBr) υ_{max}: 3110, 1641, 1530, 1470, 1359 cm^{-1}. ^1H NMR (400 MHz, $CDCl_3$) δ = 3.80 (s, 3H), 7.33 – 7.30 (m, 3H), 7.60 (s, 1H), 8.27 – 8.30 (m, 1H), 9.92 (s, 1H) ppm. ^{13}C NMR (100 MHz, $CDCl_3$) δ = 33.7 (CH_3), 109.9 (CH), 118.0 (Cq), 122.0 (CH), 122.9 (CH), 124.0 (CH), 125.2 (Cq), 137.9 (Cq), 139.4 (CH), 184.5 (Cq) ppm. Spectral data is in accordance with the literature.[79]

3.5.26: 1-Benzyl-1*H*-indole-3-carboxaldehyde (3c):

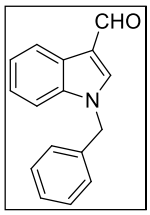

Following the similar procedure as described in experiment 3.5.24 gave the white solid product in 78% yield.

White solid, m.p. 105 °C. IR (KBr) υ_{max}: 3134, 2819, 1621, 1536, 1387, 1170 cm^{-1}. ^1H NMR (400 MHz, $CDCl_3$) δ = 5.34 (s, 2H), 7.17 (d, *J* = 8 Hz, 2H), 7.36 – 7.25 (m, 6H), 7.70 (s, 1H), 8.33 (d, *J* = 8 Hz, 1H), 9.98 (s, 1H) ppm. ^{13}C NMR (100 MHz, $CDCl_3$) δ = 50.9 (CH_2), 110.4 (CH), 118.5 (Cq), 122.2 (2XCH), 123.1 (CH), 124.2 (CH), 125.5 (Cq), 127.4 (2XCH), 128.4 (CH), 129.1 (2XCH), 137.5 (Cq), 138.6 (Cq), 184.70 (Cq) ppm. Spectral data is in accordance with the literature.[79]

3.5.27: 5-Methoxy-1*H*-indole-3-carboxaldehyde (3d):

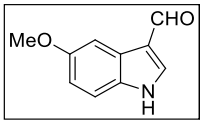

Following the similar procedure as described in experiment 3.5.24 gave the pale pink solid product in 71% yield.

Pale pink solid, m.p. 179 °C. IR (KBr) υ_{max}: 3462, 2945, 1660, 1578, 1456 cm^{-1}. ^{1}H NMR (400 MHz, DMSO-d_6) δ = 3.79 (s, 3H), 6.88 (dd, *J* = 8.8, 2.6 Hz, 1H), 7.41 (d, *J* = 8.8 Hz, 1H), 7.59 (d, *J* = 2.8 Hz, 1H), 8.22 (s, 1H), 9.90 (s, 1H), 12.03 (s, 1H) ppm. ^{13}C NMR (100 MHz, DMSO-d_6) δ = 55.7 (OCH_3), 102.9 (CH), 113.7 (CH), 113.8 (CH), 118.5 (Cq), 125.4 (Cq), 132.3 (Cq), 138.9 (CH), 156.1 (Cq), 185.3 (Cq) ppm. Spectral data is in accordance with the literature.[81]

3.5.28: 6-Chloro-1*H*-indole-3-carbaldehyde (3e):

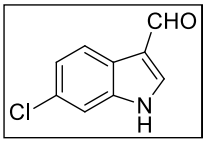

Following the similar procedure as described in experiment 3.5.24 gave the white solid product in 75% yield.

White solid, m.p. 205 °C. IR (KBr) υ_{max}: 3111, 2978, 2918, 1639, 1567, 1534, 1492, 1457, 1430 cm^{-1}. ^{1}H NMR (400 MHz, DMSO-d_6) δ = 7.26 (d, *J* = 8.4Hz, 1H), 7.58 (s, 1H), 8.08 (d, *J* = 8 Hz, 1H), 8.34 (s, 1H), 9.94 (s, 1H), 12.23(s, 1H) ppm. ^{13}C NMR (100 MHz, DMSO-d_6) δ = 117.4 (CH), 123.1 (CH), 127.2 (CH), 127.7 (Cq), 128.1 (Cq), 133.1 (Cq), 142.7 (CH), 144.5 (Cq), 190.5 (Cq) ppm. Spectral data is in accordance with the literature.[82]

3.5.29: 5-Nitro-1*H*-indole-3-carboxaldehyde (3f):

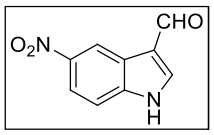

Following the similar procedure as described in experiment 3.5.24 gave the yellow solid product in 79% yield.

Yellow solid, m.p. 290 °C. IR (KBr) υ_{max}: 2931, 1703, 1536, 1528 cm^{-1}. ^{1}H NMR (400 MHz, DMSO-d_6) δ = 7.72 (d, *J* = 9.2 Hz, 1H), 8.16 (d, *J* = 8.8 Hz, 1H), 8.58 (s, 1H), 8.94 (s, 1H), 10.03 (s, 1H), 12.73 (s, 1H) ppm. ^{13}C NMR (100 MHz, DMSO-d_6) δ = 113.7 (CH), 117.5 (CH), 119.3 (CH), 119.5 (Cq), 124.0 (Cq), 140.6 (Cq), 142.0 (CH), 143.3 (Cq), 186.0 (Cq) ppm. Spectral data is in accordance with the literature.[79]

3.5.30: 3-Formyl-1*H*-indole-5-carbonitrile (3g):

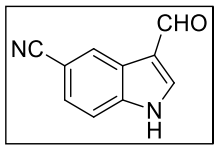

Following the similar procedure as described in experiment 3.5.24 gave the yellow solid product in 61% yield.

Yellow solid, m.p. 259 °C. IR (KBr) υ_{max}: 3196, 2245, 1649, 1598 cm^{-1}. ^{1}H NMR (400 MHz, DMSO-d_6) δ = 7.65 – 7.63 (m, 2H), 7.68 (d, *J* = 8.4 Hz, 1H), 8.46 (s, 1H), 8.51 (s, 1H), 10.00 (s, 1H) ppm. ^{13}C NMR (100 MHz, DMSO-d_6) δ = 104.9 (Cq), 114.4 (CH), 118.4 (Cq), 120.4 (Cq), 124.4 (Cq), 126.2 (CH), 126.9 (CH), 139.3 (Cq), 140.8 (CH), 185.9 (Cq) ppm. Spectral data is in accordance with the literature.[81]

3.5.31: 2-Methyl-1*H*-indole-3-carboxaldehyde (3i):

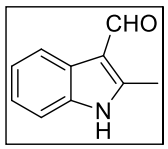

Following the similar procedure as described in experiment 3.5.24 gave the yellow solid product in 43% yield.

Yellow solid, m.p. 196 °C. IR (KBr) υ_{max}: 3391, 2631, 1769, 1564 cm^{-1}. ^{1}H NMR (400 MHz, DMSO-d_6): δ = 2.68 (s, 3H), 7.19 – 7.13 (m, 2H), 7.40 – 7.37 (m, 1H), 8.04 (t, *J* = 6.8 Hz, 1H), 10.06 (s, 1H), 11.98 (bs, 1H) ppm. ^{13}C NMR (100 MHz, DMSO-d_6): δ = 11.9 (CH_3), 111.8 (CH), 114.1 (Cq), 120.4 (CH), 122.3 (CH), 123.1 (CH), 126.0 (Cq), 135.8 (Cq), 149.0 (Cq), 184.7 (Cq) ppm. Spectral data is in accordance with the literature.[81]

3.5.32: Ethyl 3-formyl-1*H*-indole-2-carboxylate (3j):

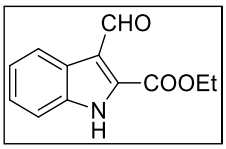

Following the similar procedure as described in experiment 3.5.24 gave the white solid product in 68% yield.

White solid, m.p. 183 °C. IR (KBr) υ_{max}: 3310, 1698, 1655, 1565 cm^{-1}. ^{1}H NMR (400 MHz, DMSO-d_6) δ = 1.42 (t, *J* = 6.8 Hz, 3H), 4.45 (q, *J* = 6.8 Hz, 2H), 7.32 – 7.28 (m, 1H), 7.42 – 7.38 (m, 1H), 7.58 (d, *J* = 8.4, 1H), 8.25 (d, *J* = 8.0 Hz, 1H), 10.62 (s, 1H), 12.84 (s, 1H) ppm. ^{13}C NMR (100 MHz, DMSO-d_6) δ = 14.5 (CH_3), 62.3 (CH_2), 113.6 (CH), 118.9 (Cq), 122.8 (CH), 124.0 (CH), 125.2 (Cq), 126.4 (CH), 133.2 (Cq), 136.2 (Cq), 160.6 (Cq), 188.0 (Cq) ppm. Spectral data is in accordance with the literature.[81]

3.5.33: 4-Hydroxy-2-oxo-2*H*-chromene-3-carboxaldehyde (3k):

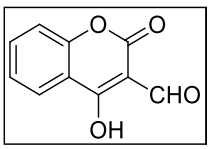

Following the similar procedure as described in experiment 3.5.24 gave the white crystalline solid product in 35% yield.

White crystals, m.p. 138 °C. IR (KBr) υ_{max}: 3329, 1736, 1645, 1573 cm^{-1}. ^{1}H NMR (400 MHz, DMSO-d_6) δ = 7.36 – 7.42 (m, 2H), 7.74 (t, *J* = 7.2, 1 H), 8.32 (d, *J* = 8.4, 1 H),

10.00 (s, 1H), 10.34 (s, 1H) ppm. ^{13}C NMR (100 MHz, DMSO-d_6): δ = 95.5 (Cq), 114.0 (Cq), 118.0 (CH), 124.7 (CH), 125.3 (CH), 135.4 (CH), 154.3 (Cq), 158.3 (Cq), 162.5 (Cq), 191.1 (Cq) ppm. Spectral data is in accordance with the literature.[80]

3.5.34: Thiophene-2-carboxaldehyde (3l):

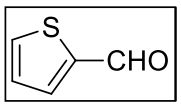

Following the similar procedure as described in experiment 3.5.24 gave the yellow liquid product in 59% yield.

Yellow liquid, b.p. 250-254 °C, yield: 59 %. IR (KBr) υ_{max}: 1668, 1514, 1423, 1219, 910, 728 cm^{-1}. ^{1}H NMR (400 MHz, $CDCl_3$), δ = 7.13–7.11 (t, *J* = 4.8 Hz, 2H), 7.68 (d, *J* = 4.8 Hz, 1H), 7.70 (d, *J* = 3.6 Hz, 1H), 9.84 (s, 1H) ppm. ^{13}C NMR (100 MHz, $CDCl_3$): δ = 128.4 (CH), 135.2 (CH), 136.6 (CH), 143.9 (Cq), 183.1 (Cq) ppm. Spectral data is in accordance with the literature.[80]

3.5.35: 2-Hydroxy-1-naphthaldehyde (3m):

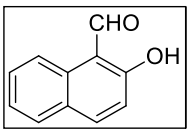

Following the similar procedure as described in experiment 3.5.24 gave the yellow solid product in 56% yield.

Yellow solid, m.p. 80-83 °C. IR (KBr) υ_{max}: 3156, 3061, 2840, 1648, 1610 cm^{-1}. ^{1}H NMR (400 MHz, $CDCl_3$), δ = 7.10–7.17 (m, 1H), 7.44–7.40 (m, 1H), 7.62–7.57 (m, 1H), 7.76–7.80 (m, 1H), 7.93–7.98 (m, 1H), 8.29 (d, *J* = 8.6 Hz, 1H), 10.76 (s, 1H), 13.15 (s, 1H) ppm. ^{13}C NMR (100 MHz, $CDCl_3$): δ = 111.3 (Cq), 118.6 (CH), 119.2 (CH), 124.5 (CH), 127.8 (Cq), 129.1 (CH), 129.5 (CH), 132.9 (Cq), 139.2 (CH), 164.9 (Cq), 193.3 (Cq) ppm. Spectral data is in accordance with the literature.[83]

3.5.36: 3,4-Dimethoxybenzaldehyde (3n):

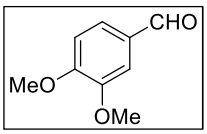

Following the similar procedure as described in experiment 3.5.24 gave the white solid product in 67% yield.

Off white solid, m.p. 46-48 °C. IR (KBr) υ_{max}: 1688, 1601, 1514, 1272, 1140, 733 cm^{-1}. ^{1}H NMR (400 MHz, $CDCl_3$): δ = 3.95 (s, 3H), 3.98 (s, 3H), 6.99 (d, *J* = 8.4 Hz, 1H), 7.42 (s, 1 H), 7.48 (d, *J* = 7.6 Hz, 1H), 9.86 (s, 1H) ppm. ^{13}C NMR (100 MHz, $CDCl_3$): δ = 56.0 (OCH_3), 56.2 (OCH_3), 108.9 (CH), 110.4 (CH), 126.9 (CH), 130.1 (Cq), 149.6 (Cq), 154.5 (Cq), 191.0 (Cq) ppm. Spectral data is in accordance with the literature.[84]

3.5.37: 2,3,4-Trimethoxybenzaldehyde (3o):

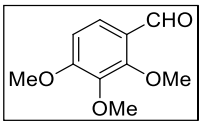

Following the similar procedure as described in experiment 3.5.24 gave the colorless oil product in 64% yield.

Colorless oil, b.p. 168-170 °C. IR (KBr) υ_{max}: 1693, 1594, 1297, 1210, 1110, 743 cm^{-1}. ^{1}H NMR (400 MHz, $CDCl_3$): δ = 3.89 (s, 1H), 3.94 (s, 1H), 4.04 (s, 1H), 6.77 (d, *J* = 8.8 Hz, 1H), 7.61 (d *J* = 8.8 Hz, 1H), 10.24 (s, 1H) ppm. ^{13}C NMR (100 MHz, $CDCl_3$) δ = 56.2 (OCH_3), 61.0 (OCH_3), 62.3 (OCH_3), 107.4 (CH), 123.3 (Cq), 124.2 (CH), 141.6 (Cq), 156.9 (Cq), 159.3 (Cq), 188.9 (Cq) ppm. Spectral data is in accordance with the literature.[85]

3.5.38: 3-Methoxybenzaldehyde (3p):

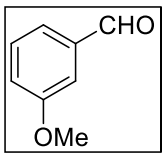

Following the similar procedure as described in experiment 3.5.24 gave the colorless oil product in 59% yield.

Colorless oil, b.p. 229-232 °C. IR (KBr) υ_{max}: 1703, 1596, 1276, 993, 778 cm^{-1}. ^{1}H NMR (400 MHz, $CDCl_3$) δ = 3.87 (s, 3H), 7.19-7.16 (m, 1H), 7.39 (s, 1H), 7.46-7.43 (m, 2H), 9.98 (s, 1H) ppm. ^{13}C NMR (100 MHz, $CDCl_3$) δ = 55.5 (OCH_3), 112.0 (CH), 121.2 (CH), 123.6 (CH), 130.0 (CH), 137.8 (Cq), 160.1 (Cq), 192.2 (Cq) ppm. Spectral data is in accordance with the literature.[85]

3.5.39: Acetophenone (3s):

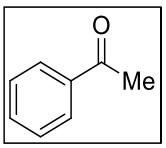

Following the similar procedure as described in experiment 3.5.24 gave the colorless oil product in 53% yield.

Colorless oil, b.p. 200-202 °C. IR (KBr) υ_{max}: 3069, 2967, 1689, 756 cm^{-1}. ^{1}H NMR (400 MHz, $CDCl_3$) δ = 2.61 (s, 3H), 7.46 (t, *J* = 7.6 Hz, 2H), 7.57 (t, *J* = 7.4 Hz, 1H), 7.96 (d, *J* = 8.0 Hz, 2H) ppm. ^{13}C NMR (100 MHz, $CDCl_3$) δ = 26.6 (CH_3), 128.3 (2XCH), 128.6 (2XCH), 133.1 (CH), 137.1 (Cq), 198.3 (Cq) ppm. Spectral data is in accordance with the literature.[85]

3.5.40: Benzophenone (3t):

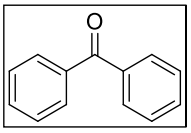

Following the similar procedure as described in experiment 3.5.24 gave the white solid product an 89% yield.

White solid, m.p. 52-54 °C. IR (KBr) υ_{max}: 3104, 3005, 1704, 980, 765 cm^{-1}. ^{1}H NMR (400 MHz, $CDCl_3$) δ = 7.47 (t, *J* = 7.8 Hz, 4H), 7.58 (t, *J* = 7.3 Hz, 2H), 7.80 (d, *J* = 8.0 Hz, 4H) ppm. ^{13}C NMR (100 MHz, $CDCl_3$) δ = 128.3 (4XCH), 130.1 (4XCH), 132.5 (2XCH), 137.6 (2XCq), 196.8 (Cq) ppm. Spectral data is in accordance with the literature.[85]

3.6 References:

1) Lee, J.-H.; Lee, J. *FEMS Microbiol Rev* **2010**, *34*, 426.
2) Elze, F. *Chem.-Ztg.* **1910**, *34*, 814.
3) (a) Cerighelli, R. *Compt. rend.* **1924**, *179*, 1193. (b) Hesse, A. *Ber.* **1904**, *37*, 1457. (c) Soden, H. V. *J. prakt. Chem.* **1904**, *69*, 256.
4) Sack, J. *Pharm. Weekblad* **1911**, *48*, 307.
5) Hesse, A.; Zeitschel, O. *J. prakt. Chem.* **1902**, *66*, 481.
6) Porcher, C. *Compt. rend.* **1908**, *147*, 214.
7) Nencki, M. *Ber.* **1874**, *7*, 1593.
8) Stockly, F. *J. prakt. Chem.* **1881**, *24*, 17.
9) Ernst, C. *J. physiol. Chem.* **1892**, *16*, 208.
10) Baeyer, A. *Ber.* **1868**, *1*, 17.
11) Fischer, E.; Jourdan, F. *Ber.* **1883**, *16*, 2241.
12) Yannai, S. Dictionary of Food Compounds with CD-ROM: Additives, Flavors, and Ingredients; CRC Press: Boca Raton, **2003**.
13) Dzurilla, M.; Kutschy, P.; Zaletova, J.; Ruzinsky, M.; Kovacik, V. *Molecules* **2001**, *6*, 716.
14) Kuramochi, K.; Osada, Y.; Kitahara, T. *Tetrahedron* **2003**, *59*, 9447.
15) Donia, M.; Hamann, M. T. *Lancet Infect. Dis.* **2003**, *3*, 338.
16) (a) Kobayashi, J.; Ishibashi, M.; Nagai, U.; Ohizumi, Y. *Experientia* **1989**, *45*, 782. (b) Kobayashi, J.; Murayama, T.; Ishibashi, M.; Kosuge, S.; Takamatsu, M.; Ohizumi, Y.; Kobayashi, H.; Ohta, T.; Nozoe, S.; Sasaki, T. *Tetrahedron* **1990**, *46*, 7699.
17) Kondo, K.; Nishi, J.; Ishibashi, M.; Kobayashi, J. *J. Nat. Prod.* **1994**, *57*, 1008.
18) Jiang, B.; Yang, C. G.; Wang, J. *J. Org. Chem.* **2002**, *67*, 1396.
19) Wang, Y. Y.; Chen, C. *J. Chin. Chem. Soc.* **2013**, *54*, 1363.
20) (a) González-Lamothe, R.; Mitchell, G.; Gattuso, M.; Diarra, M. S.; Malouin, F.; Bouarab, K. *Int. J. Mol. Sci.* **2009**, *10*, 3400. (b) Burnett, J. C.; Rossi, J. *J. Cell Chem. Biol.* **2012**, *19*, 60.
21) Herrmann, J.; Fayad, A. A.; Müller, R. *Nat. Prod. Rep.* **2017**, *34*, 135.
22) Davyt, D.; Entz, W.; Fernandez, R.; Mariezcurrena, R.; Mombrú, A. W.; Saldaña, J.; Domínguez, L.; Coll, J.; Manta, E. *J. Nat. Prod.* **1998**, *61*, 1560.

23) Lewellyn, K.; Bialonska, D.; Chaurasiya, N. D.; Tekwani, B. L.; Loria, M. J.; White, S. W.; Sufka, K. J.; Zjawiony, J. K. *Planta Med.* **2012**, *78*, CL22.

24) Cimanga, K.; De Bruyne, T.; Pieters, L.; Vlietinck, A. J.; Turger, C. A. *J. Nat. Prod.* **1997**, *60*, 688.

25) Pedras, M. S. C.; Sarwar, M. G.; Suchy, M.; Adio, A. M. *Phytochemistry* **2006**, *67*, 1503.

26) Nandha K. R.; Suresh T.; Mohan P. S. *Tetrahedron Lett.* **2002**, *43*, 3327.

27) Griffiths-Jones, C. M.; Knight, D. W. *Tetrahedron* **2011**, *67*, 8515.

28) (a) Yang, M. R.; Qin, Y. J.; Chen, C.; Zhang, Y. L.; Li, B. Y.; Liu, T. B.; Gong, H. B.; Wang, B. Z.; Zhu, H. L. *RSC Adv.* **2016**, *6*, 30412. (b) Netz, N.; Opatz, T. *J. Org. Chem.* **2016**, *81*, 1723. (c) Mukherjee, D. D.; Kumar, N. M.; Tantak, M. P.; Das, A.; Ganguly, A.; Datta, S.; Kumar D.; Chakrabarti, G. *Biochemistry* **2016**, *55*, 3020. (d) Sundaree, S.; Vaddula, B. R.; Tantak, M. P.; Khandagale, S. B.; Shi, C.; Shah, K.; Kumar, D. *Med. Chem. Res.* **2016**, *25*, 941. (e) Pedada, S. R.; Yarla, N. S.; Tambade, P. J.; Dhananjaya, B. L.; Bishayee, A.; Arunasree, K. M.; Philip, G. H.; Dharmapuri, G.; Aliev, G.; Rangaiah, G. *Eur. J. Med. Chem.* **2016**, *112*, 289. (f) Zhang, Y. L.; Qin, Y. J.; Tang, D. J.; Yang, M. R.; Li, B. Y.; Wang, Y. T.; Cai, H. Y.; Wangand, B. Z.; Zhu, H. L. *ChemMedChem* **2016**, *11*, 1446. (g) El-labbad, E. M.; Ismail, M. A. H.; Ei Ella, D. A. A.; Ahmed, M.; Wang, F.; Barakat K. H.; Abouzid, K. A. M. *Chem. Bio. Drug Des.*,**2015**, *86*, 1518. (h) Chen, C. H.; Genapathy, S.; Fischer P. M.; Chan, W. C. *Org. Biomol. Chem.* **2014**, *12*, 9764. (i) Sashidhara, K. W.; Dodda, R. P.; Sonkar, R.; Palnati G. R.; Bhatia, G. *Eur. J. Med. Chem.* **2014**, *81*, 499. (j) Jin, H.; Zhang, P.; Bijian, K.; Ren, S.; Wan, S.; Alaoui-Jamali, M. A.; Jiang, T. *Mar. Drugs.* **2013**, *11*, 1427.

29) (a) Bennasar, M. L.; Zulaica, E.; Sole O.; Alonso, O. *Tetrahedron* **2007**, *63*, 861. (b) Tohyama, S.; Choshi, T.; Matsumoto, K.; Yamabuki, A.; Ikegata, K.; Nobuhiro, J.; Hibino, S. *Tetrahedron Lett.* **2005**, *46*, 5263. (c) Mayer, S.; Joseph, B.; Guillaumet, G.; Merour, J. Y. *Synthesis* **2002**, *13*, 1871.

30) (a) Van Niel, M. B.; Collins, I.; Beer, M. S.; Broughton, H. B.; Cheng, S. K. F.; Goodacre, S. C.; Heald, A.; Locker, K. L.; MacLeod, A. M.; Morrison, D.; Moyes, C. R.; O'Connor, D.; Pike, A.; Rowley, M. L.; Russell, M. G. N.; Sohal, B.; Stanton, J. A.; Thomas, S.; Verrier, H.; Watt, A. P.; Castro, J. L. *J. Med. Chem.* **1999**, *42*, 2087. (b) Charterjee A.; Biswas, K. M. *J. Org. Chem.* **1973**, *38*, 4002.

31) (a) Wynberg, H. *Chem. Rev.* **1960**, *60*, 169. (b) Blume R. C.; Lindwall, H. G. *J. Org. Chem.* **1945**, *10*, 255.

32) Mei, Q.; Liu, H.; Yang, Y.; Liu, H.; Li, S.; Zhang, P.; Han, B. *ACS Sustain. Chem. Eng.* **2018**, *6*, 2362.

33) Baruah, D.; Saikia, U. P.; Pahari, P.; Konwar, D. *Tetrahedron Lett.* **2015**, *56*, 2543.

34) Steves, J. E.; Stahl, S. S. *J. Am. Chem. Soc.* 2013, *135*, 15742.

35) Yan, Q.; Fang, Y. C.; Jia, Y. X.; Duan, X. *New J. Chem.* **2017**, *41*, 2372.

36) Jiang, J. A.; Du, J. L.; Wang, Z. G.; Zhang, Z. N.; Xu, X.; Zheng, G. L.; Ji, Y. F. *Tetrahedron Lett.* **2014**, *55*, 1677.

37) Sarmah, K.; Pal, J.; Maji, T. K.; Pratihar, S. *ACS Sustain. Chem. Eng.* **2017**, *5*, 11504.

38) Fernandes, R. A.; Bethi, V. *RSC Adv.* **2014**, *4*, 40561.

39) Zhang, Y.; Schilling, W.; Riemer, D.; Das, S. *Nat. Protoc.* **2020**, *15*, 822.

40) Schilling, W.; Riemer, D.; Zhang, Y.; Hatami, N.; Das, S. *ACS Catal.* **2018**, *8*, 5425.

41) Ang, W. J.; Chng, Y. S.; Lam, Y. *RSC Adv.* **2015**, *5*, 81415.

42) Rathore, P. S.; Patidar, R.; Thakore, S. *RSC Adv.* **2014**, *4*, 41111.

43) Sheriff Shah, S.; Pradeep Singh, N. D. *Tetrahedron Lett.* **2018**, *59*, 247.

44) Kumar, K.; Kumar, P.; Joshi, P.; Rawat, D. S. *Tetrahedron Lett.* **2020**, *61*, 151749.

45) Misztal, S.; Mokrosz, J. L.; Bielecka, Z. *J. for Prakt. Chemie* **1989**, *331*, 751.

46) Niu, G. H.; Huang, P. R.; Chuang, G. J. *Asian J. Org. Chem.* **2016**, *5*, 57.

47) Yin, Z.; Wang, Z.; Wu, X. F. *Org. Biomol. Chem.* **2018**, *16*, 3707.

48) Huang, H.; Yu, C.; Li, X.; Zhang, Y.; Zhang, Y.; Chen, X.; Mariano, P. S.; Xie, H.; Wang, W. *Angew. Chemie - Int. Ed.* **2017**, *56*, 8201.

49) Bonesi, S. M.; Torriani, R.; Mella, M.; Albini, A. *Eur. J. Org. Chem.* **1999**, *7*, 1723.

50) Fei, H.; Yu, J.; Jiang, Y.; Guoa, H.; Cheng, J. *Org. Biomol. Chem.* **2013**, *11*, 7092.

51) Betterley, N. M.; Kongsriprapan, S.; Chaturonrutsamee, S.; Deelertpaiboon, P.; Surawatanawong, P.; Pohmakotr, M.; Soorukram, D.; Reutrakul, V.; Kuhakarn, C. *Synthesis* **2018**, *50*, 2033.

52) Jia-Qin L.; Hui-Lin T.; Dan-Dan M.; Xin-Xin Z.; Hai-Lei C. *J. Org. Chem.* **2021**, *86*, 10118.

53) (a) Wang, Q.-D.; Yang, J.-M.; Fang, D.; Ren, J.; Zeng B.-B. *Tetrahedron Lett.* **2017**, *58*, 2877. (b) Tongkhan, S.; Radchatawedchakoon, W.; Kruanetr, S.; Sakee, U. *Tetrahedron Lett.* **2014**, *55*, 3909.

54) Li, X.; Gu, X.; Li, Y.; Li, P. *ACS Catal.* **2014**, *4*, 1897.

55) Zhang, L.; Peng, C.; Zhao, D.; Wang, Y.; Fu, H. J.; Shen, Q.; Li, J. X. *Chem. Commun.* **2012**, *48*, 5928.

56) Zhang, B.; Liu, B.; Chen, J.; Wang, J.; Liu, M. *Tetrahedron Lett.* **2014**, *55*, 5618.

57) Lu, L.; Xiong, Q.; Guo, S.; He, T.; Xu, F.; Gong, J.; Zhu, Z.; Cai, H. *Tetrahedron* **2015**, *71*, 3637.

58) Chen, J.; Liu, B.; Liu, D.; Liu, S.; Cheng, J. *Adv. Synth. Catal.* **2012**, *354*, 2438.

59) Zhang, W.; Tang, J.; Yu, W.; Huang, Q.; Fu, Y.; Kuang, G.; Pan, C.; Yu, G. *ACS Catal.* **2018**, *8*, 8084.

60) Ye, Y.; Cheung, K. P. S.; He, L.; Tsui, G. C. *Org. Lett.* **2018**, *20*, 1676.

61) Yan, M.; Hider, R. C.; Ma, Y. *Org. Chem. Front.* **2019**, *6*, 1168.

62) Wu, W.; Su, W. *J. Am. Chem. Soc.* **2011**, *133*, 11924.

63) Li, L. T.; Huang, J.; Li, H. Y.; Wen, L. J.; Wang, P.; Wang, B. *Chem. Commun.* **2012**, *48*, 5187.

64) Sun, L.; Yao, A.; Wang, H.; Zhang, L.; Zeng, L.; Huang, Z.; Gao, M.; Lei, A. *Asian J. Org. Chem.* **2018**, *7*, 1571.

65) Li, L. T.; Li, H. Y.; Xing, L. J.; Wen, L. J.; Wang, P.; Wang, B. *Org. Biomol. Chem.* **2012**, *10*, 9519.

66) Wang, Q. D.; Zhou, B.; Yang, J. M.; Fang, D.; Ren, J.; Zeng, B. B. *Synlett* **2017**, *28*, 2670.

67) Yang, L.; Liu, Z.; Li, Y.; Lei, N.; Shen, Y.; Zheng, K. *Org. Lett.* **2019**, *21*, 7702.

68) Xiao, J.; Li, Q.; Chen, T.; Han, L. B. *Tetrahedron Lett.* **2015**, *56*, 5937.

69) Iranpoor, N.; Firouzabadi, H.; Rizi, Z. T.; Erfan, S. *RSC Adv.* **2014**, *4*, 43178.

70) Li, L. H.; Niu, Z. J.; Liang, Y. M. *Org. Biomol. Chem.* **2018**, *16*, 7792.

71) Ding, S.; Jiao, N. *J. Am. Chem. Soc.* **2011**, 12374.

72) Iranpoor, N.; Panahi, F.; Erfan, S.; Roozbin, F. *J. Heterocycl. Chem.* **2017**, *54*, 904.

73) Zhang, L.; Wen, Q.; Jin, J.; Wang, C.; Lu, P.; Wang, Y. *Tetrahedron* **2013**, *69*, 4236.

74) Ganesan, B.; Senadi, G. C.; Guo, B. C.; Hung, M. Y.; Lin, W. Y. A *RSC Adv.* **2018**, *8*, 40968.

75) Itoh, T.; Abe, T.; Nakamura, S.; Ishikura, M. *Heterocycles* **2015**, *91*, 1423.

76) Desjardins, S.; Jacquemot, G.; Canesi, S. *Synlett* **2012**, *23*, 1497.

77) Stanek, F.; Pawłowski, R.; Mlynarski, J.; Stodulski, M. *Eur. J. Org. Chem.* **2018**, *2018*, 6624.

78) Volvoikar, P. S.; Tilve, S. G. *Org. Lett.* **2016**, *18*, 892.

79) Wang, Q. D.; Yang, J. M.; Ren, D. F. J.; Zeng, B. B. *Tetrahedron Lett.* **2017**, *58*, 2877.

80) Ibrahim, M. A. *Tetrahedron* **2009**, *65*, 7687.

81) Lu, L.; Xiong, Q.; Guo, S.; He, T.; Xu, F.; Gong, J.; Zhu, Z.; Cai, H. *Tetrahedron* **2015**, *71*, 3637.

82) Zhang, B.; Liu, B.; Chen, J.; Wang, J.; Liu, M. *Tetrahedron Lett.* **2014**, *55*, 5618.

83) Deb, M. L.; Pegu, C. D.; Borpatra, P. J.; Baruah, P. K. *RSC Adv.* **2016**, *6*, 40552.

84) Das, A. K.; Goswami, S.; Quah, C. K.; Fun, H. K. *New J. Chem.* **2015**, *39*, 5669.

85) Adil, S. F.; Assal, M. E.; Rafi, M.; Kuniyil, S. M. A.; Khan, H. M.; Khan, A.; Tahir, M. N.; Al-Warthan, A.; Siddiqui, M. R. H. *Appl.Organomet. Chem.* **2020**, *34*, e5718.

NMR Spectra

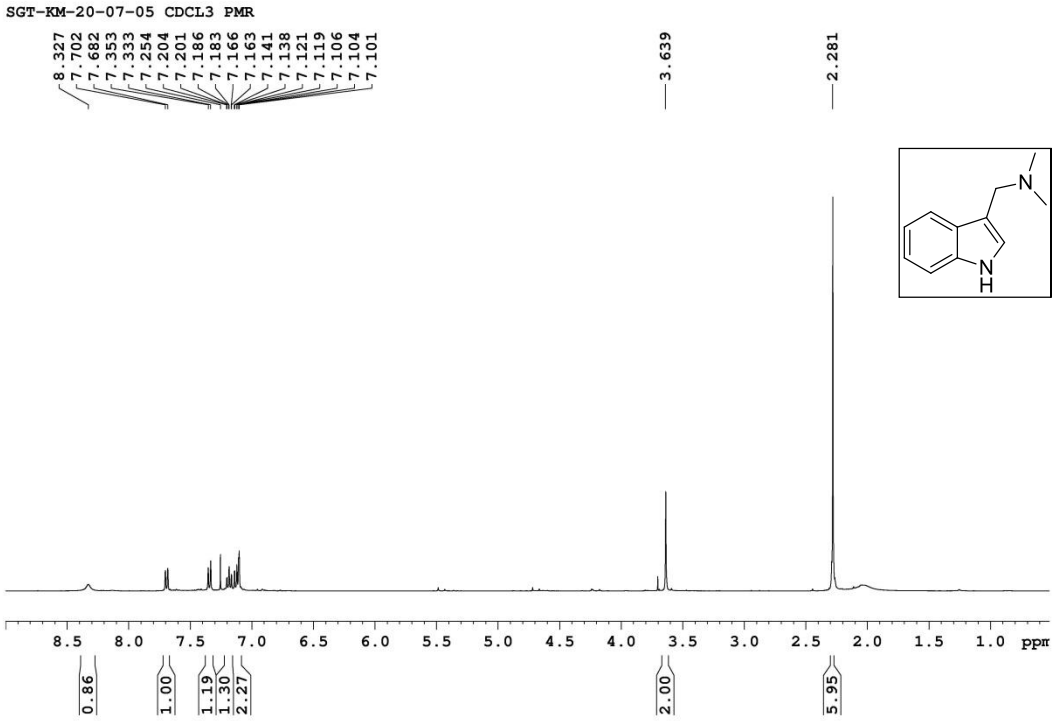
SGT-KM-20-07-05 CDCL3 PMR
8.327
7.702
7.682
7.353
7.333
7.254
7.204
7.201
7.186
7.183
7.166
7.163
7.141
7.138
7.121
7.119
7.106
7.104
7.101
3.639
2.281
N
N
H
8.5 8.0 7.5 7.0 6.5 6.0 5.5 5.0 4.5 4.0 3.5 3.0 2.5 2.0 1.5 1.0 ppm
0.86
1.00
1.19
1.30
2.27
2.00
5.95

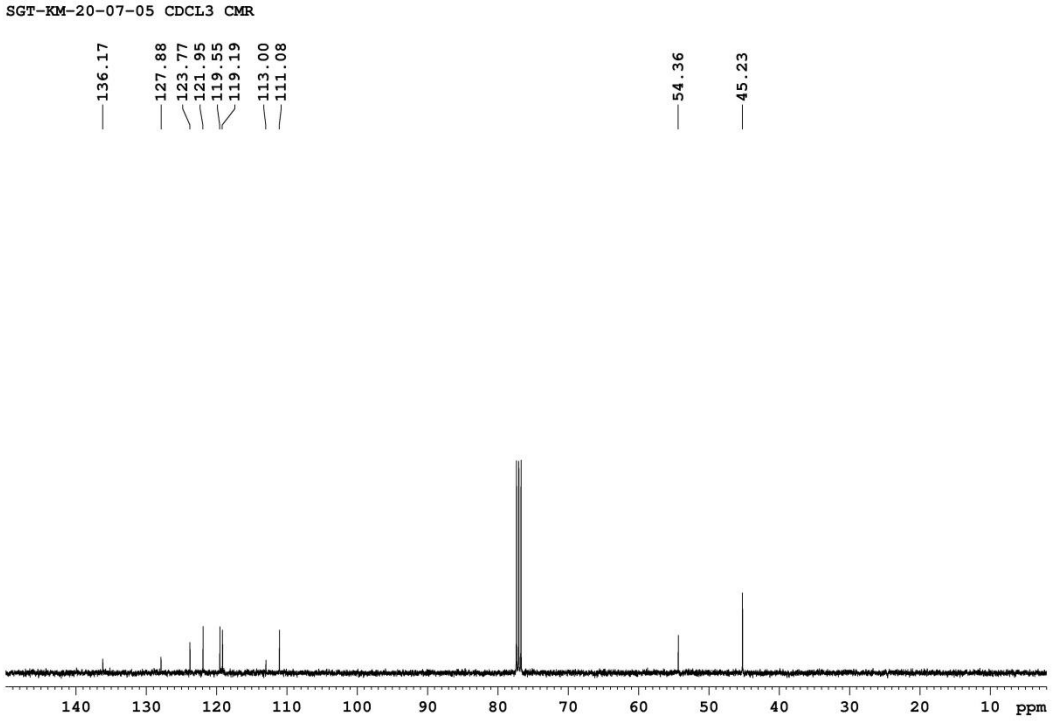
SGT-KM-20-07-05 CDCL3 CMR
136.17
127.88
123.77
121.95
119.55
119.19
113.00
111.08
54.36
45.23
140 130 120 110 100 90 80 70 60 50 40 30 20 10 ppm

SGT-KM-20-07-05 CDCL3 DEPT

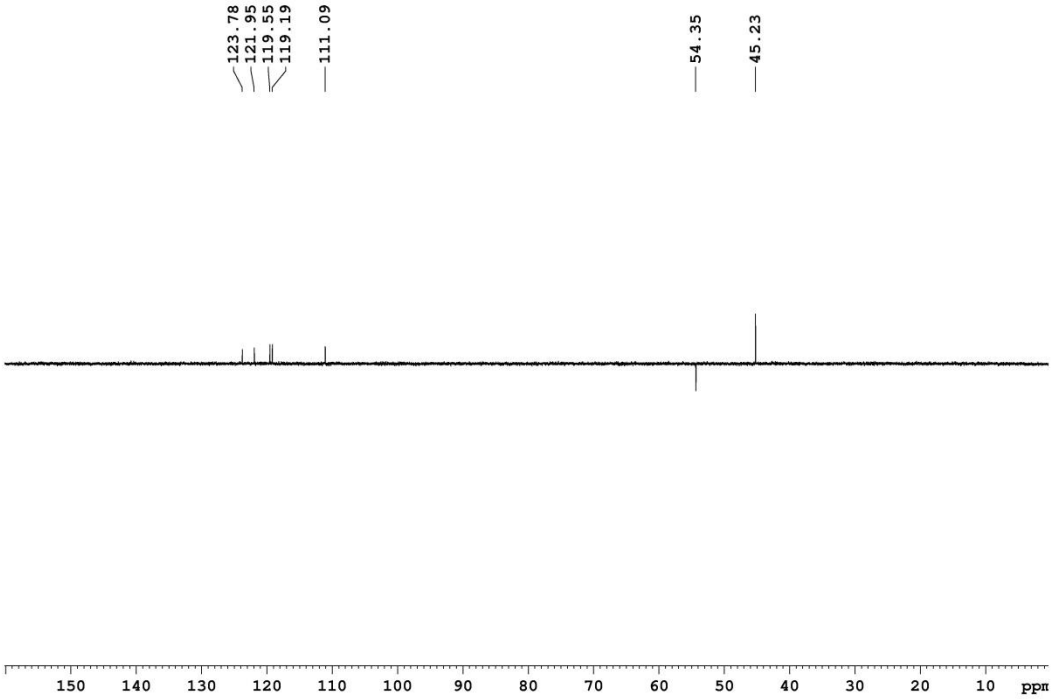

SGT-KM-20-19 CDCL3 PMR

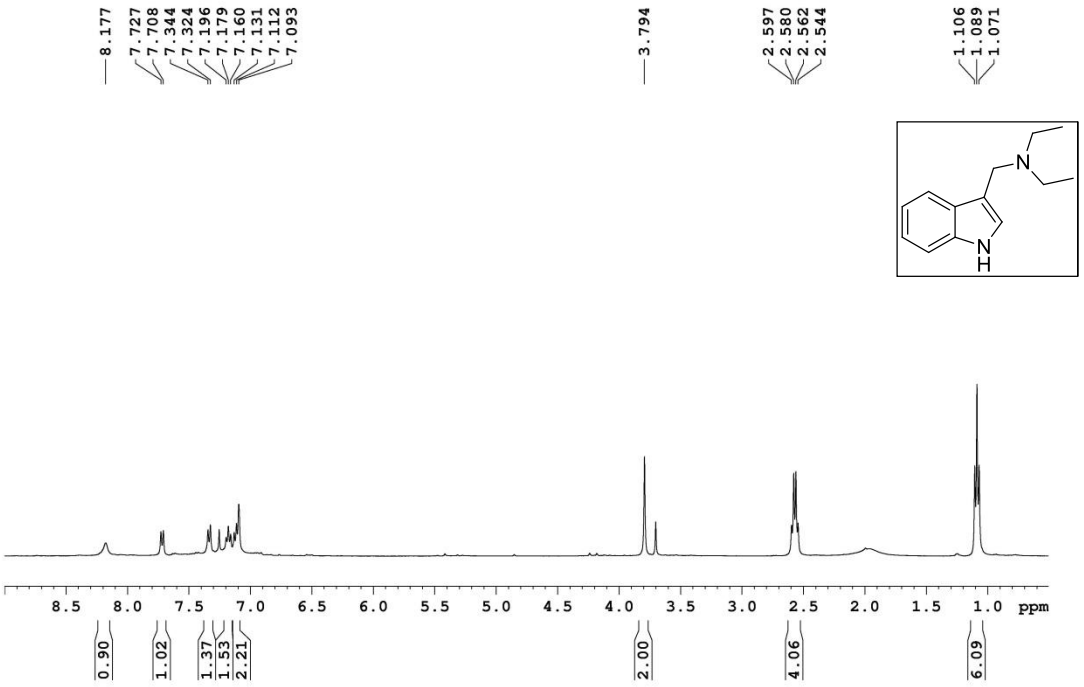

SGT-KM-20-19 CDCL3 CMR

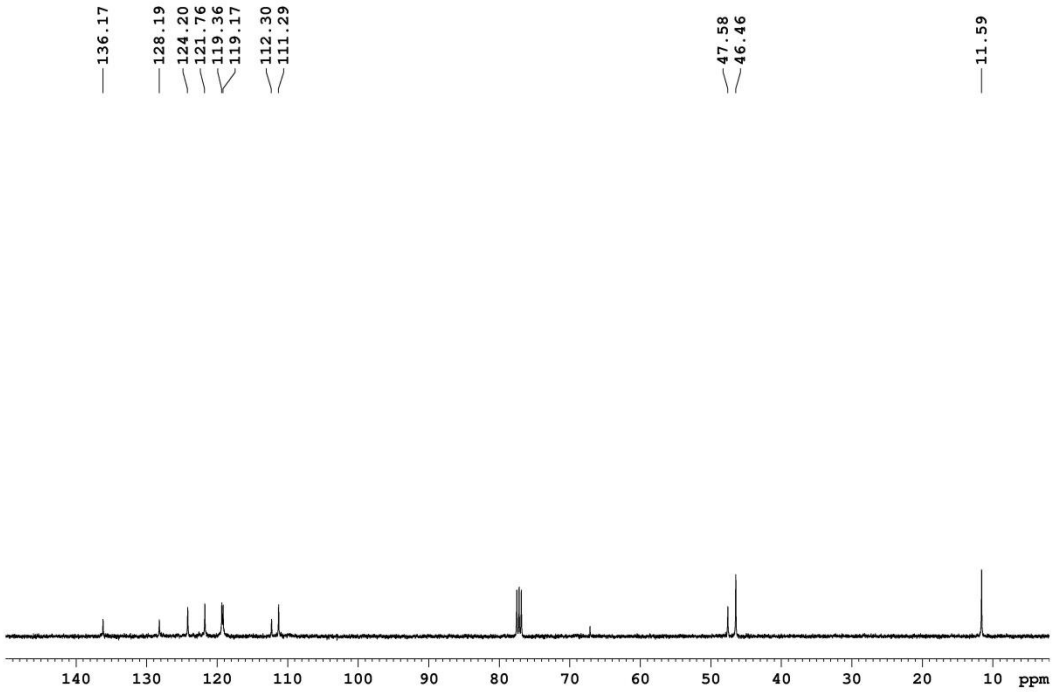

SGT-KM-20-19 CDCL3 DEPT

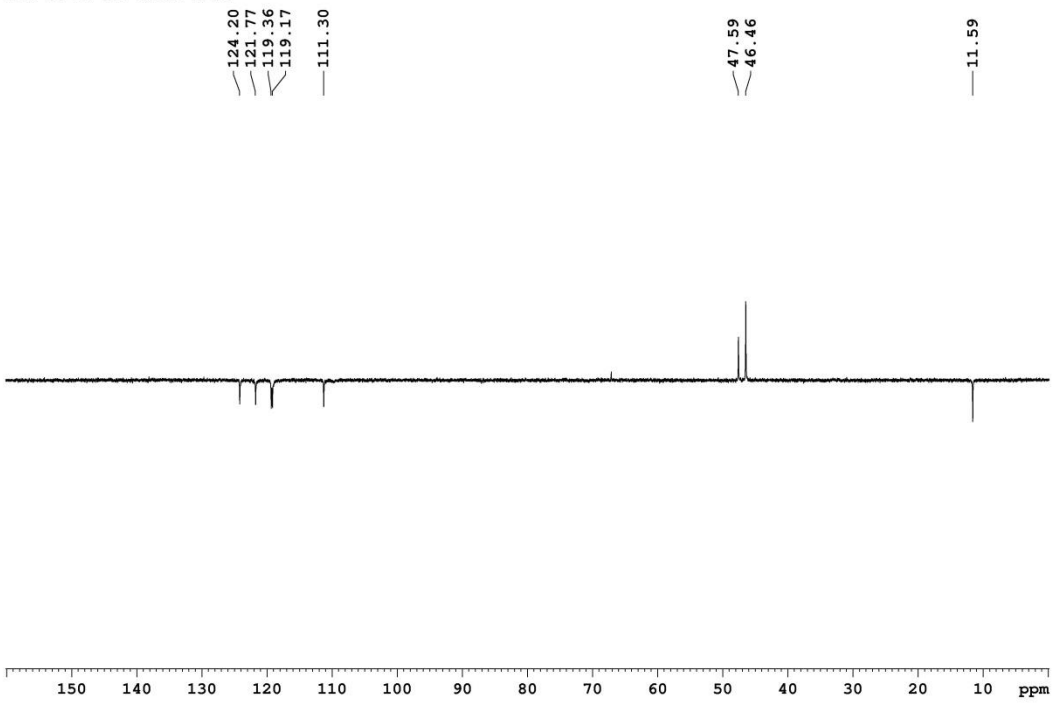

SGT-KM-20-05-01 CDCL3 PMR

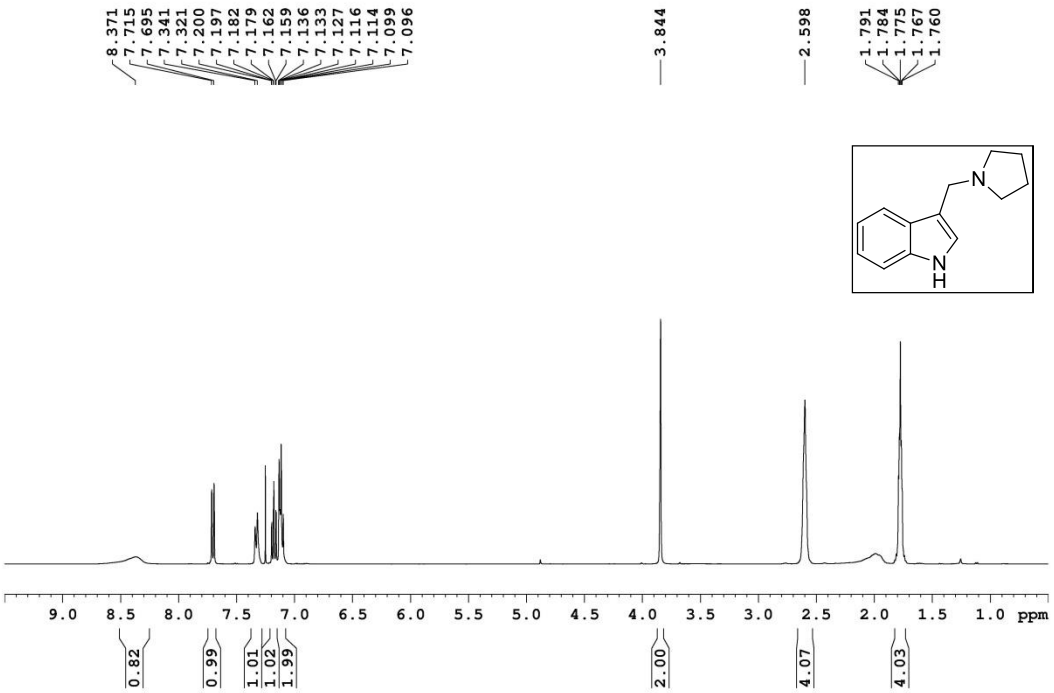

SGT-KM-20-05-01 CDCL3 CMR

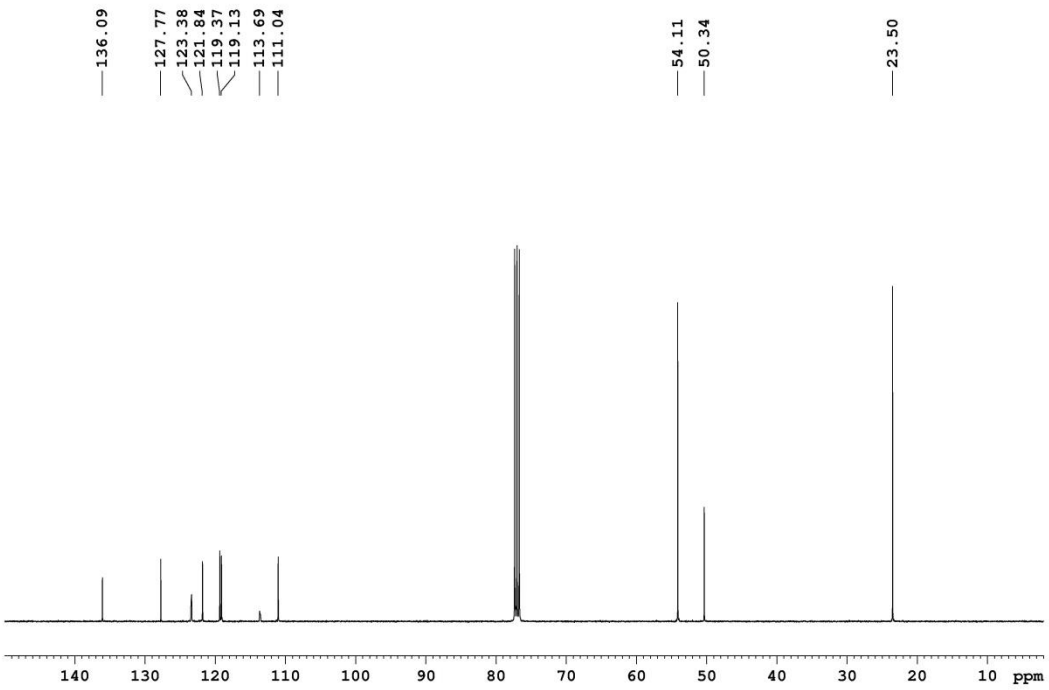

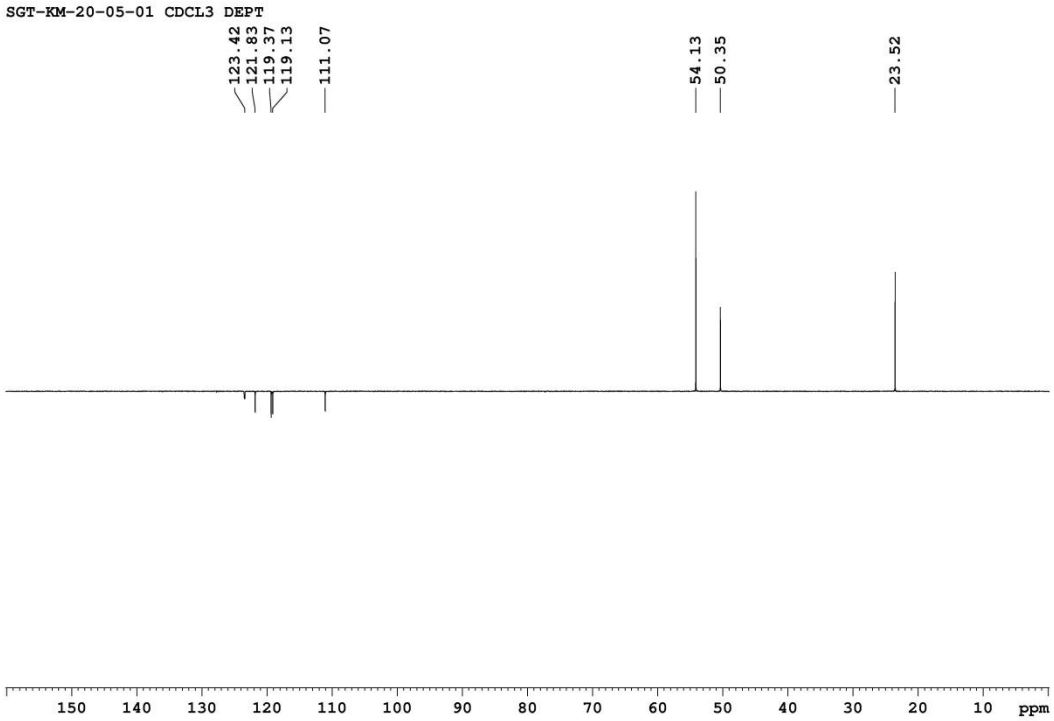
SGT-KM-20-05-01 CDCL3 DEPT
123.42
121.83
119.37
119.13
111.07
54.13
50.35
23.52
150 140 130 120 110 100 90 80 70 60 50 40 30 20 10 ppm

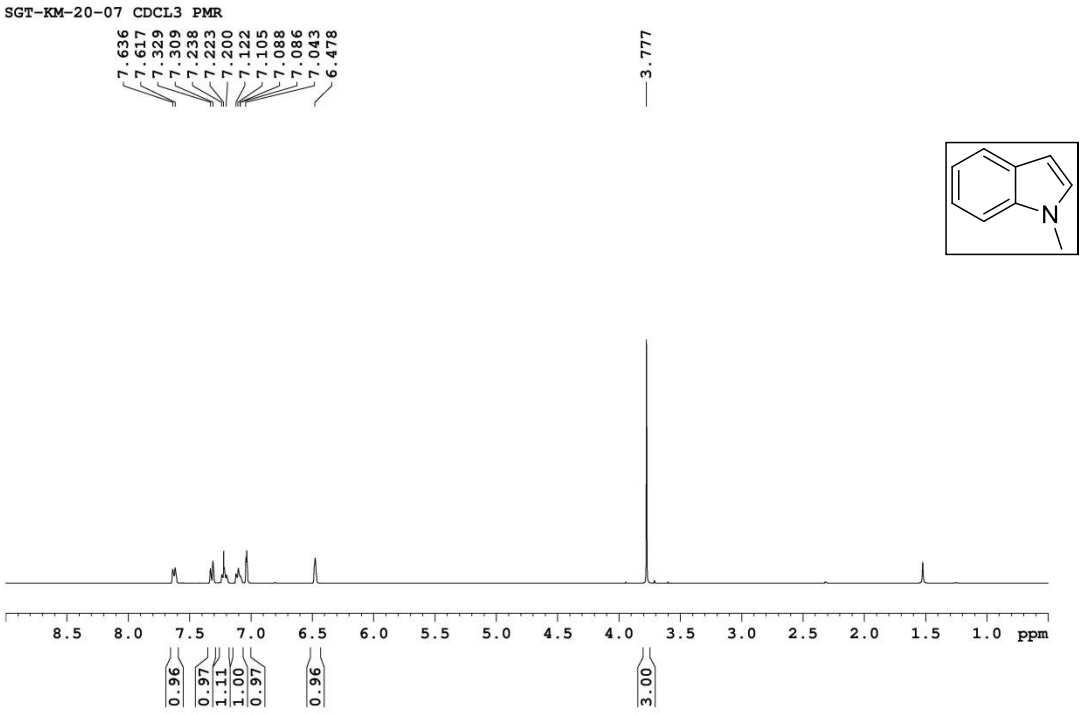
SGT-KM-20-07 CDCL3 PMR
7.636
7.617
7.329
7.309
7.238
7.223
7.200
7.122
7.105
7.088
7.086
7.043
6.478
3.777
N
8.5 8.0 7.5 7.0 6.5 6.0 5.5 5.0 4.5 4.0 3.5 3.0 2.5 2.0 1.5 1.0 ppm
0.96
0.97
1.11
1.00
0.97
0.96
3.00

SGT-KM-20-07 CDCL3 CMR

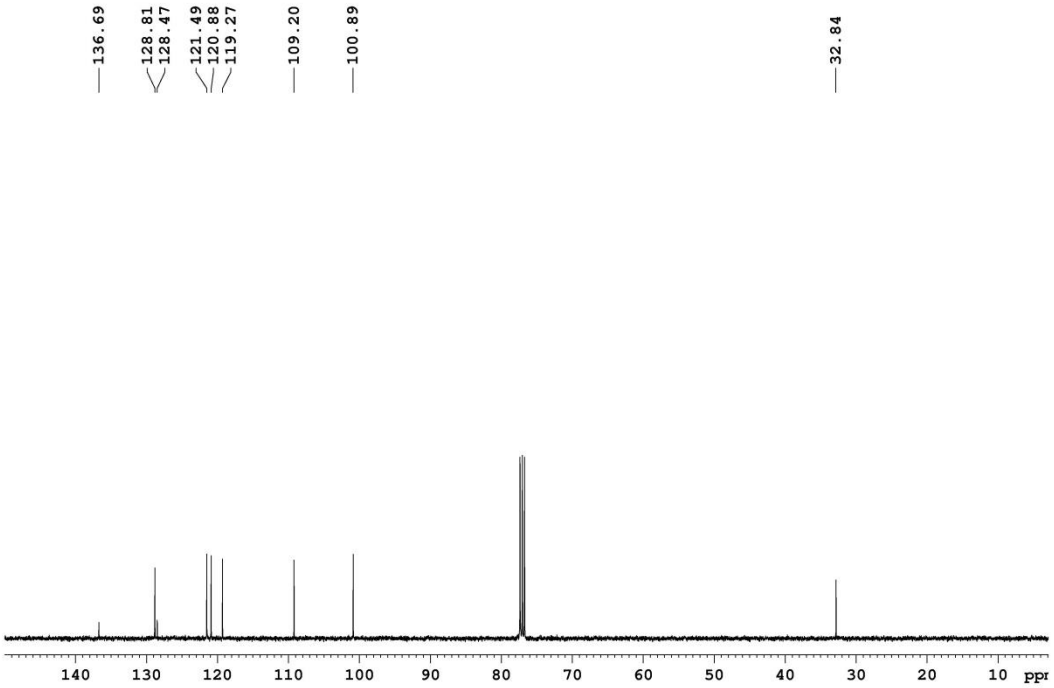

SGT-KM-20-07 CDCL3 DEPT

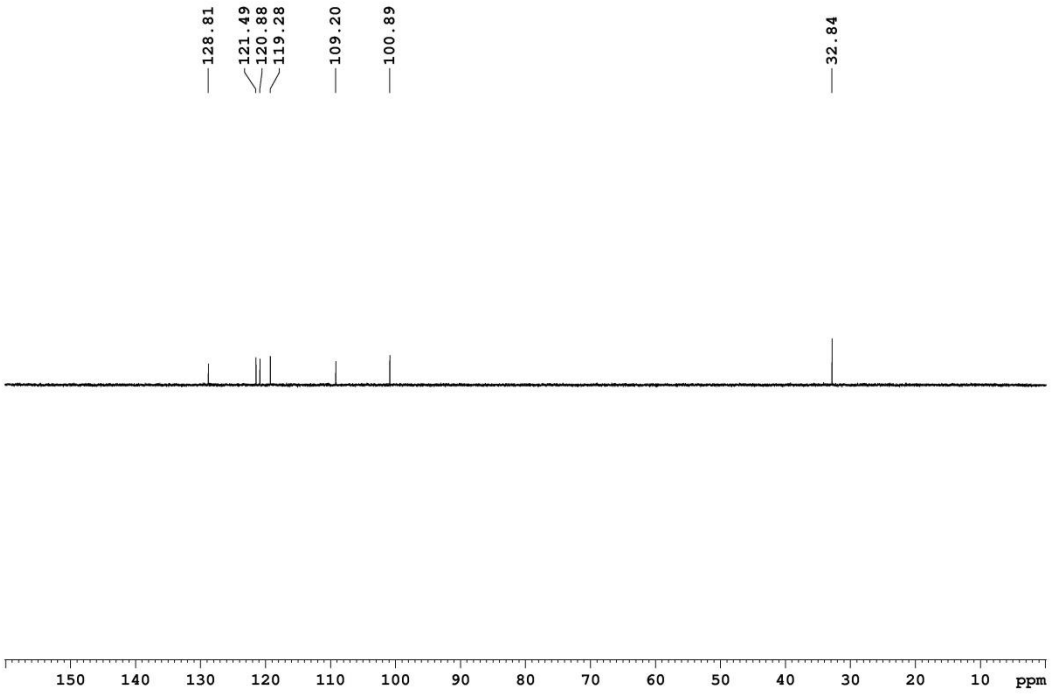

SGT-KM-20-06 CDCL3 PMR

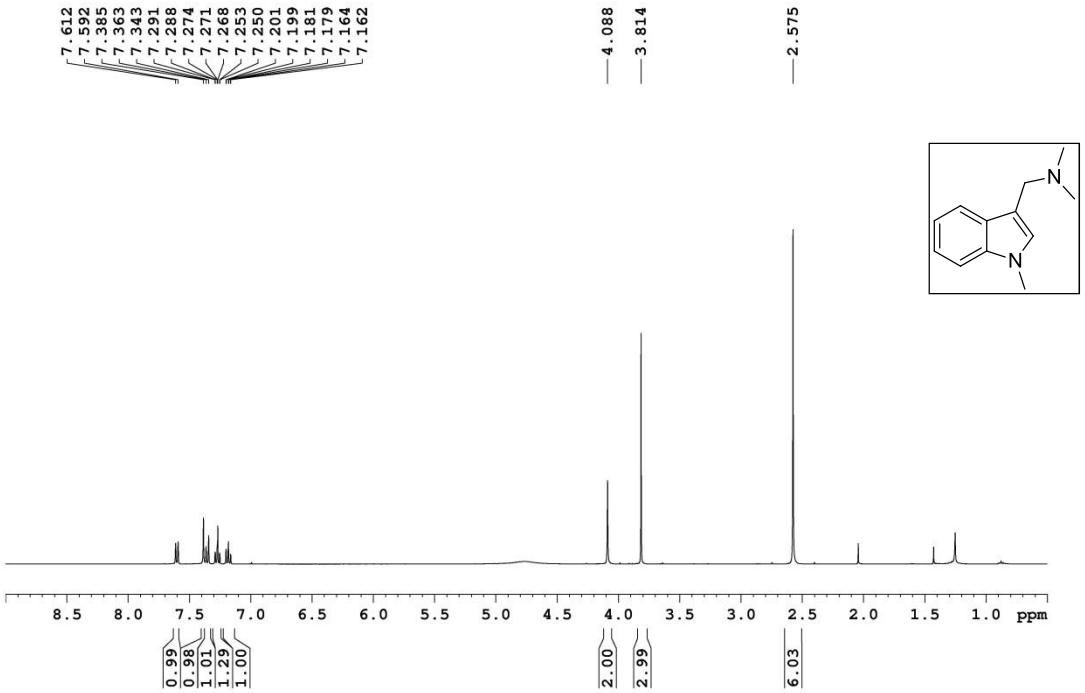

SGT-KM-20-06 CDCL3 CMR

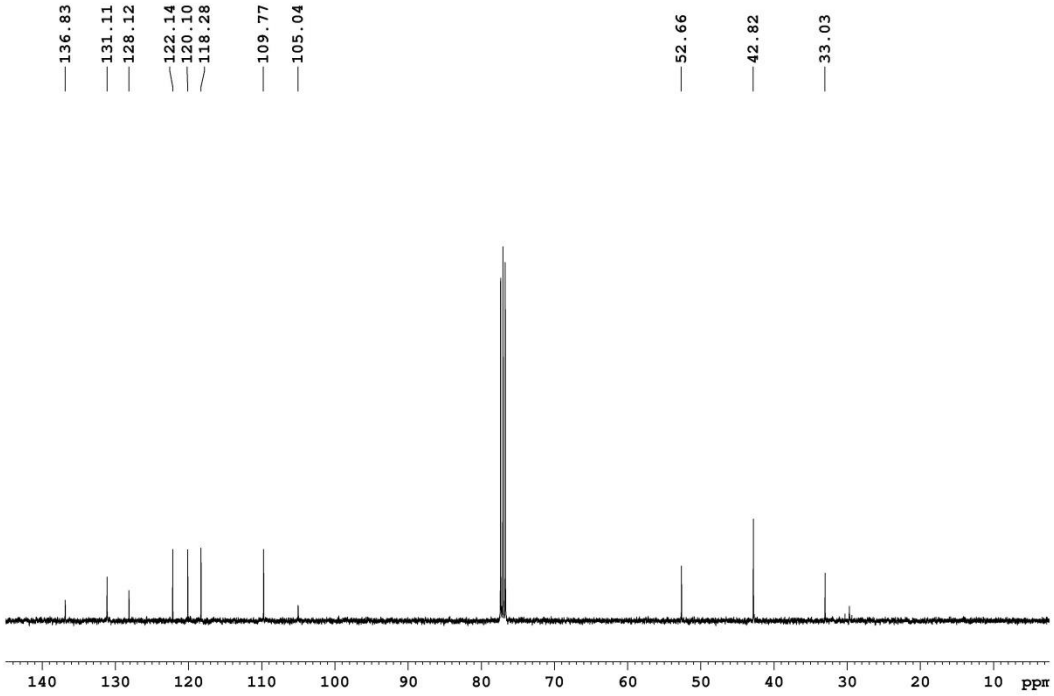

SGT-KM-20-06 CDCL3 DEPT

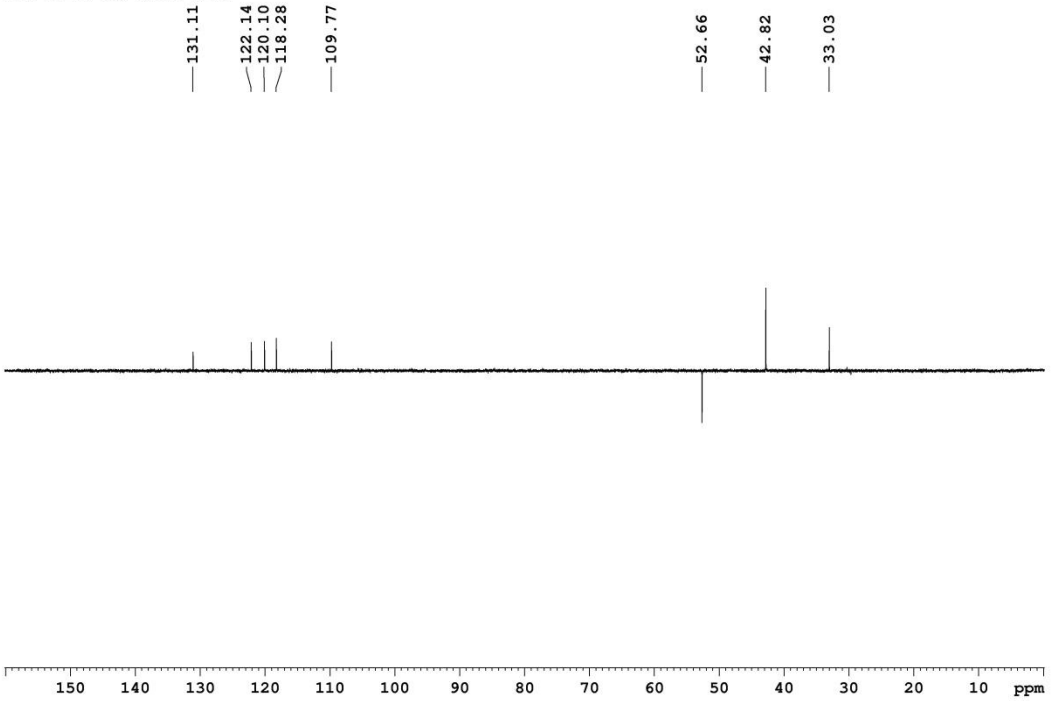

SGT-KM-20-03 CDCL3 PMR

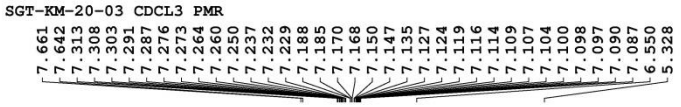

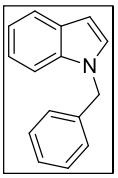

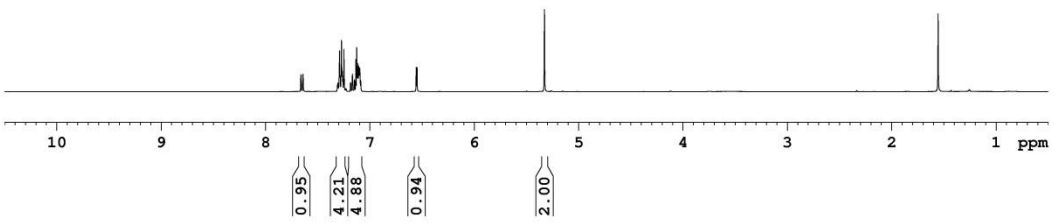

SGT-KM-20-03 CDCL3 CMR

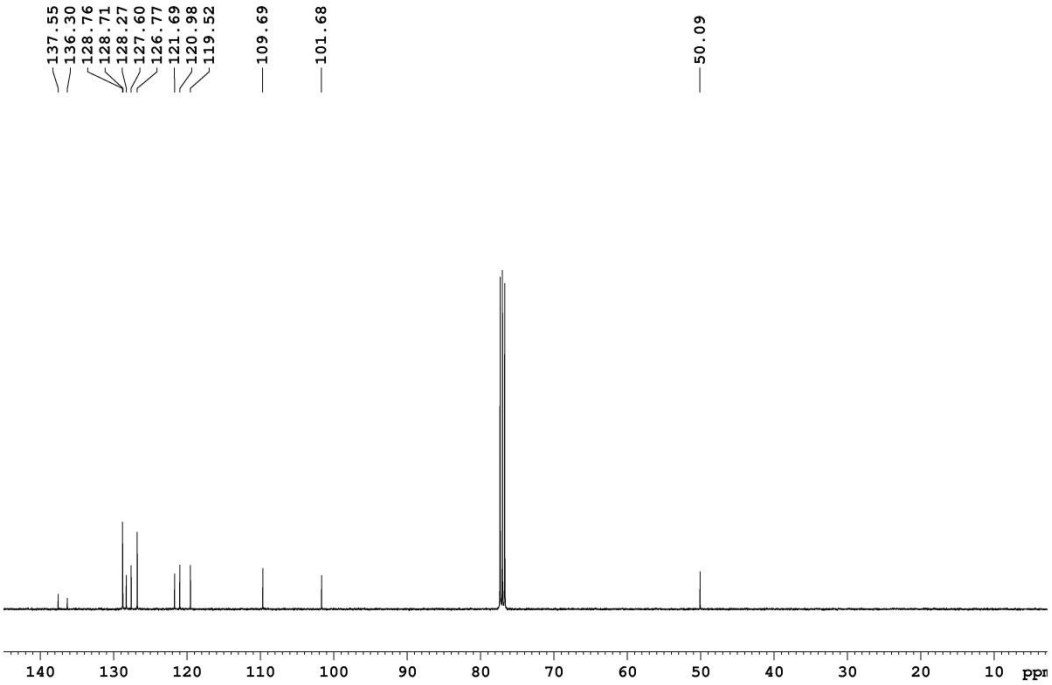

SGT-KM-20-033 CDCL3 DEPT

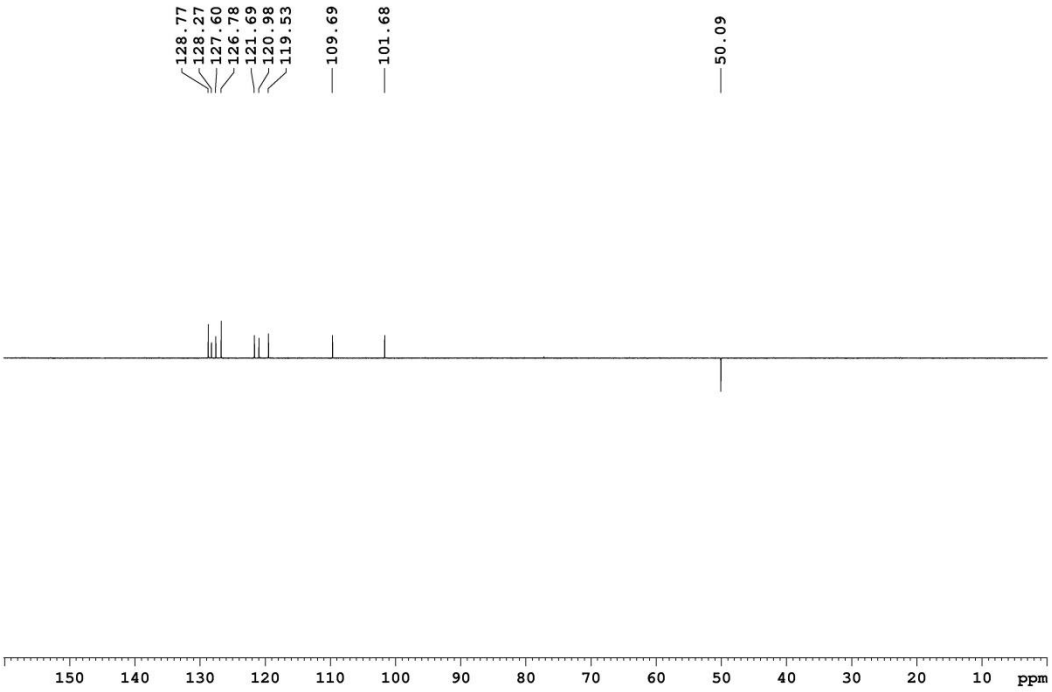

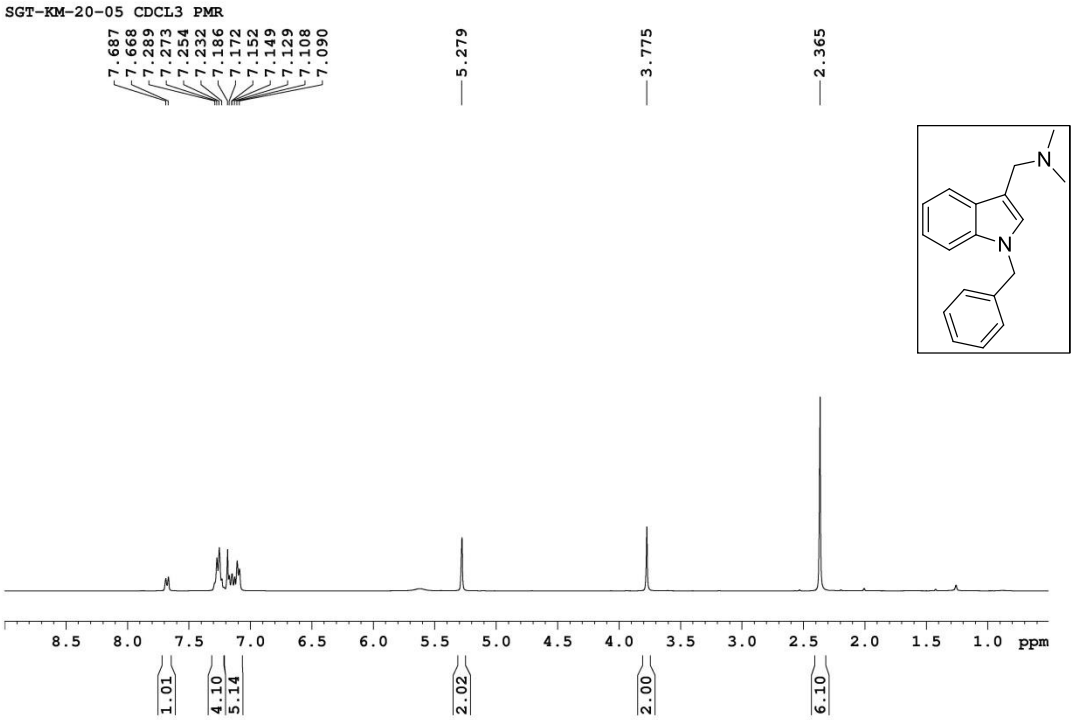
SGT-KM-20-05 CDCL3 PMR
7.687
7.668
7.289
7.273
7.254
7.232
7.186
7.172
7.152
7.149
7.129
7.108
7.090
5.279
3.775
2.365
N
N
8.5 8.0 7.5 7.0 6.5 6.0 5.5 5.0 4.5 4.0 3.5 3.0 2.5 2.0 1.5 1.0 ppm
1.01
4.10
5.14
2.02
2.00
6.10

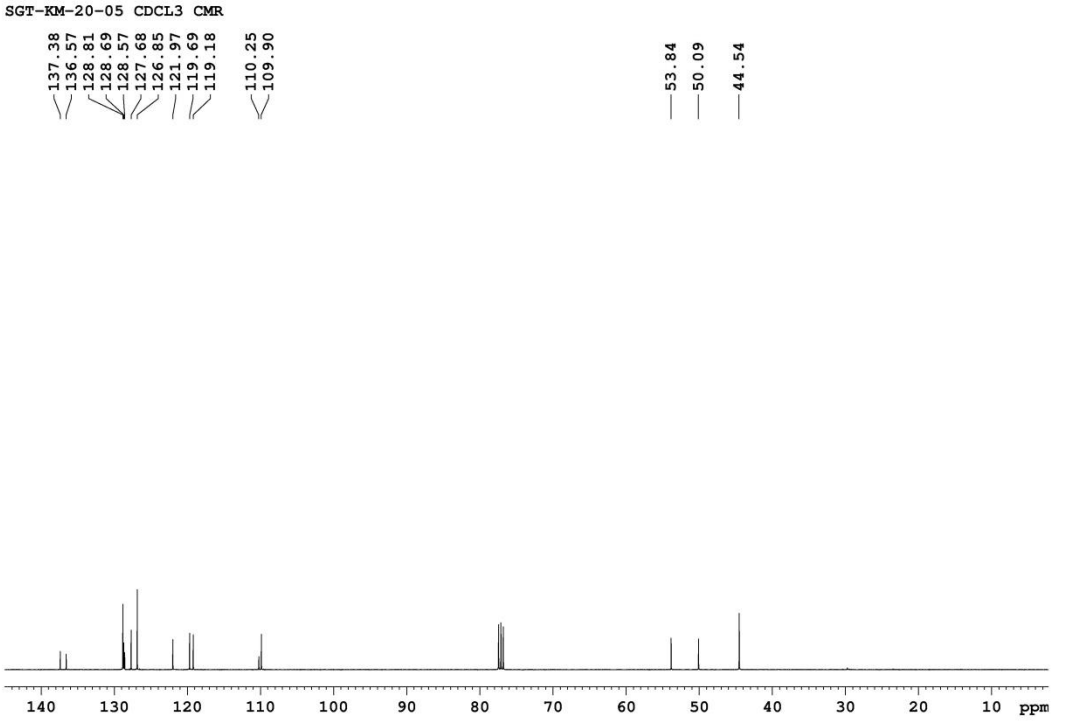
SGT-KM-20-05 CDCL3 CMR
137.38
136.57
128.81
128.69
128.57
127.68
126.85
121.97
119.69
119.18
110.25
109.90
53.84
50.09
44.54
140 130 120 110 100 90 80 70 60 50 40 30 20 10 ppm

SGT-KM-20-05 CDCL3 DEPT

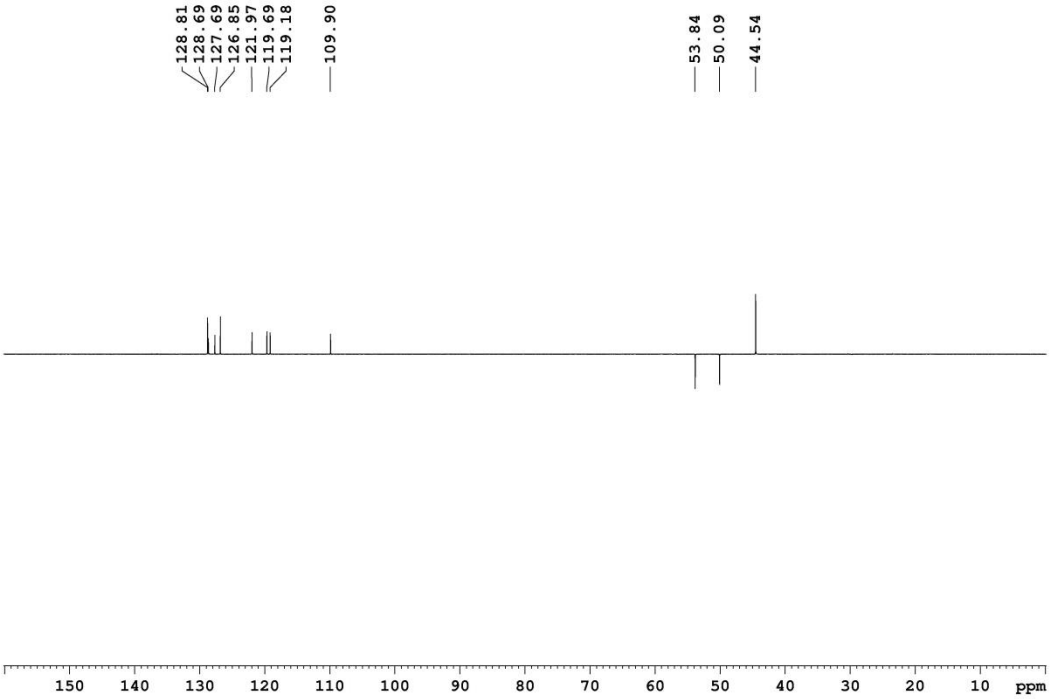

SGT-KM-19-31 CDCL3 PMR

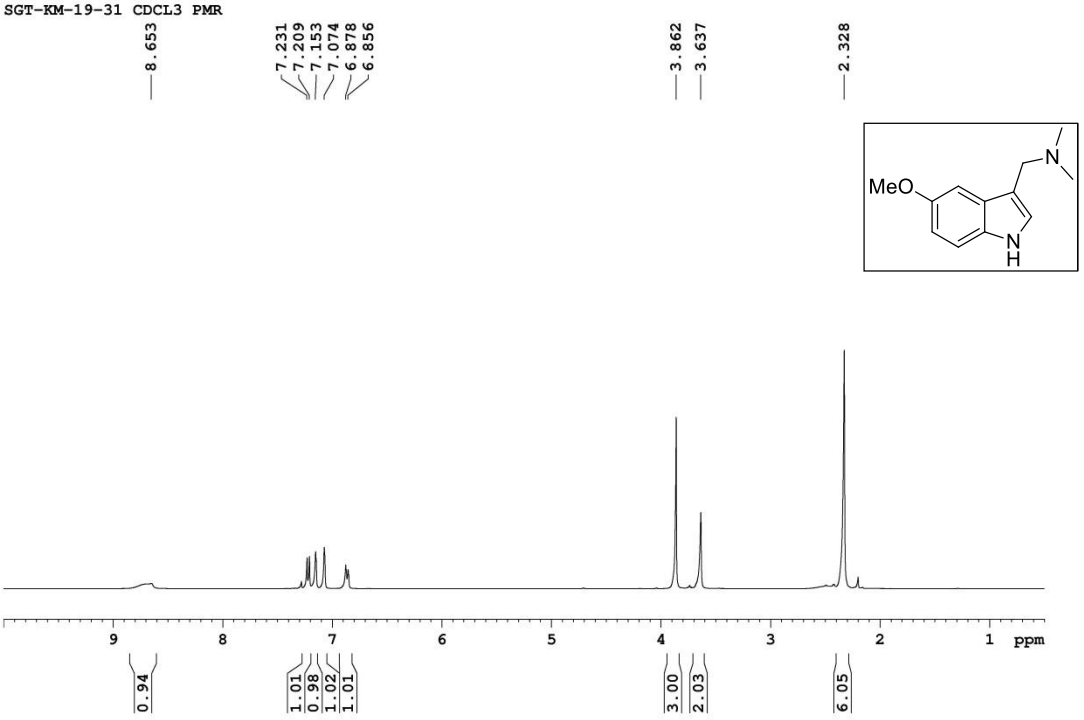

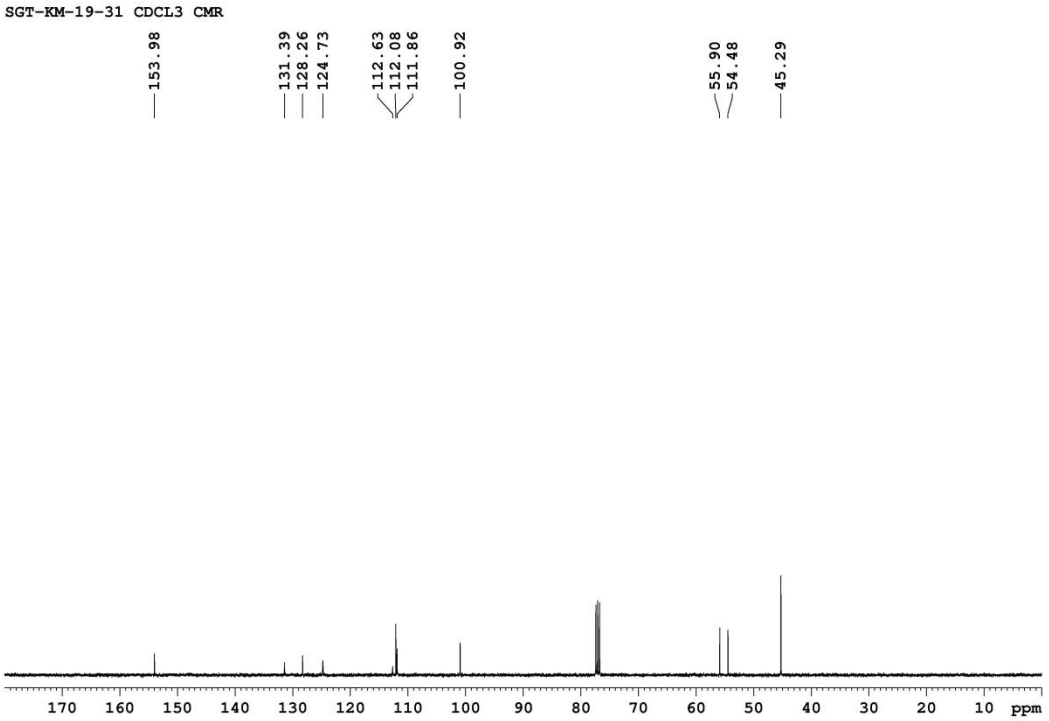
SGT-KM-19-31 CDCL3 CMR
153.98
131.39
128.26
124.73
112.63
112.08
111.86
100.92
55.90
54.48
45.29
170 160 150 140 130 120 110 100 90 80 70 60 50 40 30 20 10 ppm

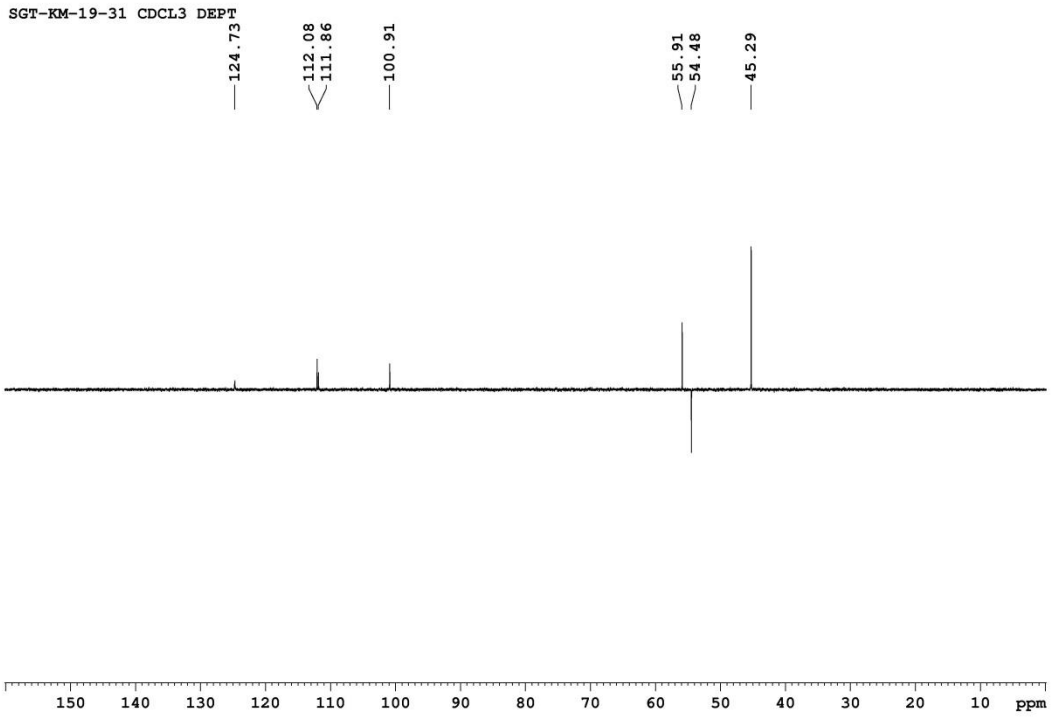
SGT-KM-19-31 CDCL3 DEPT
124.73
112.08
111.86
100.91
55.91
54.48
45.29
150 140 130 120 110 100 90 80 70 60 50 40 30 20 10 ppm

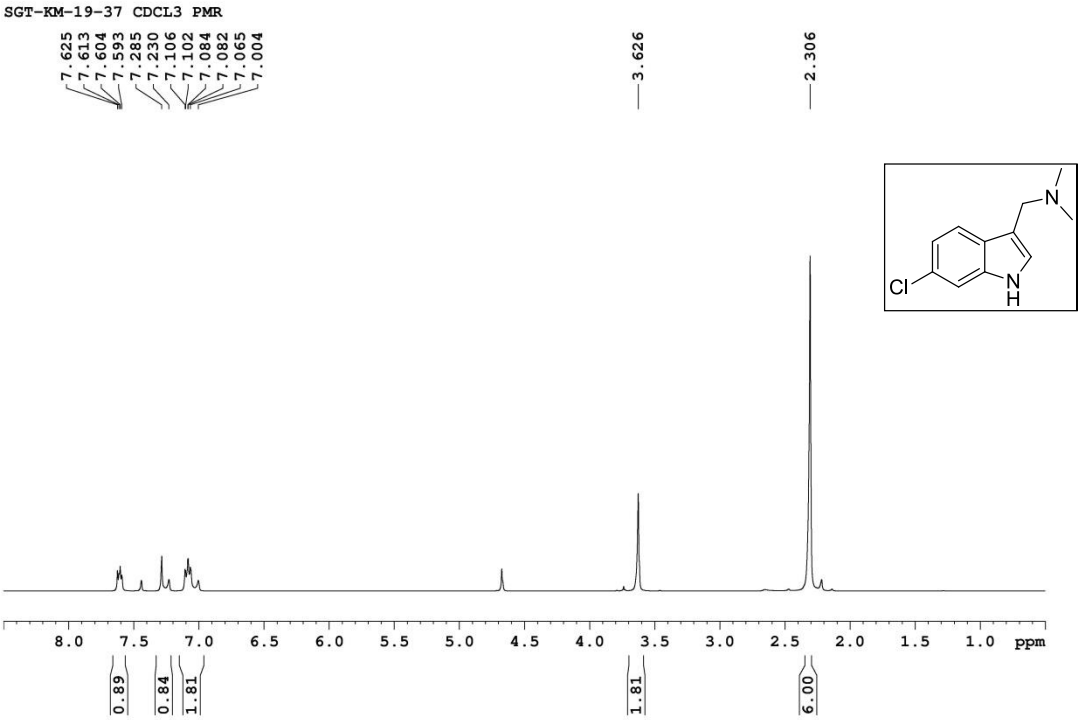
SGT-KM-19-37 CDCL3 PMR
7.625
7.613
7.604
7.593
7.285
7.230
7.106
7.102
7.084
7.082
7.065
7.004
3.626
2.306
Cl
N
H
8.0
7.5
7.0
6.5
6.0
5.5
5.0
4.5
4.0
3.5
3.0
2.5
2.0
1.5
1.0
ppm
0.89
0.84
1.81
1.81
6.00

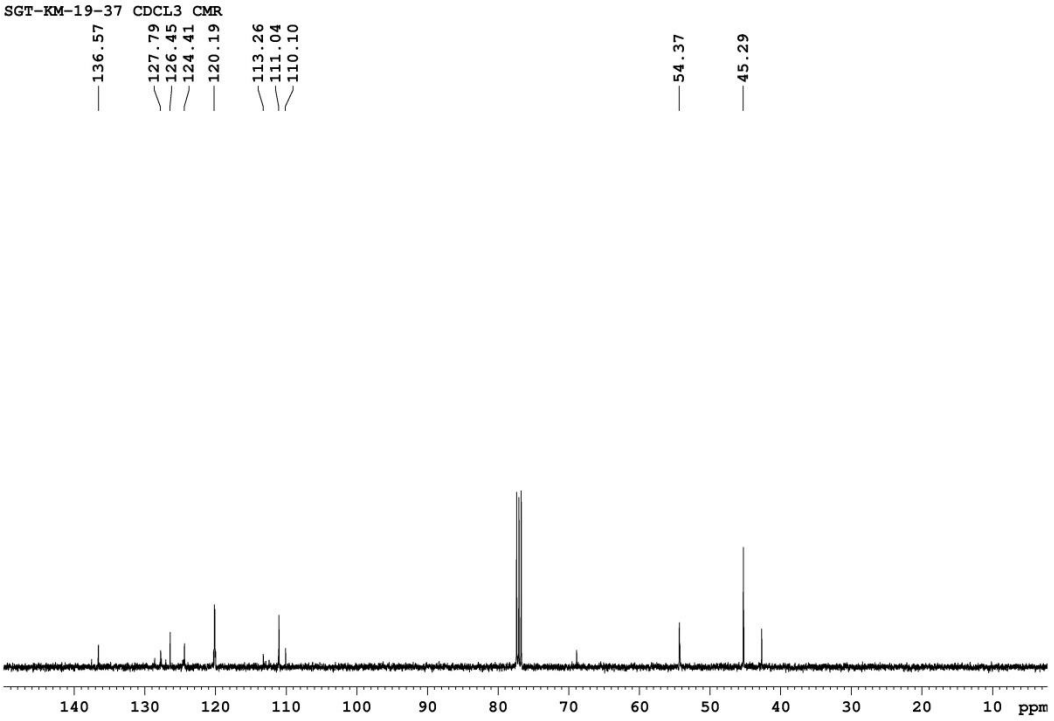
SGT-KM-19-37 CDCL3 CMR
136.57
127.79
126.45
124.41
120.19
113.26
111.04
110.10
54.37
45.29
140
130
120
110
100
90
80
70
60
50
40
30
20
10
ppm

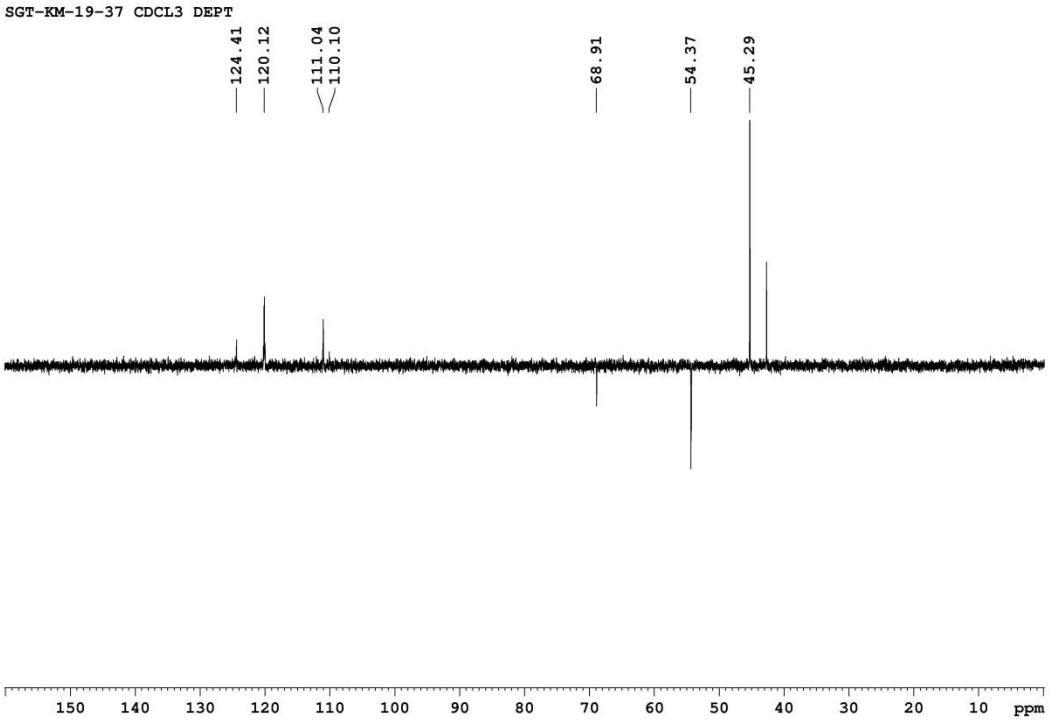
SGT-KM-19-37 CDCL3 DEPT
124.41
120.12
111.04
110.10
68.91
54.37
45.29
150 140 130 120 110 100 90 80 70 60 50 40 30 20 10 ppm

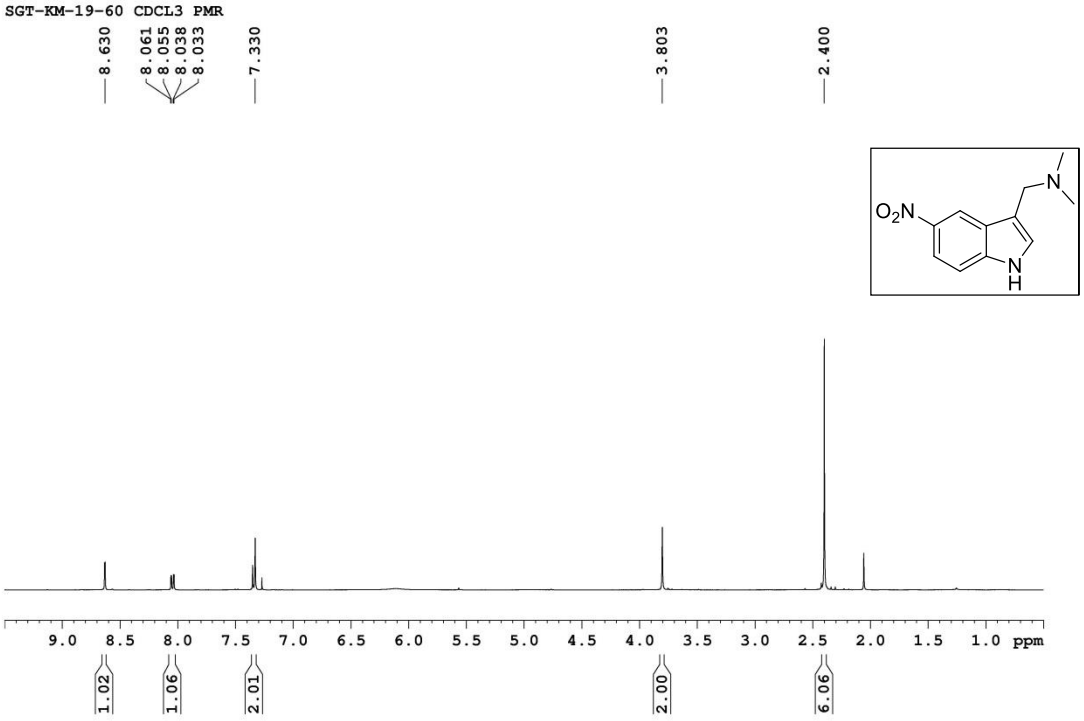
SGT-KM-19-60 CDCL3 PMR
8.630
8.061
8.055
8.038
8.033
7.330
3.803
2.400
O2N
N
N
H
9.0 8.5 8.0 7.5 7.0 6.5 6.0 5.5 5.0 4.5 4.0 3.5 3.0 2.5 2.0 1.5 1.0 ppm
1.02
1.06
2.01
2.00
6.06

SGT-KM-19-60-A CDCL3 CMR

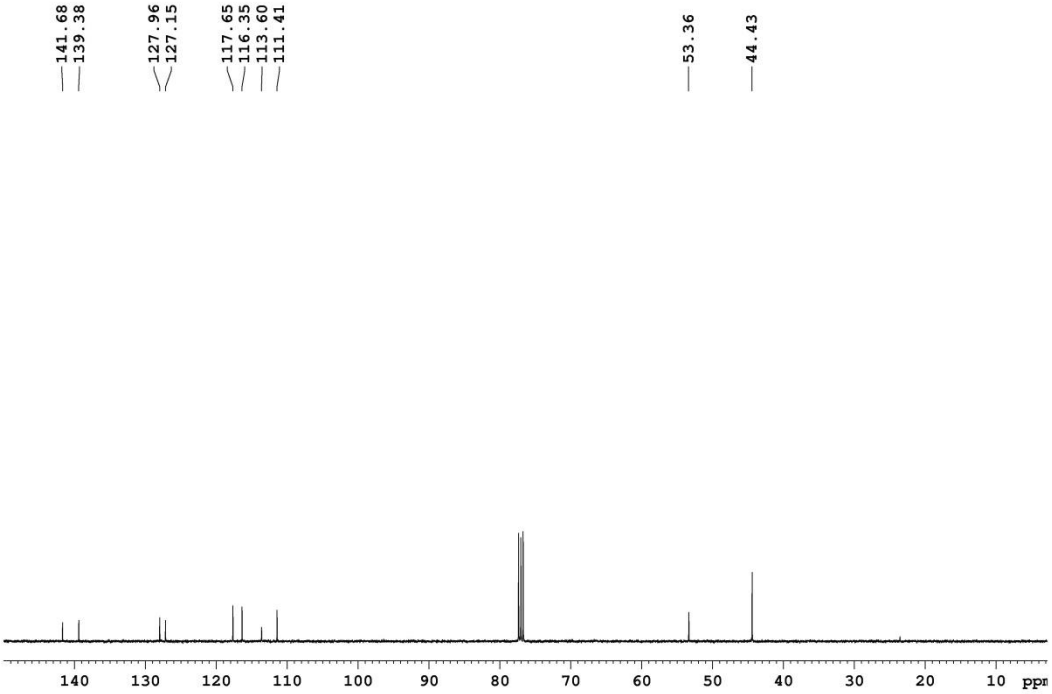

SGT-KM-19-60-A CDCL3 DEPT

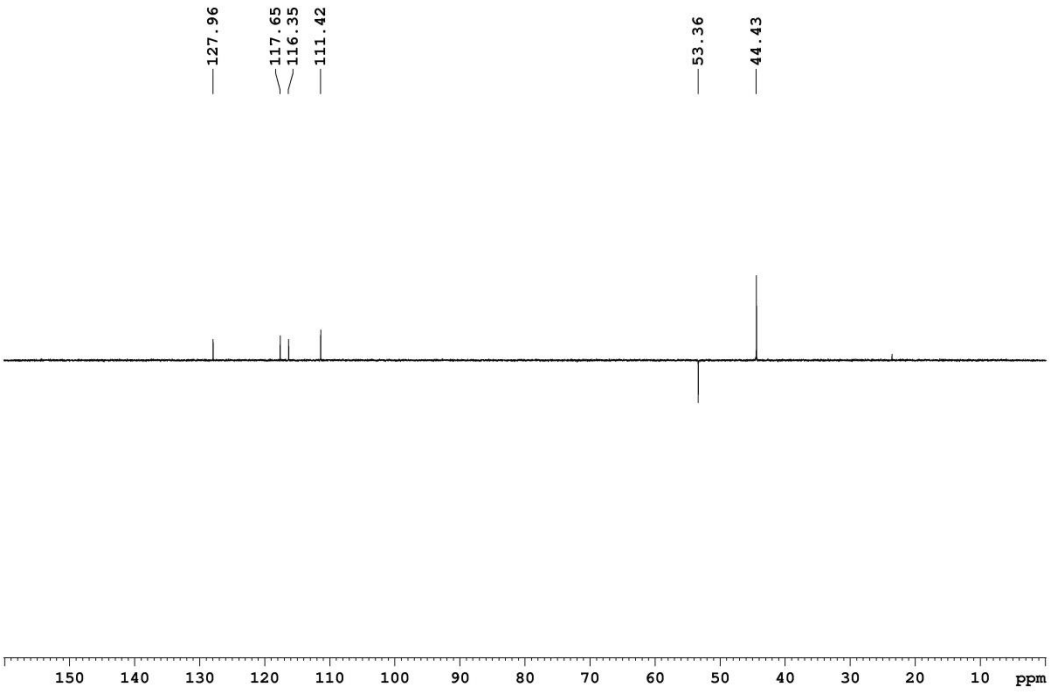

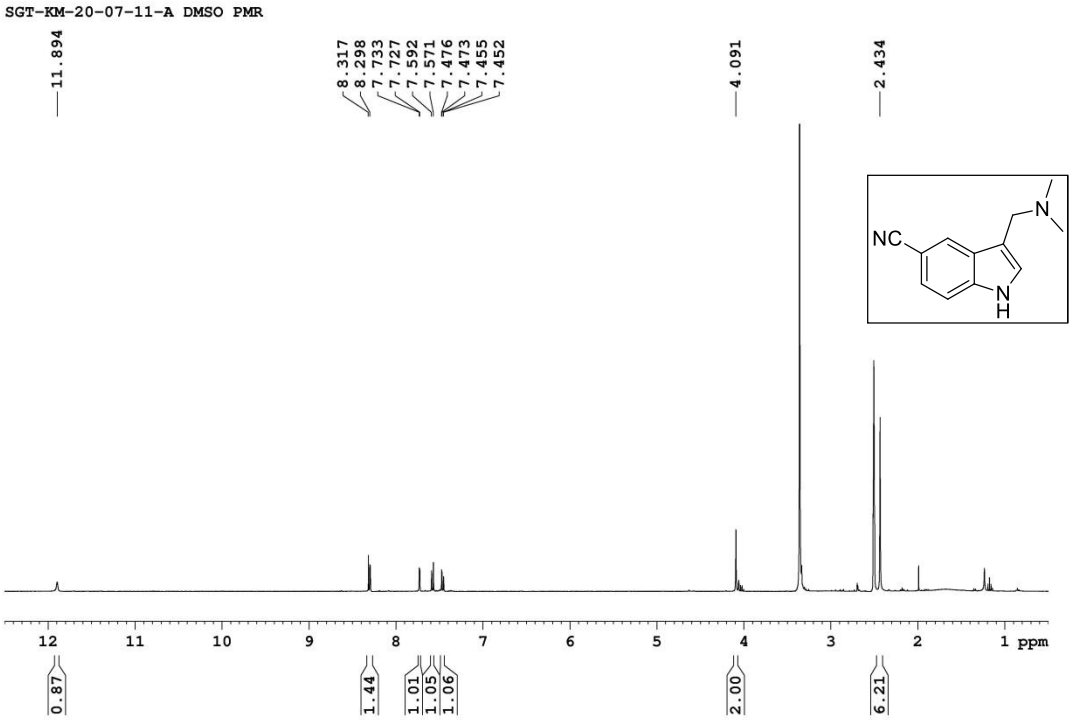
SGT-KM-20-07-11-A DMSO PMR
11.894
8.317
8.298
7.733
7.727
7.592
7.571
7.476
7.473
7.455
7.452
4.091
2.434
NC
N
N
H
12
11
10
9
8
7
6
5
4
3
2
1 ppm
0.87
1.44
1.01
1.05
1.06
2.00
6.21

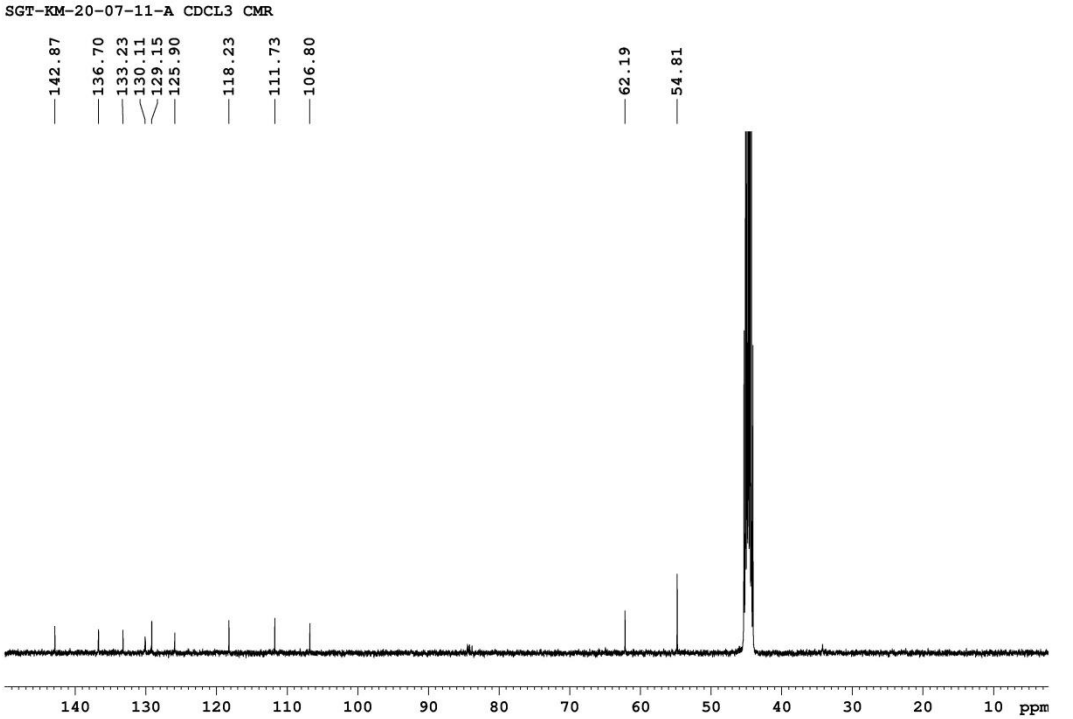
SGT-KM-20-07-11-A CDCL3 CMR
142.87
136.70
133.23
130.11
129.15
125.90
118.23
111.73
106.80
62.19
54.81
140
130
120
110
100
90
80
70
60
50
40
30
20
10 ppm

SGT-KM-20-07-11-B DMSODEPT

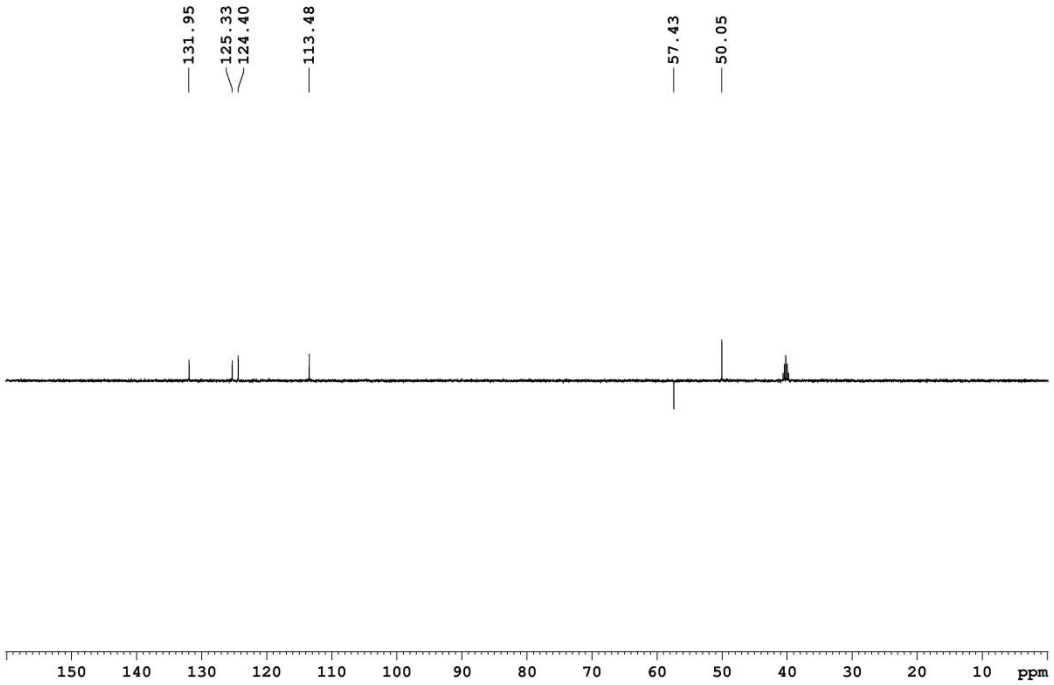

SGT-KM-20-11 CDCL3 PMR

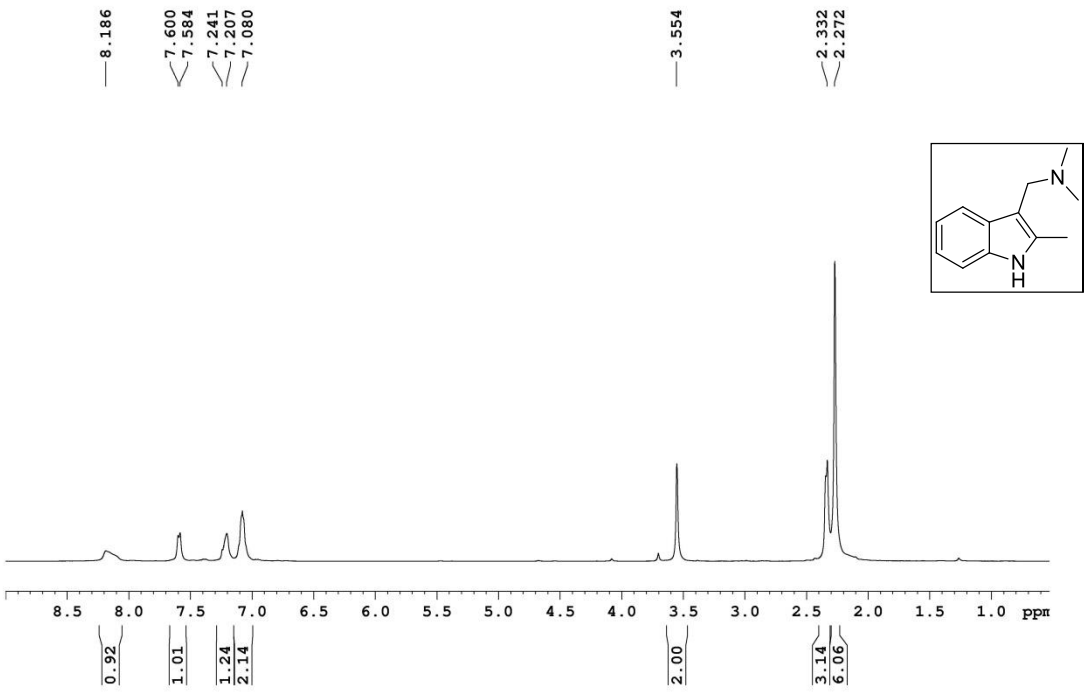

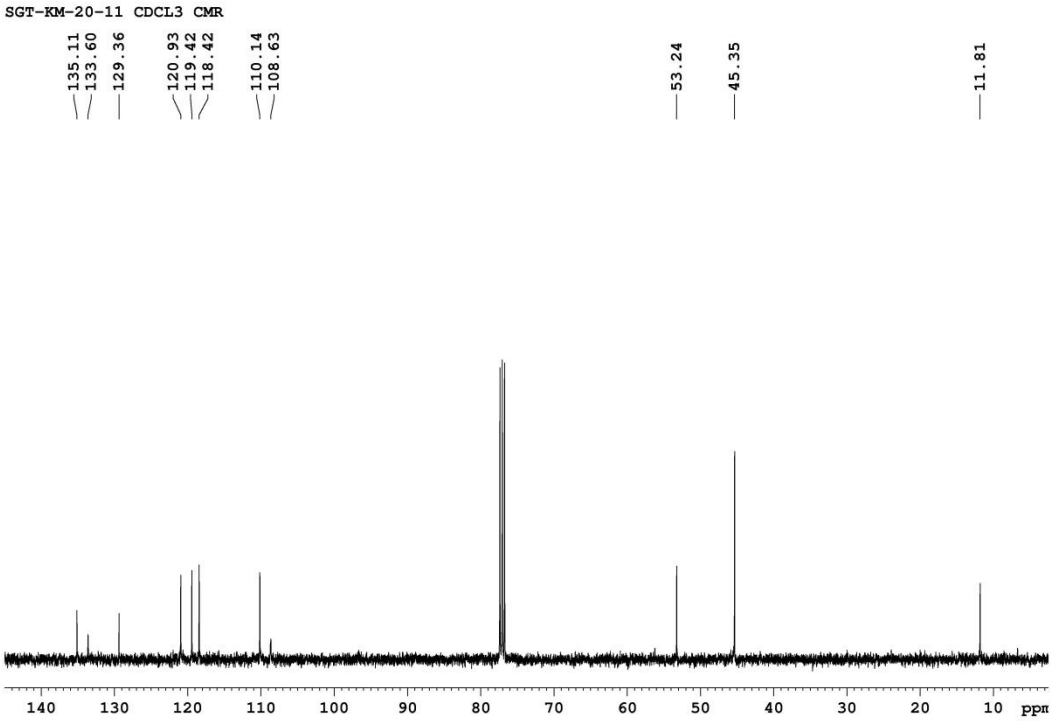
SGT-KM-20-11 CDCL3 CMR
135.11
133.60
129.36
120.93
119.42
118.42
110.14
108.63
53.24
45.35
11.81
140
130
120
110
100
90
80
70
60
50
40
30
20
10
ppm

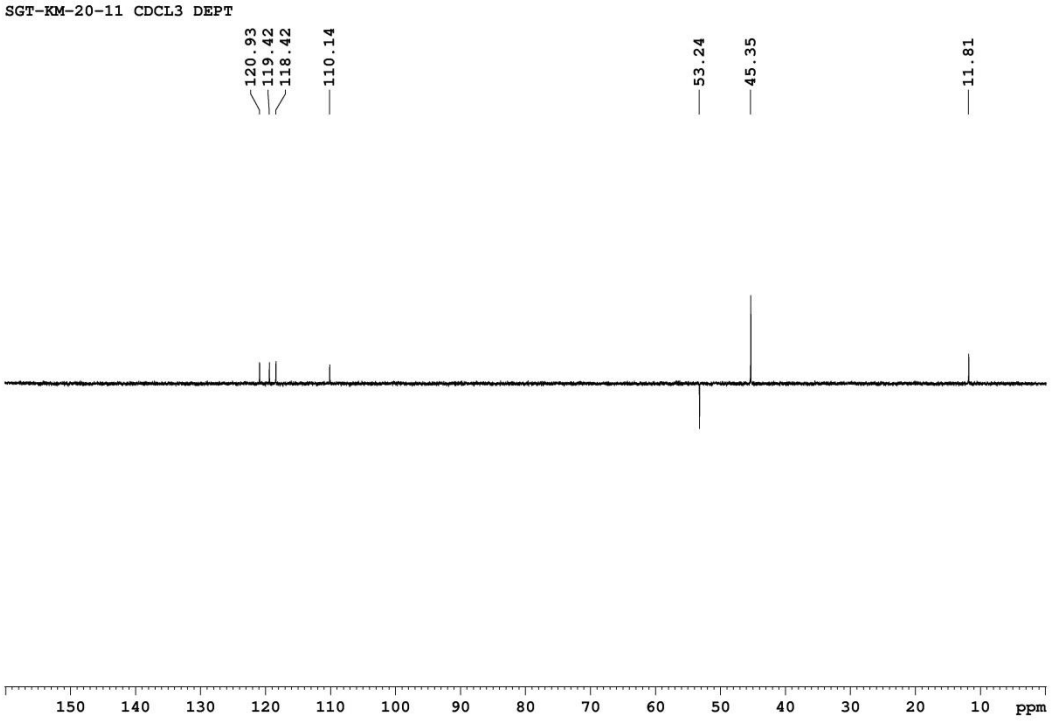
SGT-KM-20-11 CDCL3 DEPT
120.93
119.42
118.42
110.14
53.24
45.35
11.81
150
140
130
120
110
100
90
80
70
60
50
40
30
20
10
ppm

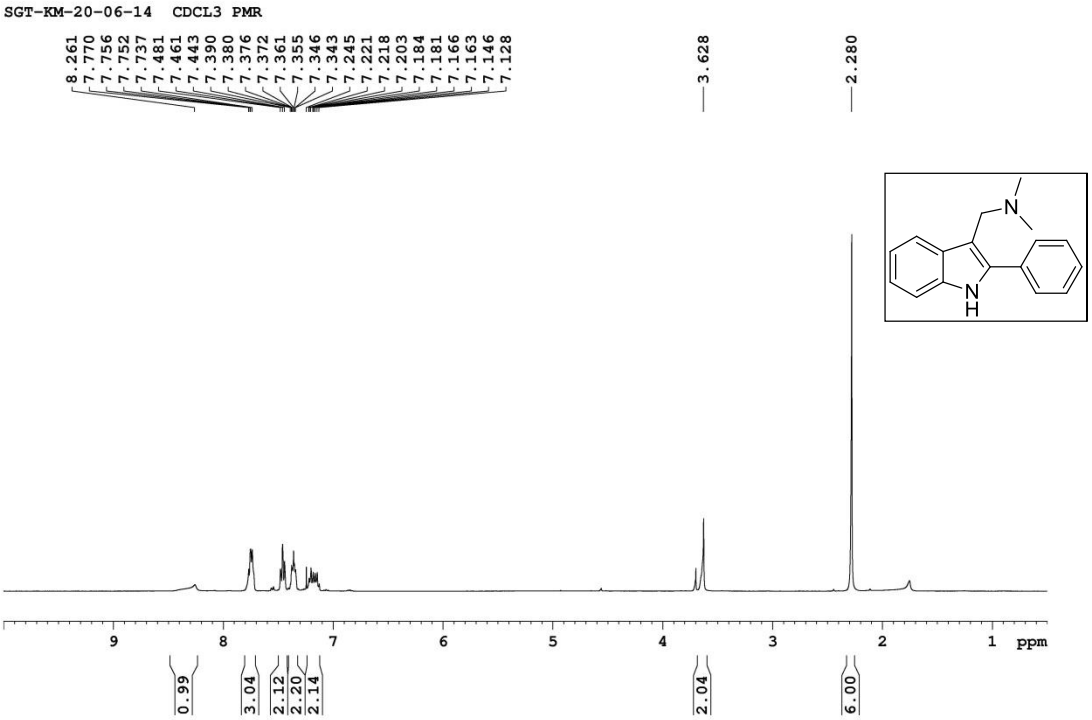
SGT-KM-20-06-14 CDCL3 PMR
8.261
7.770
7.756
7.752
7.737
7.481
7.461
7.443
7.390
7.380
7.376
7.372
7.361
7.355
7.346
7.343
7.245
7.221
7.218
7.203
7.184
7.181
7.166
7.163
7.146
7.128
3.628
2.280
N
N
H
9
8
7
6
5
4
3
2
1
ppm
0.99
3.04
2.12
2.20
2.14
2.04
6.00

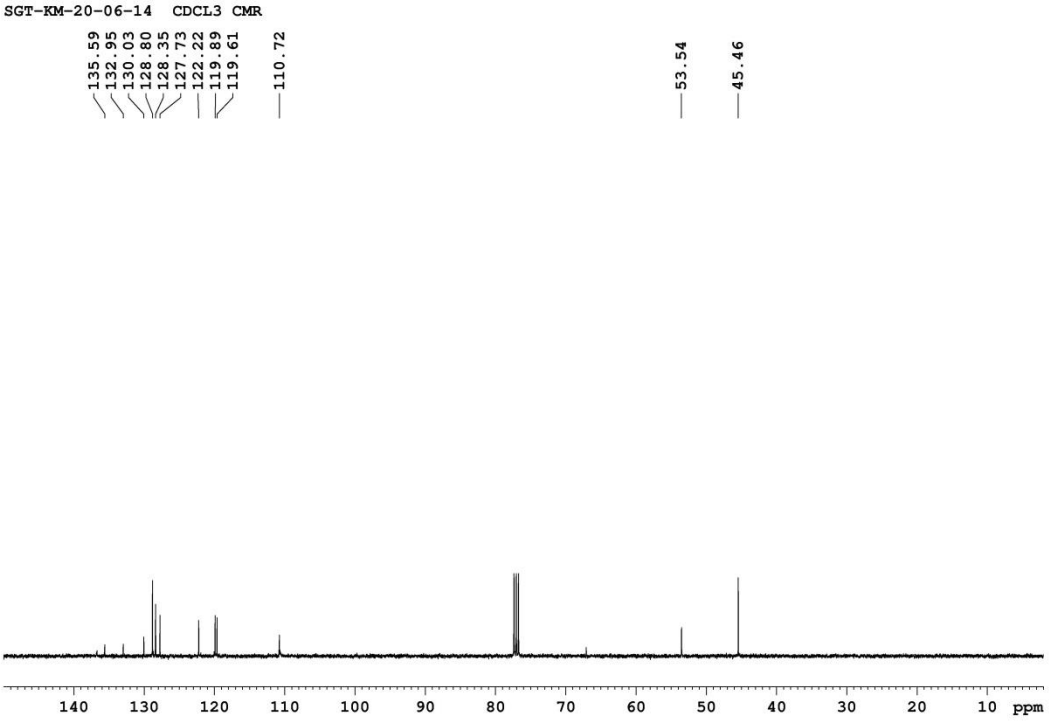
SGT-KM-20-06-14 CDCL3 CMR
135.59
132.95
130.03
128.80
128.35
127.73
122.22
119.89
119.61
110.72
53.54
45.46
140
130
120
110
100
90
80
70
60
50
40
30
20
10
ppm

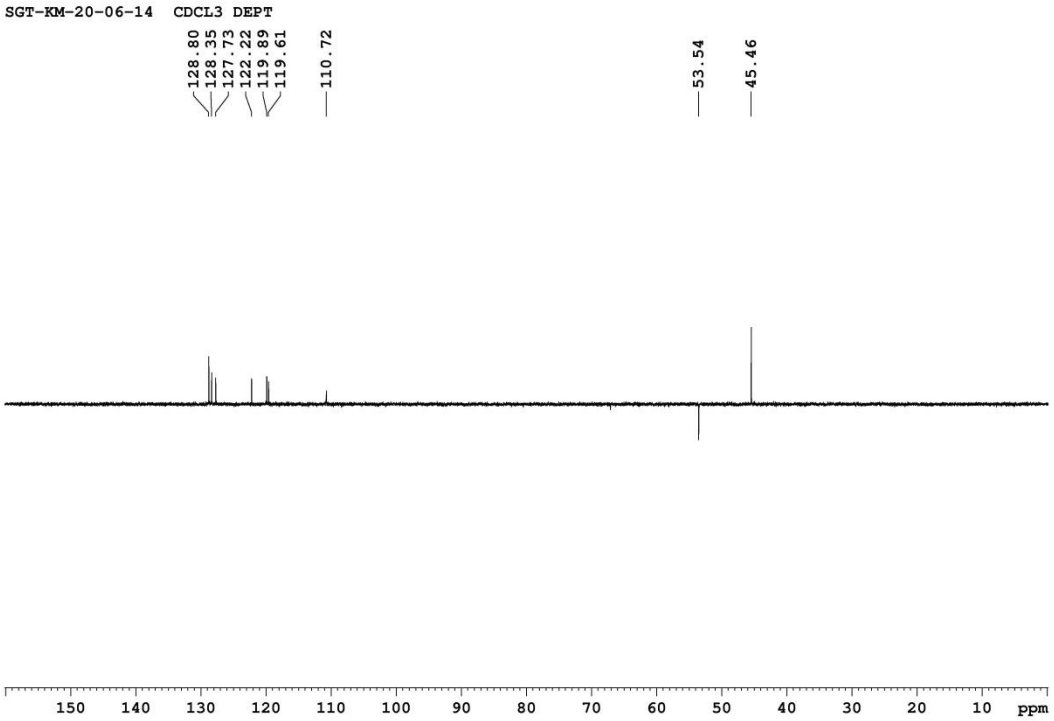
SGT-KM-20-06-14 CDCL3 DEPT
128.80
128.35
127.73
122.22
119.89
119.61
110.72
53.54
45.46
150 140 130 120 110 100 90 80 70 60 50 40 30 20 10 ppm

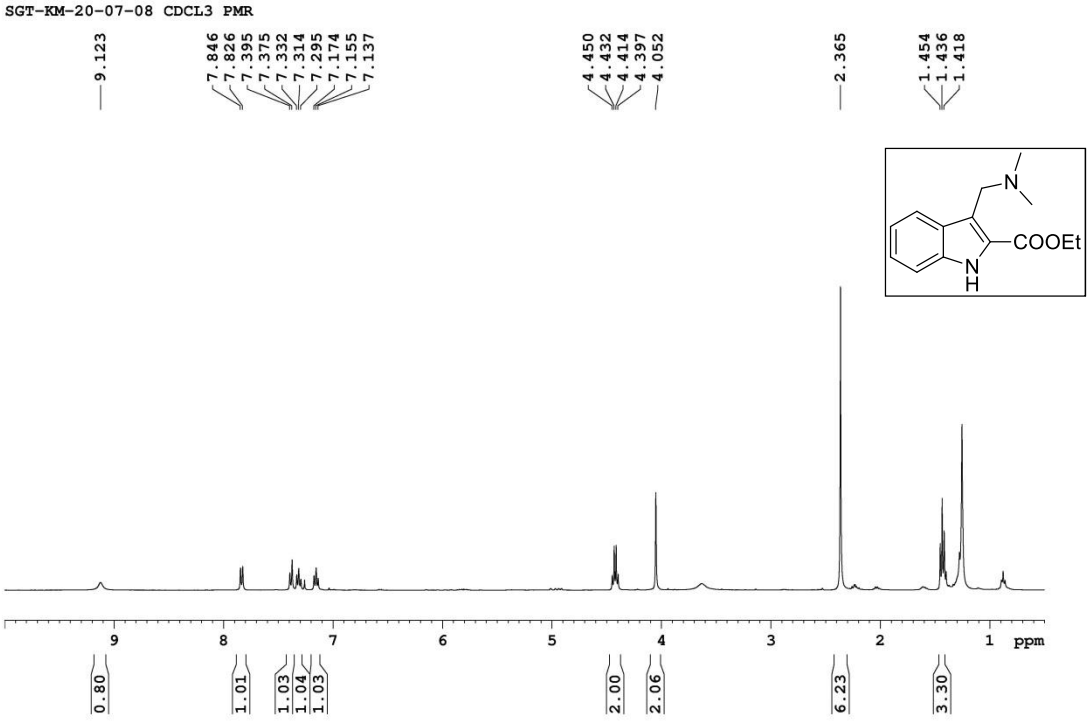
SGT-KM-20-07-08 CDCL3 PMR
9.123
7.846
7.826
7.395
7.375
7.332
7.314
7.295
7.174
7.155
7.137
4.450
4.432
4.414
4.397
4.052
2.365
1.454
1.436
1.418
N
COOEt
N
H
9 8 7 6 5 4 3 2 1 ppm
0.80
1.01
1.03
1.04
1.03
2.00
2.06
6.23
3.30

SGT-KM-20-07-08 CDCL3 CMR

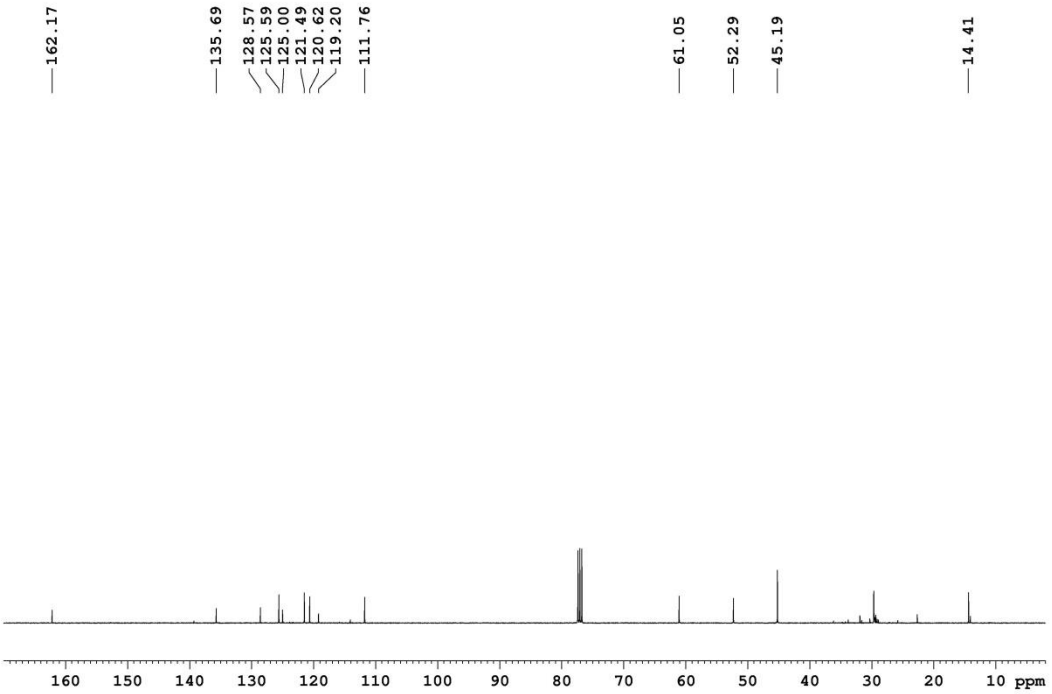

SGT-KM-20-07-08 CDCL3 DEPT

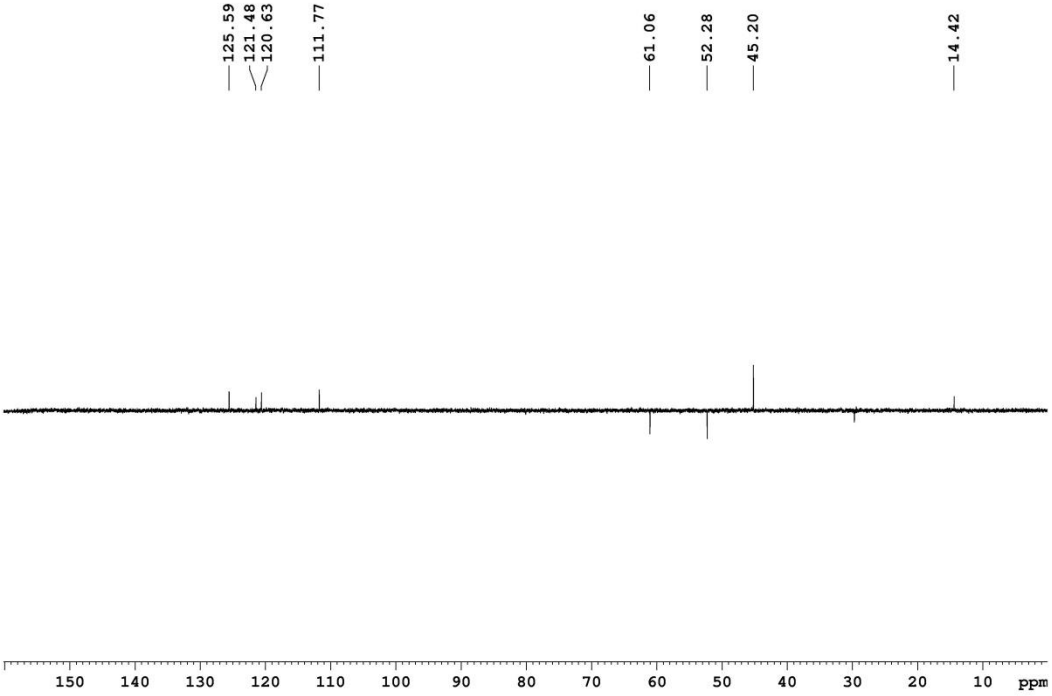

SGT-KM-19-54 CDCL3 PMR

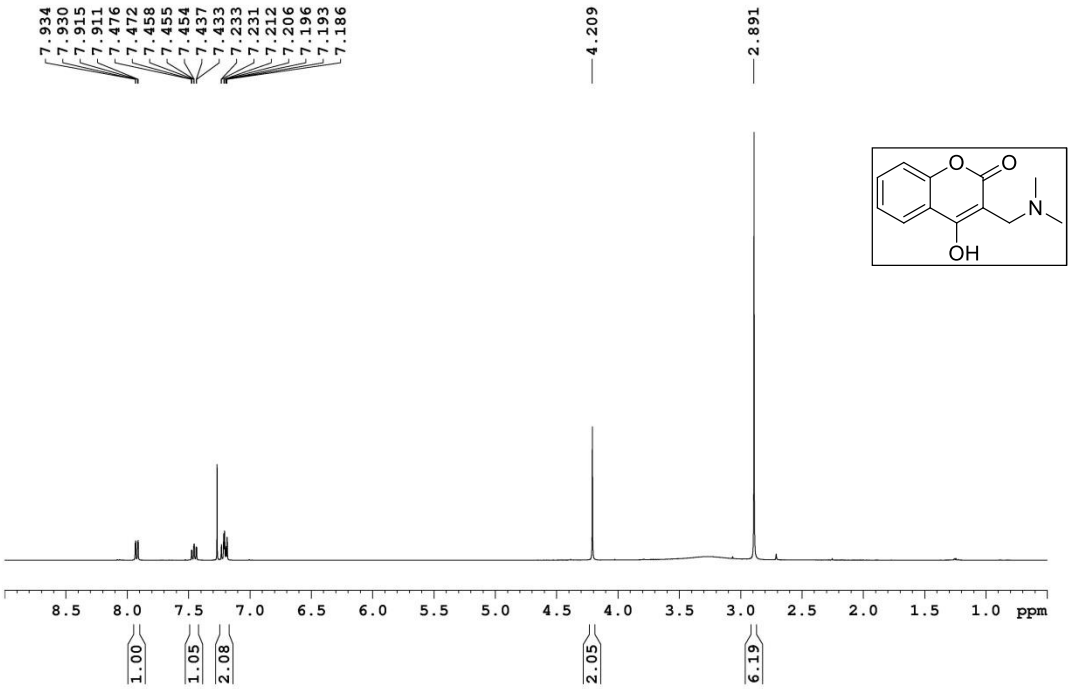

SGT-KM-19-55 CDCL3 CMR

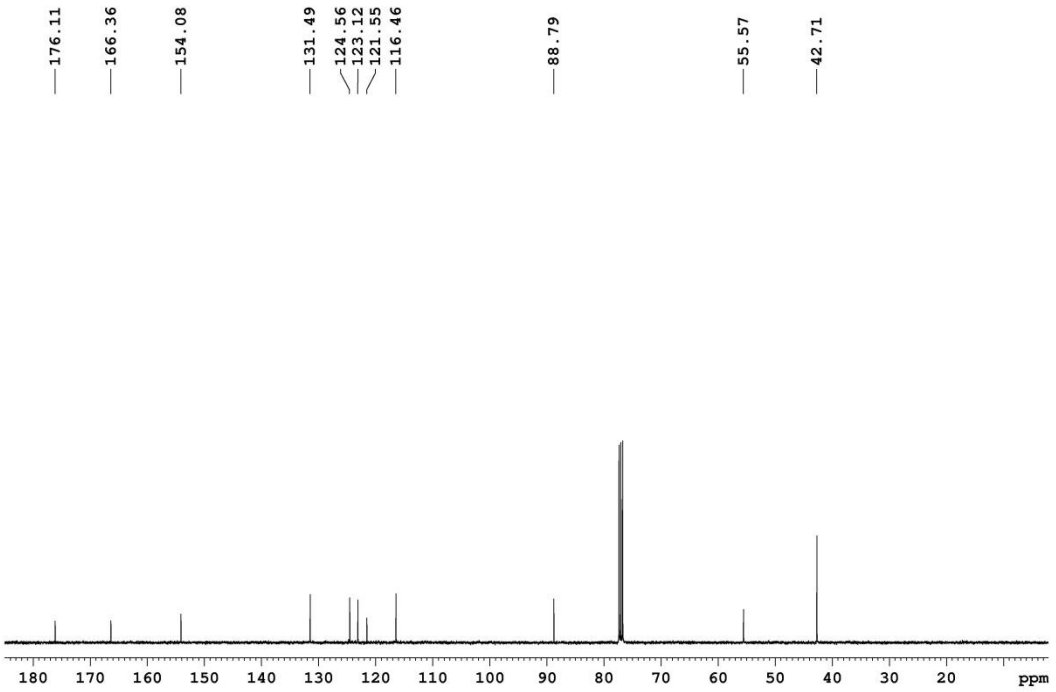

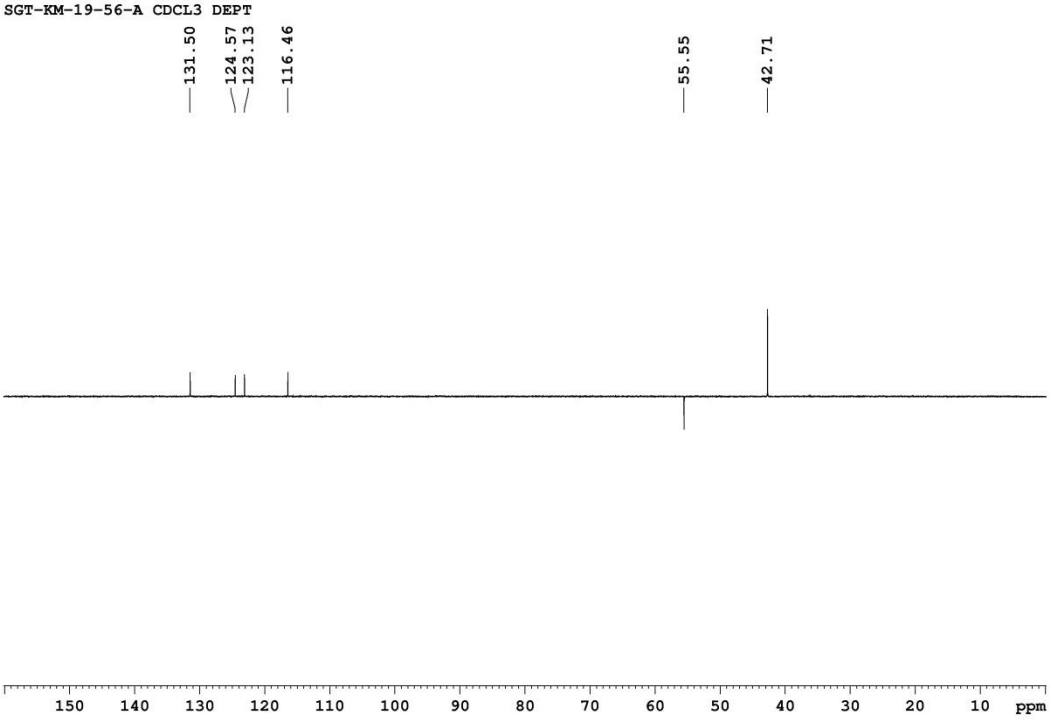
SGT-KM-19-56-A CDCL3 DEPT
131.50
124.57
123.13
116.46
55.55
42.71
150 140 130 120 110 100 90 80 70 60 50 40 30 20 10 ppm

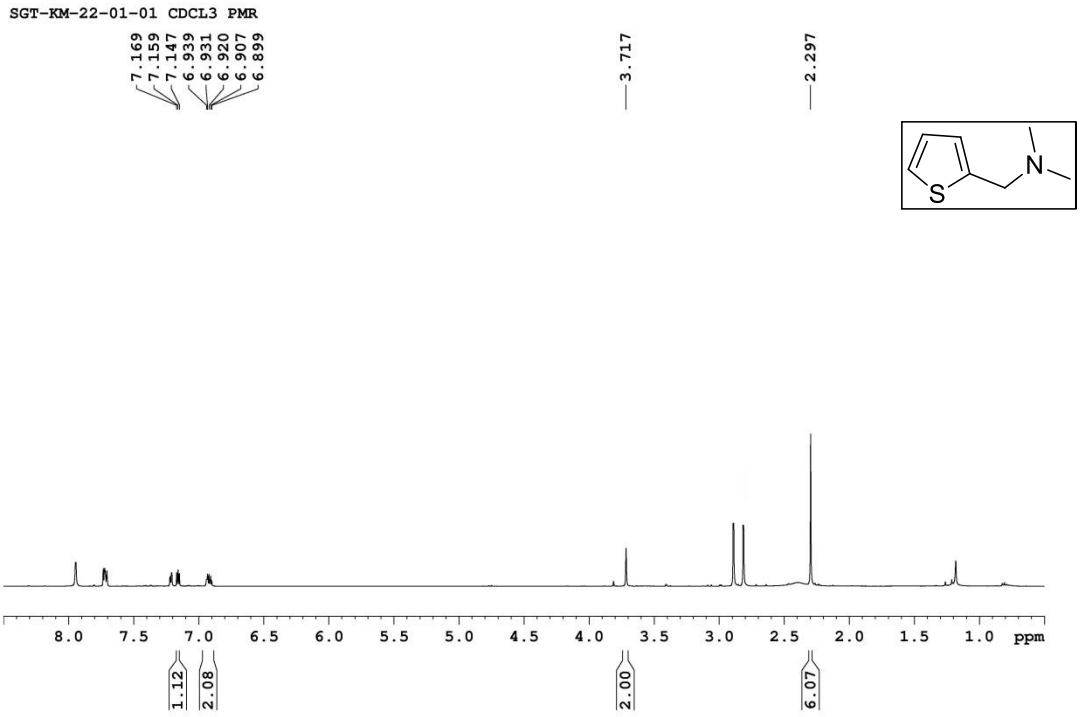
SGT-KM-22-01-01 CDCL3 PMR
7.169
7.159
7.147
6.939
6.931
6.920
6.907
6.899
3.717
2.297
N
S
8.0 7.5 7.0 6.5 6.0 5.5 5.0 4.5 4.0 3.5 3.0 2.5 2.0 1.5 1.0 ppm
1.12
2.08
2.00
6.07

SGT-KM-20-12 CDCL3 PMR

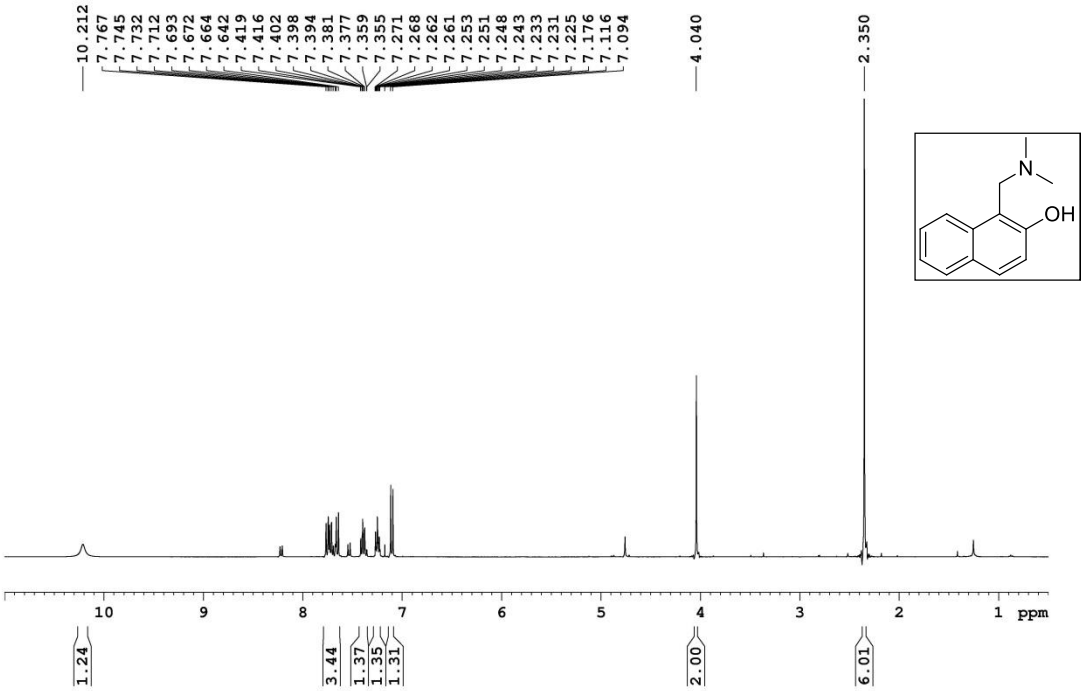

SGT-KM-20-12 CDCL3 CMR

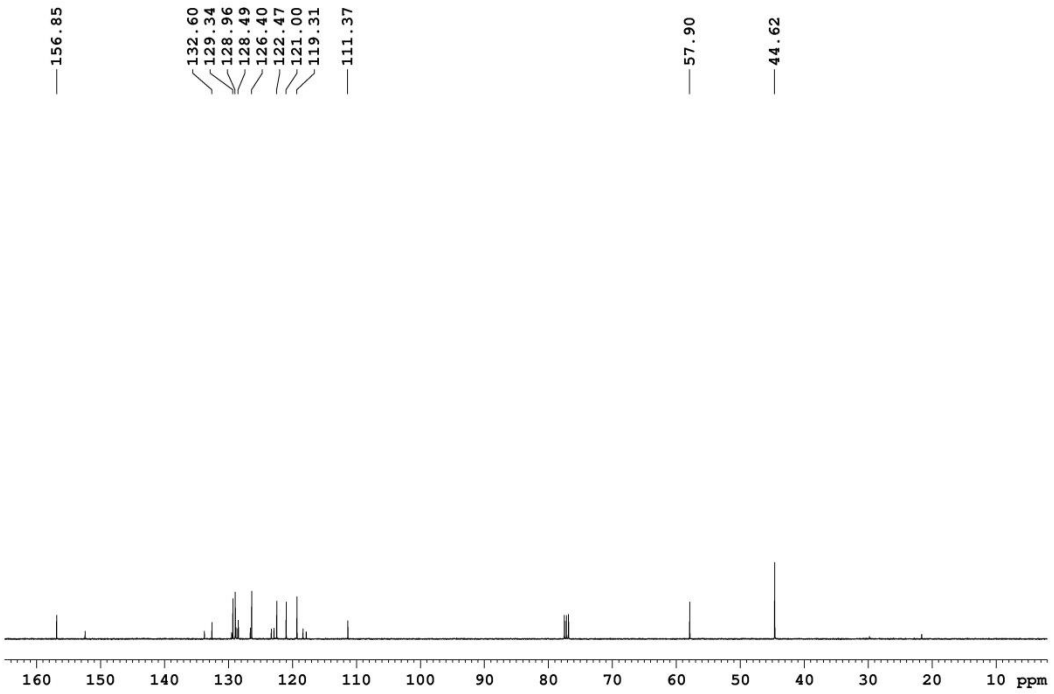

SGT-KM-20-12 CDCL3 DEPT

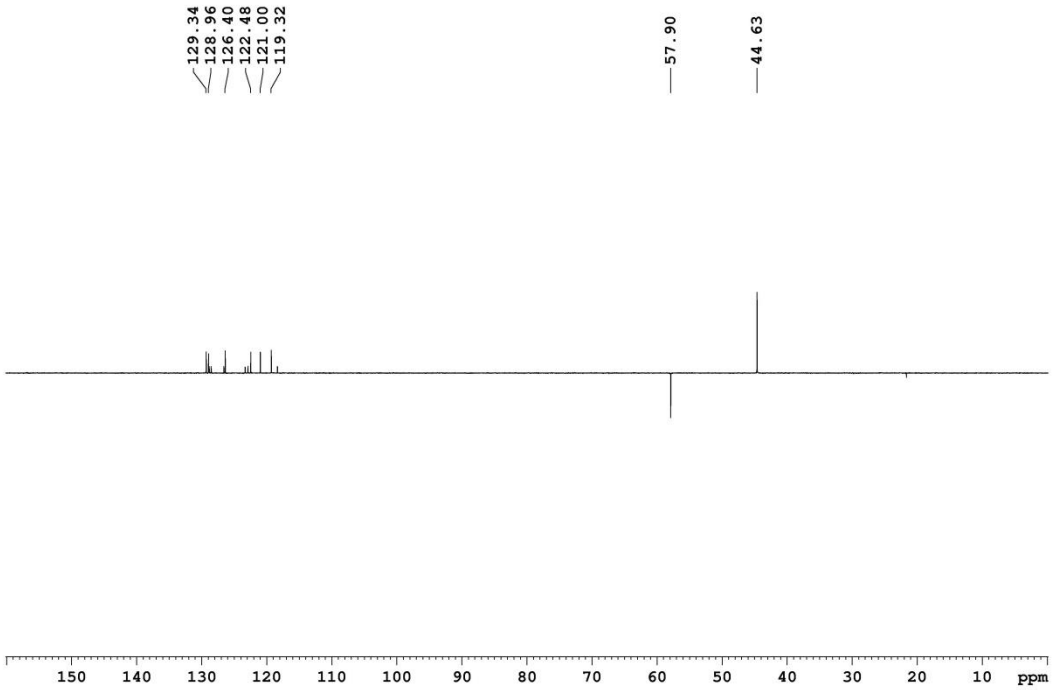

SGT-KM-20-09 CDCL3 PMR

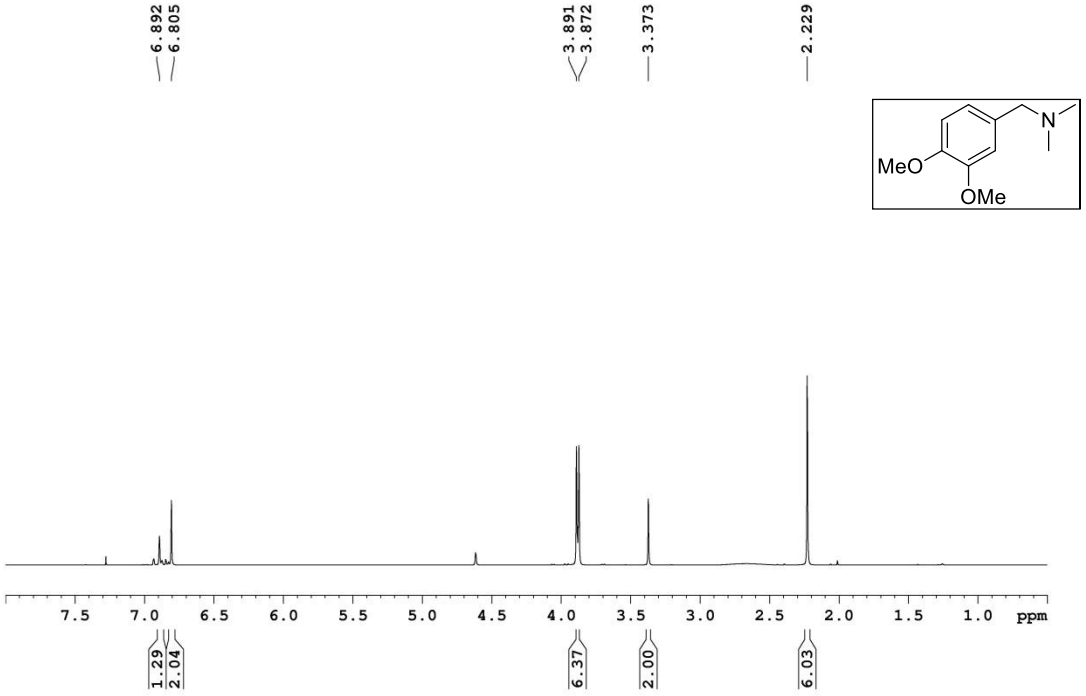

SGT-KM-20-09 CDCL3 CMR

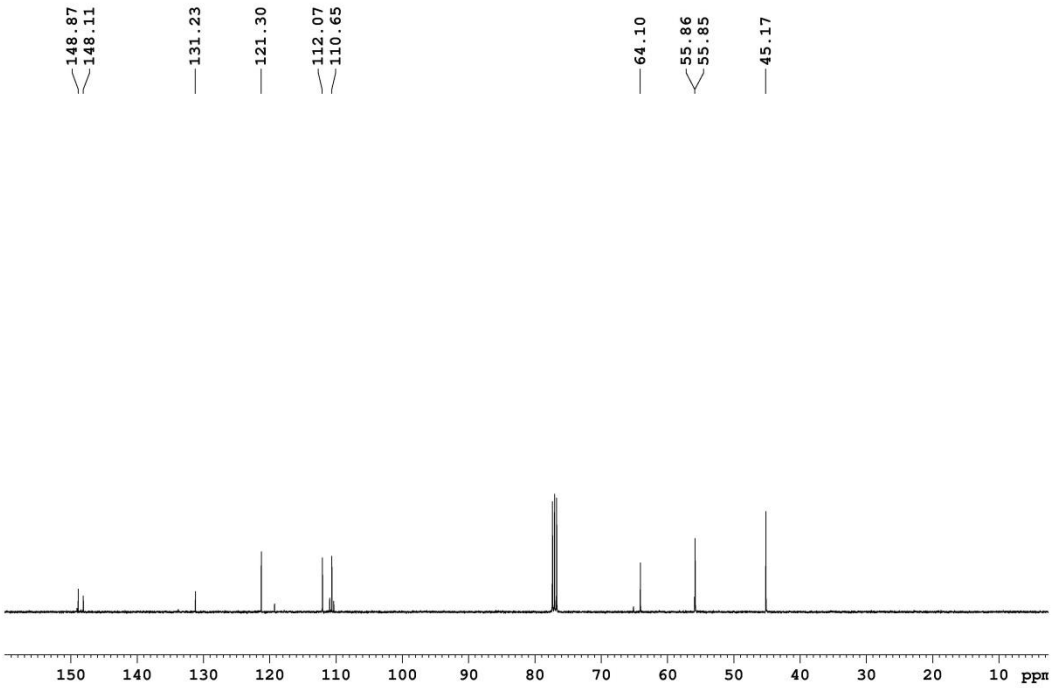

SGT-KM-20-09 CDCL3 DEPT

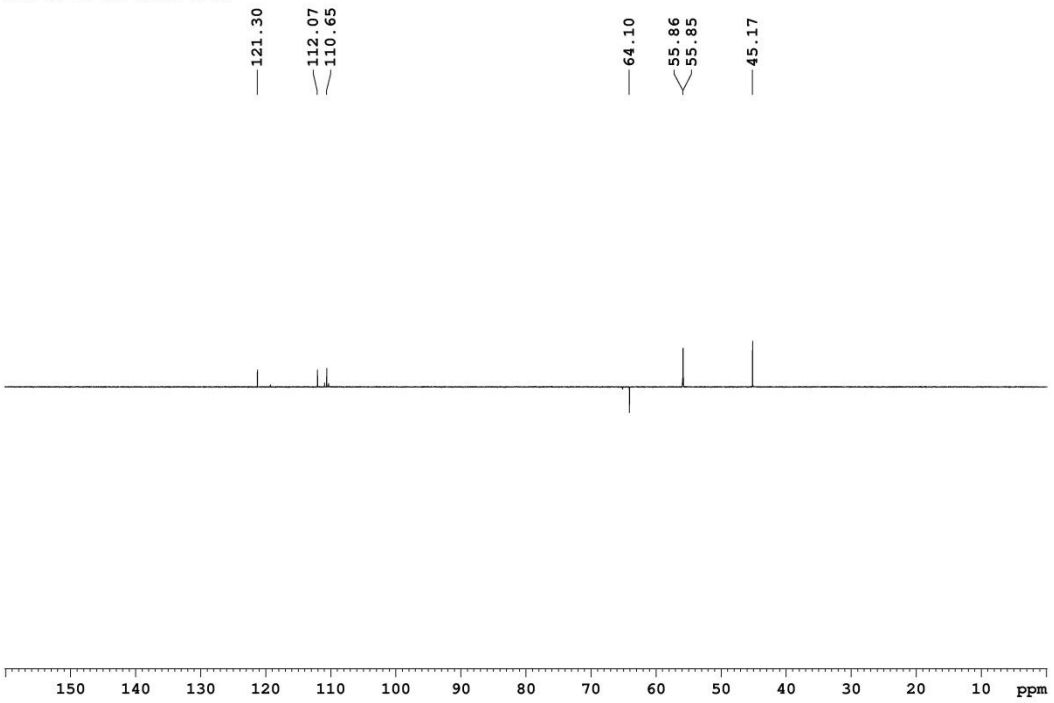

SGT-KM-20-10 CDCL3 PMR

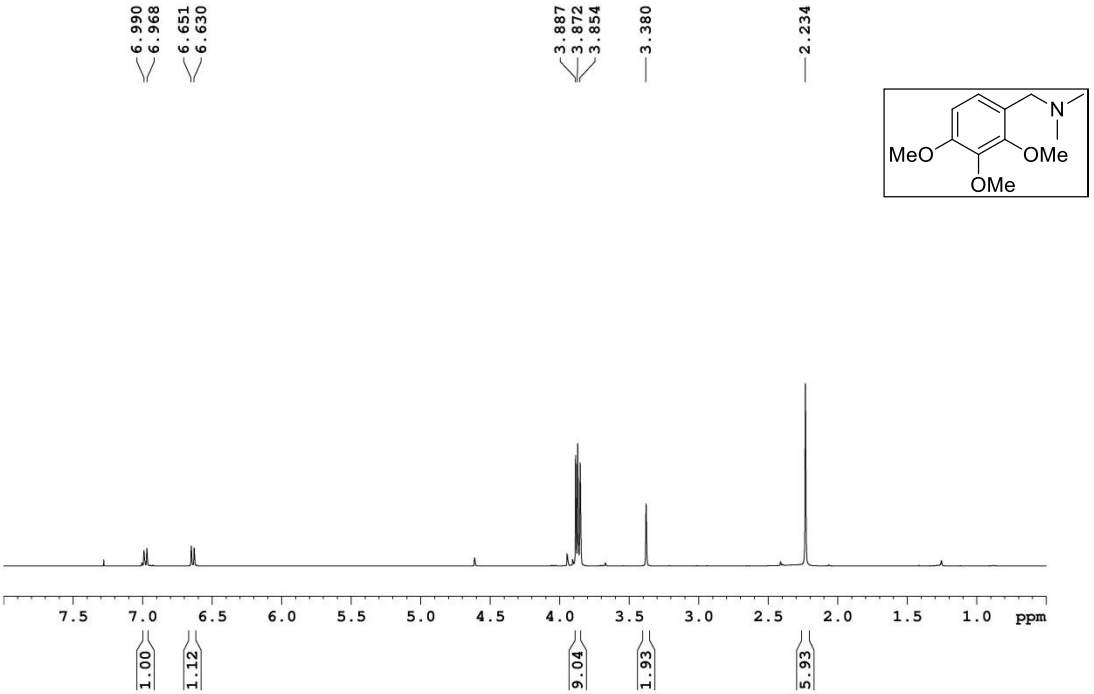

SGT-KM-20-06-05 CDCL3 CMR

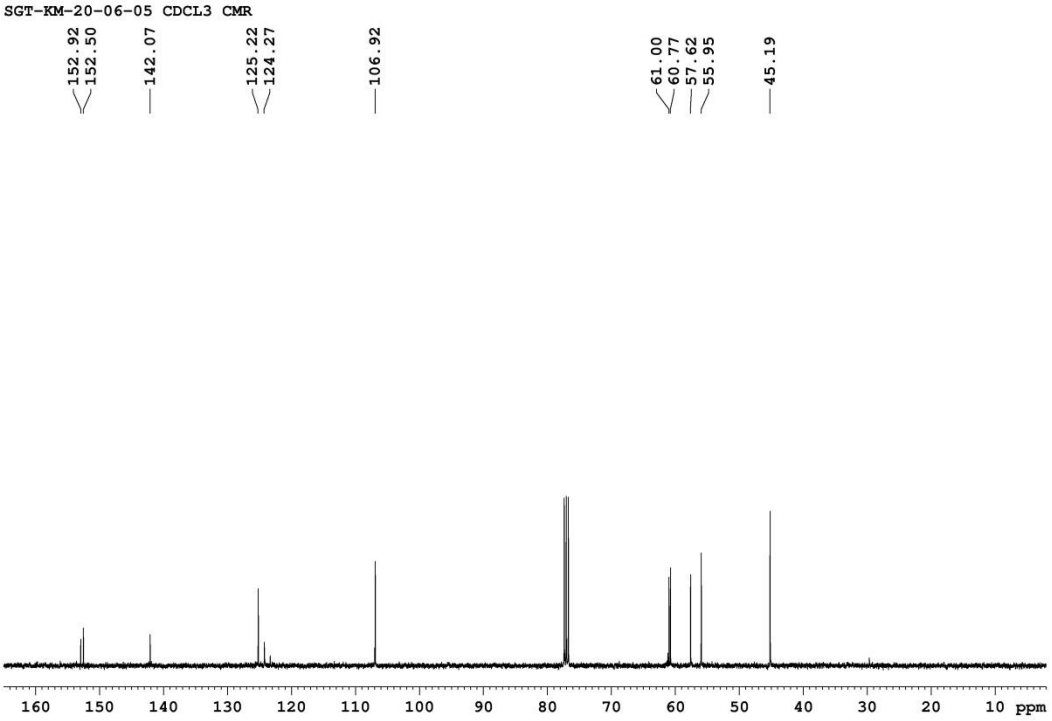

SGT-KM-20-06-05 CDCL3 DEPT

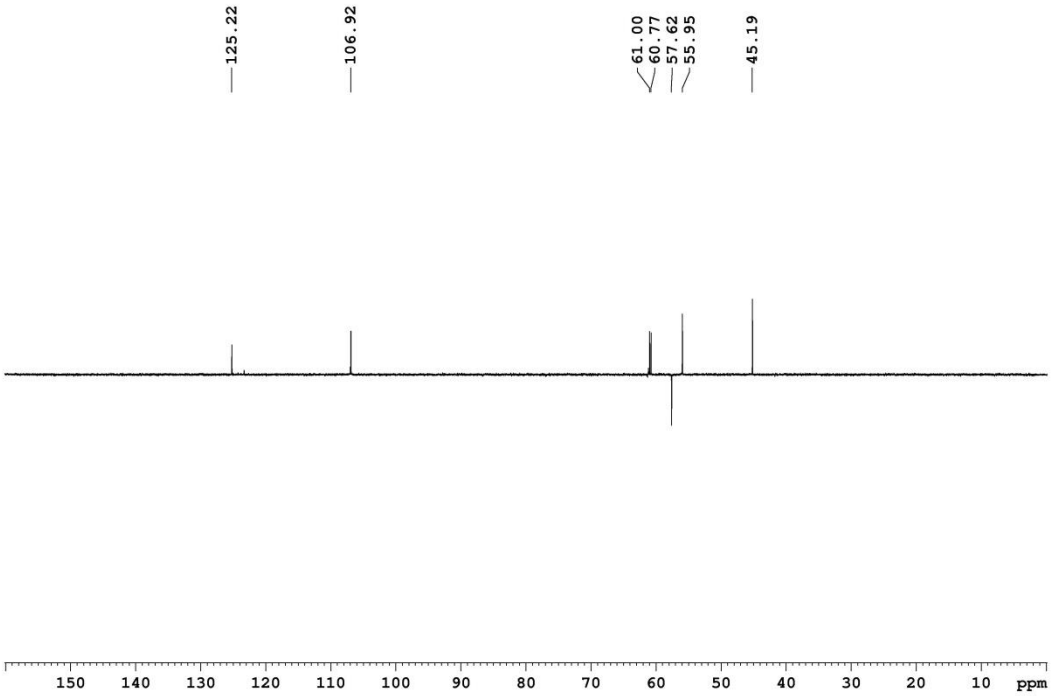

SGT-KM-20-08 CDCL3 PMR

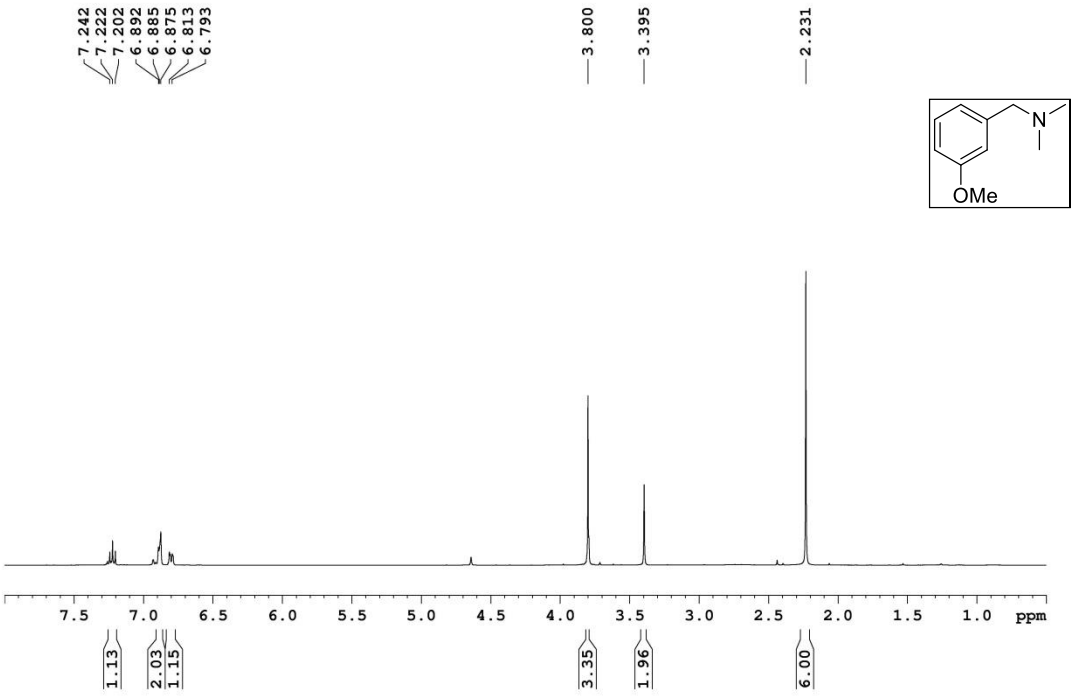

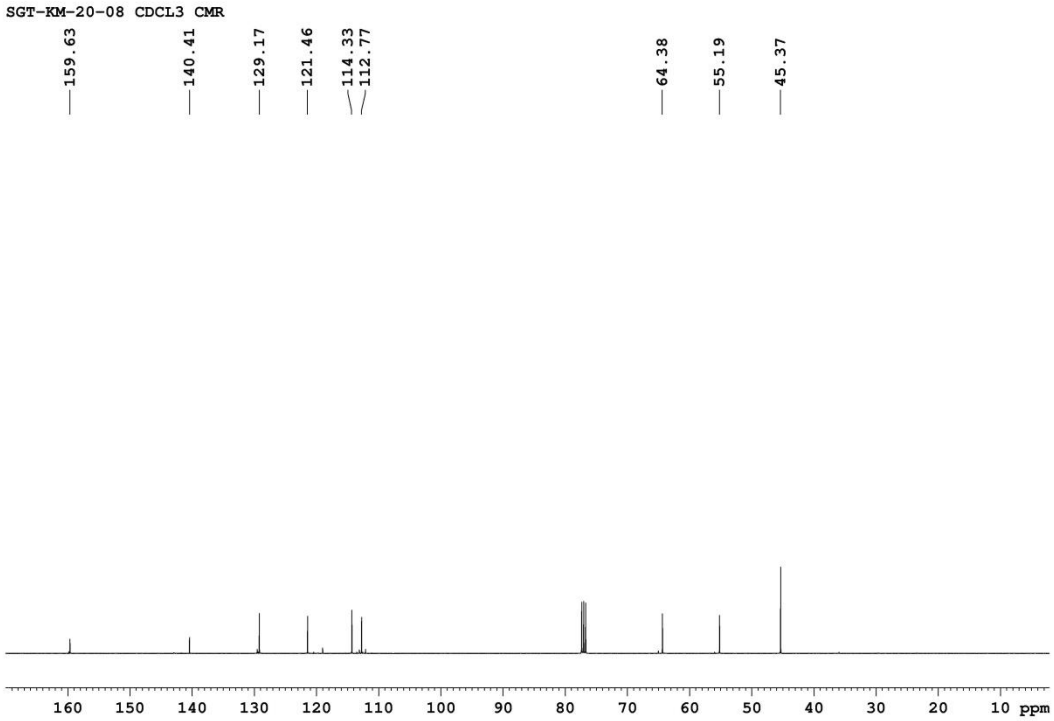
SGT-KM-20-08 CDCL3 CMR
159.63
140.41
129.17
121.46
114.33
112.77
64.38
55.19
45.37
160 150 140 130 120 110 100 90 80 70 60 50 40 30 20 10 ppm

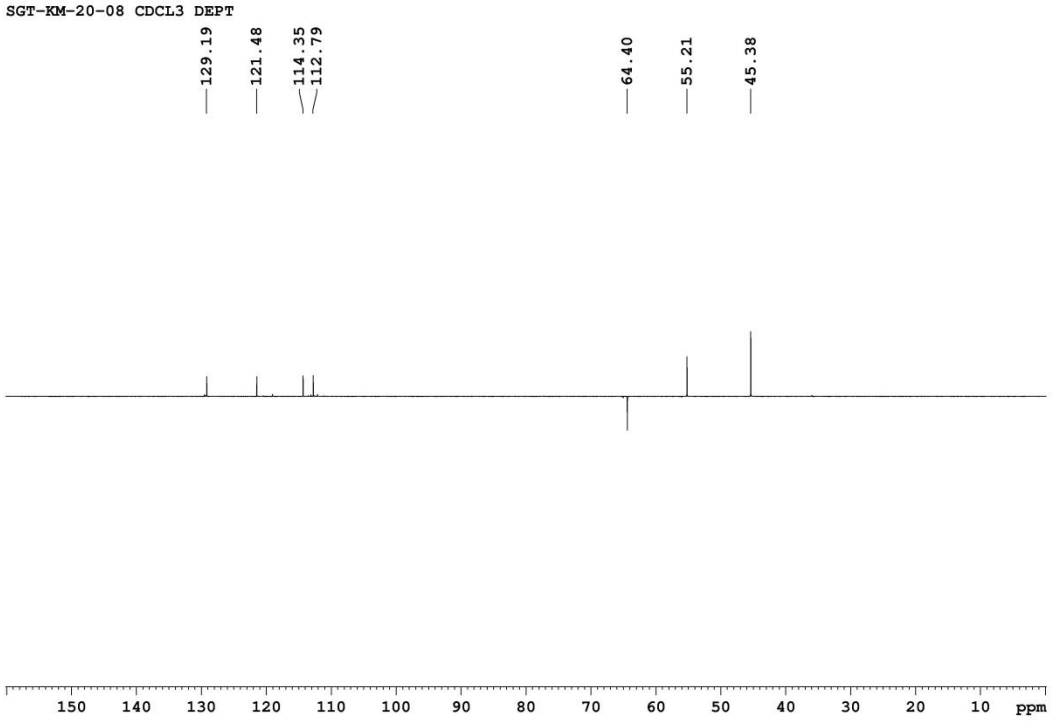
SGT-KM-20-08 CDCL3 DEPT
129.19
121.48
114.35
112.79
64.40
55.21
45.38
150 140 130 120 110 100 90 80 70 60 50 40 30 20 10 ppm

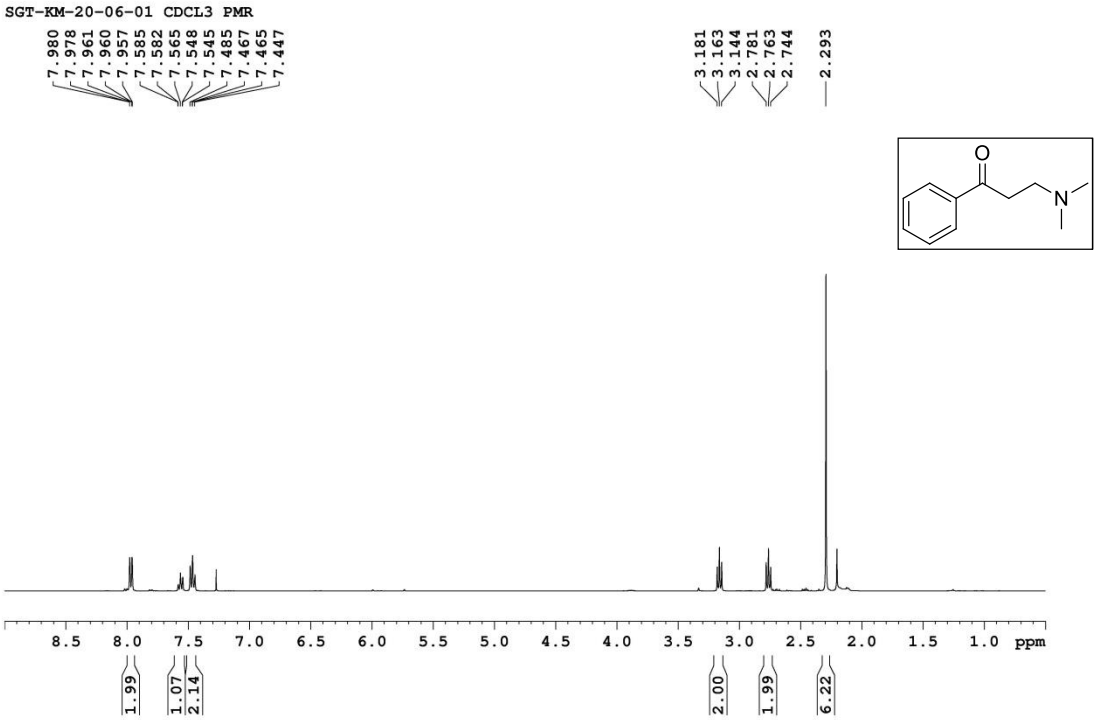
SGT-KM-20-06-01 CDCL3 PMR
7.980
7.978
7.961
7.960
7.957
7.585
7.582
7.565
7.548
7.545
7.485
7.467
7.465
7.447
3.181
3.163
3.144
2.781
2.763
2.744
2.293
O
N
8.5 8.0 7.5 7.0 6.5 6.0 5.5 5.0 4.5 4.0 3.5 3.0 2.5 2.0 1.5 1.0 ppm
1.99
1.07
2.14
2.00
1.99
6.22

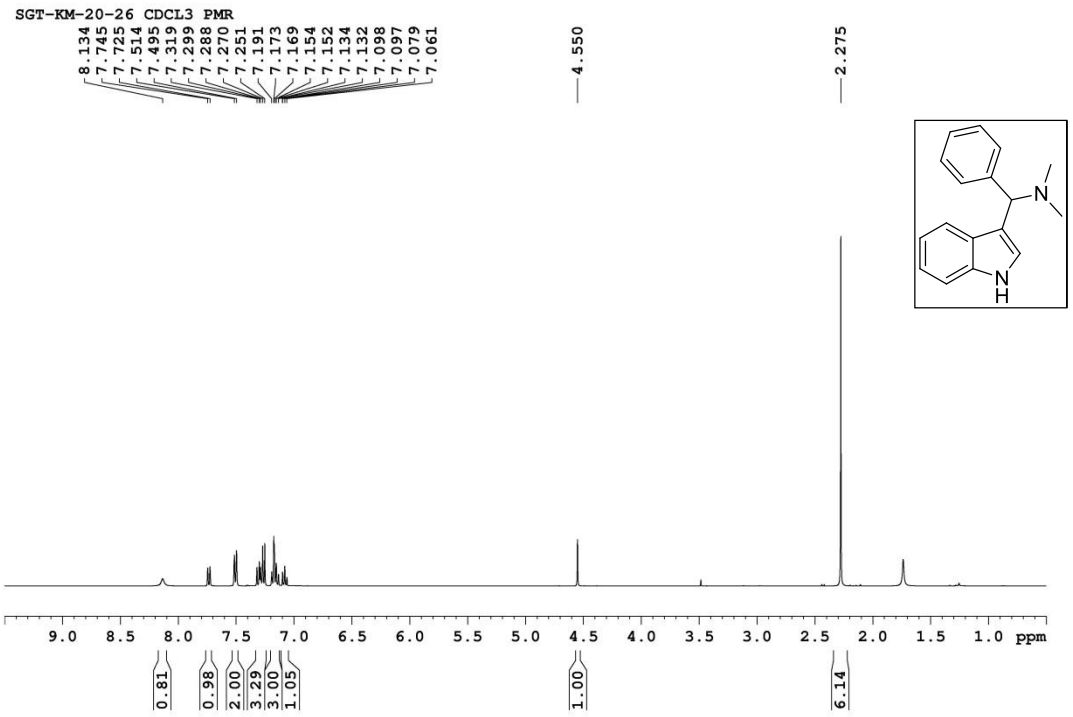
SGT-KM-20-26 CDCL3 PMR
8.134
7.745
7.725
7.514
7.495
7.319
7.299
7.288
7.270
7.251
7.191
7.173
7.169
7.154
7.152
7.134
7.132
7.098
7.097
7.079
7.061
4.550
2.275
N
H
9.0 8.5 8.0 7.5 7.0 6.5 6.0 5.5 5.0 4.5 4.0 3.5 3.0 2.5 2.0 1.5 1.0 ppm
0.81
0.98
2.00
3.29
3.00
1.05
1.00
6.14

SGT-KM-20-07-26 CDCL3 CMR

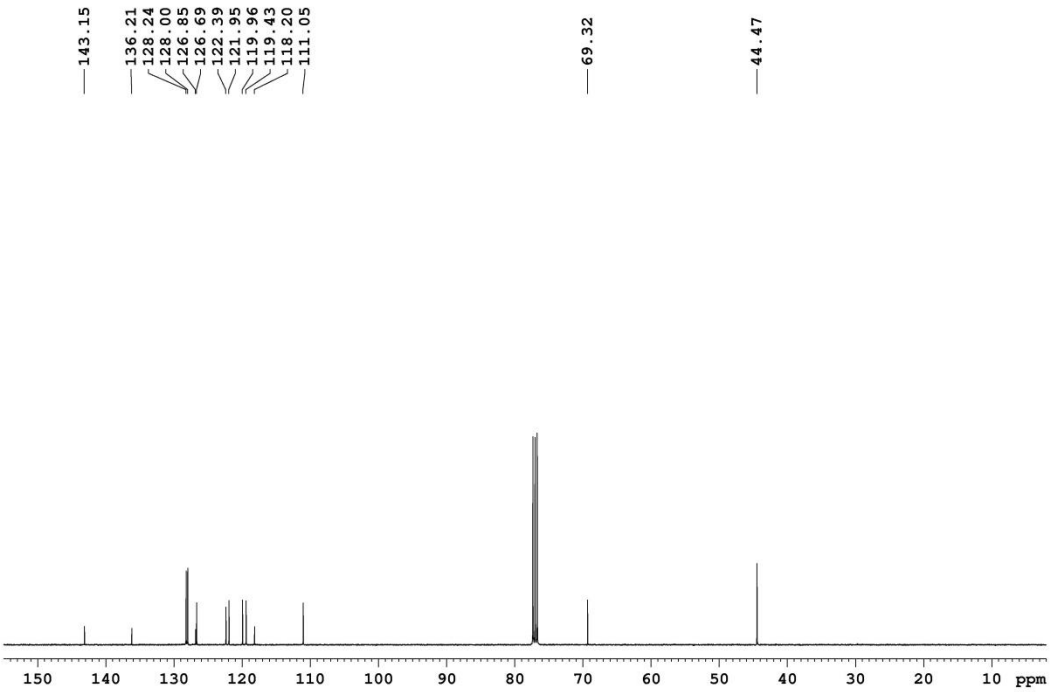

SGT-KM-20-07-26 CDCL3 DEPT

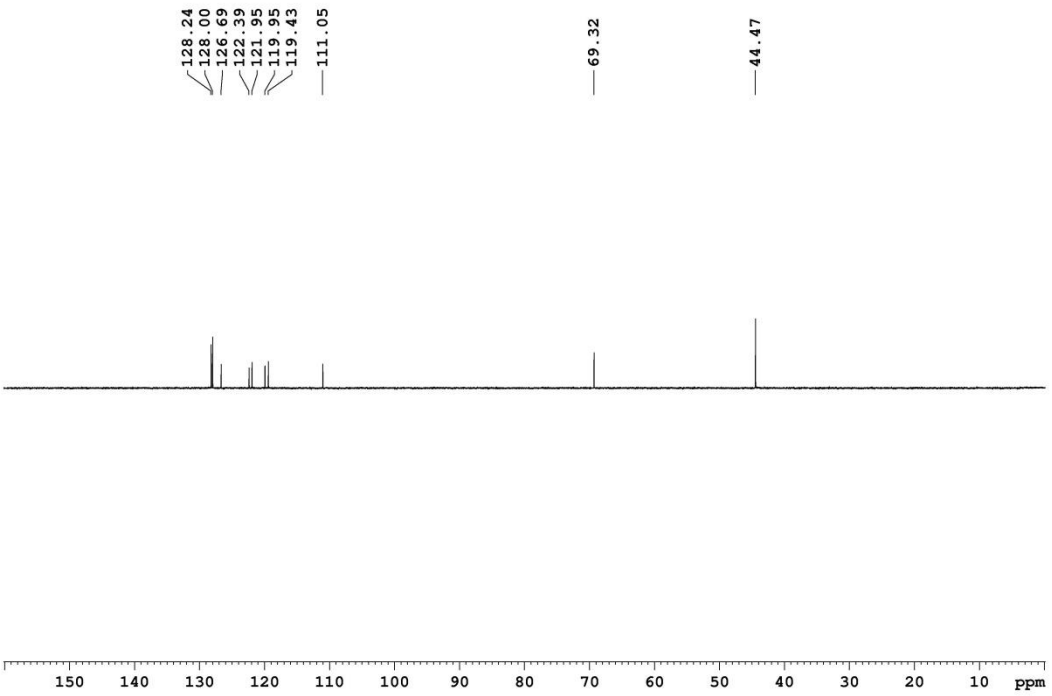

SGT-KM-20-09-02 CDCL3 PMR

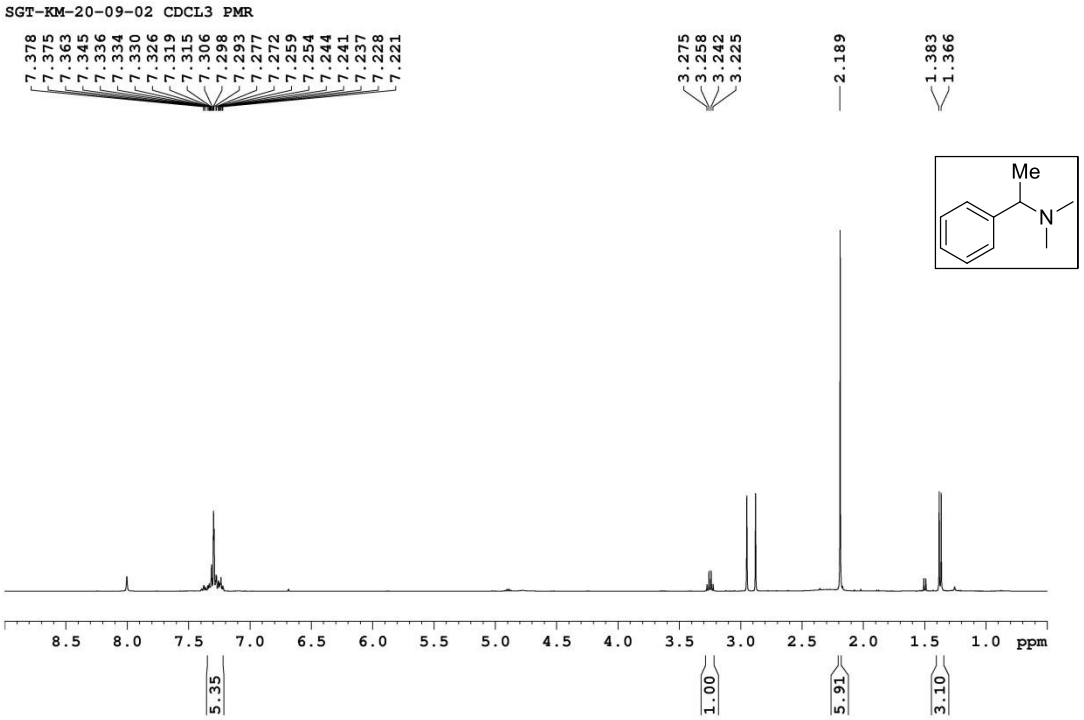

SGT-KM-20-07-22 CDCL3 PMR

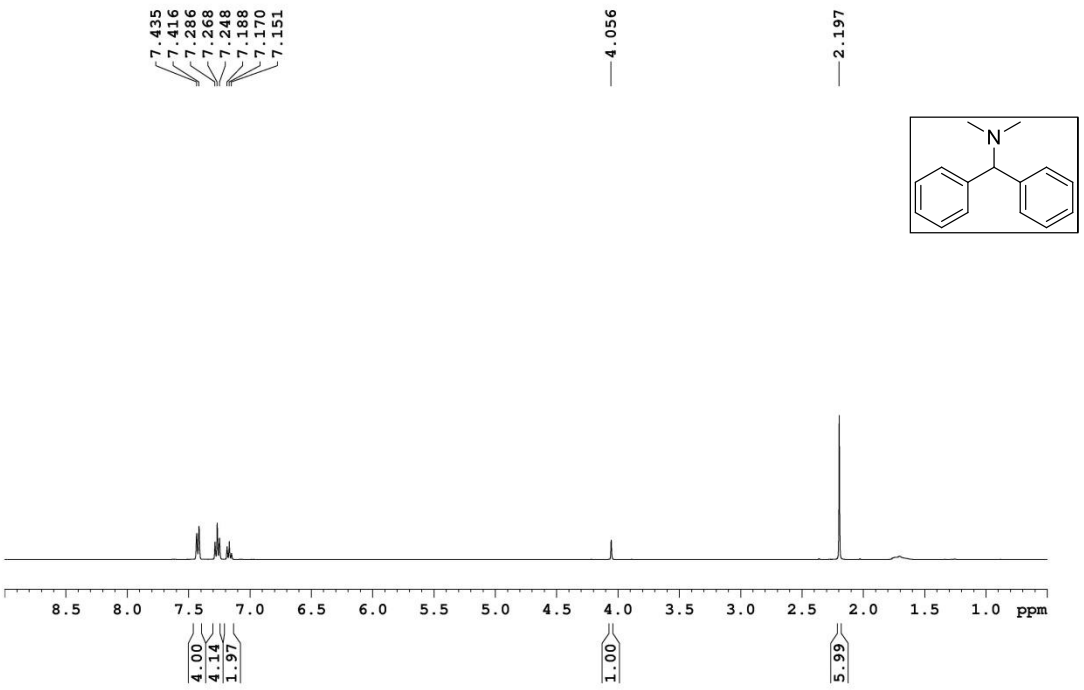

SGT-KM-20-07-22 CDCL3 CMR

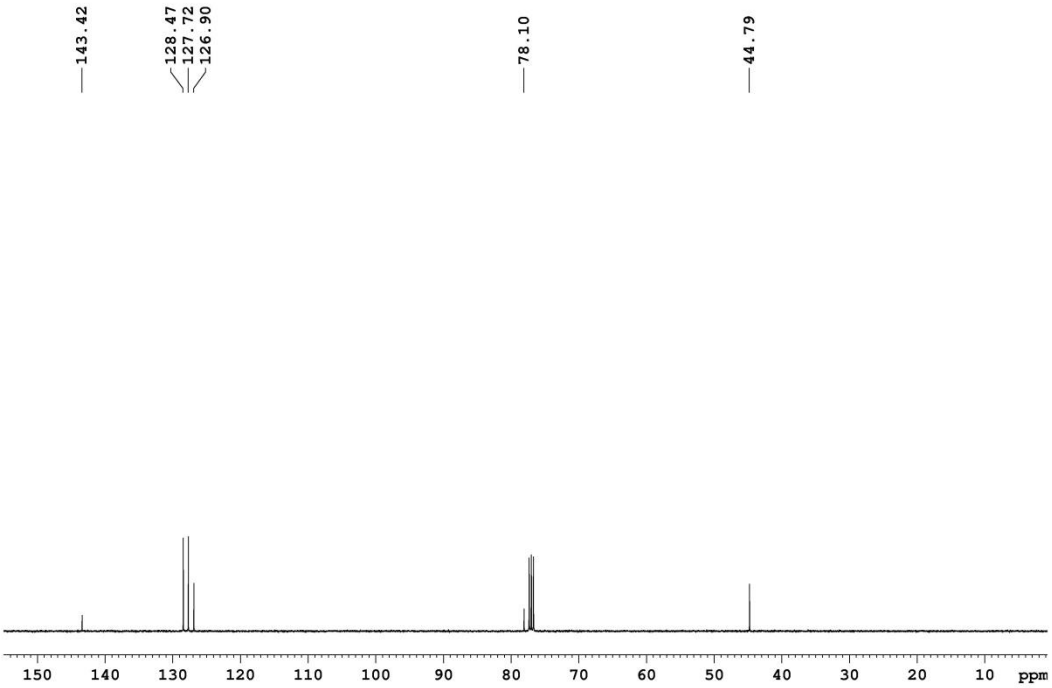

SGT-KM-20-07-22 CDCL3 DEPT

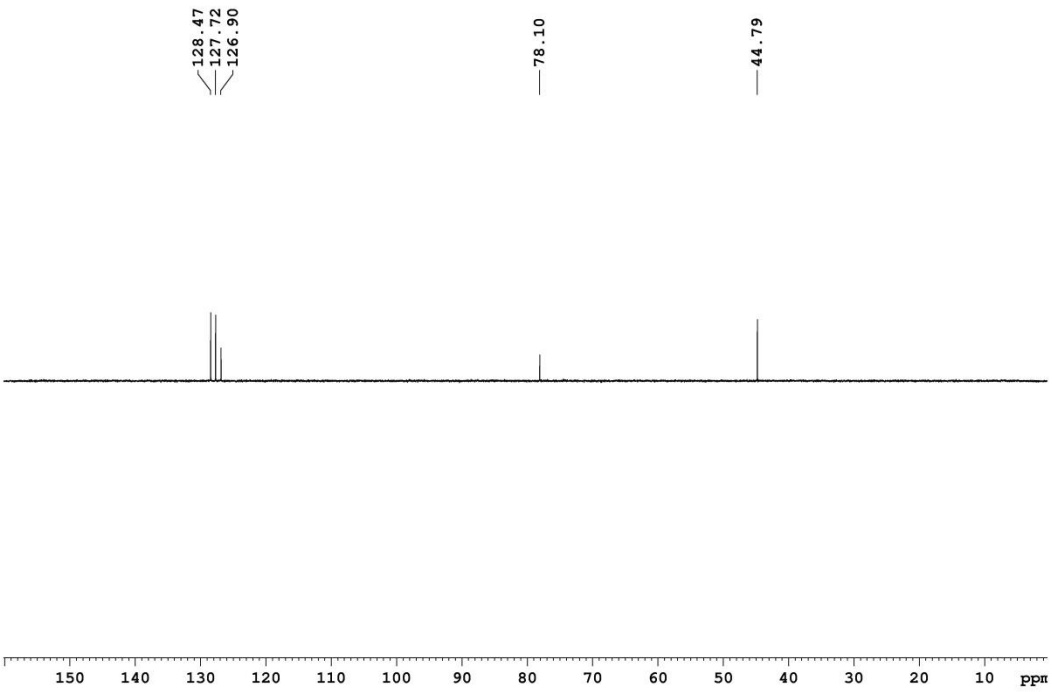

SGT-KM-20-07-04 DMSO PMR

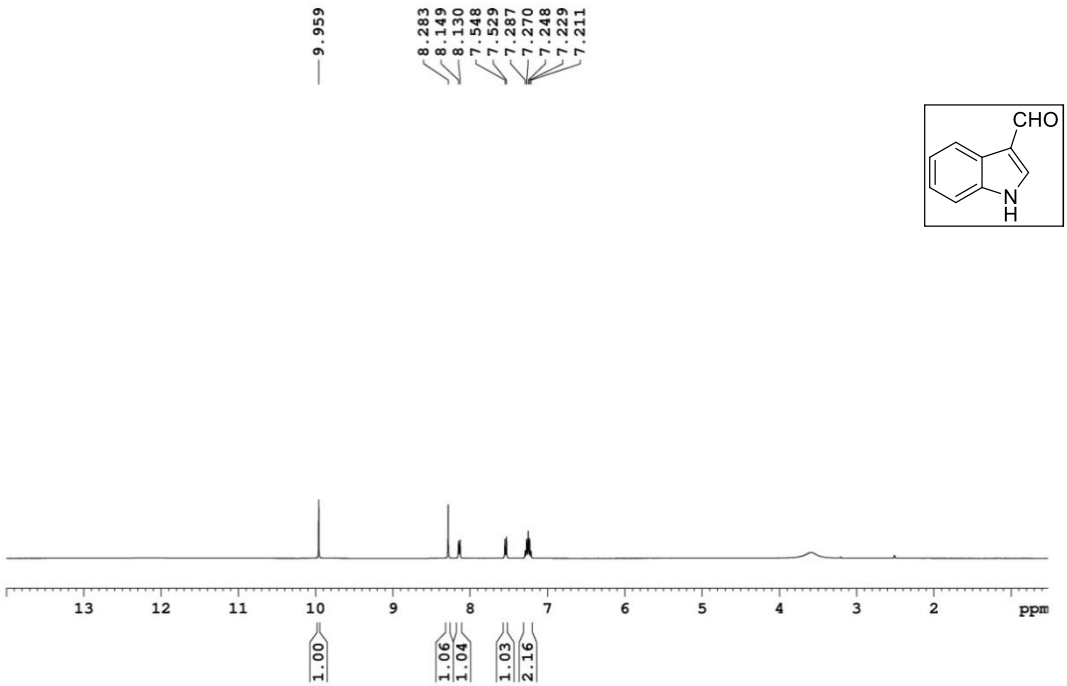

SGT-KM-20-07-04 DMSO CMR

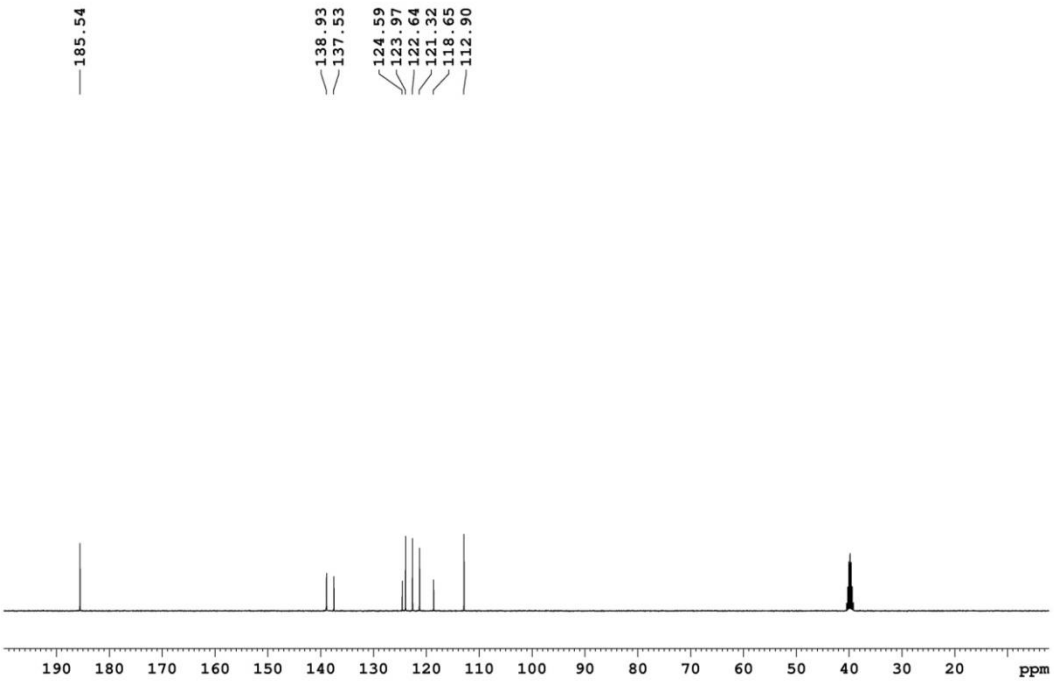

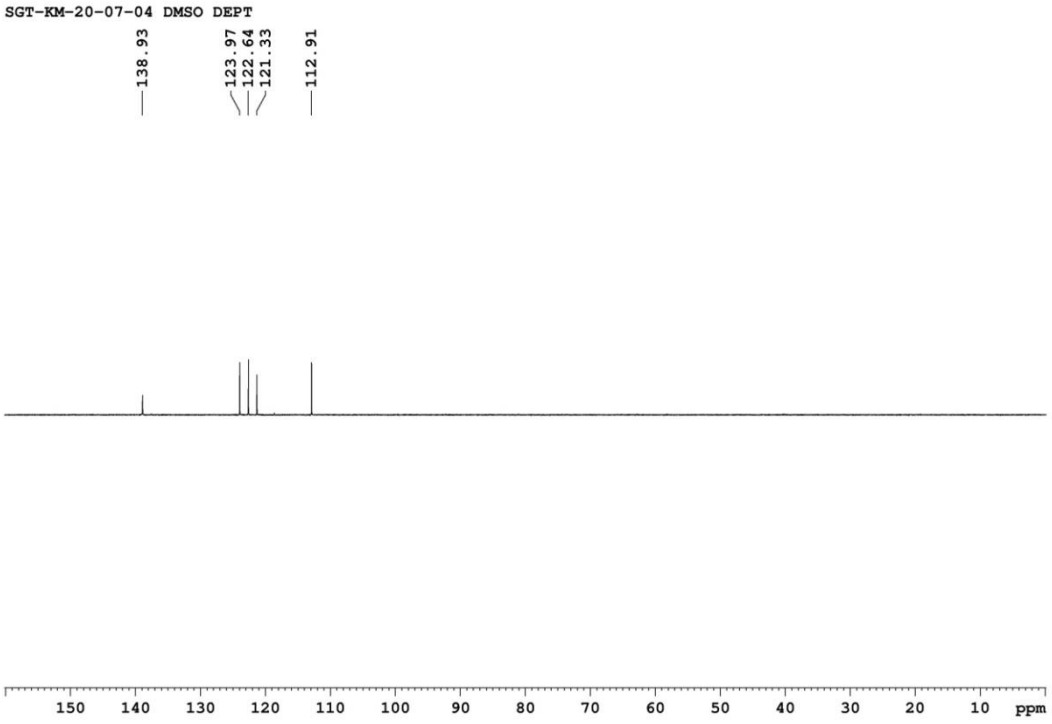
SGT-KM-20-07-04 DMSO DEPT
138.93
123.97
122.64
121.33
112.91
150 140 130 120 110 100 90 80 70 60 50 40 30 20 10 ppm

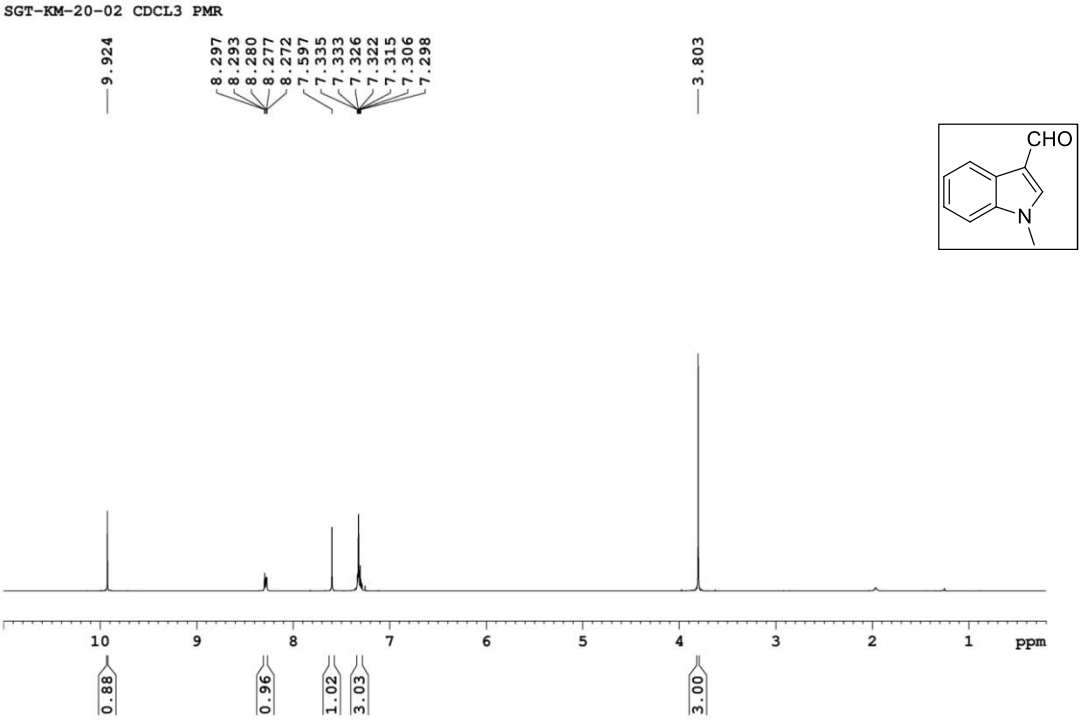
SGT-KM-20-02 CDCL3 PMR
9.924
8.297
8.293
8.280
8.277
8.272
7.597
7.335
7.333
7.326
7.322
7.315
7.306
7.298
3.803
CHO
N
10 9 8 7 6 5 4 3 2 1 ppm
0.88
0.96
1.02
3.03
3.00

SGT-KM-20-02 CDCL3 CMR

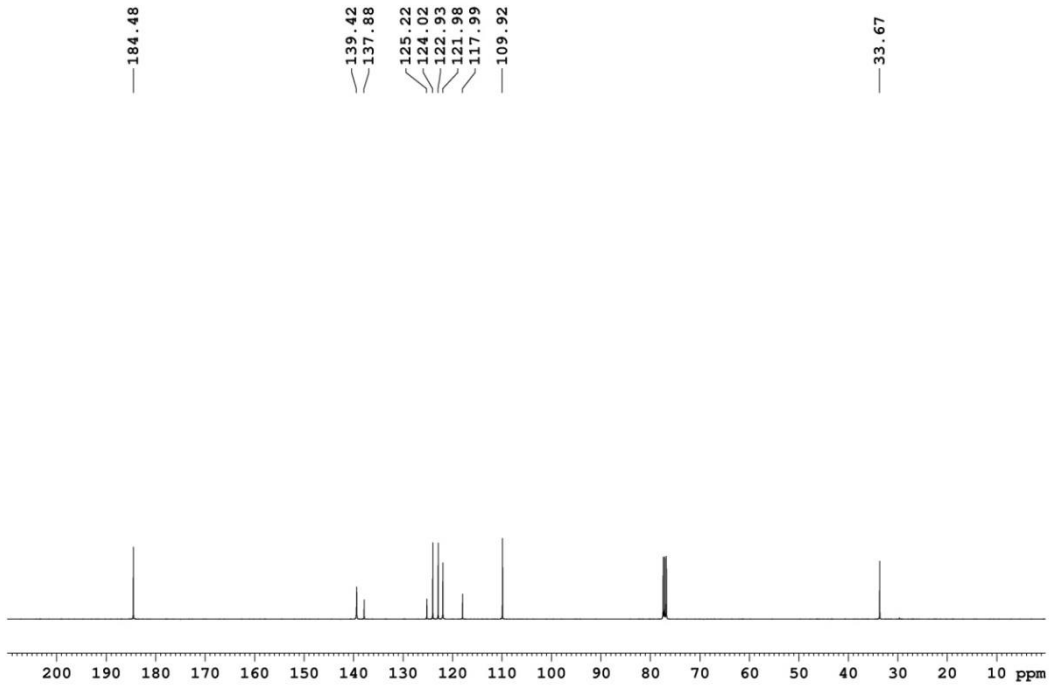

SGT-KM-20-02 CDCL3 DEPT

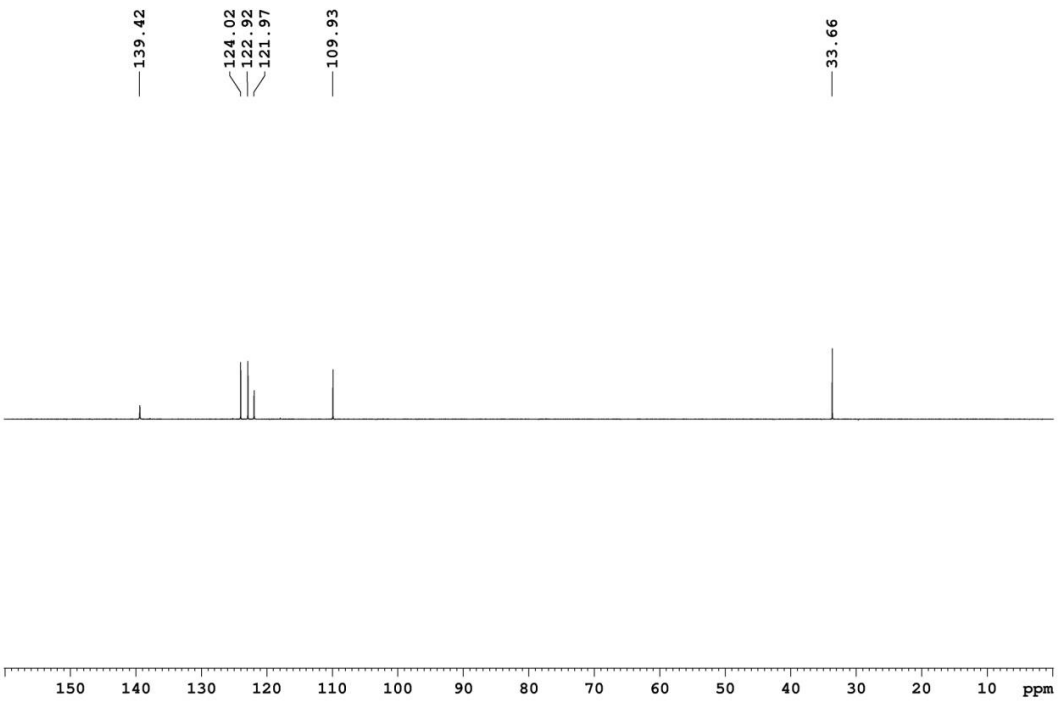

SGT-KM-20-06-13 CDCL3 PMR

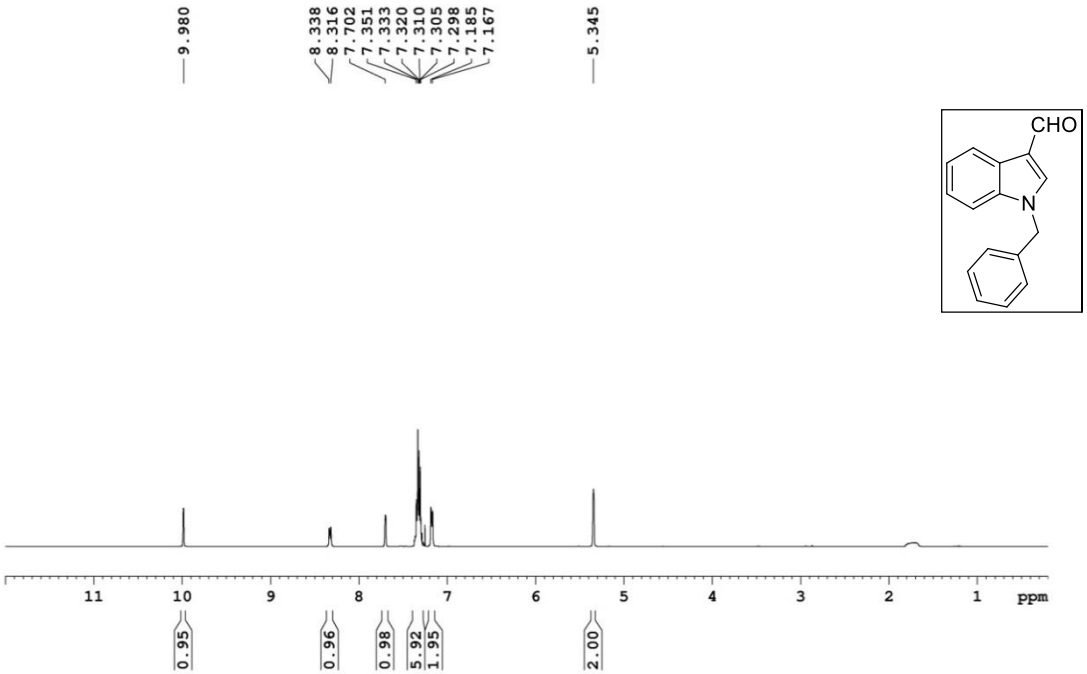

SGT-KM-20-06-13 CDCL3 CMR

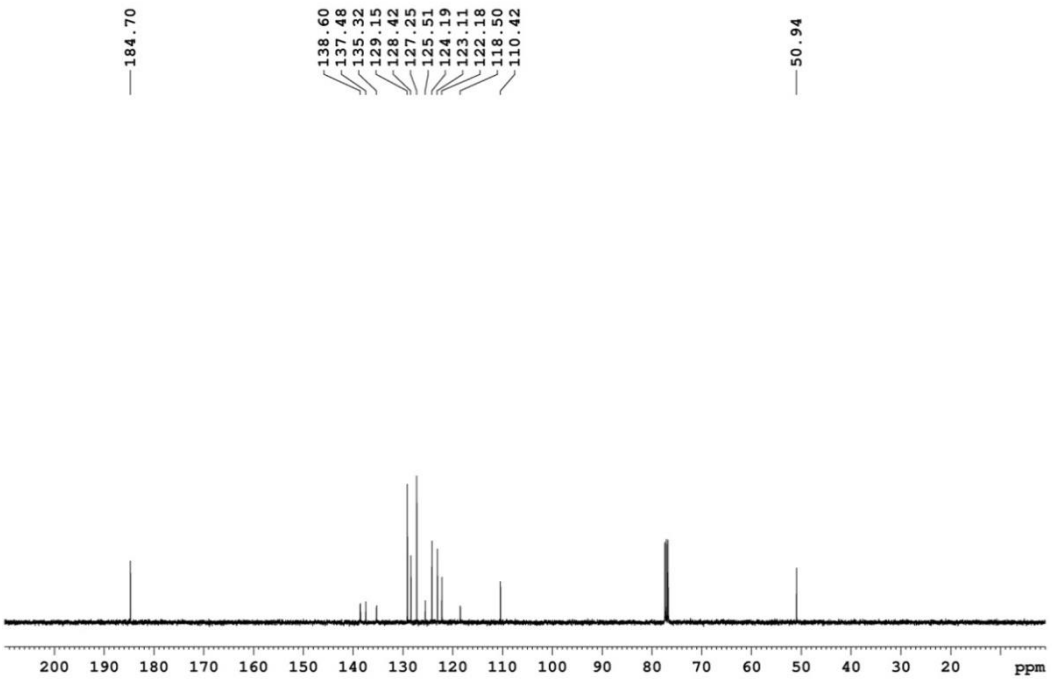

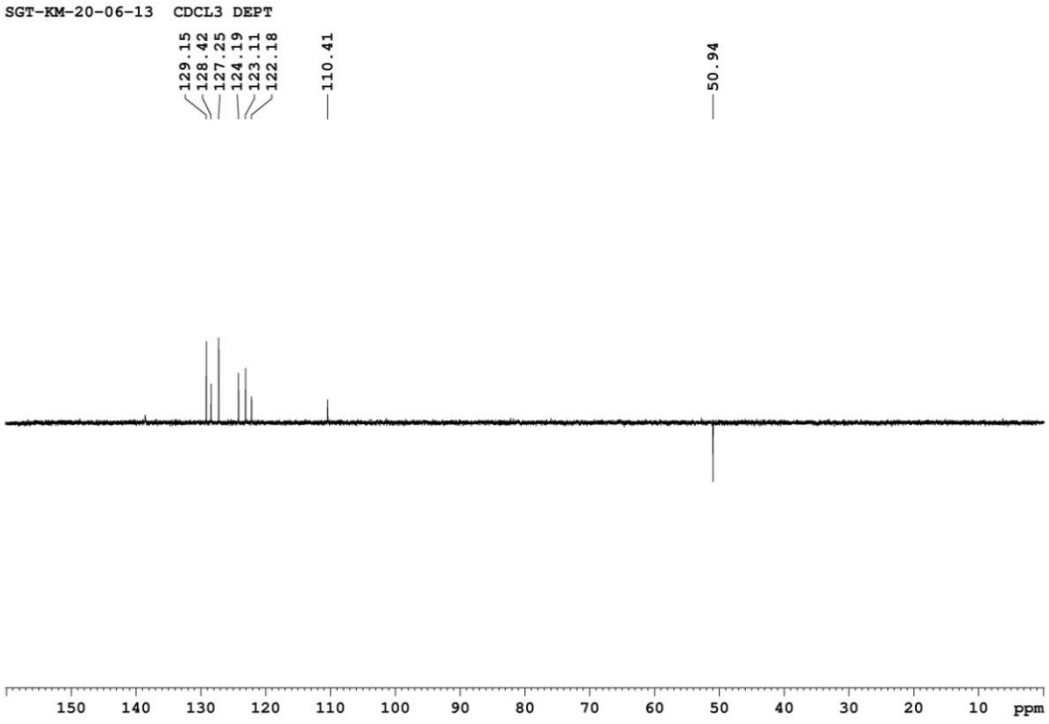
SGT-KM-20-06-13 CDCL3 DEPT
129.15
128.42
127.25
124.19
123.11
122.18
110.41
50.94
150 140 130 120 110 100 90 80 70 60 50 40 30 20 10 ppm

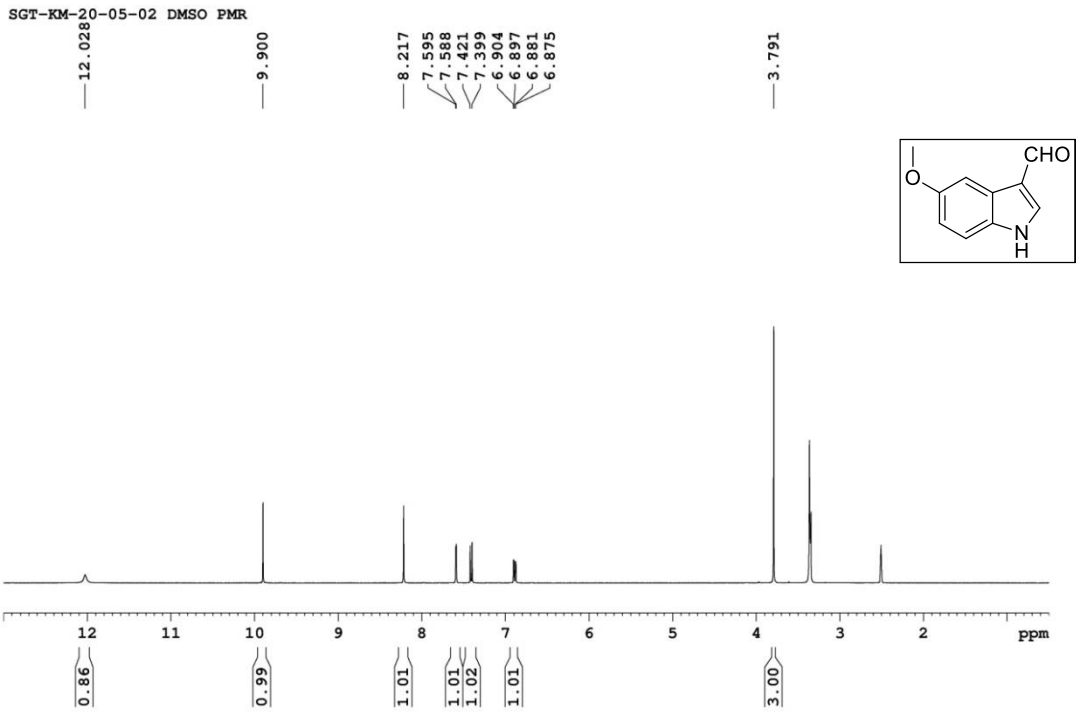
SGT-KM-20-05-02 DMSO PMR
12.028
9.900
8.217
7.595
7.588
7.421
7.399
6.904
6.897
6.881
6.875
3.791
CHO
O
N
H
12 11 10 9 8 7 6 5 4 3 2 ppm
0.86
0.99
1.01
1.01
1.02
1.01
3.00

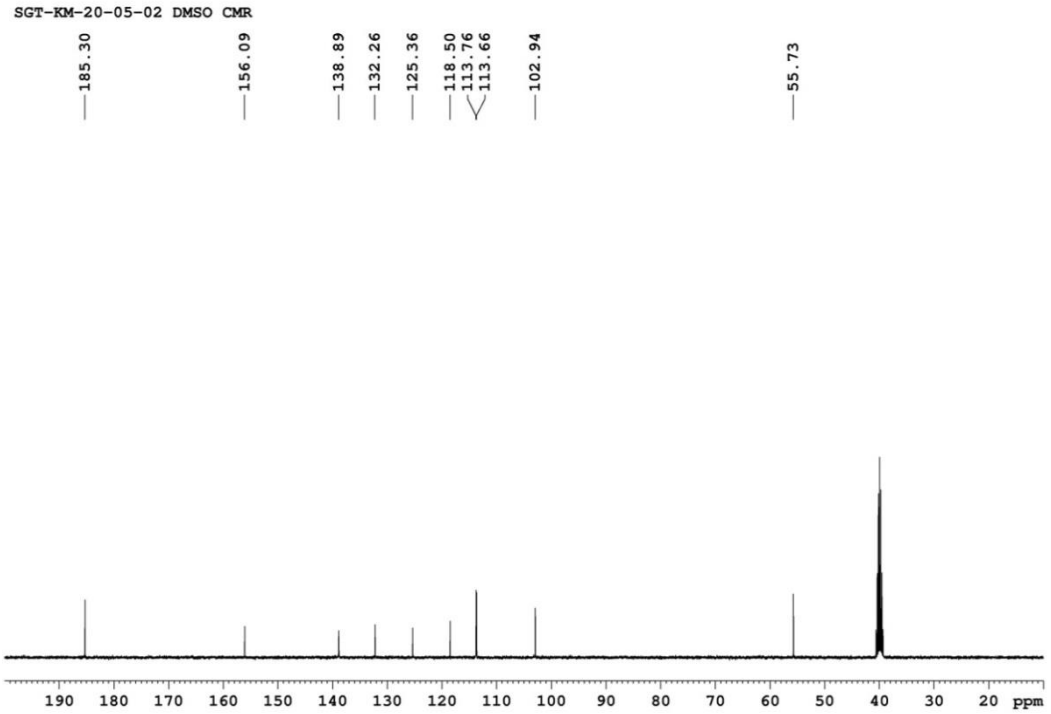
SGT-KM-20-05-02 DMSO CMR
185.30
156.09
138.89
132.26
125.36
118.50
113.76
113.66
102.94
55.73
190 180 170 160 150 140 130 120 110 100 90 80 70 60 50 40 30 20 ppm

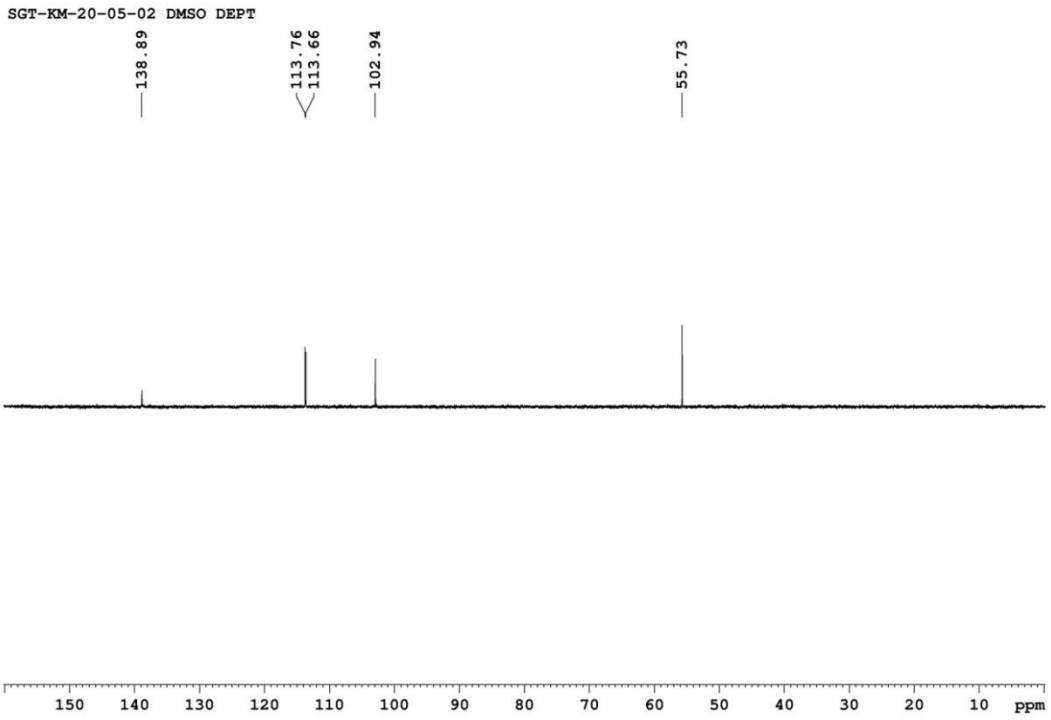
SGT-KM-20-05-02 DMSO DEPT
138.89
113.76
113.66
102.94
55.73
150 140 130 120 110 100 90 80 70 60 50 40 30 20 10 ppm

SGT-KM-19-59 DMSO PMR

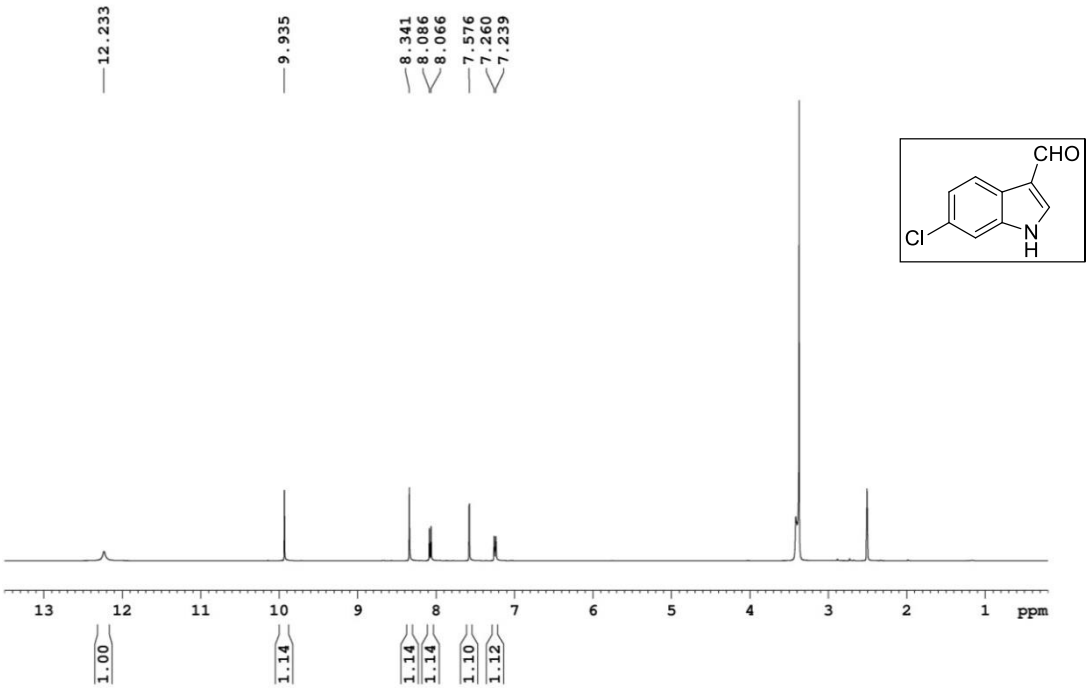

SGT-KM-19-59 DMSO CMR

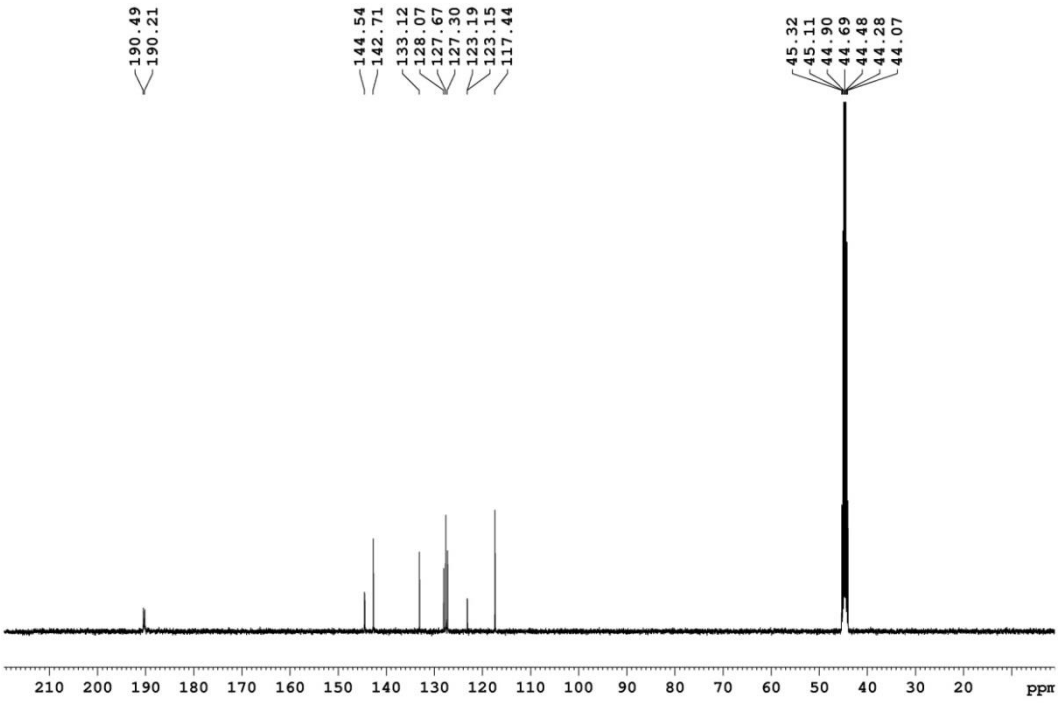

SGT-KM-19-59 DMSO DEPT

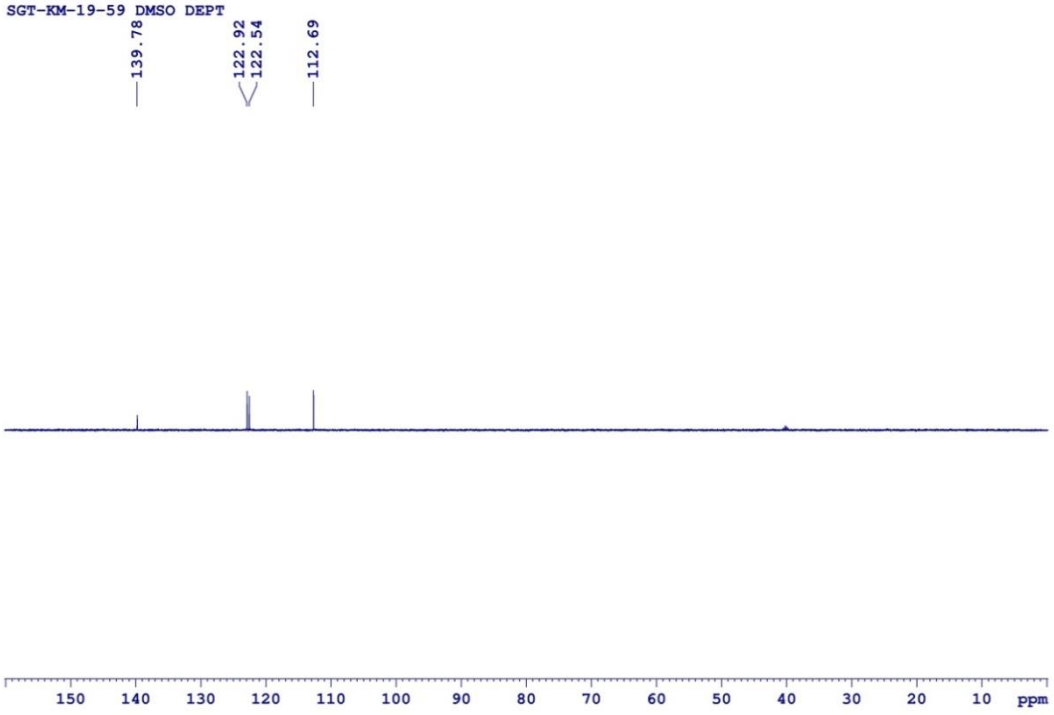

SGT-KM-19-61 DMSO PMR

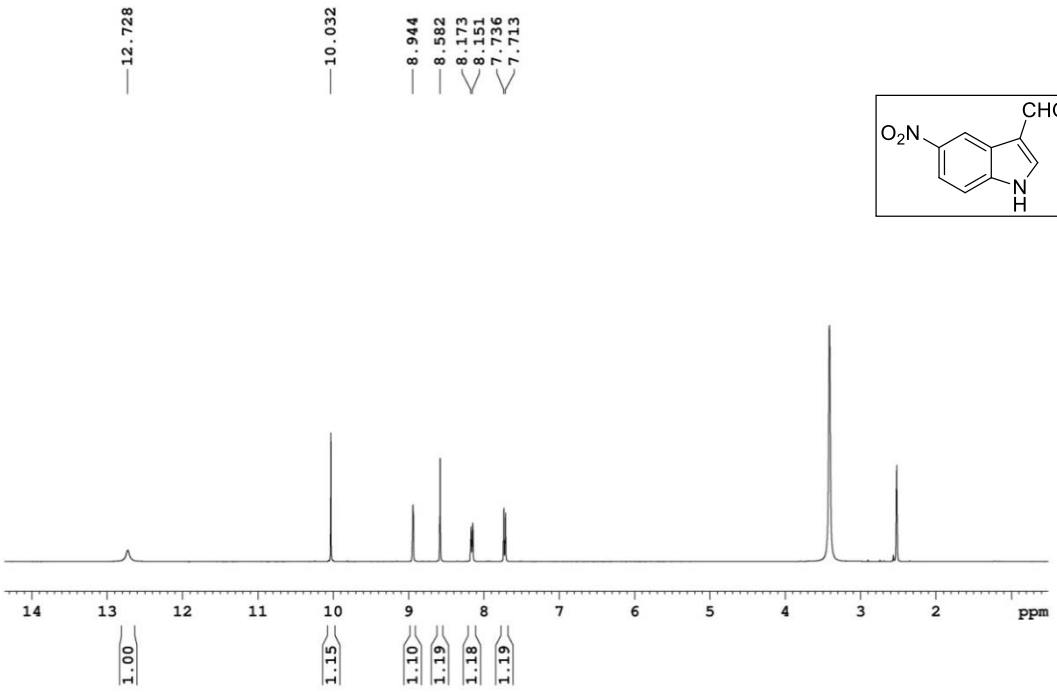

SGT-KM-19-61-A DMSO CMR

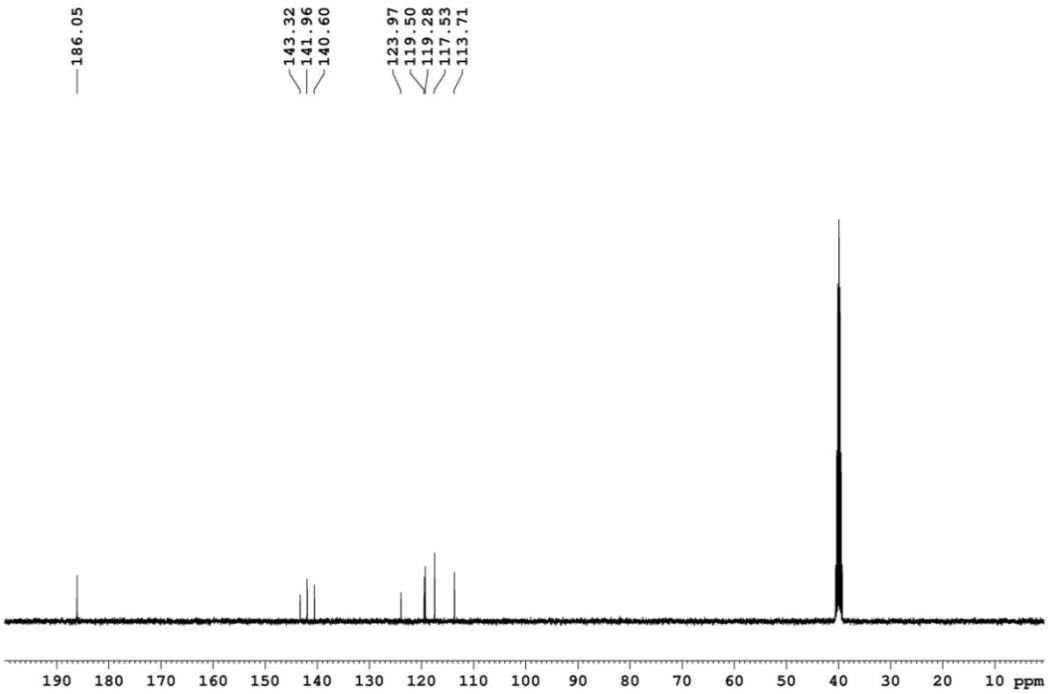

SGT-KM-19-61-A DMSO DEPT

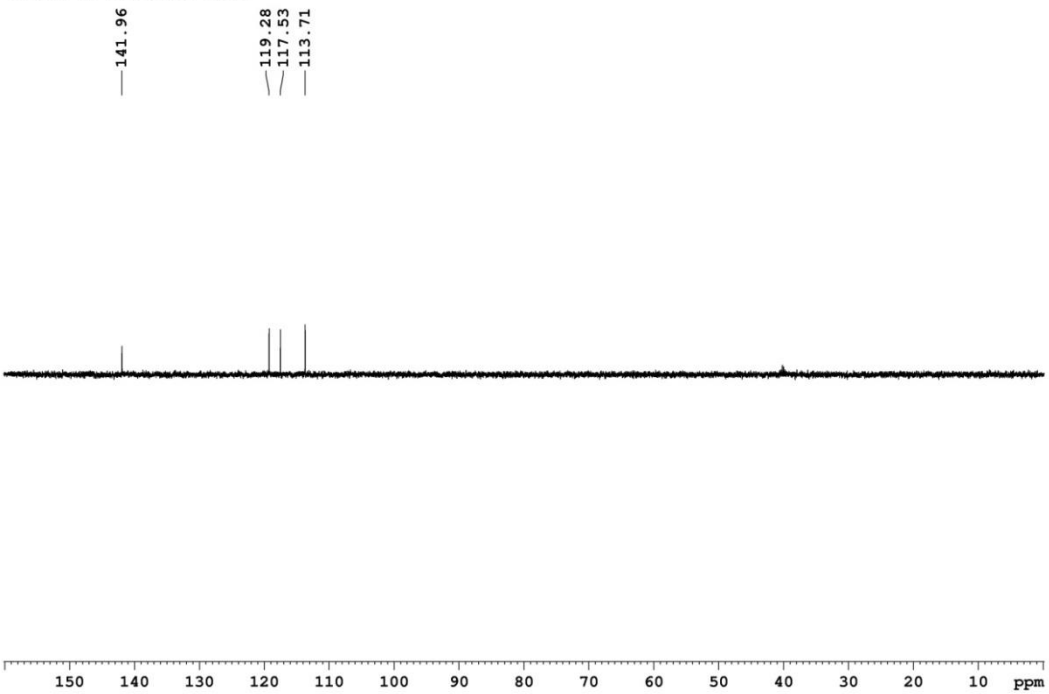

SGT-KM-20-05-03 DMSO PMR

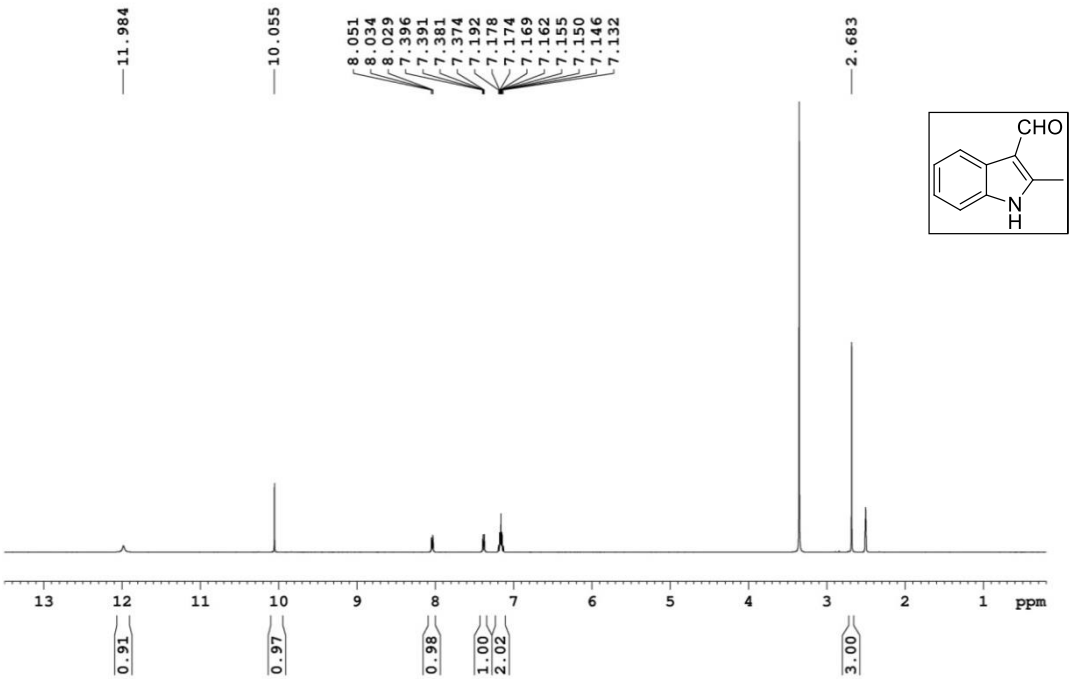

SGT-KM-20-05-03 DMSO CMR

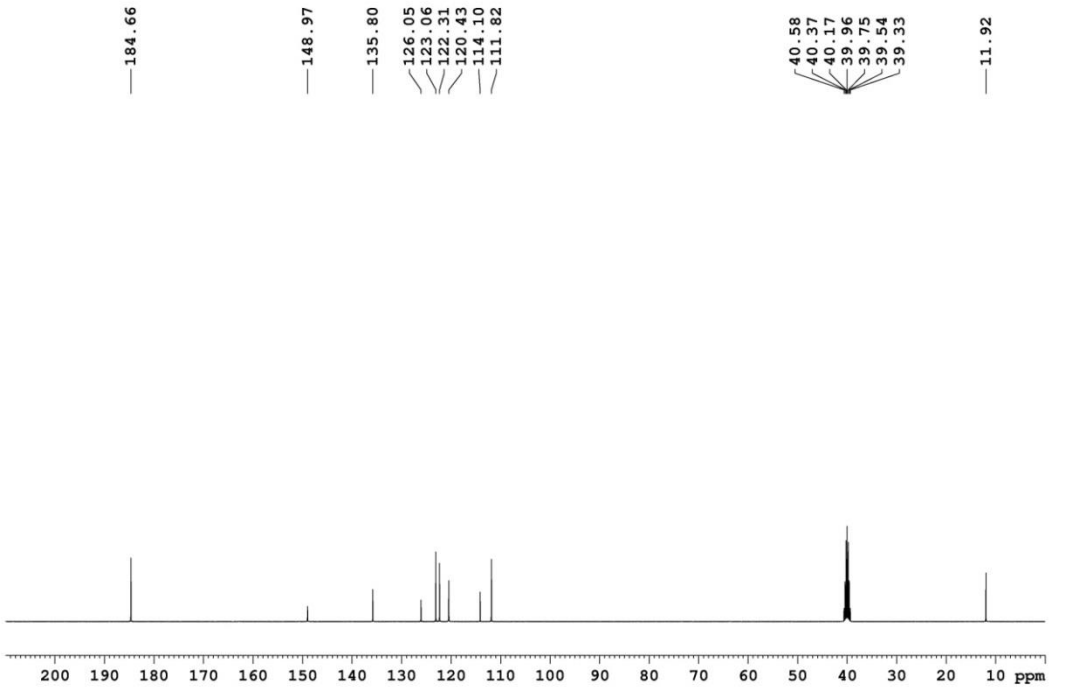

SGT-KM-20-05-03 DMSO DEPT

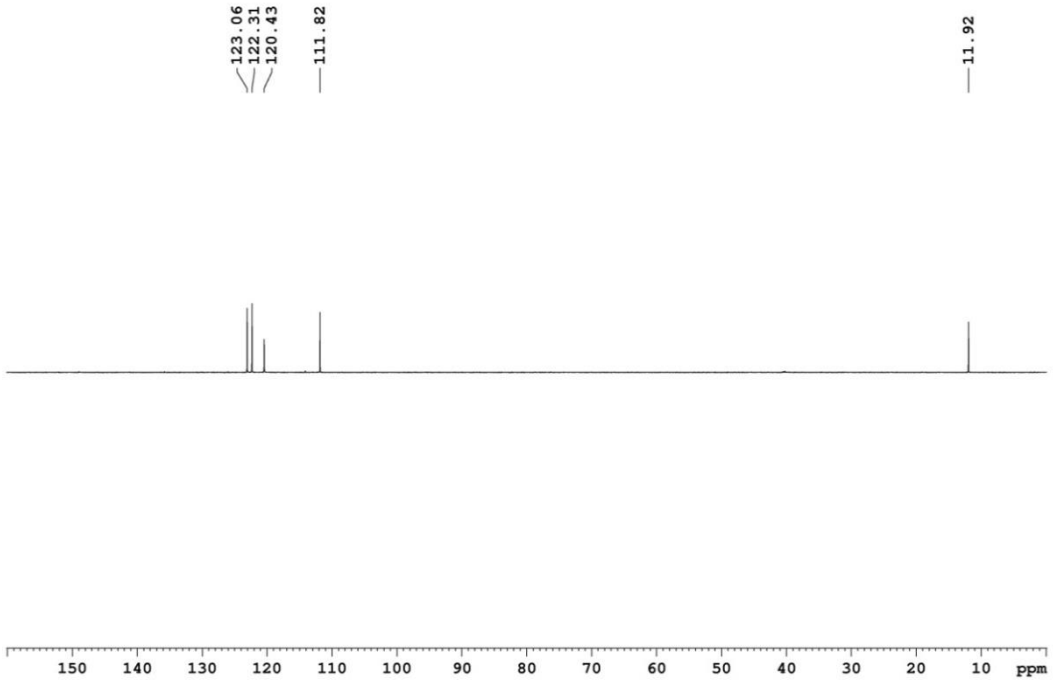

SGT-KM-19-15-TT19 DMSO PMR

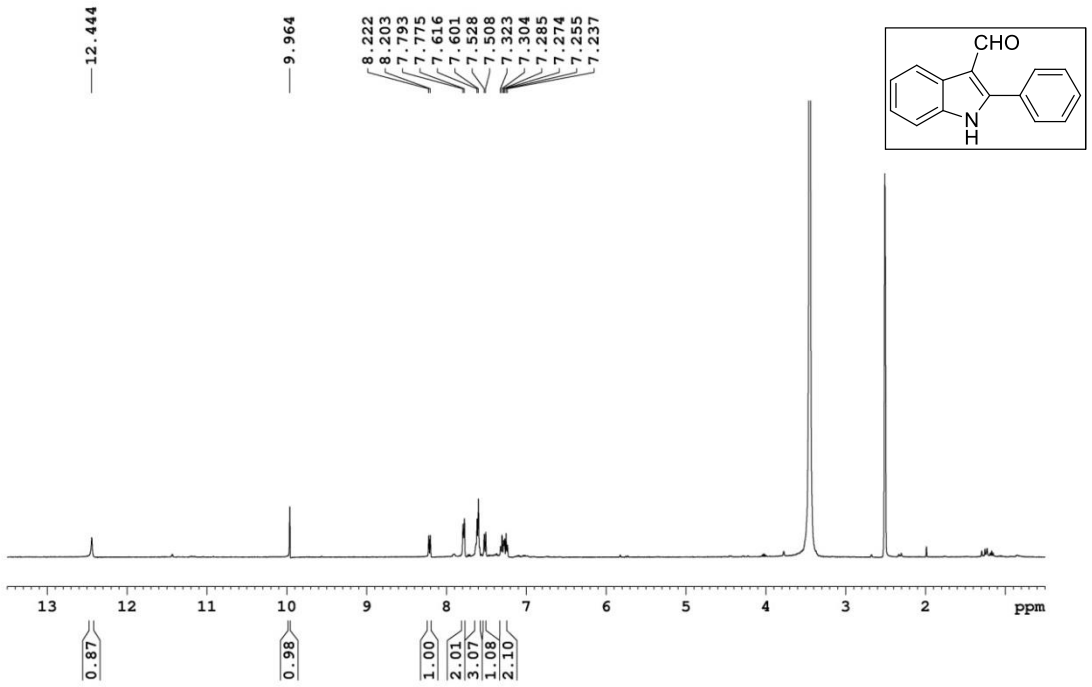

SGT-KM-19-15-TT9-A DMSO CMR

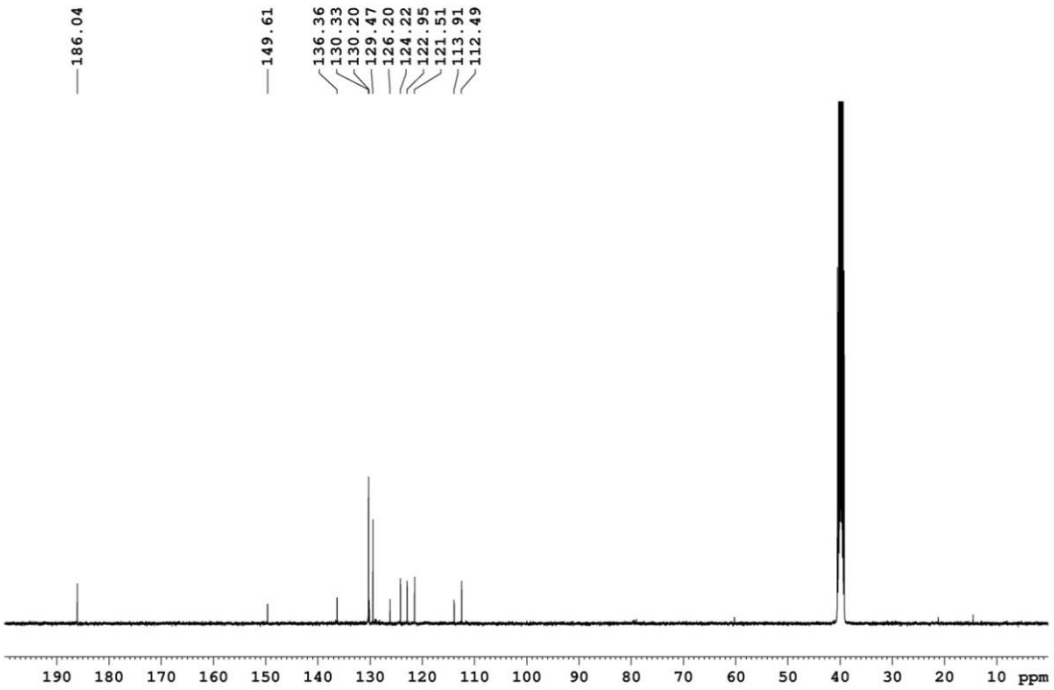

SGT-KM-19-15-TT9 DMSO DEPT

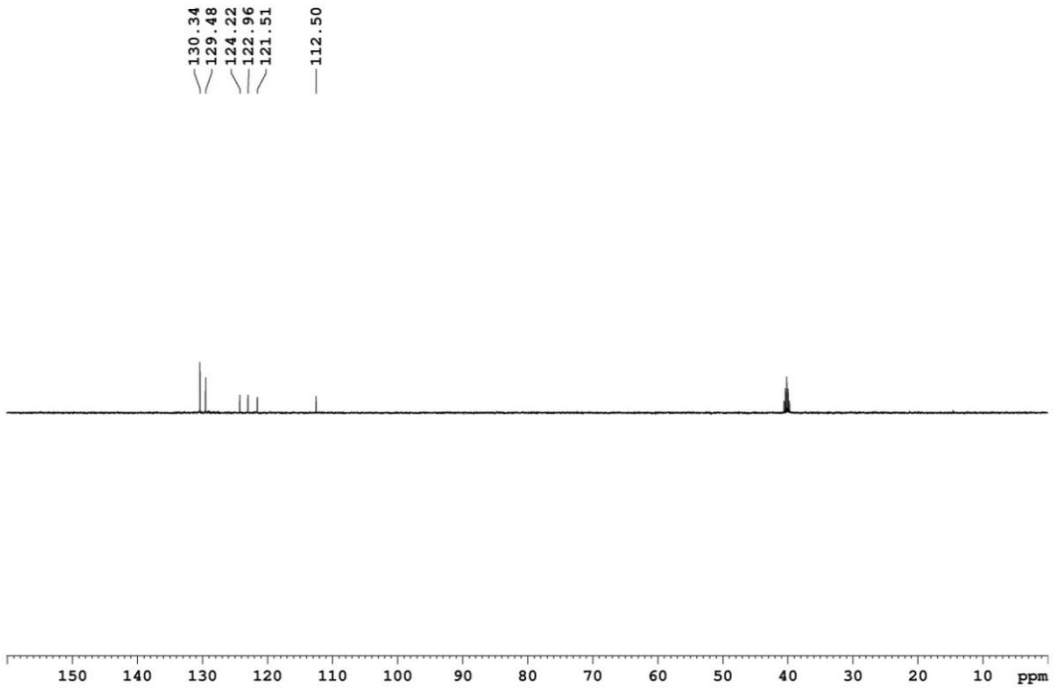

SGT-KM-20-06-10 DMSO PMR

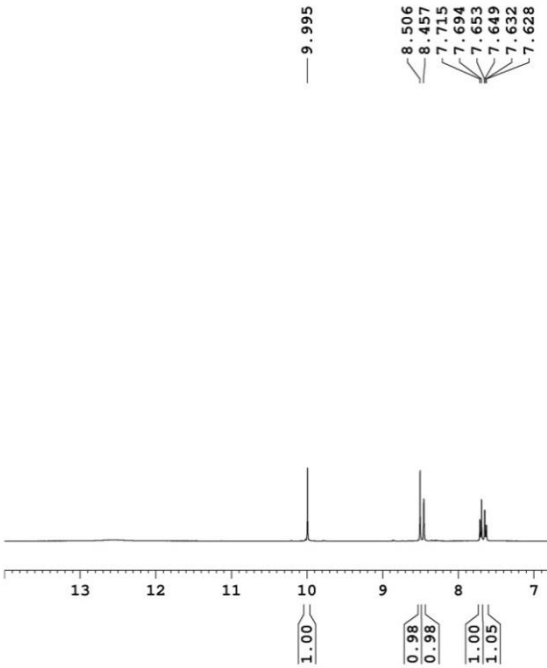

SGT-KM-20-06-10 DMSO CMR

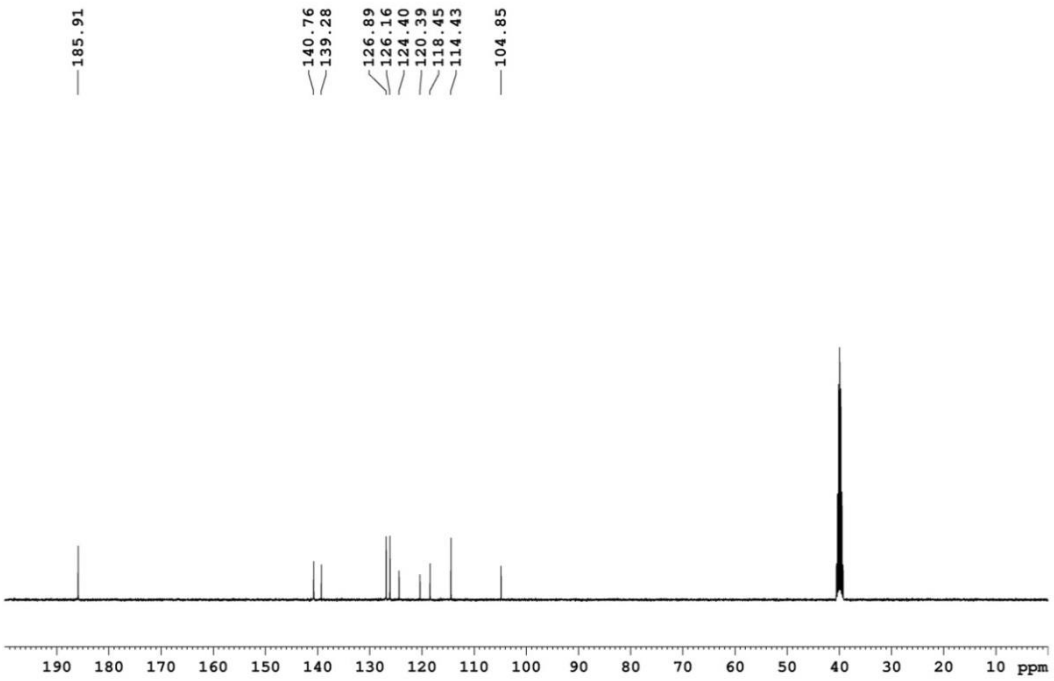

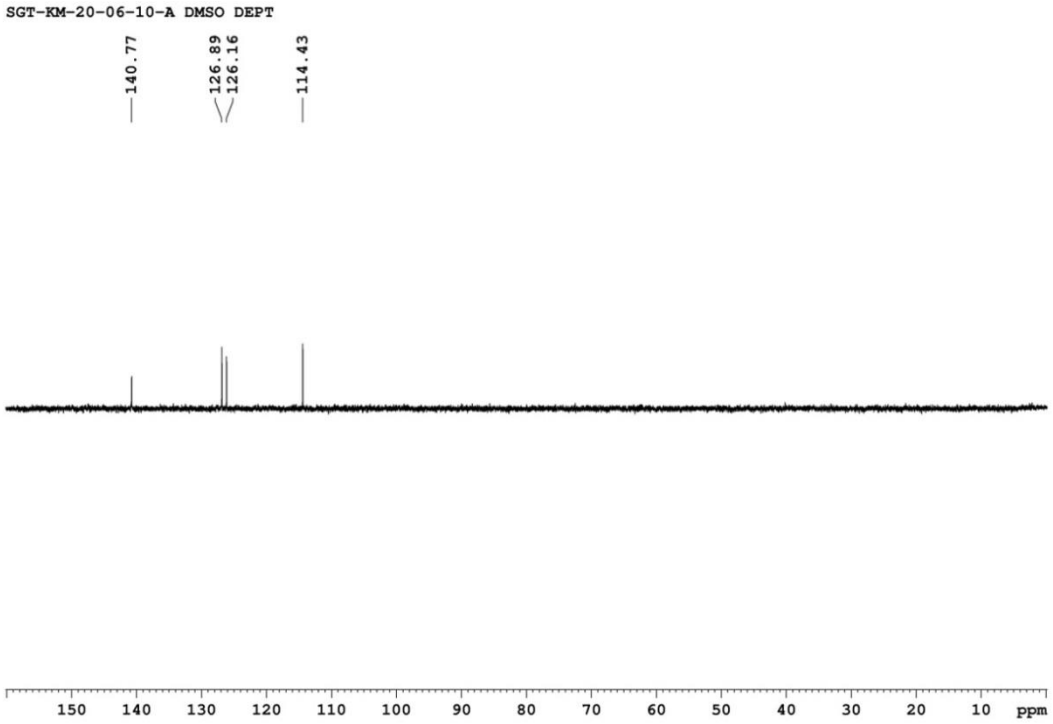
SGT-KM-20-06-10-A DMSO DEPT
140.77
126.89
126.16
114.43
150 140 130 120 110 100 90 80 70 60 50 40 30 20 10 ppm

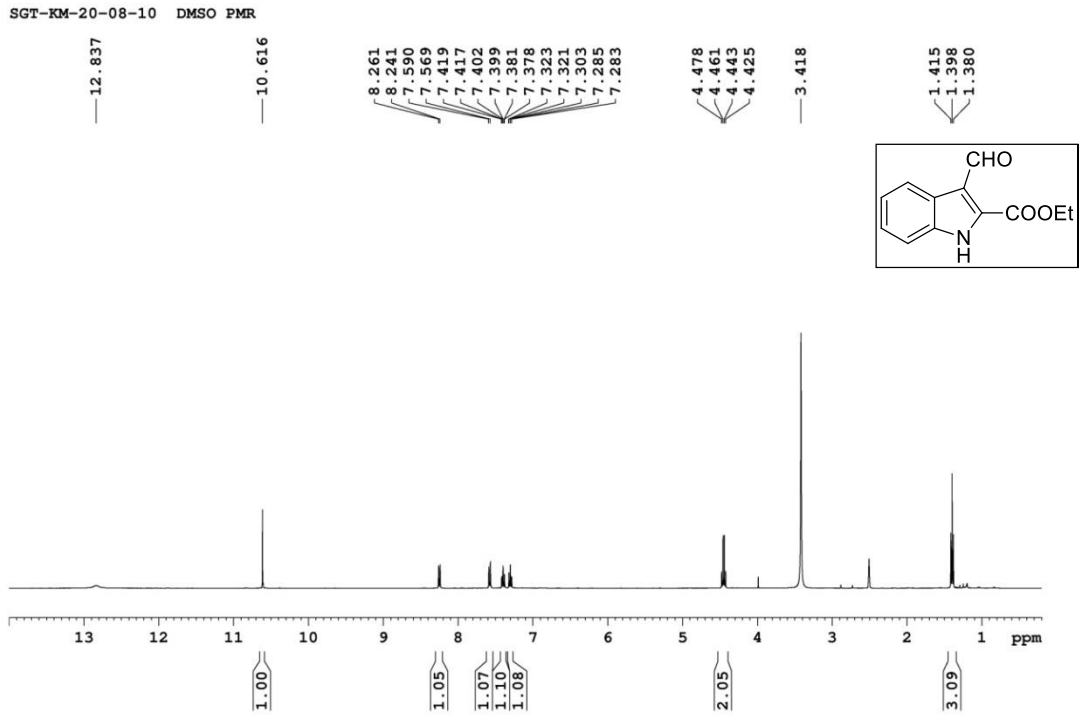
SGT-KM-20-08-10 DMSO PMR
12.837
10.616
8.261
8.241
7.590
7.569
7.419
7.417
7.402
7.399
7.381
7.378
7.323
7.321
7.303
7.285
7.283
4.478
4.461
4.443
4.425
3.418
1.415
1.398
1.380
CHO
COOEt
N
H
13 12 11 10 9 8 7 6 5 4 3 2 1 ppm
1.00
1.05
1.07
1.10
1.08
2.05
3.09

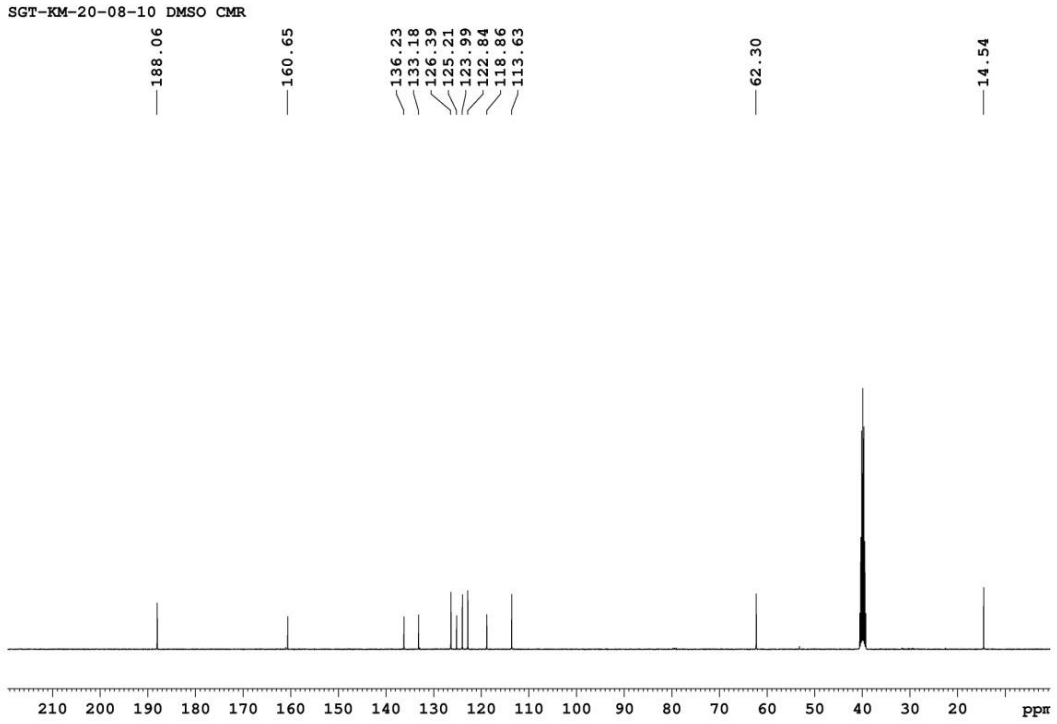
SGT-KM-20-08-10 DMSO CMR
188.06
160.65
136.23
133.18
126.39
125.21
123.99
122.84
118.86
113.63
62.30
14.54
210 200 190 180 170 160 150 140 130 120 110 100 90 80 70 60 50 40 30 20 ppm

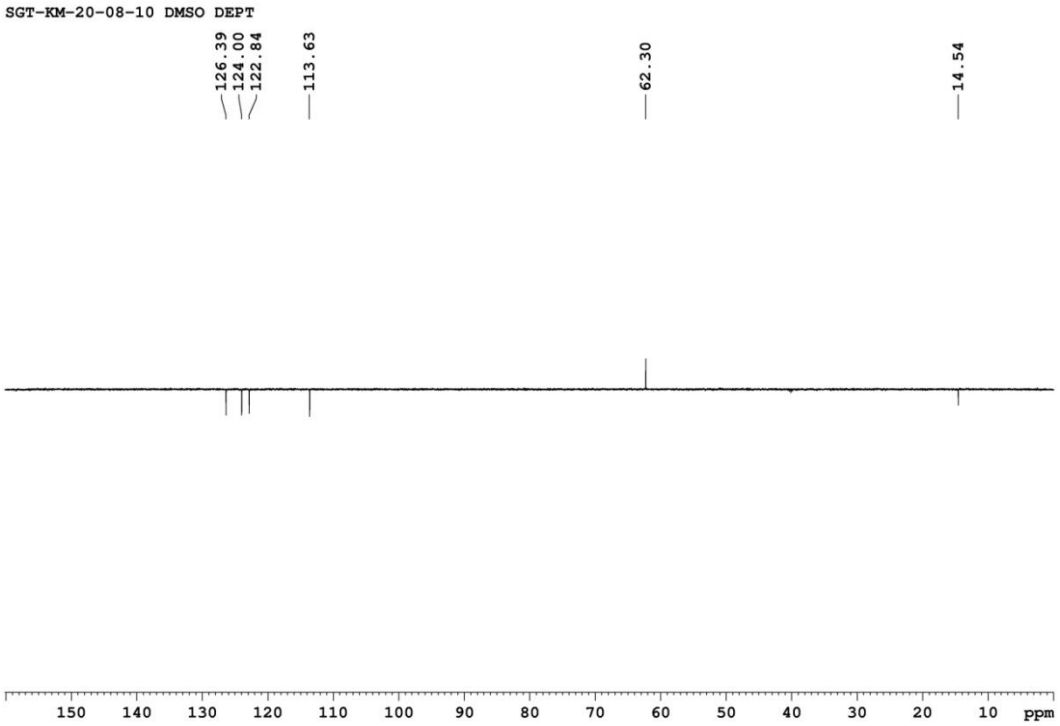
SGT-KM-20-08-10 DMSO DEPT
126.39
124.00
122.84
113.63
62.30
14.54
150 140 130 120 110 100 90 80 70 60 50 40 30 20 10 ppm

SGT-KM-19-62 DMSO PMR

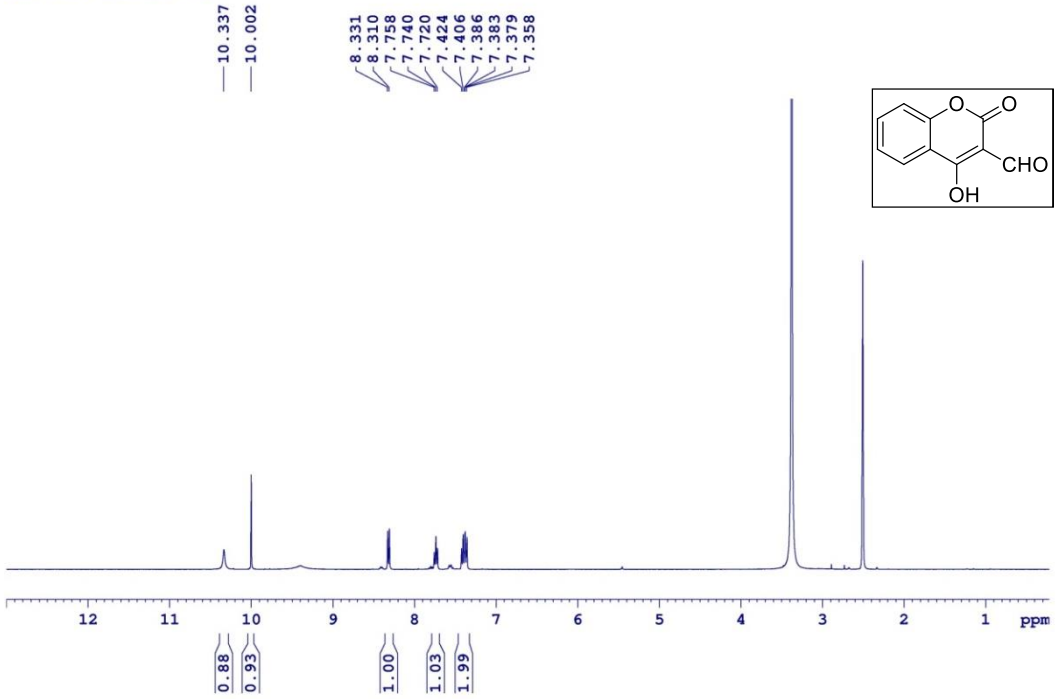

SGT-KM-19-62 DMSO CMR

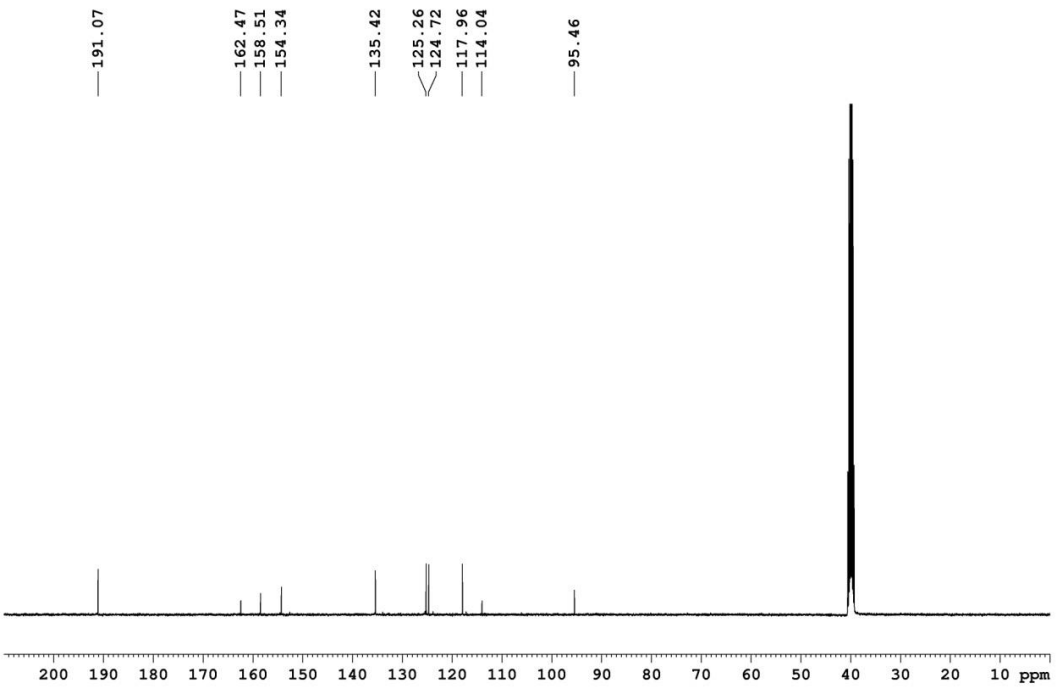

SGT-KM-19-62 DMSO DEPT

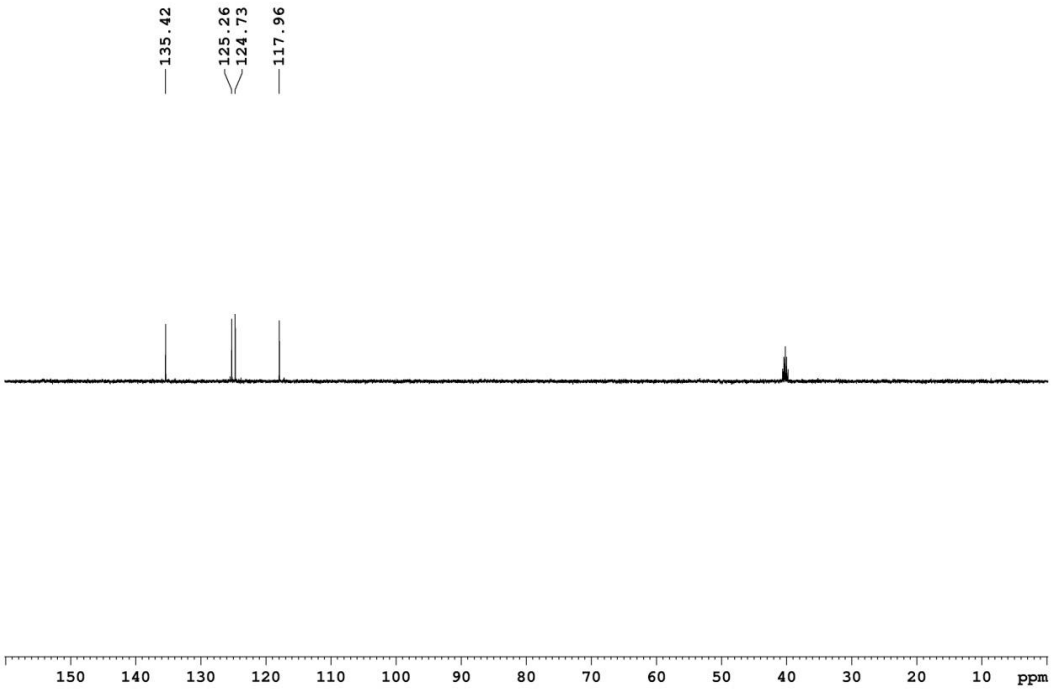

SGT-KM-21-01-11 CDCL3 PMR

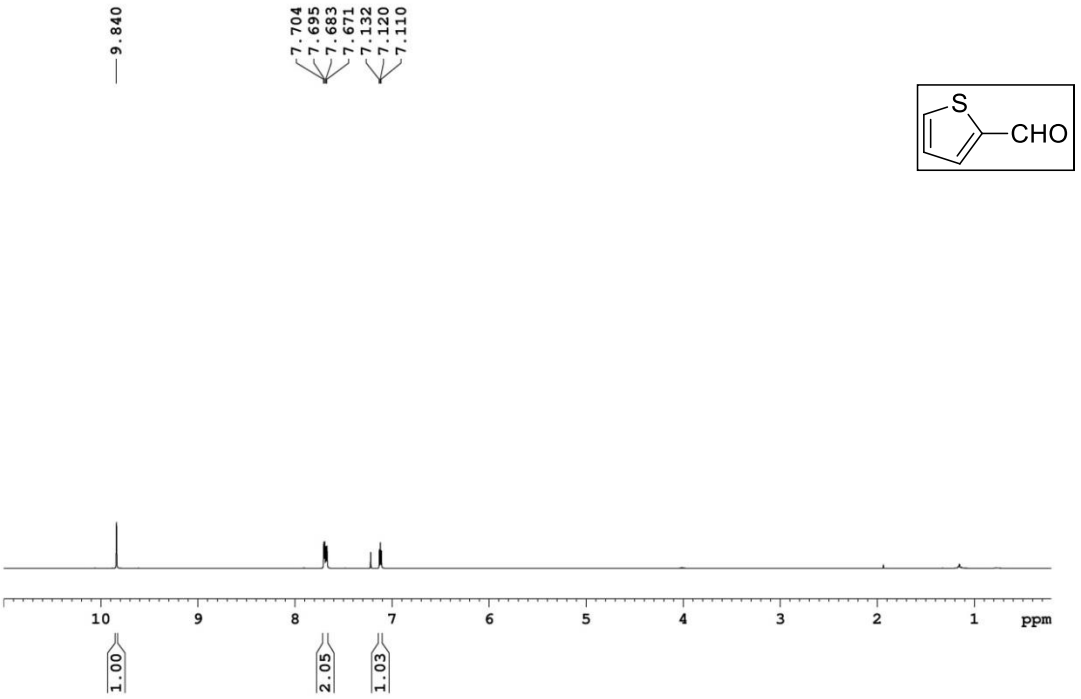

SGT-KM-21-01-11 CDCL3 CMR

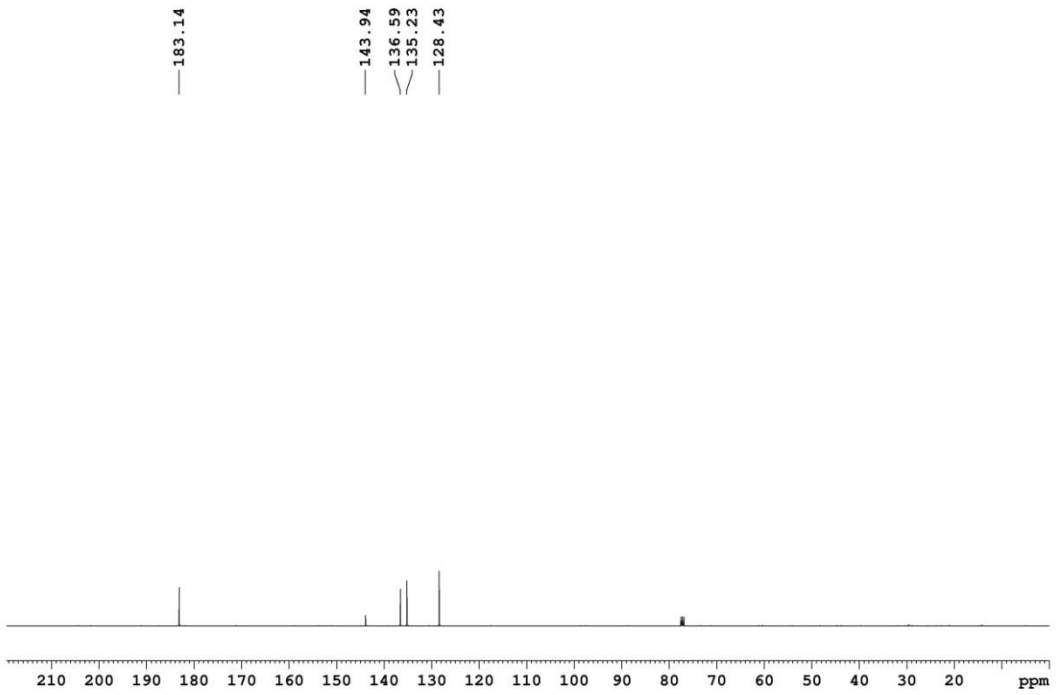

SGT-KM-21-01-11 CDCL3 DEPT

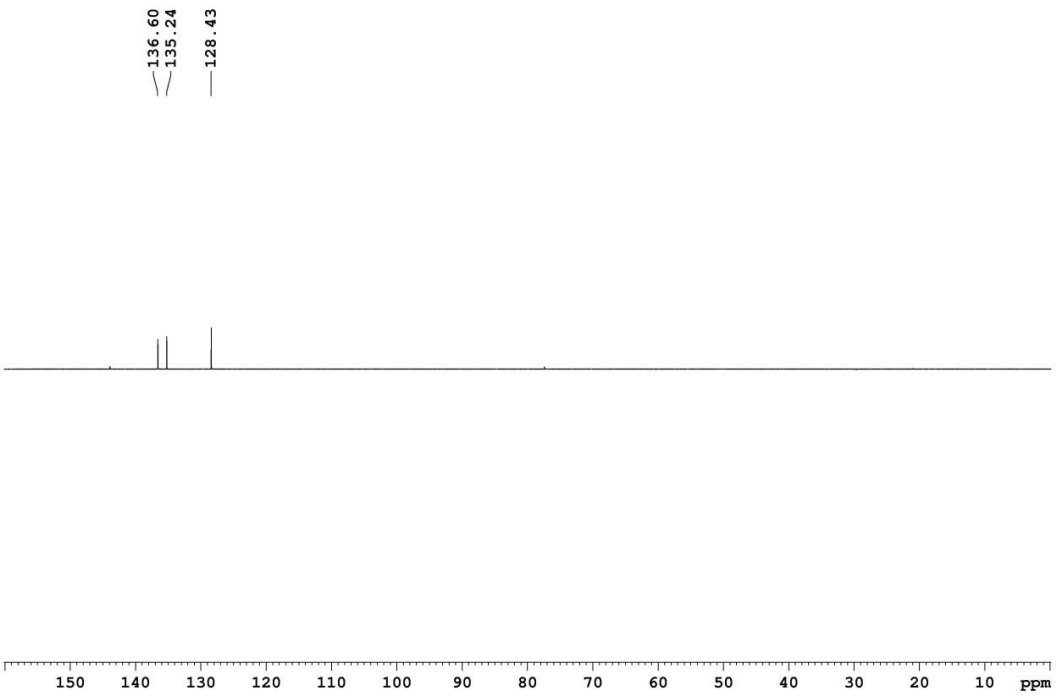

SGT-KM-20-06-12 CDCL3 PMR

13.150
10.756
8.305
8.284
7.974
7.952
7.930
7.795
7.779
7.762
7.621
7.611
7.607
7.604
7.593
7.590
7.586
7.572
7.569
7.442
7.436
7.434
7.418
7.416
7.405
7.398
7.396
7.137
7.122
7.116
7.099

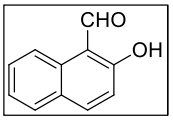

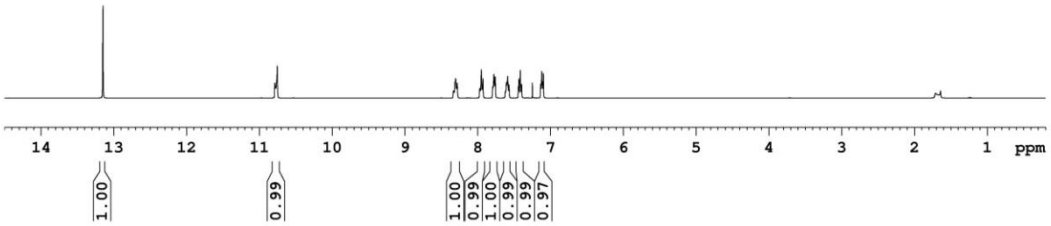

SGT-KM-20-06-12 CDCL3 CMR

193.31
164.93
139.18
132.87
129.50
129.14
127.79
124.53
119.18
118.61
111.27

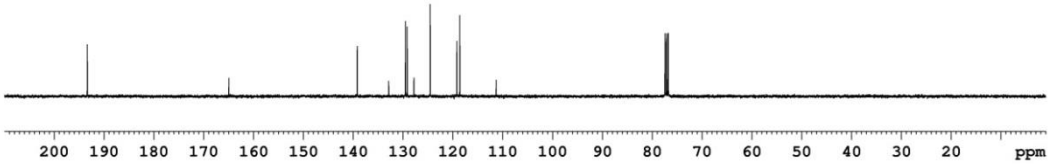

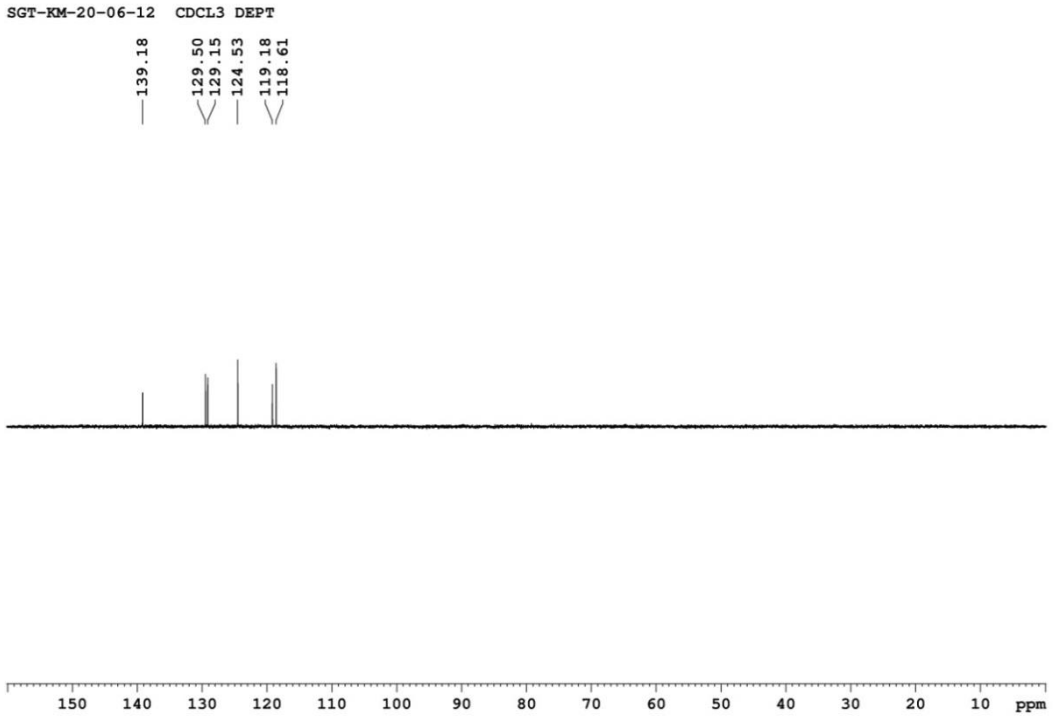
SGT-KM-20-06-12 CDCL3 DEPT
139.18
129.50
129.15
124.53
119.18
118.61
150 140 130 120 110 100 90 80 70 60 50 40 30 20 10 ppm

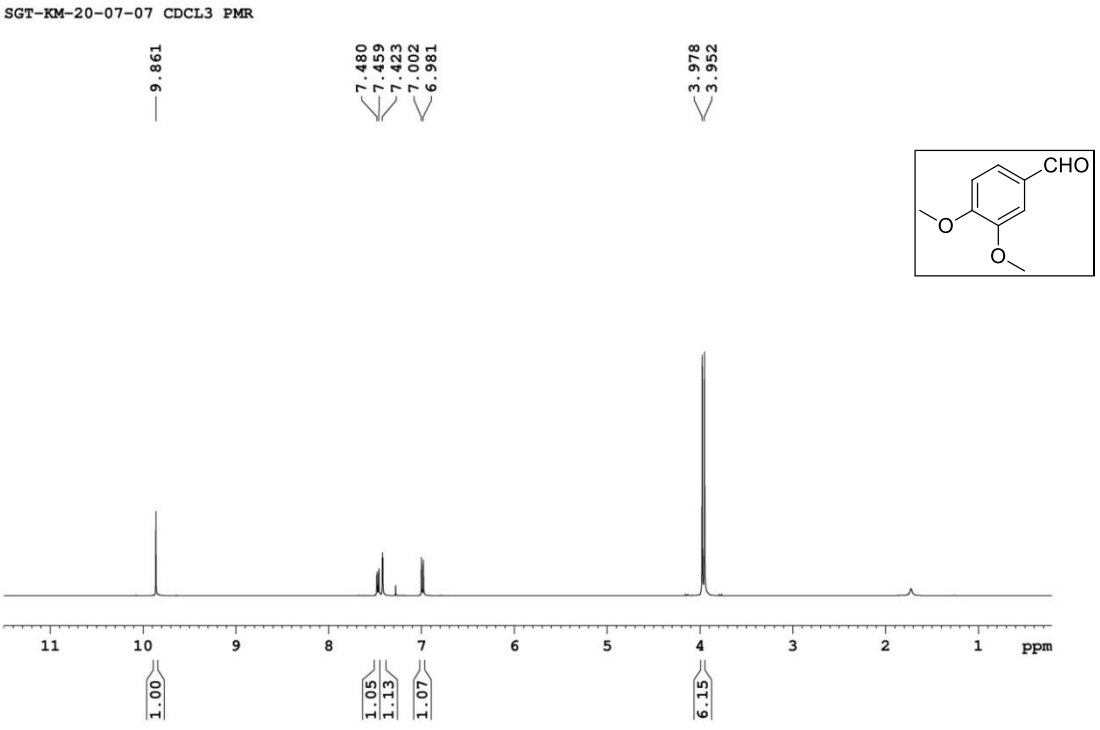
SGT-KM-20-07-07 CDCL3 PMR
9.861
7.480
7.459
7.423
7.002
6.981
3.978
3.952
CHO
O
O
11 10 9 8 7 6 5 4 3 2 1 ppm
1.00
1.05
1.13
1.07
6.15

SGT-KM-20-07-07 CDCL3 CMR

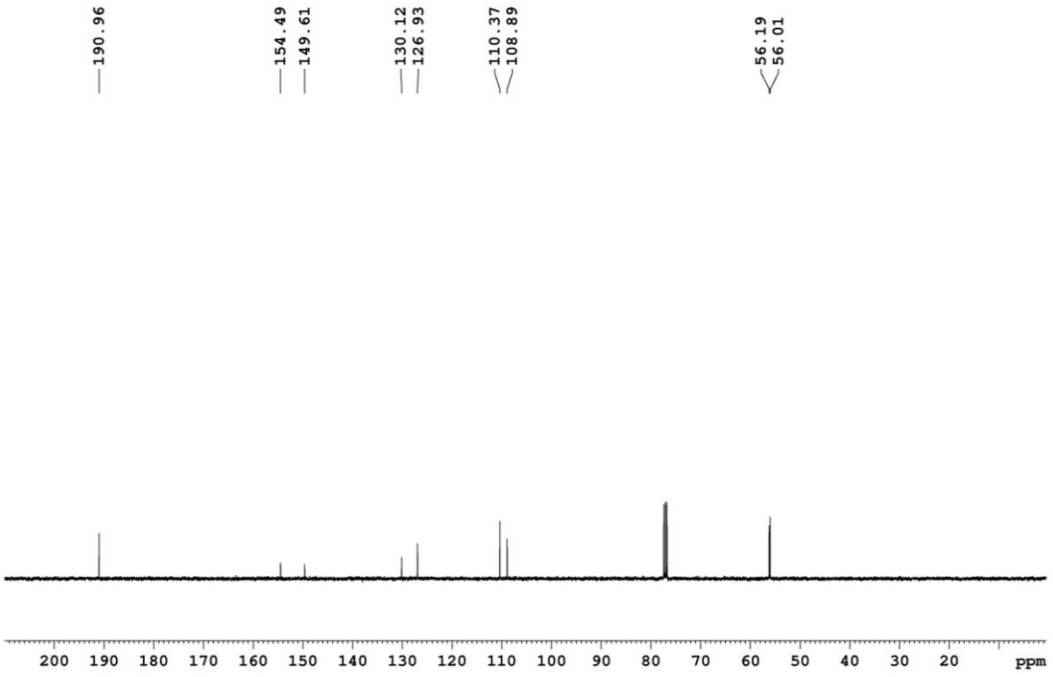

SGT-KM-20-07-07 CDCL3 DEPT

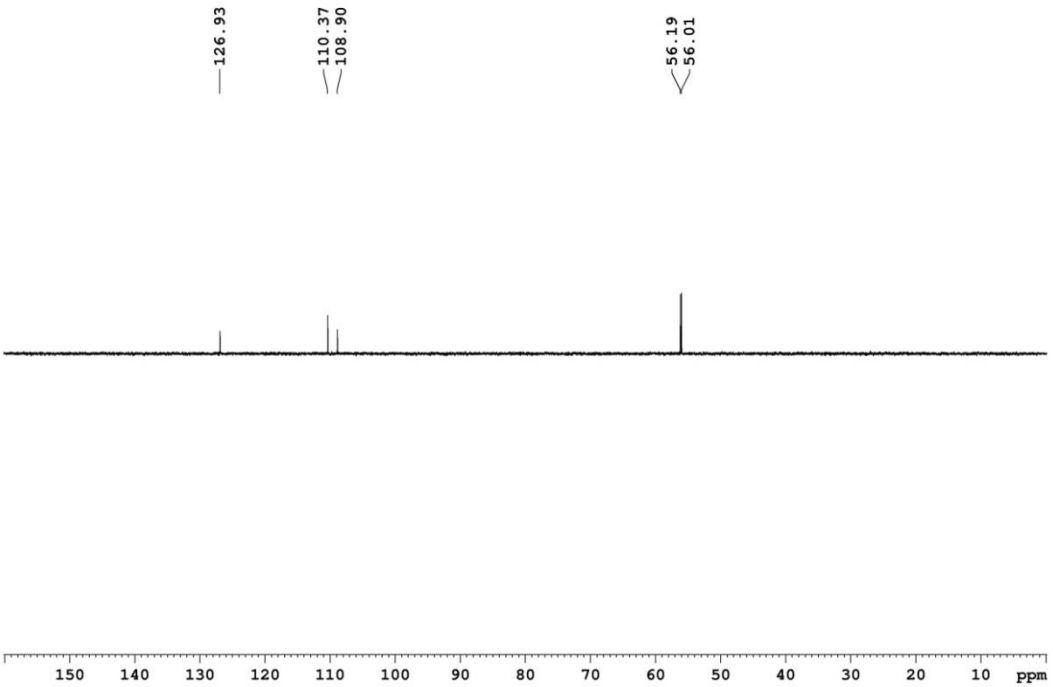

SGT-KM-20-07-06 CDCL3 PMR

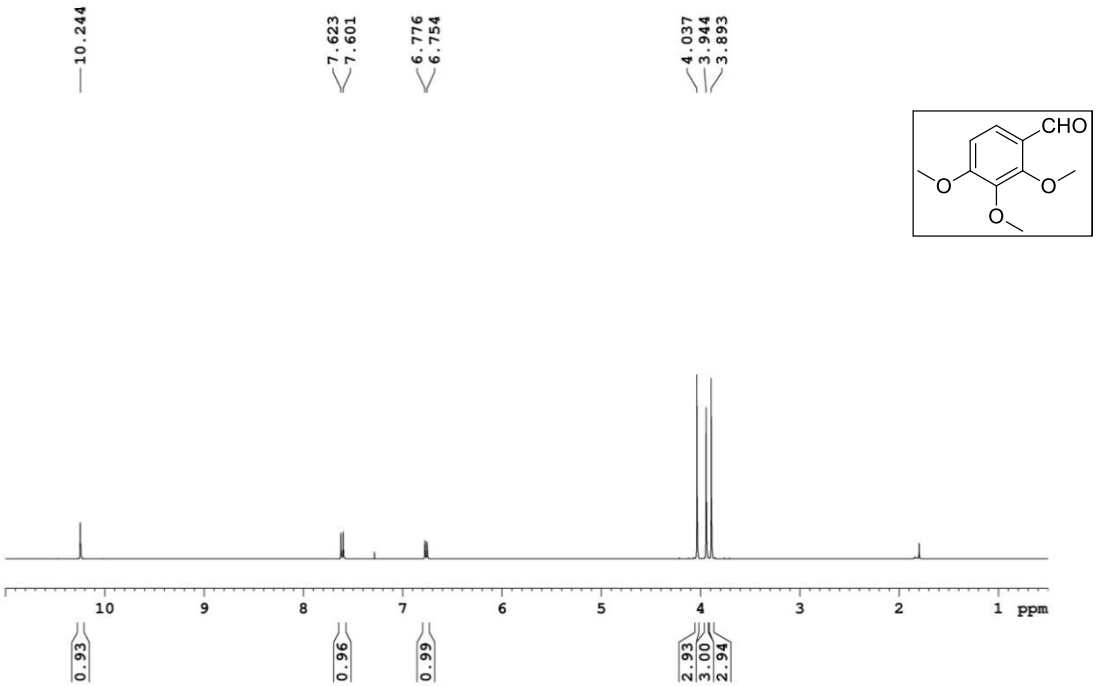

SGT-KM-20-07-06 CDCL3 CMR

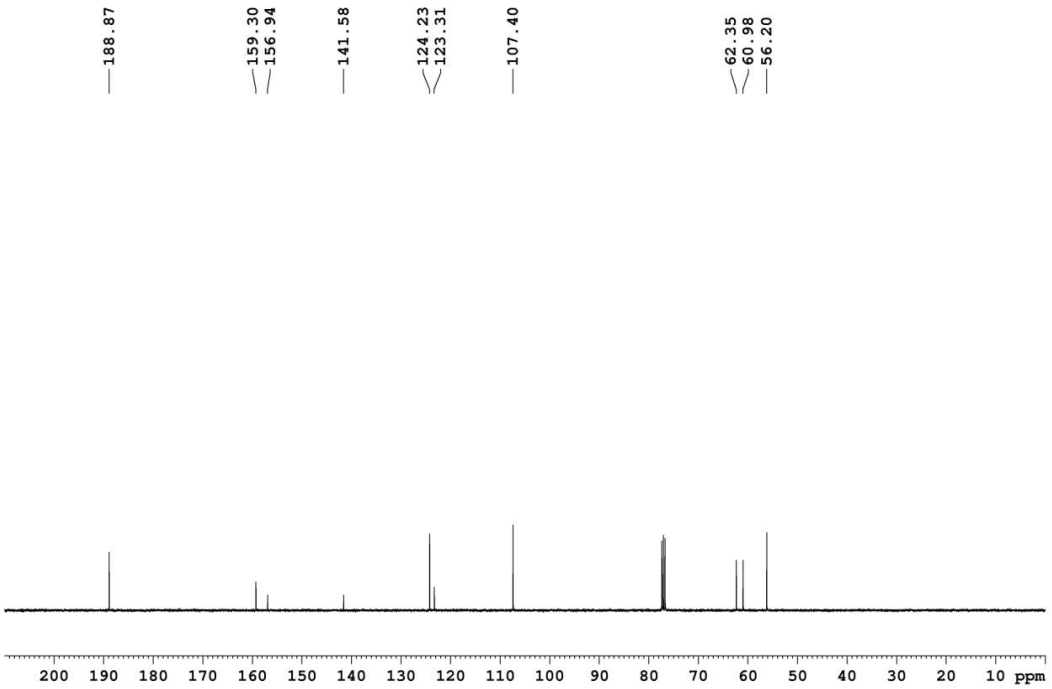

SGT-KM-20-07-06 CDCL3 DEPT

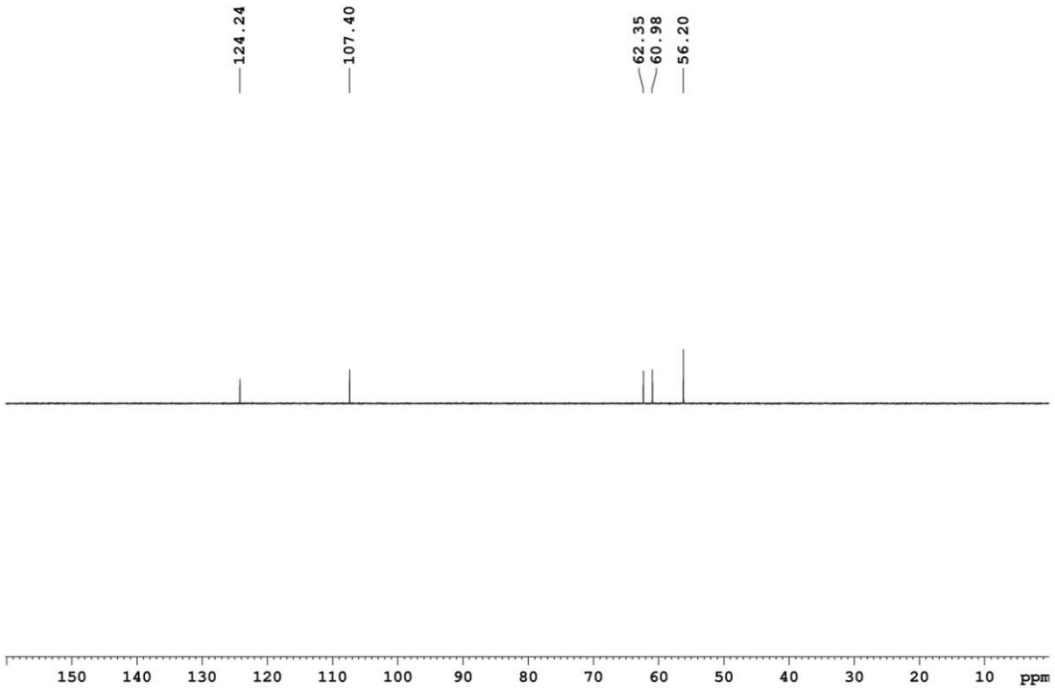

SGT-KM-20-07-03 CDCL3 PMR

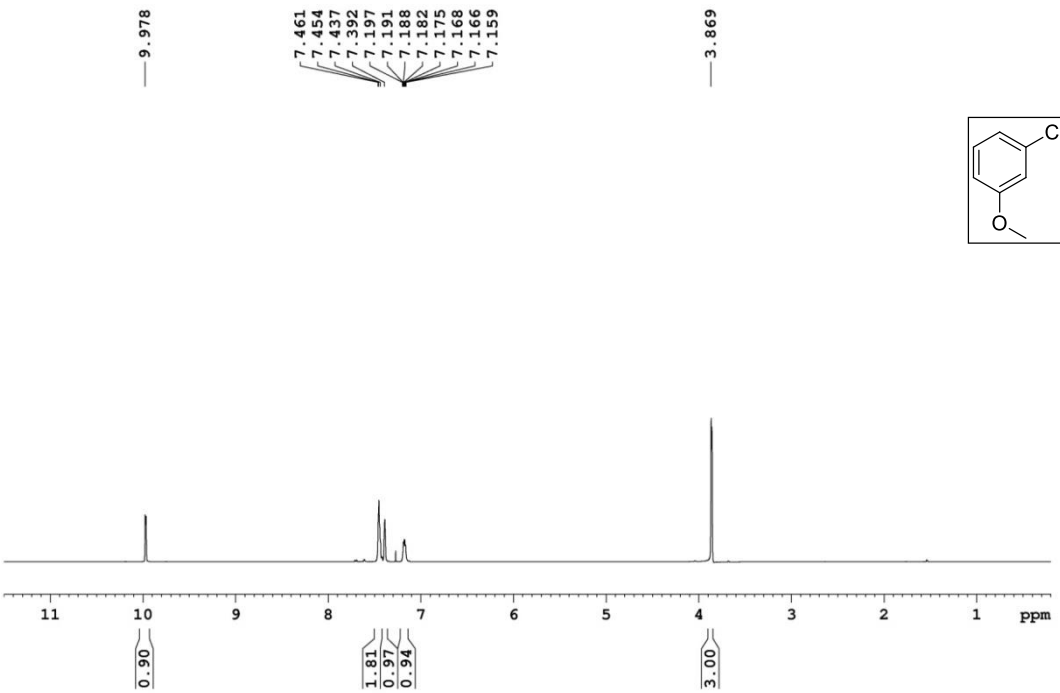

SGT-KM-20-07-03 CDCL3 CMR

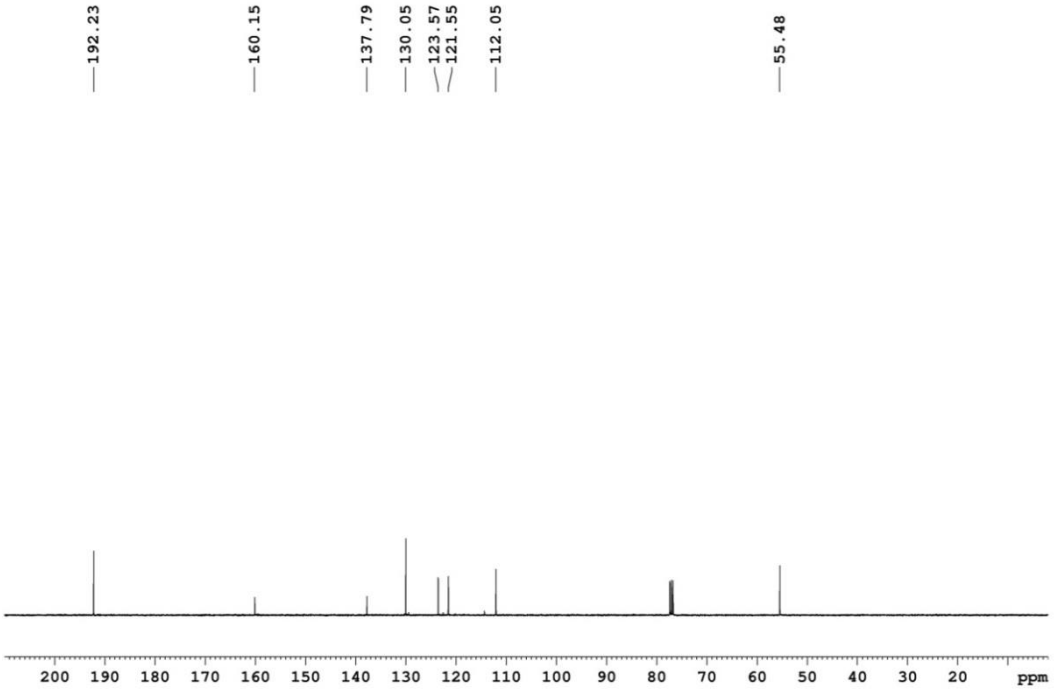

SGT-KM-20-07-03 CDCL3 DEPT

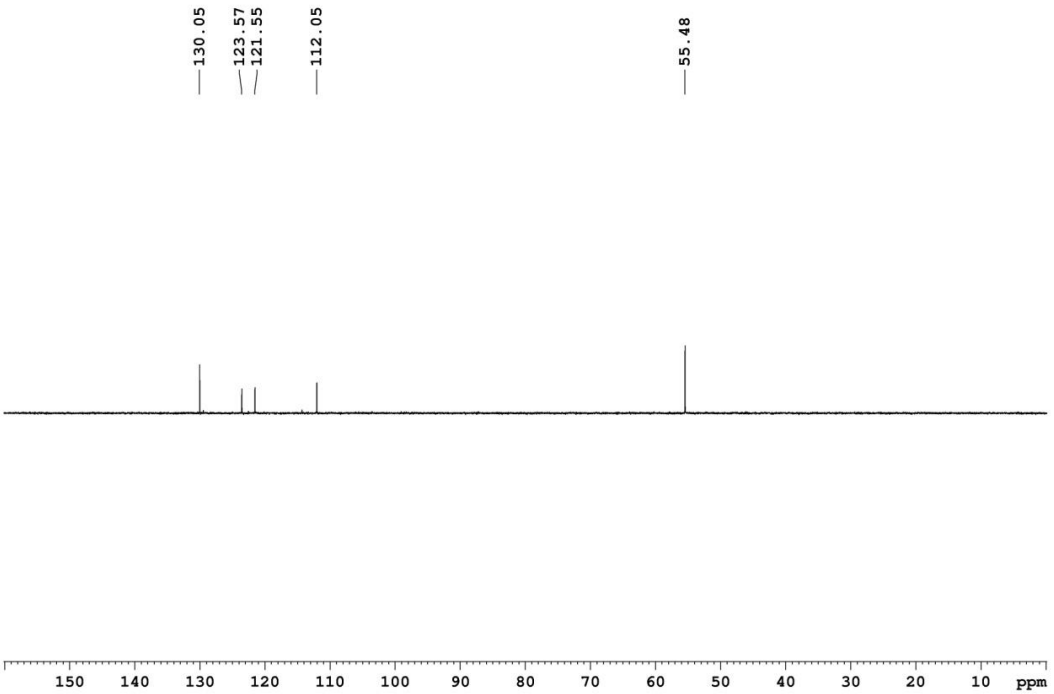

SGT-KM-20-08-31 CDCL3 PMR

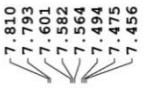

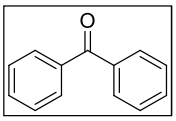

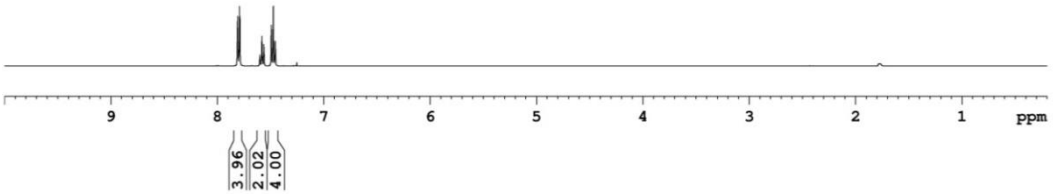

SGT-KM-20-08-31 CDCL3 CMR

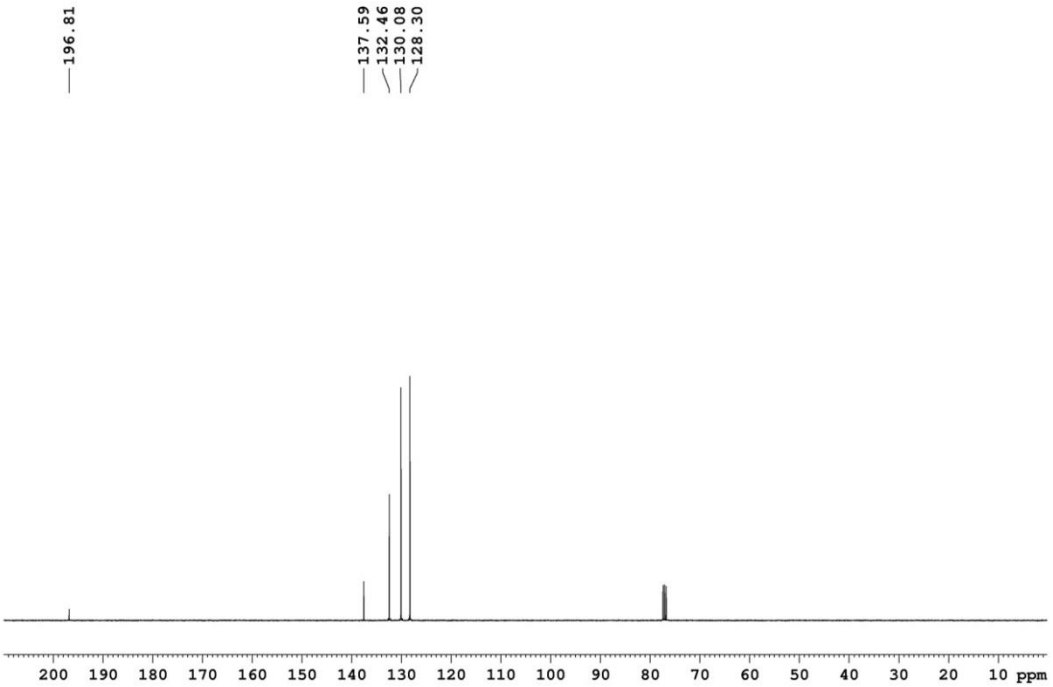

SGT-KM-20-08-31 CDCL3 DEPT

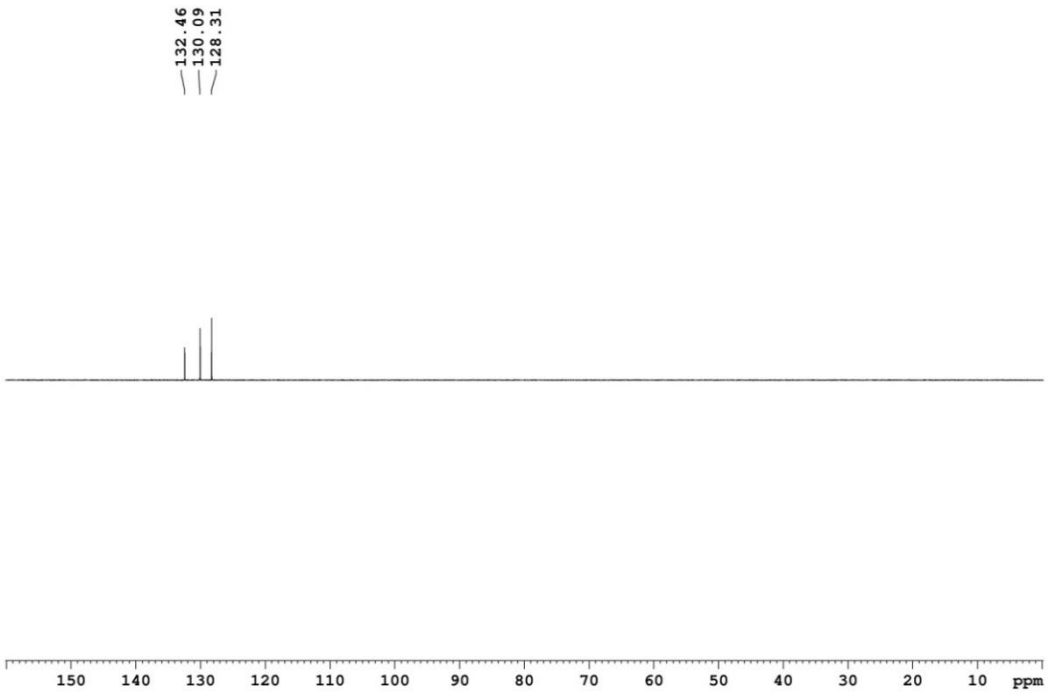

SGT-KM-20-08-32 CDCL3 PMR

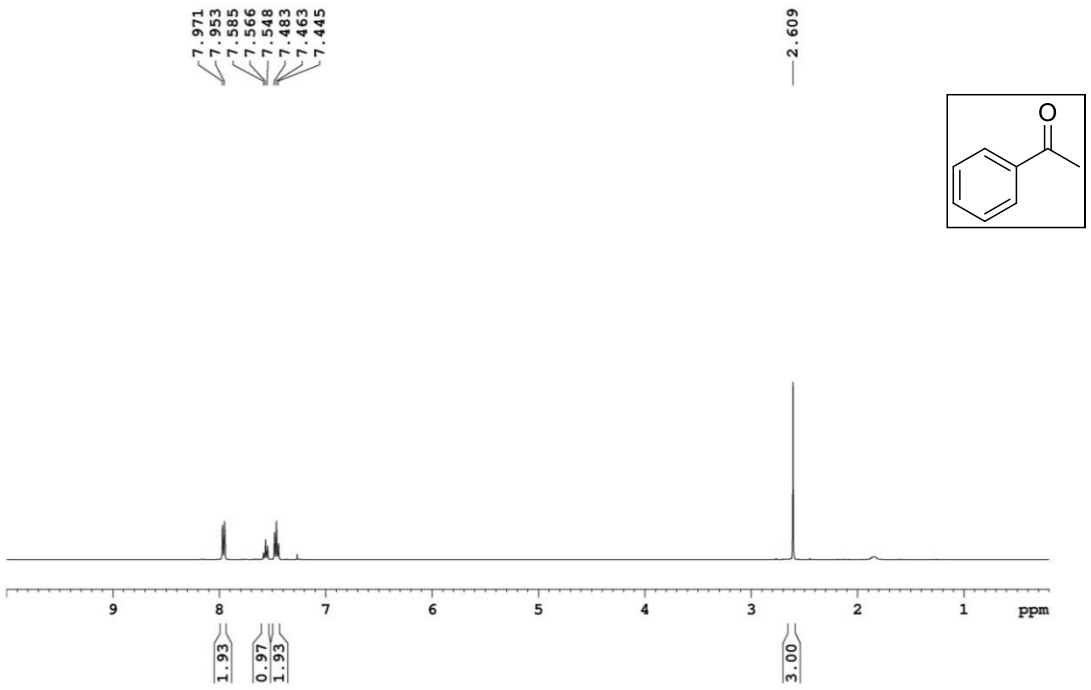

SGT-KM-20-08-32 CDCL3 CMR

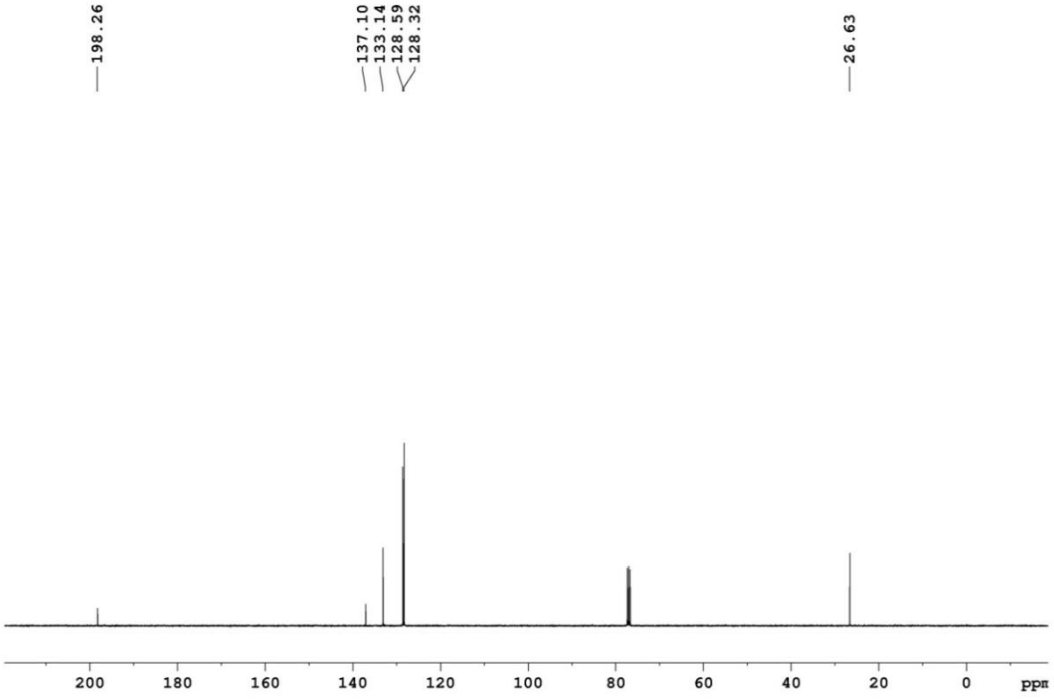

SGT-KM-20-08-32 CDCL3 DEPT

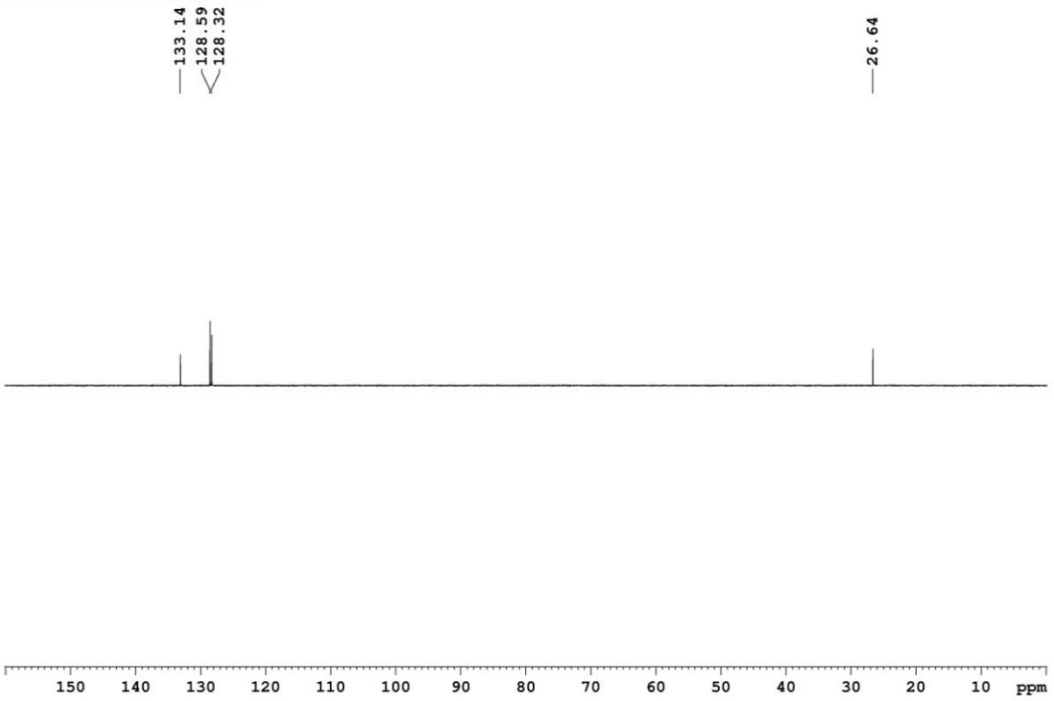

Chapter 4

Intermolecular cross dehydrogenative Csp^3-Csp^3 coupling reactions of *N*-phenyl-THIQ employing ternary oxide nanocomposite of $CuO{\cdot}NiO{\cdot}TiO_2$

4.1 Introduction:

The carbonyl group, the promising electrophilic moiety among the carbon chemical compounds, was the only means of forming the C-C bond in the past years. Inspired from the excellent enolization property of carbonyl compounds with their α-C-H they were made to attack other carbonyl moieties to construct a new bond, and that is where the first aldol condensation reaction came into existence in 1872.[1] This reaction is still developing from the basic concepts and is a valuable tool in forming large molecules.[2] Many scientists have explored this reaction to the further extent that helped other researchers with their proper terminologies. The direct attack on a carbonyl group is also a more excellent way to prepare functionalized C-C bonds. Wherein, Friedel-Craft's reaction tops the list chronologically. Discovered in 1877, this reaction of alkylation and acylation served to form a C-C bond across the benzene ring.[3] Reformatsky first showed the involvement of transition metal in C-C bond formation in 1887 by using zinc dust to facile the reaction between an alkyl halide with a carbonyl compound.[4] The output of the reaction was not that productive, so a noble prize rewarded reaction of C-C bond formation using alkylmagnesiumbromide reagents given by Victor Grignard became more famous with time.[5]

Since it was easy using carbonyl compounds for the simple C-C bond formation, it is suitable only to construct aliphatic compounds and lacks to form cyclization products. That is when in 1928, Diels and Alder gave the world the best method to synthesize six-membered cyclic compounds by just heating two unsaturated moieties (diene and dienophile).[6] Although all the reactions were based on the formation of the C-C single bond, in 1954, the first C-C double bond formation reaction between carbonyl compounds and phosphorane ylides of alkyl halides was published by a German Scientist George Wittig, which went on to achieve Noble prize in 1981.[7] Later in the 21st century, imitation of the same process was performed and studied thoroughly by Yves Chauvin, Robert H. Grubbs, and Richard R. Schrock, which also rewarded them with a Noble prize.[8] This metathesis reaction composites various other reactions, namely, ring-closing metathesis, ring-opening metathesis, cross metathesis, ring-opening metathesis polymerization, etc. Even though it is an excellent method to form a double bond from two different double bonds, it lacks a point on making a double bond across benzene rings. And that novel strategy came in front of the world in 1972, when Richard F. Heck introduced a versatile

kind of reaction wherein simple geminal alkene halide was coupled with aryl halide in the presence of transition metal catalysts to construct any aliphatic or cyclic compounds.[9] This reaction later got its variants developed by other scientists, including different aryl substituents instead of alkyl halide. Suzuki coupling describes the coupling of boronic acid with an aryl halide.[10] Similarly, Hiyama,[11] Kumada,[12] Negishi,[13] Stille[14] worked on organosilicon, organomagnesium, organozinc, and organotin reactants, respectively. Heck, Suzuki and Negishi were awarded the Noble prize in 2010 for their outstanding contribution to the chemistry field. Well, most of the Noble prizes awarded to the C-C bond formation reaction work imply how important those reactions are in the day-to-day life of chemists.

The importance of C-C bond formation of Csp3 or Csp2 is well known, but they are only limited to some functionalized systems that comprise prefunctionalization or defunctionalization steps. So a need for direct C-C bond formation is fulfilled by cross dehydrogenative coupling reactions (CDC) or C-H activation reaction methods. Although it is hard to mention a pioneer for CDC reaction, historically, Carl Andreas Glaser gave copper-mediated oxidative homodimerization of alkynes producing C-C bond by activating two C-H bonds.[15] Later, Eglinton and Hay reproduced the same reaction in their way.[16] Over the past years, scientists have been playing with various reactants and reagents to generate discrete kinds of C-C bonds that lead to Csp^3-Csp^3, Csp^3-Csp^2, Csp^3-Csp, Csp^2-Csp^2, Csp^2-Csp, Csp-Csp bonds which are represented in figure 1.[17]

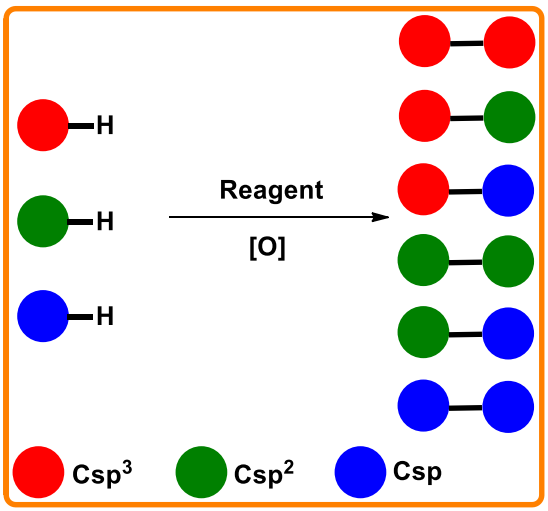

Figure 1. Pictorial representation of various C-C bond coupling

As per the recently published review in Green Chemistry journal, it can be seen that over the past two decades, the amount of work published defines the employment of CDC reactions in the world (Figure 2). This data has been recorded depending upon SciFinder search on CDC reactions.[18]

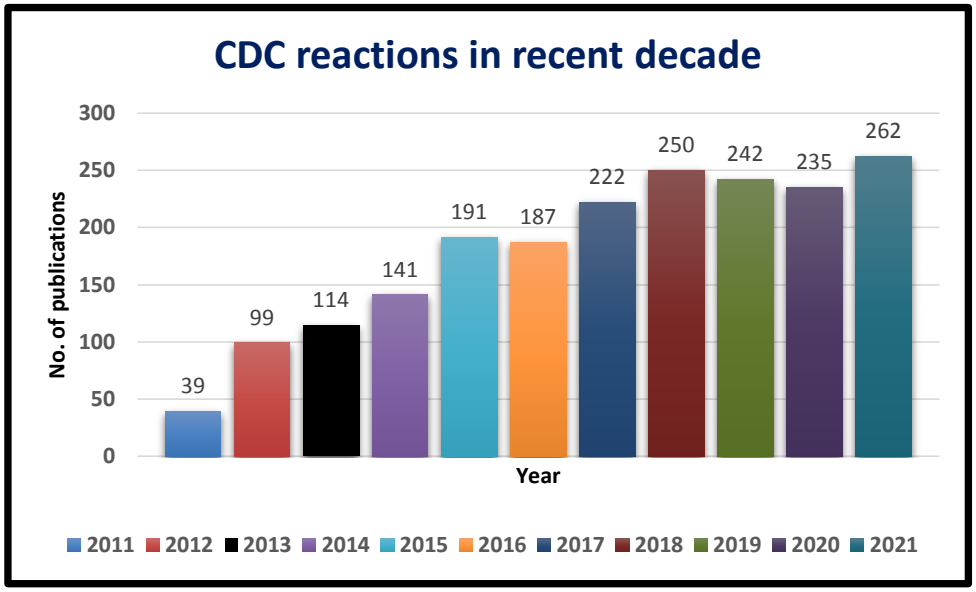

Figure 2. Advancement in CDC reaction over the past decade

The graph mentioned above suggests the vast array of work done in the CDC reaction field. So it is not possible to summarize every reaction in our literature report. Instead, we have focused mainly on CDC reactions between *N*-aryl tetrahydroisoquinoline and various nucleophiles using photocatalysts, transition metal catalysts, and normal organocatalysts or reagents.

4.2 Literature review:

The aza-Henry type reaction is very feasible utilizing cross-dehydrogenative coupling reactions *via* excellent methodologies.[19] Scientists have worked in distinct fields to develop new catalyst systems and screen their applicability in CDC reactions. Over the last two years, more than 80 such methods have been published, which shows the excellent producibility of reagents and catalysts in CDC reactions, and the same is mentioned in the tabular form (Table 1).

The Csp^3-Csp^3, Csp^3-Csp^2, and Csp^3-Csp couplings are prominent in CDC reactions, that has also been applied on *N*-aryl-1,2,3,4-tetrahydroisouinoline type of compounds, having them coupled with various nucleophiles using various sorts of reagents. The table below shows the use of photocatalytic reaction conditions in higher amounts than the other reaction conditions. The use of transition metal catalysts, various supramolecular assisted reagents, photoredox reaction conditions, oxidizing agents, solid-supported catalysts is briefly shown in table 1. Scientists have enormously demonstrated the employment of different nucleophiles, which tend to undergo enolization or resonance in thermal or photochemical reaction conditions.

Table 1. Inter/intramolecular CDC reactions

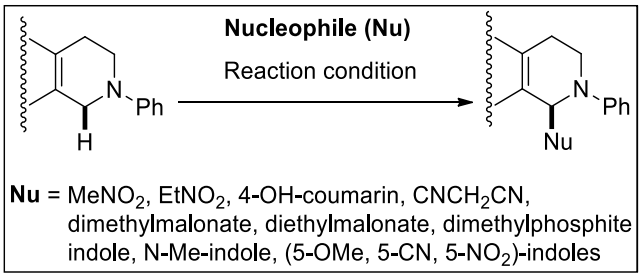

Entry	Reaction conditions	Examples	%Yields	References
1	4 mol% Fe_3O_4-RB/LDH, green LED's, H_2O, rt, 24 h	7 examples	62-89%	Zhang et al. [20]
2	Rose Bengal, green LED's, CH_3CN	22 examples	71-93%	Stubb et al. [21]
3	CsF, CH_3CN, 70 °C, 12 h	24 examples	46-97%	Su et al. [22]
4	i)$Ir(ppy)_2(bpy)PF_6$, O_2, rt, *hv*, CH_2Cl_2 ii)D-α-phenylglycine, 15 °C, toluene	12 examples	37-67%	Rueping et al. [23]
5	CPOP-28, air, white LED	8 examples	80-96%	Han et al. [24]
6	2 mol% $Co(OAc)_2 \cdot 4H_2O$, 20 mol% NHPI, 0.2 M CH_3CN, air, rt	43 examples	0-91%	Kumar et al. [25]
7	10 mol% $Co(OAc)_2$, 30 mol% NHPI, CH_3CN, air, 80 °C	27 examples	Trace-90%	Zhao et al. [26]
8	B-COP, O_2, rt, blue LED	7 examples	70-97%	Wu et al. [27]
9	In_2S_3/MoS_2 composite, O_2, rt, 24 h, green	6	57-77%	Fan et al.

	LED	examples		[28]
10	NHPI, DEAD, CH_2Cl_2, rt, 6 h	15 examples	49-91%	Zhen et al. [29]
11	20 mol% TBPB, EtOAc, 110 °C, under Ar, 12 h	28 examples	30-98%	Zhang et al. [30]
12	1.2 equiv BI-OH, 2 equiv $TMSN_3$, 2 equiv $N_2CHCOOEt$, CH_3CN, rt, N_2 atm., 72 h	27 examples	17-87%	Shi et al. [31]
13	TBHP (70% in water), CH_3CN, Ar atm., 80 °C, 24 h	33 examples	Trace-95%	Zhao et al. [32]
14	2 mol% Cot-RB, green LED, EtOH, rt, 24 h	18 examples	55-96%	Zhang et al. [33]
15	1 mol% $CsPbBr_3$, toluene, white LED, air, rt, 4 h	15 examples	0-96%	Wu et al. [34]
16	1 mol% $Ru(bpy)_3(PF)_6$, 40 mol% *o*-F-BA, DMPU, Ar atm, rt	19 examples	41-97%	Yang et al. [35]
17	1 mol% Sponge nano-Au, TBHP (70% in water), water, 80 °C	27 examples	Trace-98%	Zhang et al. [36]
18	2.6 mol% $Ru(bpy)_3Cl_2$, 25 °C	5 examples	73-93%	Jamison et al. [37]
19	1 mol% $Ir(ppy)_3$, 1 equiv TMSCN, DMA, rt, blue LED, 2 h	10 examples	20-97%	Hamashima et al. [38]
20	DHMIQ-TiO_2, TMSCN, CH_3CN, O_2, *hv* (462 nm)	9 examples	0-97%	Opatz et al. [39]
21	0.5 mol% erythrosine B, 160 mg P25, TFE, 40 °C, blue LED, 14 h	18 examples	44-90%	Cong et al. [40]
22	2 mol% Rose Bengal, toluene, air, blue LED, 24 h	31 examples	74-91%	Hajra et al. [41]
23	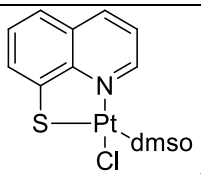 1 mol% , O_2, blue LED, CH_3CN, rt, 8-24 h	11 examples	47-82%	Aleman et al. [42]
24	Cu–TPA, 26 W fluorescent lamp, O_2, 30 h	1 example	79%	Zhao et al. [43]
25	5 mol% AuNP@EDGA, CH_3CN, 80 °C, 24 h	1 example	94%	Xu et al. [44]

26	CoNiFe-LDH, 1,4-dioxane, 80 °C, O_2 atm., 22-36 h	18 examples	36-86%	He et al. [45]
27	0.5% Pt-TzH, 50% TFA, CH_3CN, N_2 atm., blue LED, 24 h	1 example	86%	Massi et al. [46]
28	DA-CMP3, visible light, O_2	21 examples	62-99%	Liu et al. [47]
29	$CuCl_2$, air, $CHCl_3$, 60 °C, 30 min	21 examples	45-70%	Zhang et al. [48]
30	Zr-OF-EY, MeOH, visible light, rt	22 examples	30-96%	Khan et al. [49]
31	Ru@DAFO@ASMNPs, CH_3CN, 10 W lamp, rt, air, 12-30 h	17 examples	69-89%	Sharma et al. [50]
32	30 mol% L-proline, 30 mol% TFA, 1.05 equiv DDQ, CH_3CN, rt	23 examples	44-78%	Bondžić et al. [51]
33	i)1.1 equiv PIFA, DCE, 80 °C, 2 h ii) $R_{alk}MgBr{\cdot}MgCl_2{\cdot}LiCl$, 25 °C, 12 h	24 examples	36-81%	Jiang et al. [52]
34	10 mol% $Cu(OTf)_2$, 30 mol% bpy, 1.2 equiv benzoic peroxyanhydride, MeCN, rt, 18 h	23 examples	10-92%	Manchen˜o et al. [53]
35	 , *n*-Bu_4NBr, CH_2Cl_2, rt	21 examples	27-91%	Xiang et al. [54]
36	 , *n*Bu_4NPF_6, MeCN, 50 °C, 6 h	29 examples	Trace-87%	Lei et al. [55]
37	CPP-PhIm-2F, CH_3NO_2, visible light, air, rt	1 example	85%	Sanchez et al. [56]
38	1 mol% 7-Se, CH_3CN/CH_3NO_2, GE 14 W, 850 lm LED light, rt	4 examples	3-84%	Detty et al. [57]
39	*α*-diazo amide, *N*, *N*-dimethylaniline/1-aryl-1,2,3,4-tetrahydroisoquinoline, PIDA, MeOH,	20 examples	21-95%	Studer et al. [58]
40	$CsPbBr_3$, TFA, blue LED, CH_2Cl_2, N_2	1 example	85%	Yan et al. [59]
41	2 mol% MNPs-eosin Y, green LED, DMSO, air, rt, 12 h	30 examples	71-97%	Wang et al. [60]
42	10 mol% 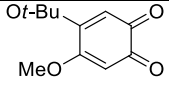 , 60 °C, O_2, 12 h	10 examples	42-90%	Luo et al. [61]
43	TBHP (70% solution in H_2O), Et_3N:H_2O,	26	75-93%	Li et al. [62]

	50 °C	examples		
44	ZJU-56-0.6, 1,4-dioxane, 660 nm LED, O_2, 32 h	6 examples	37-78%	Duan et al. [63]
45	Thiourea, TBHP, TMSCN, MeOH, rt-60 °C, 5-24 h	15 examples	20-86%	Zhang et al. [64]
46	3 mol% NiTPP, 18 W blue LED, air, rt, 12 h	4 examples	82-93%	Sarkar et al. [65]
47	DEAD, CH_2Cl_2, rt, 12 h	22 examples	50-82%	Ding et al. [66]
48	30 W purple LED, O_2, CH_3CN, rt, 24 h	18 examples	0-92%	Lan et al. [67]
49	$TMSCCl_3$, DDQ, KF, CH_3CN, rt, 1 min	25 examples	0-100%	Dong et al. [68]
50	Alkyl-SiF_5K_2, 2.2 equiv $Cu(OTf)_2$, 3 equiv Et_2NH, 10 mol% TBAF, $KHCO_3$, H_2O/CCl_4, N_2, 80 °C	31 examples	35-87%	Wang et al. [69]
51	$(R_{alkyl}COO)_2$, CH_3CN, Ar atms., rt, 24 h	33 examples	0-92%	Wang et al. [70]
52	3.5 mol% $[Rh(cod)Cl_2]$, 10 mol% DPEPhos, 2 mol% $[Ir(ppy)_2(dtbbpy)]PF_6$, 20 mol% $PhMe_2CCOOH$, DCE, 4.8 W blue LED, rt	75 examples	21-96%	Breit et al. [71]
53	2.5 mol% $[Ru(phd)_3](PF_6)$, 5 mol% Co(salophen), MeOH, O_2, 40 °C, 24 h	3 examples	87-99%	Stahl et al. [72]
54	1 mol% DPZ, royal blue LED, air, 25 °C, 24 h	1 example	96%	Bureˇs et al. [73]
55	15 mol% *o*-NQ2, 80 °C, 12 h	42 examples	Trace-88%	Oh et al. [74]
56	1% $[Ru(bpy)_3](PF)_6$, 50% TFA, CH_3CN, N_2, blue LED, 24 °C, 8 h	1 example	95%	Bissember et al. [75]
57	i) 2 mol% $Ru(Phen)_3Cl_2$, 4 equiv CCl_4, blue LED, CH_3CN, rt ii) 2 equiv NEt_3, 50 °C	23 examples	55-92%	Li et al. [76]
58	s-CD, 34 W blue LED, 25 °C, O_2, 5-8 h	6 examples	74-87%	Sarma et al. [77]
59	2 mol% $[Ir(dtbbpy)(ppy)_2]PF_6$, DMA:H_2O, blue LED,	28 examples	21-91%	Lou et al. [78]

60	*N*-ethoxy-2-methylpyridinium tetrafluoroborate, $NaHCO_3$, blue LED, DMF, 40 °C	12 examples	71-91%	Lakhdar et al. [79]
61	Hypericum vesiculosum, blue LED, DIPEA, DMSO, N_2, 25 °C	11 examples	30-90%	Weigand et al. [80]
62	10 wt% ZIF-9, hυ, 40 °C, 6 h	6 examples	39-92%	Raja et al. [81]
63	 , 10 mol% $Cu(OTf)_2$, 13 mol% **L**, 20 mol% TEMPO, *n*-Bu_4NPF_6, CF_3COOH, I= 1.5 mA, CH_3CN, rt, 12 h **L** = 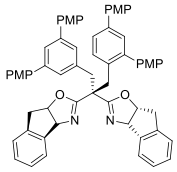	43 examples	Treace-98%	Mei et al. [82]
64	CuMgAl-LDH, O_2, 17-72 h	14 examples	40-85%	Chen et al. [83]
65	Ni_3Ga-LDO, 1,4-dioxane, 80 ℃, O_2, 16-48 h	19 examples	23-88%	He et al. [84]
66	Benzoyl cyanide, Li_2CO_3, CH_3CN, purple LED, rt, 24 h	37 examples	30-99%	Wang et al. [85]
67	10 mol% $B(C_6H_5)_3$, 405 nm LED, CH_3CN, rt, 36 h	10 examples	0-90%	Ooi et al. [86]
68	10 mol% $CuCl_2 \cdot 2H_2O$, O_2 (balloon), acetone, rt, 13 h - 16 days	4 examples	4-94%	Klussmann et al. [87]
69	In situ 1.5 mol% [Cu(dmphen)(P^P)](PF_6), O_2, hυ, CH_3NO_2, rt, 16 h	1 example	94%	Kamer et al. [88]
70	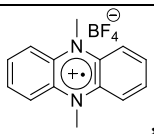 , CH_3NO_2, O_2, 90 °C, 15 h	4 examples	4-75%	Mejía et al. [89]
71	Cs_2CO_3, DMF, 3 W LED, rt, 15 h	20 examples	32-86%	Zhang et al. [90]
72	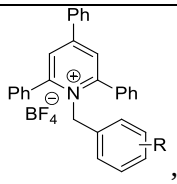 , 2-3 mol% $[Ru(bpy)_3]Cl_2$, DMA/ACN, blue LED, 6 h, rt	11 examples	25-64%	Schnürch et al. [91]

73	2 mol% $[Ir(dF(CF_3)ppy)_2(dtbbpy)(PF_6)]$, Na_2CO_3, acetone, 450 nm, 24 °C, 24 h	6 examples	66-80%	Ready et al. [92]
74	PCN-808-BDBR, CH_3NO_2, visible light	3 examples	94-100%	Zhou et al. [93]
75	OH-TFP−TTA, 460 nm LED, MeOH, 25 °C	7 examples	59-91%	Yang et al. [94]
76	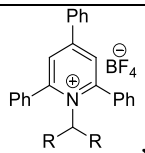 , K_2CO_3, CH_2Cl_2, purple LED, Ar, rt, 24 h	24 examples	0-83%	Zhang et al. [95]
77	Malanonitrile, TBHP, Ni_3Ga-LDO, MeOH, 80 °C, 24 h	24 examples	0-88%	Chen et al. [96]
78	20 mol% TBA, 20 mol% K_3PO_4, blue LED, DMF, rt, 12 h	33 examples	42-98%	Hamashima et al. [97]
79	$RB(OH)_2$, TFA, O_2, DCE, 100 °C, 10 min	17 examples	38-86%	Liu et al. [98]
80	5 equiv **Nu**, 6 W blue LED, O_2 (balloon), DMF, rt	5 examples	54-75%	Wang et al. [99]
81	Cs_2CO_3, DMA, 427 nm LED, rt, 40 h	38 examples	11-97%	Jin et al. [100]

4.3 Results and discussion:

Although various reagents have been employed to perform CDC reactions on *N*-aryl-1,2,3,4-tetrahydroisoquinoline compounds, we envisaged exploring our own catalyst $CuO{\cdot}NiO{\cdot}TiO_2$ in this field. The catalyst preparation and characterization are published along with a few application reactions in organic chemistry.[101] Among them, one application depicts the α-oxidation of *N*-phenyl-1,2,3,4-tetrahydroisoquinoline using 5 mol% of 5% of Cu-Ni in $CuO{\cdot}NiO{\cdot}TiO_2$ catalyst (Scheme 1). That work indicated the imine formation of *N*-phenyl-1,2,3,4-tetrahydroisoquinoline moiety with our catalyst in an open-air, further with the attack of oxygen at C1 position lead to the formation of 2-phenyl-3,4-dihydroisoquinolin-1(2*H*)-one. We further explored the applicability of our said catalyst in CDC reactions with this knowledge.

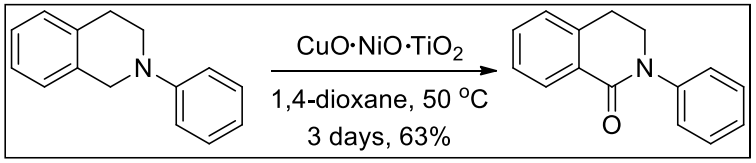

Scheme 1. Synthesis of 2-phenyl-3,4-dihydroisoquinolin-1(2*H*)-one using 5% CuO·NiO·TiO$_2$

Various reported methods are available to synthesize *N*-phenyl-1,2,3,4-tetrahydroisoquinoline, so we picked one simple, high yielding, time-reliable reported reaction and synthesized **3a** from **1a** and **2** using KTBT, TBAF in dry DMSO (Scheme 2).

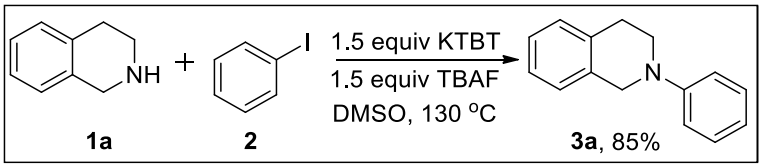

Scheme 2. Synthesis of *N*-phenyl-1,2,3,4-tetrahydroisoquinoline

Many researchers have stressed the CDC reaction between *N*-aryl-1,2,3,4-tetrahydroisoquinoline with nitromethane by employing their reagents. To know whether there is any synergistic effect of the metal oxides (CuO & NiO) in our system we also tested individual metal oxides on TiO_2 in various solvents and differentiating temperature levels.

We have performed comparative studies of three catalysts in the same environment of the sealed tube at a constant 100 °C temperature. A stoichiometric amount of **3a** and **4a** was heated in different polar and non-polar solvents to see the formation of **5a** over **6a** in the large amount. The reported oxidation reaction was carried out in a 1,4-dioxane solvent, so commencing with the same solvent, we heated **3a** with **4a** in an air-tight sealed tube at 100 °C under an oxygen atmosphere (Table 2, entry 1). After around 36 hours of constant heating, the disappearance of starting **3a** was observed on TLC, which upon normal workup of dilution with CH_2Cl_2 and filtration, we could isolate two analytically pure spots indicating them as compounds **5a** and **6a**. As for the 5% CuO·TiO_2 catalyst, compound **5a** was formed in 35% yield, which was also seen the same for the 5% CuO·NiO·TiO_2 catalyst. It was observed that the use of 5% NiO·TiO_2 catalyst gave a trace amount of **5a**. Even, we checked the productivity of our reaction by increasing the temperature up to 150 °C, but it only helped in the generation of **6a** more than **5a**. So relying on the exact

temperature of 100 °C, we later studied the reaction in a polar aprotic solvent like acetonitrile and saw that it also supports the formation of **6a** substantially than **5a** (Table 2, entry 2). Polar solvents like methanol and isopropanol were also compared to the polar aprotic solvents and found that they are much worse to support the formation of **5a** (Table 2, entry 3, 4). That could be due to the solvation factor of atmospheric oxygen in polar solvent causing more of the amidation reaction than the CDC reaction. Above boiling water temperature, non-polar solvents like toluene and xylene were studied for CDC reaction, which failed to help form **5a** and only supported the amidation reaction to some extent (Table 2, entry 5, 6).

The quick interaction of **3a** with catalyst and attack of **4a** must be hampered in the solvent, so directly, increasing the amount of nitromethane **4a** by five-fold excess, we could synthesize **5a** in more than **6a** using 5% $CuO{\cdot}NiO{\cdot}TiO_2$ catalyst at the same temperature and time interval (Table 2, entry7). But, 5% $CuO{\cdot}TiO_2$ and 5% $NiO{\cdot}TiO_2$ didn't give much of compound **5a**.

Table 2. Optimization of catalysts and solvents

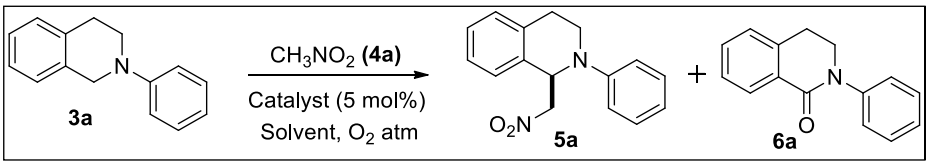

Entry	Solvent	5 wt% $CuO{\cdot}TiO_2$ (%Yield)		5 wt% $NiO{\cdot}TiO_2$ (%Yield)		5 wt% $CuO{\cdot}NiO{\cdot}TiO_2$ (%Yield)	
		5a	**6a**	**5a**	**6a**	**5a**	**6a**
1	1,4-dioxane	25	50	12	45	35	53
2	Acetonitrile	12	66	14	45	16	65
3	Methanol	5	35	5	40	20	35
4	Isopropanol	15	45	4	38	18	37
5	Toluene	-	27	-	23	-	45
6	p-Xylene	-	30	-	24	-	43
7	**-**	**15**	**67**	**5**	**47**	**83**	**7**

From the above comparative study, we excluded both 5% $CuO{\cdot}TiO_2$, and 5% $NiO{\cdot}TiO_2$ and only considered the 5% $CuO{\cdot}NiO{\cdot}TiO_2$ catalyst for further reactions. We could not conclude the best yield by employing 5 mol% of the catalyst, so the catalyst loading study

was also considered with different stoichiometries of catalyst.

The above study showed the formation of **5a** in 87% yields while heating in excess of **4a** at 100 °C (Table 3, entry 1), so we emphasized the employment of catalysts more than 5 mol%. When 10 mol% of catalyst was used, it helped reduce the reaction time but simultaneously imbalanced the formation of the **5a** and **6a** ratios (Table 3, entry 2). A similar observation was made for 15 mol% and 20 mol% catalyst loading, supporting more amidation reaction than CDC reaction (Table 3, entry 3, 4).

Table 3. Catalyst loading study

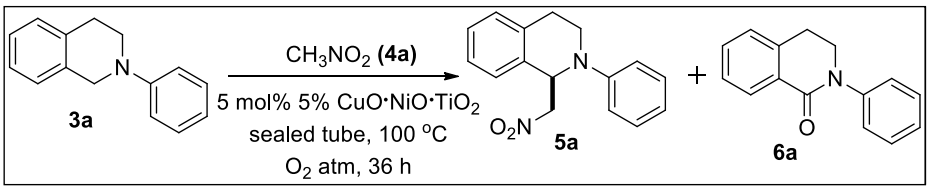

Entry	Catalyst loading	5a (%Yield)	6a (%Yield)
1	5 mol%	83	07
2	10 mol%	65	34
3	15 mol%	49	56
4	**20 mol%**	**23**	**72**

Even though everything was settled with less catalyst loading, optimum temperature, and solvent-free measures for the CDC reaction, we thought of incorporating various organic oxidants to see which serves better.

We could synthesize **5a** in an 83% yield using molecular oxygen as an oxidant (Table 4, entry 1). Instead of carrying out the reaction in a sealed tube with molecular oxygen, it was done in the open air, and substantially we could isolate **5a** in 67% yield (Table 4, entry 2). Organic oxidants like 70% TBHP in decane and *N*-Methylmorpholine *N*-oxide were also explored as co-oxidants but couldn't do much for the CDC reaction (Table 4, entry 3, 4).

Table 4. Productivity study using various oxidants

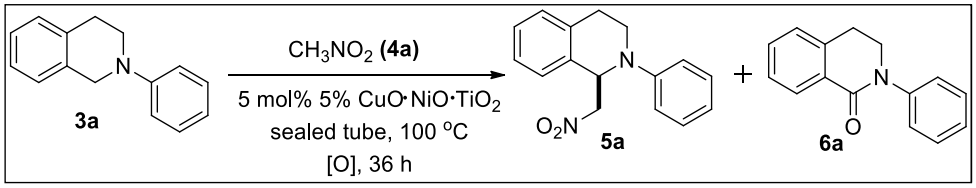

Entry	Oxidants [O]	5a (%Yield)
1	**Molecular oxygen**	**83**
2	Open-air	67
3	70% TBHP in decane	45
4	*N*-Methylmorpholine *N*-oxide	33

We got a precisely standardized condition for our CDC reaction between *N*-aryl-1,2,3,4-tetrahydroisoquinoline surrogates with various nucleophiles from all the above studies. The **3a** was reacted with nitroethane **4b** to construct a Csp^3-Csp^3 bond. We could successfully isolate **5b** in 78% yield, which analytical data matches the reported data (Scheme 3).

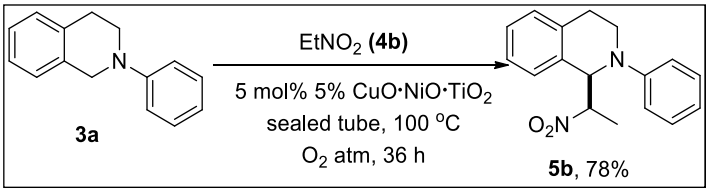

Scheme 3. CDC reaction of *N*-phenyl-1,2,3,4-tetrahydroisoquinoline with nitromethane

Along with the nitroalkane compounds, we fused active methylene compounds like dimethyl malonate **4c**, diethyl malonate **4d**, and malononitrile **4e** to **3a** (Scheme 4). The **4c** and **4d** went smoothly to furnish **5c** and **5d** in 67% and 62% yields, respectively. But the reaction of **4e** with **3a** gave an unexpected product **5e'**, i.e., cyano adduct of **3a** in 63% yield. The **5e** was not seen in our reaction mixture, which made us go through the literature reports for the answers. As per the reports, most of the CDC reactions on malononitrile **4e** with **3a** in heating conditions have shown the formation of **5e'** along with the **5e** but **5e** in higher amount. That could be possible only if malononitrile decomposes at a certain temperature level giving rise to cyano species which causes the formation of cyano adduct **5e'**. And just because we heat our reaction mixture in an oxidizing atmosphere at 100 °C for 36 h, it must be decomposing malononitrile into its corresponding cyano species, which explains why our reaction only forms **5e'** and **5e**.

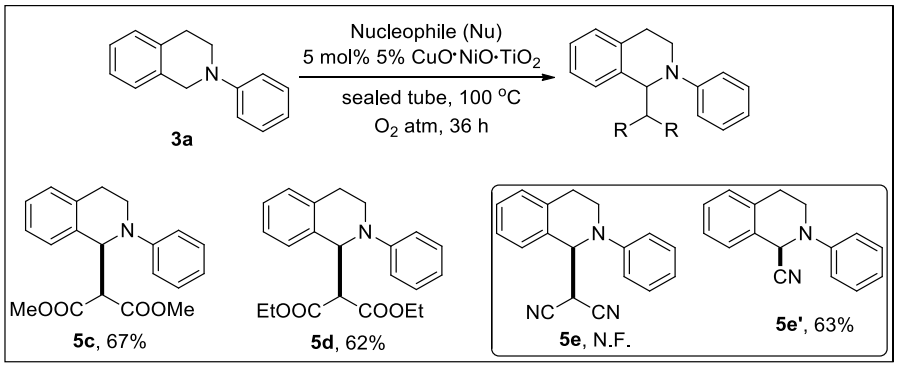

Scheme 4. CDC reactions of *N*-phenyl-1,2,3,4-tetrahydroisoquinoline with activated methylene compounds

With the liquid nucleophiles, we could efficiently perform our CDC reactions with *N*-phenyl-1,2,3,4-tetrahydroisoquinoline. So phosphite compounds like dimethyl phosphite were attached to **3a** in 76% yield (Scheme 5). As it is a high boiling liquid, we used only three-fold excess to avoid any complication during column purification. Its characterized data matches that to the reported data.

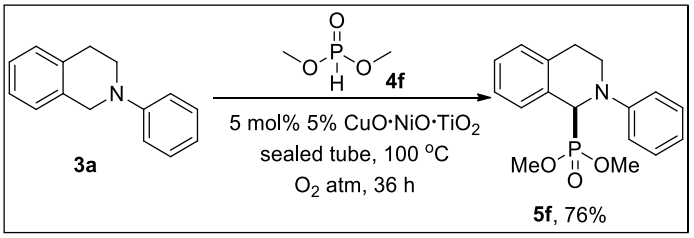

Scheme 5. CDC reactions of *N*-phenyl-1,2,3,4-tetrahydroisoquinoline with dimethyl phosphite

Researchers have also fused coumarin derivatives to **3a** in an efficient manner and high yield. So to check the diversity of our strategy, we planned to carry out the reaction between 4-hydroxy coumarin **4g** with **3a** (Scheme 6). But in this case, the nucleophile is in solid-state, so we have taken **3a** in excess than that of **4g**. So when after the reaction, we could isolate the remaining amount of **3a** and use it for another reaction. Our reaction productivity didn't disturb with such modification, and we synthesized compound **5g** in a 79% yield.

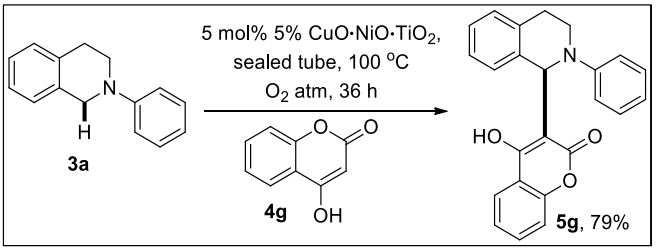

Scheme 6. CDC reactions of *N*-phenyl-1,2,3,4-tetrahydroisoquinoline with 4-hydroxycoumarin

Unlike coumarin compound, we envisaged attacking indole proxies on **3a**, which can help us, build a library of compounds. Similar to **4g,** we used more **3a** than the employed indole compounds and synthesized various C1-indole substituted *N*-phenyl-1,2,3,4-tetrahydroisoquinoline molecules. The reaction of indole **4h** with **3a** was transformed into **5h** in a 78% yield (Table 5, entry 1). Indole containing electron-donating group also favored our strategy and yielded compound **5i** in 77% (Table 5, entry 2).

Table 5. Csp^3-Csp^3 coupling of *N*-phenyl-1,2,3,4-tetrahydrosiqouinoline with indole proxies

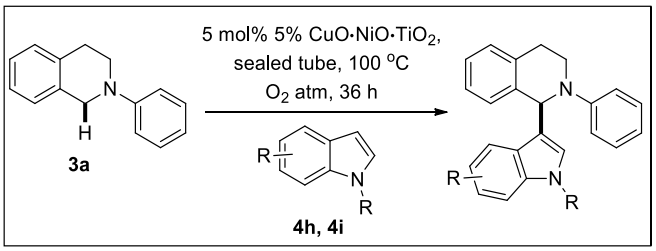

Entry	Starting indole	Product	% yield
1	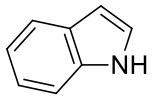 **4h**	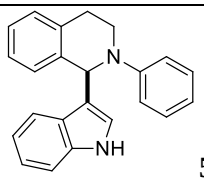 **5h**	78%
2	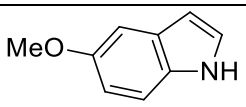 **4i**	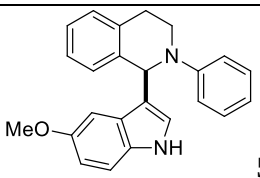 **5i**	77%

After successfully varying nucleophiles, we changed compound **3a** with different other substrates like 5-phenyl-4,5,6,7-tetrahydrothieno[3,2-*c*]pyridine **3b**. The required **3b** was prepared using the similar reported procedure to **3a** in 67% yield (Scheme 7).

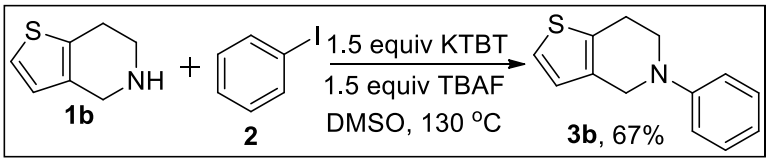

Scheme 7. Synthesis of 5-phenyl-4,5,6,7-tetrahydrothieno[3,2-*c*]pyridine

Later, **3b** was heated with **4a** in the presence of our catalyst in the sealed tube as per the standard procedure (Scheme 8). As expected, we achieved the nitromethane adduct of 5-phenyl-4,5,6,7-tetrahydrothieno[3,2-*c*]pyridine **5j** in 75% yield along with its amide derivative **6b** in 11% yield after the column purification. Though compounds like **3b** are not much explored in CDC reactions, all analytical data of nitromethane adduct **5j** suggests its formation.

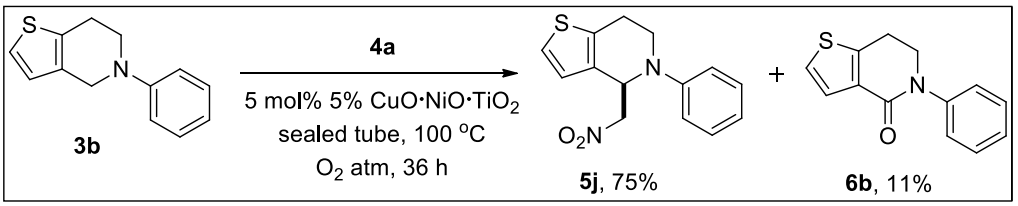

Scheme 8. CDC reaction of 5-phenyl-4,5,6,7-tetrahydrothieno[3,2-*c*]pyridine with nitromethane

The crystallographic structure was deduced using single crystal X-ray diffraction method of compound **5j**, which confirms the formation of nitromethane adduct with **3b** (Figure 3). Supplementarily, we could get the existence of **5j** in dimer form due to intermolecular hydrogen bonding between C8 - methylene protons with O2- oxygen of N2- nitro group (Figure 4). The crystallographic data are exhibited in experimental section **4.5.16**.

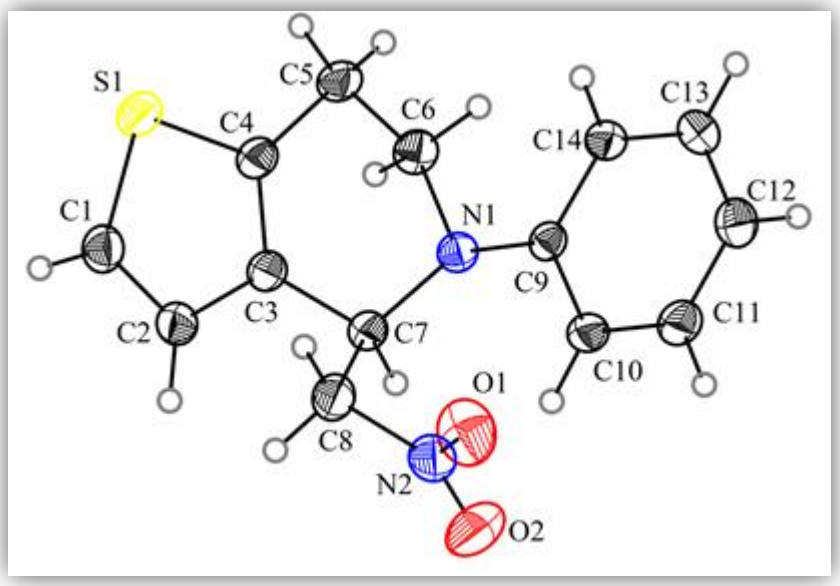

Figure 3. Single crystal X-ray structure of 5j

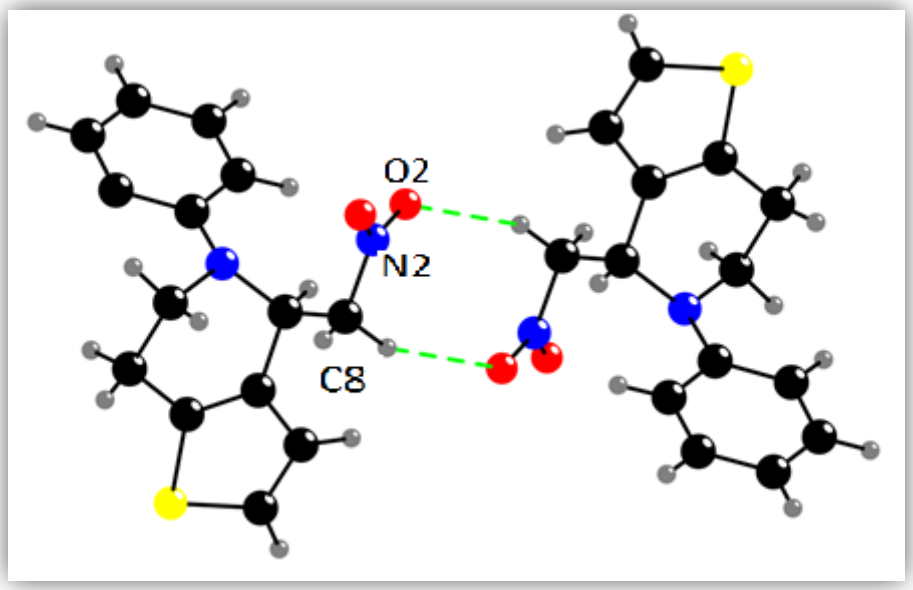

Figure 4. Single crystal X-ray structure of 5j showing intermolecular hydrogen bonding

Along with this, it was also subjected to indole addition reaction with **4h** in a similar reaction condition and found it forms white color solid upon purification, which analytical data matches to the expected structure (Scheme 9).

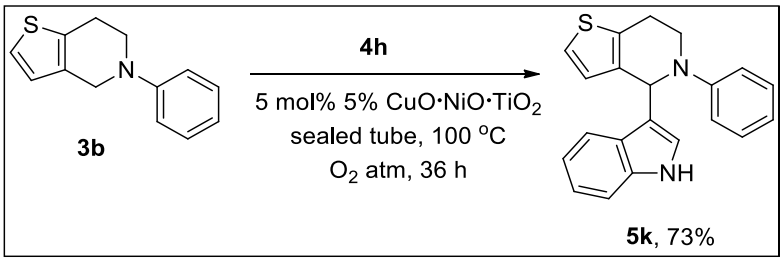

Scheme 9. CDC reaction of 5-phenyl-4,5,6,7-tetrahydrothieno[3,2-*c*]pyridine 5k with indole

Preparing different products of various nucleophiles with **3a** and **3b**, we checked the efficiency of the catalyst for the subsequent reaction after its recovery (Chart 1). The used catalyst was dried in an oven at 100 °C after filtering it from the reaction mixture and was used for another reaction with **3a** and **4a**. We observed a substantial decrease in the yield of the product, and even the starting material remained untouched in the reaction mixture. As per that, the yield ratio of both **5a** and **6a** shifted more towards the amidation reaction.

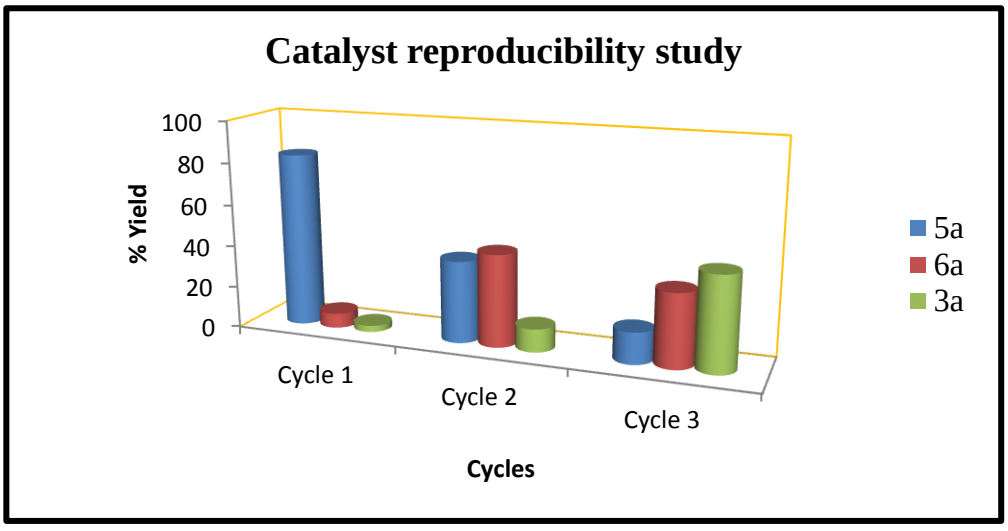

Figure 5. Catalyst recycling study

We could easily generate more of **5a** in an 83% yield than **6a** (7%) and **3a** (3%) with the freshly synthesized catalyst in the first cycle. For the second cycle, although we could isolate a little less catalyst from the first cycle, we set the reaction accordingly and traced the yields of all three compounds. Production of **5a** decreased to 39%, whereas **6a** gained the productivity to 44%. We could recover more of our starting **3a** in 11% even though we prolonged the reaction time. A researcher must always try one thing in three parts to make a precise observation, and we also tried the third cycle for our catalyst. Apparently, in the third cycle, we could achieve only 15% of **5a** whereas, **6a** productivity increased to 35%,

and the remaining starting **3a** was isolated in 45%. The failure of the reuse of the catalyst could be probably due to the loss of CuO·NiO from the surface of the catalyst during filtration.

4.4 Conclusion:

We demonstrated the utility of our 5% of Cu-Ni in $CuO{\cdot}NiO{\cdot}TiO_2$ catalyst for the CDC reactions on *N*-phenyltetrahydroisoquinoline moieties with various liquid as well as solid nucleophiles. An aerobic and solvent-free CDC reaction strategy is been developed to synthesize various compounds in good yields.

We have prepared nitroalkane, compounds having activated methylene group, indoles, dimethylphosphite, 4-hydroxycoumarin adducts with 2-phenyl-1,2,3,4-tetrahydroisoquinoline and 5-phenyl-4,5,6,7-tetrahydrothieno[3,2-*c*]pyridine. The adducts of 5-phenyl-4,5,6,7-tetrahydrothieno[3,2-*c*]pyridine with nitromethane and 1*H*- indole are novel and the spectroscopic analysis is done using IR, NMR, and HRMS. The crystallographic data of 4-(nitromethyl)-5-phenyl-4,5,6,7-tetrahydrothieno[3,2-*c*]pyridine proves the formation and elemental arrangement of the compound.

4.5 Experimental:

4.5.1: 2-phenyl-1,2,3,4-tetrahydroisoquinoline (3a):

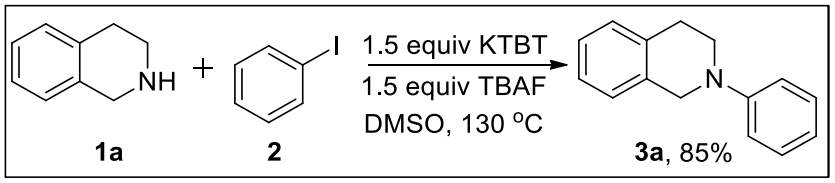

In a 10 mL sealed tube, 2 mmol of bromobenzene was added and 3 mmol of 1,2,3,4-tetrahydroisoquinoline **1a** in 3 mL DMSO, followed by 5 mol% of TBAB and 3 mmol of KTBT, and the whole mixture was heated at 130 °C for 1 hour. After the disappearance of **1a** on TLC, the reaction was cooled to room temperature and poured in 15 mL of H_2O, and stirred for 30 mins. The aqueous solution was then extracted using ethyl acetate (4 X 10 mL), which was then dried over anhydrous Na_2SO_4 and concentrated on the rotary evaporator to give crude thick liquid. The crude compound was then purified over flash chromatography on silica gel (Pet. ether and ethyl acetate) to provide pale brown oil in an 85% yield.

Pale brown oil. IR υ_{max}: 3030, 2963, 1667, 1613, 1117, 1049 cm^{-1}. ^1H NMR (400 MHz, $CDCl_3$) δ = 2.99 (t, *J* = 6 Hz, 2H), 3.56 (t, *J* = 6 Hz, 2H), 4.41 (s, 2H), 6.83 (t, *J* = 7.2 Hz, 1H), 6.98 (d, *J* = 8 Hz, 2H), 7.15-7.19 (m, 4H), 7.24-7.31 (m, 2H) ppm. ^{13}C NMR (100 MHz, $CDCl_3$) δ = 29.1 (CH_2), 46.6 (CH_2), 50.8 (CH_2), 115.2 (2XCH), 118.7 (CH), 126.0 (CH), 126.3 (CH), 126.6 (CH), 128.5 (CH), 129.2 (2XCH), 134.5 (Cq), 134.9 (Cq), 150.6 (Cq) ppm.

4.5.2: 5-phenyl-4,5,6,7-tetrahydrothieno[3,2-*c*]pyridine (3b):

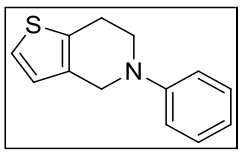

Following the similar procedure, as described in experiment 4.5.1, it is prepared using 4,5,6,7-tetrahydrothieno[3,2-*c*]pyridine and bromobenzene in 67% yield as a colorless liquid.

Colorless liquid. IR υ_{max}: 3038, 2979, 1693, 1614, 1197, 1079 cm^{-1}. ^{1}H NMR (400 MHz, $CDCl_3$) δ = 2.99 (t, *J* = 6 Hz, 2H), 3.63 (t, *J* = 6 Hz, 2H), 4.31 (s, 2H), 6.84-6.87 (m, 2H), 7.00 (d, *J* = 8.4 Hz, 2H), 7.12-7.14 (m, 1H), 7.28-7.31 (m, 2H) ppm. ^{13}C NMR (100 MHz, $CDCl_3$) δ = 25.3 (CH_2), 47.5 (CH_2), 49.0 (CH_2), 116.0 (2XCH), 119.3 (CH), 122.9 (CH), 125.1 (CH), 129.2 (2XCH), 133.3 (Cq), 133.6 (Cq), 150.7 (Cq) ppm.

4.5.3: 1-(nitromethyl)-2-phenyl-1,2,3,4-tetrahydroisoquinoline (5a):

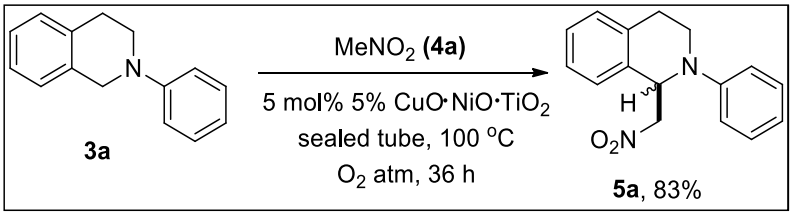

In a 5 mL sealed tube equipped with a stirring bar, was added 1 mmol of **3a** followed by 3 mL of nitroethane **4a** and 5 mol% of 5% $CuO{\cdot}NiO{\cdot}TiO_2$ catalyst. To that mixture, oxygen was purged, and the tube was tightly packed using Teflon. The resultant mixture was then heated at 100 °C for 36 hours till the starting material disappeared on TLC. The mixture was cooled to room temperature, and dry CH_2Cl_2 was added and stirred vigorously for 15 minutes. The catalyst was then filtered and subsequently washed using CH_2Cl_2 and dried for another batch reaction. The filtrate was then dried over anhydrous Na_2SO_4 and evaporated over a rotary evaporator. The resultant crude was purified over flash chromatography on silica gel (Pet. ether and ethyl acetate) to furnish compound **5a** in 83% as pale brown solid.

Pale brown solid, m.p. 72 °C. IR υ_{max}: 2928, 1601, 1557, 1513, 1493, 1389, 757, 696 cm^{-1}. ^{1}H NMR (400 MHz, $CDCl_3$) δ = 2.76-2.82 (m, 1H), 3.05-3.12 (m, 1H), 3.58-3.68 (m, 2H), 4.54-4.59 (m, 1H), 4.87-4.90 (m, 1H), 5.55 (t, *J* = 7.2 Hz, 1H), 6.83-6.87 (m, 1H), 6.98 (d, *J* = 8 Hz, 2H), 7.12-7.14 (m, 1H), 7.18-7.29 (m, 5H) ppm. ^{13}C NMR (100 MHz, $CDCl_3$) δ = 26.5 (CH_2), 42.1 (CH_2), 58.2 (CH), 78.8 (CH_2), 115.1 (2XCH), 119.4 (CH), 126.7 (CH), 127.0 (CH), 128.2 (CH), 129.2 (CH), 129.5 (2XCH), 132.9 (Cq), 135.3 (Cq), 148.4 (Cq) ppm. Spectral data is in accordance with the literature.[25]

4.5.4: 2-phenyl-3,4-dihydroisoquinolin-1(2*H*)-one (6a):

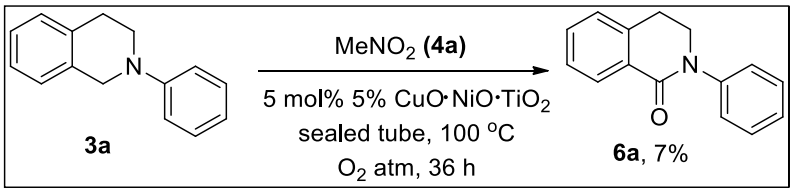

Following the similar procedure described in experiment 4.5.3, it is isolated as a side product in 7% yield as a light brown oil.

Light brown oil. IR υ_{max}: 3050, 2912, 1651, 1598, 1413, 1317, 1168, 1071, 753, 690 cm^{-1}. ^{1}H NMR (400 MHz, $CDCl_3$) δ = 3.15 (t, *J* = 8 Hz, 2H), δ 4.00 (t, *J* = 6.4 Hz, 2H), 7.24-7.29 (m, 2H), 7.36-7.49 (m, 6H), 8.16 (d, *J* = 7.6 Hz, 1H) ppm. ^{13}C NMR (100MHz, $CDCl_3$): δ = 28.6 (CH_2), 49.4 (CH_2), 125.3 (2XCH), 126.3 (CH), 127.0 (CH), 127.2 (CH), 128.8 (CH), 128.9 (2XCH), 129.3 (Cq), 129.7 (Cq), 132.1 (CH), 138.3 (Cq), 143.1 (Cq), 164.2 (Cq) ppm. Spectral data is in accordance with the literature. [25]

4.5.5: 1-(1-nitroethyl)-2-phenyl-1,2,3,4-tetrahydroisoquinoline (5b):

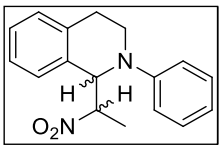

Following the similar procedure, as described in experiment 4.5.3, it is prepared using nitroethane in 78% yield as a yellow oil.

Yellow oil. IR υ_{max}: 2923, 1597, 15482, 1513, 1367, 1244, 1125, 953, 750 cm^{-1}. ^{1}H NMR (400 MHz, $CDCl_3$) δ = 1.46 & 1.62 (2Xd, *J* = 6.8, 7.2 Hz, 3H), 2.81 & 2.98 (2Xm, 2H), 3.50 & 3.51 (2Xm, 2H), 4.83 & 4.97 (2Xm, 1H), 5.14-5.19 (m, 1H), 6.72-7.92 (m, 9H) ppm. ^{13}C NMR (100 MHz, $CDCl_3$) δ = 16.4 [17.5] (CH_3), 26.4 [26.8] (CH_2), 42.7 [43.6] (CH_2), 62.2 [62.8] (CH), 85.5[(89.0] (CH), 114.5 [115.4] (2XCH), 118.8 [119.3] (CH), 126.1 [126.6] (CH), 127.7 [128.2] (CH), 128.4 [128.7] (CH), 129.1 [129.3] (2XCH), 129.4 [132.0] (CH), 133.8 [134.7] (Cq), 134.8 [135.6] (Cq), 148.9 [149.2] (Cq) ppm. Spectral data is in accordance with the literature.[25]

4.5.6: Dimethyl 2-(2-phenyl-1,2,3,4-tetrahydroisoquinolin-1-yl)malonate (5c):

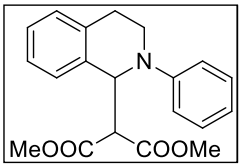

Following the similar procedure, as described in experiment 4.5.3, it is prepared using dimethylmalonate in 67% yield as a thick yellow liquid.

Yellow thick liquid. IR υ_{max}: 3384, 2967, 2393, 2181, 2003, 1738, 1500, 1266, 763, 689 cm^{-1}. ^{1}H NMR (400 MHz, $CDCl_3$) δ = 2.84-2.90 (m, 1H), 3.03-3.11 (m, 1H), 3.55 (s, 3H), 3.55-3.88 (m, 2H), 3.66 (s, 3H), 3.95 (d, *J* = 9.6 Hz, 1H), 5.70 (d, *J* = 9.6 Hz, 1H), 6.76 (t, *J* = 7.2 Hz, 1H), 6.98 (d, *J* = 8 Hz, 2H), 7.11-7.13 (m, 2H), 7.16-7.23 (m, 4H) ppm. ^{13}C NMR (100 MHz, $CDCl_3$) δ = 26.1 (CH_2), 42.2 (CH_2), 52.5 (CH), 52.6 (CH), 58.2(CH), 59.1 (CH), 115.2 (2XCH), 118.6 (CH), 126.0 (CH), 127.1 (CH), 127.6 (CH), 128.9 (CH), 129.1 (2XCH), 134.8 (Cq), 135.7 (Cq), 148.8 (Cq), 167.4 (Cq), 168.3 (Cq) ppm. Spectral data is in accordance with the literature.[25]

4.5.7: Diethyl 2-(2-phenyl-1,2,3,4-tetrahydroisoquinolin-1-yl)malonate (5d):

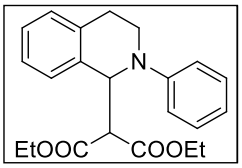

Following the similar procedure described in experiment 4.5.3, it is prepared using diethylmalonate in 62% yield as pale orange oil.

Pale orange oil. IR υ_{max}: 3359, 2971, 2380, 2194, 1993, 1751, 1483, 1293, 789, 667 cm^{-1}. ^{1}H NMR (400 MHz, $CDCl_3$) δ = 1.08 (t, *J* = 7.2 Hz, 3H), 1.17 (t, *J* = 7.2 Hz, 3H), 2.86-2.90 (m, 1H), 3.03-3.07 (m, 1H), 3.63-3.74 (2H), 3.89 (d, *J* = 9.2 Hz, 1H), 3.95-4.22 (m, 4H), 5.71 (d, *J* = 9.2 Hz, 1H), 6.75 (t, *J* = 7.2 Hz, 1H), 6.97 (d, *J* = 8.4 Hz, 2H), 7.10-7.24 (m, 6H) ppm. ^{13}C NMR (100 MHz, $CDCl_3$) δ = 13.9 (CH_3), 13.9 (CH_3), 26.1 (CH_2), 42.3 (CH_2), 57.9 (CH), 59.6 (CH), 61.6 ($2XCH_2$), 115.1 (2XCH), 118.4 (CH), 126.0 (CH), 127.2 (CH), 127.5 (CH), 128.9 (CH), 129.1 (2XCH), 134.8 (Cq), 136.0 (Cq), 148.9 (Cq), 167.1 (Cq), 168.0 (Cq) ppm. Spectral data is in accordance with the literature. [25]

4.5.8: 2-phenyl-1,2,3,4-tetrahydroisoquinoline-1-carbonitrile (5e'):

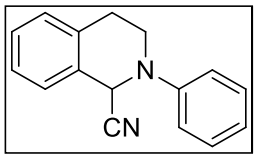

Following the similar procedure, as described in experiment 4.5.3, it is prepared using malanonitrile in 63% yield as white solid.

White solid, m.p. 94-98 °C. IR υ_{max}: 3067, 3040, 2930, 2832, 2239, 1589, 1513, 1392, 1222, 946, 742, 701 cm^{-1}. ^{1}H NMR (400 MHz, $CDCl_3$) δ = 2.88-2.94 (m, 1H), 3.06-3.14 (m, 1H), 3.38-3.45 (m, 1H), 3.68-3.73 (m, 1H), 5.45 (s, 1H), 6.95 (t, *J* = 7.2 Hz, 1H), 7.02 (d, *J* = 8.0 Hz, 2H), 7.16-7.32 (m, 6H) ppm. ^{13}C NMR (100 MHz, $CDCl_3$) δ = 28.6 (CH_2), 44.2 (CH_2), 53.3 (CH), 117.6 (2XCH), 121.9 (CH), 126.9 (CH), 127.1 (CH), 128.8 (CH), 129.4 (CH), 129.6 (2XCH), 134.6 (2XCq), 148.4 (2XCq) ppm. Spectral data is in accordance with the literature.[25]

4.5.9: Dimethyl (2-phenyl-1,2,3,4-tetrahydroisoquinolin-1-yl)phosphonate (5f):

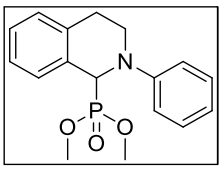

Following the similar procedure, as described in experiment 4.5.3, it is prepared using dimethylphosphite in 76% yield as a pale yellow liquid.

Pale yellow liquid. IR υ_{max}: 30566, 30290, 2945, 2903, 2867, 1600, 1513, 1242, 1062, 987, 723 cm^{-1}. ^{1}H NMR (400 MHz, $CDCl_3$) δ = 2.87-3.03 (m, 2H), 3.55-3.59 (m, 1H), 3.56 (d, *J* = 7.2 Hz, 3H), 3.58 (d, *J* = 7.2 Hz, 3H) 3.89-3.96 (m, 1H), 5.12 (d, *J* = 20 Hz, 1H), 6.73 (t, *J* = 7.2 Hz, 1H), 6.89 (d, *J* = 8.4 Hz, 2H), 7.06-7.11 (m, 3H), 7.12-7.18 (m, 2H), 7.20-7.28 (m, 1H) ppm. ^{13}C NMR (100 MHz, $CDCl_3$) δ = 26.7 (CH_2), 43.6 (CH_2), 53.0 & 54.0 (P-CH), 58.0 (CH_3), 59.6 (CH_3), 114.8 (2XCH), 118.7 (CH), 126.1 (CH), 127.6 (CH), 127.9 (CH), 128.9 (CH), 129.3 (2XCH), 130.4 (Cq), 136.4 (Cq), 149.2 (Cq) ppm. Spectral data is in accordance with the literature.[25]

4.5.10: 4-hydroxy-3-(2-phenyl-1,2,3,4-tetrahydroisoquinolin-1-yl)-2*H*-chromen-2-one (5g):

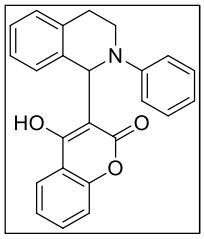

Following the similar procedure, as described in experiment 4.5.3, it is prepared using 4-hydroxy coumarin in 79% yield as pale yellow solid.

Pale yellow solid, m.p. 136−138 °C. IR υ_{max}: 3712, 2924, 2873, 2858, 2643, 2071, 1630 cm^{-1}. ^{1}H NMR (400 MHz, $CDCl_3$) δ = 2.86-2.90 (m, 1H), 3.14-3.21 (m, 1H), 3.42-3.50 (m, 1H), 3.59-3.64 (m, 1H), 6.09 (s, 1H), 7.04-7.09 (m, 5H), 7.11-7.17 (m, 1H), 7.23-7.30 (m, 2H), 7.32-7.57 (m, 4H), 7.58 (d, 1H) ppm. ^{13}C NMR (100 MHz, $CDCl_3$) δ = 30.4 (CH_2), 55.0 (CH_2), 58.3 (CH), 104.8 (Cq), 116.5 (CH), 122.4 (2XCH), 123.3 (CH), 123.7 (CH), 126.2 (CH), 127.0 (2XCH), 127.4 (CH), 128.3 (CH), 129.7 (2XCH), 132.0 (CH), 132.7 (2XCq), 135.7 (Cq), 148.5 (Cq), 153.4 (Cq), 164.1 (Cq), 165.2 (Cq) ppm. Spectral data is in accordance with the literature.[25]

4.5.11: 1-(1*H*-indol-3-yl)-2-phenyl-1,2,3,4-tetrahydroisoquinoline (5h):

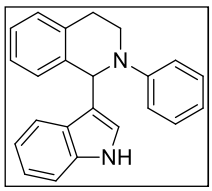

Following the similar procedure, as described in experiment 4.5.3, it is prepared using indole in 78% yield as white solid.

White solid, m.p. 167−169 °C. IR υ_{max}: 3406, 2928, 1621, 1613, 1507, 1345, 1223, 1109, 1043, 943, 756cm^{-1}. ^{1}H NMR (400 MHz, $CDCl_3$) δ = 2.73-2.77 (m, 1H), 2.96-3.03 (m, 1H), 3.33-3.36 (m, 2H), 6.09 (s, 1H), 6.53 (s, 1H), 6.71 (t, *J* = 7.2 Hz, 1H), 6.92-6.97 (m, 3H), 7.04-7.11 (m, 4H), 7.13-7.21 (m, 4H), 7.44 (d, *J* = 7.6 Hz, 1H), 7.87 (bs, 1H) ppm. ^{13}C NMR (100 MHz, $CDCl_3$) δ = 26.7 (CH_2), 42.4 (CH_2), 56.8 (CH), 111.1 (2XCH), 116.0

(CH), 118.5 (CH), 119.7 (CH), 120.0 (CH), 122.1 (CH), 124.3 (CH), 125.8 (CH), 126.5 (CH), 126.7 (CH), 128.1 (CH), 128.8 (2XCq), 129.5 (2XCH), 135.5 (Cq), 136.6 (Cq), 137.3 (Cq), 149.7 (Cq) ppm. Spectral data is in accordance with the literature.[25]

4.5.12: 1-(5-methoxy-1*H*-indol-3-yl)-2-phenyl-1,2,3,4-tetrahydroisoquinoline (5i):

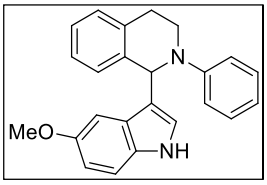

Following the similar procedure, as described in experiment 4.5.3, it is prepared using 5-methoxy indole in 77% yield as white solid.

White solid, m.p. 143-147 °C. IR υ_{max}: 3412, 2930, 1604, 1510, 1387, 1289, 1183, 1110, 1059, 969, 778, 756 cm^{-1}. ^{1}H NMR (400 MHz, $CDCl_3$) δ = 2.94 (m, 1H), 3.04-3.12 (m, 1H), 3.62-3.65 (s, 2H), 3.63 (s, 3H), 6.25 (s, 1H), 6.70-6.73 (m, 3H), 6.95 (s, 1H), 7.08 (d, *J* = 8 Hz, 2H), 7.16-7.25 (m, 5H), 7.35 (d, *J* = 5.6 Hz, 1H), 9.97 (bs, 1H) ppm. ^{13}C NMR (100 MHz, $CDCl_3$) δ = 28.7 (CH_2), 43.6 (CH_2), 56.2 (CH_3), 58.3 (CH), 103.3 (CH), 113.2 (CH), 113.6 (CH), 113.6 (CH), 117.4 (CH), 119.6 (CH), 127.0 (CH), 128.3 (CH), 128.8 (CH), 129.8 (Cq), 130.3 (2XCq), 130.8 (2XCq), 133.9 (Cq), 137.2 (Cq), 139.9 (Cq), 155.5 (Cq) ppm.

4.5.13: 4-(nitromethyl)-5-phenyl-4,5,6,7-tetrahydrothieno[3,2-*c*]pyridine (5j):

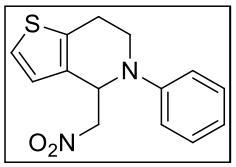

Following the similar procedure, as described in experiment 4.5.3, it is prepared using 5-phenyl-4,5,6,7-tetrahydrothieno[3,2-c]pyridine and nitromethane in 75% yield as a light yellow solid.

Light tan solid, m.p. 82 °C. IR υ_{max}: 2936, 1593, 1555, 1503, 1473, 1307, 601 cm^{-1}. ^{1}H NMR (400 MHz, $CDCl_3$) δ = 2.71-2.76 (m, 1H), 3.00-3.09 (m, 1H), 3.45-3.52 (m, 1H), 3.92-3.97 (m, 1H), 4.60-4.64 (m, 1H), 4.74-4.80 (m, 1H), 5.54-5.57 (m, 1H), 6.80 (d, *J* =

5.2 Hz, 1H), 6.87 (t, *J* = 7.2 Hz, 1H), 6.97 (d, *J* = 8 Hz, 2H), 7.14 (d, *J* = 5.2 Hz, 1H), 7.23-7.27 (m, 2H) ppm. ^{13}C NMR (100 MHz, $CDCl_3$) δ = 22.6 (CH_2), 42.0 (CH_2), 56.7 (CH), 77.6 (CH_2), 117.2 (2XCH), 120.5 (CH), 123.5 (CH), 124.5 (CH), 129.4 (2XCH), 131.1 (Cq), 136.7 (Cq), 148.9 (Cq) ppm.

4.5.14: 5-phenyl-6,7-dihydrothieno[3,2-*c*]pyridin-4(5*H*)-one (6b):

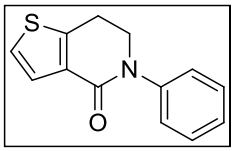

Following the similar procedure, as described in experiment 4.5.3, it is isolated as a side product in 13% yield as a colorless oil.

Pale brown oil. IR υ_{max}: 3049, 2935, 1660, 1593, 1421, 1342, 1120, 1079, 792 cm^{-1}. ^{1}H NMR (400 MHz, $CDCl_3$) δ = 3.22 (t, *J* = 6.8 Hz, 2H), δ 4.09 (t, *J* = 6.8 Hz, 2H), 7.11 (d, *J* = 5.2 Hz, 1H), 7.26 (d, *J* = 6.4 Hz, 1H), 7.34-7.43 (m, 4H), 7.49 (d, *J* = 5.2 Hz, 1H) ppm. 13C NMR (100MHz, CDCl3): δ = 24.8 (CH_2), 50.6 (CH_2), 123.4 (CH), 125.6 (2XCH), 126.2 (CH), 126.8 (CH), 128.9 (2XCH), 133.2 (Cq), 142.7 (Cq), 145.3 (Cq), 161.6 (O=Cq) ppm. LCMS $[M+H]^+$: 229.2975; Found: 229.31. HRMS (m/z): calculated for $C_{14}H_{14}N_2O_2SH$ $[M+H]^+$ 275.0854; found 275.0851.

4.5.15: 4-(1*H*-indol-3-yl)-5-phenyl-4,5,6,7-tetrahydrothieno[3,2-*c*]pyridine (5k):

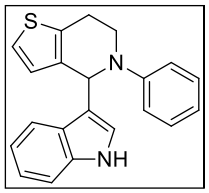

Following the similar procedure, as described in experiment 4.5.3, it is prepared using indole in 73% yield as light yellow solid.

White solid, m.p. 132-135 °C. IR υ_{max}: 3310, 2923, 1634, 1605, 1498, 1355, 1229, 1115, 1080, 960, 740 cm^{-1}. ^{1}H NMR (400 MHz, $CDCl_3$) δ = 2.71-2.76 (m, 1H), 3.03-3.11 (m, 1H), 3.50-3.57 (m, 1H), 3.72-3.77 (m, 1H), 6.18 (s, 1H), 6.68 (d, *J* = 2.4 Hz, 1H), 6.81-6.86 (m, 2H), 7.02 (t, *J* = 7.6 Hz, 1H), 7.07-7.09 (m, 3H), 7.16 (t, *J* = 7.6 Hz, 1H), 7.25 (t, *J*

= 8.8 Hz, 2H), 7.31 (d, *J* = 8.1 Hz, 1H), 7.49 (d, *J* = 7.9 Hz, 1H), 7.95 (bs, 1H) ppm. ^{13}C NMR (100 MHz, $CDCl_3$) δ = 23.1 (CH_2), 42.3 (CH_2), 54.7 (CH), 111.0 (CH), 117.4 (2XCH), 118.0 (Cq), 119.1 (CH), 119.7 (CH), 120.0 (CH), 121.9 (CH), 122.2 (CH), 124.2 (CH), 126.4 (CH), 126.7 (Cq), 129.2 (2XCH), 134.9 (Cq), 135.8 (Cq), 136.5 (Cq), 150.0 (Cq) ppm. HRMS (m/z): calculated for $C_{21}H_{18}N_2SH$ $[M+H]^+$ 331.1269; found 331.1267.

4.5.16: Single crystal X-ray data of 4-(nitromethyl)-5-phenyl-4,5,6,7-tetrahydrothieno[3,2-*c*]pyridine (5j):

Table 6. Crystal data and structure refinement for SGT-KM-21-01

Empirical formula	$C_{14}\ H_{14}\ N_2\ O_2\ S$
Formula weight	274.33
Temperature	296(2) K
Wavelength	0.71073 Å
Crystal system	Monoclinic
Space group	*P* $2_1/n$
Unit cell dimensions	a = 9.6651(4) Å
	b = 8.4684(3) Å
	c = 16.2104(6) Å
Volume	1320.90(9) $Å^3$
Z	4
Density (calculated)	1.379 Mg/m^3
Absorption coefficient	0.244 mm^{-1}
F(000)	576
Crystal size	0.27 x 0.14 x 0.10 mm^3
Theta range for data collection	2.564 to 28.290°.
Index ranges	$-12\leq h\leq 12$, $-11\leq k\leq 11$, $-21\leq l\leq 21$
Reflections collected	44215
Independent reflections	3270 [R(int) = 0.0443]
Completeness to theta = 25.242°	99.7 %
Absorption correction	Semi-empirical from equivalents
Refinement method	Full-matrix least-squares on F^2
Data / restraints / parameters	3270 / 0 / 172
Goodness-of-fit on F^2	1.059
Final R indices [I>2sigma(I)]	R1 = 0.0359, wR2 = 0.0919
R indices (all data)	R1 = 0.0470, wR2 = 0.1029
Largest diff. peak and hole	0.206 and -0.318 $e.Å^{-3}$

Table 7. Atomic coordinates (x 10^4) and equivalent isotropic displacement parameters ($Å^2$x 10^3) for km_0m_a. U(eq) is defined as one third of the trace of the orthogonalized U^{ij} tensor

Atom	x	y	z	U(eq)
S1	3259(1)	6496(1)	5212(1)	52(1)
N1	2620(1)	2316(1)	3516(1)	39(1)
N2	58(2)	635(2)	3636(1)	61(1)
O1	-498(2)	740(2)	2935(1)	90(1)
O2	400(2)	-613(2)	3969(1)	93(1)
C1	2557(2)	5384(2)	5951(1)	51(1)
C2	2065(2)	3985(2)	5646(1)	47(1)
C3	2281(1)	3785(2)	4793(1)	39(1)
C4	2896(1)	5058(2)	4471(1)	41(1)
C5	3248(2)	5174(2)	3593(1)	48(1)
C6	2482(2)	3852(2)	3098(1)	45(1)
C7	1956(1)	2301(2)	4292(1)	40(1)
C8	379(2)	2116(2)	4114(1)	54(1)
C9	3856(1)	1448(1)	3472(1)	34(1)
C10	4081(1)	14(2)	3894(1)	41(1)
C11	5261(2)	-871(2)	3815(1)	49(1)
C12	6252(2)	-379(2)	3311(1)	54(1)
C13	6043(2)	1021(2)	2889(1)	51(1)
C14	4870(2)	1930(2)	2964(1)	43(1)

Table 8. Bond lengths [Å] and angles [°] for SGT-KM-21-01

S1-C1	1.7133(17)
S1-C4	1.7228(14)
N1-C9	1.4107(16)
N1-C7	1.4647(17)
N1-C6	1.4671(17)
N2-O1	1.214(2)
N2-O2	1.217(2)
N2-C8	1.491(2)

C1-C2	1.353(2)
C1-H1	0.9300
C2-C3	1.4279(19)
C2-H2	0.9300
C3-C4	1.3594(19)
C3-C7	1.5126(19)
C4-C5	1.4974(19)
C5-C6	1.528(2)
C5-H5A	0.9700
C5-H5AB	0.9700
C6-H6A	0.9700
C6-H6AB	0.9700
C7-C8	1.532(2)
C7-H7	0.9800
C8-H8A	0.9700
C8-H8AB	0.9700
C9-C14	1.3988(18)
C9-C10	1.4005(18)
C10-C11	1.381(2)
C10-H10	0.9300
C11-C12	1.380(2)
C11-H11	0.9300
C12-C13	1.374(2)
C12-H12	0.9300
C13-C14	1.385(2)
C13-H13	0.9300
C14-H14	0.9300

C1-S1-C4	91.79(7)
C9-N1-C7	118.76(10)
C9-N1-C6	118.60(11)
C7-N1-C6	112.11(11)
O1-N2-O2	123.81(18)
O1-N2-C8	118.44(18)
O2-N2-C8	117.73(16)
C2-C1-S1	111.99(12)
C2-C1-H1	124.0
S1-C1-H1	124.0

C1-C2-C3	112.32(14)
C1-C2-H2	123.8
C3-C2-H2	123.8
C4-C3-C2	112.74(13)
C4-C3-C7	121.94(12)
C2-C3-C7	125.22(12)
C3-C4-C5	124.29(13)
C3-C4-S1	111.14(11)
C5-C4-S1	124.55(11)
C4-C5-C6	108.03(12)
C4-C5-H5A	110.1
C6-C5-H5A	110.1
C4-C5-H5AB	110.1
C6-C5-H5AB	110.1
H5A-C5-H5AB	108.4
N1-C6-C5	112.86(11)
N1-C6-H6A	109.0
C5-C6-H6A	109.0
N1-C6-H6AB	109.0
C5-C6-H6AB	109.0
H6A-C6-H6AB	107.8
N1-C7-C3	111.62(11)
N1-C7-C8	110.31(12)
C3-C7-C8	109.81(11)
N1-C7-H7	108.3
C3-C7-H7	108.3
C8-C7-H7	108.3
N2-C8-C7	109.81(12)
N2-C8-H8A	109.7
C7-C8-H8A	109.7
N2-C8-H8AB	109.7
C7-C8-H8AB	109.7
H8A-C8-H8AB	108.2
C14-C9-C10	117.07(12)
C14-C9-N1	121.48(12)
C10-C9-N1	121.33(12)
C11-C10-C9	121.17(13)
C11-C10-H10	119.4

C9-C10-H10	119.4
C12-C11-C10	121.02(14)
C12-C11-H11	119.5
C10-C11-H11	119.5
C13-C12-C11	118.54(14)
C13-C12-H12	120.7
C11-C12-H12	120.7
C12-C13-C14	121.27(14)
C12-C13-H13	119.4
C14-C13-H13	119.4
C13-C14-C9	120.93(13)
C13-C14-H14	119.5
C9-C14-H14	119.5

Symmetry transformations used to generate equivalent atoms:

Table 9. Anisotropic displacement parameters ($Å^2$x 10^3)for km_0m_a. The anisotropic displacement factor exponent takes the form: $-2\pi^2[h^2a^{*2}U^{11} + ... + 2 h k a^* b^* U^{12}]$

Atom	U^{11}	U^{22}	U^{33}	U^{23}	U^{13}	U^{12}
S1	62(1)	40(1)	53(1)	-4(1)	5(1)	-6(1)
N1	42(1)	36(1)	38(1)	4(1)	3(1)	4(1)
N2	49(1)	62(1)	75(1)	-15(1)	17(1)	-16(1)
O1	76(1)	112(1)	79(1)	-25(1)	-2(1)	-11(1)
O2	122(1)	51(1)	107(1)	-9(1)	16(1)	-18(1)
C1	62(1)	49(1)	44(1)	-4(1)	7(1)	5(1)
C2	55(1)	42(1)	44(1)	3(1)	11(1)	5(1)
C3	39(1)	36(1)	41(1)	2(1)	3(1)	4(1)
C4	45(1)	35(1)	43(1)	2(1)	2(1)	3(1)
C5	65(1)	36(1)	44(1)	8(1)	7(1)	0(1)
C6	53(1)	42(1)	39(1)	9(1)	-2(1)	8(1)
C7	41(1)	35(1)	45(1)	1(1)	7(1)	2(1)
C8	45(1)	48(1)	72(1)	-12(1)	13(1)	-4(1)
C9	39(1)	32(1)	31(1)	-3(1)	0(1)	-1(1)

C10	43(1)	37(1)	43(1)	4(1)	6(1)	0(1)
C11	52(1)	39(1)	56(1)	5(1)	4(1)	8(1)
C12	48(1)	52(1)	64(1)	-3(1)	12(1)	10(1)
C13	52(1)	53(1)	52(1)	-3(1)	19(1)	-1(1)
C14	52(1)	39(1)	40(1)	2(1)	9(1)	-2(1)

Table 10. Hydrogen coordinates (x 10^4) and isotropic displacement parameters ($Å^2$x 10^3) for SGT-KM-21-01

Atom	x	y	z	U(eq)
H1	2518	5705	6497	61
H2	1635	3239	5957	56
H5A	4242	5065	3571	58
H5AB	2964	6193	3362	58
H6A	1504	4122	3004	54
H6AB	2844	3769	2561	54
H7	2312	1393	4621	48
H8A	-48	2079	4631	65
H8AB	1	3016	3798	65
H10	3424	-348	4233	49
H11	5391	-1814	4107	59
H12	7044	-981	3259	65
H13	6701	1364	2546	62
H14	4756	2875	2673	52

Table 11. Torsion angles [°] for SGT-KM-21-01

C4-S1-C1-C2	-0.17(13)
S1-C1-C2-C3	1.06(17)
C1-C2-C3-C4	-1.70(18)
C1-C2-C3-C7	174.82(13)
C2-C3-C4-C5	179.92(13)
C7-C3-C4-C5	3.3(2)

C2-C3-C4-S1	1.54(15)
C7-C3-C4-S1	-175.11(10)
C1-S1-C4-C3	-0.80(12)
C1-S1-C4-C5	-179.18(13)
C3-C4-C5-C6	14.09(19)
S1-C4-C5-C6	-167.75(10)
C9-N1-C6-C5	-79.43(16)
C7-N1-C6-C5	64.96(16)
C4-C5-C6-N1	-46.91(17)
C9-N1-C7-C3	100.51(13)
C6-N1-C7-C3	-43.82(15)
C9-N1-C7-C8	-137.11(12)
C6-N1-C7-C8	78.56(14)
C4-C3-C7-N1	11.14(18)
C2-C3-C7-N1	-165.07(13)
C4-C3-C7-C8	-111.51(15)
C2-C3-C7-C8	72.27(18)
O1-N2-C8-C7	-115.18(17)
O2-N2-C8-C7	63.2(2)
N1-C7-C8-N2	57.84(17)
C3-C7-C8-N2	-178.73(13)
C7-N1-C9-C14	-149.50(12)
C6-N1-C9-C14	-7.48(18)
C7-N1-C9-C10	34.58(17)
C6-N1-C9-C10	176.60(12)
C14-C9-C10-C11	0.6(2)
N1-C9-C10-C11	176.69(13)
C9-C10-C11-C12	-0.7(2)
C10-C11-C12-C13	0.2(2)
C11-C12-C13-C14	0.2(2)
C12-C13-C14-C9	-0.2(2)
C10-C9-C14-C13	-0.2(2)
N1-C9-C14-C13	-176.25(13)

Symmetry transformations used to generate equivalent atoms:

Table 12. Hydrogen bonds for SGT-KM-21-01 [Å and °]

D-H...A	d(D-H)	d(H...A)	<(DHA)	d(D...A)	A
C8-H8A	0.970	2.637	149.24	3.506	O2 [-x, -y, -z+1]

4.6 References:

1) Wurtz, C. A. *Bulletin de la Société Chimique de Paris* **1872**, *17*, 436. (b) Wurtz, C. A. *Journal für Praktische Chemie* **1872**, *5*, 457. (c) Wurtz, C. A. *Comptes rendus de l'Académie des sciences* **1872**, *74*, 1361.
2) Mahrwald, R. Modern Aldol Reactions, Vol. 1: *Enolates, Organocatalysis, Biocatalysis and Natural, Product Synthesis*, WILEY-VCH Verlag GmbH & Co. KGaA, Weinheim, **2004**.
3) P. Y. Bruce, Organic Chemistry; 4th edn; Pearson Education, **2004**.
4) Reformatsky, S. *Ber.* **1887**, *20*, 1210.
5) Grignard, V. *Compt. Rend.* **1900**, *130*, 1322.
6) Diels, O.; Alder, K. *Justus Liebigs Ann. Chem.* **1928**, *460*, 98.
7) Wittig, G. *Angew. Chem.* **1956**, *68*, 505.
8) Schrock, R. R. *Acc.Chem. Res.* **1986**, *19*, 342.
9) (a) Heck, R. F. *J. Am. Chem. Soc.* **1968**, *90*, 5526. (b) Heck, R. F. *J. Am. Chem. Soc.* **1968**, *90*, 5531. (c) Heck, R. F. *J. Am. Chem. Soc.* **1968**, *90*, 5535.
10) (a) Miyaura, N.; Yamada, K.; Suzuki, A. *Tetrahedron Lett.* **1979**, *20*, 3437. (b) Miyaura, N.; Suzuki, A. *Chem. Comm.* **1979**, *19*, 866. (c) Miyaura, N.; Suzuki, A. *Chem. Rev.*. **1995**, *95*, 2457.
11) Hatanaka, Y.; Hiyama, T. *J. Org. Chem.* **1988**, *53*, 918.
12) Amao, K.; Sumitani, K.; Kumada, M. *J. Am. Chem. Soc.* **1972**, *94*, 4374.
13) King, A. O.; Okukado, N.; Negishi, E. *J. Chem. Soc., Chem. Comm.* **1977**, *19*, 683.
14) Stille, J. K. *Angew. Chem. Int. Ed. Engl.* **1986**, *25*, 508.
15) Glaser, C. *Ber. Dtsch. Chem. Ges.*, **1869**, *2*, 422. (b) Hay, A.S. *J. Org. Chem.* **1962**, *27*, 3320.
16) (a) Eglinton, A.; Galbraith, G. R. *Chem. Ind.* **1956**, 737.
17) (a) Girard, S. A.; Knauber, T.; Li, C-J. The Evolution of the Concept of Cross-Dehydrogenative-Coupling Reactions, RSC, **2015**. (b) Li, C.-J.; Li, Z. *Pure Appl. Chem.* **2006**, *78*, 935.
18) Tian, T.; Li, Z.; Li, C.-J. *Green Chem.* **2021**, *23*, 6789.
19) (a) Penga, K.; Dong, Z-B. *Adv. Synth. Catal*. **2021**, *363*, 1185. (b) Li, C.-J. *Acc.Chem.Res.* **2009**, *42*, 335.
20) Huang, Y.; Xin, Z.; Yao, W.; Hu, Q.; Li, Z.; Xiao, L.; Yang, B.; Zhang, *J. Chem. Commun.* **2018**, *54*, 13587.

21) Ho, L. A.; Raston, C. L.; Stubbs, K. A. *Chem. - A Eur. J.* **2018**, *24*, 8869.

22) Tan, J.; Liu, B.; Su, S. *Org. Chem. Front.* **2018**, *5*, 3093.

23) Hou, H.; Zhu, S.; Atodiresei, I.; Rueping, M. *Eur. J. Org. Chem.* **2018**, *2018*, 1277.

24) Liang, H. P.; Chen, Q.; Han, B. H. *ACS Catal.* **2018**, *8*, 5313.

25) Patil, M. R.; Dedhia, N. P.; Kapdi, A. R.; Kumar, A.V. *J. Org. Chem.* **2018**, *83*, 4477.

26) Lin, B.; Shi, S.; Lin, R.; Cui, Y.; Fang, M.; Tang, G.; Zhao, Y. *J. Org. Chem.* **2018**, *83*, 6754.

27) Liu, W.; Wu, S.; Su, Q.; Guo, B.; Ju, P.; Li, G.; Wu, Q. *J. Mater. Sci.* **2019**, *54*, 1205.

28) Li, Z.; Zhou, Z.; Ma, J.; Li, Y.; Peng, W.; Zhang, G.; Zhang, F.; Fan, X. *Appl. Catal. B Environ.* **2018**, *237*, 288.

29) Wang, J.; Sun, Y.; Jiang, M.-H.; Hu, T.-Y.; Zhao, Y.-J.; Li, X.; Wang, G.; Hao, K.; Zhen, L. *J. Org. Chem.* **2018**, *83*, 13121.

30) Sun, M. X.; Wang, Y. F.; Xu, B. H.; Ma, X. Q.; Zhang, S. J. *Org. Biomol. Chem.* **2018**, *16*, 1971.

31) Zhu, D.; Yao, Y.; Zhao, R.; Liu, Y.; Shi, L. *Chem. - A Eur. J.* **2018**, *24*, 4805.

32) Lin, B.; Lu, G.; Lin, R.; Cui, Y.; Liu, Y.; Tang, G.; Zhao Y. *Synlett* **2018**, *29*, A-D.

33) Xiao, L.; Huang, Y.; Luo, Y.; Yang, B.; Liu, Y.; Zhou, X.; Zhang, J. *ACS Sustain. Chem. Eng.* **2018**, *6*, 14759.

34) Wu, W.-B.; Wong, Y.-C.; Tan, Z.-K.; Wu, J. *Catal. Sci. Technol.* **2018**, *8*, 4257.

35) Wang, C. M.; Song, D.; Xia, P. J.; Ye, Z. P.; Xiao, J. A.; Xiang, H. Y.; Chen, X. Q.; Yang, H. *Org. Chem. Front.* **2018**, *5*, 1608.

36) Liang, W.; Zhang, T.; Liu, Y.; Huang, Y.; Liu, Z.; Liu, Y.; Yang, B.; Zhou, X.; Zhang, J. *ChemSusChem* **2018**, *11*, 3586.

37) Bédard, A.; Adamo, A.; Aroh, K. C.; Russell, M. G.; Bedermann, A. A.; Torosian, J.; Yue, B.; Jensen, K. F.; Jamison, T. F. *Chemical Reactions* **2018**, *1225*, 1220.

38) Ide, T.; Shimizu, K.; Egami, H.; Hamashima, Y. *Tetrahedron Lett.* **2018**, *59*, 3258.

39) Nauth, A.; Schechtel, E.; Dören, R.; Tremel, W.; Opatz, T. *J. Am. Chem. Soc.* **2018**, *140*, 14169.

40) Ren, L.; Cong, H. *Org. Lett.* **2018**, *20*, 3225.

41) Kibriya, G.; Bagdi, A. K.; Hajra, A. *J. Org. Chem.* **2018**, *83*, 10619.

42) Casado-Sánchez, A.; Uygur, M.; González-Muñoz, D.; Aguilar-Galindo, F.; Nova-Fernández, J. L.; Arranz-Plaza, J.; Díaz-Tendero, S.; Cabrera, S.; Mancheño, O. G.; Alemán, J. *J. Org. Chem.* **2019**, *84*, 6437.

43) Shi, D.; Guo, X.; Lai, T.; Zheng, K.; Wu, Q.; Sun, C.; He, C.; Zhao, J. *Inorg. Chem. Commun.* **2019**, *105*, 9.

44) Zhao, Y.; Sun, T.; Liao, W.; Wang, Y.; Yu, J.; Zhang, M.; Yu, Z.; Yang, B.; Gui, D.; Zhu, C.; Xu, J. *ACS Appl. Mater. Interfaces* **2019**, *11*, 22794.

45) Xia, Z.; Qin, L.; Zhou, W.; Wang, H.; Yu, B.; Sun, Z.; Qian, J.; He, M. *Tetrahedron Lett.* **2019**, *60*, 151121.

46) Ranieri, A. M.; Burt, L. K.; Stagni, S.; Zacchini, S.; Skelton, B. W.; Ogden, M. I.; Bissember, A. C.; Massi, M. *Organometallics* **2019**, *38*, 1108.

47) Zhi, Y.; Ma, S.; Xia, H.; Zhang, Y.; Shi, Z.; Mu, Y.; Liu, X. *Appl. Catal. B Environ.* **2019**, *244*, 36.

48) Tan, Q.; Yang, Z.; Jiang, D.; Cheng, Y.; Yang, J.; Xi, S.; Zhang, M. *Angew. Chemie - Int. Ed.* **2019**, *58*, 6420.

49) Kumar, G.; Solanki, P.; Nazish, M.; Neogi, S.; Kureshy, R. I.; Khan, N. ul H. *J. Catal.* **2019**, *371*, 298.

50) Rana, P.; Gaur, R.; Gupta, R.; Arora, G.; Jayashree, A.; Sharma, R. K. *Chem. Commun.* **2019**, *55*, 7402.

51) Džambaski, Z.; Bondžić, B. P. *Org. Biomol. Chem.* **2019**, *17*, 6420.

52) Peng, Z.; Wang, Y.; Yu, Z.; Wu, H.; Fu, S.; Song, L.; Jiang, C. *Adv. Synth. Catal.* **2019**, *361*, 2048.

53) Brandhofer, T.; Gini, A.; Stockerl, S.; Piekarski, D. G.; Mancheño, O. G. *J. Org. Chem.* **2019**, *84*, 12992.

54) Xie, W.; Liu, N.; Gong, B.; Ning, S.; Che, X.; Cui, L.; Xiang, J. *Eur. J. Org. Chem.* **2019**, *2019*, 2498.

55) Yuan, Y.; Qiao, J.; Cao, Y.; Tang, J.; Wang, M.; Ke, G.; Lu, Y.; Liu, X.; Lei, A. *Chem. Commun.* **2019**, *55*, 4230.

56) Monterde, C.; Navarro, R.; Iglesias, M.; Sánchez, F. *ACS Appl. Mater. Interfaces* **2019**, *11*, 3459.

57) Clark, J. L.; Hill, J. E.; Rettig, I. D.; Beres, J. J.; Ziniuk, R.; Ohulchanskyy, T. Y.; McCormick, T. M.; Detty, M. R. *Organometallics* **2019**, *38*, 2431.

58) Döben, N.; Yan, H.; Kischkewitz, M.; Mao, J.; Studer, A. *Org. Lett.* **2018**, *20*, 7933.

59) Zhu, X.; Lin, Y.; San Martin, J.; Sun, Y.; Zhu, D.; Yan, Y. *Nat. Commun.* **2019**, *10*, 1.

60) Li, P.; Wang, G. W.; Zhu, X.; Wang, L. *Tetrahedron* **2019**, *75*, 3448.

61) Zhang, R.; Qin, Y.; Zhang, L.; Luo, S. *J. Org. Chem.* **2019**, *84*, 2542.

62) Ji, J.; Chen, L. Y.; Qiu, Z. Bin; Ren, X.; Li, Y. *Synth.* **2020**, *52*, 471.

63) Li, H.; Yang, Y.; He, C.; Zeng, L.; Duan, C. *ACS Catal.* 2019, *9*, 422.

64) Ullah, B.; Zhou, Y.; Chen, J.; Bao, Z.; Yang, Y.; Yang, Q.; Ren, Q.; Zhang, Z. *Tetrahedron Lett.* **2019**, *60*, 348.

65) Mandal, T.; Das, S.; De Sarkar, S. *Adv. Synth. Catal.* **2019**, *361*, 3200.

66) Sun, M.; Zhao, L.; Ding, M.-W. *J. Org. Chem.* **2019**, *84*, 14313.

67) Yi, B.; Yan, N.; Yi, N.; Xie, Y.; Wen, X.; Au, C. T.; Lan, D. *RSC Adv.* **2019**, *9*, 29721.

68) Xu, C.; Zhu, Z.; Wang, Y.; Jing, Z.; Gao, B.; Zhao, L.; Dong, W.-K. *J. Org. Chem.* **2019**, *84*, 2234.

69) Wang, T.; Wang, D. H. *Org. Lett.* **2019**, *21*, 3981.

70) Tian, H.; Xu, W.; Liu, Y.; Wang, Q. *Chem. Commun.* **2019**, *55*, 14813.

71) Zheng, J.; Breit, B. *Angew. Chemie - Int. Ed.* **2019**, *58*, 3392.

72) Li, B.; Wendlandt, A. E.; Stahl, S. S. *Org. Lett.* **2019**, *21*, 1176.

73) Hloušková, Z.; Klikar, M.; Pytela, O.; Almonasy, N.; Růžička, A.; Jandová, V.; Bureš, F. *RSC Adv.* **2019**, *9*, 23797.

74) Si, T.; Kim, H. Y.; Oh, K. *ACS Catal.* **2019**, *9*, 9216.

75) Nicholls, T. P.; Burt, L. K.; Simpson, P. V.; Massi, M.; Bissember, A. C. *Dalt. Trans.* **2019**, *48*, 12749.

76) Ji, J.; Chen, L. Y.; Qiu, Z. Bin; Ren, X.; Li, Y. *A. J. Org. Chem.* **2019**, *8*, 1436.

77) Sarma, D.; Majumdar, B.; Sarma, T. K. *Green Chem.* **2019**, *21*, 6717.

78) Xu, Y.; Xu, Z. J.; Liu, Z. P.; Lou, H. *Org. Chem. Front.* **2019**, *6*, 3902.

79) Quint, V.; Chouchène, N.; Askri, M.; Lalevée, J.; Gaumonta, A.-C.; Lakhdar, S. *Org. Chem. Front.* **2019**, *6*, 41.

80) Wang, J. J.; Schwedtmann, K.; Liu, K.; Schulz, S.; Haberstroh, J.; Schaper, G.; Wenke, A.; Naumann, J.; Wenke, T.; Wanke, S.; Weigand, J. J. *Green Chem.* **2021**, *23*, 881.

81) Potter, M. E.; Ross, C. P.; Gianolio, D.; Rios, R.; Raja, R. *Catal. Sci. Technol.* **2020**, *10*, 7262.

82) Gao, P. Sen; Weng, X. J.; Wang, Z. H.; Zheng, C.; Sun, B.; Chen, Z. H.; You, S. L.; Mei, T. S. *Angew. Chemie - Int. Ed.* **2020**, *59*, 15254.

83) Zhou, W.; Lu, W.; Wang, H.; Xia, Z.; Zhai, S.; Zhang, Z.; Ma, Y.; He, M.; Chen, Q. *Appl. Catal. A Gen.* **2020**, *604*, 117771.

84) Sun, Z.; Xia, Z.; Wang, A.; Wang, H.; Zhang, Z.; Zhou, W.; Qian, J.; He, M. *Tetrahedron Lett.* **2020**, *61*, 152254.

85) Xia, Q.; Li, Y.; Cheng, L.; Liang, X.; Cao, C.; Dai, P.; Deng, H.; Zhang, W.; Wang, Q. *Org. Lett.* **2020**, *22*, 9638.

86) Aramaki, Y.; Imaizumi, N.; Hotta, M.; Kumagai, J.; Ooi, T. *Chem. Sci.* **2020**, *11*, 4305.

87) Boess, E.; Hoof, M. V.; Birdsall, S. L.; Klussmann, M. *J. Org. Chem.* **2020**, *85*, 1972.

88) Li, C.; Dickson, R.; Rockstroh, N.; Rabeah, J.; Cordes, D. B.; Slawin, A. M. Z.; Hünemörder, P.; Spannenberg, A.; Bühl, M.; Mejía, E.; Zysman-Colman, E.; Kamer, P. C. *J. Catal. Sci. Technol.* **2020**, *10*, 7745.

89) Unglaube, F.; Hünemörder, P.; Guo, X.; Chen, Z.; Wang, D.; Mejía, E. *Helv. Chim. Acta* **2020**, 103.

90) Li, Z.; Ma, P.; Tan, Y.; Liu, Y.; Gao, M.; Zhang, Y.; Yang, B.; Huang, X.; Gao, Y.; Zhang, J. *Green Chem.* **2020**, *22*, 646.

91) Schönbauer, D.; Sambiagio, C.; Noël, T.; Schnürch, M. Beilstein *J. Org. Chem.* **2020**, *16*, 809.

92) Leng, L.; Ready, J. M. *ACS Catal.* **2020**, *10*, 13196.

93) Pang, J.; Di, Z.; Qin, J. S.; Yuan, S.; Lollar, C. T.; Li, J.; Zhang, P.; Wu, M.; Yuan, D.; Hong, M.; Zhou, H. C. *J. Am. Chem. Soc.* **2020**, *142*, 15020.

94) Liu, H.; Li, C.; Li, H.; Ren, Y.; Chen, J.; Tang, J.; Yang, Q. *ACS Appl. Mater. Interfaces* **2020**, *12*, 20354.

95) Xia, Q.; Li, Y.; Wang, X.; Dai, P.; Deng, H.; Zhang, W.-H. *Org. Lett.* **2020**, *22*, 7290.

96) Wang, H.; Lu, W.; Sun, Z.; Wang, A.; Zhou, W.; He, M.; Chen, Q. *Asian J. Org. Chem.* **2020**, *9*, 1769.

97) Kobayashi, F.; Fujita, M.; Ide, T.; Ito, Y.; Yamashita, K.; Egami, H.; Hamashima, Y.; *ACS Catal.* **2021**, *11*, 82.

98) Yang, L.; Qiu, Z.; Wu, J.; Zhao, J.; Shen, T.; Huang, X.; Liu Z.-Q. *Org. Lett.* **2021**, *23*, 3207.

99) Chao Lin, Peiwu Li, Lin Wang *Tetrahedron Lett.* **2021**, *73*, 153102.

100) Chang Xu, Fang-Qi Shen, Gaofeng Feng, Jian Jin *Org. Lett.* **2021**, *23*, 3913.

101) Bakre P. V.; Kamat D. P.; Mandrekar K. S.; Tilve S. G.; Ghosh N. N. *Mol. Catal.* **2020**, *496*, 111193.

NMR Spectra

SGT-KM-19-46 CDCL3 PMR

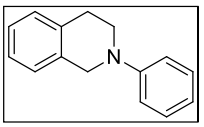

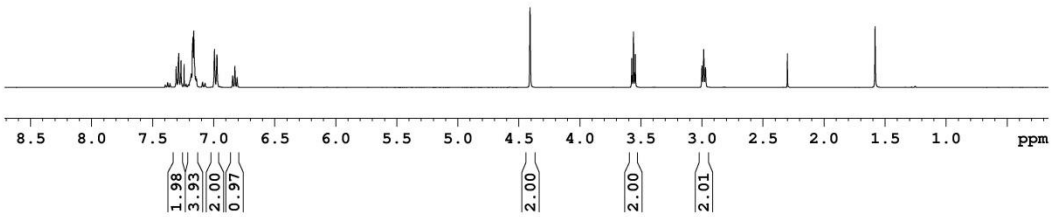

SGT-KM-19-46 CDCL3 CMR

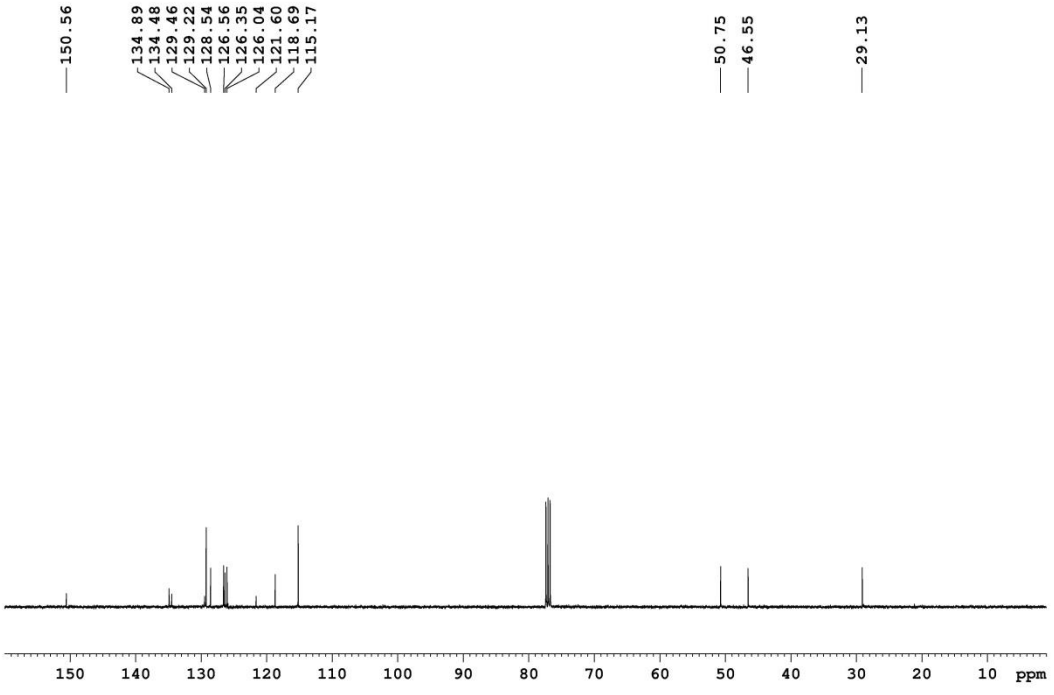

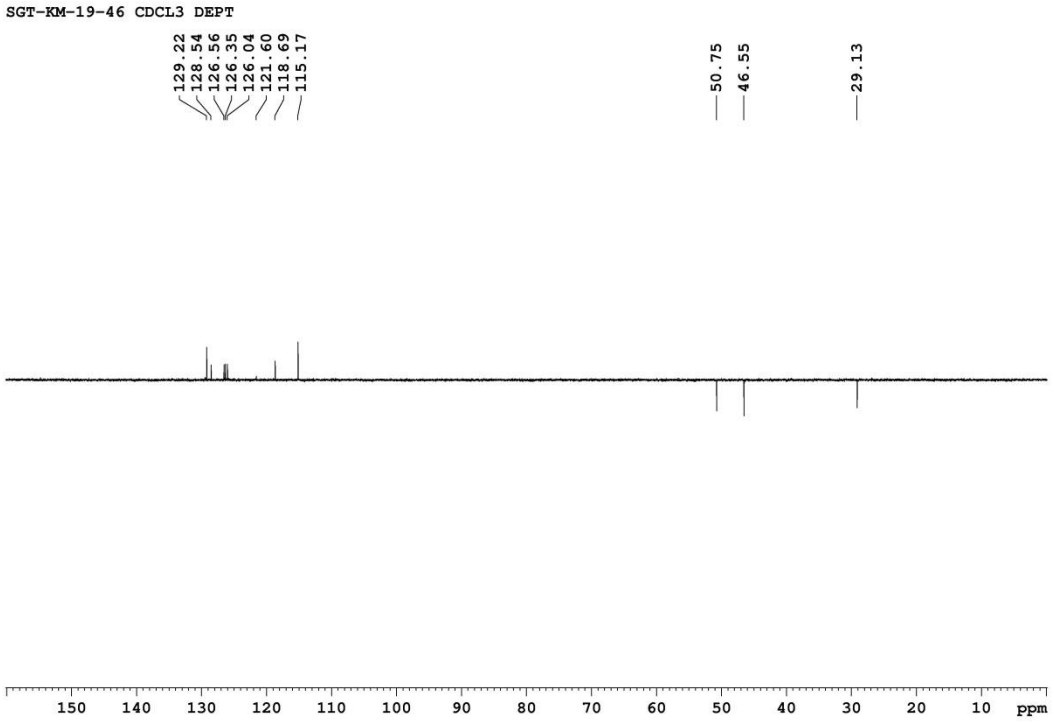
SGT-KM-19-46 CDCL3 DEPT
129.22
128.54
126.56
126.35
126.04
121.60
118.69
115.17
50.75
46.55
29.13
150 140 130 120 110 100 90 80 70 60 50 40 30 20 10 ppm

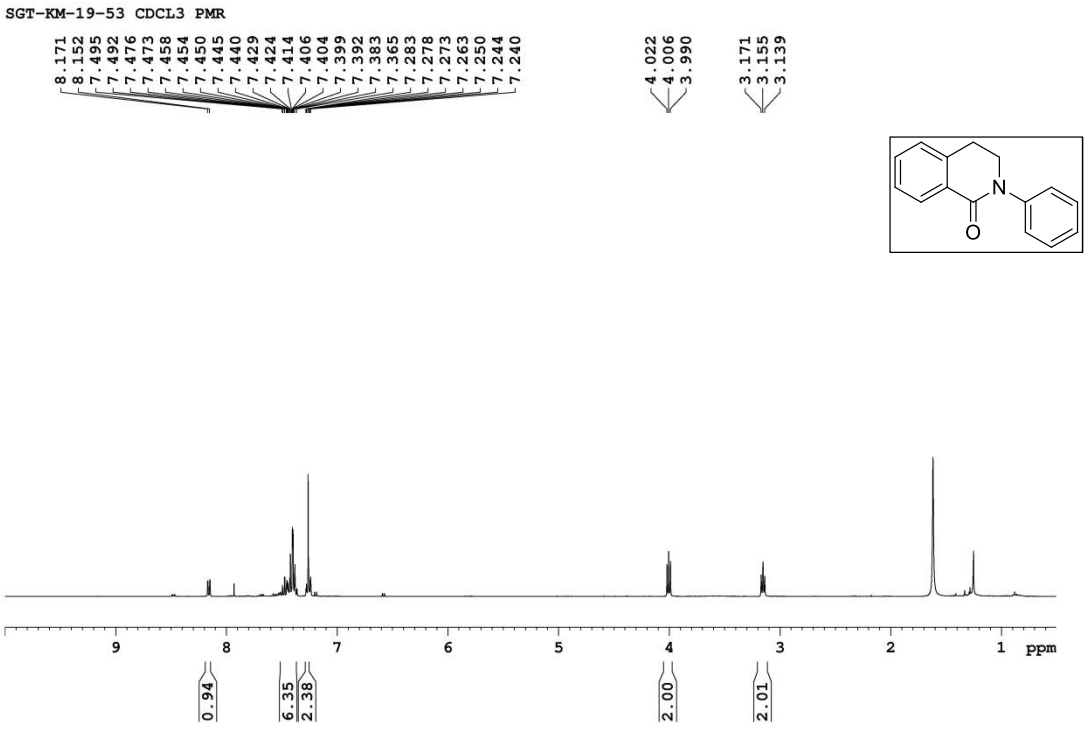
SGT-KM-19-53 CDCL3 PMR
8.171
8.152
7.495
7.492
7.476
7.473
7.458
7.454
7.450
7.445
7.440
7.429
7.424
7.414
7.406
7.404
7.399
7.392
7.383
7.365
7.283
7.278
7.273
7.263
7.250
7.244
7.240
4.022
4.006
3.990
3.171
3.155
3.139
N
O
9 8 7 6 5 4 3 2 1 ppm
0.94
6.35
2.38
2.00
2.01

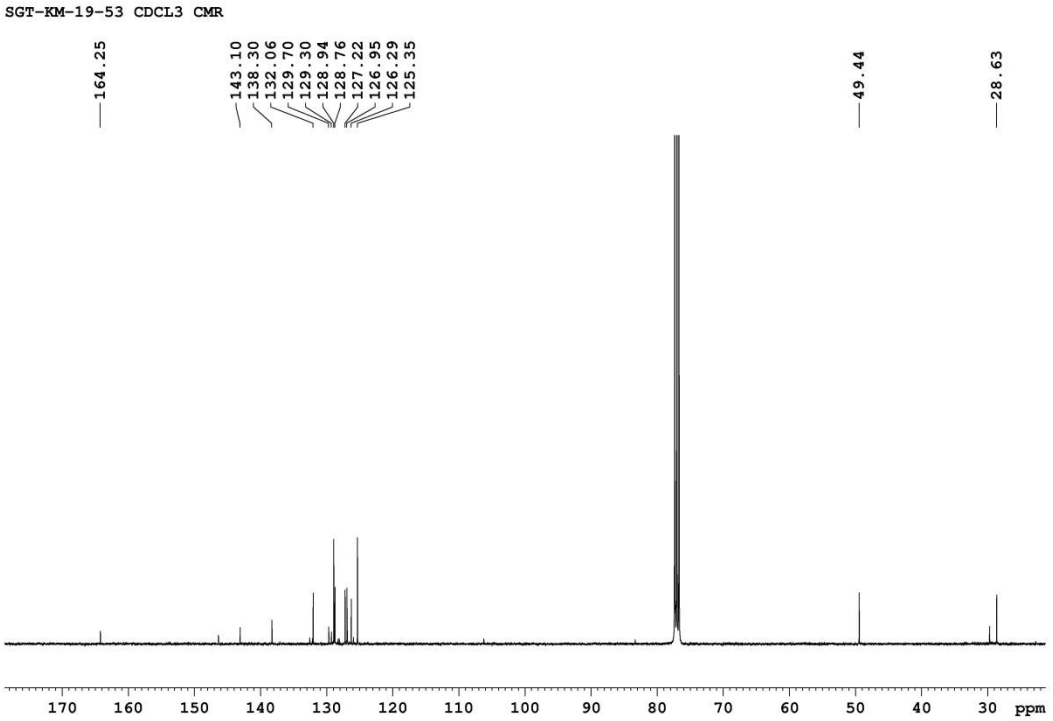
SGT-KM-19-53 CDCL3 CMR
164.25
143.10
138.30
132.06
129.70
129.30
128.94
128.76
127.22
126.95
126.29
125.35
49.44
28.63
170
160
150
140
130
120
110
100
90
80
70
60
50
40
30
ppm

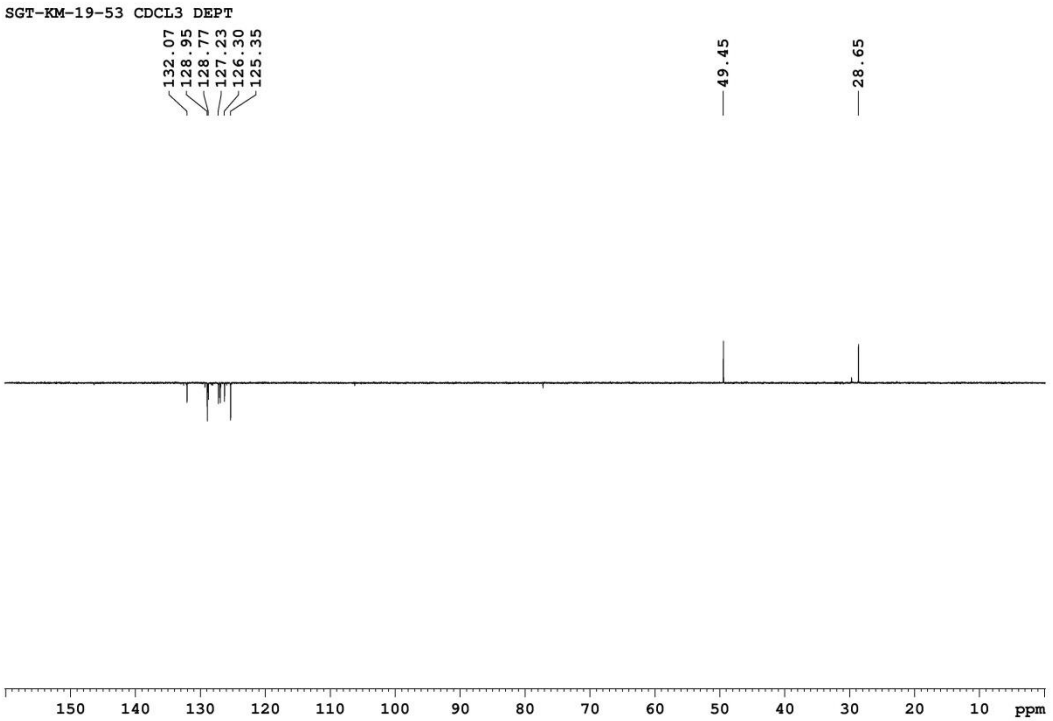
SGT-KM-19-53 CDCL3 DEPT
132.07
128.95
128.77
127.23
126.30
125.35
49.45
28.65
150
140
130
120
110
100
90
80
70
60
50
40
30
20
10
ppm

SGT-KM-20-11-02 CDCL3 PMR

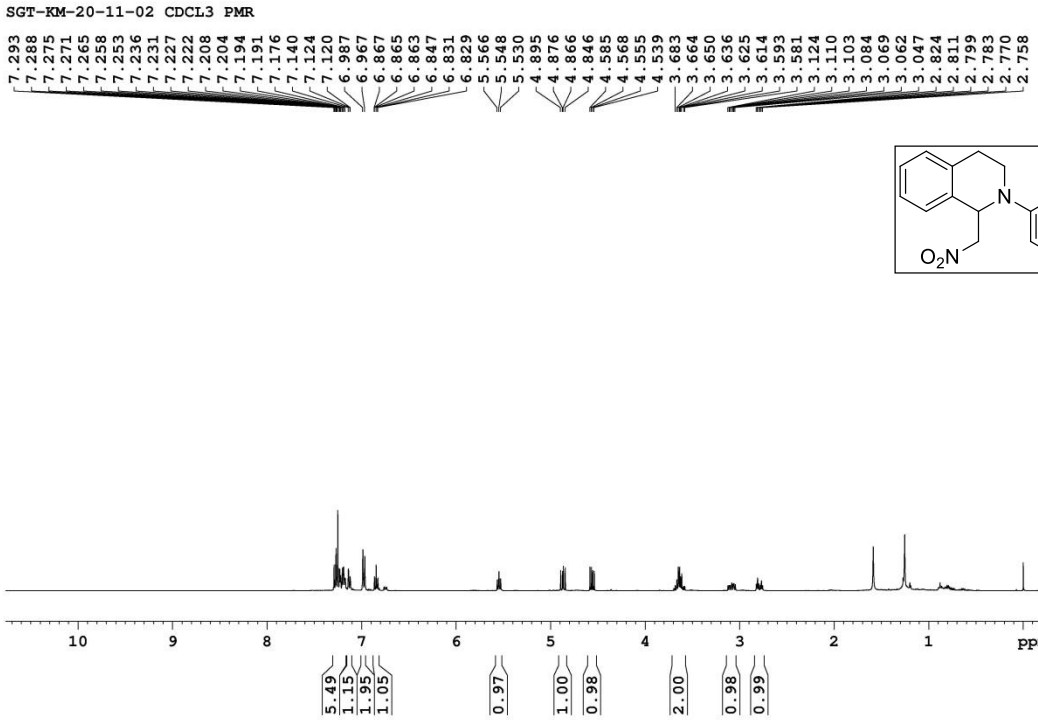

SGT-KM-20-11-02 CDCL3 CMR

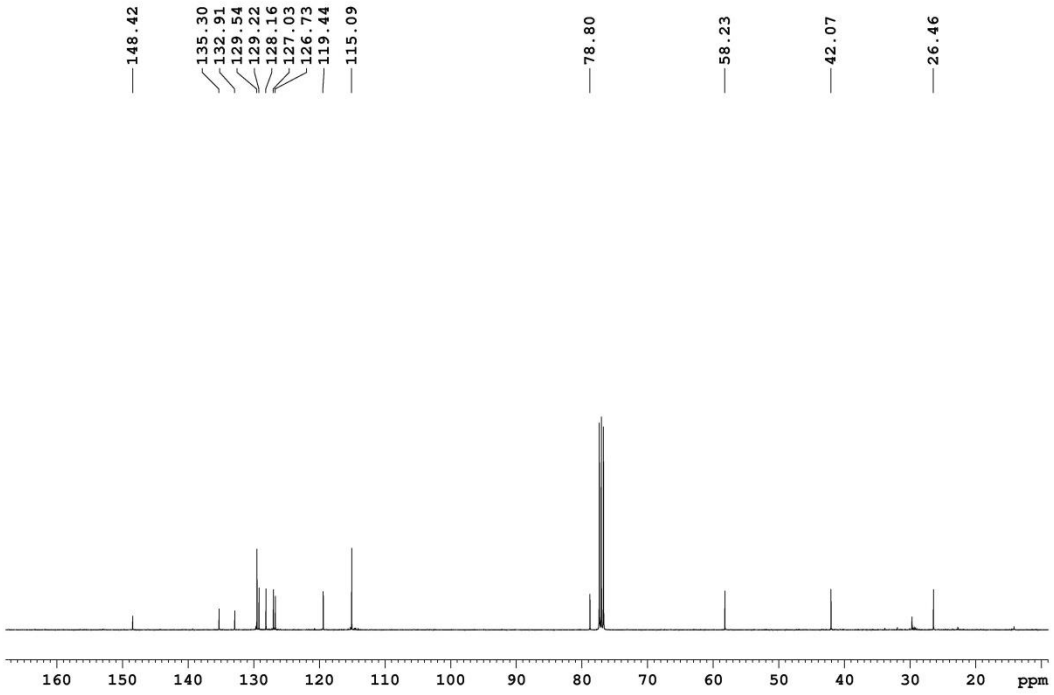

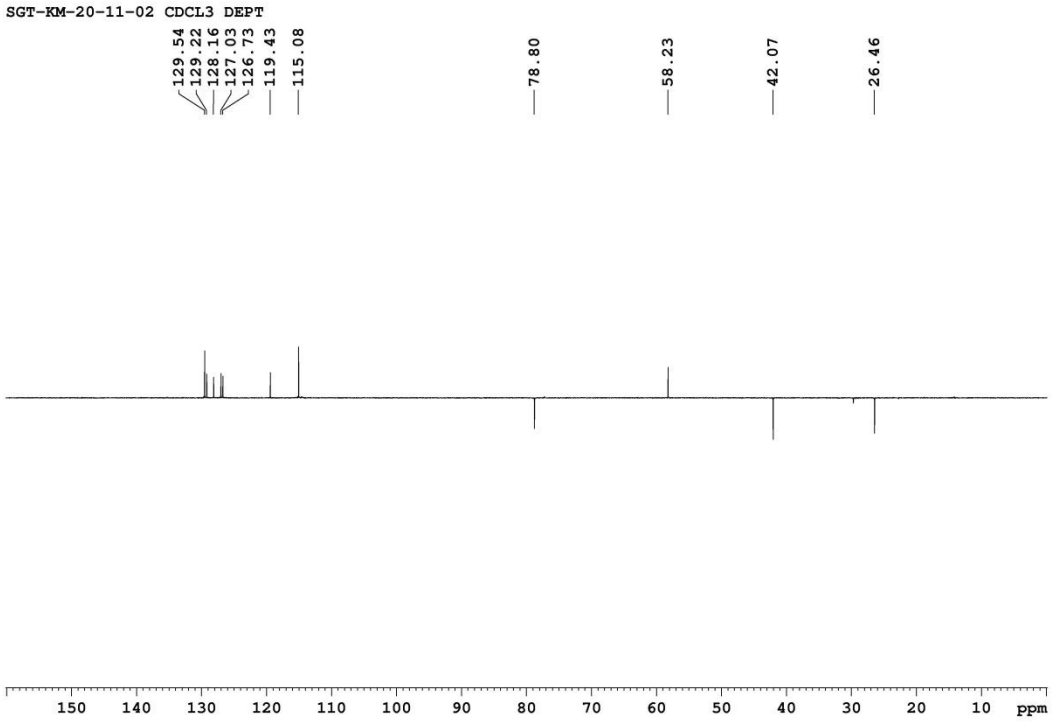
SGT-KM-20-11-02 CDCL3 DEPT
129.54
129.22
128.16
127.03
126.73
119.43
115.08
78.80
58.23
42.07
26.46
150 140 130 120 110 100 90 80 70 60 50 40 30 20 10 ppm

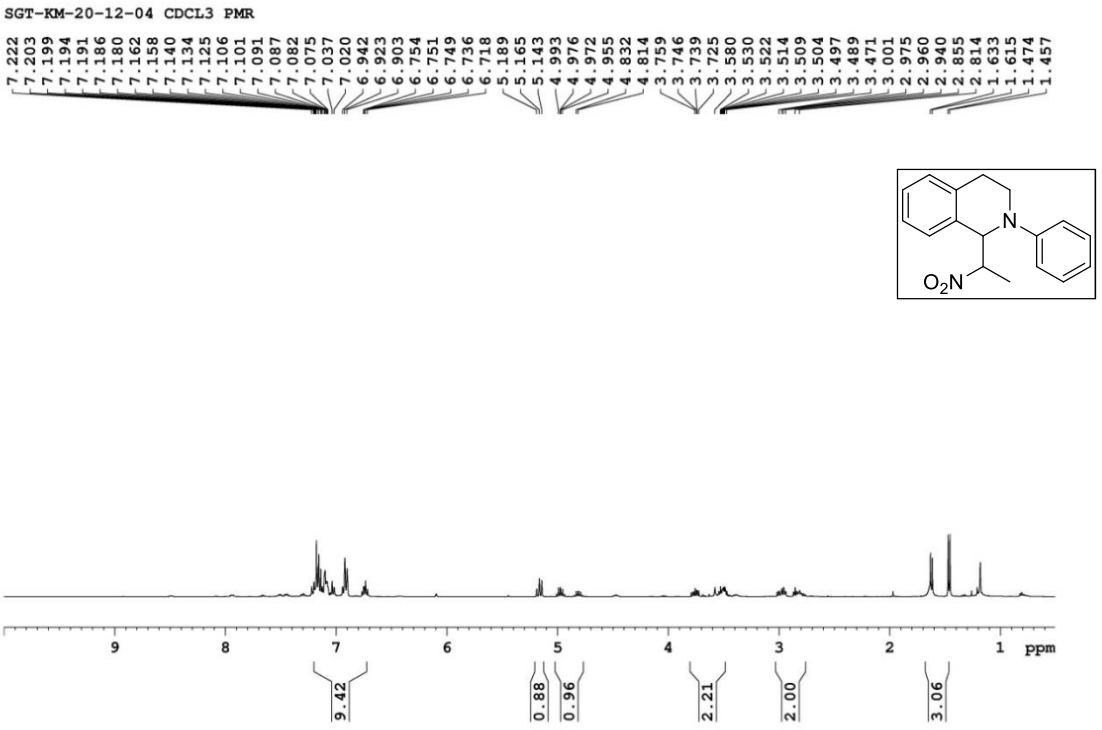
SGT-KM-20-12-04 CDCL3 PMR
7.222 7.203 7.199 7.194 7.191 7.186 7.180 7.162 7.158 7.140 7.134 7.125 7.106 7.101 7.091 7.087 7.082 7.075 7.037 7.020 6.942 6.923 6.903 6.754 6.751 6.749 6.736 6.718 5.189 5.165 5.143 4.993 4.976 4.972 4.955 4.832 4.814 3.759 3.746 3.739 3.725 3.580 3.530 3.522 3.514 3.509 3.504 3.497 3.489 3.471 3.001 2.975 2.960 2.940 2.855 2.814 1.633 1.615 1.474 1.457
N
O2N
9 8 7 6 5 4 3 2 1 ppm
9.42
0.88
0.96
2.21
2.00
3.06

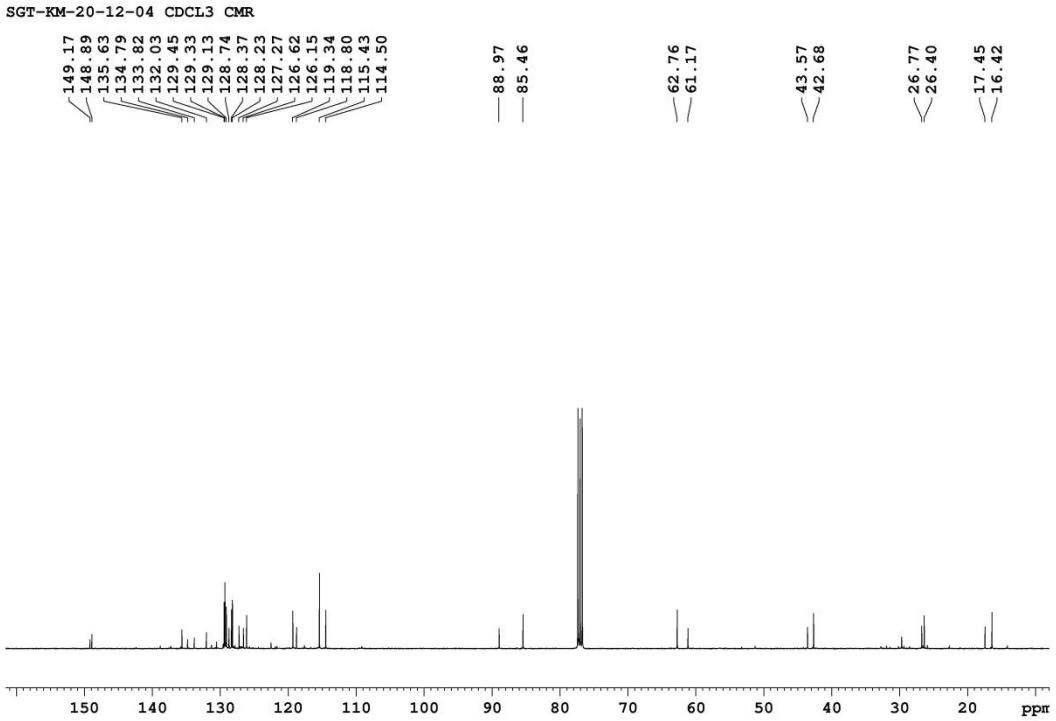
SGT-KM-20-12-04 CDCL3 CMR
149.17
148.89
135.63
134.79
133.82
132.03
129.45
129.33
129.13
128.74
128.37
128.23
127.27
126.62
126.15
119.34
118.80
115.43
114.50
88.97
85.46
62.76
61.17
43.57
42.68
26.77
26.40
17.45
16.42
150 140 130 120 110 100 90 80 70 60 50 40 30 20 ppm

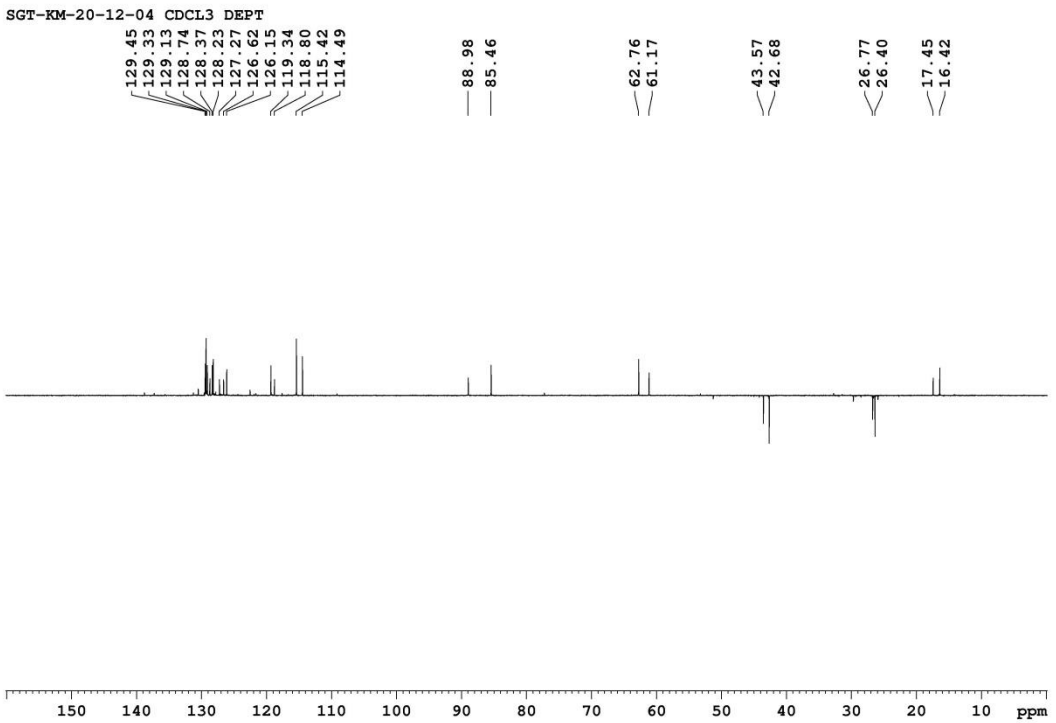
SGT-KM-20-12-04 CDCL3 DEPT
129.45
129.33
129.13
128.74
128.37
128.23
127.27
126.62
126.15
119.34
118.80
115.42
114.49
88.98
85.46
62.76
61.17
43.57
42.68
26.77
26.40
17.45
16.42
150 140 130 120 110 100 90 80 70 60 50 40 30 20 10 ppm

SGT-KM-20-12-01 CDCL3 PMR

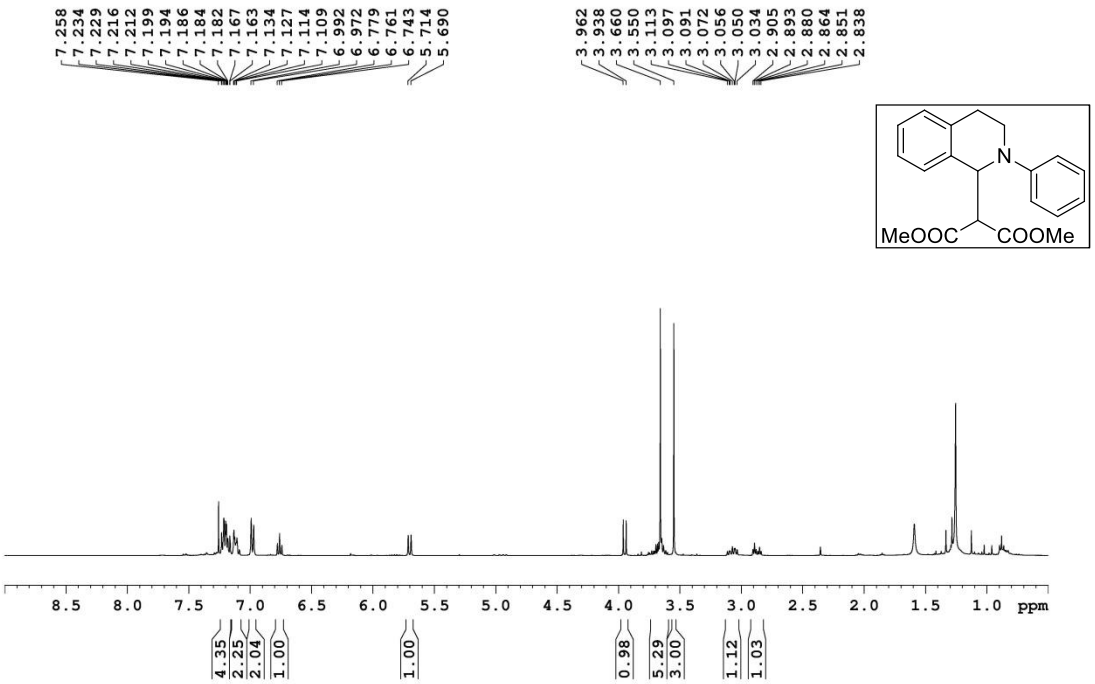

SGT-KM-20-12-01 CDCL3 CMR

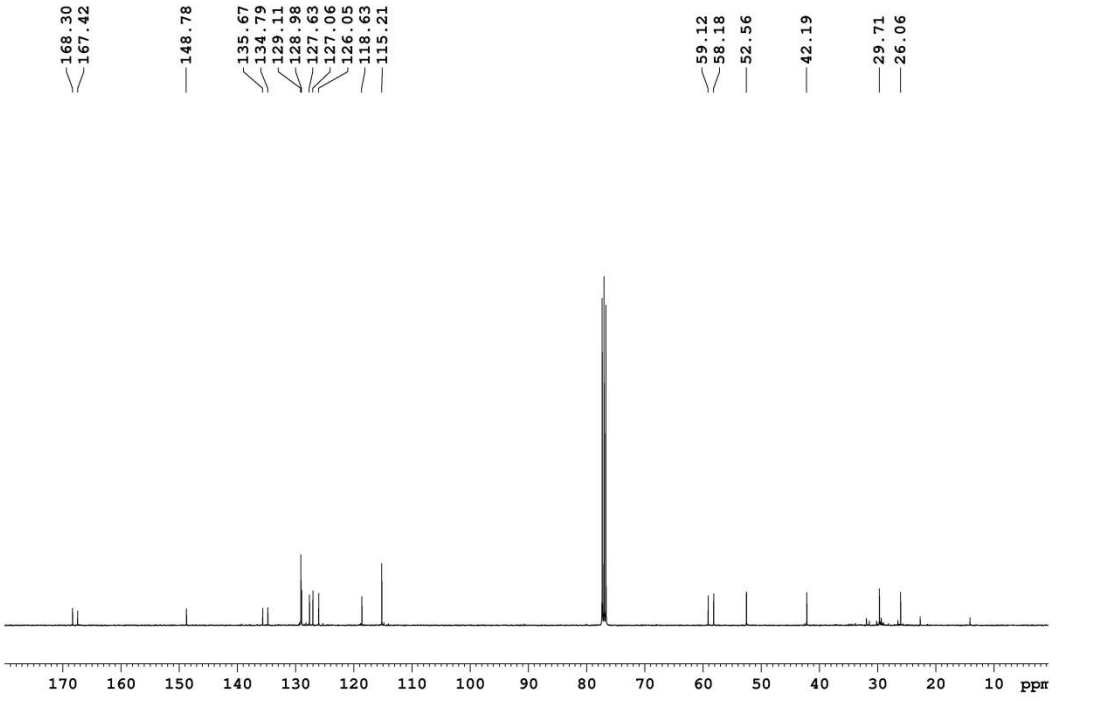

SGT-KM-20-12-01 CDCL3 DEPT

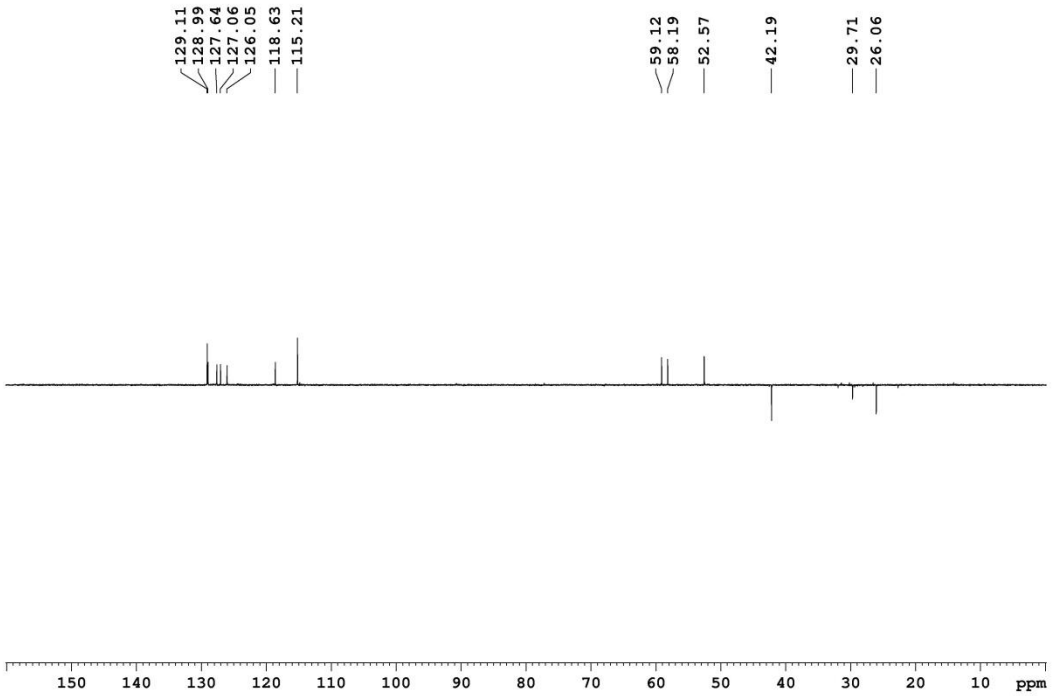

SGT-KM-20-11-21 CDCL3 PMR

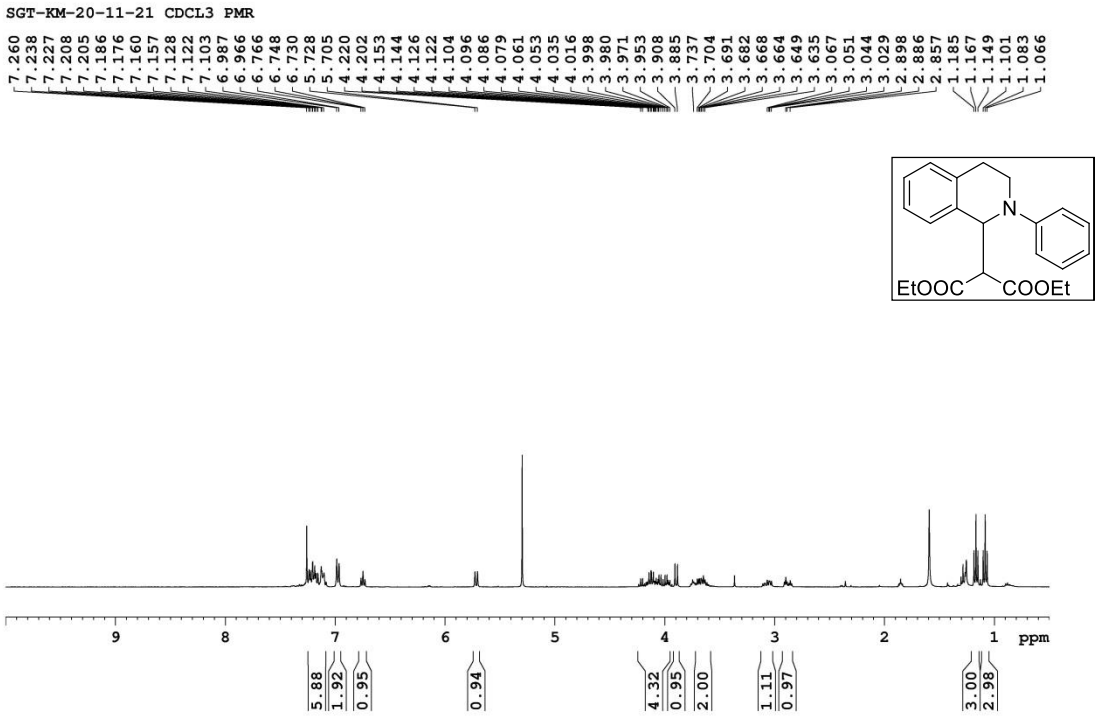

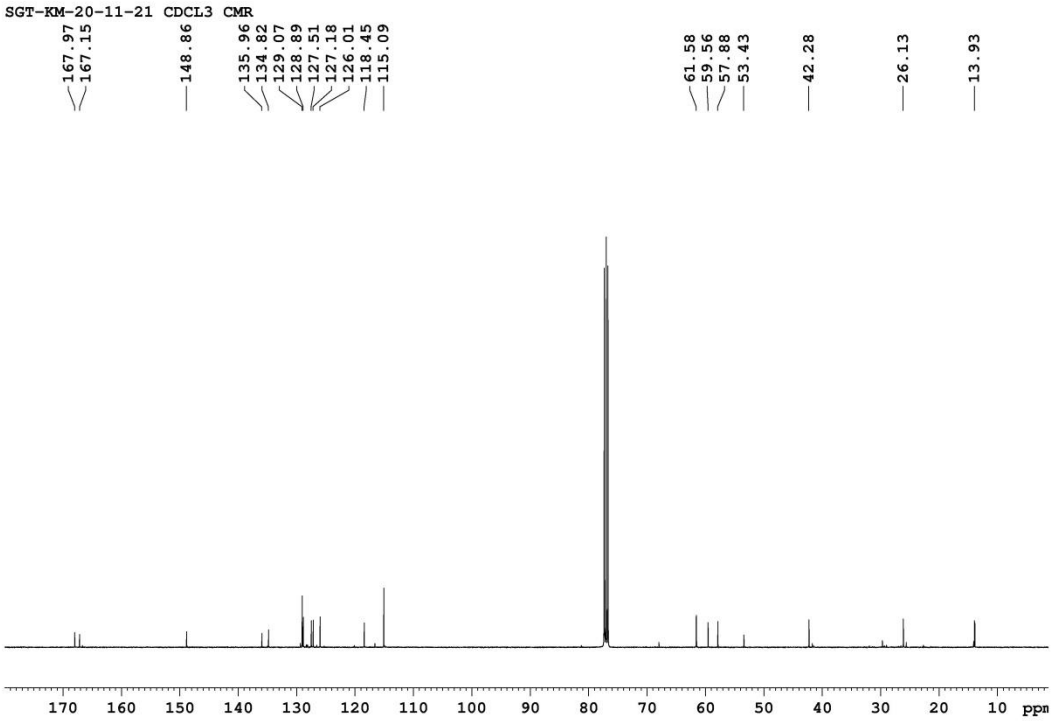
SGT-KM-20-11-21 CDCL3 CMR
167.97
167.15
148.86
135.96
134.82
129.07
128.89
127.51
127.18
126.01
118.45
115.09
61.58
59.56
57.88
53.43
42.28
26.13
13.93
170 160 150 140 130 120 110 100 90 80 70 60 50 40 30 20 10 ppm

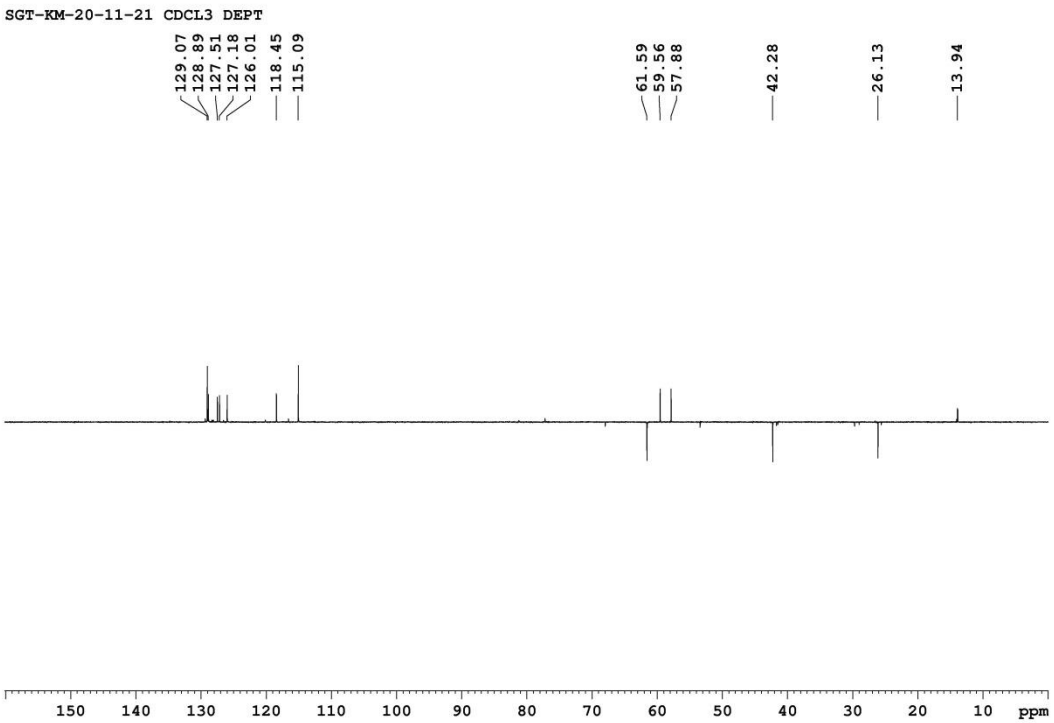
SGT-KM-20-11-21 CDCL3 DEPT
129.07
128.89
127.51
127.18
126.01
118.45
115.09
61.59
59.56
57.88
42.28
26.13
13.94
150 140 130 120 110 100 90 80 70 60 50 40 30 20 10 ppm

SGT-KM-21-04-06 CDCL3 PMR

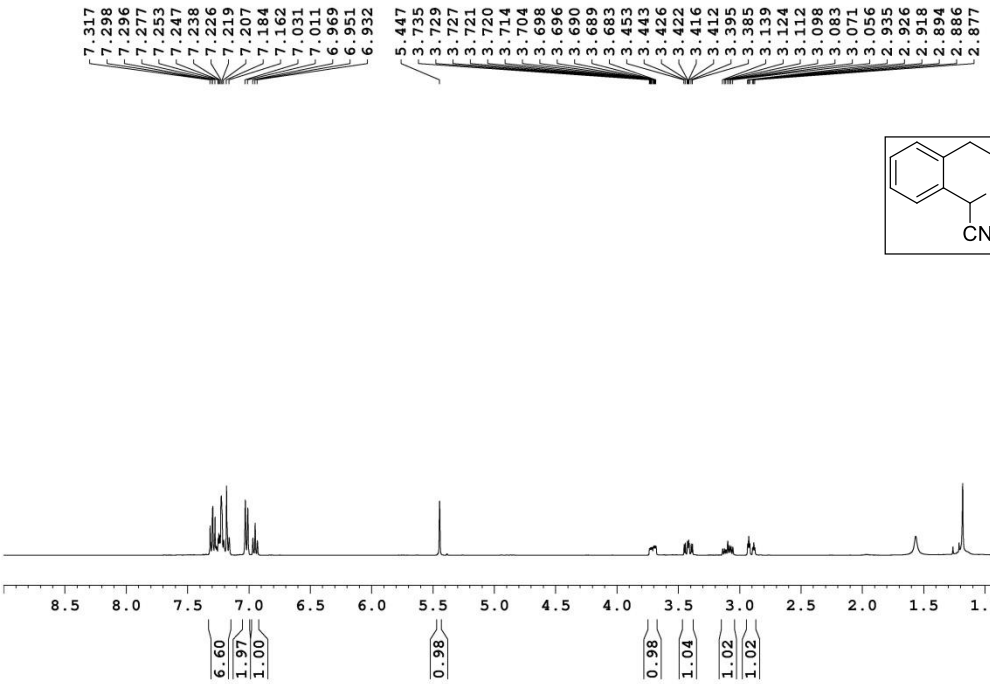

SGT-KM-21-04-06 CDCL3 CMR

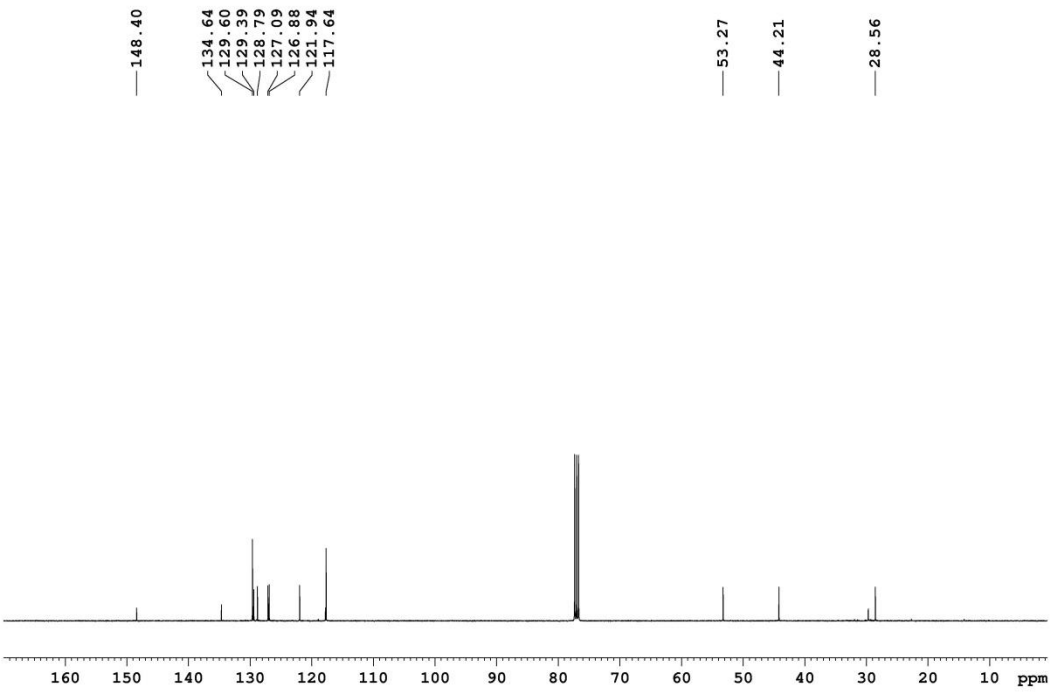

SGT-KM-21-04-06 CDCL3 DEPT

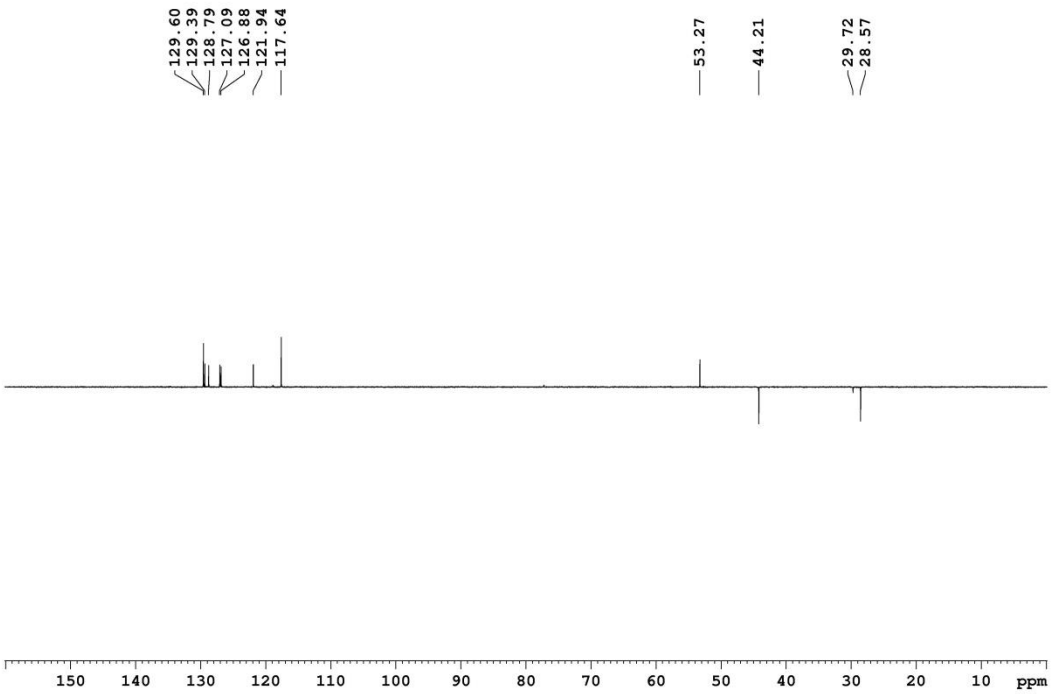

SGT-KM-21-03-03 CDCL3 PMR

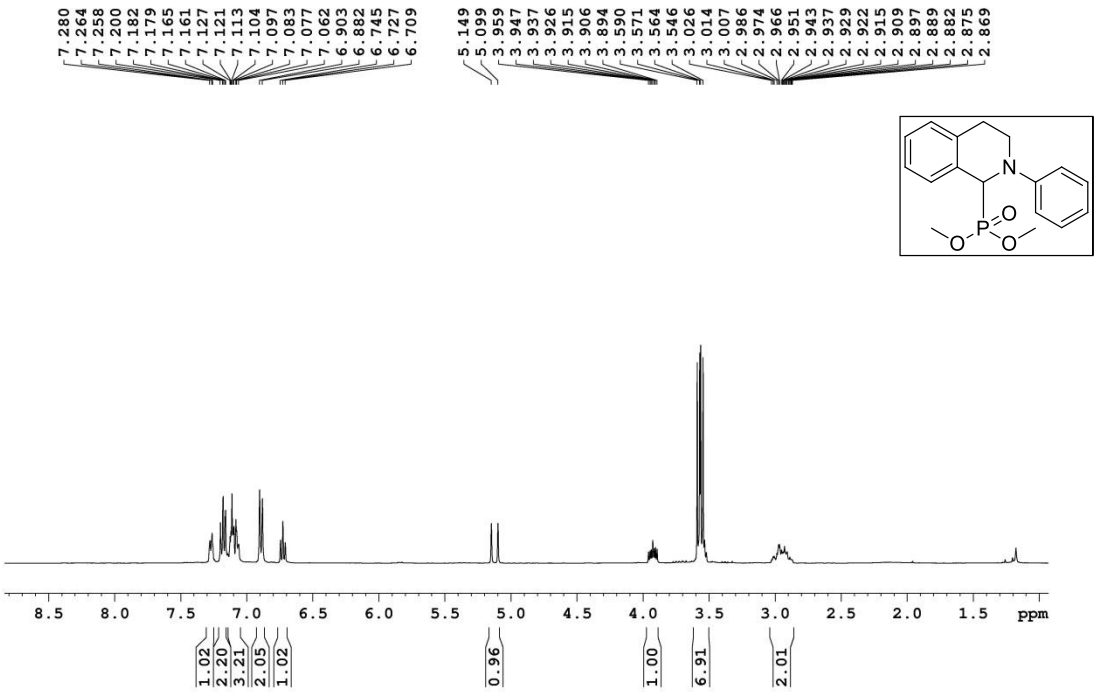

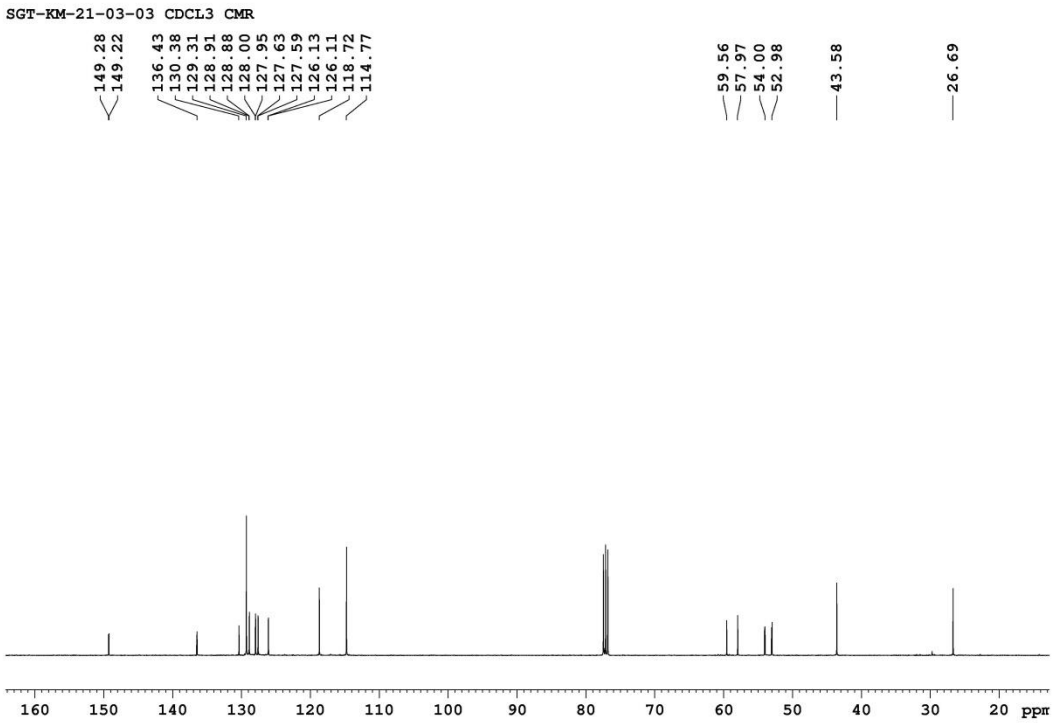
SGT-KM-21-03-03 CDCL3 CMR
149.28
149.22
136.43
130.38
129.31
128.91
128.88
128.00
127.95
127.63
127.59
126.13
126.11
118.72
114.77
59.56
57.97
54.00
52.98
43.58
26.69
160 150 140 130 120 110 100 90 80 70 60 50 40 30 20 ppm

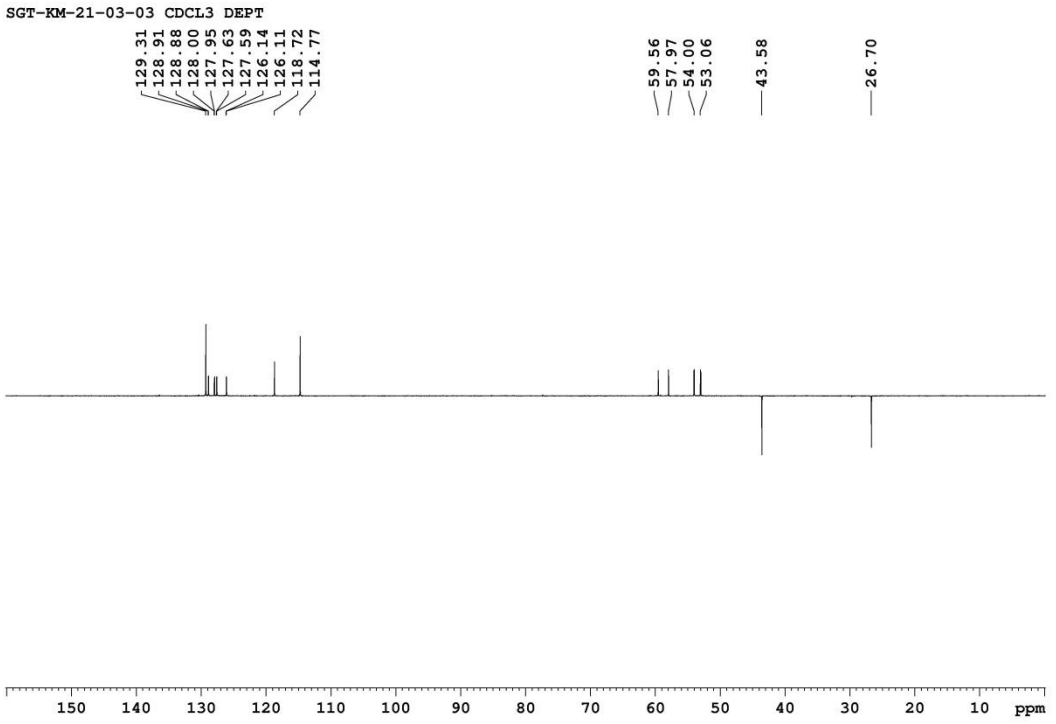
SGT-KM-21-03-03 CDCL3 DEPT
129.31
128.91
128.88
128.00
127.95
127.63
127.59
126.14
126.11
118.72
114.77
59.56
57.97
54.00
53.06
43.58
26.70
150 140 130 120 110 100 90 80 70 60 50 40 30 20 10 ppm

SGT-KM-21-04-02 CDCL3 PMR

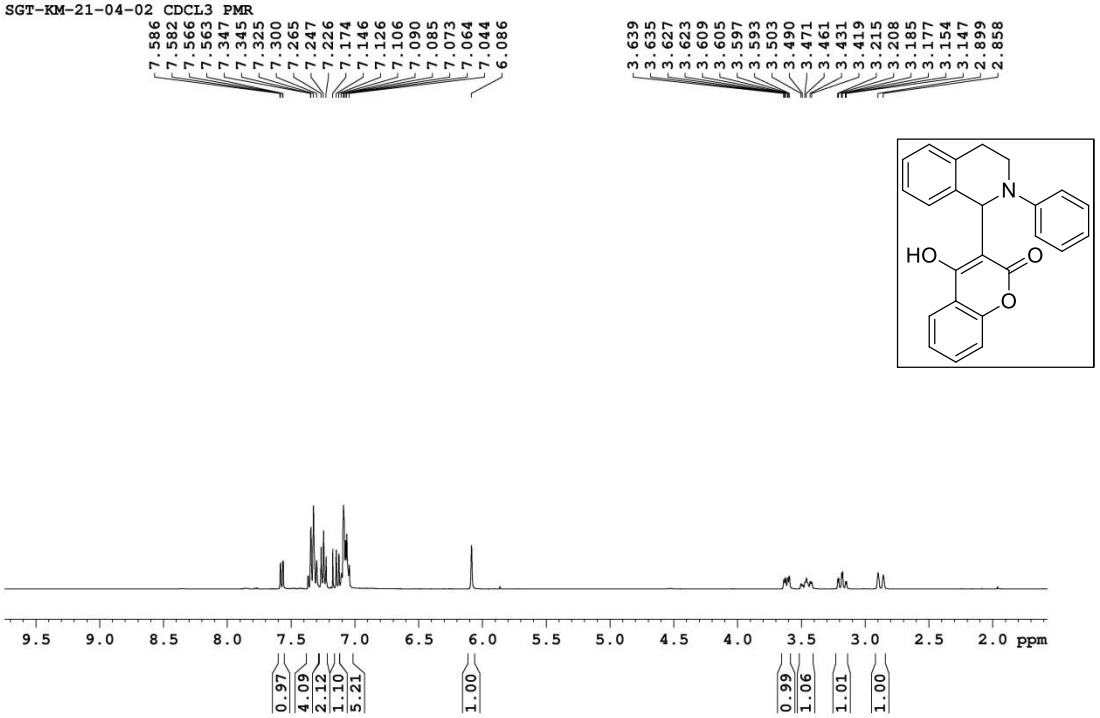

SGT-KM-21-04-02-B CDCL3 CMR

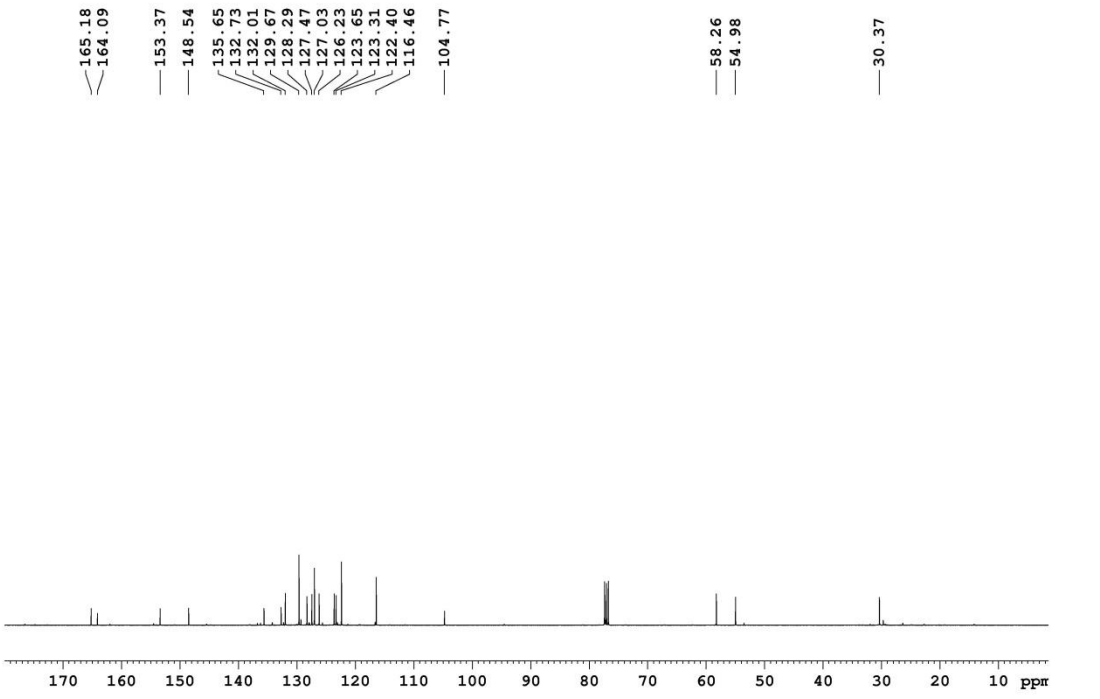

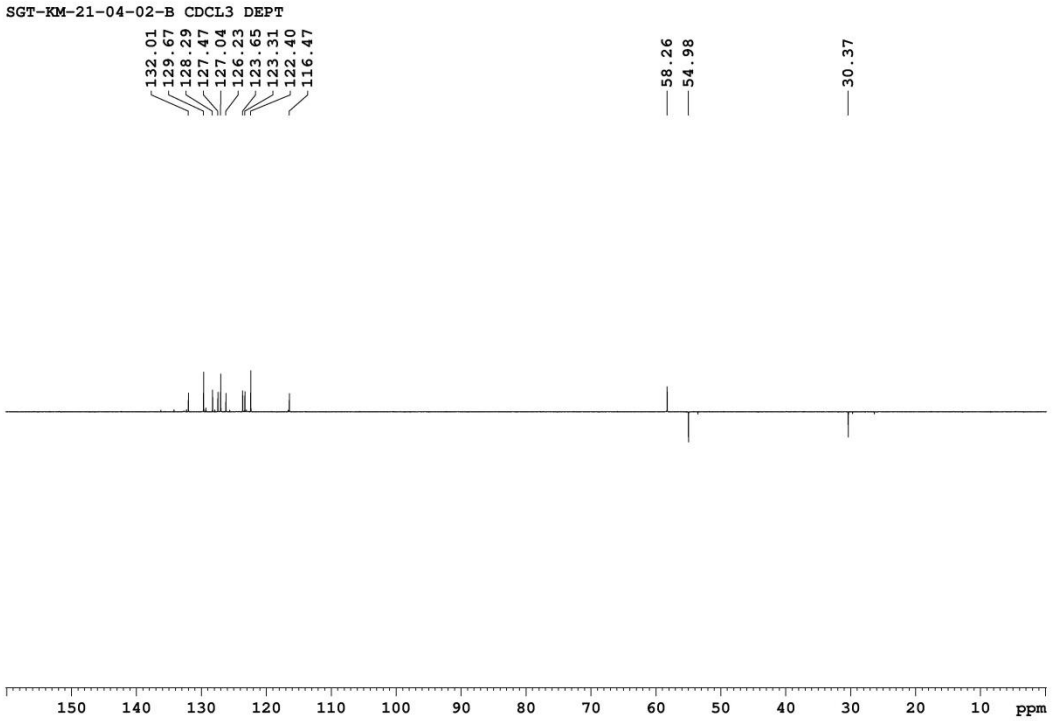
SGT-KM-21-04-02-B CDCL3 DEPT
132.01
129.67
128.29
127.47
127.04
126.23
123.65
123.31
122.40
116.47
58.26
54.98
30.37
150
140
130
120
110
100
90
80
70
60
50
40
30
20
10
ppm

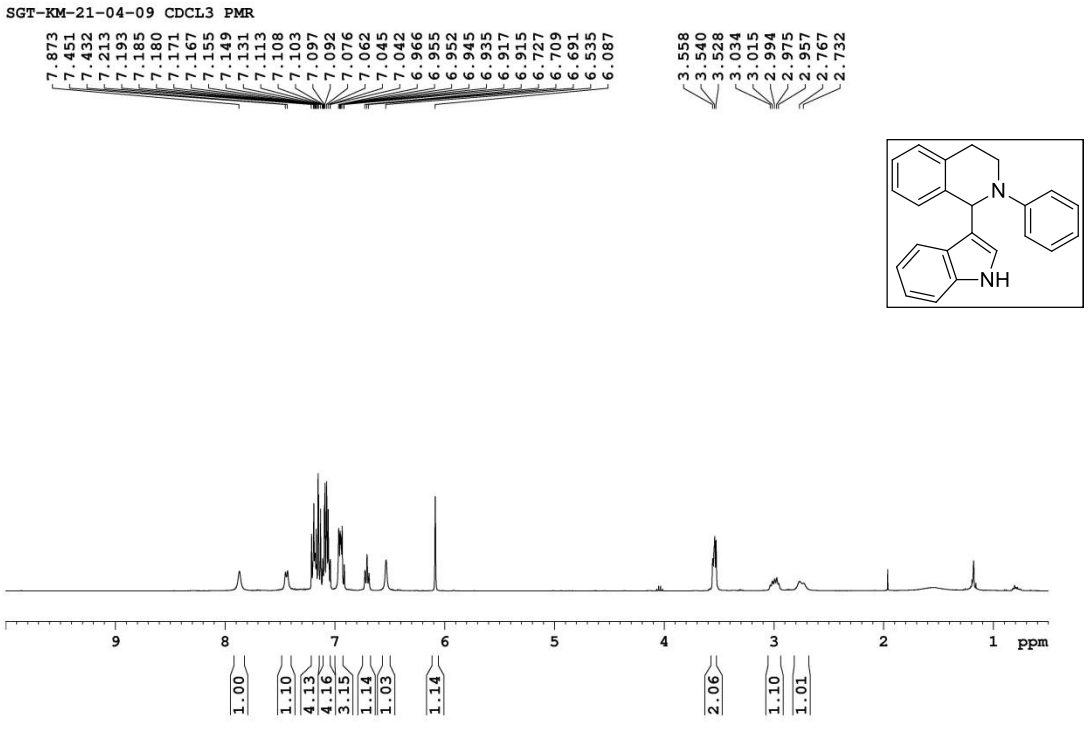
SGT-KM-21-04-09 CDCL3 PMR
7.873
7.451
7.432
7.213
7.193
7.185
7.180
7.171
7.167
7.155
7.149
7.131
7.113
7.108
7.103
7.097
7.092
7.076
7.062
7.045
7.042
6.966
6.955
6.952
6.945
6.935
6.917
6.915
6.727
6.709
6.691
6.535
6.087
3.558
3.540
3.528
3.034
3.015
2.994
2.975
2.957
2.767
2.732
N
NH
9
8
7
6
5
4
3
2
1
ppm
1.00
1.10
4.13
4.16
3.15
1.14
1.03
1.14
2.06
1.10
1.01

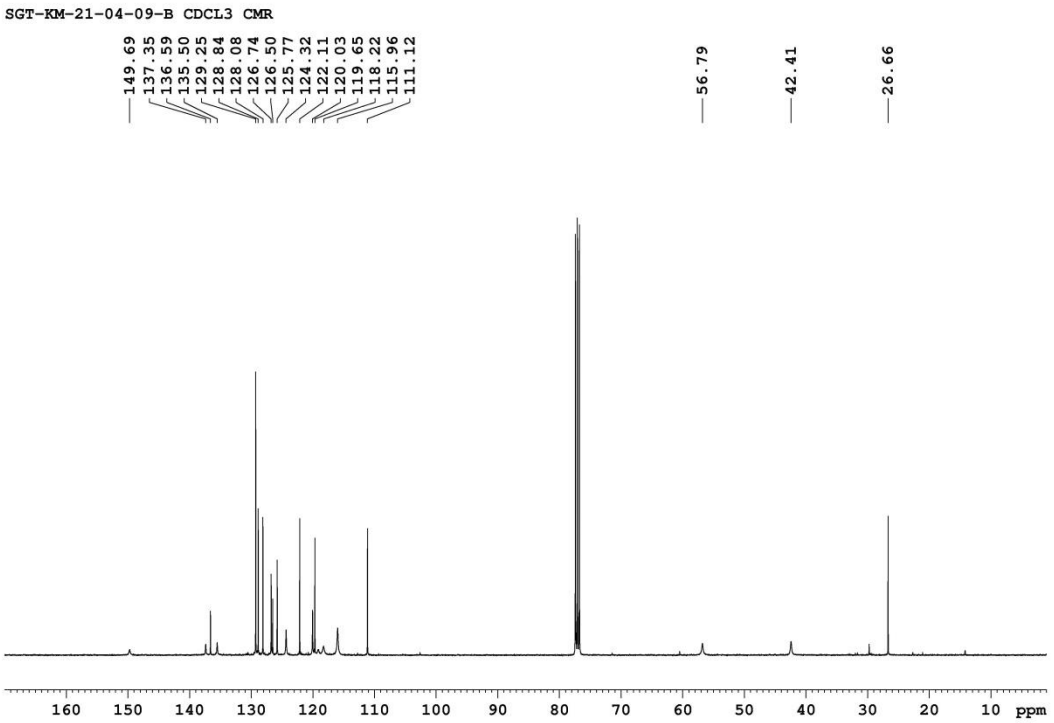
SGT-KM-21-04-09-B CDCL3 CMR
149.69
137.35
136.59
135.50
129.25
128.84
128.08
126.74
126.50
125.77
124.32
122.11
120.03
119.65
118.22
115.96
111.12
56.79
42.41
26.66
160 150 140 130 120 110 100 90 80 70 60 50 40 30 20 10 ppm

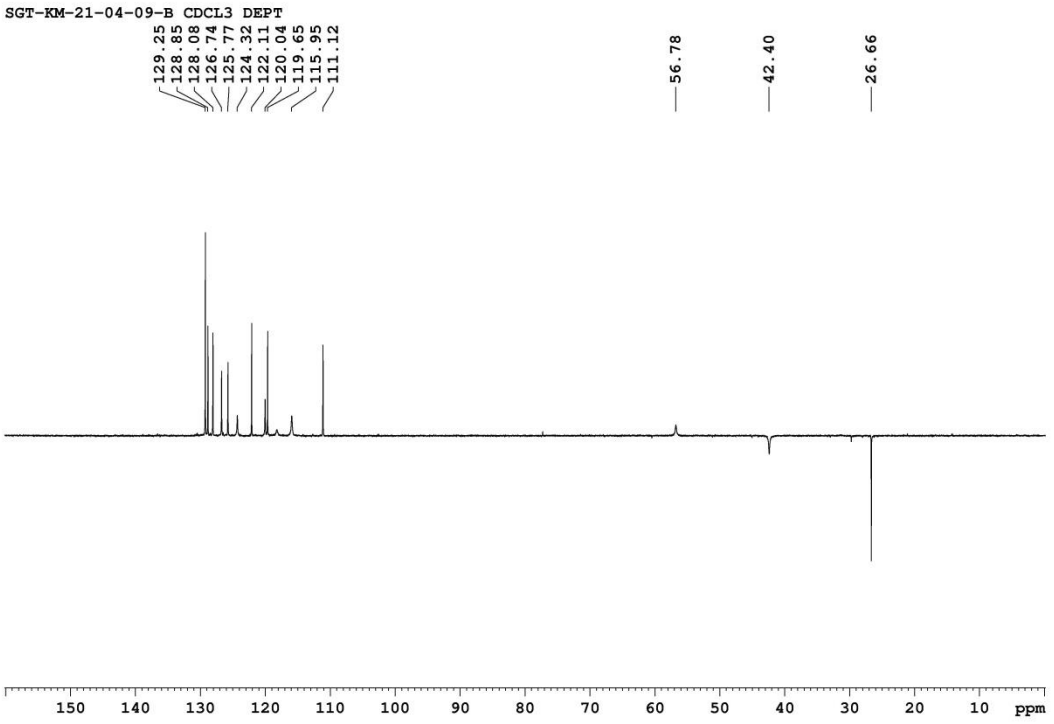
SGT-KM-21-04-09-B CDCL3 DEPT
129.25
128.85
128.08
126.74
125.77
124.32
122.11
120.04
119.65
115.95
111.12
56.78
42.40
26.66
150 140 130 120 110 100 90 80 70 60 50 40 30 20 10 ppm

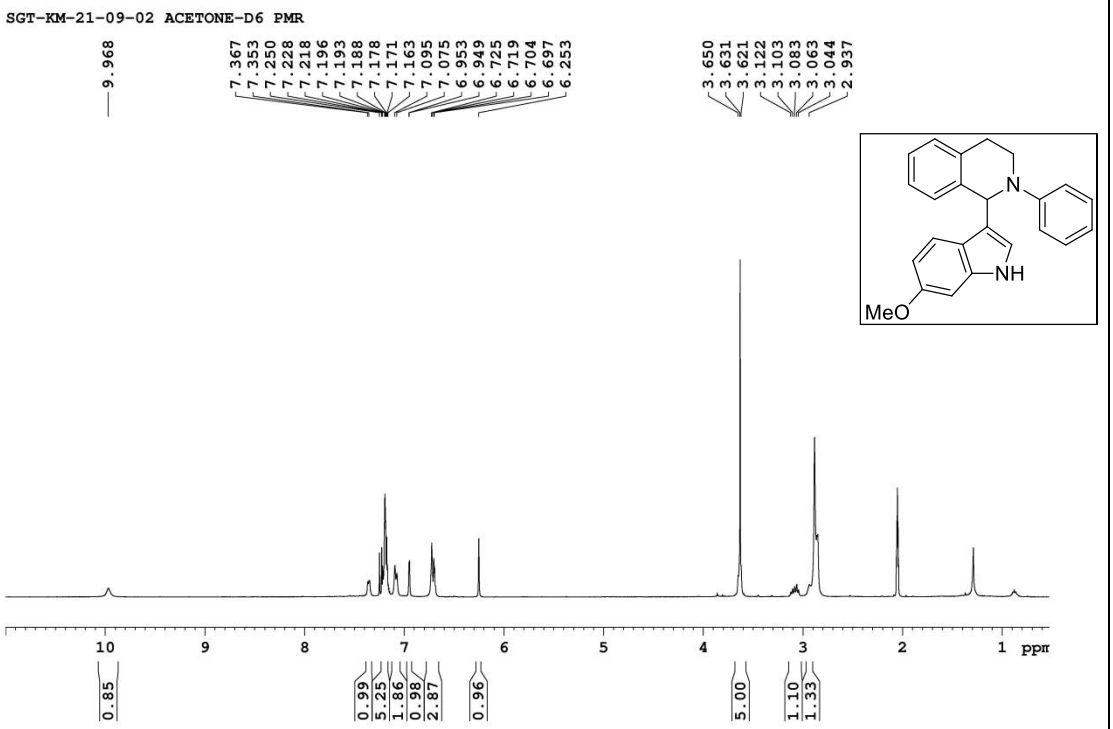
SGT-KM-21-09-02 ACETONE-D6 PMR
9.968
7.367
7.353
7.250
7.228
7.218
7.196
7.193
7.188
7.178
7.171
7.163
7.095
7.075
6.953
6.949
6.725
6.719
6.704
6.697
6.253
3.650
3.631
3.621
3.122
3.103
3.083
3.063
3.044
2.937
N
NH
MeO
10
9
8
7
6
5
4
3
2
1 ppm
0.85
0.99
5.25
1.86
0.98
2.87
0.96
5.00
1.10
1.33

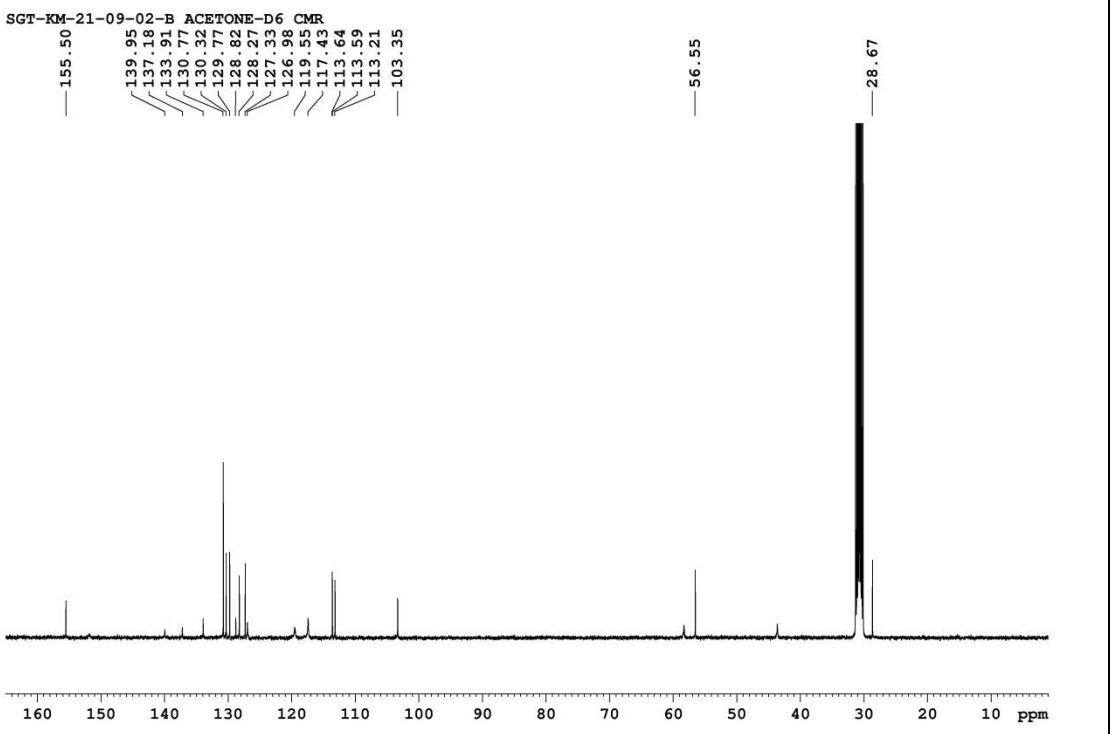
SGT-KM-21-09-02-B ACETONE-D6 CMR
155.50
139.95
137.18
133.91
130.77
130.32
129.77
128.82
128.27
127.33
126.98
119.55
117.43
113.64
113.59
113.21
103.35
56.55
28.67
160
150
140
130
120
110
100
90
80
70
60
50
40
30
20
10 ppm

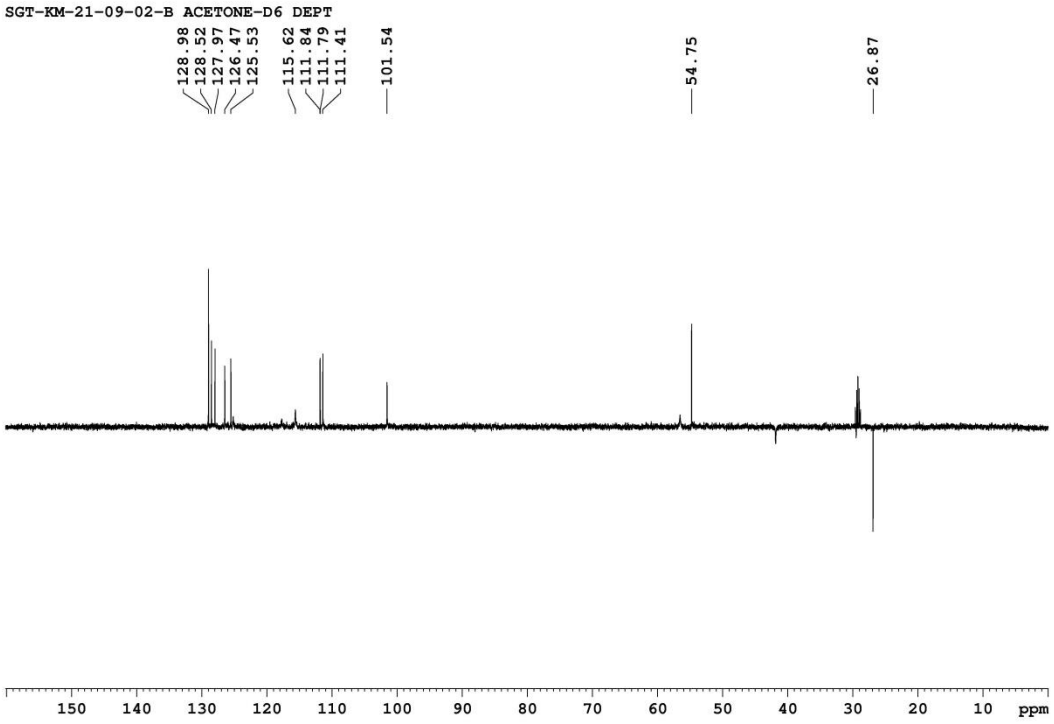
SGT-KM-21-09-02-B ACETONE-D6 DEPT
128.98
128.52
127.97
126.47
125.53
115.62
111.84
111.79
111.41
101.54
54.75
26.87
150 140 130 120 110 100 90 80 70 60 50 40 30 20 10 ppm

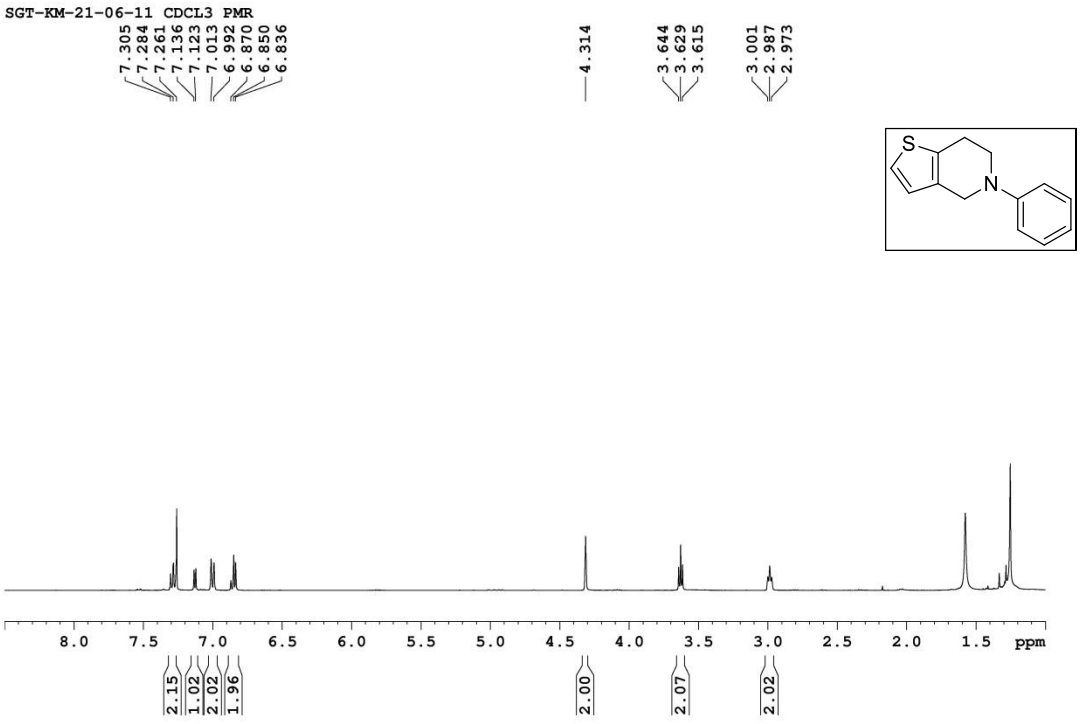
SGT-KM-21-06-11 CDCL3 PMR
7.305
7.284
7.261
7.136
7.123
7.013
6.992
6.870
6.850
6.836
4.314
3.644
3.629
3.615
3.001
2.987
2.973
S
N
8.0 7.5 7.0 6.5 6.0 5.5 5.0 4.5 4.0 3.5 3.0 2.5 2.0 1.5 ppm
2.15
1.02
2.02
1.96
2.00
2.07
2.02

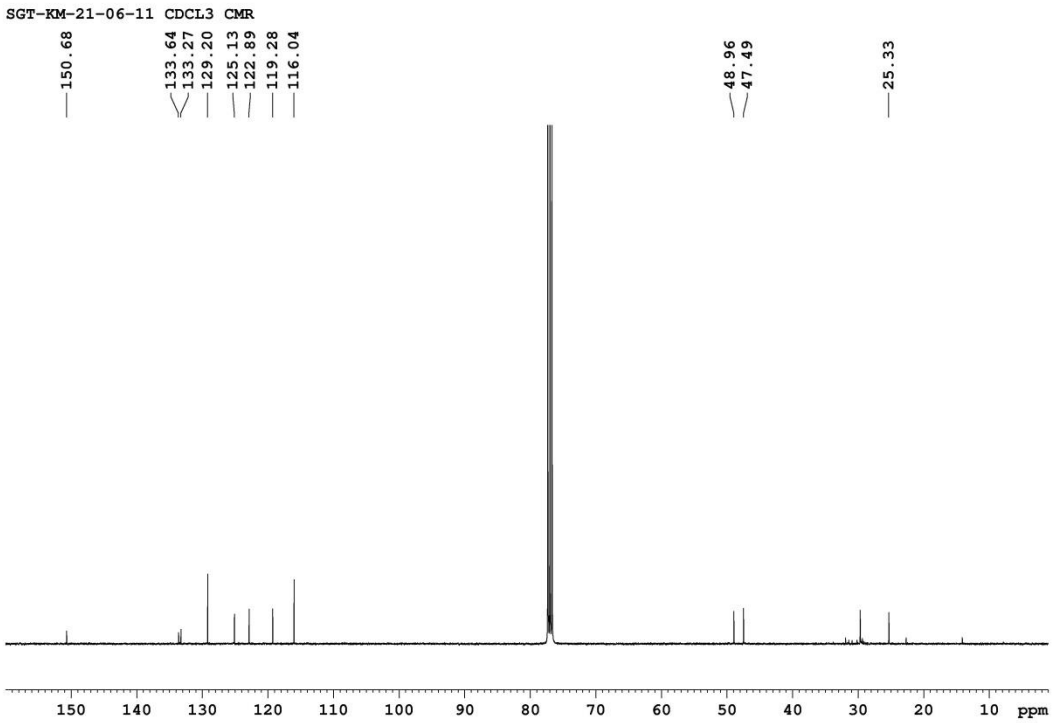
SGT-KM-21-06-11 CDCL3 CMR
150.68
133.64
133.27
129.20
125.13
122.89
119.28
116.04
48.96
47.49
25.33
150 140 130 120 110 100 90 80 70 60 50 40 30 20 10 ppm

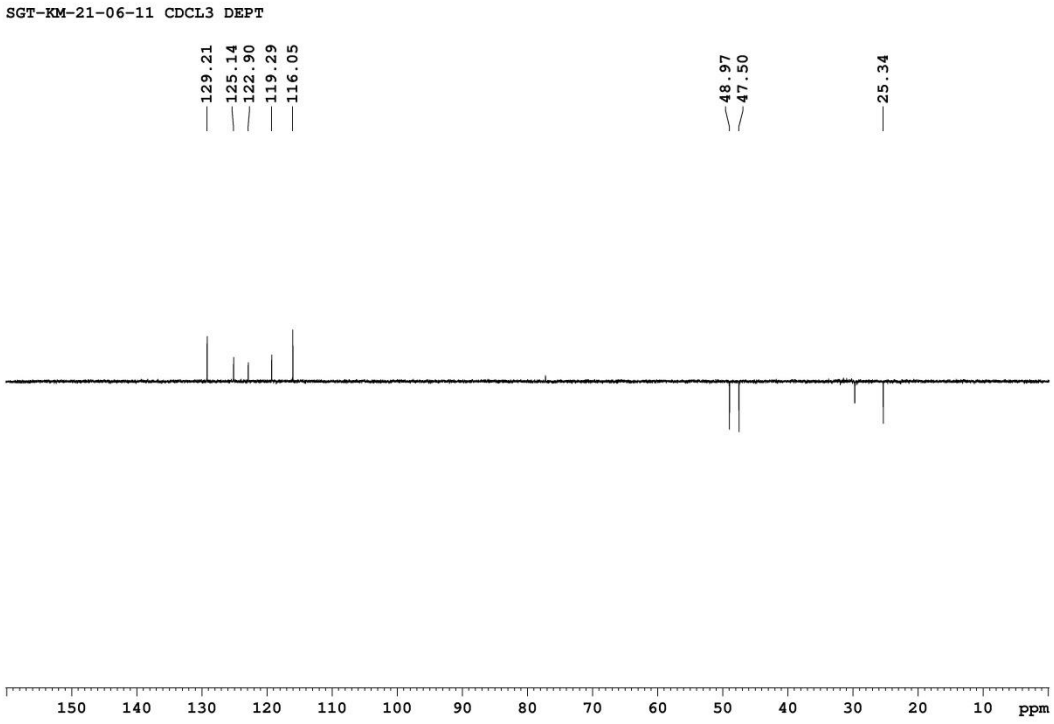
SGT-KM-21-06-11 CDCL3 DEPT
129.21
125.14
122.90
119.29
116.05
48.97
47.50
25.34
150 140 130 120 110 100 90 80 70 60 50 40 30 20 10 ppm

KM-22-01-CDCl3 PMR

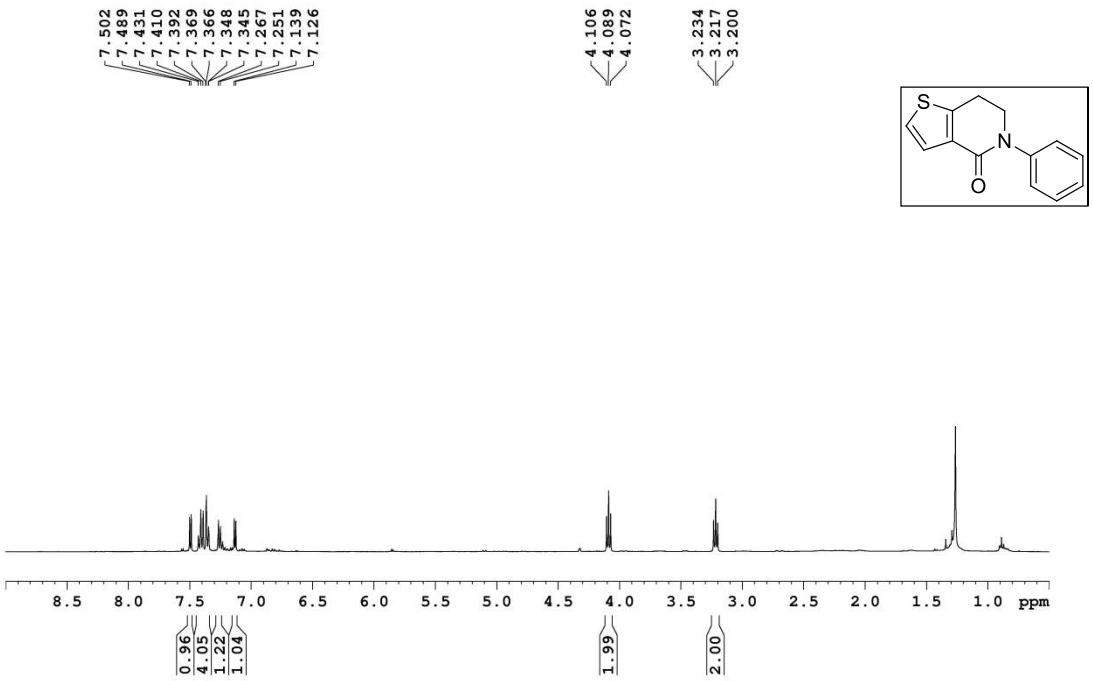

KM-22-01 CDCL3 CMR

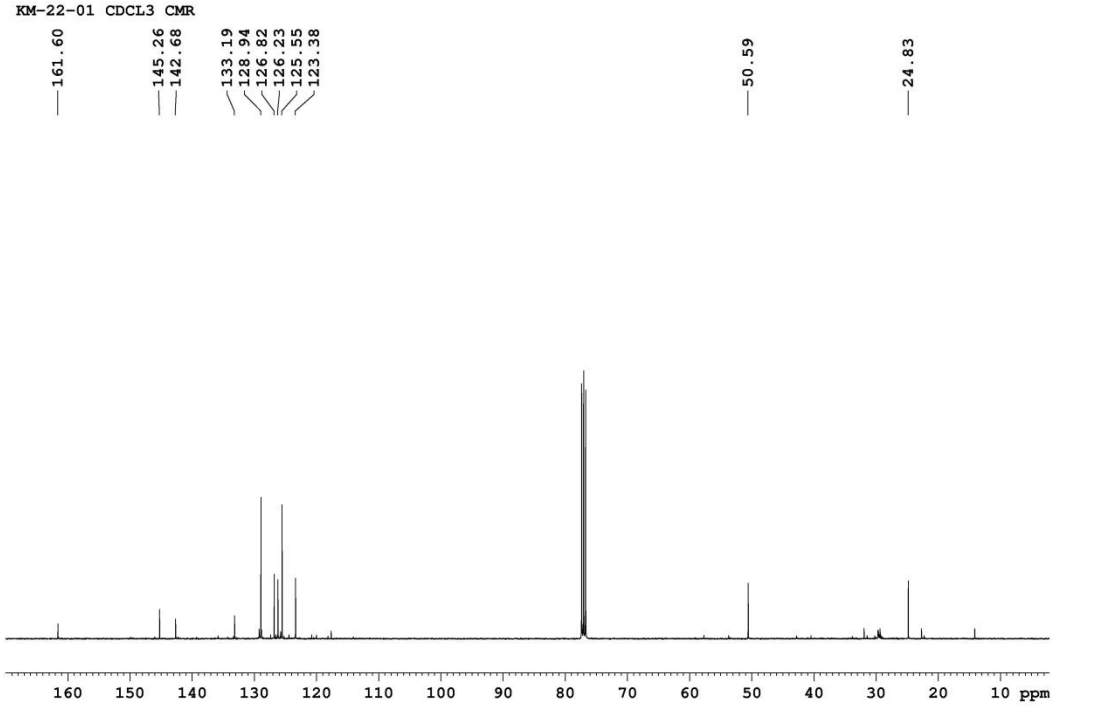

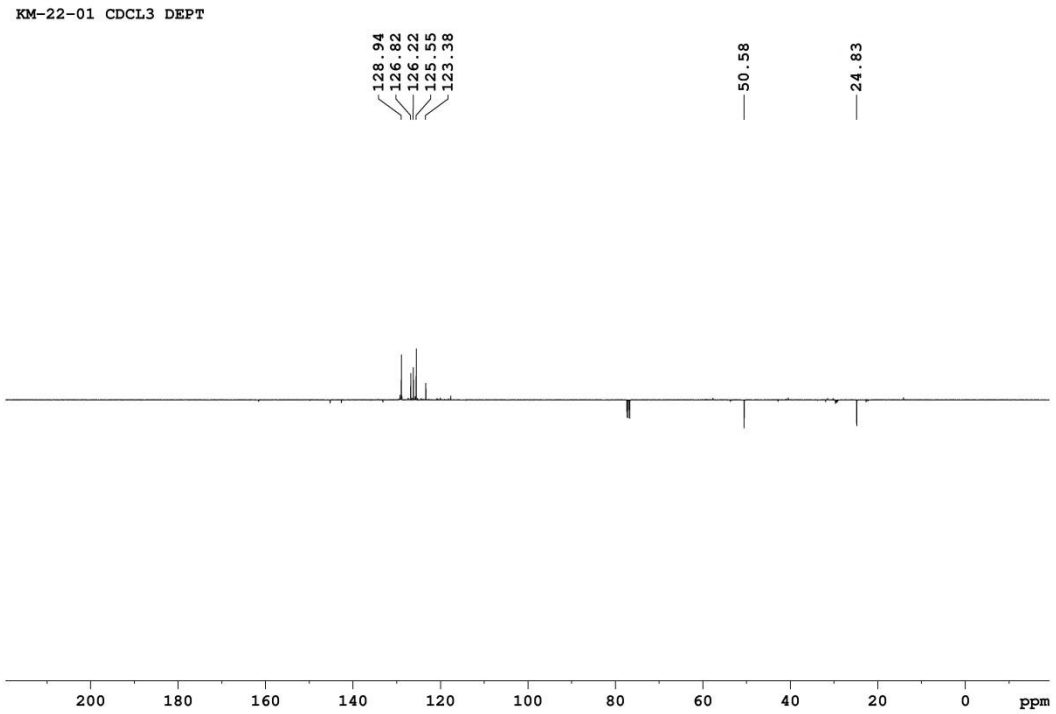
KM-22-01 CDCL3 DEPT
128.94
126.82
126.22
125.55
123.38
50.58
24.83
200
180
160
140
120
100
80
60
40
20
0
ppm

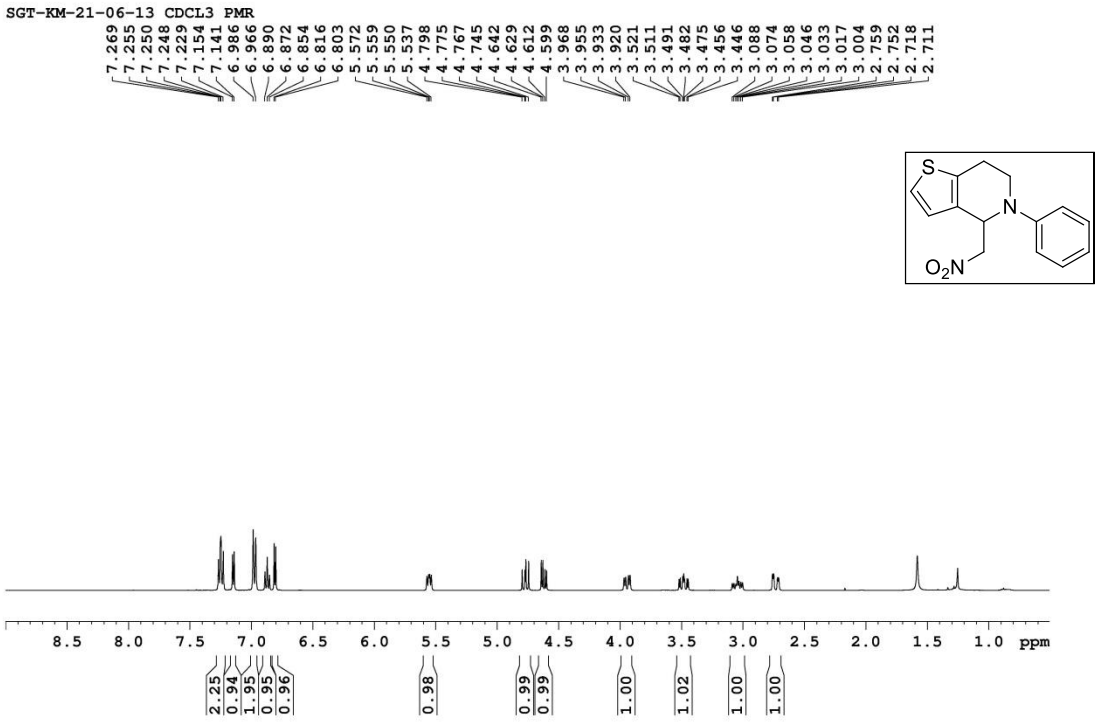
SGT-KM-21-06-13 CDCL3 PMR
7.269
7.255
7.250
7.248
7.229
7.154
7.141
6.986
6.966
6.890
6.872
6.854
6.816
6.803
5.572
5.559
5.550
5.537
4.798
4.775
4.767
4.745
4.642
4.629
4.612
4.599
3.968
3.955
3.933
3.920
3.521
3.511
3.491
3.482
3.475
3.456
3.446
3.088
3.074
3.058
3.046
3.033
3.017
3.004
2.759
2.752
2.718
2.711
S
N
O2N
8.5
8.0
7.5
7.0
6.5
6.0
5.5
5.0
4.5
4.0
3.5
3.0
2.5
2.0
1.5
1.0
ppm
2.25
0.94
1.95
0.95
0.96
0.98
0.99
0.99
1.00
1.02
1.00
1.00

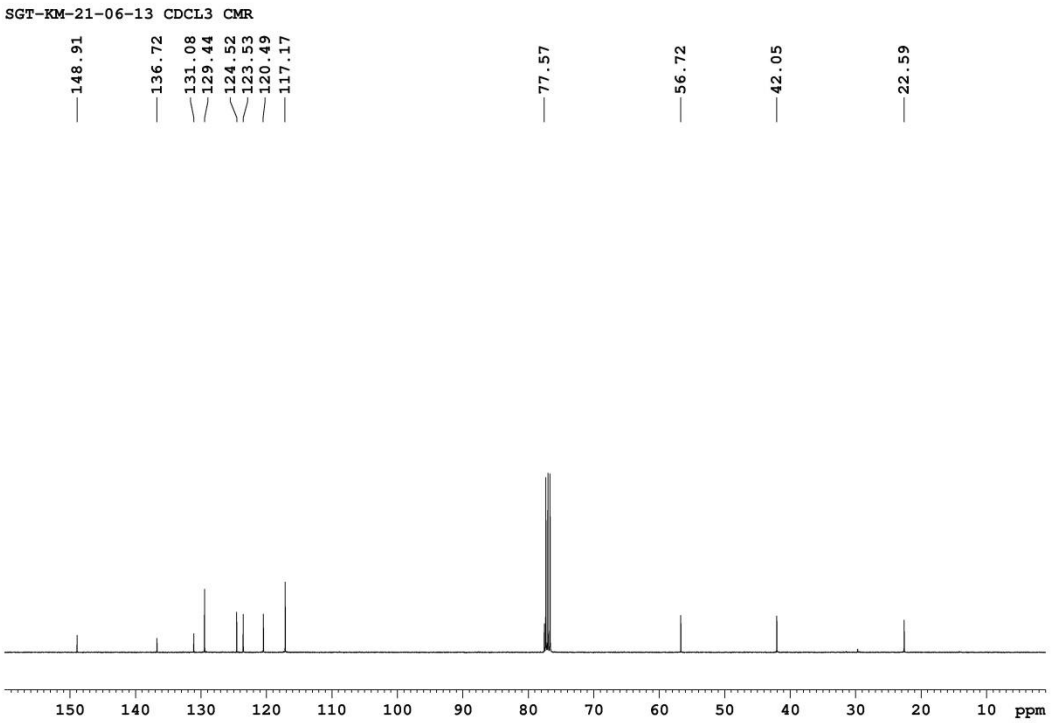
SGT-KM-21-06-13 CDCL3 CMR
148.91
136.72
131.08
129.44
124.52
123.53
120.49
117.17
77.57
56.72
42.05
22.59
150 140 130 120 110 100 90 80 70 60 50 40 30 20 10 ppm

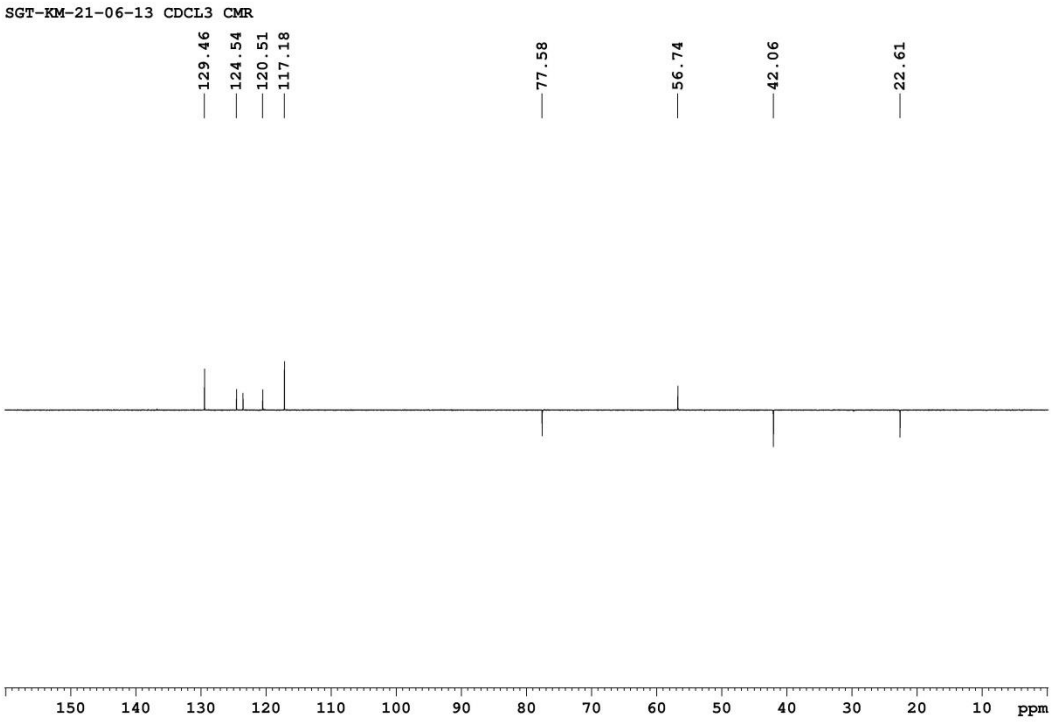
SGT-KM-21-06-13 CDCL3 CMR
129.46
124.54
120.51
117.18
77.58
56.74
42.06
22.61
150 140 130 120 110 100 90 80 70 60 50 40 30 20 10 ppm

SGT-KM-21-06-14 CDCL3 PMR

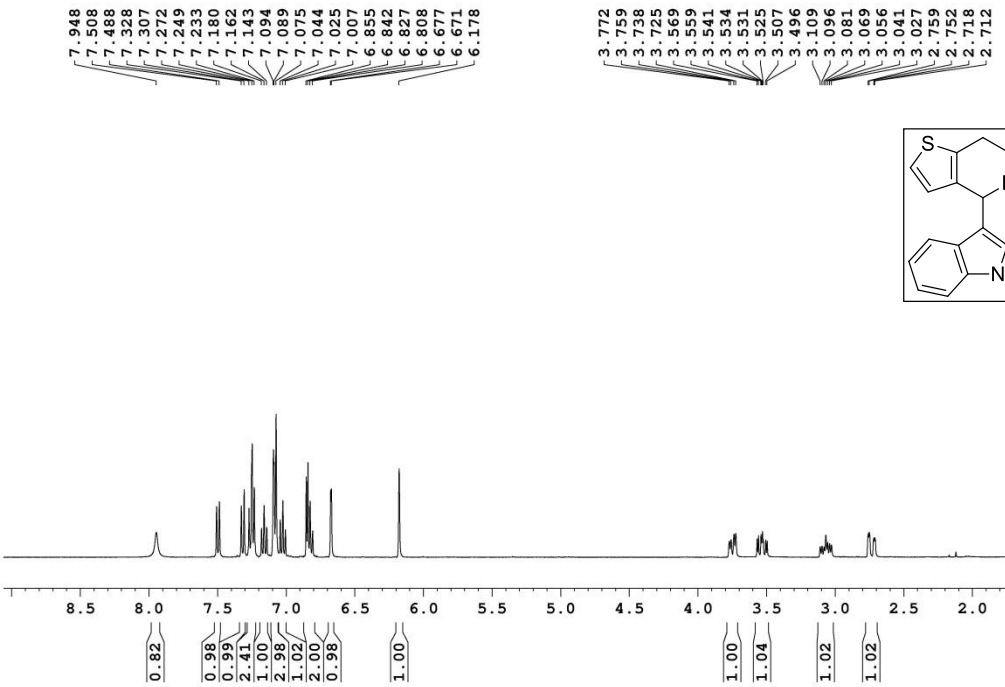

SGT-KM-21-06-14 CDCL3 CMR

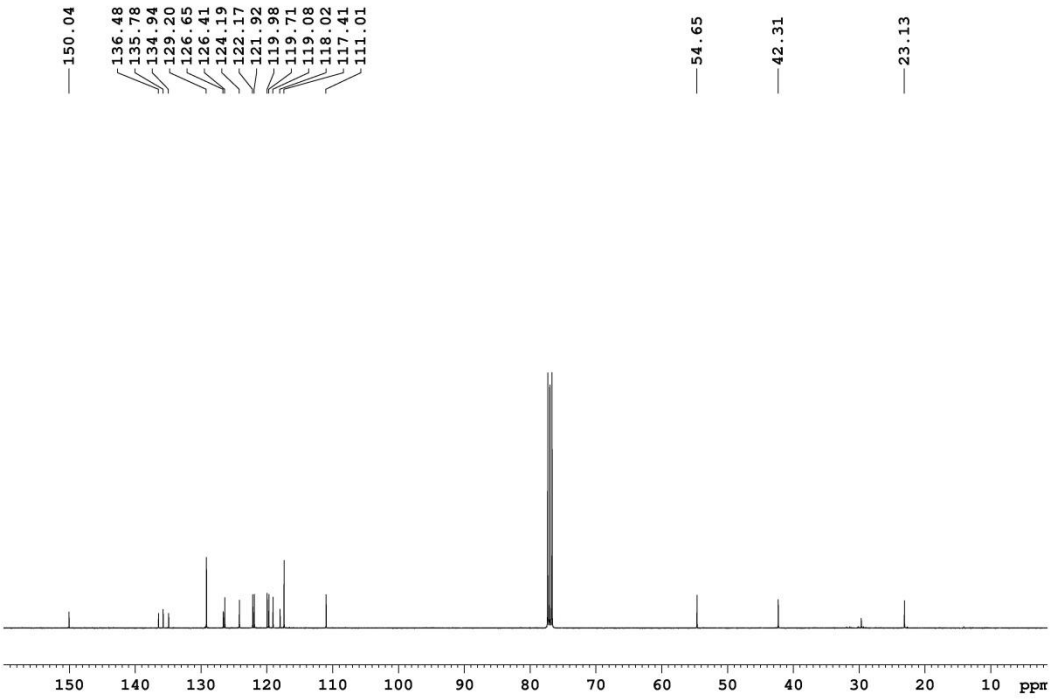

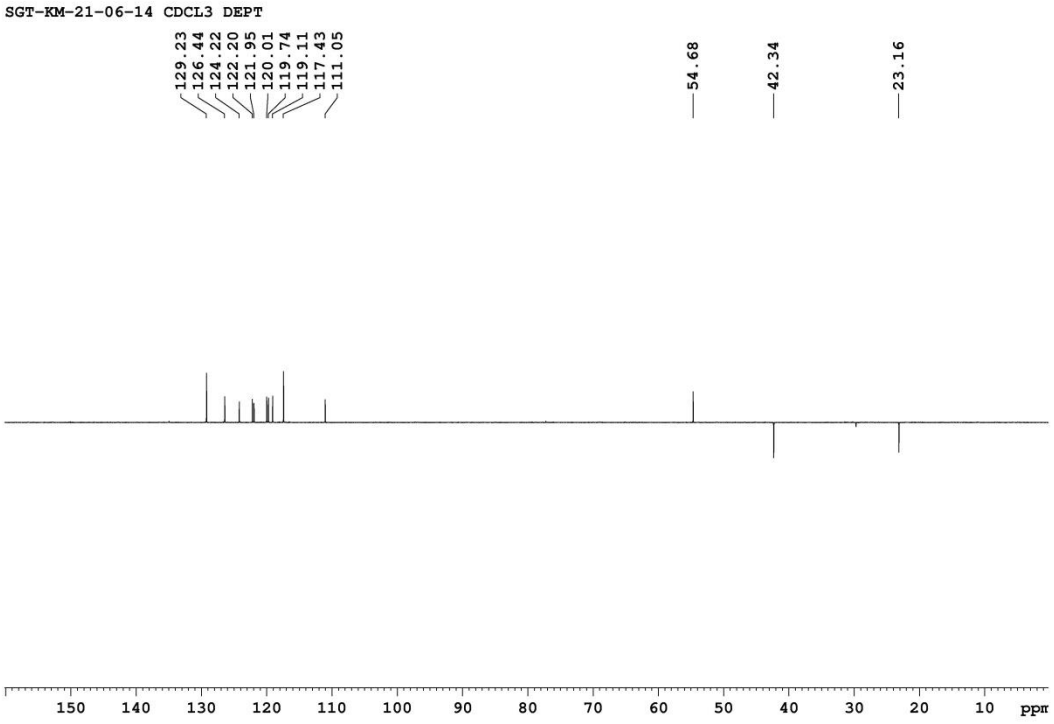
SGT-KM-21-06-14 CDCL3 DEPT
129.23
126.44
124.22
122.20
121.95
120.01
119.74
119.11
117.43
111.05
54.68
42.34
23.16
150
140
130
120
110
100
90
80
70
60
50
40
30
20
10
ppm